Hydroclimatic drought and its impacts on vegetation in south-eastern Romania

Maria-Alexandra Chelu

THESE DE DOCTORAT DE

L'UNIVERSITE RENNES 2 EN CO-TUTELLE AVEC
UNIVERSITATEA BUCUREȘTI

ECOLE DOCTORALE N° 645
Espaces, Sociétés, Civilisations
Spécialité : *Géographie*

Par

Maria-Alexandra CHELU

Hydroclimatic drought and its impacts on vegetation in south-eastern Romania

Thèse présentée et soutenue à Rennes, le 19 décembre 2023
Unité de recherche : LETG (Littoral - Environnement - Télédétection - Géomatique) UMR 6554

Rapporteurs avant soutenance :

Nadège MARTINY	Maître de Conférences-HDR, Université Bourgogne-Franche-Comté, Dijon
Iulian-Horia HOLOBÂCĂ	Professeur, Universitatea Babeș-Bolyai, Cluj-Napoca

Composition du Jury :

Examinateurs : Sylvain BIGOT	Professeur, Université Grenoble Alpes, Grenoble
Nadège MARTINY	Maître de Conférences-HDR, Université Bourgogne-Franche-Comté, Dijon
Iuliana ARMAȘ	Professeure, Universitatea din București, Bucarest
Iulian-Horia HOLOBÂCĂ	Professeur, Universitatea Babeș-Bolyai, Cluj-Napoca
Dir. de thèse : Vincent DUBREUIL	Professeur, Université Rennes 2, Rennes
Co-dir. de thèse : Liliana ZAHARIA	Professeure, Universitatea din București, Bucarest

University of Bucharest

Faculty of Geography

Doctoral School Simion Mehedinți - Nature and Sustainable Development

Rennes 2 University

LETG UMR 6554

Doctoral School Espaces, Sociétés, Civilisations

Hydroclimatic drought and its impacts on vegetation in south-eastern Romania

COTUTELLE THESIS

by

Maria-Alexandra Chelu

SUPERVISORS

Prof. univ. dr. Liliana Zaharia

Prof. univ. dr. Vincent Dubreuil

ACKNOWLEDGEMENTS

I would like to express my thanks and gratitude to my scientific supervisors, Prof. Liliana Zaharia and to Prof. Vincent Dubreuil, for their trust, patience, and support throughout my doctoral journey. I was greatly encouraged by their guidance and collaboration.

I am thankful for the discussions and suggestions from the members of my guiding committees in Romania and France, Prof. Nicoleta Ionac, Prof. Valentina-Mariana Mănoiu and Prof. Georgeta Bandoc, as well as Prof. Gabriela Ioana-Toroimac and Prof. Sylvain Bigot. I thank the members of the defense committee, Prof. Nadège Martiny and Prof. Iulian-Horia Holobâcă. I would also like to thank my colleagues at LETG Rennes for welcoming me.

I am grateful for the support from Ioana Sîrbu and for my fruitful discussions with Nicu Ciobotaru and Gabriela Moroșanu.

I am grateful to Prof. Ionuț Șandric and Prof. Cristian Iojă for my early formative training in environmental sciences.

I acknowledge the funding from the "Bourse du Gouvernement Français" through the Institut Français and the scholarship from the University of Bucharest.

I acknowledge the agencies and organizations providing the data for the thesis: ROCADA and the Water Basins Administrations, ECA&D and E-OBS, EEA, CRU, ESA, NOAA, and NASA.

I am deeply grateful for the support of my family and my friends in Romania, France and elsewhere that constantly encouraged me during this time.

SUMMARY

The south-eastern part of Romania is particularly vulnerable to drought due to its specific physical-geographical and socio-economic features. The present study aimed to investigate hydroclimatic drought in this region and its impact on natural and cultivated vegetation. After an introductory first part, the second part of the thesis was dedicated to two main aspects regarding this hazard's characteristics in south-eastern Romania. Firstly, the variability of hydroclimatic parameters relevant to drought was analysed, focusing on precipitation, temperatures, evapotranspiration, and streamflow. Secondly, drought was investigated using standardized drought indices and the climatic water deficit, obtained through a water balance method. Results have shown that all stations had significant positive trends between 1961 – 2020 in annual and summer months temperatures and potential evapotranspiration. Precipitation did not have a very clear trend in the region. There was a reduction of streamflow (analysed in the 1966 – 1910 interval) in basins in the study area, determined mainly by climatic factors. Between 1961 – 2020, the climatic water deficit showed a higher frequency of arid months in the summer, particularly in August, and a significant positive trend of the water deficit in August at all meteorological stations, probably related to the increased evapotranspiration due to higher temperatures. The climatic water deficit, the Standardized Precipitation Index (SPI) and the Standardized Precipitation Evapotranspiration Index (SPEI) were used to identify and characterise important periods of drought. The third part of the thesis focused on the assessment of vegetation response to drought, based on the Normalized Difference Vegetation Index (NDVI), in different land cover types and ecoregions. At the regional level, the NDVI trends and the interannual variability in NDVI anomalies were examined in different land covers (arable lands, forests, pastures and grasslands). Finally, the NDVI variability was investigated in detail in the broadleaf forests in five study areas. Results highlighted variations in vegetation condition and phenological metrics in response to drought between 2001 – 2020, particularly in two selected dry periods (2007 – 2008 and 2019 – 2020). The phenological analysis showed varied responses depending on the phenological phase identification algorithm. The results of this thesis could contribute to a better understanding of the hydroclimatic drought occurrence and features in south-eastern Romania, as well as its relation to vegetation health. They could be used for further research or drought mitigation and preparedness measures.

REZUMAT

Partea de sud-est a României este deosebit de vulnerabilă la secetă din cauza caracteristicilor sale fizico-geografice și social-economice specifice. Studiul de față a avut ca scop investigarea secetei hidroclimatice din această regiune și impactul acesteia asupra vegetației naturale și cultivate. După o primă parte introductivă, a doua parte a tezei abordează două aspecte principale privind caracteristicile acestui hazard în sud-estul României. În primul rând, a fost analizată variabilitatea a parametrilor hidroclimatici relevanți pentru secetă, cu accent pe precipitații, temperatura aerului, evapotranspirație și debitul râurilor. În al doilea rând, seceta a fost investigată cu ajutorul indicilor standardizați de secetă și al deficitului de evaporație, obținut prin metoda bilanțului hidric. Rezultatele au arătat că toate stațiile meteorologice au avut tendințe pozitive semnificative între 1961 - 2020 în ceea ce privește temperaturile anuale și ale lunilor de vară și evapotranspirația potențială. Precipitațiile nu au avut o tendință foarte clară în regiune. S-a înregistrat o diminuare a debitului cursurilor de apă (în intervalul 1966 – 1910) în bazine hidrografice din zona de studiu, determinată în principal de factori climatici. În perioada 1961 – 2020, deficitul de evaporație a înregistrat o frecvență mai mare a lunilor aride în timpul verii, în special în luna august, și o tendință pozitivă semnificativă a deficitului de evaporație în luna august la toate stațiile meteorologice, probabil legată de creșterea evapotranspirației din cauza temperaturilor mai ridicate. Deficitul de evaporație, Indicele Standardizat de Precipitații și Indicele Standardizat de Precipitații-Evapotranspirație au fost utilizate pentru a identifica și caracteriza perioadele semnificative de secetă. Cea de-a treia parte a tezei s-a axat pe evaluarea răspunsului vegetației la secetă, pe baza Indicelui Normalizat de Diferențiere a Vegetației (NDVI), în diferite tipuri de acoperire a terenurilor și ecoregiuni. La nivel regional, au fost examinate tendințele NDVI și variabilitatea interanuală a anomaliilor NDVI în diferite tipuri de acoperire a terenului (terenuri arabile, păduri, pășuni și pajiști). În final, variabilitatea NDVI a fost investigată în detaliu în pădurile de foioase din cinci zone de studiu. Rezultatele au evidențiat variații în starea vegetației și în metricile fenologice ca răspuns la secetă între 2001 – 2020, în special în două perioade secetoase selectate (2007 – 2008 și 2019 – 2020). Analiza fenologică a arătat răspunsuri variate în funcție de algoritmul de identificare a fazei fenologice. Rezultatele acestei teze pot contribui la o mai bună înțelegere a apariției secetei hidroclimatice în sud-estul României, precum și a relației acesteia cu starea de sănătate a vegetației. Acestea ar putea fi utilizate pentru cercetări ulterioare sau pentru măsuri de atenuare și pregătire în caz de secetă.

RÉSUMÉ

La partie sud-est de la Roumanie est particulièrement vulnérable à la sécheresse en raison de ses caractéristiques physiques géographiques et socio-économiques spécifiques. La présente étude a pour objectif d'analyser la sécheresse hydroclimatique dans cette région et son impact sur la végétation naturelle et cultivée. Après une première partie introductive, la deuxième partie de la thèse est consacrée à deux aspects principaux concernant les caractéristiques de cet aléa dans le sud-est de la Roumanie. Tout d'abord, la variabilité des paramètres hydroclimatiques pertinents pour la sécheresse est analysée, en se focalisant sur les précipitations, les températures de l'air, l'évapotranspiration et le débit des rivières. Deuxièmement, la sécheresse est étudiée en utilisant des indices de sécheresse standardisés et le déficit d'évaporation obtenu par la méthode du bilan hydrique. Les résultats montrent que toutes les stations météorologiques présentent des tendances positives significatives entre 1961 et 2020 en ce qui concerne les températures annuelles et estivales et l'évapotranspiration potentielle. Les précipitations n'ont pas de tendance très claire dans la région. Le débit des cours d'eau (dans la période 1966 – 1910) a diminué dans les bassins versants de la zone d'étude, principalement en raison de facteurs climatiques. Entre 1961 – 2020, le déficit d'évaporation montre une plus grande fréquence de mois secs en été, en particulier en août, et une tendance positive significative en août pour toutes les stations météorologiques, probablement liée à l'augmentation de l'évapotranspiration due à des températures plus élevées. Le déficit d'évaporation, l'indice standardisé des précipitations et l'indice standardisé des précipitations et de l'évapotranspiration sont utilisés pour identifier et caractériser les périodes de sécheresse importantes. La troisième partie de la thèse est focalisée sur l'évaluation de la réponse de la végétation à la sécheresse, basée sur l'indice de végétation par différence normalisée (NDVI), dans différents types de couverture terrestre et écorégions. Au niveau régional, les tendances du NDVI et la variabilité interannuelle des anomalies du NDVI dans différents types de couverture terrestre sont examinées (terres arables, forêts, pâturages et prairies). Enfin, la variabilité du NDVI est étudiée en détail dans les forêts à feuilles caduques de cinq zones d'étude. Les résultats révèlent des variations de l'état de la végétation et des paramètres phénologiques en réponse à la sécheresse entre 2001 et 2020, en particulier au cours de deux périodes sèches sélectionnées (2007 – 2008 et 2019 – 2020). L'analyse phénologique montre des réponses variées en fonction de l'algorithme d'identification de la phase phénologique. Les résultats de cette thèse peuvent contribuer à une meilleure compréhension de l'occurrence de la sécheresse hydroclimatique dans le sud-est de la Roumanie et de sa relation avec la santé de la végétation. Ils pourraient être utilisés pour d'autres recherches ou pour des mesures d'atténuation et préparation pour la sécheresse.

TABLE OF CONTENTS

ABBREVIATIONS

AET	Actual Evapotranspiration
AWC	Available Water Capacity
CDD	Consecutive Dry Days
CLC	Corine Land Cover
CRU	Climatic Research Unit
CWD	Climatic Water Deficit
ECA&D	European Climate Assessment & Dataset
ECDF	Empirical Cumulative Distribution Functions
EEA	European Environment Agency
E-OBS	European Daily High-Resolution Gridded Dataset
EOS	End of Season
HILDA	Historic Land Dynamics Assessment
IPCC	Intergovernmental Panel on Climate Change
LAI	Leaf Area Index
MODIS	Moderate Resolution Imaging Spectroradiometer
NAO	North Atlantic Oscillation
NDVI	Normalized Difference Vegetation Index
P	Precipitation
PET	Potential Evapotranspiration
Q	Streamflow
ROCADA	Romanian Climatic Dataset
SCI	Site of Community Importance
SLP	Sea Level Pressure
SM	Soil Moisture
SOS	Start of Season

SPEI	Standardized Precipitation Evapotranspiration Index
SPI	Standardized Precipitation Index
SRTM	Shuttle Radar Topography Mission
SSI	Standardized Streamflow Index
ST	Soil Water Storage

GENERAL INTRODUCTION

Drought is one of the natural hazards that generate the highest damage costs in Europe, considering that water stress negatively influences an average of 30% of the population every year (EEA, 2021a). It affects multiple socio-economic sectors and natural ecosystems and disproportionately impacts the most vulnerable members of society (UNDRR, 2021). The impacts of drought-related water deficit can be far-reaching: decreases in crop yield (Jacobs et al., 2019), loss of livelihood of farmers (Lupu et al., 2018; Sima et al., 2015), river flow reduction with consequences on water resources and energy production (Van Vliet et al., 2015, 2016) and on aquatic life (Crausbay et al., 2020), increases in tree mortality (Allen et al., 2010) and alteration of vegetation functions. In the last decades, climate change has impaired the water cycle globally (IPCC, 2022), compounded by human influence, with implications for all water-dependent sectors.

Drought is a natural hazard in Romania that frequently occurs, especially in the southern and eastern parts. These areas are particularly vulnerable to drought due to their specific geographic features, such as a negative climatic water balance during the vegetation period (Prăvălie et al., 2019), a trend of increased temperatures and heat waves that can enhance drought intensity (Bojariu et al., 2021; Dumitrescu et al., 2015) and aridization (Bojariu et al., 2019; World Bank, 2018). The National Strategy for Climate Change for 2013 – 2020 highlights that these parts of Romania are the most vulnerable to drought (MMSC, 2012). In the European Union, Romania has one of the lowest rankings regarding water availability per capita (World Bank, 2018). Moreover, climatic scenarios project decreases in mean streamflow and increased frequency of hydrological drought in Romania (Van Vliet et al., 2015) with consequences on water resources and supply.

An analysis between 1970 – 2013 based on the European Drought Impact Report Inventory (EDII) showed that the most important impact of drought in Romania (from a total of 155 reports) was on agriculture and livestock farming, followed by impacts on human health and on the energy and industry fields (Stahl et al., 2016). Stahl et al. (2016) also showed that decreased productivity of annual and perennial crops represented more than half of Romania's "agriculture and livestock farming" impact. For example, maize yield decreased by approximately 46.1%, wheat by 18.3%,

and sunflower by about 15.7% in 2012 (a year with drought) compared to the previous three years' average (Mateescu et al., 2013).

Water deficit, higher temperatures, and pests adapted to droughts are also recognized as threats to forest function and structure (Bastrup-Birk et al. 2016; MMSC 2012). For example, droughts and warmer temperatures after the 1980s had significant impacts on forests in Romania, such as defoliation and tree mortality, particularly on broadleaves such as *Quercus pedunculiflora*, *Quercus pubescens* and *Quercus frainetto* (Badea and Neagu, 2007; Petriţan et al., 2021). The potential effects on forests caused by the projected drought and rising temperature stress during the vegetation season in many parts of Europe might include increases in tree mortality and pests or decreased resilience (Bates et al., 2008).

Given the risks induced by droughts on natural ecosystems, ecosystem services, and human societies, it is crucial to deepen the knowledge of this physical process in the context of environmental change and climate warming. Furthermore, understanding the local and regional vulnerability can support the sustainable management of drought and mitigate the related impacts, one of the most critical issues worldwide. This is particularly interesting in areas with a high vulnerability to drought due to the climatic and geographic particularities, such as the south-east of Romania.

Objectives

In the aforementioned context, this thesis aims to investigate the temporal and spatial drought variability in south-eastern Romania and explore how the water deficit influences vegetation in this particular geographic context. Three major specific objectives can be summarized:

1. Analysing the variability of hydroclimatic parameters relevant to drought in south-eastern Romania.

2. Analysing drought variability at different temporal and spatial scales and identifying particular features (e.g., drought occurrence, frequency changes and trends, drought events characteristics).

3. Investigating the response of vegetation to drought at different spatial and temporal scales considering different land covers and ecoregions based on remote sensing data.

Thesis structure

The thesis is organised into three major parts. **Part I** outlines introductory aspects: the **first chapter** introduces the contextual and conceptual framework, while **Chapter 2** presents the study area and its main geographical features based on a review of relevant literature and available data processing.

The next two parts are devoted to the investigation of hydroclimatic drought and its impact on vegetation in the study area. The methodology of each of the two parts is presented separately —**Chapter 3** describes the methodology for **Part II** and **Chapter 6** describes the methodology for **Part III**.

Part II is dedicated to analysing the hydroclimatic variability and drought in south-eastern Romania. **Chapter 3** presents the general data and methodology for investigating hydroclimatic variability and estimating drought indices. Furthermore, it discusses the evaluation of the gridded precipitation datasets used in the analysis. **Chapter 4** first explores the variability of the hydroclimatic parameters relevant to drought at meteorological and gauging stations, based on measured data and data modelling through the water balance method. The hydrological analysis focuses only on surface water due to the difficulty of obtaining groundwater data. It is followed by the analysis of soil moisture data derived from satellite products. Moreover, several catchment case studies were selected to investigate streamflow's long-term variability in relation to climatic variation, human influence, and vegetation ad land cover dynamics. Finally, **Chapter 5** investigates drought in the study area using the climatic water deficit (obtained through a water balance method) and standardized drought indices.

Part III focuses on the assessment of vegetation response to drought. **Chapter 6** presents the general data and methodology for exploring the impact of drought on vegetation**.** Two approaches were considered: firstly, a regional, larger scale approach that allowed finding a general effect of drought on vegetation while distinguishing between different land covers and secondly, a smaller-scale comparative analysis of drought impact on broadleaf forests considering several case studies corresponding to different ecoregions. At the regional level, trends in the

Normalized Difference Vegetation Index (NDVI) were examined in the different land covers while discussing phenological changes due to climate change (**Chapter 7**). Moreover, the interannual variability in NDVI anomalies was explored to highlight the temporal and spatial distribution of stressed vegetation. The last chapter (**Chapter 8**) investigated the differences in vegetation response to drought in several case studies and the results regarding variations in vegetation condition and phenological metrics were analysed particularly in two dry periods (2007 – 2008 and 2019 – 2020) and discussed in the context of drought occurrence.

The spatial and temporal scales considered in the approaches of this thesis are summarized in **Figure 1**.

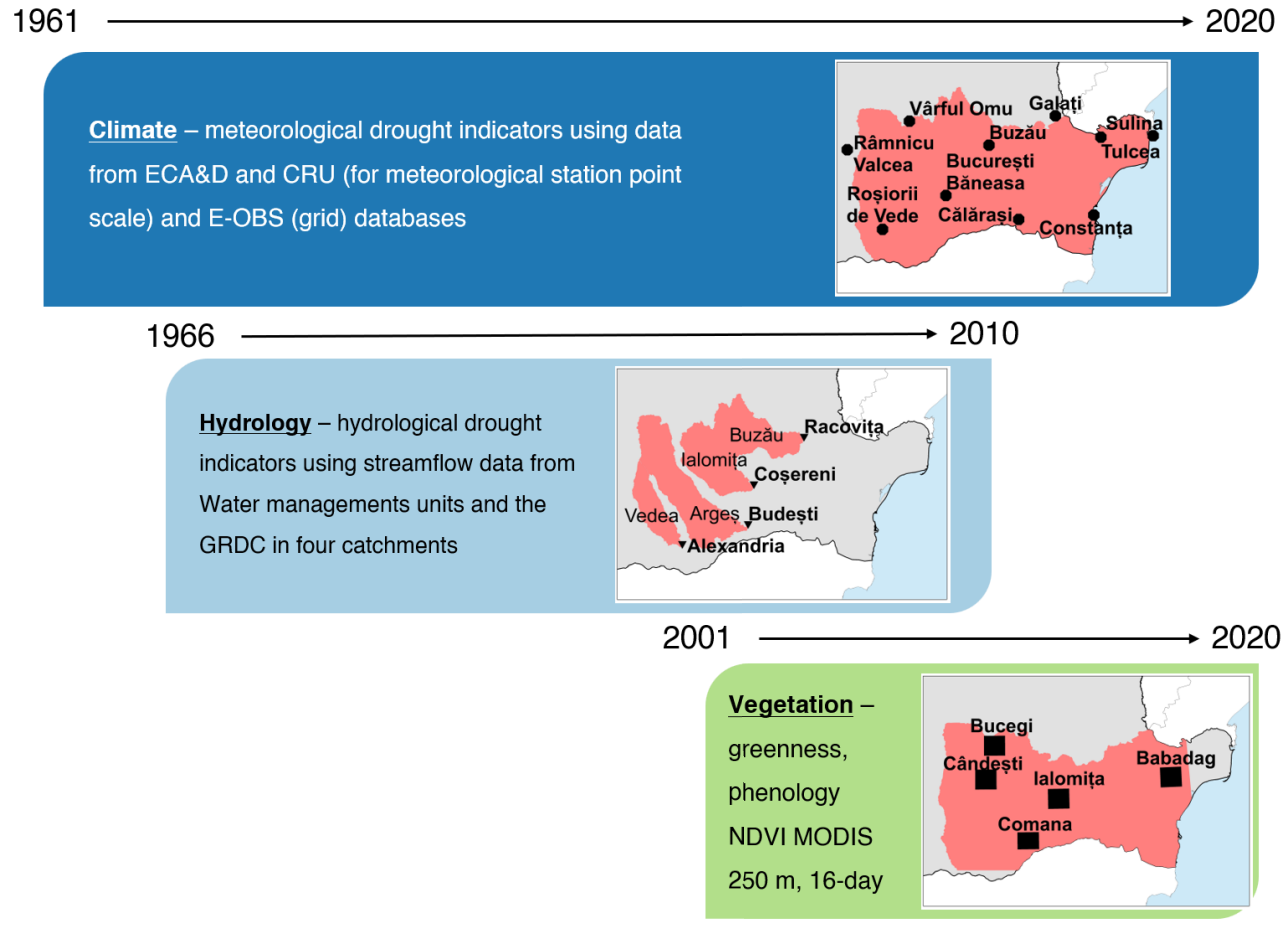

Figure 1 Overview of temporal and spatial scales and data used in this study

PART I

INTRODUCTION AND CONTEXTUAL FRAMEWORK

This part establishes the foundation of the thesis by setting up the contextual theoretical framework for the subsequent chapters and outlining the general geographical features of the study area. **Chapter 1** provides a review of the relevant literature on three main topics: i) drought definitions, approaches, and monitoring; ii) drought in the context of climate change and human influence, and iii) an overview of drought impacts on vegetation in relation to climate change. **Chapter 2** presents the study area and its main geographical characteristics (location, landforms, climate, hydrology, vegetation, and land covers) and highlights the relevance of researching drought within this study area.

1. THEORETICAL FRAMEWORK AND LITERATURE REVIEW

1.1. Drought definitions, approaches, and monitoring

Drought is a temporary, recurring feature in any climate and is not synonymous with aridity. Conceptually, drought is defined as a precipitation deficit relative to average conditions (IPCC, 2021; Monacelli et al., 2005), with high temperatures and high saturation deficit (Ciulache and Ionac, 2003), generating an impact on human activities and the environment, while aridity is a permanent characteristic of a climate manifested by low average rainfall (Hounam et al., 1975; Monacelli et al., 2005). Drought occurrence is mainly associated with the persistence of anticyclonic conditions (Holobâcă, 2010). Droughts unfold gradually over an extensive period and across large areas, and identifying their onset is challenging (Wilhite, 2000). It has a progressive and diffuse spatial and temporal nature (Sorocovschi, 2009). Therefore, a regional approach is recommended in defining drought by considering regional climatic, geographic, and socio-economic conditions that increase drought risk (Dubreuil, 1996; Mutti, 2020; Wilhite and Glantz, 1985). The intensity of drought is controlled by multiple factors such as the characteristics of the Earth's surface (e.g., topography, land cover, water surfaces), climate particularities, physiological and phenological characteristics of vegetation and human activities (Bogdan and Țîștea, 1983; Dubreuil, 2004). The occurrence of droughts in areas with aridity tendencies, such as south-eastern Romania, imposes more severe issues related to regional water resources than in other regions (Păltineanu et al., 2007b). While drought can occur every season, a long spring drought following a winter drought can be the most damaging type (Ciulache and Ionac, 1995).

Outlining a universal definition of drought is problematic due to the complexity and interconnections between its multiple facets at multiple spatial and temporal scales (Dubreuil, 1996; Heim, 2002). However, operational definitions address the characteristics of drought events, thus helping to identify and analyse them in time and space and relating them to historical conditions (Monacelli et al., 2005). Droughts are usually classified into four main types, depending on where the water deficit manifests: *meteorological drought*, *soil moisture (agricultural) drought*, *hydrological drought, socio-economic drought* (**Figure 1.1**) and *ecological drought* (Crausbay et al., 2017; Kallis, 2008; Lambert, 1977; Mishra and Singh, 2011; Wilhite, 2000; Wilhite and Glantz, 1985; Zargar et al., 2011).

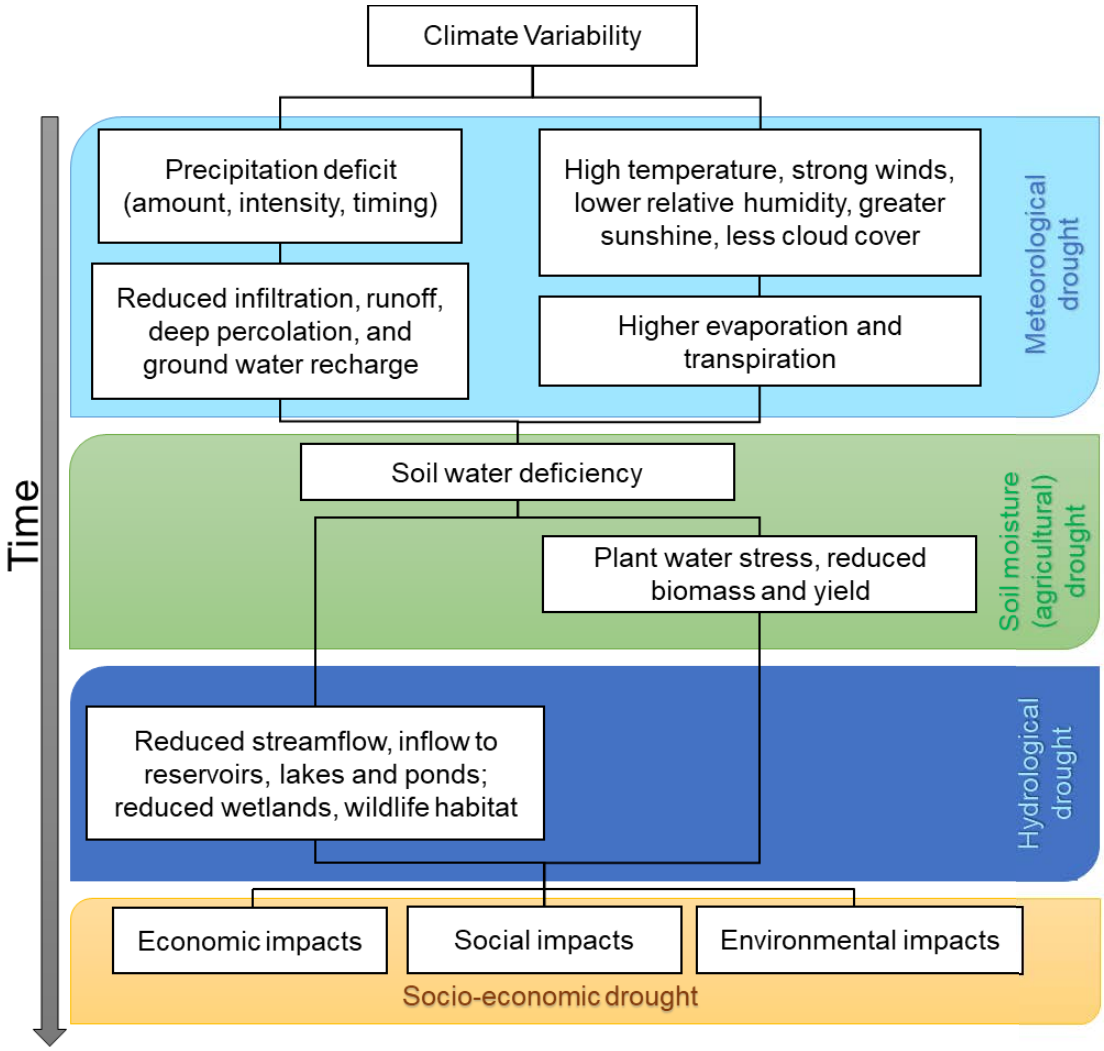

Figure 1.1 Drought types and their cascading effects in time (adapted from Wilhite, 2000)

- *Meteorological drought* is generally defined by a precipitation deficit relative to the regional climate within a specific time frame or by an indicator also considering potential evapotranspiration. The main factors that enhance drought intensity are high temperatures, strong winds and decreased cloudiness and humidity (**Figure 1.1**). In Romania, meteorological drought is considered to set in after ten consecutive days of no rainfall (ANM, 2014). Meteorological drought could also occur when actual evapotranspiration is higher than precipitation and lower than potential evapotranspiration (Lambert, 1977). During meteorological drought, hydrological processes such as infiltration, runoff, percolation, and groundwater recharge are reduced while evaporation and transpiration increase (**Figure 1.1**).

- *Soil moisture drought* (*agricultural drought* or *agricultural and ecological drought*, as defined in the 2021 IPCC report) is defined as a period when plant water requirements are not met due to reduced soil moisture as a consequence of meteorological drought, reducing biomass and yield in natural and agricultural vegetation (Lambert, 1977; Monacelli et al., 2005; van der Molen et al., 2011). It occurs after the onset of meteorological drought due to the soil water reserve that sustains plants during rainfall deficits (Trzpit, 1978). When the available water reserves decrease, a lower transpiration rate is sustained by the extension of roots (Hounam et al., 1975). The water requirements of plants depend on meteorological conditions, species' biological characteristics, life stages, and bio-physical features of the soil (Wilhite and Glantz, 1985). The climatic water deficit can highlight periods of both meteorological and soil moisture drought (Lamy, 2014; Mutti, 2020).
- *Hydrological drought* refers to a decrease in streamflow, water volume in lakes, reservoirs and ponds, and groundwater, compared to average values. Some authors have proposed groundwater drought as a distinct type of drought (Mishra and Singh, 2010). Hydrological drought is influenced by climatic factors and the basin's geomorphology, lithology and soil texture (INHGA, 2015). An operational definition can be given based on exceedance probability thresholds on the flow duration curve (Croitoru and Toma, 2011; Ștefan et al., 2004).
- *Socio-economic drought* occurs when the water supply does not satisfy water demands (water as an economic good). Meteorological, soil moisture and hydrological drought impacts cascade effects on social, economic and environmental systems. It reflects both drought as a natural hazard and the vulnerability of a socio-economic system (Maskey and Trambauer, 2015).

More recently, *ecological drought* has been defined as a water deficit that negatively impacts ecosystems and ecosystem services, driving ecological communities beyond vulnerability thresholds (Crausbay et al., 2017). From an ecological perspective, an extreme climatic event such as a severe drought alters ecosystem structure and function beyond the normal variability after passing an "extreme response threshold", which can lead to responses such as a longer recovery time or a permanent shift in species composition (Smith, 2011). In this context, the ecosystem response to drought depends on its resilience (Ingrisch and Bahn, 2018). Many studies on ecological drought focused on impacts related to water bodies (Bachmair et al., 2016).

Drought monitoring and early warning systems are essential to national and international drought risk management strategies, and they identify hydroclimatic trends for detecting drought occurrence and estimating its severity (WMO, 2006). Monitoring drought involves the continuous use of indicators and indices, estimated based on the current climate, hydrological and vegetation conditions (WMO and GWP, 2016). More specifically, drought indices represent a quantitative measure of estimating drought and are calculated using climatic, hydrometeorological or vegetation indicators, such as precipitation, air temperature, streamflow, soil moisture, groundwater levels, or vegetation greenness (WMO and GWP, 2016). A vast body of literature is available on this subject, with more than 150 drought indices identified until 2011 (Chelu, 2019; Zargar et al., 2011).

New indices have been developed to represent local geographic conditions better, apply different statistical methods, or integrate multiple variables. However, when considering drought impact on vegetation, hydrometeorological indices represent only an indirect measurement and should be complemented by remote sensing indices (Norman et al., 2016), which can generate a spatialization of this hazard (Dubreuil, 1996). For instance, integrating hydrometeorological drought indicators such as the climatic water deficit with vegetation indices could describe the extent and intensity of drought (Dubreuil, 1995, 2004; Holobâcă et al., 2003; Lecerf et al., 2008). Moreover, the anomalous seasonal variations in land surface phenology have the potential to be an early indicator of drought stress, especially for drought-sensitive species or phenological phases (Norman et al., 2016). Nevertheless, choosing a remote sensing product involves compromising between temporal and spatial resolution and considering the relevance of the product for the observed phenomenon.

Various quantitative methods of analysing drought events have been developed based on these indices. One widely used method for characterizing droughts is based on the *theory of runs* (Yevjevich, 1967). Drought events are identified as sequences of consecutive elements below a threshold (a negative run) in a relevant drought variable. This method allows the characterization of drought events by identifying different parameters (Dracup et al., 1980; Yevjevich, 1967; Zargar et al., 2011): duration, severity (a measure of deficit accumulation), intensity (the ratio between severity and duration, which highlights an average deficit), onset and end of the drought event and frequency (number of cases in a specific interval, for example in a decade) (**Figure 1.2**).

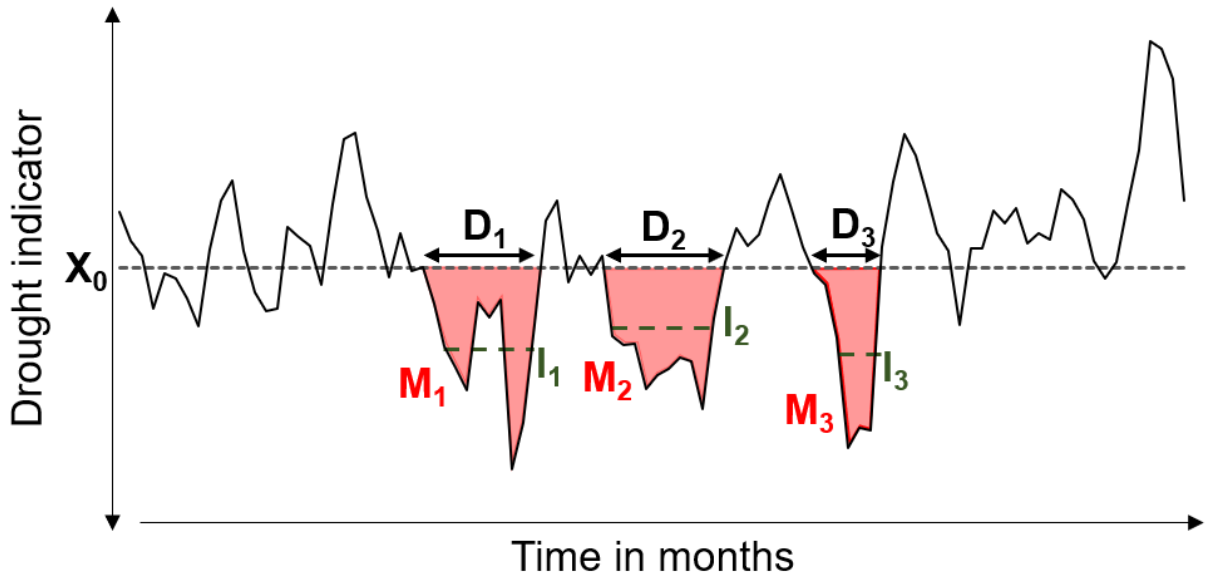

Figure 1.2 Definition of drought characteristics using the run theory and a drought indicator (adapted from Yevjevich, 1967). The drought event starts when the indicator crosses a threshold (X_0), and it is characterized by duration (D), magnitude (M) and intensity (I) (terminology from Zargar et al. 2011).

1.2. Drought, climate change and human influence

While droughts are a regular occurrence following variations in atmospheric circulation, global warming has increased drying trends in many parts of the world (Dai, 2011), which amplified the likelihood and severity of drought impact on society and economy (Pörtner et al., 2022).

The spatial distribution of drought trends is heterogeneous globally (IPCC, 2021). On the European continent, a spatial north-south opposition in trends was observed, with southern Europe experiencing increasing drought frequency, in contrast to northern Europe (Stagge et al., 2017). The projected trends for the 21st century are predicted to follow a similar structure due to the continuing warming (IPCC, 2021).

Even though drought distribution or frequency might not have changed substantially, this phenomenon became more intense due to global warming. The influence of temperatures, cloudiness and solar radiation on the variability of the global water budget became higher,

especially after the 1980s, alongside precipitation (Dai, 2011). The increase in average global temperature due to greenhouse gas concentrations is an essential factor influencing local hydroclimatic variability.

The observed and projected warming might exacerbate extreme events such as droughts; the onset might be sooner and more intense (Baronetti et al., 2022; Trenberth et al., 2014), which increases the potential impact on water resources and vegetation. The association of dry periods with high temperatures drives a higher evaporative demand (increased potential evapotranspiration) and increases surface drying (IPCC, 2021; Trenberth et al., 2003), which defines the "hotter drought" concept (Allen et al., 2015; Breshears et al., 2005).

The increase in water deficit and drought severity caused by higher temperatures is likely to influence negatively plant physiological processes faster during drought events and therefore increase tree mortality (Allen et al., 2015) or affect crop yield (Füssel et al., 2017). In addition, the increasing risk of heatwaves and wildfires (Trenberth et al., 2003) also compounds the vulnerability of ecosystems to drought.

Furthermore, because of the warming in winter, snowpack accumulation might generally decrease ("warm snow drought") and could contribute to lower soil moisture and streamflow later in the year, with implications for ecosystems, agriculture, water management, flood risk and hydropower (Harpold et al., 2017; Huning and AghaKouchak, 2020).

Moreover, drought development is influenced by human activities that directly or indirectly affect the water cycle (**Figure 1.3**), such as land use, irrigation, dams or water abstractions (Van Loon et al., 2016). As examples of land use change, deforestation and urbanisation influence water resources at the catchment scale (Dey and Mishra, 2017; Wang et al., 2020) and responses to drought. Van Loon et al. (2016) proposed to differentiate between climate and human-induced droughts, as well as human-modified droughts. For example, the Nuntași-Tuzla Lake, located in the Dobrogea region, adjacent to the Black Sea, dried up in 2020 (**Figure 1.4**) due to severe drought on the background of modifications of the hydrological system and inadequate management (Șerban et al., 2022).

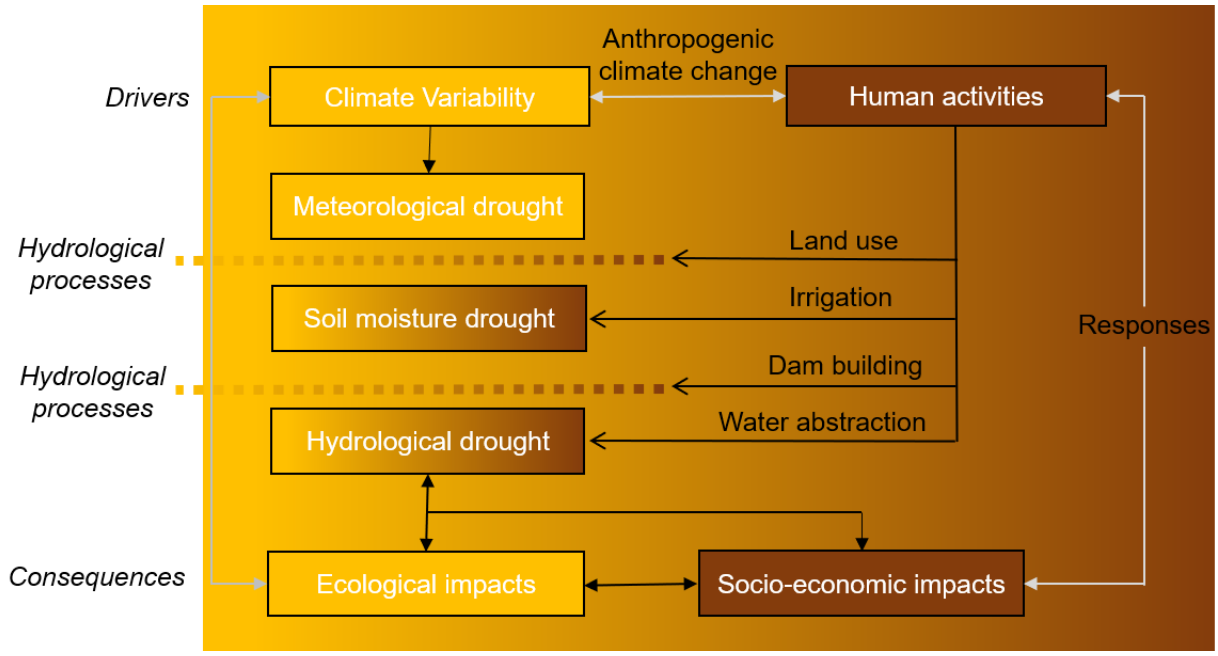

Figure 1.3 Drought development and the role of human impact (adapted from Van Loon et al., 2016). The climatic influence is represented by yellow (on the left), while human influences are brown (on the right). Human activities that impact land and hydrological processes inherent to drought are represented with black arrows, and feedbacks by white arrows.

Figure 1.4 Dried Nuntași-Tuzla Lake in September 2020 (drone photography taken by Maria-Alexandra Chelu)

1.3. Drought impacts on vegetation in the context of climate change

During drought, plants induce stomatal closure that decreases the photosynthetic and transpiration rates and increases the water use efficiency (Chaves et al., 2009; Peñuelas et al., 2013; Trzpit, 1978). High temperatures during water deficit periods, and therefore higher rates of

potential evapotranspiration, exacerbate the stress on plant physiology and lead to increased mortality (Ciulache and Ionac, 1995; Reichstein et al., 2013). Moreover, some structural responses in vegetation during drought, such as reduced leaf area, negatively affect productivity (van der Molen et al., 2011).

Drought can influence vegetation communities at the ecosystem level by reducing primary productivity (Ciais et al., 2005), induced through direct physiological damage or lagged plant mortality (Frank et al., 2015). In addition, extreme droughts could generate shifts in plant communities when critical points are reached, which can occur more frequently under climate change (Frank et al., 2015; Harris et al., 2018). Carbon sequestration and storage, a regulating ecosystem service vital for the mitigation of climate change (Millennium Ecosystem Assessment, 2005; UNDRR, 2021), is affected by drought due to increased mortality and impeded plant growth (Reichstein et al., 2013). For carbon balance in forests, drought is the most common influencing factor on the global scale (Reichstein et al., 2013). For example, the reduction in primary productivity due to the heatwave and drought of 2003 determined ecosystems in Western Europe to release a quantity of CO_2 roughly similar to the amount stored in the previous four years (Ciais et al., 2005). Forests in Romania sequester about 25% of national total annual emissions, about 42.9 Mt CO_2 equivalent, and about 40% of them are considered to have an environmental protection role (MMSC 2012). Another regulating service that can be disturbed by drought is water purification and water storage in wetlands and riverine forests (UNDRR, 2021).

Warming has influenced phenology, the most evident effect being the advance of spring phenological stages (Füssel et al., 2017), which has implications for the ecosystem water balance (Richardson et al., 2013). In this context, drought can also influence annual phenology by advancing or delaying phenological stages (Frank et al., 2015; Jentsch et al., 2009). Plant phenological adjustment can help avoid drought periods (Allen et al., 2015; Bodner et al., 2015). The relations and feedbacks between climate variability, the water budget, vegetation productivity and phenology are complex. In years with an earlier spring onset, soil water reserves might be depleted faster, enhancing the risk of soil moisture drought in summer (Richardson et al., 2013), and potentially reducing productivity. Some studies found that water stress in summer advanced the date of the end of the growing season in drier areas (Bórnez et al., 2021). On the other hand, some species showed later autumn phenology in other sites (Xie et al., 2018).

There is a debate about whether some favourable effects of global warming compensate for the increased risk of vegetation mortality attributed to hotter droughts (Allen et al., 2015). Higher rates of photosynthesis and increased water use efficiency due to the CO_2 fertilization effect could benefit vegetation growing in drought-prone regions. Moreover, warmer temperatures at high-latitudes might encourage plant growth (Allen et al., 2015) or have minor contributions to crop yield growth in northern Europe (IPCC, 2014). For example, greening trends were observed globally and regionally in the last decades, including in grasslands, broadleaf and coniferous forests, as a response to climate change and land use/land cover change (Buitenwerf et al., 2018; Forkel et al., 2015). The positive effects of higher CO_2 concentration are expected rather for C3[1] species (most of the plant species), while C4 species (such as maize and sorghum) are less sensitive (Ainsworth and Long, 2005). Studies have suggested that photosynthesis enhancement, resulting from CO_2 fertilization, depends on water availability (Bates et al., 2008). Fischer et al. (2006) estimated increases in net irrigation requirements at the global scale by 2080, despite including the positive effect of CO_2 (Bates et al., 2008). While the CO_2 fertilization effect is beneficial during moderate drought, hydraulic failure or insufficient carbon supply due to excessive stomatal closure during extreme drought can increase plant mortality (Allen et al., 2015; Hartmann et al., 2022). The potential beneficial effects of CO_2 have often been negatively compensated by other factors (such as drought or limited nutrients), as shown in different sites worldwide (Peñuelas et al., 2011). Generally, most studies point towards an adverse effect of climate change on crops (IPCC, 2014). Furthermore, adaptations of plants to more severe droughts might not be fast enough compared to the rate of climate warming (Allen et al., 2010).

In addition, the combined effect of water deficit, high temperature, drought-related dryness and litter accumulation, as well as human-induced forest degradation, amplifies the risk of

[1] C3 and C4 are types of photosynthesis; the numbers three and four represent the number of carbons in the first stable product of carbon fixation during photosynthesis (Hopkins and Huner, Norman, 2008). While plants that use the C3 pathway are the most common, photorespiration can occur in this type of plants under hot and dry conditions, defined as the loss of CO_2 and energy due to O_2 being taken up instead of CO_2 by the enzyme responsible of capturing CO_2 (Evert and Eichhorn, 2012; Hopkins and Huner, Norman, 2008). During hot and dry conditions, plants close stomata for conserving water, limiting the concentrations of CO_2, and increasing the levels of O_2, promoting photorespiration. Plants that utilize the C4 pathway are more adapted to these conditions because the processes involved in this type of photosynthesis are more efficient, reducing photorespiration and maintaining CO_2 uptake (Hopkins and Huner, Norman, 2008). The increase of CO_2 concentration in the atmosphere might reduce photorespiration, which could benefit the C3 plants and decrease the competitive advantage of C4 plants (Evert and Eichhorn, 2012).

wildfires (Aragão et al., 2007; Bigot et al., 2019, 2021; Laurance and Williamson, 2001; Seidl et al., 2017). For instance, during the severe drought in 2018, wildfires occurred over large areas in Europe, including the centre and north (EEA, 2021b). In turn, the vulnerability to drought could be higher in the forests degraded by wildfire (Le Roux et al., 2022). Wildfires are more frequent during drought years: the largest burnt area occurred in 2012 and 2020, and the highest numbers of fires were in 2012, 2000, and 2020 (San-Miguel-Ayanz et al., 2021). The convergence of climatic and anthropogenic factors can enhance the wildfire risk during drought. Agricultural land clearings by burning during the dry and warm season (**Figure 1.5**), increased fuel load due to land abandonment, and the loss of traditional practices are determinants in fire spread from agricultural to forest land (Mallinis et al., 2019).

Figure 1.5 Agricultural land clearing by burning in southern Romania in September 2020 and August 2021 (drone photography taken by Maria-Alexandra Chelu)

Many previous results regarding drought impact on forests were provided in dendrochronological studies (Levanič et al., 2013; Mihai et al., 2021; Nechita and Chiriloaei, 2018; Nechita et al., 2017, 2019a,b; Petriţan et al., 2021). They showed that the response of trees to drought depends on local conditions, but in general, there are positive correlations with rainfall and negative correlations with temperatures. A study on *Quercus robur* at a site in the Romanian Plain showed that precipitation, drought and aridity are limiting factors (Nechita and Chiriloaei, 2018). Another dendrochronological study on *Quercus* spp. in southern Romania showed that drought, especially during the vegetation period, is the main climatic limitation for radial growth, but the response varies between species (Popa et al., 2013). A study on *Quercus petraea* in western Romania indicated that tree dieback and growth decline were associated with the frequent hot drought events since the 1980s, and they showed a higher sensitivity to hot droughts in managed

compared to old-growth forests (Petriţan et al., 2021). As observed in the Romanian forest monitoring system between 1990 – 2006, the impact of the prolonged drought conditions starting from the 1980s was noticed in the very high percentage of defoliated trees between 1993 – 1994 (Badea and Neagu, 2007). Their analysis showed that coniferous forests exhibited a smaller percentage of damaged trees than broadleaved due to the geographical conditions in Romania that drive a higher water deficit at the lower altitudes where broadleaved are situated. Among the broadleaves, they found that xerophilous oaks (*Quercus pedunculiflora* and *Quercus pubescens*), *Robinia pseudoacacia,* and *Quercus frainetto* were the most affected (for example, the highest defoliation of about 45.5% for *Q. frainetto* in 1994) (Badea and Neagu, 2007).

Drought's impact on crops depends on the species, the timing relative to their sensitive phenological stages, and agricultural planning (Ciulache and Ionac, 1995; Wilhite, 2000). For grain crops, the reproductive stage is susceptible to drought and heat stress (Saini and Westgate, 1999). For example, maize is vulnerable to drought associated with temperatures above 35ºC during flowering-fertilization (Roman et al., 2011). However, new genotypes might reduce their sensitivity (Amigues et al., 2006).

Multiple studies focused on the impact of drought on agricultural vegetation using remote sensing methods (Angearu et al., 2020; Dobri et al., 2021; Gouveia et al., 2017; Onţel et al., 2021; Páscoa et al., 2020) and other statistical methods related to crop yields (Lupu et al., 2018; Onţel and Vlăduţ, 2015; Prăvălie et al., 2016; Zaharia et al., 2012). Páscoa et al. (2020) analysed the Normalized Difference Vegetation Index (NDVI) – Standardized Precipitation Evapotranspiration Index (SPEI) correlations at multiple scales in the main land cover types. They showed that cropland had a more sensitive response to drought than forests and grasslands. In the Dobrogea region, an analysis of drought indices, vegetation indices and fire locations showed that agricultural land is the most frequently affected by fire (particularly in August, July, and March) compared to forests (Angearu et al., 2018).

2. STUDY AREA

This chapter provides an overview of the study area and its geographical features, based on the synthesis of the existing literature and on the processing of available datasets.

First, the main geographical features are introduced, particularly the location and boundaries of the study area and the landforms overlapping it (**Chapter 2.1**). Next, **Chapter 2.2** presents the general climatic characteristics of the study area: the major climate types; the main atmospheric systems that influence climate variability and drought occurrence in the region, the general temporal and spatial characteristics of the primary climate parameters that influence drought; changes in the main climatic parameters and drought indices. **Chapter 2.3** provides an overview of the main hydrographical and hydrological features in the study area, including its river network, groundwater, and lakes. Finally, the distribution of ecoregions, the main vegetation formations and land covers are presented in **Chapter 2.4**.

2.1. Main geographical features

The study area is located in the south-east of Romania (**Figure 2.1**), approximately bounded by the following coordinates: 45° 51' 47" N, 26° 21' 9" E (north), 43° 37' 36" N, 25° 26' 18" E (south), 44° 36' 60" N, 24° 27' 32" E (west), and 44° 52' 50" N, 29° 36' 58" E (east).

The study area is bordered by the Black Sea to the east and the Danube to the south and north-east (**Figure 2.1** and **Figure 2.2**). The borders of the major river catchments in the region (Argeș, Ialomița and Buzău) were considered as the western and northern limits. Therefore, it comprises most of the Muntenia and the entire Dobrogea historical Romanian regions. The study area overlaps parts of several major landforms (**Figure 2.2** and **Table 2.1**).

The total area of the study region is approximately 63,820 km^2 (about 26% of the Romanian territory). Altitudes decrease from the north-west (where the maximum elevation is 2544 m in the Făgăraș Mts. in the Southern Carpathians) towards the south and east (until the 0 m level of the Black Sea) (**Figure 2.2**).

The elevation gradient, the latitudinal zonation, the distribution of landforms and the vicinity of the Black Sea generate a range of different climate and biotic characteristics in the study area, which makes this region interesting for drought research. The large variety of geographical

features, socio-economic conditions, and intensities of environmental pressures allow the study of the drought dynamics in relation to the hydroclimatic variability and vegetation cover.

This region also includes areas with high water supply requirements, such as the Bucharest metropolitan region and multiple localities, cities, and county capitals (Alexandria, Pitești, Ploiești, Târgoviște, Buzău, Călărași, Constanța, Tulcea). Moreover, it is one of the main agricultural regions of Romania, due to the extensive croplands, which are another factor generating high water requirements.

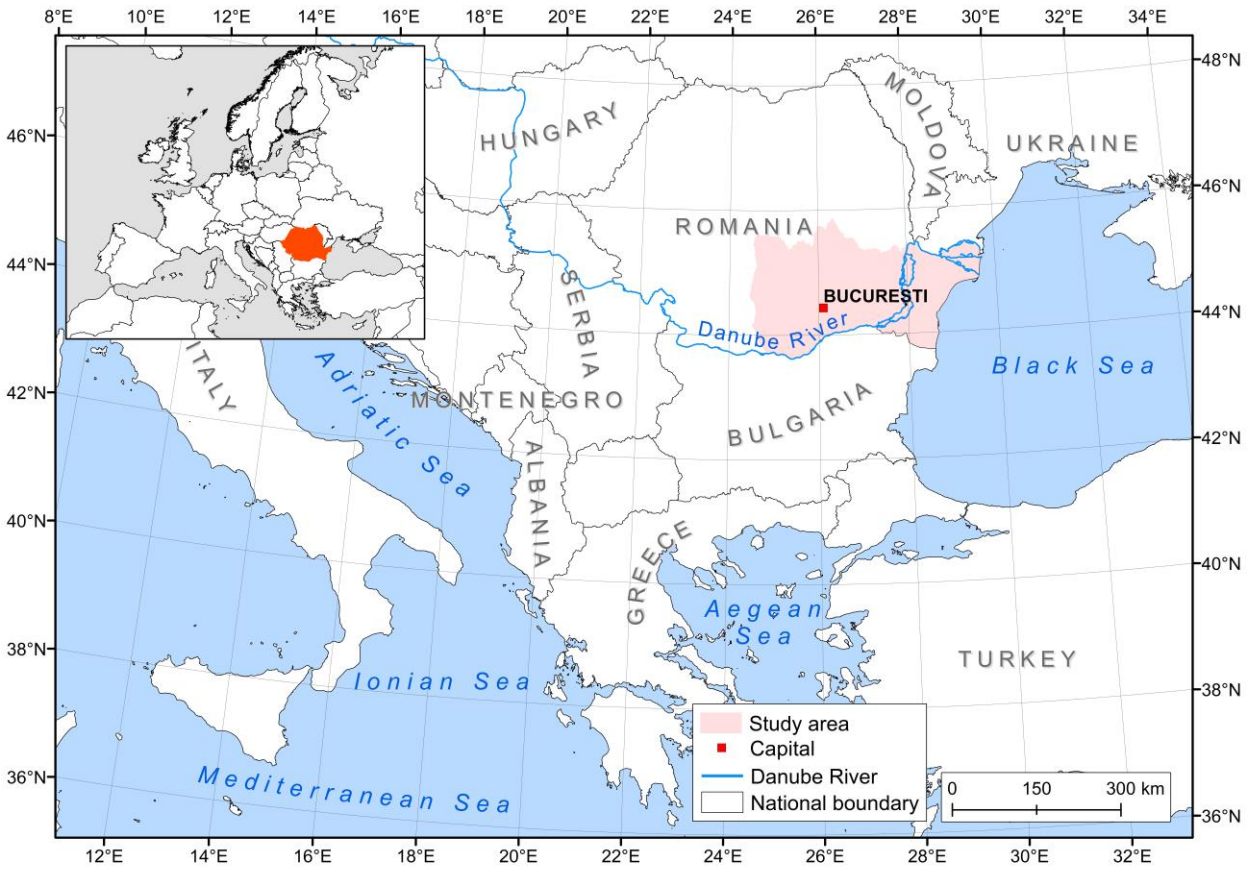

Figure 2.1 Location of the study area in Romania and relative to countries in south-eastern Europe and the neighbouring seas

Table 2.1 Major landforms and their divisions in the study area (according to Posea, 2005)

Major landforms	Landform divisions and sub-divisions in the study area
Carpathian Mountains	➢ **Southern Carpathians:** *Făgăraș-Iezer Mts.* (Făgăraș M., Iezer-Păpușa M., Loviștea M.) ➢ **Curvature Carpathians:** *Bucegi-Piatra Craiului Mts.* (Bucegi Mts., Leaota Mts., Rucăr-Bran Corridor); *Teleajen Mts.* (Ciucaș M., Grohotișu Mts., Baiu Mts.); *Buzău Mts.* (Penteleu M., Podul Calului M., Siriu M., Întorsura Buzăului M.).
Subcarpathians	➢ **Getic Subcarpathians:** specifically, most of *Muscelele Argeșului* ➢ **Curvature Subcarpathians:** *Prahova Subcarp*., *Buzău Subcarp.*
Getic Piedmont	➢ **Cândești Piedmont** ➢ **Argeș Hills** ➢ part of **Cotmeana Piedmont**
Romanian Plain	➢ **Teleorman Plain:** *Piteşti P., Boianu P., Găvanu-Burdea P., Burnas P.* ➢ **Ialomița Plain:** *Prahova Piedmont P., Titu-Sărata P., Vlăsia P.* ➢ **Bărăgan Plain:** *Mostiștea Bărăgan, Ialomița Bărăgan, Brăila P.* ➢ part of **Buzău-Siret Plain:** part of *Râmnic Piedmont P*., part of *Buzău P.*
Dobrogea Plateau	➢ **Northern Dobrogea Plateau:** *Măcin Mts., Niculițel Plt., Nalbant Depression, Tulcea Hills, Măcin Glacis, North-Dobrogea Glacis, Babadag Plt.* ➢ **Central Dobrogea Plateau:** *Casimcea Plt., Istria Plt., Gârlici Plt*. ➢ **Southern Dobrogea Plateau:** *Carasu Plt., Oltina Plt., Cobadin Plt., Mangalia Plt.*
Danube Delta	

Plt. = plateau; P. = plain, Mts. = mountains; M. = massif

Figure 2.2 Main landforms in the study area, based on the Romanian landform map, Candrea et al. (2008), according to Posea and Badea (1984)

2.2. General climate characteristics

This chapter first presents the major climate types overlapping the study area, according to several classifications (**Chapter 2.2.1**). Next, the main atmospheric drivers of climate and drought occurrence in south-eastern Romania are described in **Chapter 2.2.2**, followed by the spatial distribution of temperature, precipitation, and potential evapotranspiration in **Chapter 2.2.3**.

2.2.1. Climate types and regional climatic influences

Due to its geographical location and the large-scale atmospheric circulation, the study area is generally characterized by a *temperate-continental climate* (Bogdan and Țîștea, 1983). Ciulache and Ionac (2004) define three *major mid-latitude climate types* that cover the Romanian territory:

transitional (between the continental and oceanic climates; covers most of the area), semi-arid (in the Dobrogea Plateau), and mountainous (in the Carpathians).

For identifying the climate types according to the *Köppen-Geiger climate classification*, the dataset calculated for the 1980 – 2016 period by Beck et al. (2018) is used. This classification uses the Russell (1931) modification, where the demarcation between temperate (type C) and continental (type D) climates is defined by the cases where the threshold for the temperature of the coldest month is 0°C instead of -3°C (Wilcock, 1968). The *Köppen-Geiger climate classification* shows that there are five classes in the study area, that are included in three major climates types (**Figure 2.3**): semi-arid (Bsk class), continental (Dfa, Dfb and Dfc classes) and tundra/alpine (ET class). The semi-arid Bsk climate, or steppe climate, has hot, dry summers but cold winters, and it is specific to the eastern part of the study area (the Dobrogea Plateau and the easternmost part of the Romanian Plain). The Dfa class, characterized by no dry season and hot summers, defines most of the Romanian Plain, while the Dfb class, with no dry season and warm summers, is specific to the hilly Subcarpathian area. The Dfc (no dry season, cold and short summers) and ET (alpine) classes characterize the higher altitudes in the Carpathians.

The annual *De Martonne aridity index* (IDM) calculated for the 1961 – 2007 period classifies the study area as *semi-arid* in eastern Dobrogea ($10 \leq IDM < 20$), *Mediterranean* in the eastern Romanian Plain, the Danube Floodplain and western Dobrogea ($20 \leq IDM < 24$), *semi-humid* ($24 \leq IDM < 28$) in the southern and centre of the Romanian Plain, and *humid* ($28 \leq IDM < 35$) in the north-western part of the Romanian Plain (Croitoru et al., 2013b). The IDM classifies the hilly areas as *humid*, while higher regions are *very* and *extremely humid*, increasing with altitude in the Carpathian Mountains (Păltineanu et al., 2007a).

In addition to the large-scale atmospheric circulation, *regional and local factors* add complexity to the climatic characteristics in the study area. Firstly, the Carpathian Mountains strongly influence the vertical distribution of climatic parameters due to landforms and elevations exceeding 2000 m.a.s.l. They also act as an orographic barrier (ANM, 2008). Thereby, due to their location and shape, moist Atlantic air masses generally influence the western and central parts of the country, while the south-eastern region has a more continental character. Mediterranean air masses influence the climate in southern and south-western parts of Romania (higher precipitation during winter) (ANM, 2008). The Black Sea induces a maritime influence on the coastland on a

strip of about 15 – 25 km by moderating temperatures, increasing air humidity and wind speed, and increasing the number of cloudless days leading to lower rainfall (ANM, 2008; Ciulache and Ionac, 2004).

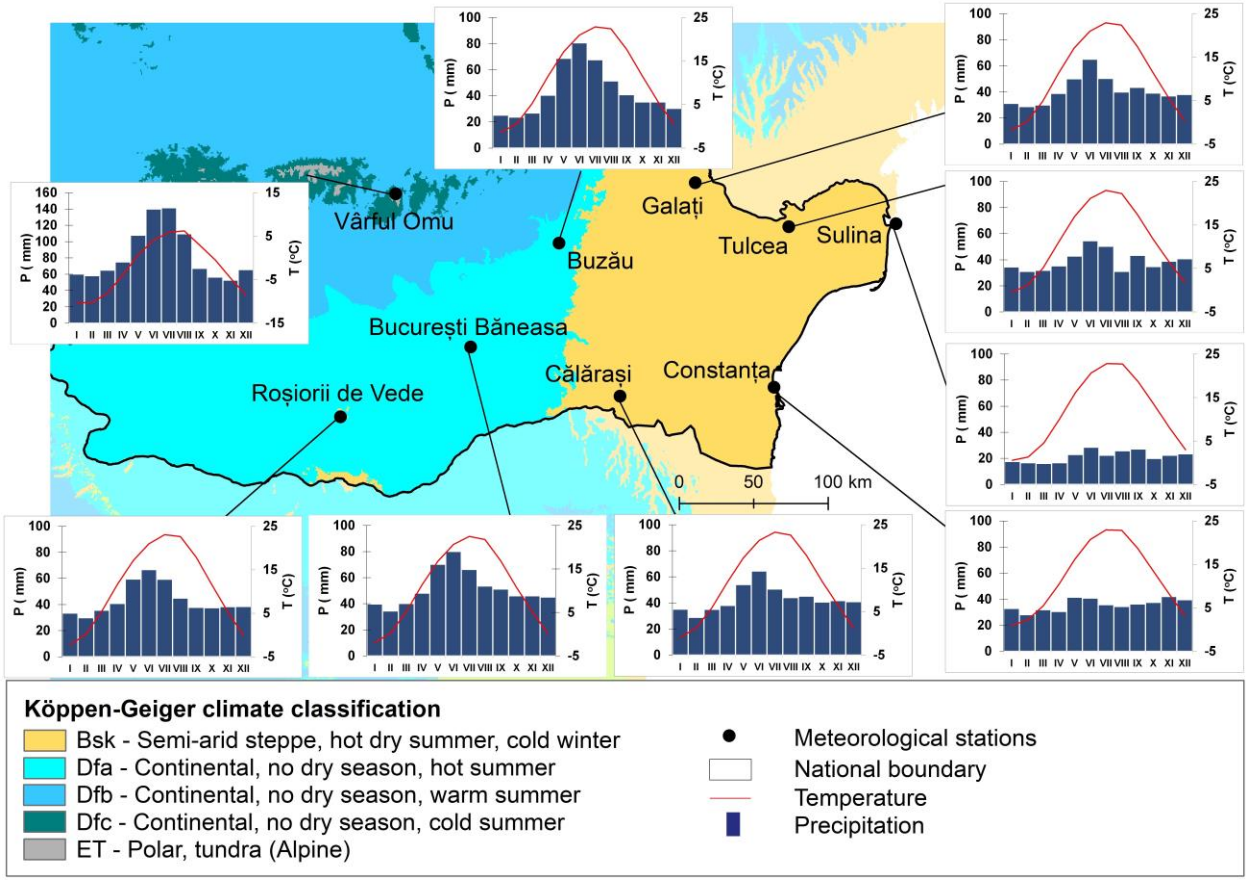

Figure 2.3 Main climate types in the Köppen-Geiger classification system calculated for the 1980 – 2016 period (Beck et al., 2018) and annual regimes of precipitation (P) and temperature (T) at the main meteorological stations in the study area (according to data from ECA&D for 1961 – 2020)

2.2.2. Atmospheric drivers of climate and drought

Atmospheric drivers play an essential role in the regional climate and development of droughts. The Romanian territory, and consequently the study area, is under the influence of several atmospheric pressure systems. The Azores and the Siberian anticyclones, as well as the Icelandic and the Mediterranean cyclones, occur more frequently, while the Greenland,

Scandinavian and North-African anticyclones and the Arabian cyclone are less frequent (Bogdan and Țîștea, 1983).

Dry periods are associated with the persistence of anticyclonic structures, namely the ridges of the Azores, Siberian, North-African and Scandinavian high-pressure systems (ANM, 2008; Ciulache and Ionac, 1995) or with a south-eastern tropical continental circulation (Bogdan and Țîștea, 1983).

Due to the orographic blocking role of the Carpathian Mountains on the air masses formed by anticyclonic structures, drought has different characteristics across Romania (Bogdan and Țîștea, 1983). Southern and south-eastern Romania is characterized by more frequent and severe drought occurrences due to the higher influence of continental anticyclonic structures (Bogdan and Țîștea, 1983).

One important large-scale determinant of meteorological and hydrological droughts is the North Atlantic Oscillation (NAO) (Ștefan et al., 2004). In particular, the positive phase of the NAO is associated in winter in Romania with negative precipitation anomalies, positive temperature anomalies, particularly in southern Romania, and less snow pack (Bîrsan and Dumitrescu, 2014b; Bojariu et al., 2015), which could reduce the soil water reserve for the growing season (Busuioc et al., 2016). The influence of NAO can also be noticed in the lowered streamflow in winter and the beginning of spring (Bîrsan, 2017). A positive phase of the East Atlantic/Western Russia Pattern (EAWR) in winter also determines drier-than-normal conditions in winter and early spring (Ioniță, 2014). The mean Sea Level Pressure (SLP) and the air humidity at 700 hPa (SH700) are the main drivers of drought variability in winter (Busuioc et al., 2015; Cheval et al., 2014), as positive anomalies of SLP represent more frequent anticyclonic structures associated to lowered precipitation.

A large-scale multi-decadal influence on drought in the summer season is also given by the Atlantic Multidecadal Oscillation (AMO) (Cheval et al., 2014). However, thermodynamic factors, such as the air temperature at 850 hPa (T850) and air humidity at the 700 hPa level (SH700), are the main determinants of drought in summer (Busuioc et al., 2016; Cheval et al., 2014). The persistence of drought duration is determined by the anomalies of both T850 and SH700 (Busuioc et al., 2015). In summer, the increase in the maximum length of dry periods and the frequency of

very warm days is related to the higher frequency of positive anomalies of T850 and negative SH700 anomalies between 1961 – 2010 (Busuioc et al., 2015, 2016).

2.2.3. Main climatic parameters controlling drought

2.2.3.1. Air temperatures

Between 1961 and 2020, based on the data from European Climate Assessment & Dataset (ECA&D) (Klein Tank et al., 2002), the eastern part of the study area was characterized by average annual air temperatures of 12.1ºC at Constanța and 11.4ºC at Tulcea meteorological stations, respectively.

The western part of the study area has slightly lower average temperatures, of about 11.1ºC at Roșiorii de Vede and 10.8ºC at București Băneasa meteorological stations, respectively. The elevational gradient induced by the Carpathian Mountains leads to a decrease in mean annual temperature at higher altitudes. For example, at the Vârful Omu meteorological station, located at an altitude of 2504 m in the Bucegi Mountains, the mean annual temperature analysed period was -2.2ºC.

Using the same dataset and for the same period, at most of the stations, the annual regime of the average air temperatures was analysed and shown in **Figure 2.3**. The temperatures reach their maximum values in summer and the lowest in winter. The lowest average temperatures are generally recorded in January (for example, -0.5ºC at Tulcea, -1.9ºC at București Băneasa and -2.3ºC at Roșiorii de Vede) and the highest average temperatures are recorded in July (such as 22.9ºC at Tulcea, 22.5ºC at București Băneasa and 23.3ºC at Călărași) (**Figure 2.3**). However, stations above 1850 m have a different temperature pattern, with the lowest monthly average temperatures in February and the highest in August. An example of this can be seen at Vârful Omu, where the average temperature in February is -10.3ºC and in August, it is 6.2ºC (**Figure 2.3**).

The spatial distribution of the annual average air temperatures in the study area, based on the E-OBS dataset at a spatial resolution of 0.1º (Cornes et al., 2018) for the 1961 – 2020 period, is illustrated in **Figure 2.4**. It highlights that most of the study area has an average annual air temperature between 10 – 12ºC. At higher altitudes, they decrease at 6 – 8ºC in the Subcarpathians and lower than 6ºC in the Carpathians.

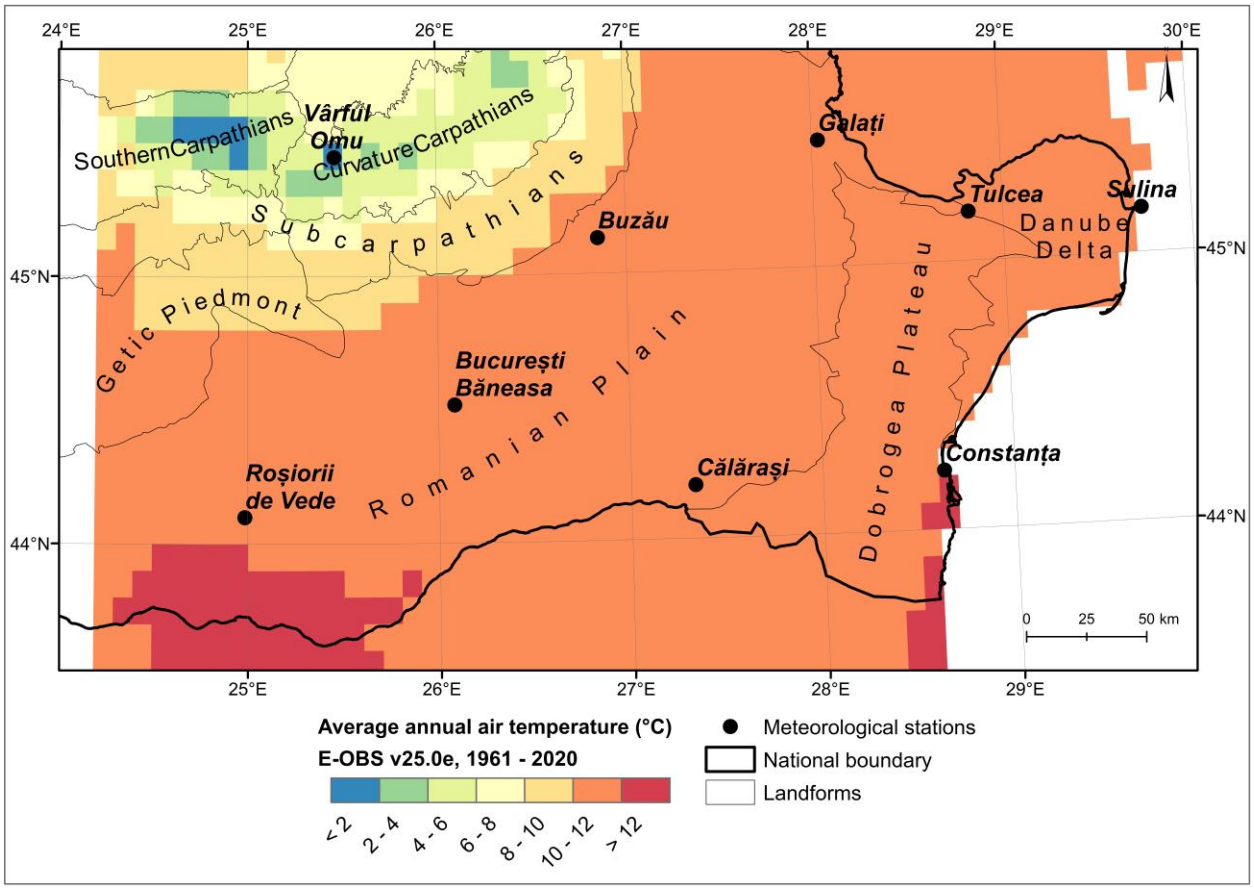

Figure 2.4 Spatial distribution of the average air temperatures (°C), based on the data from E-OBS v25.0e for the 1961 – 2020 period

2.2.3.2. Precipitation

Between 1961 and 2020, based on the ECA&D data, the eastern part of the study area was characterized by average annual precipitation of 432 mm at Constanța and 470 mm at Tulcea meteorological stations, respectively. The Danube Delta experiences lower annual rainfall, with an average of 260 mm recorded at the Sulina meteorological station. The western part of the study area is wetter, with an average annual precipitation of 523 mm at Roșiorii de Vede and 622 mm at București Băneasa meteorological stations, respectively. In addition, the Carpathian Mountains influence the precipitation distribution, increasing the mean annual precipitation with elevation. In particular, at the Vârful Omu meteorological station, an average annual precipitation of about 1000 mm was recorded between 1961 – 2020.

The spatial distribution of the annual average precipitation in the study area, based on the Romanian Climatic Dataset (ROCADA) dataset at a spatial resolution of 0.1° (Bîrsan and Dumitrescu, 2014a; Dumitrescu and Bîrsan, 2015), available for the 1961 – 2013 period, is presented in **Figure 2.5**. This dataset was chosen to illustrate precipitation distribution due to its higher accuracy compared to other gridded precipitation products (**Chapter 3.2**). The map highlights the high rainfall values occurring in the mountainous areas (>700 mm/year) compared to the eastern part of the Romanian Plain and the Dobrogea region (<500 mm/year). The Danube Delta region has the lowest values (<400 mm/year).

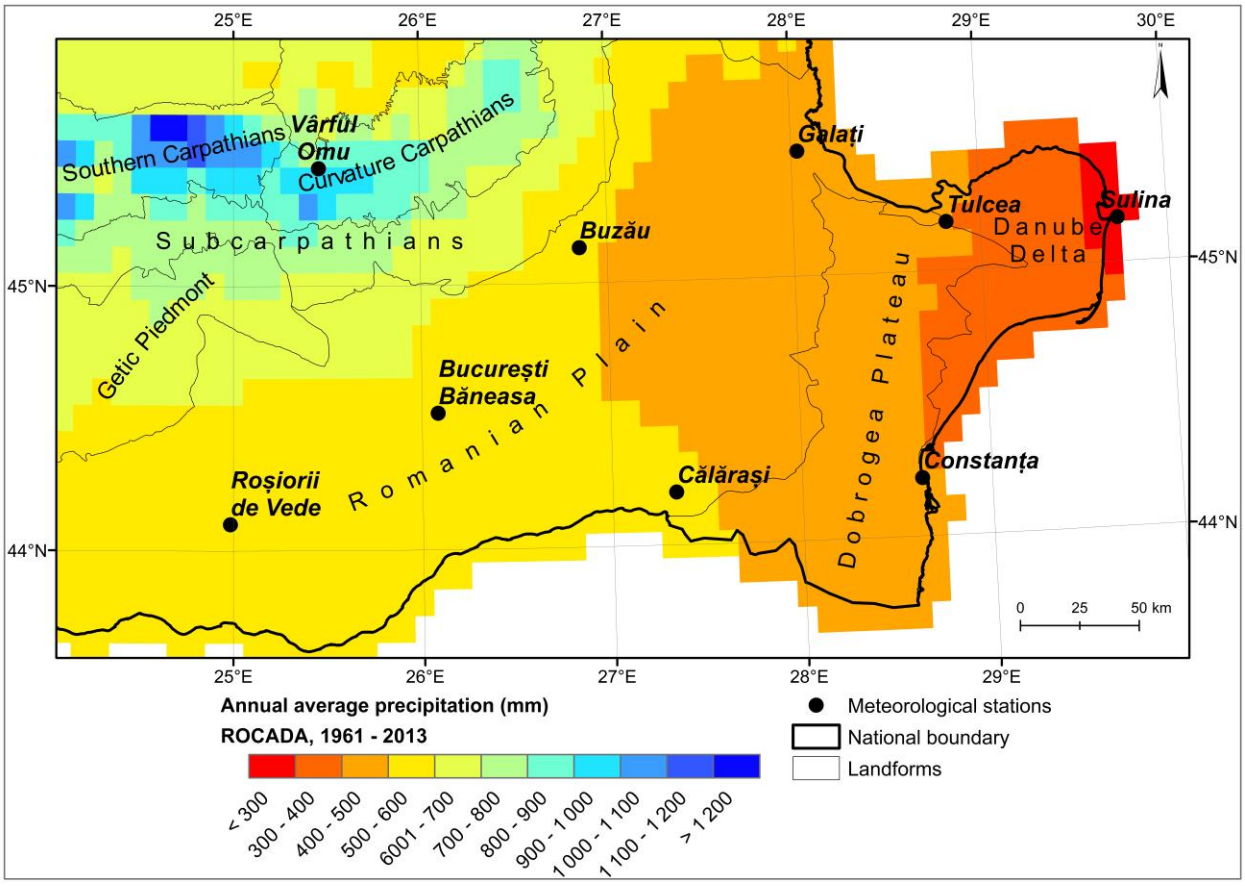

Figure 2.5 Spatial distribution of the average annual precipitation (mm), based on the data from ROCADA for the 1961 – 2013 period

The rainfall regime in the study area shows important monthly amplitudes. Precipitation increases from February to June, when it reaches a maximum at most stations (for example, 80 mm at București Băneasa, 67 mm at Roșiorii de Vede), and decreases until the minimum in February (for example, 35 mm in București Băneasa and 30 mm at Roșiorii de Vede) (**Figure 2.3**).

On the coastland, due to the influence of the Black Sea, there is a second maximum in November – December and a second minimum at the end of the summer season, the rainfall regime having here a lower amplitude of monthly precipitation. In the mountainous area, monthly precipitation exceeds 100 mm during summer and often has a torrential character.

2.2.3.3. Potential evapotranspiration

The annual potential evapotranspiration estimated for the 1961 – 2020 period, based on the data from the Climatic Research Unit (CRU), version CRU TS4.05 (Harris et al., 2020), is shown in **Figure 2.6**.

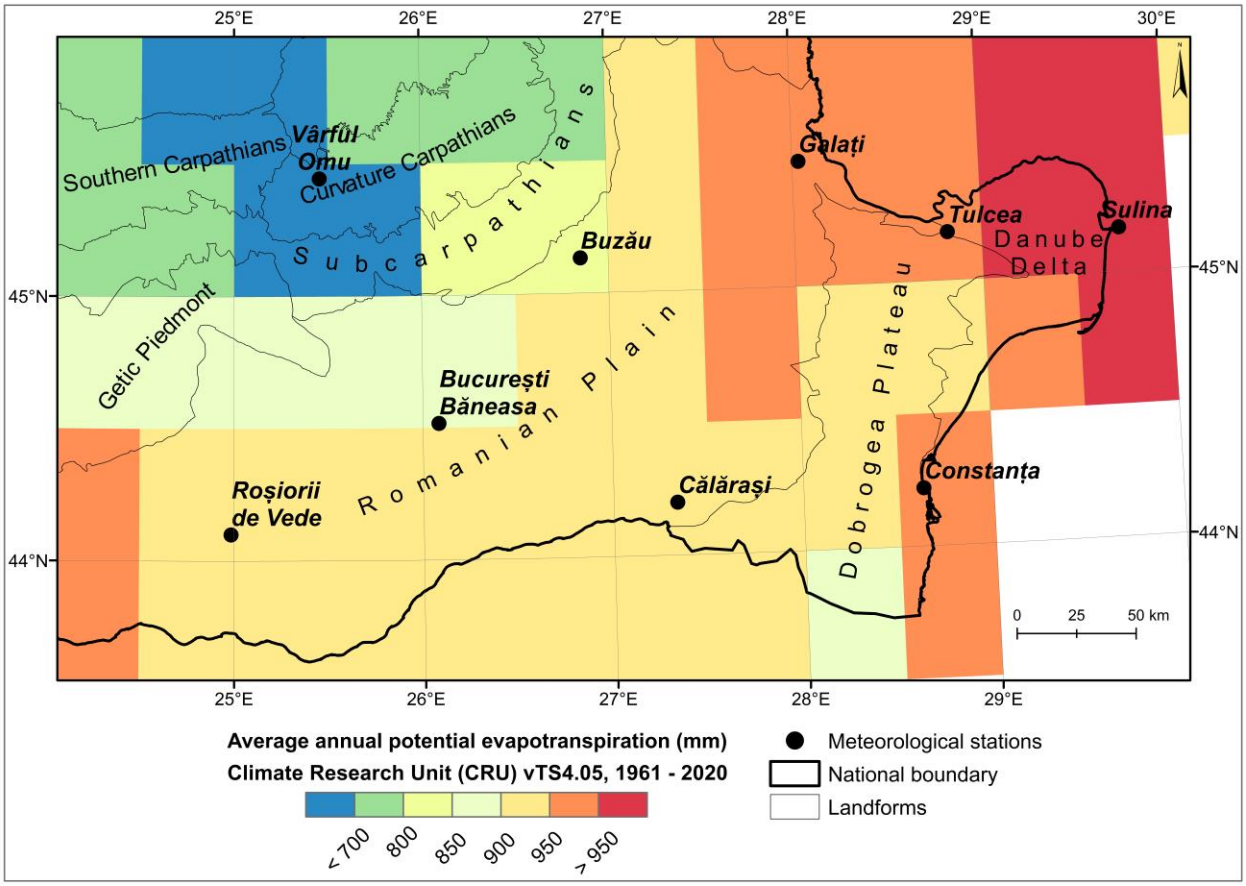

Figure 2.6 Spatial distribution of the average annual potential evapotranspiration (mm), based on the data from the Climate Research Unit (CRU) for the 1961 – 2020 period

The CRU potential evapotranspiration dataset uses a version of the Penman-Monteith method for calculating potential evapotranspiration. As shown in **Figure 2.6**, this parameter ranges between more than 900 mm in the eastern part of the study area (Danube Delta, Galați region),

800 mm in most of the Romanian Plain and Dobrogea Plateau to less than 650 mm in the mountainous areas. The highest values are in summer, particularly in July, when average potential evapotranspiration can range from more than 160 mm in the easternmost part of the study area, more than 140 mm/month in most of the Romanian Plain, to about 100 mm at higher altitudes.

Potential evapotranspiration exceeds precipitation by almost double in spring and triple in summer in south-eastern Romania (Croitoru et al., 2013a), leading to a monthly water deficit of more than 100 m in some areas (Stan et al., 2015). The annual climatic water balance, or the difference between annual precipitation and potential evapotranspiration, averaged between 1961 – 2013, ranges from less than -400 mm in the Dobrogea region to more than 200 mm in the Carpathian region (Păltineanu et al., 2007a; Prăvălie et al., 2019).

2.2.3.4. Changes in the main climatic parameters

Several studies have highlighted significant changes in the parameters influencing drought development in Romania, particularly in southern and south-eastern Romania. The general upward *trend in annual average temperatures* was highlighted, especially after the 1980s (Marin et al., 2014; Zaharia et al., 2020). A 1ºC increase in mean annual temperature was measured between 1901 and 2020 in Romania (Bojariu et al., 2021). At the seasonal level, between 1961 – 2020, there are significant increasing trends which are stronger in summer and winter, lesser in spring and the weakest in autumn (Bojariu et al., 2021). At most stations in south-eastern Romania, these trends range between 0.3 – 0.4ºC/decade in winter, 0.2 – 0.4ºC/decade in spring, 0.4 – 0.5ºC/decade in summer and 0.1 – 0.3ºC/decade in autumn. Between 1961 – 2020, there were more stations with significant increasing trends in winter and autumn temperatures than in the 1961 – 2013 period, while in summer, these were sustained in the entire area (Bojariu et al., 2015, 2021; Dumitrescu et al., 2015). In addition, Busuioc et al. (2015) noticed an increase between 1961 – 2010 in temperature extremes, such as the frequency of very warm days, especially in summer and particularly in south-eastern and southern areas of Romania.

Heatwave-related indices, computed using maximum and minimum daily temperatures, such as the annual heatwave number or the number of days in heatwaves, have increased between May – September, particularly when calculated based on the maximum temperature (Croitoru et al., 2016b). Furthermore, the highest number of heatwaves was observed in the last two decades, from 2001 to 2020 (Nagavciuc et al., 2022).

Moreover, increases in *projected average air temperatures* are anticipated in all forcing scenarios for winter and summer. Summer average temperature increases are higher in the southern part of Romania, while in the mountains, these have high magnitudes in both seasons (Bojariu et al., 2021). The EURO-CORDEX regional simulations show an average temperature increase of more than 2.5^{o}C in August for the 2021 – 2050 period in the Representative Concentration Pathways (RCP) 8.5 scenario, while global simulations show an increase of more than 3^{o}C in the same scenario (Bojariu et al., 2021).

The increase in air temperatures led to an *increase in the annual potential evapotranspiration* between 1961 – 2007, especially in southern Romania, in all seasons except autumn (Croitoru et al., 2013a). Prăvălie et al. (2019) highlighted decreasing trends in the annual climatic water balance over south-eastern Romania.

The trend in the total annual precipitation in Romania showed that this parameter was relatively stable between 1901 – 2013 (Mateescu, 2014). Seasonally, significant increasing trends were found only in autumn between 1961 – 2020, particularly in some stations in the Romanian Plain, southern Dobrogea and Subcarpathians (Bojariu et al., 2021). Decreasing precipitation trends were sparse, such as in winter and spring in the Danube Delta (Dumitrescu et al., 2015).

It is interesting to note that at most of the meteorological stations in Romania, observations point towards an increase in the frequency of *rain showers* in spring and summer, which indicates a more torrential character of precipitation in those seasons (Bojariu et al., 2021; Busuioc et al., 2016). Regarding *projected precipitation*, climatic scenarios indicate a decline in summer, relative to the 1971 – 2000 period, which is stronger towards the end of the century, with the most substantial decreases in the Dobrogea and Bărăgan regions (Bojariu et al., 2021).

Bojariu et al. (2021) highlighted that *mean monthly snow depth* between December – April decreased by up to 5 cm in the 1990 – 2021 period compared to 1961 – 1990 at most of the stations in the study area. They also showed that, in Romania, there were increasing trends in mean monthly snow depth above 800 m between October – April, while below this altitude, there were decreasing trends between December – March.

Between 1961 – 2010, the *maximum duration of dry periods* increased in summer over most of the study area, particularly in the Danube Delta, southern Dobrogea and Călărași region (Busuioc et al., 2015).

2.2.4. Drought indices

Croitoru et al. (2016a) analysed several precipitation-based indices of the Expert Team on Climate Change Detection, Monitoring and Indices (ETCCDMI), among which the index of Consecutive Dry Days (CDD) and the number of precipitation days, for the 1961 – 2013 period. The CDD showed generally decreasing trends in south-eastern Romania (except Danube Delta and at the high altitude isolated station of Vârful Omu), which are mainly insignificant (except in the Călărași region) (Croitoru et al., 2016a). At the same time, a decrease in the number of precipitation days in the southern half of Romania was noticed, suggesting a shift towards more frequent isolated days of higher precipitation (Croitoru et al., 2016a).

The Standardized Precipitation Index (SPI) did not show extensive significant trends in the warm season, except in some areas such as the Danube Delta, while in autumn, mainly increasing trends were found between 1961 – 2010 (Bojariu et al., 2015; Cheval et al., 2014). SPI indicated wetting trends in southern Dobrogea between 1962 – 2013, similar to the precipitation trends (Ioniță et al., 2016). In summer, however, when including the influence of the potential evapotranspiration, such as in the Standardized Precipitation Evapotranspiration Index (SPEI), decreasing trends (drying phenomenon) are found between 1950 – 2020 in south-eastern Romania, generally non-significant in June – July, but significant in August in the semi-arid zone (Dobrogea and easternmost part of the Romanian Plain) (Nagavciuc et al., 2022). The highest frequency of dry summers was registered in the last decade (2011 – 2020), according to SPEI (Nagavciuc et al., 2022). Similarly, the Palmer Drought Severity Index also showed a significant intensification of dryness in the warm season months between 1961 – 2010 in the study area, but it indicated the opposite tendency in southern Dobrogea (Bojariu et al., 2015).

Despite the unclear trends in precipitation and precipitation-based drought indices in the study area, the observed warming trend suggests the rise of drought risk due to the increase in atmospheric water demand during the drought events.

2.3. Hydrography and hydrology

This chapter describes the main hydrographic and hydrologic features in the study area. Firstly, the river network and the hydrological characteristics are presented, followed by an overview of groundwater bodies and lakes.

2.3.1. River network and hydrological characteristics

Most rivers draining the study area are tributary to the Danube which borders most of the southern limit of the study area and forms the border with Bulgaria up to Călărași (**Figure 2.7**).

Figure 2.7 River network and the main catchments and lakes in the study area (based on the EU-Hydro database[2])

[2] Copernicus Land Monitoring Service, EU-Hydro - River Network Database, https://land.copernicus.eu/imagery-in-situ/eu-hydro/eu-hydro-river-network-database?tab=metadata

Between Călărași and Brăila, the Danube River flows northward, including two large islands: Balta Ialomiței and Balta Brăilei. This sector is characterized by a high degree of river branching. Downstream from Galați city, the Danube River changes the flow direction eastwards, where it borders the Republic of Moldova and Ukraine, representing the north-eastern limit of the study area. Downstream from Tulcea city, there is the Danube Delta, which includes three main branches (Chilia, Sulina and Sfântul Gheorghe).

Vedea, Argeș and Ialomița rivers are the major tributaries of the Danube River in the study area. They have the largest catchments, their surface totalling about 28,330 km^2 (**Table 2.2**). In the north-eastern part, the region is drained by the Buzău River which flows into the Siret River. Its catchment has an area of 5,264 km^2. The large rivers in the study area are major sources of freshwater in the region. Cities rely heavily on these rivers for water supply. For example, Argeș and Dâmbovița (its most important tributary) rivers provide water for large cities (e.g., Bucharest, Pitești), Ialomița River for Târgoviște city and Buzău River for the homonymous city.

Table 2.2 Main morphometric and hydrological characteristics of Vedea, Argeș, Ialomița and Buzău catchments: area (A), mean altitude (H), river length (L) and multiannual average streamflow (Q) (ANAR, 2015a,b; Ministerul Mediului, 1992; Ujvári, 1972). Q for the 1966 – 2010 period is computed based on data from Water Basin Administrations and the Global Runoff Data Center.

Catchment	A (km^2)	H (m.a.s.l.)	L (km)	Main tributaries (L [km] / A [km^2])	Q (m^3/s)
Vedea	5,430	166	224	Teleorman (169/1,427)	7.39
Argeș	12,550	379	350	Râul Doamnei (107/1,836) Neajlov (186/3,720) Dâmbovița (286/2,824)	45.23
Ialomița	10,350	327	417	Cricov (80/579) Prahova (193/3,738)	40.96
Buzău	5,264	479	302	Bâsca Chiojdului: (42/340) Slănic (73/425)	28.02

Besides the mentioned rivers, small Danube tributaries drain approximately 24,540 km^2 and rivers on the coastland that flow into the Black Sea drain an area of 5,439 km^2. The main rivers flowing to the Black Sea are Taița (catchment area of 591 km^2 and mean annual streamflow of

0.486 m^3/s) and Casimcea (catchment area of 740 km^2 and mean annual streamflow of 0.632 m^3/s) (ANAR, 2015c).

The rivers are supplied predominantly from surface sources. At the highest altitudes, there is a moderately nival and nivo-pluvial regime, the latter also characteristic of the lowlands (Ujvári, 1972). The other regions generally have a pluvio-nival or pluvial moderate regime. The groundwater contribution to streamflow is, on average, about 30%, but it is lower in the drier flatlands and the Getic Piedmont; in the Bărăgan Plain, groundwater is the main supply source for rivers (Ujvári, 1972). In the Vedea catchment, water resources are generally low, and the groundwater is deep due to the high substrate permeability (Ujvári, 1972). The seasonal pattern of streamflow is mainly characterized by high waters in spring, induced by snowmelt and high precipitation, and low waters in autumn (in the lowlands and hill areas) and winter (at altitudes above 1200 m.a.s.l. in the Carpathians) (Gâștescu et al., 1983). However, the rivers on the Black Sea coastland generate high waters in winter because of the Black Sea's influence (Zaharia, 2004).

The river network density decreases from the highest values at altitudes of 1200 – 1400 m.a.s.l. towards the plain (Bîrsan, 2017). The highest densities are in the Southern Carpathians (Făgăraș, Iezer, Lotru Mts.), between 0.7 – 1 km/km^2, while lower densities (between 0.3 – 0.5 km/km^2) are in the Getic Piedmont and Curvature Carpathians (Gâștescu et al., 1983). The lowest densities are in the Romanian Plain and Dobrogea Plateau: 0.2 – 0.3 km/km^2 in the Argeș and upper Ialomița catchments and 0 – 0.1 km/km^2 in the remaining areas of the Romanian Plain and in the Dobrogea Plateau. Several semi-endorheic areas are found in the Bărăgan Plain (Ujvári, 1972).

Due to climatic conditions, altitudinal variation, vegetation, soil characteristics and anthropic influence, streamflow yield varies within the region. Generally, streamflow yield increases with altitude (Ujvári, 1972). In the Dobrogea region and southern and eastern parts of the Romanian Plain, the annual streamflow yield is below 50 mm (semi-endorheic areas generating less than 5 mm), gradually increasing towards more than 1000 mm/year at the highest altitudes (Bîrsan, 2017; Ujvári, 1972).

The climatic continental influences in southern Romania lead to generally lower rainfall, lowered streamflow and a slower recovery from drought periods (Zaharia, 2004). In Dobrogea,

due to the karst lithology (favouring permeability) and the semi-arid climate, there are non-perennial streams that frequently dry up (Pișota and Zaharia, 2003). This process occurs also in the Getic Plateau or the Subcarpathian glacis due to water infiltration, but only during drought periods (Pișota and Zaharia, 2003). In the flatlands, significant evaporative losses occur in summer, reducing runoff and water reserves (Ujvári, 1972).

During drought years, the average annual streamflow has decreased in Argeș River from the multiannual average streamflow of 65 m^3/s to 36.4 m^3/s in 1990 or 53.5 m^3/s in 2007, in Vedea River from an average of 11 m^3/s to 4 m^3/s in 1990 and 7 m^3/s in 2007, and in Ialomița River from 44 m^3/s to 22.3 m^3/s in 1990 and 32 m^3/s in 2007 (ANAR, 2013). The coastland rivers had an average multiannual streamflow of 3.4 m^3/s which increased in 1990 to 3.7 m^3/s and decreased to 1.7 m^3/s in 2007 (ANAR, 2013).

Changes in streamflow variability attributed to climate change were noticed in the observational records of the last decades (Zaharia et al., 2020). Some rivers in southern Romania experienced decreased annual streamflow (Bîrsan, 2015), such as Ialomița and Buzău (Borcan et al., 2014; Mitof and Prăvălie, 2014; Retegan and Borcan, 2011). The streamflow seasonality was impacted by the general warming trends. Higher temperatures led to less snow and encouraged more rainfall in winter, thus increasing streamflow in some rivers in December – January, while the thinner snowpack could have induced the negative trends in spring streamflow in southern Romania (Bîrsan, 2015; Bîrsan et al., 2014). From the end of spring to mid-summer, higher temperatures have determined an increase in evaporation and a decrease in river flow (Bîrsan, 2015). On the other hand, the trends of increasing precipitation in autumn have led to increased streamflow (September – October), as shown by the same authors.

Various hydrotechnical engineering works influence the streamflow regime in the rivers in the study area, but their presence varies among catchments. For example, the Argeș River is one of the most engineered catchments in Romania, considering the 13 reservoirs built along its course between 1965 – 1997, as well as the canals for water diversion and water supply (Zaharia et al., 2016). Rivers in the Bucharest region have been modified with hydrotechnical works for flood protection. The contributions of human and climate factors to streamflow change have been investigated in **Chapter 4.3**.

2.3.2. Groundwater

In the Argeș – Vedea hydrographic district (h. d.), there are 1037 million m^3 usable groundwater resources, while in the Buzău – Ialomița, 675 million m^3 usable groundwater resources (ANAR, 2015a,b). About 45% of the usable groundwater resources in Romania are located in the Romanian Plain area (the resources at the national scale totalling about 149.4 m^3/s in phreatic and 155.5 m^3/s in deep aquifers), contrasting with Dobrogea where only 4.7% are found (Pișota and Zaharia, 2003).The basin management plans mention the presence of 11 groundwater bodies in the Argeș – Vedea h. a., 18 in the Buzău – Ialomița h. a. and 10 in the Dobrogea – Littoral h. a. (ANAR, 2015c, b,a).

In the Argeș-Vedea and Buzău – Ialomița h. d., most aquifers developed in Quaternary porous-permeable deposits in floodplains and terraces of the main rivers. Other aquifer types in these two areas (karstic-fissure, fissure, fissure-porous, fissure-karstic) develop in the mountainous regions. In the Dobrogea – Littoral h. d., four aquifers are porous-permeable, four are fissure-karstic, and two are karstic-fissure. Some of the aquifers in the study area have a substantial economic value due to high groundwater extraction for public water supply, agriculture and industry — *Platforma Valahă* (Dobrogea – Littoral h. d.), *Conul aluvial Prahova* (Buzău – Ialomița h. d.), *București-Slobozia*, *Estul Depresiunii Valahe* and *București* (Argeș – Vedea h. d.) (ANAR, 2015c, b,a).

Groundwater exhibits interconnectivity with surface waters and ecosystems, highlighting the importance of groundwater levels. Among the main habitats dependent on aquifers are: riparian mixed forests with *Quercus robur*, Euro-Siberian steppic woods with *Quercus* spp., Pannonian – Balkanic turkey oak – sessile oak forests and Pannonic salt steppes and salt marshes and lowland hay meadows (ANAR, 2015c, b,a).

2.3.3. Lakes

The basin management plans provide a synthesis of lakes with a surface > 0.5 km^2 in the study area: in the Argeș – Vedea h. d. there are 40 reservoirs (a volume of 860 million m^3) and one natural lake, in the Buzău – Ialomița h. d. there are 13 reservoirs (489 million m^3) and 26 natural lakes, and in the Dobrogea – Littoral h. d. there are four main reservoirs (24.45 million m^3) and 75 natural lakes (ANAR, 2015a–c).

There is a large diversity of lake types in the study area. Besides the largest artificial reservoirs, such as Vidraru (450 million m^3) and Mihăilești (52.7 million m^3) on the Argeș River, Dridu (22.7 million m^3) on the Ialomița River, Siriu (51.9 million m^3) on the Buzău River (ABA Argeș-Vedea, 2015; ABA Buzău-Ialomița, 2015), there are numerous smaller reservoirs and various types of natural lakes.

The origin of the natural lakes depends on landscape environmental conditions. In the highest mountainous areas, in the Southern Carpathians, glacial lakes can be found in the Făgăraș Mts., and nivation lakes in the Iezer-Păpușa Mts., while lakes formed in structural geomorphology landscapes can be found in the Curvature Carpathians (Penteleu, Siriu Mts.) (Gâștescu et al., 1983). The presence of landslide induced lakes and lakes developed in salt formations is typical for the Subcarpathian and piedmont regions. On the other hand, mainly floodplain lakes are found in the lowlands, such as Balta Comana on the Neajlov river. Specifically, fluvial *liman* lakes are characteristic (e.g., Oltina, Bugeac, Amara, Snagov). A complex network of lakes develops in the Danube Delta. Southwards from the delta, on the coastland, the large Razim – Sinoe lagoon and the fluvial-maritime *liman* lakes such as Tașaul or Techirghiol are found.

2.4. Ecoregions, vegetation, and land cover

The relationships between climate, geology and soil have created particular conditions and have influenced the spatial distribution of vegetation ecoregions in the study area (**Figure 2.8**). As shown in previous studies, vegetation in the study is generally water-limited at lower altitudes and energy-limited at higher altitudes, where more humid conditions prevail (Páscoa et al., 2020; Prăvălie et al., 2022).

The semi-arid climate zone, covering the eastern part of the study area (the Dobrogea Plateau and the eastern part of the Romanian Plain), is characterized by the Pontic steppe ecoregion, which is part of the Temperate Grasslands, Savannas and Shrublands biome (Olson et al., 2001).

In most of the areas characterised by the continental climate type (the central and western parts of the Romanian Plain and in the hilly areas), the Temperate Broadleaf and Mixed Forests biome is specific: the *East European Forest Steppe* which appears as a transitional area towards the *Central European Mixed Forests* and the *Balkan Mixed Forests*. The mountainous areas are

overlapped by the *Carpathian Montane Forest* ecoregion (part of the Temperate Coniferous Forests biome) (Olson et al., 2001).

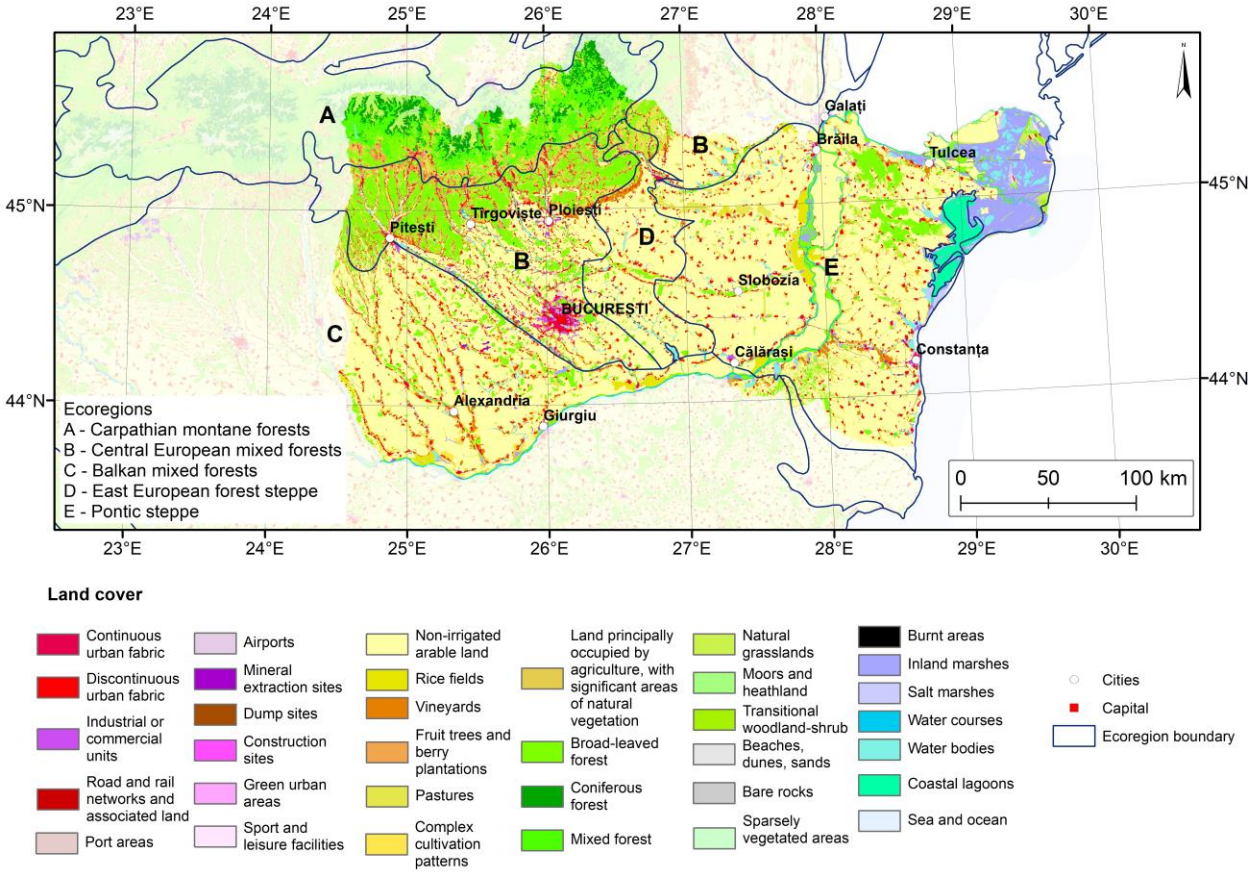

Figure 2.8 Terrestrial ecoregions (Olson et al., 2001) and land cover based on the Corine Land Cover (CLC) 2018 (EEA, 2019b) in south-eastern Romania

Within the *Pontic Steppe ecoregion*, most of the area is currently covered by cropland. The Dobrogea region has a rich diversity of agricultural land covers — arable land, pastures, vineyards, and fruit trees plantations. The remaining dry grasslands in Dobrogea, where grazing and mowing are specific, are representative of the steppe zone and are found mainly within the limits of protected areas (Hopkins, 2010). Larger forested areas are found in the northern Dobrogea Plateau, and some in the south-west, also within protected areas. These hilly areas of the Dobrogea region, particularly the northern part, are also characterized by vegetation formations distributed due to the altitudinal zonation: the forest-steppe, the *Quercus pubescens* (downy oak) sub-Mediterranean forests and the nemoral *Quercus petraea* (sessile oak) forests (Doniță et al., 2005). The easternmost part of the Romanian Plain (most of the Bărăgan Plain), located in the steppe ecoregion, is mainly

covered by agricultural land — predominantly arable land (non-irrigated) but also pastures and rice fields. Natural areas here are sparser and are mostly found along the main rivers, such as Danube and Ialomița (characterized by riparian mixed forests and galleries) or Călmățui (with salt steppes).

The *East European Forest Steppe ecoregion* borders the steppe region to the west, on a strip that transitions towards the temperate forests (**Figure 2.8**). This southern forest-steppe occurs at altitudes between 50 – 150 m.a.s.l., and it is naturally characterized by grasslands interspersed with thermophilous – xerophilous oak forests with *Q. pubescens* and *Q. pedunculiflora* (Doniță et al., 2005; Popova-Cucu et al., 1983). However, most of this ecoregion is presently covered by agricultural land.

The *Central European Mixed Forests ecoregion* overlaps parts of the Romanian Plain (the Ialomița Plain) and hilly areas (in the Getic and Curvature Subcarpathians and the Getic Piedmont). The largest urban centre and capital of Romania (Bucharest) is located here, as well as its metropolitan region and several other county seats (e.g., Ploiești, Târgoviște, Pitești), increasing the share of artificial surfaces. The low plains within this ecoregion mainly have an agricultural land cover, as deforestation occurred on extensive surfaces through time. In the Bucharest metropolitan area, forests were significantly affected by anthropic pressures such as land cover change or topographic, soil and hydraulic artificialization (Iojă, 2008). However, the remaining forests are characterized mainly by the nemoral latitudinal zone of thermophilous sub-mezophilous oak forests of *Q. cerris* and *Q. frainetto,* and *Q. robur* in the Vlăsia Plain, mixed with *Carpinus betulus* (Doniță et al., 2005; Grecu, 2010; Popova-Cucu et al., 1983). In the hilly areas, forest cover is predominant, characterized by the nemoral altitudinal zones of sessile oak forests (*Q. petraea*) and of beech forests (*Fagus sylvatica*) (Doniță et al., 2005). Larger surfaces of pastures, grasslands, vineyards, and transitional woodland-shrubs are also present (**Figure 2.8**).

The *Balkan Mixed Forest ecoregion* overlaps the western part of the area. It is mainly covered by cropland in the lowlands (Găvanu-Burdea Plain, Burnas Plain, Pitești Plain), while forest coverage increases at higher altitudes (in the Cotmeana subdivision of the Getic Piedmont). In the study area within this ecoregion, the vegetation distribution is influenced only by the latitudinal zonation, corresponding to the zone of thermophilous sub-mezophilous oak forests.

Local regionalizations indicate that the southernmost areas continue the forest-steppe ecoregion (Doniță et al., 2005; Popova-Cucu et al., 1983).

In the *Carpathian Montane Forests ecoregion*, forests are predominant, but there are also grasslands and some agricultural areas (pastures, heterogeneous agricultural areas, and fruit trees plantations). Altitude highly influences the vegetation distribution — beech forests and mixed (beech and coniferous) forests are specific between 400 – 1450 m, while higher altitudes are characterized by the boreal vegetation, dominated by *Picea abies* (between 1450 m and 1850 m), the subalpine vegetation with rare trees and subalpine scrub (1850 – 2200 m) and the alpine vegetation of heaths and grasslands (>2200 m) (Doniță et al., 2005).

In southern Romania, the average climatic growing season length between 1961 – 2010, based on mean temperatures, was 252.8 days long, and it ranged from 240 days in Ploiești to 275 days in Constanța meteorological stations (Bandoc et al., 2022).

The percentages of land covers within the study area, based on the Corine Land Cover (CLC) 2018 (EEA, 2019b), are shown in **Figure 2.9**. Agricultural areas represent the largest share (66%), followed by forest and semi-natural areas (20%). Artificial surfaces represent 6% of the study area, while wetlands and water bodies each have a share of 4%.

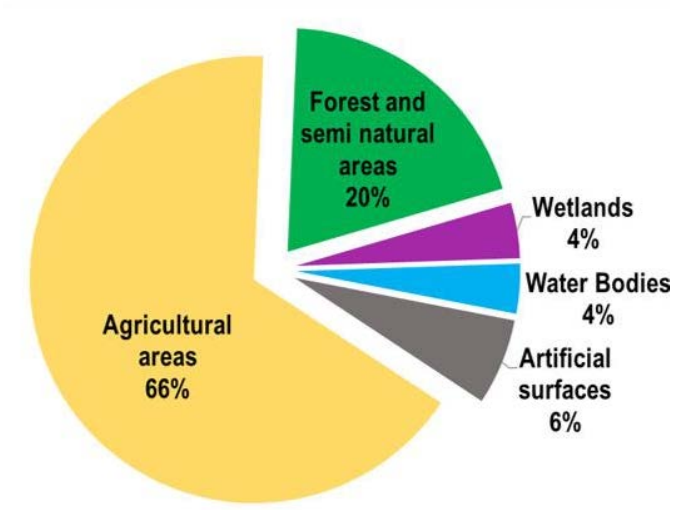

Figure 2.9 Shares of land covers in the study area, based on the Corine Land Cover (CLC) 2018 (EEA, 2019b)

Conclusion

This part focused on introducing the theoretical framework addressed in this thesis and on providing an overview of the geographical characteristics of the study area. At the same time, the susceptibility to drought was highlighted.

Generally, the location of the study area determines the characteristics of a temperate continental climate. More particularly, within the Köppen-Geiger climate classification, the semi-arid (Bsk class), continental (Dfa, Dfb and Dfc classes) and tundra/alpine (ET class) climates are present. The higher influence of continental anticyclonic structures in southern and south-eastern Romania results in more frequent and severe drought occurrences.

The average annual air temperature for most of the study area is between 10 – 12ºC, decreasing to 6 – 8ºC in the Subcarpathians and to lower than 6ºC in the Carpathians. The annual precipitation values increase from the Danube Delta and the Dobrogea regions (less than 400 mm/year and 500 mm/year, respectively) towards more than 700 mm/year at higher altitudes. Potential evapotranspiration has high values within the lowlands of the region (>800 mm/year) and decreases to less than 650 mm in the higher altitude areas. The vulnerability to drought of this region is amplified by the higher potential evapotranspiration compared to precipitation in spring and summer. This generates a high climatic water deficit, especially in the Dobrogea region.

Despite the uncertain trends in precipitation and precipitation-based drought indices in many parts of the studied area, the observed and projected warming trends indicate a higher intensity during drought events. Moreover, the interplay between factors such as increasing annual and seasonal air temperature trend, potential evapotranspiration, heatwave-related indices, and the maximum duration of dry periods as well as decreasing snow depth contribute to a predisposition towards drought-related impacts.

Regarding the hydrology, most of the rivers draining the study area are tributary to the Danube (Vedea, Argeș and Ialomița rivers are among the major tributaries). These are major sources of freshwater in the region and are supplied predominantly from surface sources. The multiannual average streamflow varies from 7.39 m^3/s (Vedea) to 45.23 m^3/s (Argeş). The annual streamflow yield is below 50 mm in the Dobrogea region and in parts of the Romania Plain, and increasing towards more than 1000 mm/year at the highest altitudes. The rivers in southern

Romania generally have a slower recovery from drought periods because of the climatic continental influences. Moreover, climate warming has impacted the streamflow seasonality by decreasing the flows in summer due to higher evapotranspiration and increasing it in some rivers in winter due to more liquid precipitation.

Groundwater bodies have a significant interrelation to many ecosystems (forests, marshes, meadows) in the study area. Furthermore, they have an important economic value for water supply.

The variety of geographic conditions in the study area have favoured the presence of multiple ecoregions: the Pontic Steppe, the East European Forest Steppe, the Central European Mixed Forests, the Balkan Mixed Forests, and the Carpathian Montane Forests. While lowlands have mainly an agricultural land cover, forest cover increases with altitude.

The vulnerability to drought is amplified by the extensive croplands that make the studied area one of the main agricultural regions in Romania and by the presence of urban agglomerations with high water supply requirements.

Having outlined the main geographical characteristics and the vulnerability to drought of the study area, the next part will focus on the methodology and analysis of climatic and hydrological data for investigating the hydroclimatic variability and drought characteristics in south-eastern Romania.

PART II

HYDROCLIMATIC VARIABILITY AND DROUGHT IN SOUTH-EASTERN ROMANIA

This part focuses on the analysis of the hydroclimatic variability and drought assessment in the study area, for identifying and characterizing the periods with water deficit and their changes over time. The first chapter (**Chapter 3**) presents the data and methods used in the analysis. In the second chapter (**Chapter 4**), the variability of the climatic and hydrological drought-related parameters at representative meteorological and gauging stations is investigated, as well as the spatio-temporal variability of soil moisture. Next, the variability of drought-related parameters is explored at the catchment scale, which led to identifying the long-term contribution of climate variations and human influence on streamflow over a long period. The last chapter of this part (**Chapter 5**) is focused on the investigation of drought events occurrence using the climatic water balance and standardized drought indicators.

3. METHODOLOGY FOR IDENTIFYING AND ANALYSING HYDROCLIMATIC VARIABILITY AND DROUGHT

This chapter first (**Chapter 3.1**) presents the different types of datasets (climatic, hydrological, land cover, soil moisture and elevation data) used in **Part II** of the thesis. It is followed by the quality assessment of several precipitation gridded datasets and their suitability for this research (**Chapter 3.2**).

Finally, **Chapter 3.3** describes in detail the methods and techniques for analysing hydroclimatic variability at meteorological and hydrological stations (**Chapter 3.3.1**), for calculating the climatic water deficit (**Chapter 3.3.2**) and the standardized drought indices (**Chapter 3.3.3**), and for estimating the contribution of climatic and human factors to streamflow change (**Chapter 3.3.4**).

3.1. Data

The analyses in **Part II** are based on a large variety of data from several sources and databases, generally freely available.

3.1.1. Climatic data

Assessing hydroclimatic variability and drought occurrence requires long-term data. In this study, a reference period of 60 years, between 1961 – 2020, was considered. This extensive period allows the characterization of droughts through time while considering the influence of climate warming.

Meteorological stations were selected based on the availability and spatial representativeness of the climate types within the region (**Figure 3.1**, **Table 3.1**). While the data for most stations presented in **Table 3.1** are used for drought analysis, the data in Craiova station are used for a better representation of spatial interpolation of drought indices, and the data in Râmnicu Vâlcea station are used in **Part III** of the thesis.

The following data sources were used: the European Climate Assessment & Dataset (ECA&D) project (Klein Tank et al., 2002), the E-OBS gridded dataset (Cornes et al., 2018), the Romanian Climatic Dataset (ROCADA) (Bîrsan and Dumitrescu, 2014a; Dumitrescu and Bîrsan, 2015) and data from the Climate Research Unit (CRU) (Harris et al., 2020).

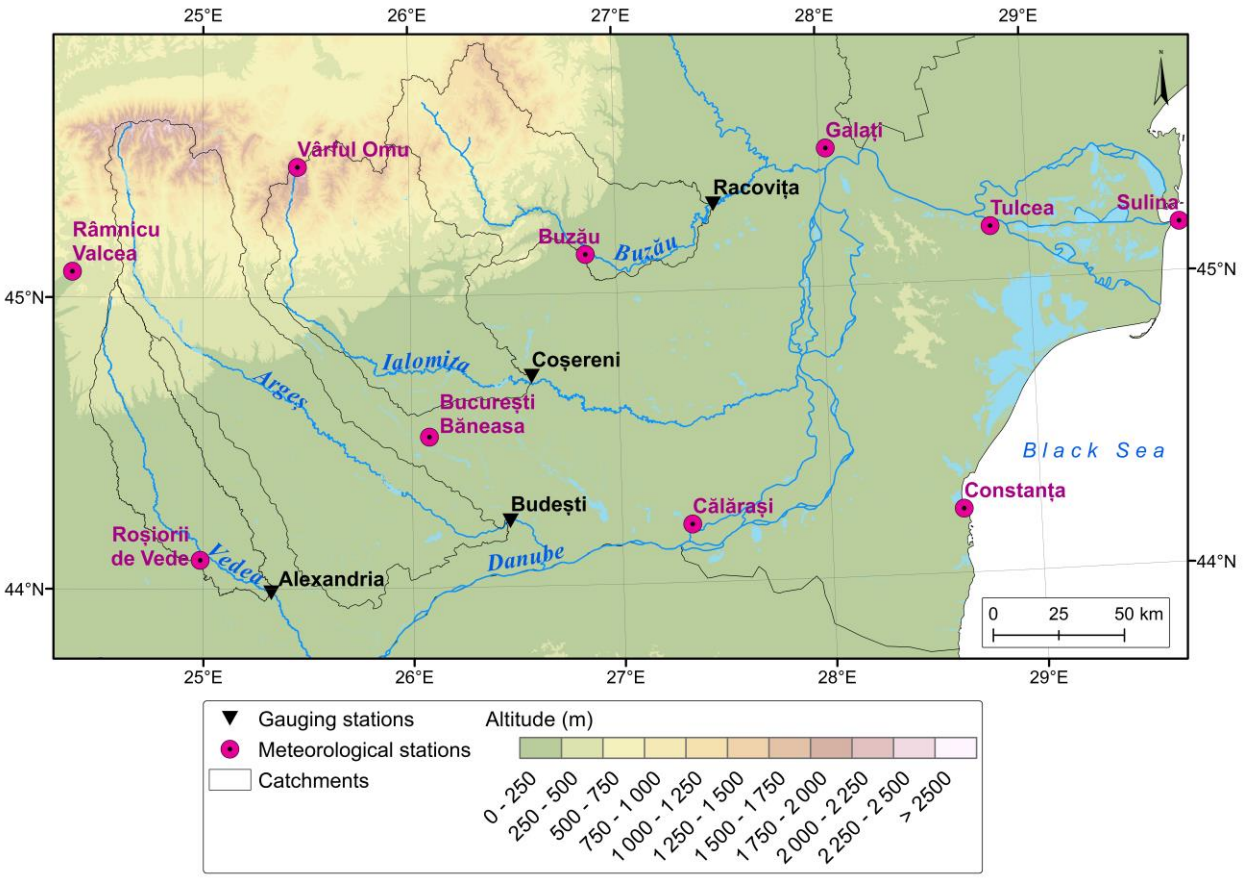

Figure 3.1 Location of meteorological and gauging stations in the study area

Table 3.1 Location and altitude of meteorological stations used in this study (data source: ECA&D)

Meteorological station	Latitude	Longitude	Altitude (m.a.s.l.)
București Băneasa	44° 31’ 00”	26° 04’ 59”	90
Buzău	45° 07’ 59”	26° 51’ 00”	97
Călărași	44° 12’ 00”	27° 19’ 59”	18
Constanța	44° 13’ 12”	28° 37’ 48”	13
Craiova	44° 19’ 00”	23° 52’ 00”	192
Galați	45° 30’ 00”	28° 01’ 12”	71
Râmnicu Vâlcea	45° 06’ 00”	24° 22’ 12”	239
Roșiorii de Vede	44° 06’ 00”	24° 58’ 59”	102
Sulina	45° 10’ 00”	29° 43’ 59”	3
Tulcea	45° 10’ 59”	28° 49’ 00”	4
Vârful Omu	45° 27’ 00”	25° 27’ 00”	2,504

Daily precipitation (mm) at each meteorological station was extracted from ECA&D[3]. Here, the blended data is used, which supplies a series where missing data was replaced by observations made in stations situated the furthest at 12.5 km and within a 25 m altitude difference[4]. The ECA&D is used as reference data throughout the study. Due to the longer time scales of the drought phenomenon, the data is aggregated at monthly and annual time steps.

Apart from the precipitation at the meteorological stations, two **gridded precipitation** products were used in this study. Firstly, the daily precipitation sum (mm) from the E-OBS (Cornes et al., 2018) was used at a spatial resolution of 0.1°. The E-OBS product has a temporal availability starting from 1950. However, the 1961 – 2020 period was considered in this study. It is built by interpolating the data from ECA&D. Additionally, precipitation data from ROCADA were used. The dataset is available daily for the Romanian territory at a spatial resolution of 0.1° for the 1961 – 2013 period (Bîrsan and Dumitrescu, 2014a; Dumitrescu and Bîrsan, 2015). The precipitation dataset is based on homogenized data from 188 stations which were interpolated using the MISH (Meteorological Interpolation based on the Surface Homogenized Data) method (Dumitrescu and Bîrsan, 2015).

Daily mean temperature (°C) at each meteorological station was extracted from ECA&D and aggregated at monthly and annual time steps.

The **potential evapotranspiration (PET) (mm)** was extracted from the gridded monthly CRU data, version CRU TS4.04 (Harris et al., 2020), **further named PET_{CRU}**, to assess the climatic influence on streamflow in the study area. These data were calculated using the Penman-Monteith equation and have a spatial resolution of 0.5°. The monthly evapotranspiration was extracted from the cells that correspond spatially to the weather stations.

Additionally, two more climatic parameters from the E-OBS version 25.0e observation dataset were used in this thesis: **the daily mean temperature (°C)** and **the surface shortwave downwelling radiation (W/m^2), or solar radiation**, representing the mean daily flux measured at the Earth's surface (van den Besselaar, 2021). These parameters were used to estimate the

[3] Royal Netherlands Meteorological Institute (KNMI), "Daily data", Accessed 3 June 2019, https://www.ecad.eu/dailydata/index.php
[4] European Climate Assessment & Dataset, "Frequently Asked Questions. What is the difference between blend and non-blend?", accessed 12 September 2022, https://www.ecad.eu/FAQ/index.php#3

potential evapotranspiration further using the Turc method (Turc, 1961), therefore providing a means of obtaining the variable at the 0.1° resolution.

For each pixel, the daily solar radiation (R) was transformed from W/m^2 to cal/cm^2 using the following procedure (Allen and Pereira, 1998). Firstly, it was converted to MJ/m^2/day using the conversion formula:

$$R[\frac{MJ}{m^2}] = R[\frac{W}{m^2}] * 0.0864 \quad \textbf{(4.1)}$$

The factor of 0.0864 (60 seconds x 60 minutes x 24 hours / 1,000,000) is used to convert the units from W/m^2 to J/m^2/day by considering 24 hours and converting from joules to megajoules. Next, because 1 cal/cm^2/day is 4.1868 x 10^{-2} MJ/m^2/day, the following formula was used to convert it to cal/cm$^{2/}$day:

$$R\ [\frac{cal}{cm^2}] = \frac{R\ [\frac{MJ}{m^2}]}{0.041868} \quad \textbf{(4.2)}$$

The Turc method of estimating the daily potential evapotranspiration was applied for each pixel using the following equation (Lu et al., 2005; Turc, 1961):

$$PET_{Turc,day} = 0.0133 * \frac{T_a}{T_a+15} * (R + 50) \quad \textbf{(4.3)}$$

where $PET_{Turc,\ day}$= daily potential evapotranspiration estimated with the Turc method and T_a = daily mean temperature. Finally, the daily PET values were aggregated on a monthly scale. The monthly PET calculated using the Turc method is denoted further as **PET_{Turc}**.

For most analyses, the calendar year is used when aggregating climatic parameters at the annual scale. For the analyses at the catchment scale regarding the contribution of climate and human influences to streamflow (methodology in **Chapter 3.3.4** and results in **Chapter 4.3)**, the ROCADA precipitation and CRU_{PET} are summed up during each hydrological year (from the 1st of October to the 30th of September of the following calendar year).

3.1.2. Hydrological data

Streamflow is an important indicator of water availability and drought impact on land at longer time scales. Therefore, the analysis of streamflow in this study aims to identify periods of severe hydrological droughts. River flow data are available for different periods for the selected

rivers, and access to these data is restricted for the most recent years. Due to the different temporal availabilities and difficult access to hydrological data, the common period between 1966 – 2010 was selected as a reference interval for analysing the hydrological variability and drought. This period reflects long-term hydrological conditions and includes human influences from the communist and post-communist periods.

In this study, four major catchments were selected for analysis, corresponding to the major rivers draining the region: Vedea, Argeș, Ialomița and Buzău (**Figure 3.1**). The choice of catchments was made to reflect the different geographical characteristics and human pressures in the study area for understanding the streamflow's regional and intra-regional responses to climate and anthropogenic impacts.

The flow data (**monthly average discharge, in m^3/s**) recorded at gauging stations (g.s.) located on the main rivers in the selected catchments were provided by the Water Basin Administrations of Argeș-Vedea and Buzău-Ialomița for three rivers: Argeș River (at Budești g.s.), the Vedea River (at Alexandria g.s.) and the Buzău River (at Racovița g.s.). For the Ialomița River (at Coșereni g.s.) the flow data were extracted from the Global Runoff Data Center (GRDC)[5]. The location of the gauging stations is shown in (**Figure 3.1**). In addition, two missing months in the Argeș River discharge series were gap-filled using linear regression with a gauging station on a tributary river (Călugăreni g.s. on the Neajlov River). The data were used at the monthly scale (in m^3/s) and the annual scale (in m^3/s and mm). The characteristics of the selected catchments at the analysed gauging stations are presented in **Table 3.2**.

For analysing the hydroclimatic variability of streamflow (methodology in **Chapter 3.3.1** and results in **Chapter 4.1.4**) and identifying hydrological droughts (methodology in **Chapter 3.3.3.3** and results in **Chapter 5.2.2**), the monthly streamflow was summed up during each calendar year.

For the analyses regarding the contribution of climate and human influences to streamflow (methodology in **Chapter 3.3.4** and results in **Chapter 4.3)**, the monthly streamflow data were calculated as streamflow depth (Q) in millimetres. These were then summed up during each

[5] Federal Institute for Hydrology, "BfG – GRDC", accessed 20 July 2020, http://www.bafg.de/GRDC

hydrological year (from the 1st of October to the 30th of September of the following calendar year) to obtain the annual series in millimetres.

Table 3.2 The selected catchments and their main characteristics (hydroclimatic parameters are averaged for the 1966 – 2010 period) (Chelu et al., 2022)

River and catchment	Gauging station	A (km^2)	H (m.a.s.l.)	P (mm)	PET (mm)	Q (mm)	PET/P
Vedea	Alexandria	3,269	166	591	847	71	1.43
Argeș	Budești	9,299	382	683	784	152	1.15
Ialomița	Coșereni	6,265	490	711	740	205	1.04
Buzău	Racovița	5,238	543	633	764	168	1.21

A = area, H = mean altitude, P = total annual precipitation, PET = total annual potential evapotranspiration, Q = annual streamflow depth, PET/P = aridity index.

3.1.3. Land cover

To understand the impact of hydroclimatic variability changes while considering land cover and vegetation dynamics, the Historic Land Dynamics Assessment (HILDA) dataset version 2.0 was used. From this database, the **land cover reconstructions** for two years (1960 and 2010) were extracted. This dataset has a spatial resolution of 1 km and a temporal resolution of 10 years (Fuchs et al., 2013). Based on the HILDA dataset, the percentages of the main land covers within each catchment were determined.

3.1.4. Vegetation data

The investigation of vegetation dynamics in the four selected catchments was based on version 5 of the National Oceanic and Atmospheric Administration Climate Data Record of **Leaf Area Index** (NOAA CDR LAI) (Claverie et al., 2016; Vermote and NOAA CDR Program, 2019). This index is an important structural property of vegetation that is significantly involved in the water balance at the catchment scale because it directly controls transpiration and evaporation processes (Donohue et al., 2007). The NOAA CDR LAI has a spatial resolution of 0.05º and a temporal resolution of one day. For this study, the dataset was processed by determining the monthly maximum values, based on which the average annual values were computed further. However, the LAI is used here only to indicate trend signs because some issues related to sensor change were reported for this LAI product (Jiang et al., 2017).

3.1.5. Soil moisture data

To analyse the variation of soil moisture, the v05.2 combined dataset from the ESA Climate Change Initiative (ESA-CCI) was used (Dorigo et al., 2017; Gruber et al., 2019). The soil moisture combined dataset is the result of data fusion algorithms from passive (radiometer) and active (radar) microwave sensors, representing approximately the first centimetres of soil (between 0 – 5 cm[6]). The spatial resolution of this daily dataset is 0.25°, and the temporal availability starts from 1978**.** Validation against *in situ* soil moisture measurements shows various degrees of agreement, depending on climate, land cover and soil type; comparisons have yielded relatively good results in agricultural areas and grasslands in the temperate zone (Dorigo et al., 2017). The volumetric **soil moisture content (in $m^3\ m^{-3}$)** characterizes the surface soil layer.

In the study area, the lack of data is a problem encountered mainly in winter. Because the quality of data from these sensors is affected by snow, frozen surfaces, very dense vegetation, storms and bodies of water, some pixels are missing. Therefore, the data from the winter season were excluded. In the other seasons, the daily data were averaged for each month.

Due to the coarse resolution of the dataset, a spatial average was performed for four extensive geomorphological units in the study area: the Bărăgan Plain, the Dobrogea Plateau, the Teleorman Plain and the Subcarpathian region, using the *Landform map of Romania* database (in Romanian: *Harta unităților de relief din România*) (Candrea et al., 2008), which was defined according to the geomorphological regionalization of Posea and Badea (1984). The z-scores (standardized anomalies) of the spatial averages were estimated on a monthly scale:

$$Z_{SM_i} = \frac{SM_i - \overline{SM_i}}{\bar{\sigma}_{SM_i}} \quad \textbf{(4.4)}$$

where Z_{SM_i} = z-score of soil moisture in month *i*, SM_i = soil moisture value in month *i*, $\overline{SM_i}$ = multiannual mean of soil moisture in month *i*, $\bar{\sigma}_{SM_i}$ = multiannual standard deviation of soil moisture in the month *i*.

[6] European Space Agency and Technische Universität Wien, "Frequently Asked Questions | ESA CCI Soil Moisture website", accessed 12 September 2022, https://www.esa-soilmoisture-cci.org/node/136

3.1.6. Elevation data

The Shuttle Radar Topography Mission (SRTM) digital elevation model (DEM)[7] data at 30 m spatial resolution was used to extract the catchment limits to represent the landscape in the study area and for morphometrical analysis.

3.2. Quality assessment of gridded precipitation datasets

Three precipitation gridded datasets (ROCADA and E-OBS at 0.1º and 0.25º) were compared to observational point measurements at meteorological stations to evaluate whether these could overestimate or underestimate precipitation, which could lead to an underestimation or overestimation of drought occurrence, respectively.

The observation dataset, considered as reference data, consists of precipitation extracted from ECA&D at representative meteorological stations in the study area, as shown in **Figure 3.1** and **Table 3.1**. The datasets are compared for a common time interval (between 1961 – 2013).

The data for the gridded datasets are compared at daily and monthly time steps with the reference dataset using descriptive statistics (e.g., minimum, maximum, median, mean, first and third quartiles, standard deviation), the Kolmogorov-Smirnov statistical test and the Pearson correlation coefficient.

Furthermore, the Călărași meteorological station is graphically compared as an example using the empirical cumulative distribution function. The differences in multiannual monthly means are also compared. The E-OBS grid at 0.1º resolution does not cover the Sulina and Constanța stations.

The descriptive statistics of daily precipitation series are presented in **Table 3.3** for București Băneasa, Buzău, and Vârful Omu meteorological stations, in **Table 3.4** for the Roșiorii de Vede, Galați and Călărași stations and in **Table 3.5** for Tulcea, Sulina and Constanța.

These tables show that E-OBS data often underestimate daily mean values compared to the reference dataset. All datasets underestimate maximum precipitation values compared to observed

[7] CGIAR - Consortium for Spatial Information, "CGIAR-CSI SRTM – SRTM 90m DEM Digital Elevation Database", accessed 20 July 2020 https://srtm.csi.cgiar.org/

values. The E-OBS underestimates and the ROCADA overestimates the number of days with precipitation when compared to the reference dataset.

Table 3.3 Descriptive statistics of daily precipitation at București Băneasa, Buzău, Călărași and Vârful Omu meteorological stations, for observed data (O), E-OBS at 0.1º (E1) and 0.25º resolution (E25) and ROCADA (R) gridded datasets between 1961 – 2013

Daily	București Băneasa				Buzău				Vârful Omu			
	O	E1	E25	R	O	E1	E25	R	O	E1	E25	R
Q1	0											
Mdn	0											0.26
M	**1.7**	1.6	1.5	1.6	**1.4**	1.3	1.3	1.4	**2.7**	2.2	1.9	2.64
Q3	**0.4**	0	0	0.6	**0.2**	0	0	0.6	**2.9**	2.4	2.3	2.68
Max	**126.4**	111.2	90.3	116.1	**90.5**	77.4	60.2	60.6	**102.4**	94.3	54	94.6
SD	**5.3**	4.7	4.2	4.8	**4.7**	4.3	3.7	4	**5.8**	4.8	3.9	5.7
DPr	**31**	22	23	46	**29**	21	22	47	**47**	37	38	64.3

Q1 = First quartile (25%); Mdn = Median; M = Mean; Q3 = Third quartile (75%); SD = Standard deviation; DPr = Days with precipitation (% of total days); Max = Maximum value

Table 3.4 Descriptive statistics of daily precipitation at Roșiorii de Vede, Galați and Călărași meteorological stations, for observed data (O), E-OBS at 0.1º (E1) and 0.25º resolution (E25) and ROCADA (R) gridded datasets between 1961 – 2013

Daily	Roșiorii de Vede				Galați				Călărași			
	O	E1	E25	R	O	E1	E25	R	O	E1	E25	R
Q1	0											
Mdn	0											
M	**1.4**	1.3	1.3	1.5	**1.3**	1.2	1.2	1.3	**1.4**	1.3	1.3	1.4
Q3	**0.3**	0	0	0.6	**0.2**	0	0	0.4	**0.3**	0	0	0.5
Max	**82.6**	67.5	61	78.3	**126.2**	94.7	77.5	99.2	**84**	80.1	81.4	68.6
SD	**4.5**	3.8	3.6	4.2	**4.7**	3.96	3.6	4.1	**4.6**	4	3.7	4.2
DPr	**30**	21.6	23.4	46.7	**30**	19.7	21.2	46	**29**	20	21	44

Q1 = First quartile (25%); Mdn = Median; M = Mean; Q3 = Third quartile (75%); SD = Standard deviation; DPr = Days with precipitation (% of total days); Max = Maximum value

Table 3.5 Descriptive statistics of daily precipitation at Tulcea, Sulina and Constanța meteorological stations, for observed data (O), E-OBS at 0.1º(E1) and 0.25º resolution (E25) and ROCADA (R) gridded datasets between 1961 – 2013

Daily	Tulcea				Sulina			Constanța		
	O	E1	E25	R	O	E25	R	O	E25	R
Q1	0									
Mdn	0									
M	**1.3**	1.2	1.1	1.1	**0.7**	0.8	0.8	**1.2**	1.1	1.1
Q3	**0.2**	0	0	0.3	**0**	0	0.2	**0.1**	0	0.3
Max	**135.5**	107.8	85.8	70.3	**84.9**	70.9	58	**201**	94	80.2

SD	**4.5**	3.9	3.5	3.6	**2.9**	2.6	2.7	**4.4**	3.4	3.7
DPr	**28**	19	19.9	44.1	**22**	17.4	36.6	**27**	18.5	41.8

Q1 = First quartile (25%); Mdn = Median; M = Mean; Q3 = Third quartile (75%); SD = Standard deviation; DPr = Days with precipitation (% of total days); Max = Maximum value

The descriptive statistics of the monthly precipitation series are presented in **Table 3.6**, **Table 3.7** and **Table 3.8**. These show that the closest values to the observed data are generally from ROCADA. The first quartile in ROCADA is almost the same as the observed value in București Băneasa, Călărași, Galați, slightly overestimated in Buzău, Roșiorii de Vede, Sulina, Constanța and Vârful Omu and slightly underestimated in Tulcea. ROCADA slightly underestimates the median value in București Băneasa, Tulcea and Vârful Omu and slightly overestimates in Buzău, Călărași, Roșiorii de Vede, Sulina, Galați and Constanța. ROCADA underestimates the mean at all stations except Roșiorii de Vede and Sulina. Except for Sulina, statistics for the Q1, median, and mean are underestimated by the E-OBS products at all stations.

Table 3.6 Descriptive statistics of monthly precipitation at București Băneasa, Buzău and Vârful Omu meteorological stations for observed data (O), E-OBS at 0.1º (E1) and 0.25º resolution (E25) and ROCADA (R) gridded datasets between 1961 – 2013

Monthly	București Băneasa				Buzău				Vârful Omu			
	O	R	E1	E25	**O**	R	E1	E25	**O**	R	E1	E25
Min	**0.1**	0.1	0	0	**0**	0.2	0	0	**1.4**	1.8	0.7	0.8
Q1	**22.5**	22.3	21.3	21.1	**18**	19.3	17.5	17.9	**40.4**	45.6	32.2	27.6
Mdn	**42.1**	41	39.8	38.1	**34.8**	35.5	33.2	33.1	**70.1**	68.9	56.7	49.3
M	**50.8**	48.8	47.3	45.1	**43.6**	42.2	41	39.4	**81.9**	80.3	66.1	56.9
Q3	**68.6**	65.8	64.3	60.6	**58.6**	56.9	54.3	52.7	**110.5**	108.1	89	77.9
Max	**269.6**	251.7	258.6	234.7	**213**	185.3	201.4	187.7	**350**	304.3	231.2	211.3

Min = Minimum value; Q1 = First quartile (25%); Mdn = Median; M = Mean; Q3 = Third quartile (75%); Max = Maximum value

Table 3.7 Descriptive statistics of monthly precipitation data at Vârful Omu and Roșiorii de Vede meteorological stations for observed data (O), E-OBS at 0.1º (E1) and 0.25º resolution (E25) and ROCADA (R) gridded datasets between 1961 – 2013

Monthly	Roșiorii de Vede				Galați				Călărași			
	O	R	E1	E25	**O**	R	E1	E25	**O**	R	E1	E25
Min	**0**	0.2	0	0	**0.4**	0.5	0	0	**0**	0.2	0	0
Q1	**19**	20.5	18.6	18.9	**18.4**	18	16.5	16.1	**20**	19.9	17.7	18
Mdn	**36**	37.7	34.9	34	**33.1**	33.8	31.5	31.3	**36.9**	37.5	34.5	33.8
M	**42.9**	44.4	40.5	39.9	**40.9**	39.9	37.5	36.3	**42.8**	42.1	39.6	38.9
Q3	**59**	59.9	54	53.2	**55.7**	54.3	51	49.3	**56.8**	54.4	54.2	53.5
Max	**232**	211.9	205.7	197.4	**240.1**	185.9	216.7	192.7	**185.2**	191.9	170.8	163.7

Min = Minimum value; Q1 = First quartile (25%); Mdn = Median; M = Mean; Q3 = Third quartile (75%); Max = Maximum value

Table 3.8 Descriptive statistics of monthly precipitation at Tulcea, Sulina, Galați and Constanța meteorological stations for observed data (O), E-OBS at 0.1º (E1) and 0.25º resolution (E25) and ROCADA (R) gridded datasets between 1961 – 2013

Monthly	Tulcea				Sulina			Constanța		
	O	R	E1	E25	**O**	R	E25	**O**	R	E25
Min	**0**	0.7	0	0	**0**	0.3	0	**0.1**	0.3	0
Q1	**16**	14.5	15.6	15.3	**7.8**	9.9	9.3	**15.3**	16.1	15.1
Mdn	**32**	29.6	29.3	28.2	**16.7**	19.3	19.2	**27.9**	28.8	26.7
M	**38.8**	34	35.9	34.1	**21.5**	23.8	23	**35.4**	34.5	32.2
Q3	**51.6**	45.4	48.7	46.2	**28.4**	32.4	30.7	**48**	46.9	42.8
Max	**191.1**	134	173.3	157.8	**129**	126.5	125.1	**259.2**	166.1	179.6

Min = Minimum value; Q1 = First quartile (25%); Mdn = Median; M = Mean; Q3 = Third quartile (75%); Max = Maximum value

In **Table 3.9** and **Table 3.10**, a synthesis of results showing the comparison between the empirical cumulative distribution functions (ECDF) of the reference (observed) dataset and gridded datasets representing monthly precipitation is presented for the meteorological stations in the study area. This evaluation was performed by visual comparison between the ECDFs for three precipitation intervals: months with 0 to 20 mm, with 20 to 40 mm and with more than 40 mm of precipitation. The first interval represents months with lower precipitation amounts, such as months in droughts.

Table 3.9 Comparison of empirical cumulative distribution functions between observed and gridded monthly precipitation datasets, ROCADA, E-OBS at 0.1º (E1) and E-OBS at 0.25º (E25), for three intervals (0 – 20 mm, 20 – 40 mm, > 40 mm) at București Băneasa, Călărași, Tulcea, Constanța and Buzău meteorological stations for the 1961 – 2013 period, showing overestimation (↑), underestimation (↓) and matching (□)

Datasets	Fraction of data	Stations				
		București Băneasa	Călărași	Tulcea	Constanța	Buzău
ROCADA	0 – 20 mm	□↓	↑	□↓	↑	↑
	20 – 40 mm	↓	□↑	↓	↑	↑
	> 40 mm	↓	↓	↓	↓	↓
E1	0 – 20 mm	↓	↓	□↓	-	↓
	20 – 40 mm	↓	↓	↓		↓
	> 40 mm	↓	↓	↓		↓
E25	0 – 20 mm	↓	↓	□↓	□	□↓
	20 – 40 mm	↓	↓	↓	↓	↓
	> 40 mm	↓	↓	↓	↓	↓

Table 3.10 Comparison of empirical cumulative distribution functions between observed and gridded monthly precipitation datasets, ROCADA, E-OBS at 0.1° (E1) and E-OBS at 0.25° (E25), for three intervals (0 – 20 mm, 20 – 40 mm, > 40 mm) at Vârful Omu, Sulina, Roșiorii de Vede and Galați meteorological stations for the 1961 – 2013 period, showing overestimation (↑), underestimation (↓) and matching (□)

Datasets	Fraction of data	Stations			
		Vârful Omu	Sulina	Roșiorii de Vede	Galați
ROCADA	0 – 20 mm	↑	↑	↑	↑
	20 – 40 mm	↓	↑	↑	↑□
	> 40 mm	↓	↑□	↑□	↓□
E1	0 – 20 mm	↓	-	□	↓□
	20 – 40 mm	↓		↓	↓
	> 40 mm	↓		↓	↓
E25	0 – 20 mm	↓	↑	□	↓□
	20 – 40 mm	↓	↑	↓	↓
	> 40 mm	↓	↑□	↓	↓

The ECDFs of reference and gridded datasets at the Călărași meteorological station for the three selected precipitation intervals are shown in **Figure 3.2**. In the first interval (0 – 20 mm, which represents about 25% of data), the ROCADA dataset generally slightly overestimates the values. In contrast, the E-OBS datasets underestimate the values. These characteristics suggest that the deficit during drought months could be underestimated by ROCADA and overestimated by E-OBS.

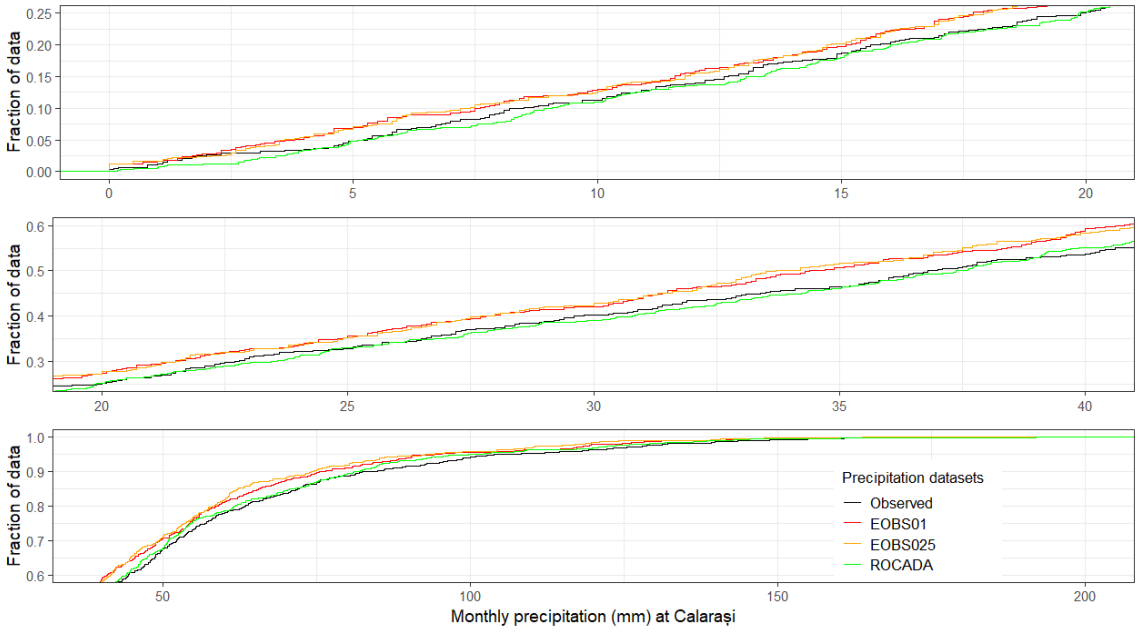

Figure 3.2 Empirical cumulative distribution functions of the gridded and observed datasets at

Călărași (1961 – 2013) for months with precipitation between 0 – 20, 20 – 40 and > 40 mm

The synthesis tables (**Table 3.9** and **Table 3.10**) highlight that E-OBS (both at 0.1º and 0.25º resolutions) generally underestimate the values at all stations (except Sulina), in all intervals of precipitation, suggesting that it could overestimate a precipitation deficit. On the other hand, overestimation occurs mainly for the ROCADA dataset and only for the first two intervals (with lower precipitation), suggesting that ROCADA might underestimate the precipitation deficit. At București Băneasa, in all intervals of precipitation, and at Vârful Omu in the last two, ROCADA also underestimated precipitation. At Sulina, all datasets overestimated precipitation. Intervals with matching periods were shown together with the general tendencies because matching did not occur along the entire series of any particular interval. At Călărași, in the 20 – 40 mm case, for example, similarities occur around the 20 mm, 25 mm and 35 mm values.

The Kolmogorov-Smirnov test is further employed to compare the distributions of the daily and monthly gridded precipitation datasets with the observed data. The null hypothesis is that the data from the gridded datasets come from the same distribution as the reference dataset (observations). With a p-value < 0.05, the null hypothesis is rejected at all stations for the three daily datasets, suggesting that the distributions are different (**Table 3.11**). The smallest maximum distance between the distribution functions is found for the E-OBS at 0.25º and the largest for ROCADA.

For the gridded precipitation datasets at a monthly scale, the lowest maximum differences between the two distribution functions are the smallest for ROCADA at most stations except Tulcea and Sulina (**Table 3.12**), where it is the largest. The distance is the largest for E-OBS at 0.25º at all stations except Tulcea and Sulina. Gridded data differ from the reference data at Vârful Omu and Sulina stations for all datasets.

Table 3.11 Kolmogorov-Smirnov test statistics to compare the daily observed and gridded precipitation datasets, ROCADA (ROC), E-OBS at 0.1º (E1) and E-OBS at 0.25º (E25), between 1961 – 2013

	București Băneasa		**Buzău**		**Călărași**		**Vârful Omu**		**Tulcea**		**Sulina**		**Roșiorii de Vede**		**Galați**		**Constanța**	
	p	D	p	D	p	D	p	D	p	D	p	D	p	D	p	D	p	D
E1	*	0.09	*	0.08	*	0.09	*	0.10	*	0.09	-	-	*	0.08	*	0.10	-	-
E25	*	0.08	*	0.07	*	0.08	*	0.09	*	0.08	*	0.05	*	0.65	*	0.08	*	0.08
ROC	*	0.14	*	0.18	*	0.15	*	0.17	*	0.16	*	0.14	*	0.17	*	0.166	*	0.15

p = the p-value of the test; D = the distance between the empirical distribution function of the comparison dataset and the cumulative distribution function of the reference dataset; * p-value < $2.2e^{-16}$

Table 3.12 Kolmogorov-Smirnov test statistics to compare the monthly observed and gridded precipitation datasets, ROCADA (ROC), E-OBS at 0.1º (E1) and E-OBS at 0.25º (E25), between 1961 – 2013

	Bucureşti Băneasa		**Buzău**		**Călăraşi**		**Vârful Omu**		**Tulcea**		**Sulina**		**Roşiorii de Vede**		**Galaţi**		**Constanţa**	
	p	D	p	D	p	D	p	D	p	D	p	D	p	D	p	D	p	D
ROC	0.8	0.04	0.84	0.03	0.99	0.025	*	0.074	*	0.086	*	0.09	0.66	0.04	0.87	0.03	0.91	0.03
E1	0.57	0.04	0.62	0.04	0.29	0.55	*	0.130	0.291	0.055	-	-	0.52	0.045	0.23	0.058	-	-
E25	0.095	0.07	0.16	0.06	0.18	0.06	*	0.212	0.02	0.085	*	0.088	0.26	0.057	*	0.077	0.16	0.06

p = the p-value of the test; D = the distance between the empirical distribution function of the comparison dataset and the cumulative distribution function of the reference dataset; * p-value < 0.05

The Pearson correlation coefficients between the reference and gridded precipitation datasets at a daily scale show high correlation coefficients (over 0.9) at most stations, except Vârful Omu in the EOBS at 0.25º and ROCADA, where correlations are lower (**Table 3.13**). The highest correlation coefficients for daily data resulted for ROCADA, except for Buzău and Vârful Omu stations, where the highest correlation coefficient was shown by E-OBS at 0.1º.

Table 3.13 Pearson correlation coefficient between daily observed and gridded precipitation datasets, ROCADA (ROC), E-OBS at 0.1º (E1) and E-OBS at 0.25º (E25) between 1961 – 2013

Observations	**Bucureşti Băneasa**	**Buzău**	**Călăraşi**	**Vârful Omu**	**Tulcea**	**Sulina**	**Roşiorii de Vede**	**Galaţi**	**Constanţa**
E1	0.98	0.97	0.96	0.95	0.97	-	0.96	0.97	-
E25	0.96	0.93	0.94	0.86	0.94	0.90	0.92	0.93	0.93
ROC	0.99	0.96	0.98	0.71	0.98	0.95	0.98	0.98	0.96

Multiannual averages (calculated for the 1961 – 2013 period) of monthly precipitation from ROCADA and E-OBS datasets at 0.1º resolution are compared to the reference dataset at the meteorological stations (**Figure 3.3**). For ROCADA, the differences are mainly between -5 and + 5 mm. In particular, average precipitation is underestimated by ROCADA at Bucureşti Băneasa, Tulcea, Buzău (except December), Galaţi (except May and July), Călăraşi (except July and October) and overestimated at Roşiorii de Vede (except June and August), Sulina (except August and September). On the other hand, E-OBS mainly underestimates average precipitation at all

stations, particularly from May to August, with the highest difference in June (between -5 and -10 mm).

Vârful Omu station is presented separately due to the large differences compared to the other stations (**Figure 3.4**). At this station, precipitation is primarily underestimated, except for some months in the ROCADA dataset (February, May, and September to December). The most considerable underestimation at Vârful Omu is in July for both the E-OBS dataset (lower than -25 mm difference) and ROCADA (lower than -10 mm difference).

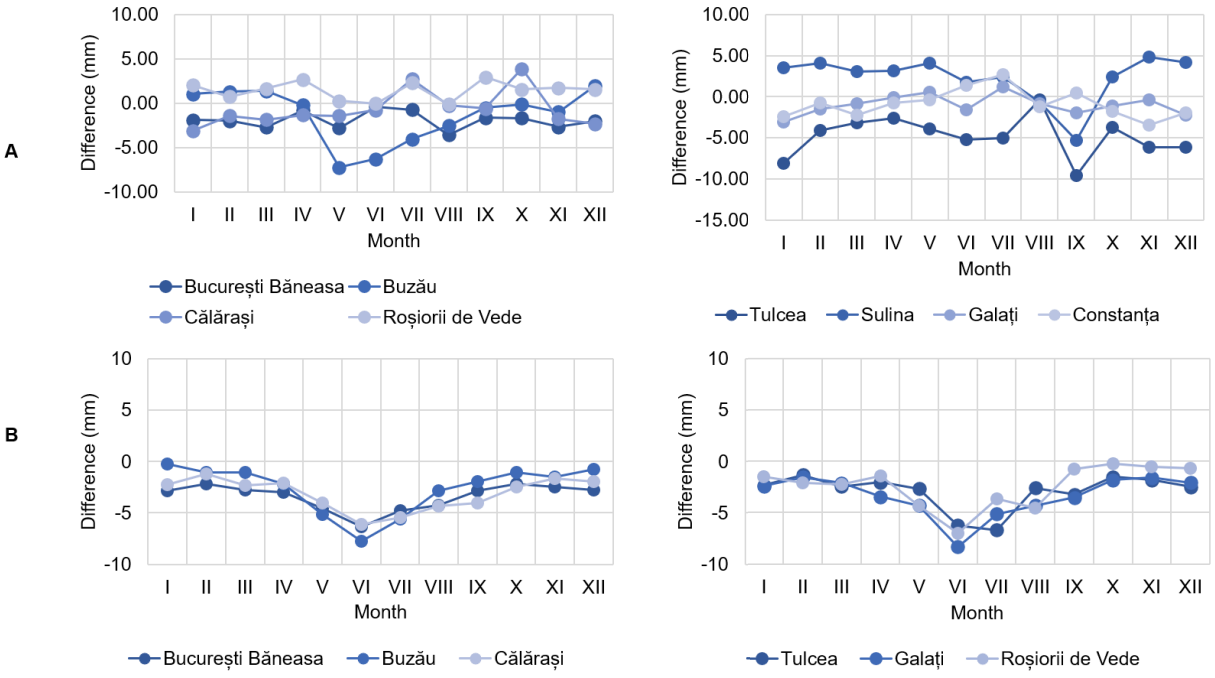

Figure 3.3 Differences between (A) ROCADA, (B) E-OBS at 0.1º resolution datasets and the observed data for the multiannual monthly precipitation average (1961 – 2013)

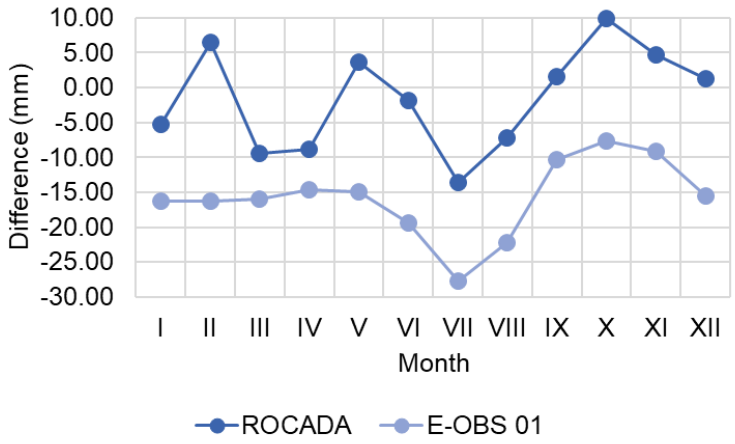

Figure 3.4 Differences between the observed and gridded datasets (ROCADA and E-OBS at 0.1° resolution) for the multiannual monthly precipitation averages at Vârful Omu meteorological station

The results of the quality assessment of the gridded precipitation datasets show that the ROCADA dataset performs best. However, the shorter availability period (1961 – 2013) compared to E-OBS (1950 – present) represents a limiting factor.

Most stations are relatively well represented by the gridded datasets at monthly time scales, except for Vârful Omu and Sulina. The disagreement between datasets at Vârful Omu could be related to topographical heterogeneity and measurement errors, as this high-altitude station is located at 2,504 m, on the Omu Peak (in Romanian: *Vârful Omu*). Sulina station is situated at the eastern extremity of the study area, on the Black Sea shore, at 3 m.a.s.l., which could impact the various interpolation methods by a scarcity of nearby stations.

The ROCADA dataset is used to analyse the climate and human influences on streamflow change (methodology in **Chapter 3.3.4** and results in **Chapter 4.3**), while the E-OBS dataset at 0.1° resolution is used to spatialise the climatic water deficit (raster-CWD) (methodology in **Chapter 3.3.2** and results in **Chapter 5.1.2**).

3.3. Methods and techniques for drought analysis

This chapter presents the methods, approaches, tests, and software tools used for drought analysis in this thesis. **Chapter 3.3.1** focuses on the methods used for analysing the variability and trends of the main climatic and hydrological parameters relevant to drought (air temperature,

precipitation, potential and actual evapotranspiration and streamflow). Next, the approach for identifying and classifying the climatic water deficit is presented in **Chapter 3.3.2**. The methodology for obtaining standardized indicators and analysing drought events is then described in **Chapter 3.3.3**. Finally, the Budyko framework and the elasticity method for analysing the contributions of climate and human factors to streamflow change are explained in **Chapter 3.3.4**.

3.3.1. Analysis of hydroclimatic variability

The variability of the main variables that play a key role role in drought occurrence — precipitation and mean temperature extracted from ECA&D, potential evapotranspiration obtained from CRU, and the actual evapotranspiration obtained from the Thornthwaite water balance (as described in **Chapter 3.3.2**) (Mounier, 1965; Thornthwaite, 1948; Thornthwaite and Mather, 1955) — were analysed at annual and monthly scale at representative meteorological stations (see **Chapter 3.1.1**) for the 1961 – 2020 period. The hydrological variability was investigated based on the average river discharges (annual and monthly) recorded at four gauging stations located on the main rivers draining the study area (presented in **Chapter 3.1.2**) in the 1966 – 2010 period. Furthermore, the Mann-Kendall test with the Sen's slope statistical tests (Kendall, 1975; Mann, 1945) are applied at monthly and annual scales to estimate trends in these parameters, by using the *mk.test* and *sens.slope* functions the *trend* package in the R programming language. For streamflow at the annual scale, the modified Mann-Kendall statistical test is used (Hamed and Ramachandra Rao, 1998; Kendall, 1975; Mann, 1945).

The variability of the main climatic parameters (precipitation, potential evapotranspiration) and that of streamflow (Q, in mm) is also explored in the major representative catchments in the study area at the annual scale between 1966 – 2010. The catchment average of gridded P and PET was estimated to obtain the monthly series for each basin. The datasets were used at their native resolution, and the values were weighted by the fraction of each pixel within the catchment boundary. The modified Mann-Kendall statistical test data is employed (Hamed and Ramachandra Rao, 1998; Kendall, 1975; Mann, 1945) in conjunction with the Sen's slope estimator to estimate trends in these hydroclimatic parameters. The modified Mann-Kendall is used due to the possible auto-correlation in the data. Breakpoints in the data series at the catchment scale are estimated using the Pettitt test (Pettitt, 1979). The *mmkh* function from the *modifiedmk* package is used to

estimate the Hamed and Rao modified Mann-Kendall test. For breakpoints, the *pettitt.test* function from the *trend* package is used.

3.3.2. Climatic water deficit (CWD)

One approach for evaluating monthly drought occurrence is the climatic water deficit (CWD), which was used in multiple studies for estimating drought conditions and changes in frequency and intensity of droughts in France, Brazil, Tunisia or the Transylvanian area (in Romania) during historical periods or in different climate scenarios (Dubreuil, 1996, 1997; Dubreuil and Planchon, 2009; Dubreuil et al., 2018; Holobâcă et al., 2003; Lamy and Dubreuil, 2013; Mjejra et al., 2015; Mounier, 1965, 1977; Mutti et al., 2022).

The CWD is defined as the difference between potential evapotranspiration (PET) and actual evapotranspiration (AET) (all parameters are in mm):

$$CWD = PET - AET \quad \textbf{(4.5)}$$

The CWD is used in this study because it is a biologically relevant drought indicator (Stephenson, 1998), which will henceforth be used for assessing for evaluating vegetation response to drought. Furthermore, because it integrates climatic variables of direct importance to vegetation, it correlates to the spatial distribution of vegetation formations (Stephenson, 1990) and vegetation response at shorter time scales, such as tree mortality (Van Mantgem and Stephenson, 2007). Therefore, the CWD indicates plant water needs during months when their requirements are not fulfilled (Mounier, 1965).

This approach to modelling the CWD shows similar results to standardized indices (e.g., SPEI) (Mutti, 2020), and it is a valuable tool for identifying dry periods. In addition, the method based on the CWD has the advantage of quantifying the water deficit in millimetres, compared to other methods using indices, which show dimensionless statistical deviations.

The CWD and the required hydrological components can be obtained through the **water balance method** introduced by Thornthwaite (1948). This methodology was further developed by Thornthwaite and Mather (1955). It requires monthly precipitation and potential evapotranspiration as input and it outputs water storage in the soil, actual evapotranspiration and surplus (available for runoff) (Liu et al., 2012; McCabe and Wolock, 2011). The model was used

in a simplified version primarily to obtain the actual evaporation at point measurements (meteorological stations).

Actual evapotranspiration is calculated using a series of relationships between water availability (precipitation) and atmospheric water demand (evapotranspiration), and it is controlled by the soil water reserve (**Table 3.14**). In the first case (wet conditions, when precipitation is higher than potential evapotranspiration), the available water can satisfy the monthly water demand because precipitation is higher than potential evapotranspiration. This situation would drive the soil water storage to recharge by the amount of available water from precipitation until the available water storage is attained (**Eq. 4.6**). Due to water availability, the AET is equal to PET, and the CWD is 0. Conversely, during a dry month (when precipitation is lower than potential evapotranspiration), the soil water storage decreases in proportion to the accumulated potential water loss (APWL) (**Eq. 4.9**), which is defined as the cumulative sum of deficits during dry months (**Eq. 4.10**), and the available water capacity (AWC). The AET is equal in this case to the sum of precipitation and the amount of water evaporated from the soil (**Eq. 4.7**). By obtaining AET, the CWD can be calculated as the difference between PET and the AET (**Eq. 4.5**), which can be further used to assess drought conditions at the monthly time scale.

Table 3.14 Calculation steps of the monthly actual evapotranspiration (AET), soil water storage (ST_m) and climatic water deficit (CWD) (Dubreuil, 1996; Thornthwaite and Mather, 1955)

Month conditions	**AET (mm)**	**ST_m (mm)**	**CWD**
$\boldsymbol{P > PET}$	PET	$ST_{m-1} + (P - PET)$ **(4.6)**	0
$\boldsymbol{P < PET}$	$P + dST$ **(4.7)**, where $dST = ST_{m-1} - ST_m$ **(4.8)**	$AWC * e^{-\frac{APWL}{AWC}}$ **(4.9)**, where $APWL = \sum(P - PET)$ **(4.10)**	PET - AET

P = precipitation; PET = potential evapotranspiration, AWC = available water capacity, APWL = accumulated water potential loss, ST_{m-1} = previous month's ST; dST = change in ST. The units for all parameters are mm.

The AWC represents the water storage in the root zone at field capacity (mm) and has high spatial variability. It depends on soil characteristics such as depth, type and structure (Thornthwaite and Mather, 1955). In this study, the value of 100 mm is held constant for the AWC at all stations, which has the advantage of characterizing deficit at the regional scale (Dubreuil, 1996). The main drawback is that setting an invariable AWC ignores the local conditions and variations.

The precipitation data from ECA&D (Klein Tank et al., 2002) and the potential evapotranspiration of PET_{CRU} (Harris et al., 2020) were used as input data in the water balance model at each meteorological station to calculate the CWD (*station-CWD_{CRU}*) between 1961 – 2020. Furthermore, the same methodology is applied using also PET_{Turc} (calculated from gridded datasets as described in **Chapter 3.1.1** and extracted at meteorological stations); the resulting CWD is further denoted as *station-CWD_{Turc}*. The station-CWD_{Turc} will be used in **Chapter 6.3.6** (**Part III**).

The resulting monthly CWD were further classified into different drought magnitude classes, providing a way to understand drought occurrence and frequency changes (Mounier, 1977) (**Table 3.15**).

Two equal study periods were selected to investigate changes at multiannual time scales (1961 – 1990 and 1991 – 2020). The frequency of each class within each period was computed and compared. The trend between 1961 – 2020 in CWD was further examined for each month using the Mann-Kendall test (Kendall, 1975; Mann, 1945) with the Sen slope estimator (Sen, 1968).

Table 3.15 Climatic water deficit (CWD) classes (Dubreuil, 1996; Mounier, 1977)

Class	Month conditions	
Very wet	**P>PET**	ST_m = AWC
Wet		ST_m < AWC
Slightly dry	**P<PET**	CWD < 30mm
Moderately dry		30 <= CWD < 60 mm
Very dry		60 <= CWD < 120 mm
Arid		CWD >= 120 mm

P = monthly precipitation (P); PET = monthly potential evapotranspiration, AWC = monthly available water capacity; ST_m = monthly soil water storage. The units for all parameters are mm.

To investigate the spatial variability of the CWD, the same approach described above for point meteorological stations was applied at the pixel level, using the E-OBS gridded dataset of

monthly precipitation at 0.1° and the potential evapotranspiration estimated using the Turc method (PET_{Turc}, **Chapter 3.1.1**). An invariable AWC of 100 mm was also adopted for the spatialised CWD. The gridded CWD was obtained by spatialising the water balance processing steps using the *raster* package in R. The obtained gridded dataset is further denoted as *raster-CWD*.

3.3.3. Standardized drought indices

The Standardized Precipitation Index (SPI), Standardized Precipitation Evapotranspiration Index (SPEI) and Standardized Streamflow Index (SSI) were calculated on a monthly scale at the meteorological and gauging stations located in the study area in order to identify trends and periods of drought.

The package *SCI* in the R programming language was used to fit the time series to the appropriate probability distribution and to calculate the three standardized indicators (SPI, SPEI, SSI) at different time scales. The *fitSCI* function in this package estimates the parameters needed for standardization, and *transformSCI* applies the standardization to the parameter values.

For each meteorological station, the *trend* package was used to calculate the Mann-Kendall trend with the Sen's trend slope estimator, using the significance level of $\alpha = 0.05$ for identifying significant trends (Kendall, 1975; Mann, 1945; Sen, 1968). The statistical tests were applied to estimate the seasonal trends on SPI-3 and SPEI-3 in February (for winter), May (for spring), August (for summer) and November (for autumn). Furthermore, they were applied on SPI-12 and SPEI-12 in September (thus reflecting conditions in the agricultural and hydrological year) and December (reflecting the calendar year conditions). The trend for SPEI-7 for October is also estimated for evaluating conditions during the growing season.

Positive values of the Sen's slope indicate upward trends (increasing wetness), and negative values indicate downward trends (decreasing wetness, or in other words, increasing drought). The Sen's slope values calculated in each meteorological station were interpolated using the Inverse Distance Weighting method in the ArcMap software to map the spatial distribution of trends.

3.3.3.1. Standardized Precipitation Index (SPI)

The Standardized Precipitation Index (SPI) (McKee et al., 1993) is a frequently used drought and wetness indicator based on precipitation. It can highlight periods of meteorological

drought by comparing the precipitation amounts received during a particular period with the long-term average during that period. It is a valuable tool for comparing drought conditions across different locations with varying climates because the values are standardized (WMO, 2012).

Calculation of SPI requires a long-term time series of monthly precipitation sum of at least 30 years (McKee et al., 1993). Precipitation is cumulated over a period *t* (3, 6, 12, 24 or 48 months are most commonly employed), including the current and previous months within the *t* interval. These aggregated time series are modelled using the suitable probability distribution (through the probability density function). The Gamma distribution (Γ) is the most used function for monthly precipitation (**Figure 3.5**). The following integral defines the Gamma distribution (Rossi et al., 2007):

$$\Gamma(\alpha) = \int_0^\infty y^{\alpha-1}\, e^{-y} dy \qquad \textbf{(4.11)}$$

The probability density function of the Gamma distribution is defined as follows (Rossi et al., 2007):

$$g(x)_= \frac{1}{\beta^\alpha \Gamma(\alpha)} x^{\alpha-1} e^{\frac{-x}{\beta}}, \text{for } x, \alpha, \beta > 0 \qquad \textbf{(4.12)}$$

where α = shape parameter, β = scale parameter, x = continuous random variable (amount of precipitation).

Other suggested distributions for modelling cumulative rainfall data series are Gumbel, log-normal, log-logistic, logistic, Weibull or Pearson-III (Stagge et al., 2015). Optimization can be performed by maximum likelihood estimation of the Gamma distribution parameters. A probability distribution function can thus represent the rainfall distribution. The cumulative probability is identified for each month and transformed into the equivalent of the standard normal distribution (mean of 0 and standard deviation of 1) (**Figure 3.5**).

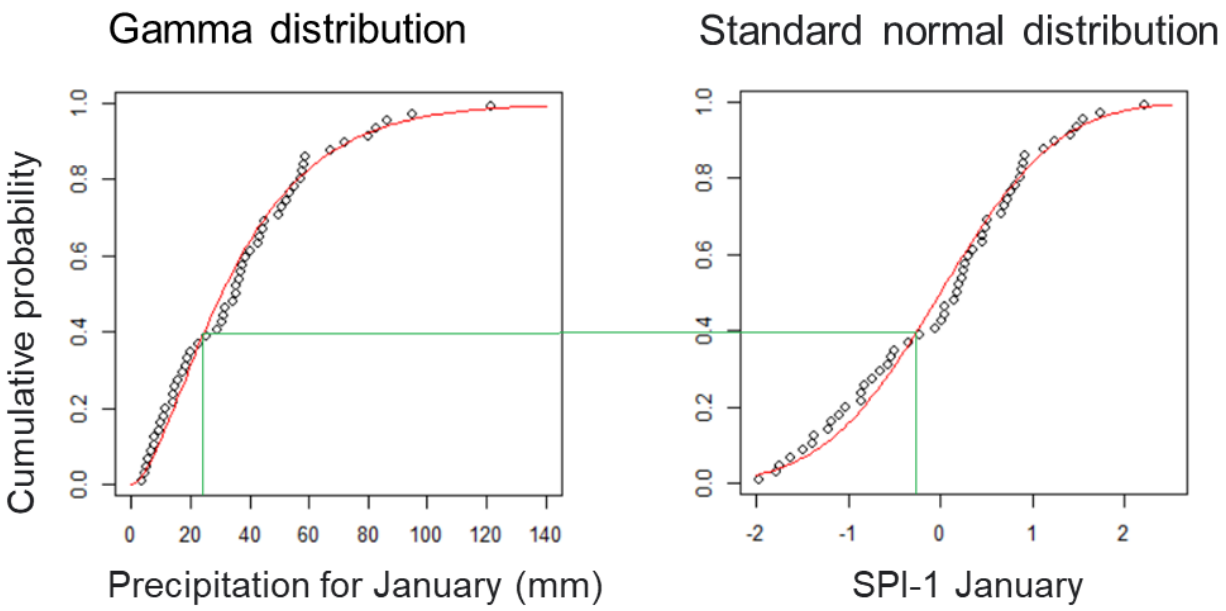

Figure 3.5 Transformation of 1-month (January) cumulative rainfall from Gamma cumulative distribution function to standard normal cumulative distribution function at București Băneasa meteorological station (data from ROCADA, 1961 – 2013)

After calculating the SPI, dry periods can be identified based on the classification according to the deviation from the mean of 0 (**Table 3.16**).

Table 3.16 Classes for SPI, SPEI and SSI (Lloyd-Hughes and Saunders, 2002; McKee et al., 1993)

Value	Class	Probability of event (%)
> 2	Extremely wet	2.3
1.5 to 2	Severely wet	4.4
1 to 1.5	Moderately wet	9.2
1 to -1	Almost normal	68.2
-1 to -1.5	Moderate drought	9.2
-1.5 to -2	Severe drought	4.4
≤ -2	Extreme drought	2.3

Due to the temporally flexible nature of the SPI, potential impacts on environmental components can be highlighted. Thus, short periods (1 to 3 months) highlight a potential impact on components with a fast response time, such as soil moisture, snow cover or flow in small rivers, and vegetation. Medium periods (3 to 12 months) highlight potential impacts on river flow and lake water volume; long periods (more than 12 months) highlight impacts on groundwater.

In this study, only short and medium time scales (3, 6 and 12 months) are used to calculate SPI using monthly precipitation from ECA&D at the meteorological stations in the study area.

3.3.3.2. Standardized Evapotranspiration Precipitation Index (SPEI)

The Standardized Evapotranspiration Precipitation Index (SPEI), developed by Vicente-Serrano et al. (2010), is a drought and wetness index that has the advantage of integrating the effects of temperature by including potential evapotranspiration. Therefore, it is more sensitive to the observed warming trends, in comparison to the SPI. The SPEI is calculated in a similar way to the SPI, and it is based on the monthly series of the climatic water balance defined for each month (Vicente-Serrano et al., 2010):

$$D_i = P_i - PET_i, \quad \textbf{(4.13)}$$

where D_i is the climatic water balance (mm), P is precipitation (mm), and PET is the potential evapotranspiration of month I (mm). D_i is then cumulated over different periods to estimate the indicator further.

This study used the generalized logistic distribution for SPEI normalization, equivalent to the three-parameter log-logistic distribution initially recommended (Stagge et al., 2015; Vicente-Serrano et al., 2010).

SPEI was calculated at 3, 6, 7 and 12 months at meteorological stations using the monthly precipitation from ECA&D and potential evapotranspiration from CRU.

The same standardized index classification is applied to SPEI as the one for SPI (**Table 3.16**).

3.3.3.3. Standardized Streamflow Index (SSI)

Hydrological droughts can be identified through a methodology similar to the one used for identifying meteorological droughts, using a standardised index applied to streamflow data: the Standardized Streamflow Index (SSI), calculated similarly to the SPI. The Gamma distribution can also be used for streamflow data (**Figure 3.6**).

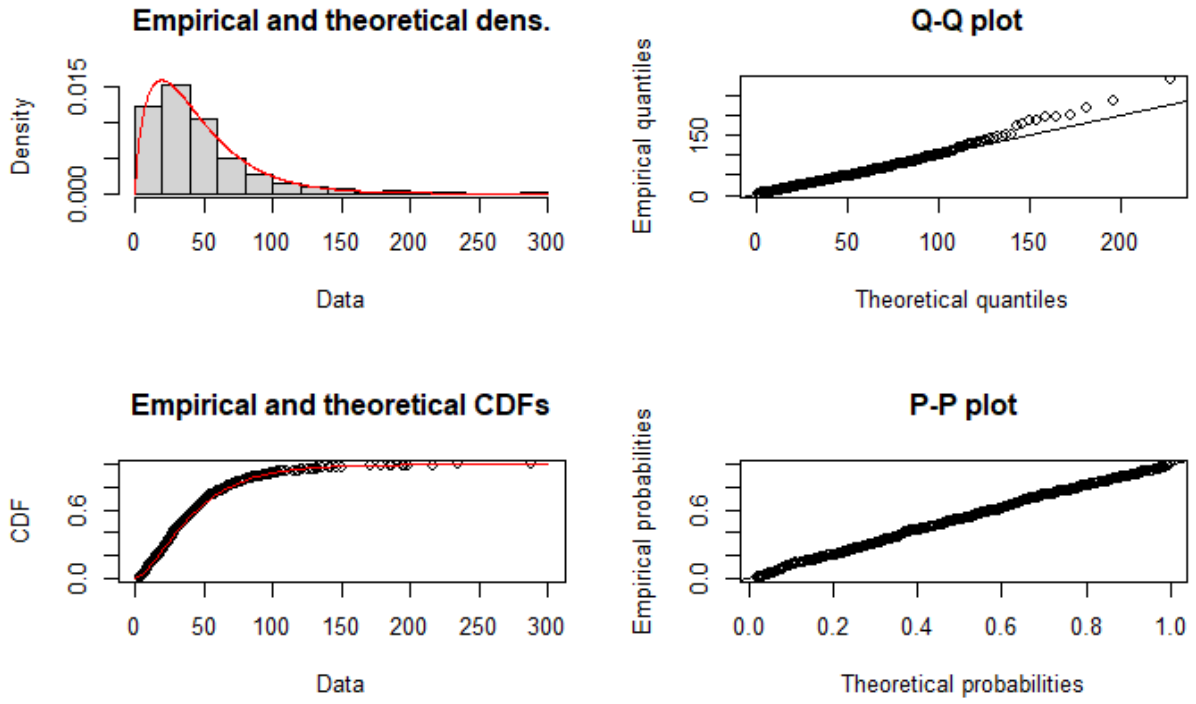

Figure 3.6 Average monthly flow at Budești station (Argeș River) between 1966 – 2010 and the Gamma statistical distribution. CDF = Cumulative distribution function; Q–Q plot = quantile-quantile plot; P–P plot = probability–probability plot.

This indicator was initially proposed by Modarres (2007) and was calculated as a standardized anomaly using monthly streamflow. Shukla and Wood (2008) applied the SPI methodology to runoff layer data in a catchment to assess hydrological drought conditions. The appropriate distribution for statistical modelling of runoff data depends on geographical conditions. Potential distributions include 2-parameter log-normal, Gamma, 3-parameter log-normal and generalized extreme value (Shukla and Wood, 2008). SSI is less variable than SPI at shorter accumulation scales due to hydrological components (snow cover, soil moisture) controlling river runoff (Shukla and Wood, 2008).

The SSI index was calculated in this study at 3- and 6-month time scales using monthly average discharges (m^3/s) data from the gauging stations of Alexandria (on the Vedea River), Budești (on the Argeș River), Coșereni (on the Ialomița River), and Racovița (on the Buzău River). The Gamma distribution was used for modelling the data and transforming it into the standard normal distribution, considering the flow data distribution (**Figure 3.6**).

The SSI was further classified using the same classes as in the case of the SPI and SPEI (**Table 3.16**).

3.3.3.4. Identification of drought events and their characteristics

The time series of the standardized indicators at each meteorological station were subsequently used to identify drought events, resulting in an inventory of droughts. A common way to identify the start of a drought event is when the drought indicator has a value ≤ -1 and the end when it becomes positive (Spinoni et al., 2015). In this study, the definition of a drought event was adapted as follows: the event starts when the indicator turns negative, reaches the value of -1 at least once, and ends when it turns positive again. The drought runs identification and characterization script was built in R programming language using run-length encoding (*rle* function). Each identified event was characterised by **duration** (calculated as the number of months during each event), **severity** as a measure of cumulated deficit (calculated as the sum of indicator values during the event) and **intensity** (calculated as the ratio of severity to duration).

3.3.4. Contribution analysis of climate and human factors to streamflow change

The methodology described in this section has been presented in Chelu et al. (2022). It was used to identify the contribution rate of climate and human factors to streamflow change, based on the Budyko model.

The Budyko model is a Darwinian approach towards understanding hydrological processes that emphasizes the co-evolution and feedback between multiple factors controlling the streamflow such as climate, topography, vegetation, and soils (Bloschl et al., 2013). In this case, it is coupled with the elasticity approach for understanding the local variability of water availability, streamflow, and drought at longer time scales due to several interacting agents. It is particularly interesting to note the contribution of natural (climate) and anthropic factors to streamflow variability, considering the political and socio-economic changes that occurred in Romania over the last century and their potential control of the landscape.

The Budyko framework expresses the relationship between water availability and energy that drives the partitioning of precipitation into streamflow and evapotranspiration (Budyko, 1961, 1974). It is based on the aridity index, the ratio between potential evapotranspiration and precipitation. At long-term averaging periods, water storage is assumed to be negligible and,

therefore, mainly the balance between the atmospheric demand (as represented by PET) and water availability from precipitation controls streamflow (Budyko, 1974).

The analytical elasticity method is often used within the Budyko framework to assess climatic and anthropogenic contributions to streamflow change (Arora, 2002; Schaake, 1990; Zheng et al., 2009). Climate elasticity, in particular, represents the streamflow response relative to the change in climate parameters, such as precipitation and evapotranspiration (Arora, 2002; Schaake, 1990; Schaake and Liu, 1989; Zheng et al., 2009). The simplicity of this method sets it apart from other methods within hydrological modelling, which require more complex parametrization.

In the following, the Budyko framework (Budyko, 1974) will be presented. The aridity index is defined, as mentioned above, as the ratio between potential evapotranspiration (PET) and precipitation (P) and denoted as φ:

$$\varphi = \frac{PET}{P} \tag{4.14}$$

It is linked through a function to the evaporation index, defined as the ratio between actual evapotranspiration (AET) and precipitation, denoted as:

$$F(\varphi) = \frac{AET}{P} \tag{4.15}$$

Multiple expressions of the Budyko equation have been put forward (Wang et al., 2016), while the framework continues to be improved at finer scales and to include non-steady water storage conditions (Mianabadi et al., 2020). However, the Fu equation, among the most frequently used, is employed in this study (Fu, 1981; Zhang et al., 2004). The Fu equation takes the following form (Fu, 1981; Zhang et al., 2004):

$$F(\varphi) = 1 + \varphi - (1 + \varphi^{\omega})^{\frac{1}{\omega}} \tag{4.16}$$

where $F(\varphi)$ = evaporation index (AET/P), φ = aridity index (PET/P), and ω = the curve shape parameter (catchment parameter).

The curve shape parameter (ω) in this equation (further called the catchment parameter) expresses the influence of other factors besides PET/P, such as topography or vegetation or, more generally, land cover. Some of the factors controlling the separation of precipitation into AET and

Q that are reflected in the catchment parameter are the average slope, the plant-extractable water capacity of soil, the share of forest or grassland cover, human influence (irrigation, dams, urbanization, population density) or climate-related influence (e.g., the snow/precipitation ratio, monthly differences between P and PET, average temperatures and seasonality) (Padrón et al., 2017). The catchment parameter can take 2.5 (Fu, 1981) or 2.63 (Zhang et al., 2004) as default values, but a local value can be obtained by fitting it to observed data.

When interpreting the Budyko curve, a higher ω for a particular aridity index would suggest a decreased streamflow (and increased evapotranspiration). For an aridity index of about 1, catchments display the greatest sensitivity to ω (Zhang et al., 2004).

The basic water balance within the catchment can be expressed as (Shaw et al., 2019):

$$P = AET + Q + \Delta S \quad \textbf{(4.17)}$$

where P is precipitation, Q is streamflow, AET is the actual evapotranspiration and ΔS represents the water storage changes. By considering water resources at multiannual time scales, water storage changes could be assumed to be negligible, and one could obtain Q from the simplified catchment water balance equation (Q = P – AET) (Pișota et al., 2010). By computing AET from the Fu's equation (**Eq. 4.15**, where F(φ) = AET/P), streamflow could therefore be calculated as:

$$Q = P(1 - F(\varphi)) \quad \textbf{(4.18)}$$

For calibrating ω to the characteristics in the study area in the four studied catchments (Vedea, Argeș, Ialomița, Buzău), the long-term averages of precipitation and potential evapotranspiration are first used to model the actual evapotranspiration by using the aridity index in the Budyko framework and to obtain the modelled streamflow through the water balance (P – AET). Further, the equation is optimized by attempting to minimize the difference between the Q obtained through the water balance and the long-term average of the observed streamflow and therefore obtaining the calibrated parameter.

To estimate how much the streamflow changes because of changes in precipitation and potential evapotranspiration, the following equation is used (Liang et al., 2015; Zheng et al., 2009):

$$dQ_c = \frac{\partial Q}{\partial P} dP + \frac{\partial Q}{\partial PET} dPET \quad \textbf{(4.19)}$$

By using the definition of elasticity by Schaake and Liu (1989) ($\varepsilon_x = \frac{\partial Q/Q}{\partial x/x}$), the change in streamflow determined by the changes in climate can otherwise be expressed as:

$$\frac{dQ_c}{Q} = \varepsilon_P \frac{dP}{P} + \varepsilon_{PET} \frac{dPET}{PET}, \quad \textbf{(4.20)}$$

where ε_P and ε_{PET} are the elasticities of streamflow to precipitation and potential evapotranspiration, respectively. These are dimensionless and provide a way to convey the proportional effect of the two climatic parameters on streamflow. In general, with an increasing aridity index, ε_P would increase (suggesting the higher sensitivity of streamflow to P in more water-limited catchments), and ε_{PET} would decrease until becoming relatively stable at an aridity index of more than 1.5 (Gao et al., 2016; Zheng et al., 2009). These can be expressed as (Arora, 2002; Zheng et al., 2009):

$$\varepsilon_P = 1 + \frac{\varphi F'(\varphi)}{1-F(\varphi)} \; ; \varepsilon_{PET} = \frac{-\varphi F'(\varphi)}{1-F(\varphi)}, \quad \textbf{(4.21)}$$

where F'(φ) is the first derivative of **Eq. 4.16**, with respect to φ:

$$F'(\varphi) = 1 - \varphi^{\omega-1}(\varphi^{\omega} + 1)^{\frac{1}{\omega}-1} \quad \textbf{(4.22)}$$

A contribution analysis is further performed to explore the possible causes behind the changes in streamflow, identified using statistical analysis (trends, breakpoints). This analysis provides a tool for a more comprehensive understanding of the impact of precipitation deficits (drought) and higher temperatures at longer time scales, using streamflow as an indicator of water availability.

The previously identified breakpoints in the Q data series at the annual time scale were used to separate between a pre- (Q_{pre}, mm) and a post-change (Q_{post}, mm) period, relative to the breakpoint, to obtain the total amount of streamflow change (ΔQ_{tot}, mm):

$$\Delta Q_{tot} = Q_{post} - Q_{pre} \quad \textbf{(4.23)}$$

Here ΔQ_{tot} is assumed to be the sum of streamflow change induced by climate (ΔQ_c, mm) and anthropic influence (ΔQ_h, mm):

$$\Delta Q_{tot} = \Delta Q_c + \Delta Q_h \quad \textbf{(4.24)}$$

Furthermore, ΔQ_c is calculated as:

$$\Delta Q_c = \Delta Q_P + \Delta Q_{PET}, \quad \textbf{(4.25)}$$

where ΔQ_P (mm) is ΔQ_{PET} represent the streamflow change resulting from precipitation and potential evapotranspiration changes. ΔQ_h represents, therefore, the cumulative influence of anthropic factors in the catchment.

The contributions of precipitation and potential evapotranspiration are calculated in millimetres using the following formula:

$$\Delta Q_x = \varepsilon_x \frac{Q}{x} \Delta x, \quad \textbf{(4.26)}$$

where x represents the average long-term P (or PET), Q is the long-term average of streamflow, and Δx is the difference of P (or PET) between the post and pre-change periods.

By calculating ΔQ_c, ΔQ_h can be obtained from **Eq. 4.23**. This anthropic influence can act indirectly on streamflow through land use/land cover conversions or directly through dam storage, water supply, withdrawal or diversions (Destouni et al., 2013; Dey and Mishra, 2017; Jaramillo and Destouni, 2015; Wang and Hejazi, 2011; Wang et al., 2020).

Finally, the contributions of each factor to streamflow change in percentages are estimated as $\frac{\Delta Q_c}{\Delta Q_{tot}} x100\%$ for climate and $\frac{\Delta Q_h}{\Delta Q_{tot}} x100\%$ for human factors.

4. HYDROCLIMATIC VARIABILITY IN SOUTH-EASTERN ROMANIA

This chapter begins by presenting the variability and trends of the main climatic and hydrological parameters relevant to drought at meteorological stations and gauging stations (air temperature, precipitation, potential and actual evapotranspiration, and river discharge) in **Chapter 4.1**. Next, an analysis of the gridded soil moisture dataset, as well as the seasonal averages and variability of this dataset, are presented in **Chapter 4.2**.

Finally, in **Chapter 4.3,** the hydroclimatic variability was investigated at the catchment scale and a contribution analysis was performed within the Budyko framework to assess the influence of climatic and human factors on streamflow changes.

4.1. Hydroclimatic variability at the station scale

4.1.1. Air temperature

As shown in **Chapter 2.2.3.1**, the average annual temperature in the study area ranges between 10 – 12°C in the lowlands to less than 2°C in the Carpathians (**Figure 2.4**).

The average annual air temperatures between 1961 – 2020 (the entire series extracted from the ECA&D dataset) show relatively small differences between stations, as they range between 10.8°C (București Băneasa) and 12.1°C (Constanța) in the lowlands (**Figure 4.1**). At the highest altitudes, the average temperatures are low, such as -2.2°C at Vârful Omu station.

As shown in **Figure 2.3**, the annual regime of temperatures is characterised by maximum values in summer (July at most stations and August at stations above 1850 m) and by the minimum values in winter (January for most stations and February for high-elevation stations).

The average temperatures in the reference period of 1991 – 2020 are higher than in the 1961 – 2020 period, as shown in **Figure 4.1**. For many stations (such as Buzău, Călărași, Constanța, Tulcea and Sulina), the annual average temperature is about 0.5°C higher in the 1991 – 2020 reference period.

The linear trends show increasing annual mean temperatures, with higher slopes at Tulcea and Constanța and a lower slope at București Băneasa. The 11-year moving average highlights a higher mean annual temperature increase since the 1990s. The last two years of the study period

(2018 and 2019) have the highest values at all stations in the time series. For example, high annual average temperatures occurred in 2020 (12.61ºC at București Băneasa, 13.53ºC in Buzău, 14.99 ºC in Sulina, and 13.98 ºC in Călărași) and 2019 (14.36 ºC at Constanța, 13.05 ºC at Roșiorii de Vede).

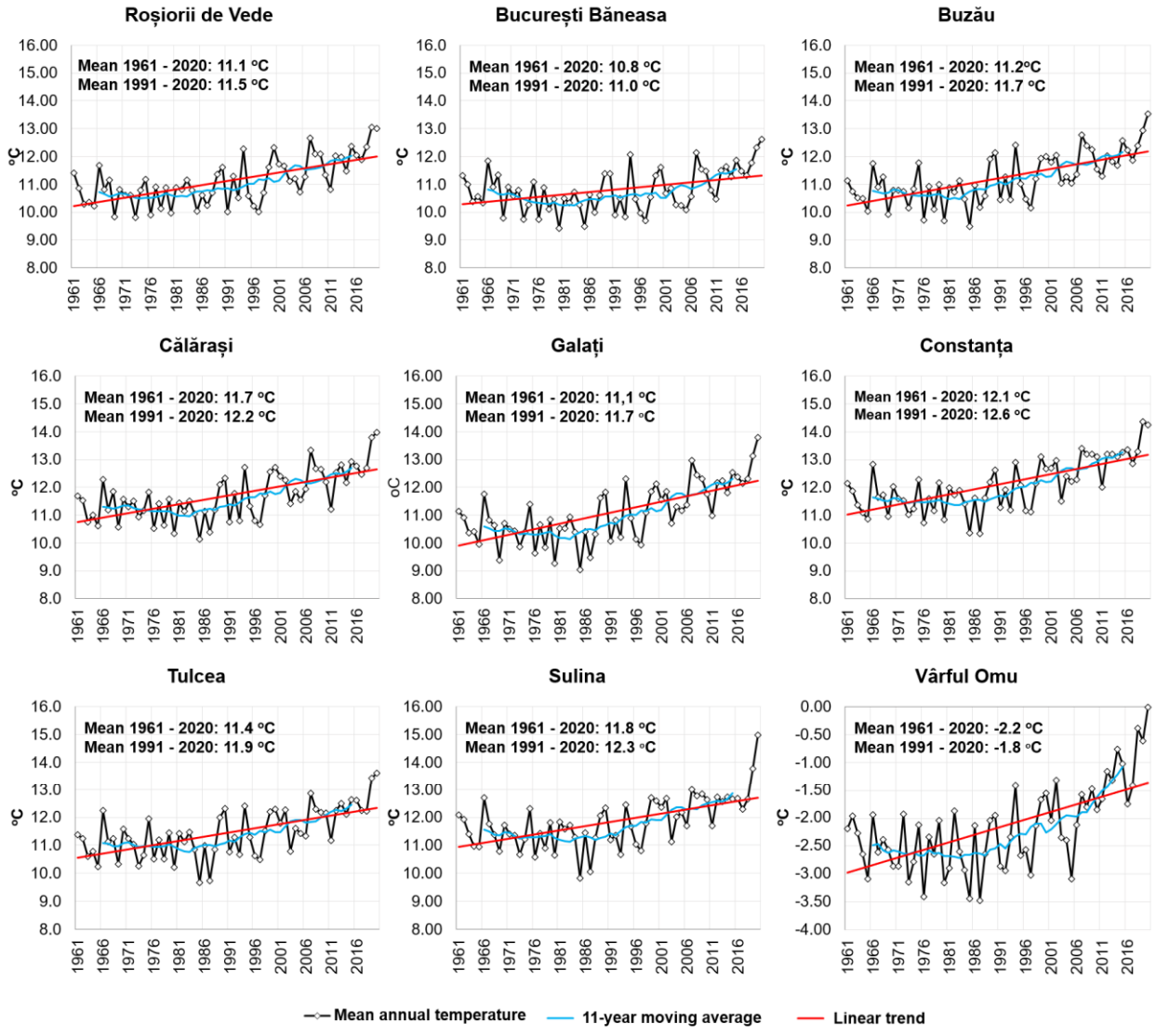

Figure 4.1 Annual average air temperatures (ECA&D), linear trends and 11-year centred moving averages at representative meteorological stations between 1961 – 2020 and multiannual averages for the 1961 – 2020 and 1991 – 2020 periods

Table A.1 in **Appendix A** presents the results of the Mann-Kendall and Sen's slope statistical tests for the trend analysis applied to the monthly and annual series of air temperature data from ECA&D, for the 1961 – 2020 period.

Annually, all stations have significant positive trends, with slopes between 0.02 and 0.04ºC/year. On the monthly scale, there are significant positive trends at all stations in the summer season (June, July, and August). Additionally, many stations also show significant upward trends in May and September. Furthermore, most stations have significant increasing trends in February and March. Galați displays a significant trend in December.

4.1.2. Precipitation

As mentioned in **Chapter 2.2.3.2**, the average annual precipitation within the study area varies from less than 500 mm in its eastern part to more than 1000 mm in the Carpathian Mountains (**Figure 2.5**).

The variation of the total annual precipitation (mm) for the 1961 – 2020 period and the averages for the 1961 – 2020 and 1991 – 2020 periods (based on the ECA&D dataset) at representative stations are shown in **Figure 4.2**. The multiannual averages for the 1961 – 2020 period vary from 260 mm at Sulina to 622 mm at București Băneasa and up to 1001 mm at Vârful Omu. The changes in time are not well defined, as seen by the linear trends that are either slightly increasing or almost stationary at most of the stations.

The lowest annual rainfall was in 1983 at Constanța and Tulcea (227 mm and 274 mm, respectively), 1985 in București Băneasa (374 mm), 1986 at Buzău (324 mm) and 1990 at Călărași (318 mm), for example. Other years with low precipitation were 1963, 1992, 2000, 2008 or 2019. The 11-year moving average emphasises a generally lower rainfall in the 1980s and 1990s.

The variation in monthly average precipitation is shown in **Figure 2.3**. It highlighted the important monthly amplitudes and the differences in rainfall regimes between locations. At most stations, monthly precipitation increases from the minimum in February reaching the maximum in June and decreasing towards February, with relatively constant values in October – January. The stations on the coastland show a second maximum in November – December and a second minimum at the end of the summer season.

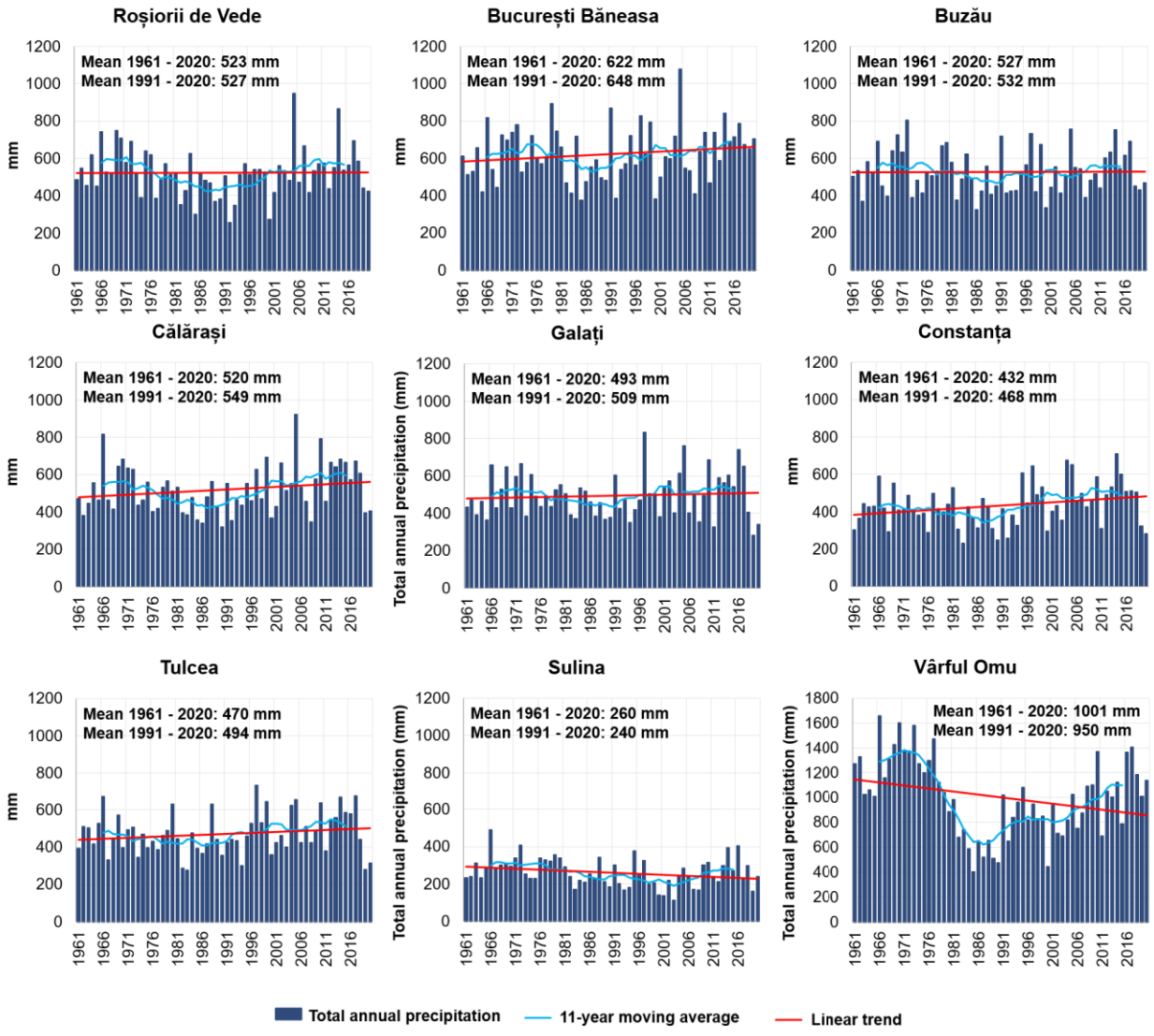

Figure 4.2 Total annual precipitation (ECA&D), linear trends and 11-year centred moving averages at representative meteorological stations between 1961 – 2020 and multiannual averages for the 1961 – 2020 and 1991 – 2020 periods.

The precipitation recorded at the Vârful Omu meteorological station should be analysed and interpreted with caution, due to potential measuring errors at high-altitude stations.

The results of the Mann-Kendall and Sen's slope statistical tests for the trend analysis applied to the monthly and annual series of precipitation data from ECA&D, for the 1961 – 2020 period, are presented in **Table A.2** in **Appendix A**.

On the annual scale, the only significant trends are in Constanța (positive, 1.7 mm/year) and Sulina (negative, -1.05 mm/year). Monthly trends show significant positive trends only in October, at most stations except Constanța and Vârful Omu. Moreover, there was a significant increasing trend in Călărași in January. Significant negative monthly trends were noticed at Sulina in February and May, at Vârful Omu in April and at Galați in August.

The multiannual averages in the 1991 – 2020 reference period were slightly higher when compared to the 1961 – 2020 reference period at most stations (differences ranging between +4 mm at Roșiorii de Vede to +36 mm at Constanța), except Sulina (-20 mm) and Vârful Omu (-51 mm) (**Figure 4.2**).

4.1.3. Evapotranspiration

The spatial distribution of the average annual PET between 1961 -2020 (**Figure 2.6**) showed that the largest values occur in the eastern part of the study area (more than 950 mm in the Danube Delta, between 900 – 950 mm/year in the eastern Romanian Plain). Annual PET decreases to less than 700 mm/year at higher altitudes, with a minimum of 357 mm at Vârful Omu.

The multiannual averages of PET (obtained from the CRU dataset) and the AET modelled with the Thornthwaite water balance (using an available water capacity of 100 mm) between 1961 – 2020 are shown in **Figure 4.3**. PET ranges from 800 mm (Buzău) to 941 mm (Tulcea), while AET ranges from 433 mm (Constanța) to 563 mm (București Băneasa). The linear trend lines of PET in **Figure 4.3** show evident increases with time. The AET trends are less certain, as most of them are slightly increasing or stationary. Only in Sulina, there is a slightly decreasing trend.

The trends in PET and AET, estimated using the Mann-Kendall and the Sen's slope statistical tests, are shown in **Table A.3** and **Table A.4** of **Appendix A**. The increasing trend in PET shown in **Figure 4.3** is also highlighted by these statistical tests (**Table A.3**). At the annual scale, there is a significant positive trend at all stations, with trend slopes ranging between 0.6 mm/year (Vârful Omu) to 3.3 mm/year (Sulina). Significant upward trends appeared between January and April at most stations (except Vârful Omu for this entire period, and Sulina and Călărași for January). Moreover, significant positive trends occur at all stations between June and September (except Vârful Omu, where the trends are not significant in June and September). In

addition, these increasing and significant trends were also estimated in December at Galați, Constanța and Tulcea.

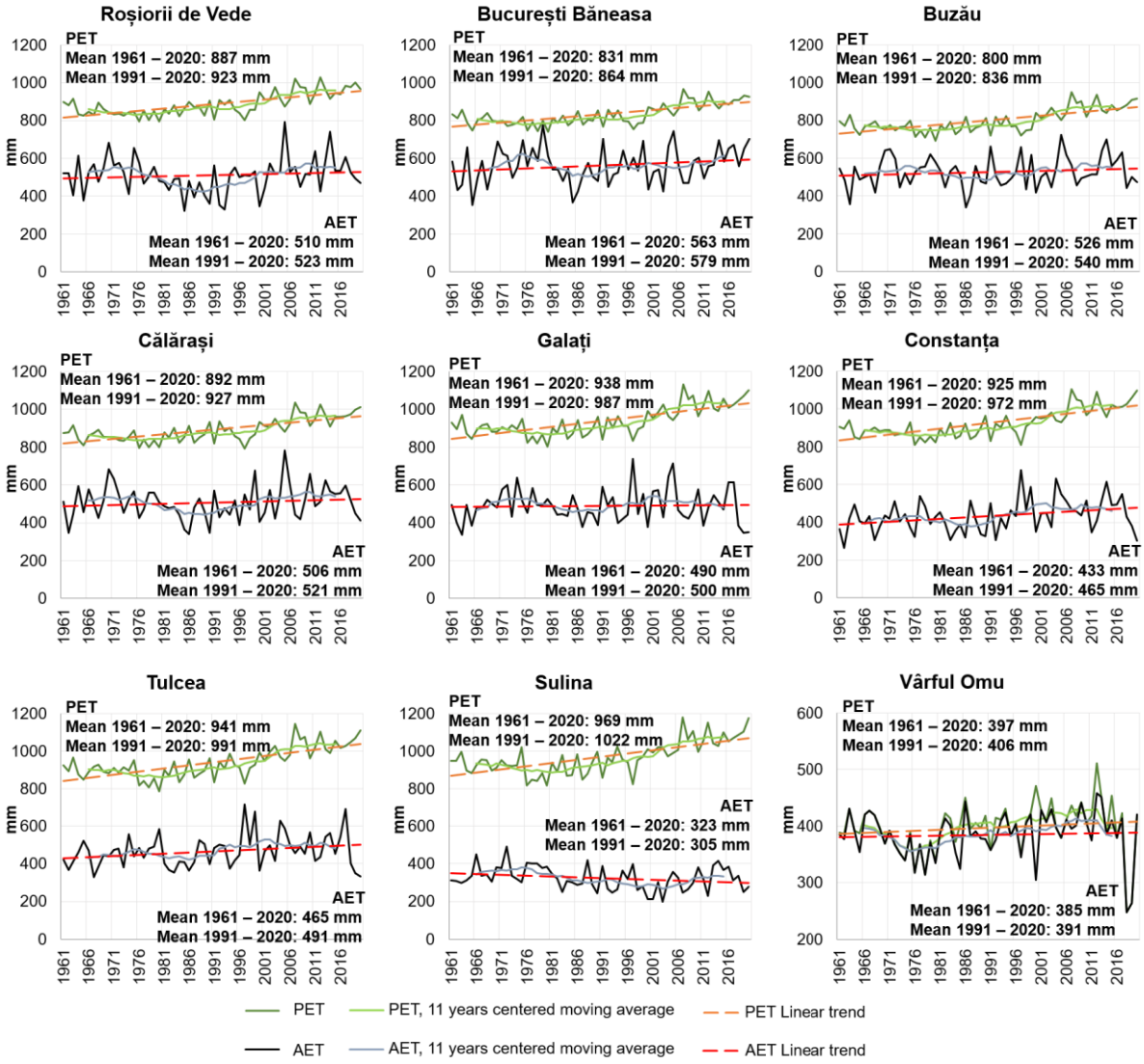

Figure 4.3 Total annual potential evapotranspiration (PET_{CRU}) and actual evapotranspiration (obtained from the Thornthwaite water balance), linear trends and 11-year centred moving averages at representative meteorological stations between 1961 – 2020 and multiannual averages for the 1961 – 2020 and 1991 – 2020 periods

Regarding AET (**Table A.4**), there are some months with significant increasing trends in the January – April period at these meteorological stations. For example, Roșiorii de Vede, Galați and Tulcea showed significant trends between January and March, while București Băneasa and

Călărași had significant trends between February – April. In October, there was a significant increasing trend at all stations except Vârful Omu and Constanța. In August, there were significant decreasing trends at Galați and Tulcea.

4.1.4. River discharge

The variability of average annual river discharges at four gauging stations (g.s.) in the study area is presented in **Figure 4.4**: Alexandria g.s. on the Vedea River, Budești g.s. on the Argeş River, Coșereni g.s. on the Ialomiţa River and Racovița g.s. on the Buzău River. These rivers had a relatively similar pattern of variability between 1966 – 2010. In the first part of this period, there were generally higher discharge values, followed by lower discharges from the 1980s. In the last part of the studied period, discharges were again slightly higher. Very high values were reached in 2005 in all rivers.

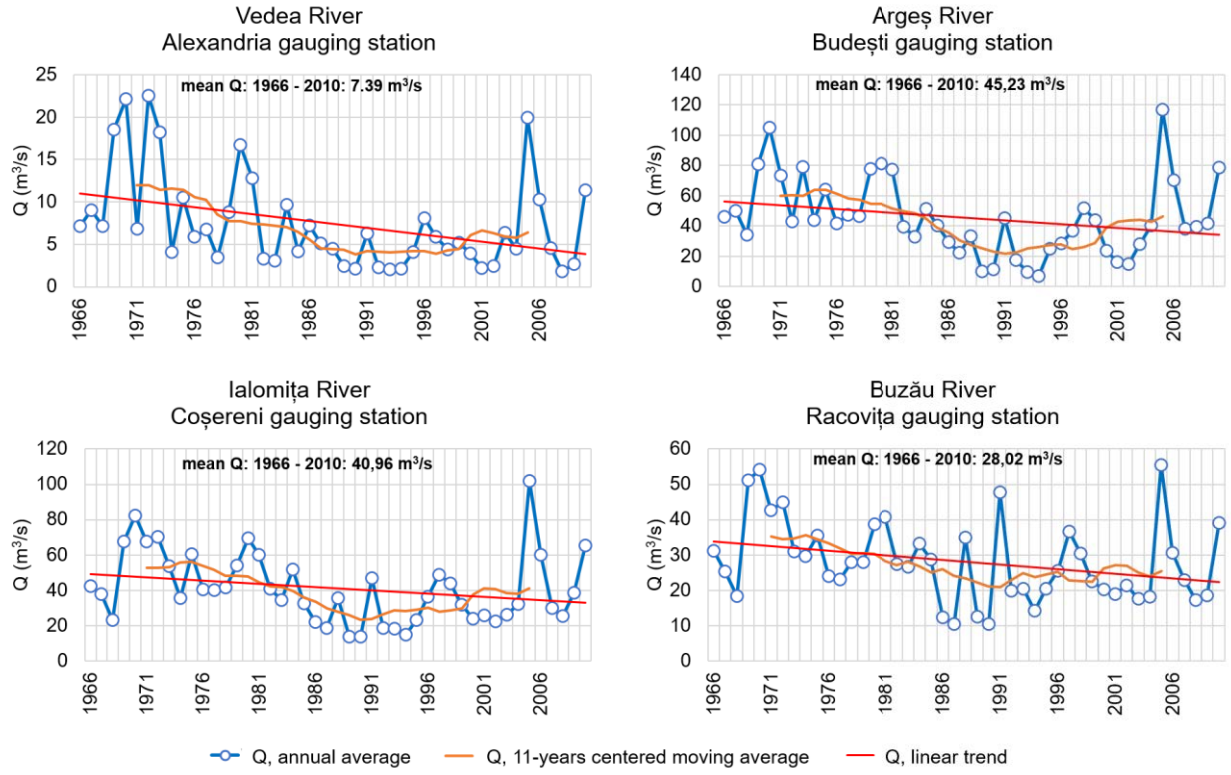

Figure 4.4 Annual average river discharge (Q) variability, multiannual average, linear trends, and 11-year centred moving averages at the selected gauging stations between 1966 – 2010

In the 1966 – 2010 period, the average discharge was 7.39 m^3/s in Vedea, 45.23 m^3/s in Argeş, 40.96 m^3/s in Ialomiţa and 28.02 m^3/s in Buzău.

The monthly average river discharges at the four g.s. are shown in **Figure 4.5**. Vedea and Argeş rivers reached the highest values in March, while in the case of Ialomiţa and Buzău rivers, the highest average monthly discharges were in April. On the other hand, the lowest average monthly discharges were in August for the Vedea River, in October for the Argeş River and in November for the Ialomița and Buzău rivers. The river discharge regime of the Argeş River is highly influenced by the numerous dams and reservoirs on both the Argeş River and its tributaries. The anthropic influences are lower in the case of the Ialomița and Buzău rivers and the lowest in the Vedea basin.

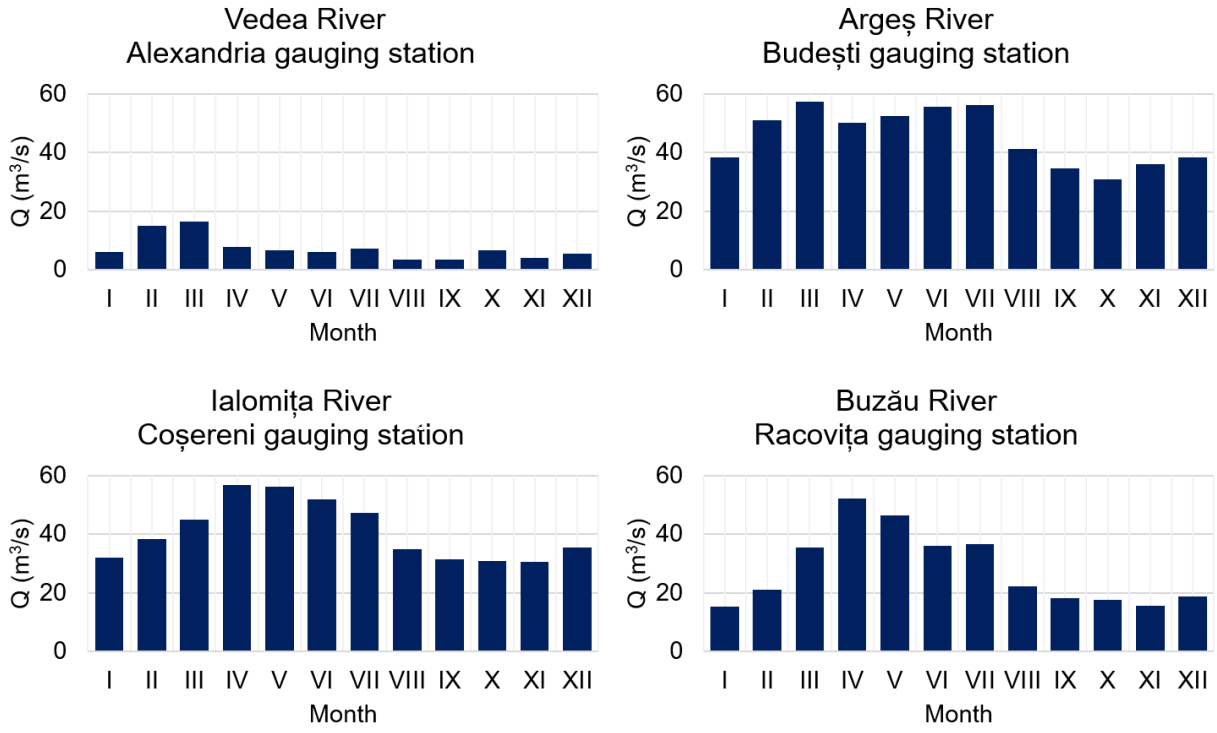

Figure 4.5 Monthly average discharges (Q) of Vedea, Argeş, Ialomiţa and Buzău rivers at the selected gauging stations between 1966 – 2010

The monthly and annual trends of river discharges between 1966 – 2010 estimated with the Mann-Kendall (or modified Mann-Kendall) and the Sen's slope statistical tests are provided in **Table A.5** in **Appendix A**. On the annual scale, the modified Mann-Kendall showed significance only in Vedea and Buzău rivers, where trends are negative (with the trend slopes of -0.114 m^3/s and -0.29 m^3/s, respectively). On the monthly scale, Vedea River showed the most months with significant trends (all negative): February and March, from May to July, September, and

November. The Argeș River registered a significant negative trend only in May, and the Ialomița River, in May and July. Buzău did not show significant trends on the monthly scale. In the case of the Argeș and Ialomița rivers, the trends may be affected by the more important anthropogenic pressures and interventions on the rivers.

4.2. Soil moisture

Soil moisture (SM) is a key component of the hydrological cycle of crucial importance for vegetation development, regulating processes at the land surface – atmosphere interface and playing an important role in biogeochemical cycles (Seneviratne et al., 2010). Decreasing soil water content limits water availability for vegetation; therefore, SM monitoring allows the spatial and temporal identification of water stress. Generally, in Europe, decreasing trends in the average and 20th percentile of soil moisture and an increase in soil moisture drought extent have been noticed over the past century, possibly due to the increased temperatures (Hanel et al., 2018). Moreover, these trends might continue, as shown by the simulations of soil moisture changes using 26 global climate models that forecast negative changes in soil moisture and increases in the frequency of low and extremely low anomalies in all seasons (2070 – 2099 relative to 1971 – 2000) in southern Europe, particularly in the Representative Concentration Pathway (RCP) 8.5 (Ruosteenoja et al., 2018).

In this study, firstly, the coverage of the ESA-CCI soil moisture dataset in the analysed area was calculated as the number of pixels within the study area with valid daily observations divided by the total number of pixels and expressed as a percentage (**Figure 4.6**).

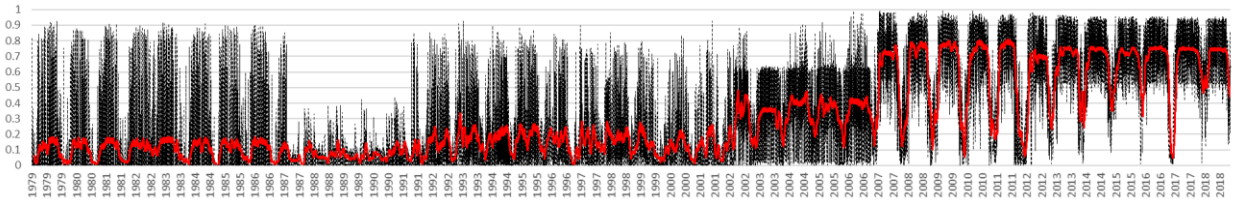

Figure 4.6 Variability of daily soil moisture availability over the 1978 – 2018 period in the study area

The daily variation of the spatial coverage from 1979 and up to 2018 in south-eastern Romania, as shown in **Figure 4.6**, highlights both the seasonal variability due to climatic

conditions and the lack of soil moisture data during winter. Data availability has increased over time, especially after 2002 and 2007. The lowest coverage can be seen between 1987 and 1991. Temporal coverage has increased in the last two decades compared to the previous periods. Due to the uncertainties related to the missing data and low resolution, the soil moisture dataset should be used with caution. This study uses the ESA-CCI soil moisture dataset only to provide an overview of the general spatial and temporal dynamics and it is not considered to reflect absolute/real soil moisture values. In the following, the soil moisture dataset is analysed for the 1992 – 2019 period. The period before 1992 was not considered due to the lower spatial coverage, as shown in **Figure 4.6**.

The spatial variation of soil moisture averaged for the 1992 – 2019 period over spring, summer, and autumn seasons, as well as annually, is shown in **Figure 4.7**.

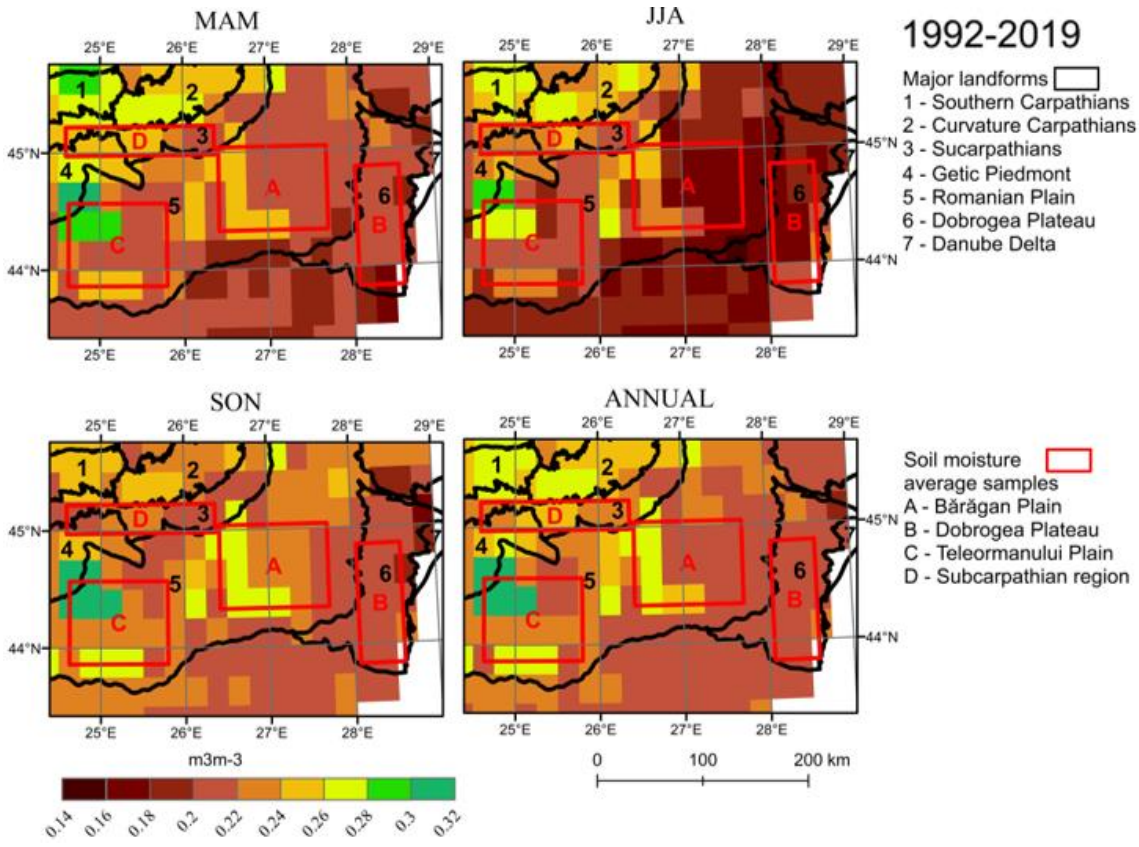

Figure 4.7 Multiannual averages of soil moisture in spring (March, April, and May [MAM]), summer (June, July, and August [JJA]), autumn (September, October, and November [SON]) and annual between 1992 – 2019. The red rectangles designate the sampling in representative geographical regions.

These values are generally lower in the study area's eastern part than in the rest of the region. Also, the lowest values are in the summer, especially in the Dobrogea Plateau and the east of the Romanian Plain. Conversely, the highest values are in the western and north-western parts of the study area, as in the Teleorman Plain.

The multiannual monthly averages (from April to November) of soil moisture in four geographical regions of the study area are represented in **Figure 4.8**. They reflected the precipitation and thermal regimes (**Figure 2.3**). The lowest values are in the Dobrogea Plateau almost throughout the year. The lowest soil moisture values occur in August in the Dobrogea Plateau and the Teleorman Plain, in July in the Bărăgan Plain, and in September in the Subcarpathians. Starting from September – October, the recharge of soil moisture is observed.

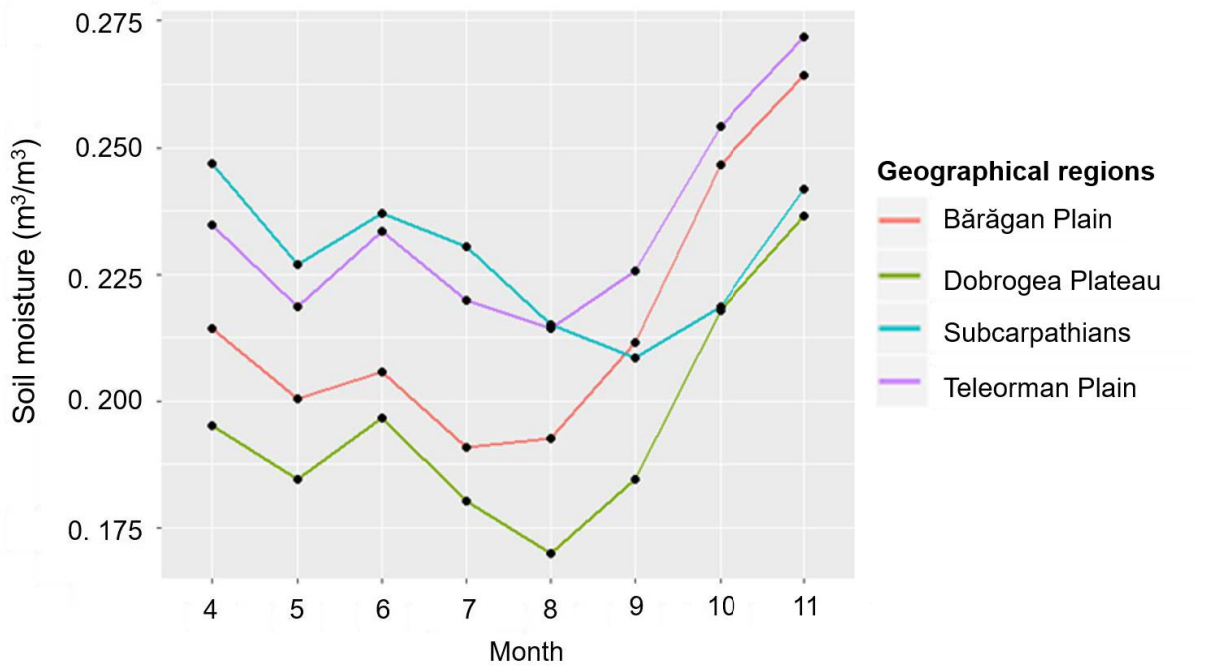

Figure 4.8 Monthly variation of soil moisture in representative regions of the study area, averaged for the 1992 – 2019 period

The variation of the standardized soil moisture anomalies (z-scores) for the 1992 – 2019 period for March – November in four areas of south-eastern Romania is shown in **Figure 4.9**. Soil moisture deficits are highlighted for the 1992 – 1993, 1994, 2000 – 2001, 2007 – 2009, 2011 – 2012 and 2019 periods. The lowest z-scores were estimated for July 2007 (Teleorman Plain), May 1996 (Subcarpathians region), November 2011 (Dobrogea Plateau) and March 2019 (Bărăgan

Plain). July 2007 appears to have the most significant anomalies in all areas. Between 1992 – 2019, the percentage of months (only including the March – November period) with standardized anomalies lower than -1 were about 17% (Bărăgan Plain), 13% (Dobrogea Plateau), 13% (Subcarpathians region), 17% (Teleorman Plain), while the months with standardized anomalies lower than -2 (extreme deficit) was about 2 – 3% in the study area.

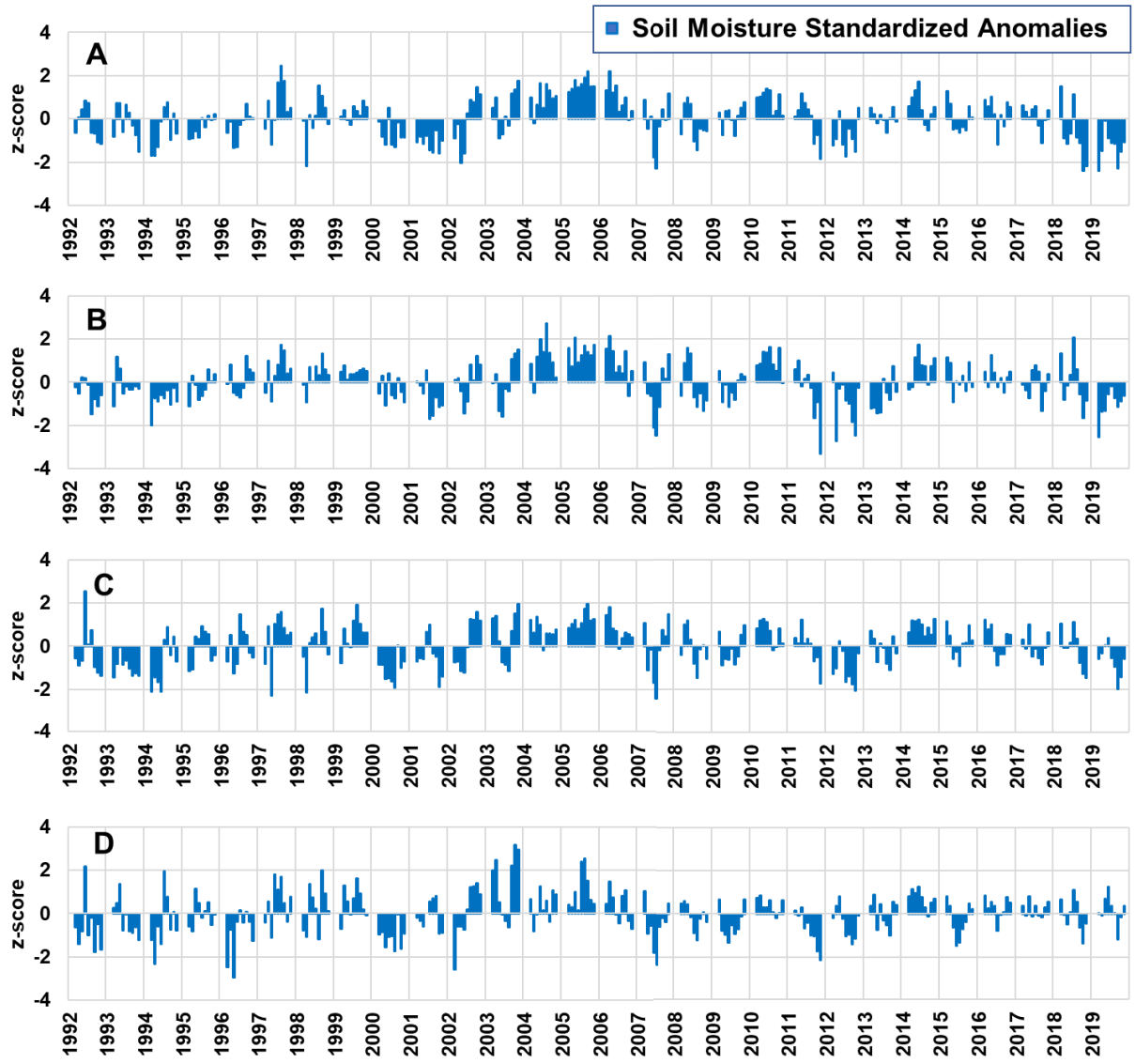

Figure 4.9 Variability of standardized soil moisture anomalies (March – November) in (A) Bărăgan Plain, (B) Dobrogea Plateau, (C) Teleorman Plain (D) Subcarpathian region between 1992 – 2019

The spatio-temporal variation of soil moisture anomalies in 2007 and 2019 (selected because these were very dry years relative to the 1992 – 2019 period) is shown in **Figure 4.10** and **Figure 4.11**. The year 2007 started with dry conditions, especially in the western part of the study area, and despite wetter conditions in the central area, May, June, and July were particularly dry in terms of soil moisture (**Figure 4.10**).

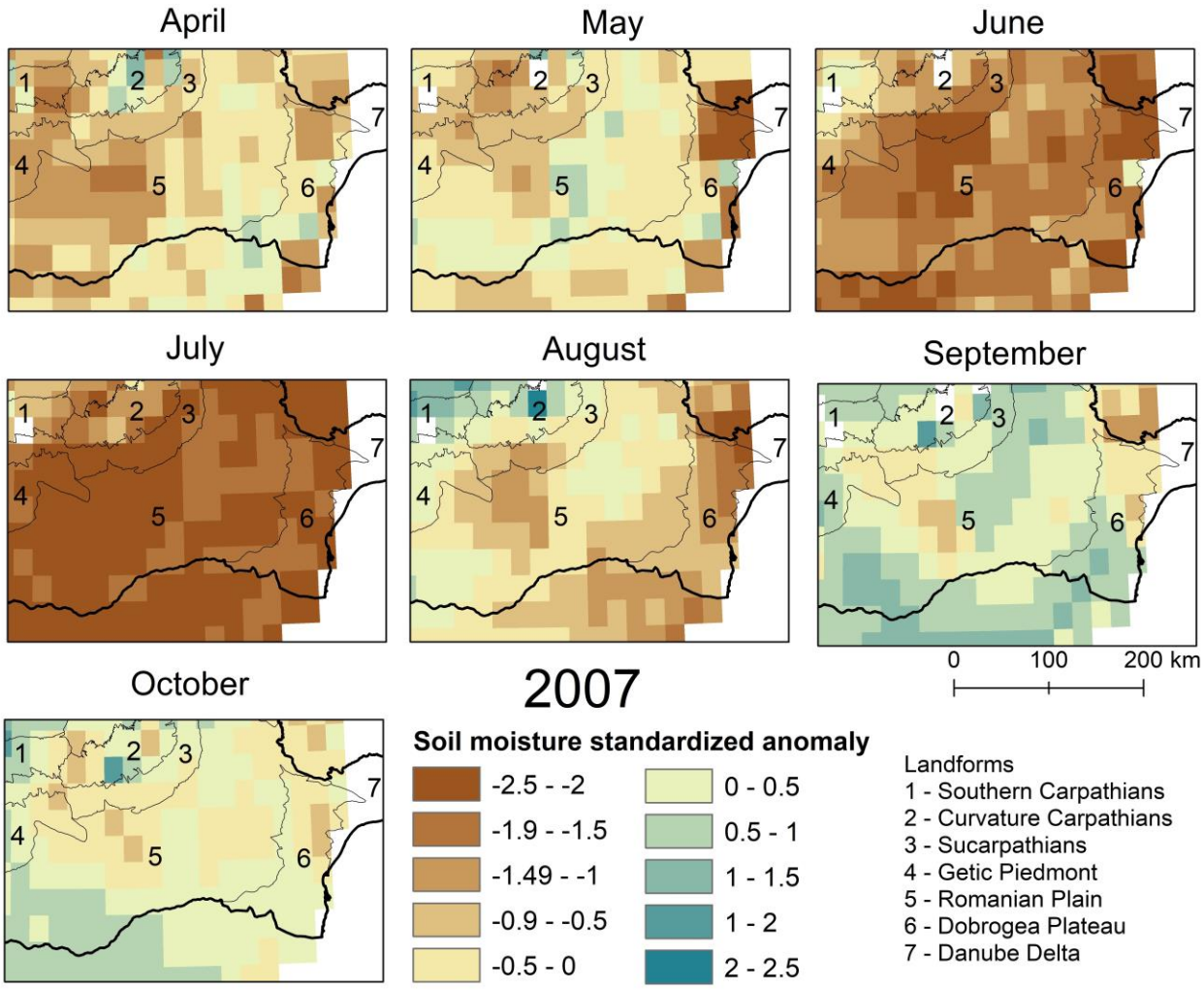

Figure 4.10 Monthly variation of standardized soil moisture anomalies from April to October in 2007, relative to 1992 – 2019

Dry conditions gradually receded from August to October, but negative soil moisture anomalies persisted in the western part of the study area and northern Dobrogea. In 2019 (**Figure 4.11**), there were wetter conditions in the western and north-western parts of the study area, but the negative soil moisture anomalies persisted in the eastern part (Dobrogea Plateau, Bărăgan

Plain). There were very dry conditions in September, but negative anomalies covered most of the study area in October.

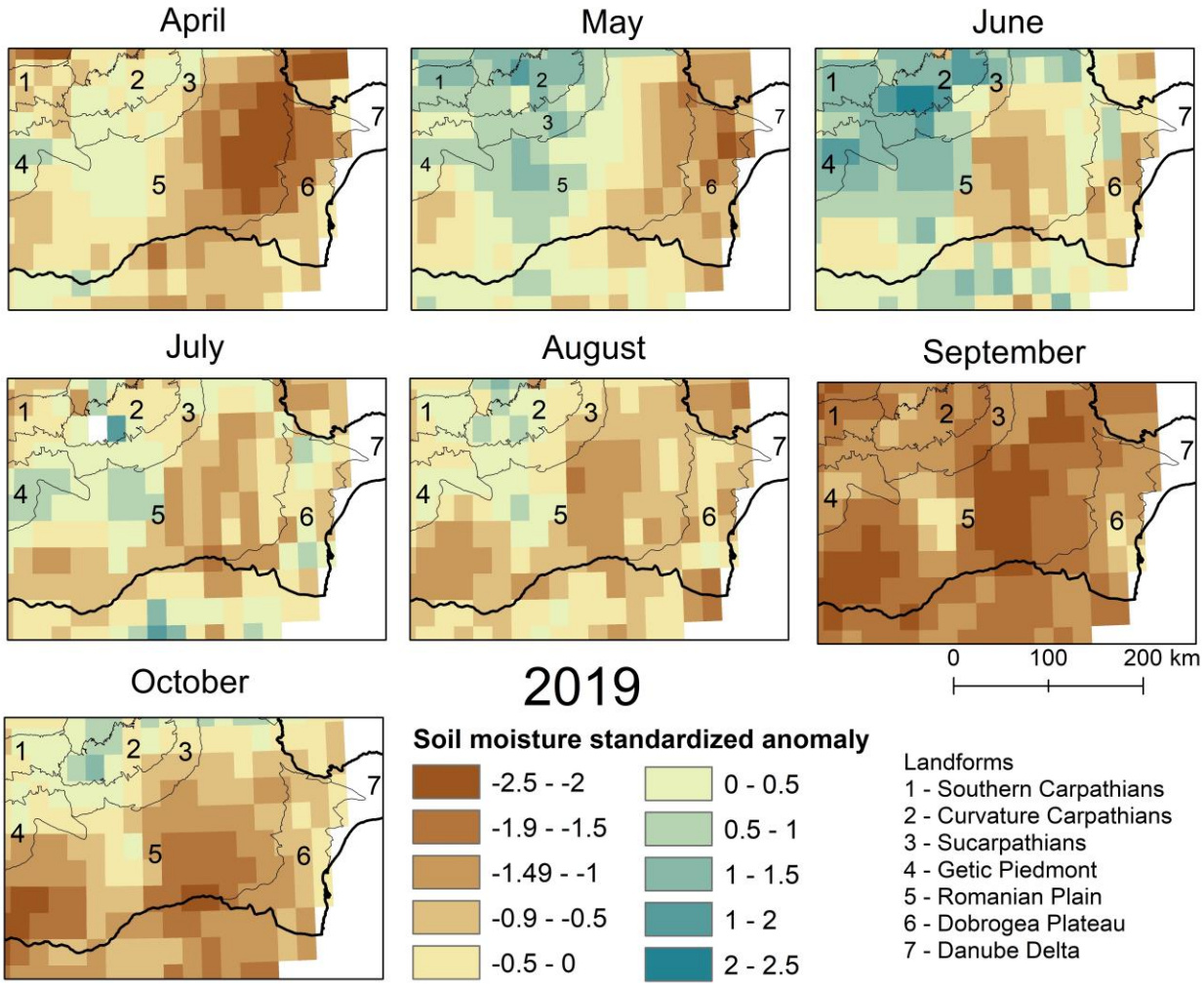

Figure 4.11 Monthly variation of standardized soil moisture anomalies from April to October 2019, relative to 1992 – 2019

4.3. Hydroclimatic variability at the catchment scale and contribution analysis of climate and human factors to streamflow changes

The following section presents the results regarding hydroclimatic variability (precipitation, potential evapotranspiration, streamflow, the aridity index, and the evaporation index) at the catchment scale, as well as a contribution analysis of climate and anthropogenic factors to streamflow changes based on the Budyko framework. The results presented in this

section have been published in Chelu et al. (2022). In this chapter, the analyses on climatic and hydrological data were performed for the 1966 – 2010 period, because of the hydrological data availability for up to 2010.

4.3.1. Variability of climatic and hydrological parameters

Variability in streamflow has in general a similar pattern in the four catchments between 1966 and 2010 (**Figure 4.12**). One common feature is that the multiannual means in streamflow are lower in the period after the breakpoint. Furthermore, because of high streamflow amounts occurring after 2004, with high historical floods in 2005, there is a positive trend in the post-change period.

In the 1966 – 2010 period, there were insignificant negative trends in precipitation and significant positive trends in PET in all four basins. The slopes of the PET trend varied between 1.9 mm/year (Ialomița, Buzău) and 2.1 mm/year (Vedea) (**Table 4.1**). Only in two catchments, significant change points in precipitation were found (Argeș and Vedea), both in 1981. In contrast, the PET in all four catchments had a significant break point in 1999. In the post-change period (as defined by the breakpoint in streamflow), precipitation decreased with values ranging from -15.8% to -7.3%, and PET increased by 6 – 7% in all catchments (**Table 4.2**). The total annual (calculated for the hydrological year, from 1st October to 30th September) precipitation anomalies (relative to the 1966 – 2010 period) that highlight the lowered amounts between 1981 – 1996 are displayed in **Figure 4.13**. Moreover, the aridity index (PET/P) trends were positive and significant, with change points occurring in 1981 and 1984.

In the same period (1966 – 2010), the modified Mann-Kendall test showed decreasing trends in measured annual streamflow, which were significant only in two catchments: Vedea and Buzău (**Table 4.1**). The slopes varied from -0.9 mm/year to -2.4 mm/year in Vedea and Ialomița, respectively. There were significant break points in the second part of the 1980s in all four basins, as shown by the Pettit test: in 1981 in Vedea, 1984 in Ialomița and 1985 in Argeș and Buzău catchments (**Table 4.1** and **Figure 4.12**). The breakpoints mark the transitions towards reduced streamflow in the basins. For this reason, the identified change years were used to distinguish between the pre-change and the post-change periods. In the second period, streamflow lowered

with a maximum of -53.4% in the Vedea catchment and a minimum of -28.1% in the Buzău catchment (**Table 4.2**) (Chelu et al., 2022).

Table 4.1 Trends and break point detection in the annual values of precipitation (P, mm/year), potential evapotranspiration (PET, mm/year), streamflow (Q, mm/year), and aridity index (PET/P, dimensionless) between 1966 – 2010 and in the annual leaf area index (LAI, m^2/m^2) between 1982 – 2010 using the modified Mann-Kendall and Pettitt tests (bold indicates statistical significance, p-value < 0.05) (Chelu et al., 2022)

Catchment	Variable	Mann-Kendall Z	Sen's Slope	Break point (Year)
Vedea	P	-1.7	-2.1	**1981**
	PET	**6**	**2.1**	**1999**
	Q	**-2.4**	**-0.9**	**1981**
	PET/P	**2.4**	**0.009**	**1981**
	LAI	**4.70**	**0.02**	**1993**
Argeș	P	-1.3	-2.0	**1981**
	PET	**4.4**	**2.0**	**1999**
	Q	-1.4	**-2.2**	**1985**
	PET/P	**2.1**	**0.006**	**1981**
	LAI	**4.75**	**0.03**	**1993**
Ialomița	P	-1.4	-2.0	1984
	PET	**4.0**	**1.9**	**1999**
	Q	-1.6	**-2.4**	**1984**
	PET/P	**2.3**	**0.006**	**1984**
	LAI	**6.5**	**0.03**	**1993**
Buzău	P	-1.2	-1.6	1981
	PET	**3.5**	**1.9**	**1999**
	Q	**-2.0**	**-1.6**	**1985**
	PET/P	**2.1**	**0.006**	**1984**
	LAI	**5.05**	**0.03**	**1993**

Table 4.2 Changes between the post and pre-change periods (as defined by the break points in Table **4.1**) in precipitation (ΔP), potential evapotranspiration (ΔPET), streamflow (ΔQ) and evaporation index (ΔAET/P) (Chelu et al., 2022)

	ΔP		ΔPET		ΔQ		ΔAET/P
Catchment	mm	%	mm	%	mm	%	
Vedea	-104.3	-15.8	49.7	6.1	-57.5	-53.4	0.06
Argeș	-63.3	-8.8	50.4	6.7	-77.2	-39.6	0.05
Ialomița	-89.2	-11.7	46.8	6.6	-90.3	-35.1	0.06
Buzău	-47.9	-7.3	50.0	6.8	-55.9	-28.1	0.04

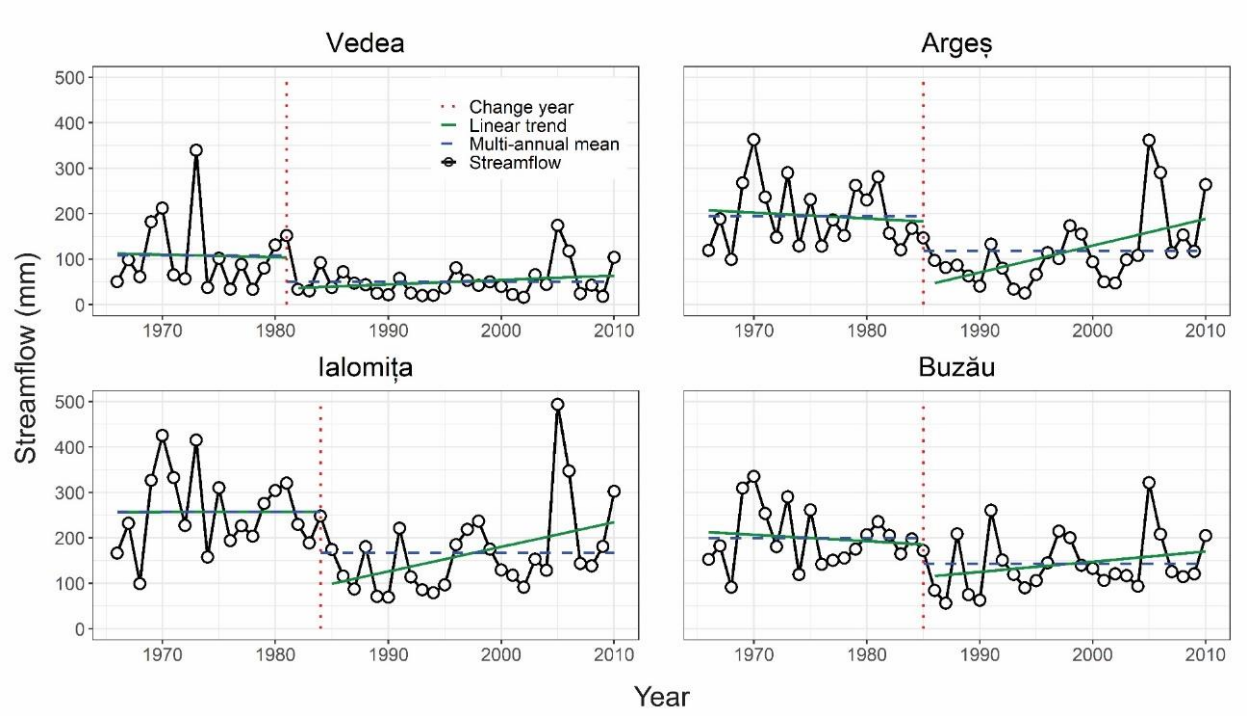

Figure 4.12 Variation, linear trends, multiannual means, and break points of the annual average streamflow in Vedea, Argeș, Ialomița and Buzău catchments (Chelu et al., 2022)

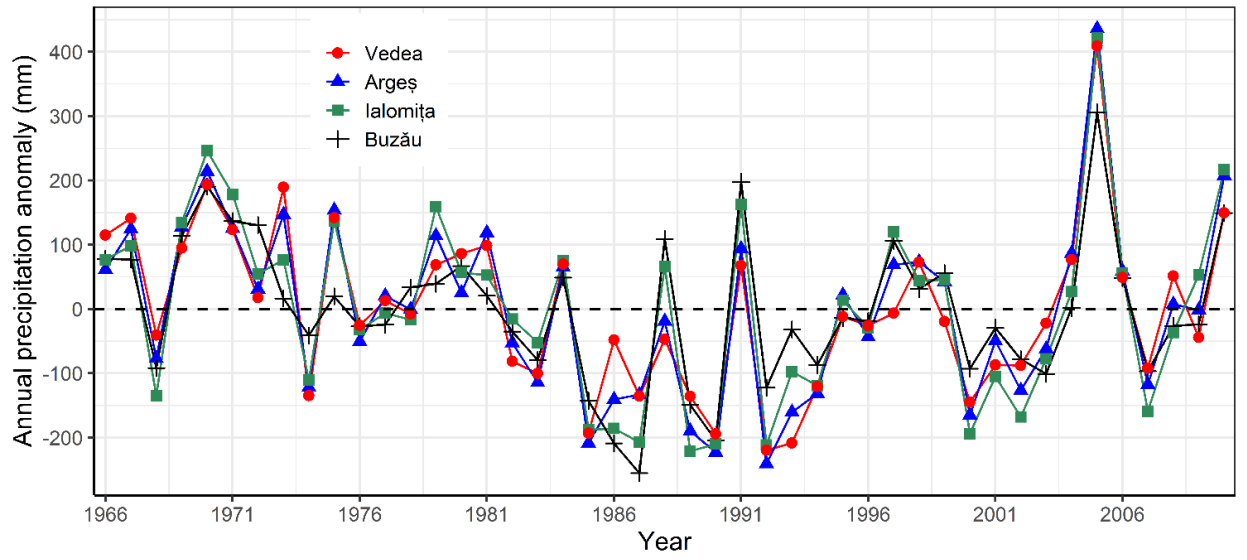

Figure 4.13 Anomalies of the catchment annual precipitation in Argeș, Buzău, Ialomița and Vedea (Chelu et al., 2022)

4.3.2. The Budyko framework and streamflow elasticity

As shown by their position in the Budyko framework (**Figure 4.14**), the four catchments are predominantly water-limited (PET/P > 1). The water yield in the catchment increases with the decrease of the catchment parameter ω (that ranges from 3.3 to 2.5), also seen by the lowering of the curves on the plot. Higher streamflow values characterized the years when the two indices were lower. The evaporation index had a higher value in the post-change period than the first one, suggesting increased evaporation and lowered streamflow.

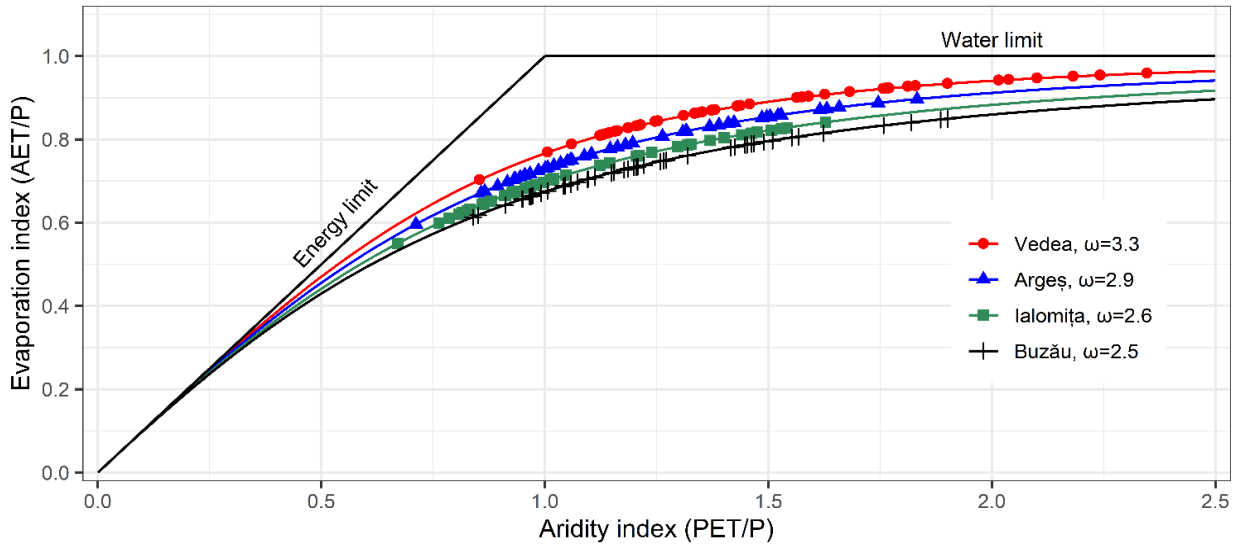

Figure 4.14 The annual aridity index (PET/P), evaporation index (AET/P) and Fu curves in the Budyko space for the Argeș, Buzău, Ialomița and Vedea catchments (Chelu et al., 2022)

Climatically, the streamflow in the four catchments is the most sensitive to precipitation, as shown by the higher values of the precipitation elasticity compared to PET elasticity (**Table 4.3**). The values of precipitation elasticity range from 2.1 to 3 and the positive values show that streamflow increases with precipitation.

On the other hand, the PET elasticity varies between -1.1 and -2, showing that the streamflow decreases with increasing PET. The most sensitive catchment to climate conditions and with the highest aridity index is Vedea. Similar to the decrease of ω, the elasticities to climate factors are lower from Vedea to Buzău catchments (**Figure 4.14**).

Table 4.3 The catchment parameter (ω) in Fu's equation and the elasticity of streamflow to precipitation (ε_P) and potential evapotranspiration (ε_{PET}) (Chelu et al., 2022)

Catchment	ω	ε_P	ε_{PET}
Vedea	3.3	3.0	-2.0
Argeș	2.9	2.4	-1.4
Ialomița	2.6	2.2	-1.2
Buzău	2.5	2.1	-1.1

4.3.3. Contribution of climate and human factors to streamflow changes

The results of the analysis based on the Budyko framework showed that climate contributed the most to streamflow decrease in the post-change period in all catchments, particularly due to precipitation (**Table 4.4**). The greatest climate contribution was estimated in the Vedea catchment (80.2%) and the smallest in the Argeș catchment (63.1%), which is the most impacted by human pressures. The highest precipitation contribution to the decrease in streamflow was in the Vedea catchment, and the lowest was in the Argeș catchment (44.8%). The highest contribution of PET was in Buzău (22.5%).

Table 4.4 The contributions of precipitation (ΔQ_P), potential evapotranspiration (ΔQ_{PET}), climatic (ΔQ_c) and human (ΔQ_h) factors to changes in streamflow between the post and pre-change periods (Chelu et al., 2022)

Catchment	ΔQ_P		ΔQ_{PET}		ΔQ_c (%)		ΔQ_h	
	mm	%	mm	%	mm	%	mm	%
Vedea	-37.7	65.6	-8.4	14.6	-46.1	80.2	-11.4	19.8
Argeș	-34.6	44.8	-14.2	18.4	-48.8	63.1	-28.5	36.9
Ialomița	-56.2	62.2	-15.4	17.0	-71.5	79.2	-18.7	20.8
Buzău	-27.3	48.8	-12.6	22.5	-39.8	71.2	-16.1	28.8

Precipitation deficits were not the only factor determining the decrease in streamflow, as human influence also impacted the catchment water balance. The human contribution varied from 19.8% (Vedea) to 36.9% (Argeș). Results regarding land cover and vegetation change in the catchments are summarised in **Table 4.5**.

The land cover resulting from the HILDA dataset shows that in 2010 compared to 1960, the cropland areas decreased while grassland, forests and settlements increased. In addition, a significant trend between 1982 – 2010 is observed using the LAI as a proxy for vegetation productivity in the catchments (**Table 4.1**).

Table 4.5 Land cover changes (%) between 1960 and 2010 in the Argeș, Buzău, Ialomița and Vedea catchments (Chelu et al., 2022)

Catchments	Settlements	Cropland	Forest	Grassland
Vedea	1.6	-5.7	0.4	3.6
Argeș	0.8	-9.1	0.5	7.8
Ialomița	2.0	-8.2	0.1	6.1
Buzău	2.4	-6.4	0.2	3.9

4.3.4. Discussion

The results of the analysis performed in **Chapter 4.3** have shown that the streamflow decrease between the 1980s and 2010 compared to the previous period was primarily due to climate variations, predominantly the decrease in precipitation. These results are in line with previous studies. Thus, in Romania, the positive NAO phase after the 1980s is associated with conditions related to drought: rainfall and streamflow reduction and higher winter temperatures (Bîrsan, 2015; Bojariu et al., 2021; Ioniță et al., 2014; Ștefan et al., 2004). Carbonnel et al. (1997) identified change points in streamflow in southern Romania in the first part of the 1980s, followed by a decrease in mean annual streamflow, which they primarily explained due to lowered winter streamflow. As shown in previous studies and analyses (**Chapter 2** and **Chapter 4.1**), temperatures have continuously increased in the last decades, contributing to the decrease in streamflow because of the increase in PET.

The human influence on the streamflow decrease could have occurred due to changes in land use/land cover, river engineering, irrigation or demographic changes (Dey and Mishra, 2017). Multiple reservoirs were built along the rivers in the four catchments during the study period, but mainly in the higher altitude area where evaporation is low; therefore, their contribution might have been limited. The highest human contribution was in the Argeș catchment (about 36.9%). This result is coherent because it has the most engineering works along the rivers (dams and reservoirs, deviations, etc.), population pressure and land cover changes between the four catchments. Regarding the influence of reservoirs on the Argeș catchment, the comparative study between reconstituted (natural) and measured (modified) discharges has shown that while there were modifications of streamflow at the monthly scale due to the reservoir regulating effect, there were non-significant influences on the multiannual mean streamflow (Zaharia et al., 2016).

The reduced precipitation after the 1980s corresponded to a period of land cover change due to the fall of communism and subsequent socio-political changes. One simulation study attributed the high freshwater stress in Romania after the 1980s to higher anthropogenic water demands, half due to agriculture (Wada et al., 2011). However, despite the large-scale irrigation systems built between 1970 – 1989, particularly in southern Romania (Lup et al., 2017), these were continuously abandoned after the 1990s, with only 5.72% used in 2013 (Popovici et al., 2016). The influence of irrigation abandonment could have been positive on streamflow by reducing AET from cropland (Wang and Hejazi, 2011). Urbanization might also determine increased streamflow because of a lower AET and reduced infiltration due to impermealization and loss of vegetation (DeWalle et al., 2000). However, an opposite effect (higher evapotranspiration and lowered streamflow) could have been produced by the cropland abandonment and grassland increase after 1989 (Griffiths et al., 2013; Kuemmerle et al., 2009; Popovici et al., 2016), slight increases in forest area due to afforestation, forest growth on abandoned land (Olofsson et al., 2011; Vanonckelen and Van Rompaey, 2015), and general greening due to CO_2 fertilization (Zhu et al., 2016). Nonetheless, the effect of vegetation on evapotranspiration decreases with increased catchment size (Donohue et al., 2007). In the more topographically complex areas in Romania, Teuling et al. (2019) attributed the streamflow changes between 1960 – 2010 to land cover change, while in lowlands, these were mainly attributed to precipitation.

Some of the uncertainties of the method chosen here to separate the climate and human contribution are related to the assumption of independence between precipitation, potential evapotranspiration, and the catchment characteristics. However, this could be violated by the changes in catchment characteristics that develop in response to climate change. Moreover, this study assumed unchanged water storage at the multiannual scale. Finally, Yang et al. (2014) showed that assessing elasticity using the first-order approximation of the Budyko equation when precipitation decreases and potential evapotranspiration decreases could overestimate the climate contribution.

5. HYDROCLIMATIC DROUGHT CHARACTERIZATION IN SOUTH-EASTERN ROMANIA

This chapter is dedicated to the analysis of the meteorological and hydrological droughts performed with two types of drought indicators: the climatic water deficit (CWD) and standardized indicators: the Standardized Precipitation Index (SPI), the Standardized Precipitation Evapotranspiration Index (SPEI) and the Standardized Streamflow Index (SSI). The analyses were performed for the 1961 – 2020 period for meteorological drought and 1966 – 2010 for hydrological drought.

Firstly (in **Chapter 5.1)**, the drought variability, trends and frequencies based on the CWD calculated at meteorological stations are presented (**Chapter 5.1.1**). Next, the results of the spatialized CWD (raster-CWD) evaluation are discussed in **Chapter 5.1.2**. The **Chapter 5.2** focuses on the variability of standardized indicators for meteorological droughts (**Chapter 5.2.1**) and for hydrological droughts (**Chapter 5.2.2**). Finally, in **Chapter 5.2.3**, a synthesis of the most important identified drought events is presented.

5.1. Drought assessment using the climatic water deficit

5.1.1. Climatic water deficit at meteorological stations

The climatic water balance method can describe average conditions in the study area and emphasize regional climatic characteristics. The multiannual averages (calculated for 1961 – 2020) for monthly modelled soil water storage (ST), potential evapotranspiration determined based on the CRU gridded data (PET_{CRU}), modelled actual evapotranspiration (AET) generated using the simplified Thornthwaite water balance and the modelled climatic water balance (CWD) are presented in **Figure 5.1**. The Vârful Omu weather station is not included in this chapter because of its limited representativeness for this indicator.

Generally, the soil water storage decreases from April to August and recharges starting in September. The same monthly pattern is inversely followed by the CWD, for which the highest average values occur in July and August.

The highest average modelled AET occurs in April in Sulina, in May in Roșiorii de Vede, Tulcea and Constanța and in June in București Băneasa, Călărași, Buzău and Galați meteorological stations.

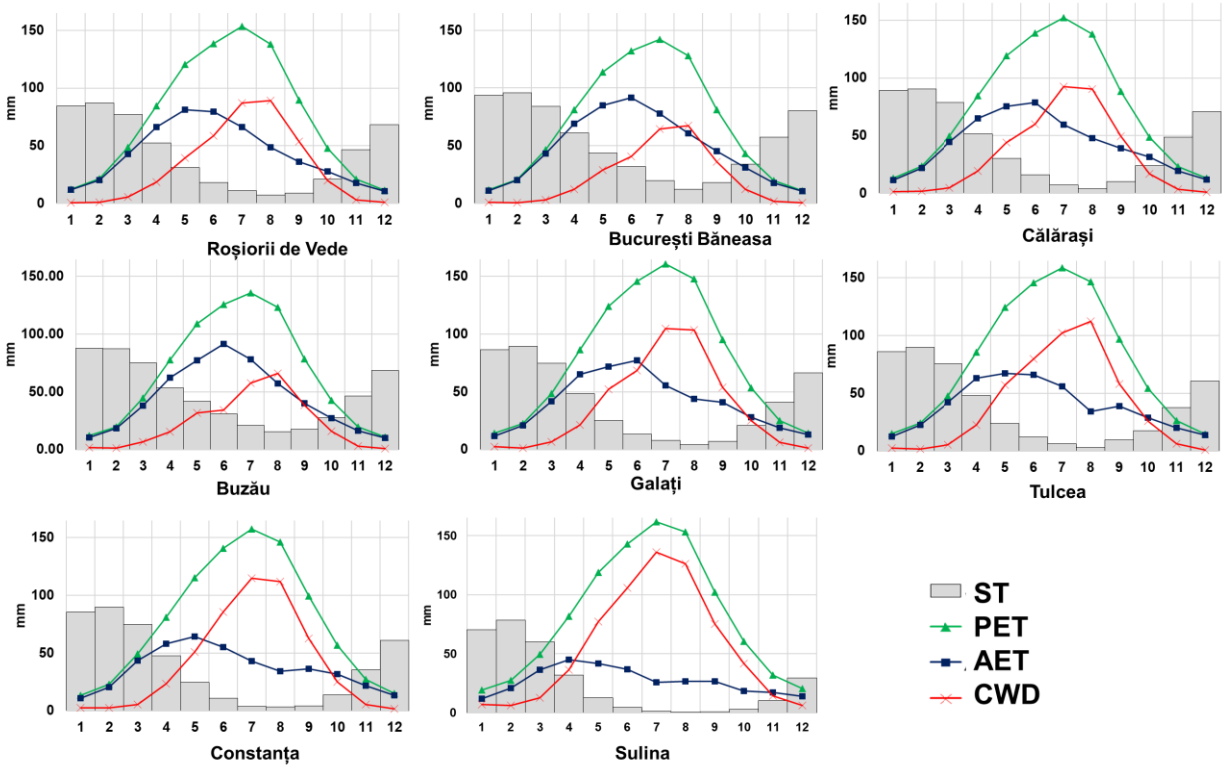

Figure 5.1 Multiannual monthly averages of soil water storage (ST), potential evapotranspiration (PET), actual evapotranspiration (AET) and the climatic water deficit (CWD) obtained through the Thornthwaite water balance for the 1961 – 2020 period

5.1.1.1. Intensity and frequency of droughts

The intensity of drought conditions between 1961 – 2020 is plotted using the classified CWD indicator (**Table 3.15**), as shown in **Figure 5.2** and **Figure 5.3**. The 1980s and 2010s had the highest count of *arid* months (CWD ≥ 120 mm).

During the summer, especially in July and August, the *arid* months (with the highest deficit) become more frequent at most stations in the latter part of the study period. Common periods of drought can be identified as 1962 – 1963, 1965, 1968, 1985 – 1990, 1992 – 1993, 1996, 2000 – 2001, 2003, 2007 – 2008, 2012, 2015 – 2016, and 2018 – 2020.

A decrease in *very wet* months (P > PET and replenished water storage) in November and December is observed from the 1980s until the early 1990s. At some stations, for example, in Roșiorii de Vede, Călărași, or Constanța, the number of *very dry* (60 ≤ CWD < 120 mm) and *moderately dry* (30 ≤ CWD < 60 mm) months slightly decreased, while the number of *arid* months increased, which could suggest a shift to a more extreme deficit. However, the total number of months with P > PET increased at Constanța, Călărași, București and Galați stations in the 1991 – 2020 interval, compared to 1961 – 1990, and it decreased at Roșiorii de Vede, Buzău, Tulcea and Sulina stations.

Regional climatic differences, in terms of frequency of *arid* months and *very dry* months, are highlighted by their percentages between 1961 – 2020, varying from 1% and 13% at Buzău (the least months) or 1% and 14% at București Băneasa, to drier locations, having percentages such as of 5% and 18% at Roșiorii de Vede, 8 % and 19% at Galați, 9% and 22% at Constanța or 14% and 24% at Sulina (the most months).

In **Figure 5.4**, the frequency of the CWD classes is compared between two 30-year intervals: 1961 – 1990 and 1991 – 2020. *Arid* months occur at most stations between June and August; *very dry* months also appear between April and September.

A remarkable change is that the frequency of *arid* months has increased in the second period at all stations in summer, particularly in August, and to a lesser degree also in June in Tulcea, Galați, Călărași and Sulina. *Arid* months appeared in the 1991 – 2020 interval in periods where they did not occur in the previous time interval, such as June at București Băneasa, Buzău, Călărași or Galați.

In October, the number of *wet* months (P > PET and storage is replenishing) increased at all stations in the second period, while the *very wet* months frequency increased in October in București Băneasa and Călărași.

Between 1991 – 2020, a drier May is found at all stations through a frequency increase in the *moderately dry* or *very dry* months, compared to the 1961 – 1991 period. The number of *slightly dry* months (CWD < 30 mm) has increased in February (București Băneasa, Tulcea, Galați, Călărași, Sulina), March (Roșiorii de Vede), or both (Buzău), with a lowering of the number of *very wet* months in February at most of the stations.

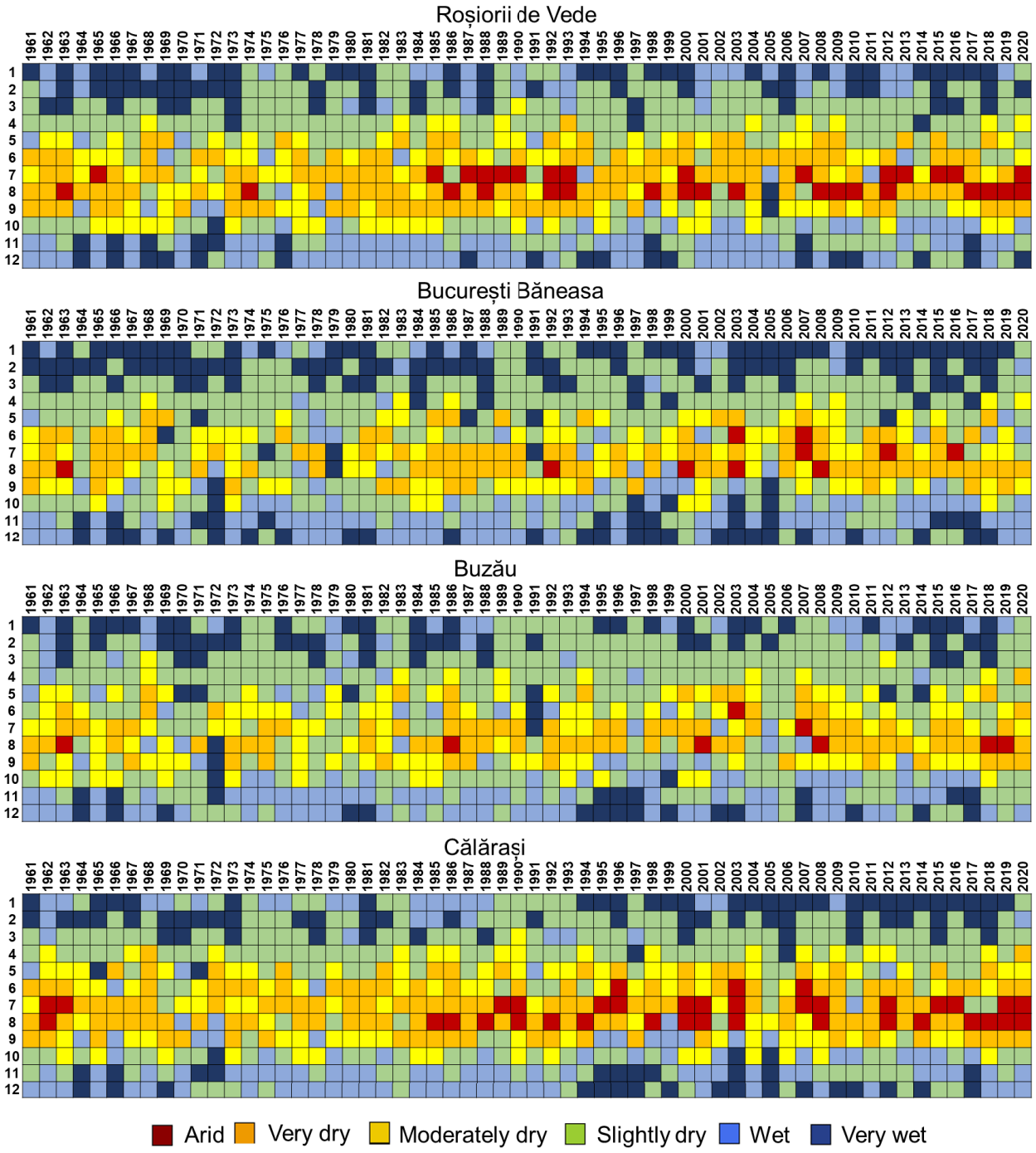

Figure 5.2 Monthly variability of the climatic water deficit (CWD) classes between 1961 –2020 at Roșiorii de Vede, București Băneasa, Buzău and Călărași meteorological stations. *Very wet* months: P > PET and water storage is at maximum; *wet* months: P > PET and storage is replenishing; *slightly dry*: CWD < 30 mm; *moderately dry*: 30 ≤ CWD < 60 mm; *very dry*: 60 ≤ CWD < 120 mm; *arid*: CWD ≥ 120 mm.

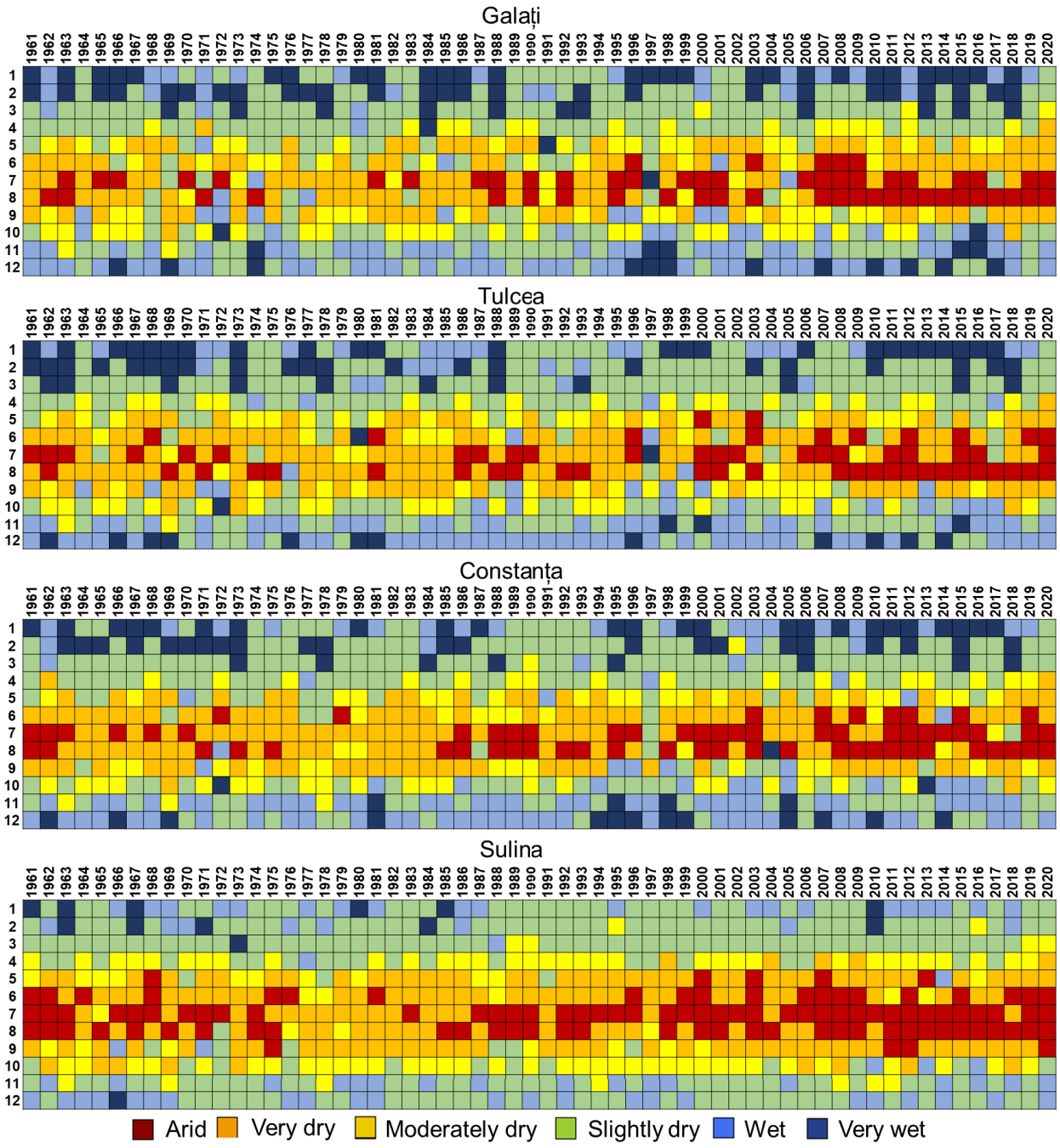

Figure 5.3 Monthly variability of the climatic water deficit classes between 1961 – 2020 at Galați, Tulcea, Constanța and Sulina meteorological stations (legend at **Figure 5.2**)

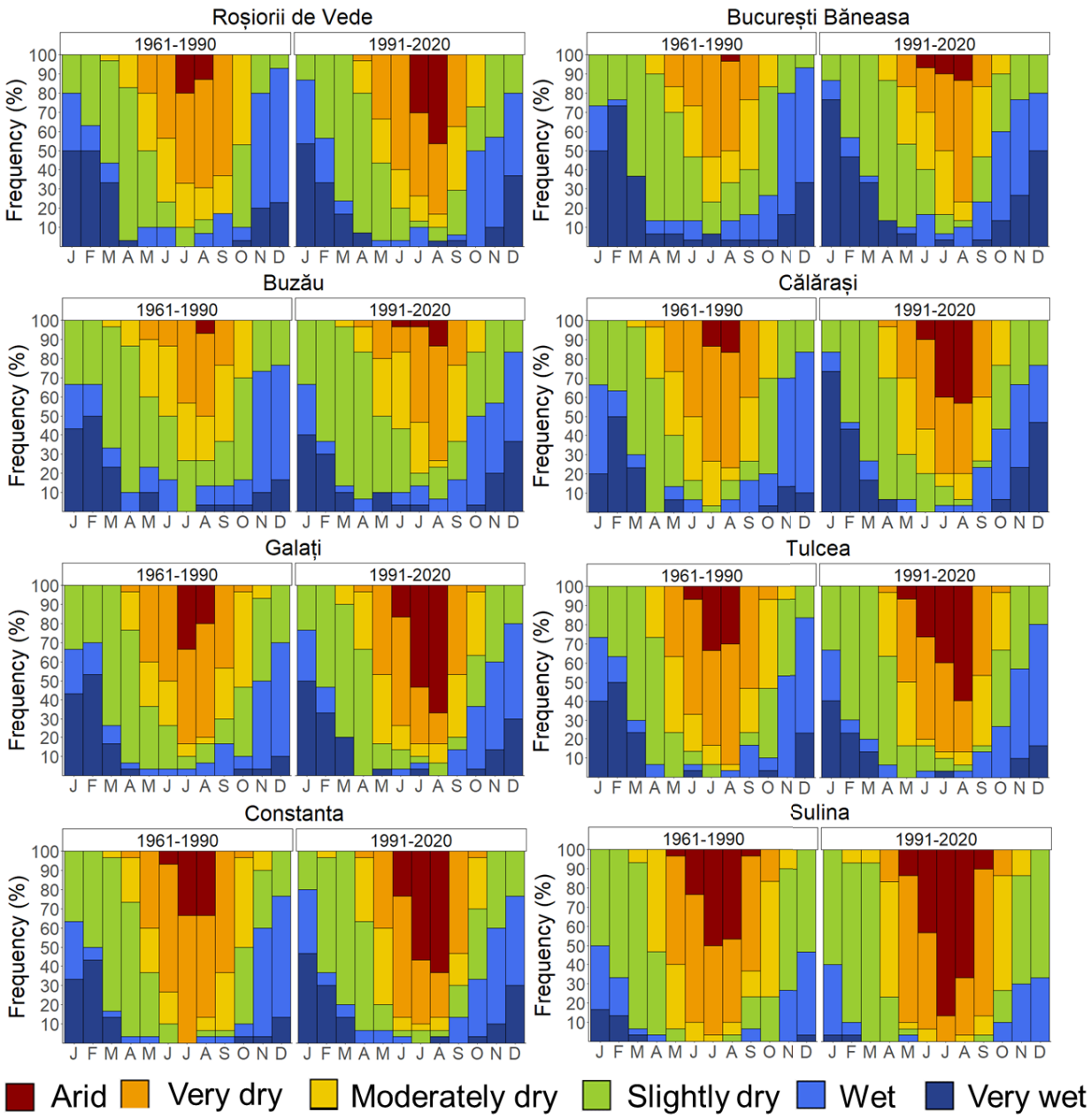

Figure 5.4 Monthly frequency (%) in CWD classes between 1961 – 1990 and 1991 – 2020 (legend at **Figure 5.2**)

5.1.1.2. Temporal variability and trends in CWD dynamics

The Sen slope and significance of trend (mm/year) for the monthly series of the CWD at the analysed meteorological stations for the spring, summer, and autumn months are shown in **Table 5.1**.

Table 5.1 Monthly Sen slopes in CWD (mm/year) between 1961 – 2020. Significance (p-value < 0.05) is shown in bold and with an asterisk.

Month	Roșiorii de Vede	București Băneasa	Buzău	Călărași	Galați	Tulcea	Constanța	Sulina
March	Ns,nt	Ns nt	0.005	Ns nt	0.0077	0.00394	0.04	**0.145***
April	**0.22***	0.01	0.067	0.06	0.136	0.194	0.163	**0.413***
May	0.21	Ns nt	0.2	0.28	**0.515***	0.338	0.317	**0.672***
June	0.13	Ns, nt	0.066	0.28	0.44	0.2245	0.156	**0.550***
July	0.67	0.36	0.538	0.63	**0.6075***	0.3264	0.357	**0.779***
August	**0.77***	**0.7***	**0.845***	**0.78***	**1.130***	**1.041***	**0.865***	**0.956***
September	Ns, nt	Ns, nt	0.088	Ns nt	0.151	0.175	0.076	**0.699***
October	**-0.298***	**-0.036***	**-0.2379***	**-0.136***	**-0.297***	**-0.350***	-0.233	-0.237
November	Ns, nt	Ns,nt	Ns nt	Ns nt	Ns nt	Ns nt	Ns nt	Ns nt

It shows that there is a significant positive trend in CWD in August at all stations (higher deficit) and a significant decreasing trend in October at most of the stations, which were also seen in the increase of the frequency of *arid* months in August and the increase of *wet* months in October. Additionally, there are significantly upward water deficit trends in May and July at Galați. Sulina station shows significant increasing trends in CWD every month from March to September.

Yearly drought conditions can be highlighted by accumulating the monthly deficit values. The total annual CWD between 1961 – 2020 at each meteorological station is illustrated in **Figure 5.5**. On average, the first ten years with the highest total CWD were 2020, 2007, 2012, 2019, 2000, 2008, 2003, 1990, 2018 and 2009, accentuating the deficit's increased intensity in the last decades. The highest deficits were reached during summer months in the previously mentioned years. At the monthly level, July 2007 had the highest CWD at all stations except Buzău, where the most intense monthly deficit was noticed in August 2018.

The increasing occurrence of arid months and frequency of dry years in the last study period is probably related to the increase in PET in all seasons except autumn (Croitoru et al., 2013a), which drives a higher deficit. Regarding this, the most significant changes appeared in the summer months at all stations. Other authors have already shown higher heat stress during this season based on the analysis of maximum temperatures, especially in the south and south-east of Romania (Micu et al., 2017), and particularly a warming-related trend towards warm/dry summers in the Romanian Plain between 1961 – 2009 (Micu et al., 2014). The results highlighting a

decreased CWD in October could be explained by the increased autumn precipitation trends (Cheval et al., 2014; Dumitrescu et al., 2015), which enhance the availability of water and, therefore, an increased AET, as well as by a decreased trend of potential evapotranspiration observed in this period (Croitoru et al., 2013a).

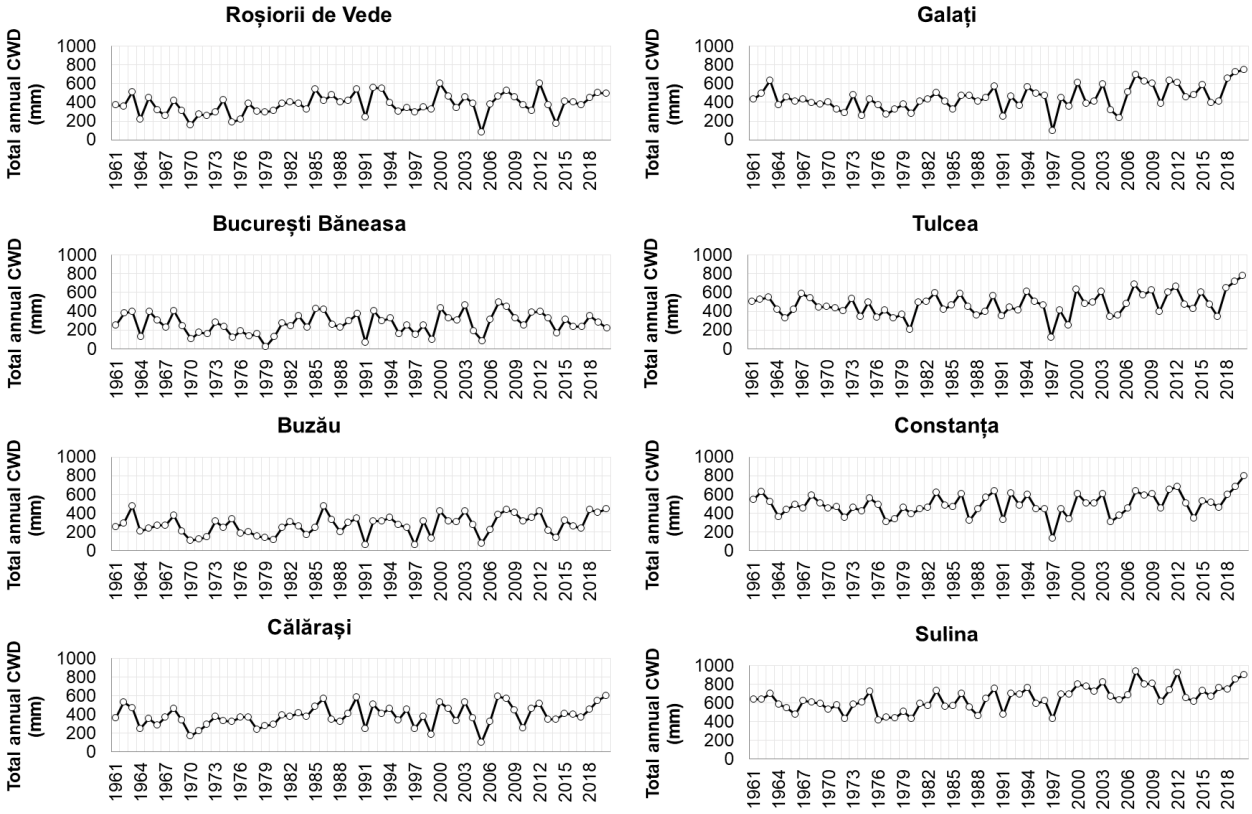

Figure 5.5 Total annual climatic water deficit (CWD) in mm between 1961 – 2020

5.1.2. Spatial analysis of the raster-CWD

5.1.2.1. Comparative analysis of raster-CWD with the climatic water deficit at meteorological stations

To highlight the spatial variability of the CWD in the study area, the monthly spatial distribution of raster-CWD was computed using the gridded rasters at 0.1º of the E-OBS dataset and the PET_{Turc}.

Firstly, the raster-CWD results were compared with the CWD at point stations (calculated using the ECA&D data and the PET_{CRU}, further called *station-*CWD_{CRU}). In this chapter, the

figures present results only from selected stations, as the findings across most lowland areas demonstrate similarities; in addition, the comparison is also presented at Vârful Omu meteorological station, to explore the variation of input parameters at the highest altitudes.

The difference between the raster-CWD and station-CWD_{CRU} is shown in **Figure 5.6**, which highlights the substantial differences in 2018 and 2019. As shown in **Figure 5.7**, the differences are related to the anomalous radiation values in 2018 and 2019 in the input data for raster-CWD. Due to this anomaly, which is propagated in the potential evapotranspiration (**Figure 5.8**) and consequently in the raster-CWD (**Figure 5.6**), **three years (2018, 2018 and 2020) are excluded from further analysis.**

The differences during the 1961 – 2017 period between raster-CWD and station-CWD_{CRU} are generally positive in Roșiorii de Vede, București Băneasa, Buzău and Călărași stations (raster-CWD overestimates the deficit), while at Tulcea and Vârful Omu, they are mostly negative (raster-CWD underestimates the deficit) (**Figure 5.6**). Seasonality is also a characteristic feature of these differences — the most considerable differences appear in June, July, and September for the first four mentioned stations and August in Tulcea. For example, the largest multiannual average differences are in July in Buzău (+13 mm) and in August in Tulcea (-17 mm).

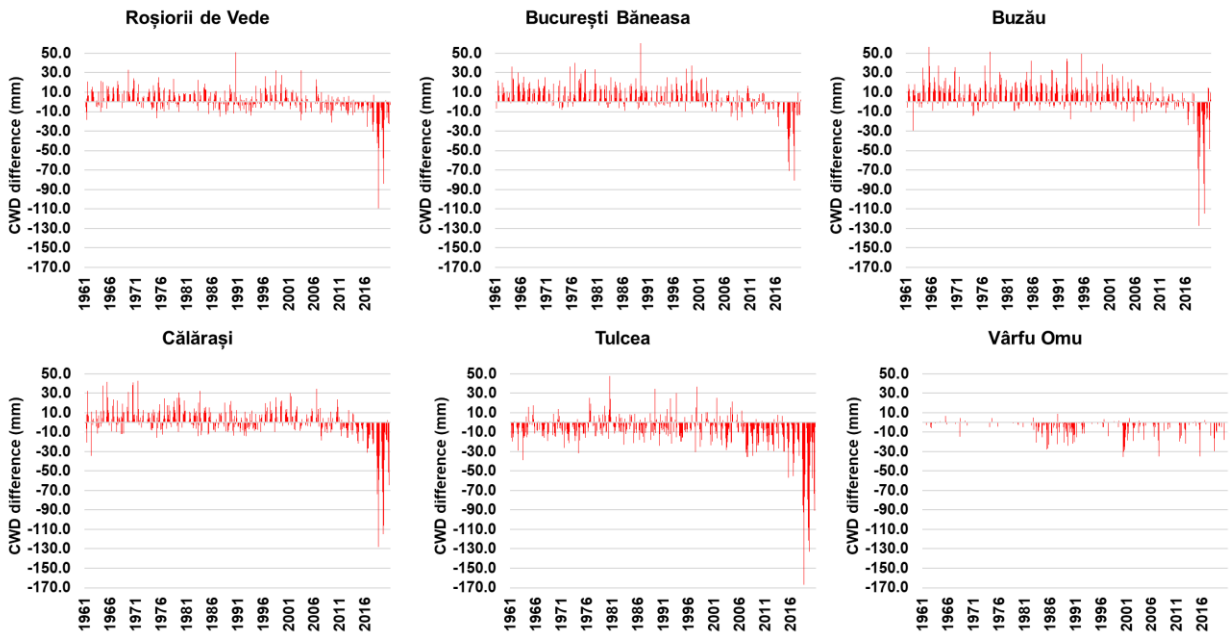

Figure 5.6 The difference in climatic water deficit (CWD) (in millimetres) between the raster-

CWD and station-CWD_{CRU} between 1961 – 2020

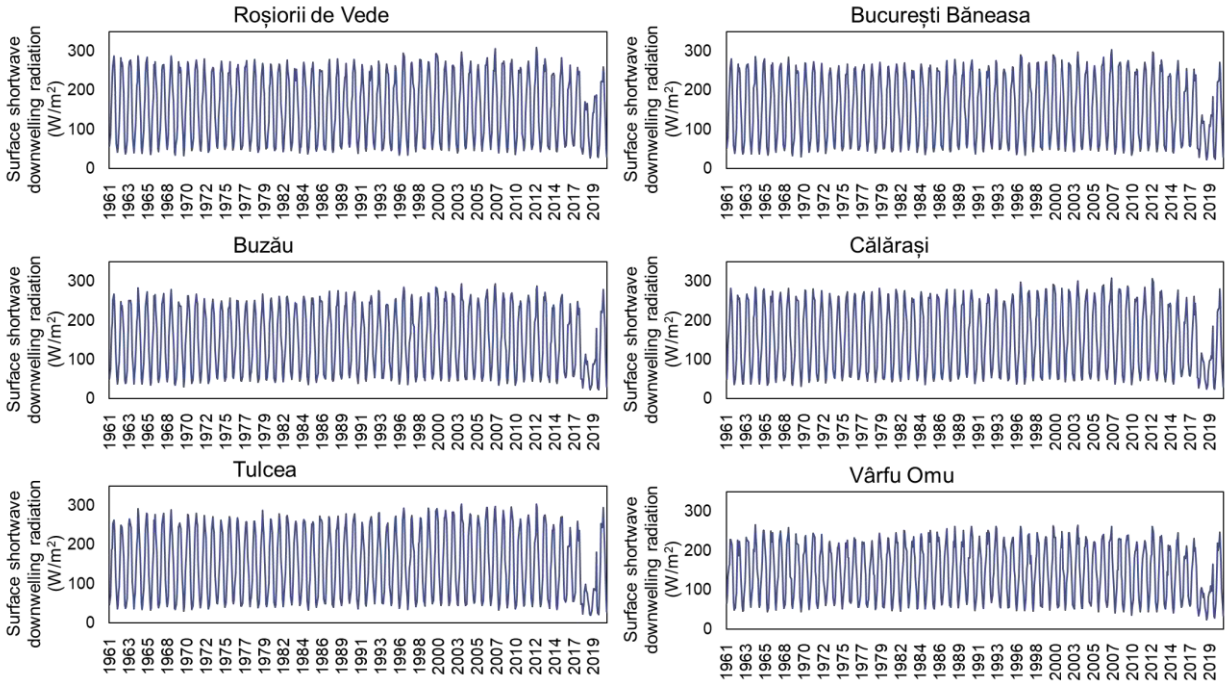

Figure 5.7 Monthly average solar radiation (surface shortwave downwelling radiation, W/m^2) between 1961 – 2020 from the E-OBS dataset in pixels representing stations

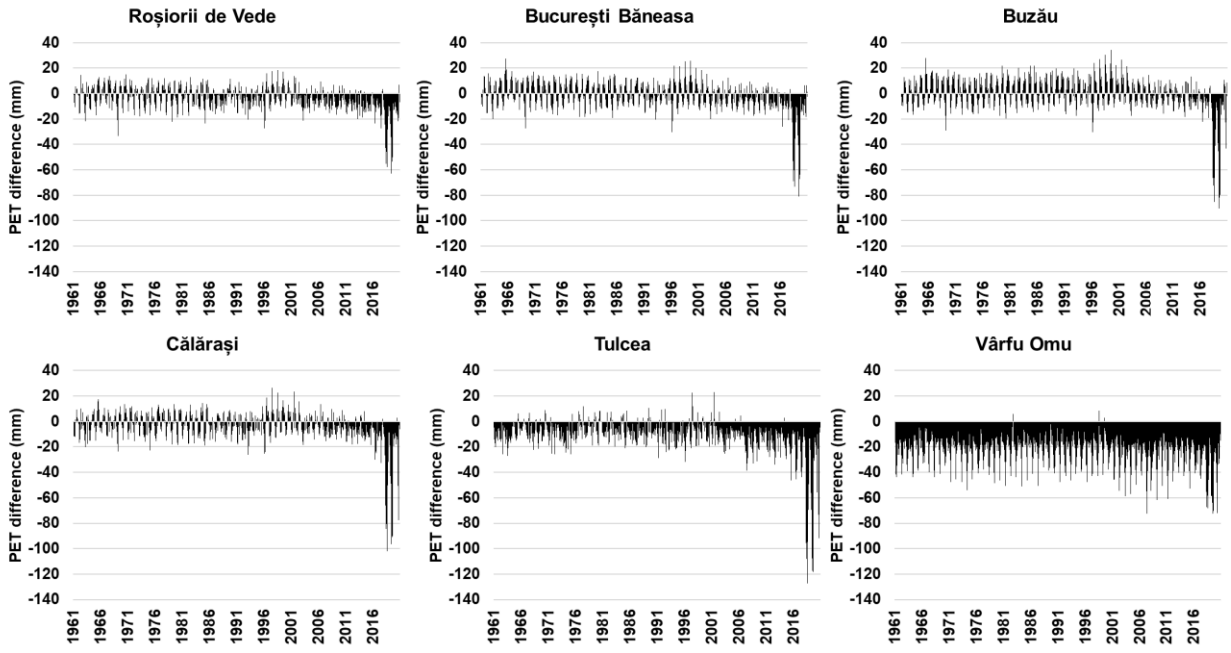

Figure 5.8 Differences in monthly potential evapotranspiration (PET) between the PET_{Turc}

method and the PET_{CRU} for the 1961 – 2020 period

The variation in the differences during the 1961 – 2017 period between raster-CWD and station-CWD_{CRU} could be explained by the different precipitation and potential evapotranspiration datasets.

The differences in monthly precipitation amounts between the E-OBS dataset in the grid points where meteorological stations are located and the reference dataset (ECA&D) are shown in **Figure 5.9**. Most monthly differences are smaller than -10 mm, but some months vastly exceed this threshold. At Vârful Omu meteorological stations, there are much larger magnitudes of this difference. Furthermore, the differences are predominantly negative (E-OBS underestimates the values), as detailed in **Chapter 3.2** *(Quality assessment of gridded precipitation)*, which could have significantly contributed to overestimating the raster-CWD.

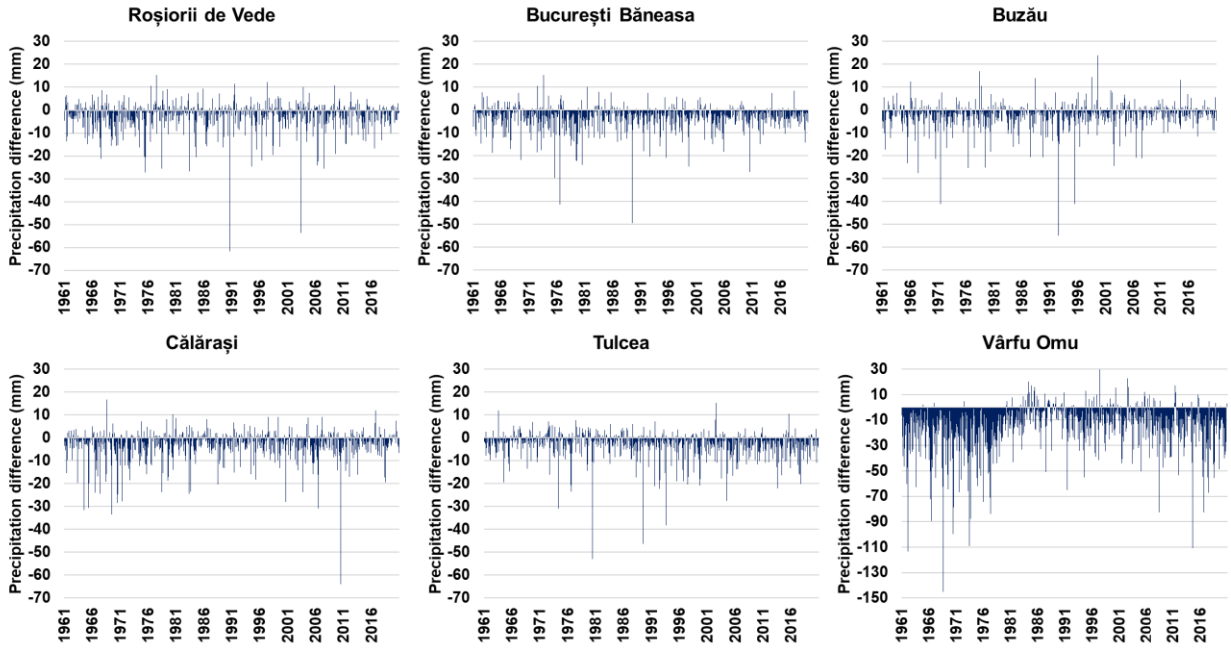

Figure 5.9 Differences in monthly precipitation between the E-OBS and the reference (ECA&D) datasets for the 1961 – 2020 period

The differences (for the 1961 – 2020 period) between PET_{Turc} and the PET_{CRU} extracted at meteorological stations are shown in **Figure 5.8**. Most of the differences for Roșiorii de Vede, București Băneasa, Buzău, Călărași and Tulcea range between ± 20 mm. The most frequent

underestimation from these four stations was found at Tulcea station (PET_{Turc} is larger than PET_{CRU}), with an average difference of about -13 mm in July and -18 mm in August.

As mentioned, 2018, 2019 and 2020 are excluded from the analysis. Two periods are selected to identify changes in time of the CWD, similar to the point-based analysis: 1961 – 1990 and 1991 – 2017. Because of the unequal periods, only the monthly means of the raster-CWD and their differences are computed for the two periods.

Taking the months between May and August at the București Băneasa station as an example, it can be seen that the coefficients of determination range from 0.86 (July) to 0.95 (May) (**Figure 5.10**).

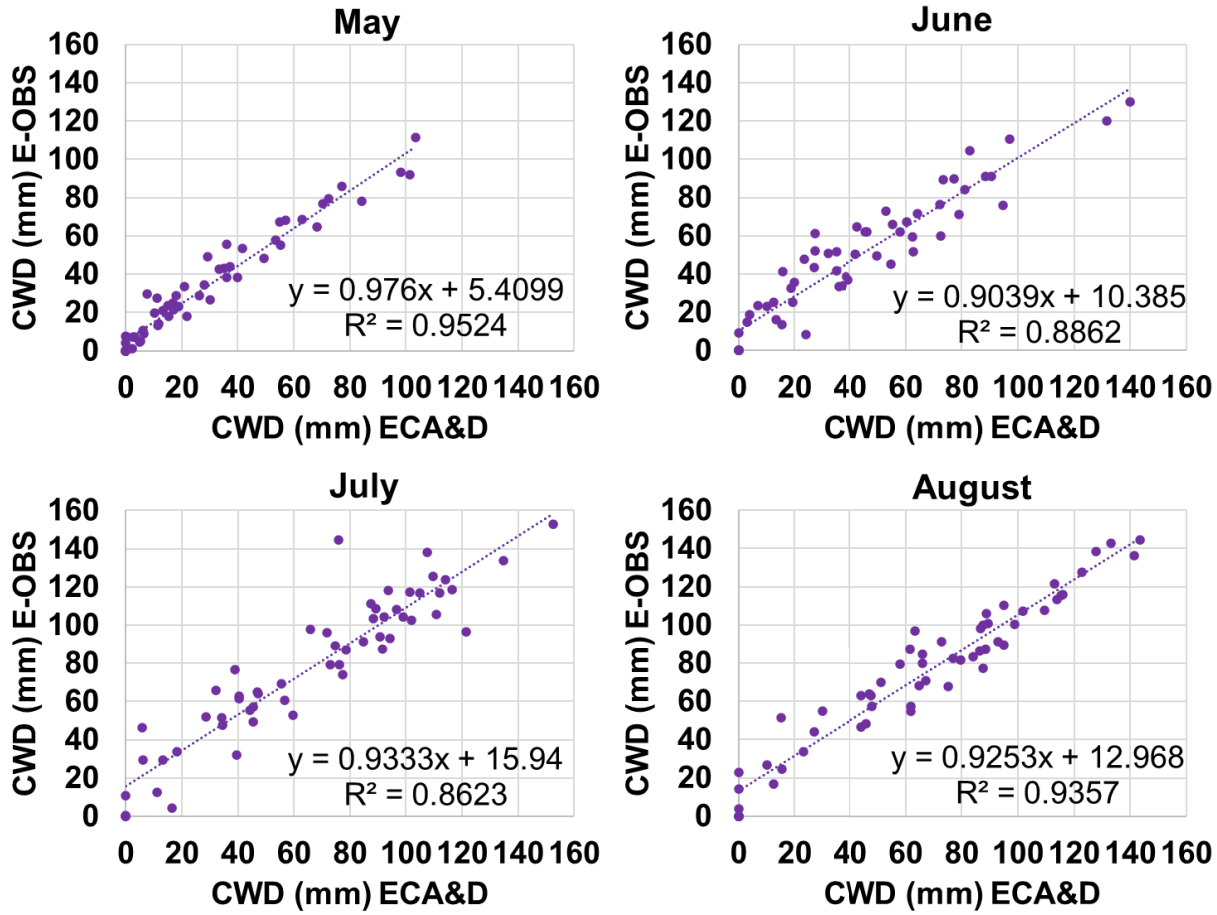

Figure 5.10 Scatter plot between station-CWD_{CRU} at București Băneasa and raster-CWD from May to August between 1961 – 2017

5.1.2.2. Changes in raster-CWD between 1991 – 2017 and 1961 – 1990

This chapter presents the average values of raster-CWD for the two analysed periods (1991 – 2017 and the 1990 – 1961) for the months of spring, summer, and autumn. Moreover, it presents the differences between the second and the first period in these months, allowing for a spatial representation of changes in CWD.

The multiannual average raster-CWD during the spring months in the two selected periods and their differences are shown in **Figure 5.11**. The average CWD is less than 10 and 30 mm in March and April, respectively. In May, the raster-CWD ranges between 30 and 60 mm in the lowlands and less than 30 mm at higher altitudes. The differences between the two periods are small in March and April (± 5 mm). Some areas of larger positive differences around Buzău city and in the Danube Delta area are shown in May.

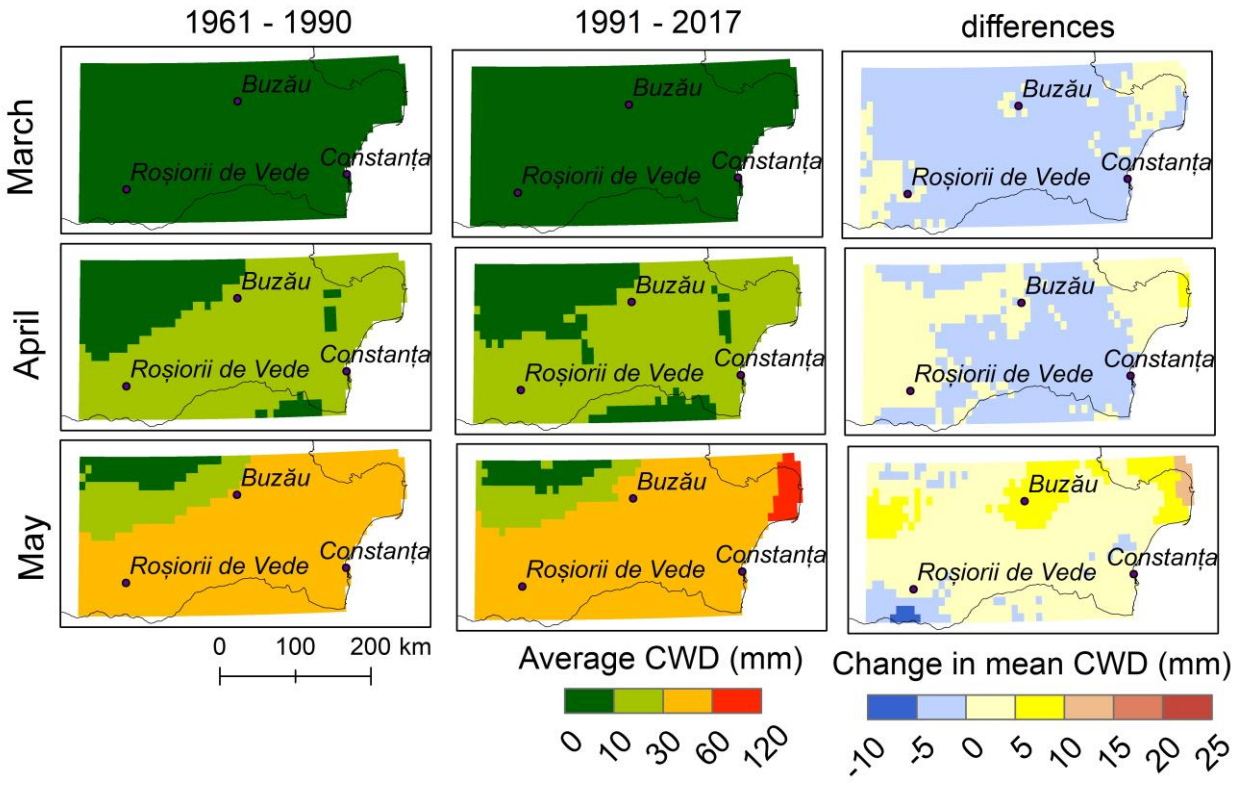

Figure 5.11 Multiannual average raster-CWD in spring and the differences between 1991 – 2017 and 1961 – 1990

In the summer months (**Figure 5.12**), climatic water deficits between 60 and 120 mm occur on average in most of the lowlands. In the Subcarpathians, these are less than 60 mm and less than 30 mm in the Carpathians. The most significant increases in average raster-CWD and with the most extensive spatial coverage are in August: 5 – 10 mm in most areas and 10 – 15 mm in the north-eastern part of the study area (Danube Delta and Galați regions). An area of decrease appears in July in the southern part of the study area. This might be explained by higher values of July average precipitation in this region in the E-OBS dataset in the 1991 – 2017 period compared to 1961 – 1990.

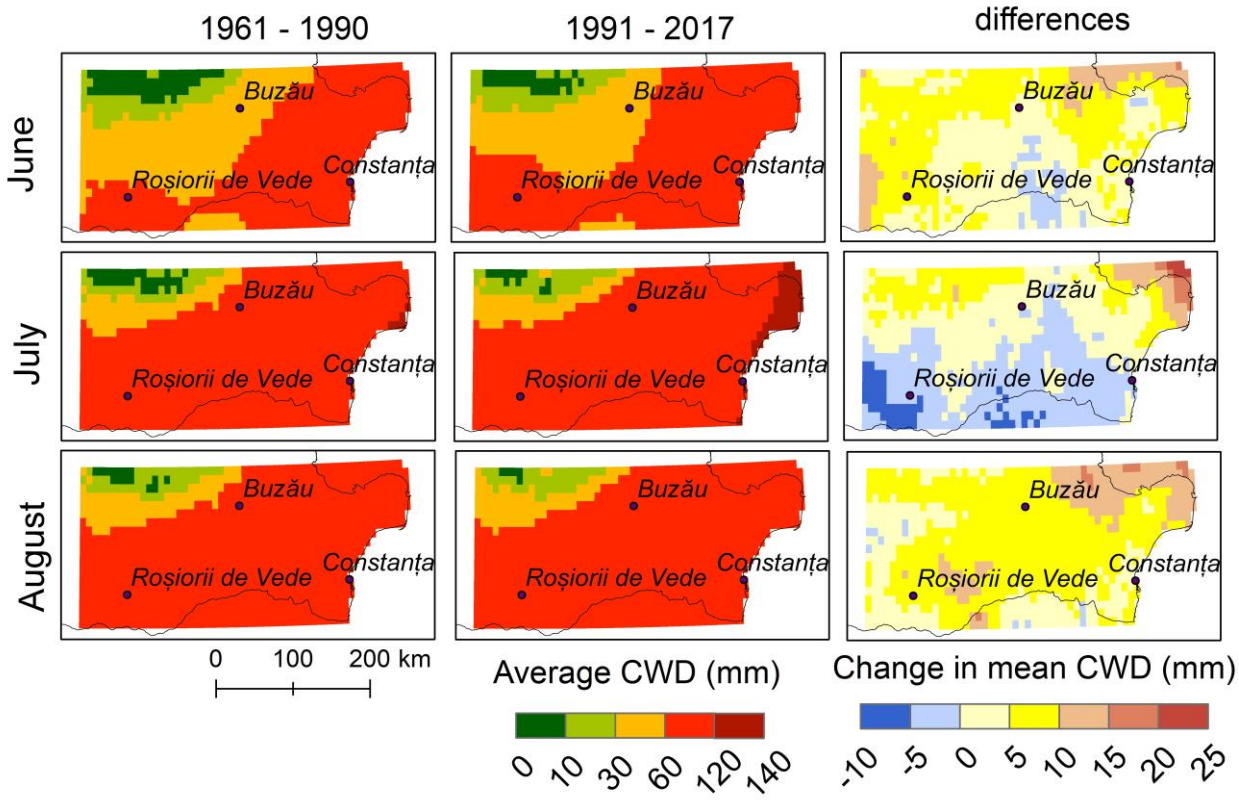

Figure 5.12 Multiannual average raster-CWD in summer and the differences between 1991 – 2017 and 1961 – 1990

In autumn (**Figure 5.13**), the differences show significant decreases in average raster-CWD for most of the area, for both September and October, in the 1991 – 2017 period compared to 1961 – 1990, reaching values of less than -15 mm. In September, the Danube Delta region shows an increase in raster-CWD. Between 1991 – 2017, in September, the Romanian Plain and most of the Dobrogea region are represented by the 30 – 60 mm class of the CWD, with decreasing values

towards the higher altitudes. On the contrary, the CWD decreases in October, most of the area being covered by the 10 – 30 mm class and by the 0 – 10 mm class at higher altitudes.

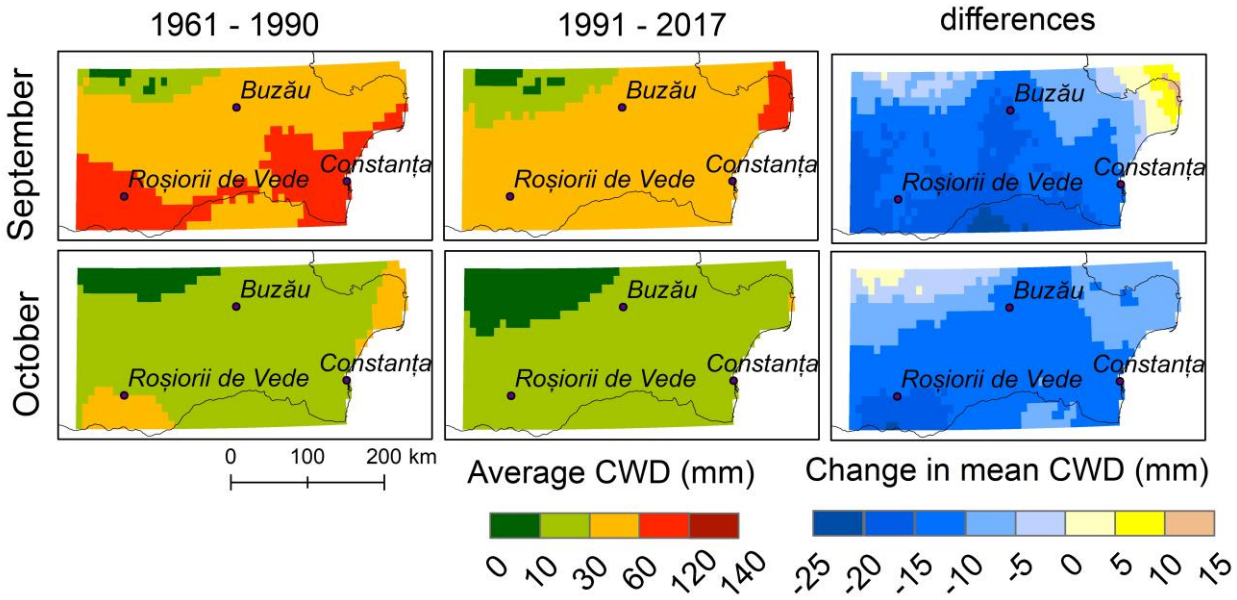

Figure 5.13 Multiannual average raster-CWD in September and October and the differences between 1991 – 2017 and 1961 – 1990

5.2. Drought assessment using standardized indicators

This chapter focuses on hydroclimatic drought assessment using specific standardized indicators: the Standardized Precipitation Index (SPI), the Standardized Precipitation Evapotranspiration Index (SPEI) and the Standardized Streamflow Index (SSI), as described in **Chapter 3.3.3**. For each indicator, their monthly variability is analysed at different time scales in the 1961 – 2020 period for climatic indicators (SPI and SPEI) (**Chapter 5.2.1**) and in 1966 – 2010 for the hydrological indicator (SSI) (**Chapter 5.2.2**). Furthermore, the seasonal trends of SPI and SPEI are also reported. Finally, in **Chapter 5.2.3**, a synthesis of drought events and an overview of the most remarkable events are highlighted.

5.2.1. Variability of drought indicators between 1961 – 2020

5.2.1.1. Standardized Precipitation Index (SPI)

The SPI was calculated and analysed as a measure of meteorological drought. The variability of SPI at meteorological stations between 1961 – 2020 is illustrated in **Figure 5.14** for

SPI-3, **Figure 5.15** for SPI-6 and **Figure 5.16** for SPI-12. These figures show the SPI value for each month for the analysed period (720 values for each time series). A period of lower SPI values, which indicates droughts, is noticed from the early 1980s to the mid-1990s at Băneasa, Călărași, Roșiorii de Vede, Galați, Buzău stations.

The months with the highest precipitation deficit relative to average conditions, identified using **SPI at 6-month time scale**, are May 1968 (București Băneasa), June 1968 (Buzău, Tulcea), December 1978 (Constanța), March 1994 (Galați), July 1996 (Călărași), July 2000 (Roșiorii de Vede), August 2000 (Vârful Omu), and May 2003 (Sulina) (**Figure 5.14**).

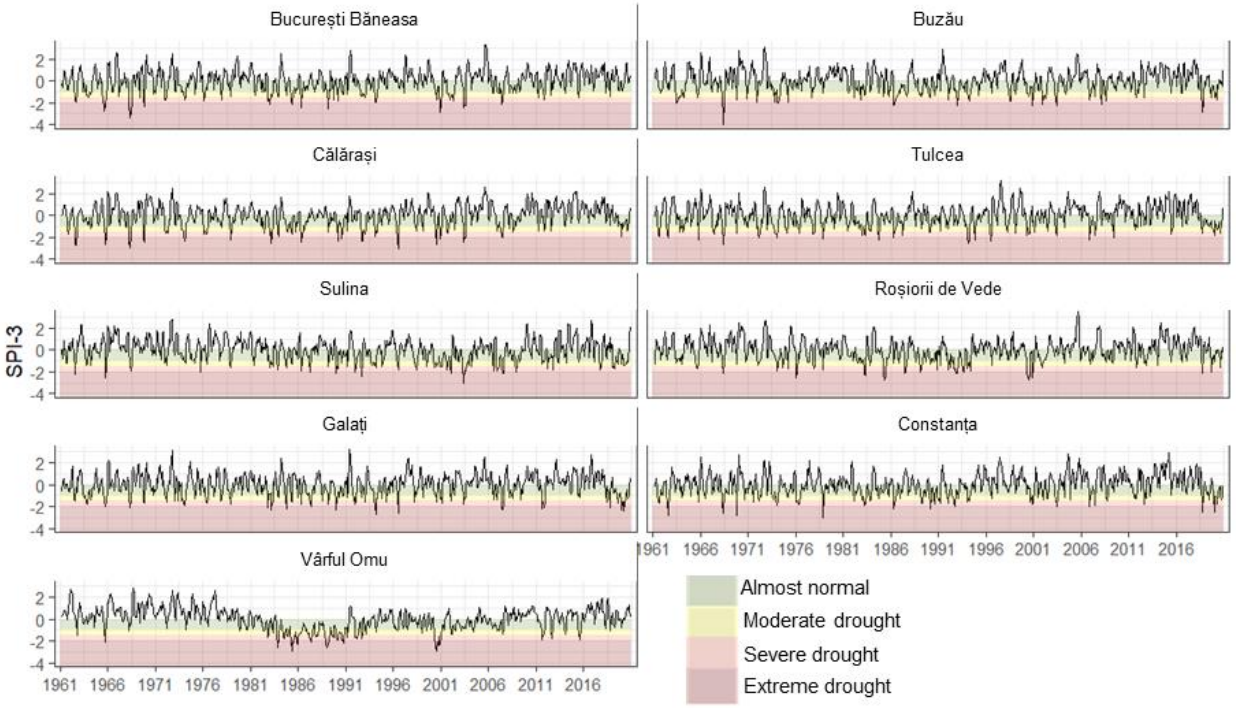

Figure 5.14 Monthly variability of SPI-3 at meteorological stations in south-eastern Romania between 1961 and 2020. Only classes indicating drought are highlighted (legend in **Table 3.16**).

Using the same index for February, May, August and November, the driest winter, spring, summer and autumn seasons can be identified. Thus, the driest winters (with the highest precipitation deficit) were in 1974 (Buzău, Călărași, Constanța), 1976 (Roșiorii de Vede), 1989 (București Băneasa, Vârful Omu), 1994 (Tulcea, Galați), and 2002 (Sulina). The driest springs were in 1968 (București Băneasa, Buzău, Călărași, Tulcea, Galați, Constanța), 1985 (Roșiorii de

Vede, Vârful Omu), and 2003 (Sulina). In summer, the years 1962 (Călărași, Tulcea, Sulina, Constanța), 1963 (Buzău), 1965 (București Băneasa), 1996 (Galați), and 2000 (Roșiorii de Vede, Vârful Omu) were remarkable. The driest autumns were in 1969 (București Băneasa, Călărași, Constanța), 1983 (Sulina, Vârful Omu), 1992 (Roșiorii de Vede), 1994 (Tulcea), 2011 (Galați), and 2018 (Buzău).

The **SPI at the 6-month time scale** can be valuable in assessing dry conditions in the warm season (April – September) and the cold season (October – March). Thus, using the SPI-6 for the warm period (April – September), dry periods were identified in 1965 (București Băneasa), 1986 (Călărași, Buzău, Constanța), 1993 (Roșiorii de Vede), 2000 (Vârful Omu), 2003 (Sulina), 2007 (Galați), and 2020 (Tulcea).

For the cold period (October – March), the driest years identified using the SPI-6 were: 1983 (București Băneasa), 2002 (Buzău, Roșiorii de Vede), 2020 (Galați), 1994 (Tulcea, Sulina), 1974 (Călărași, Constanța), and 1989 (Vârful Omu).

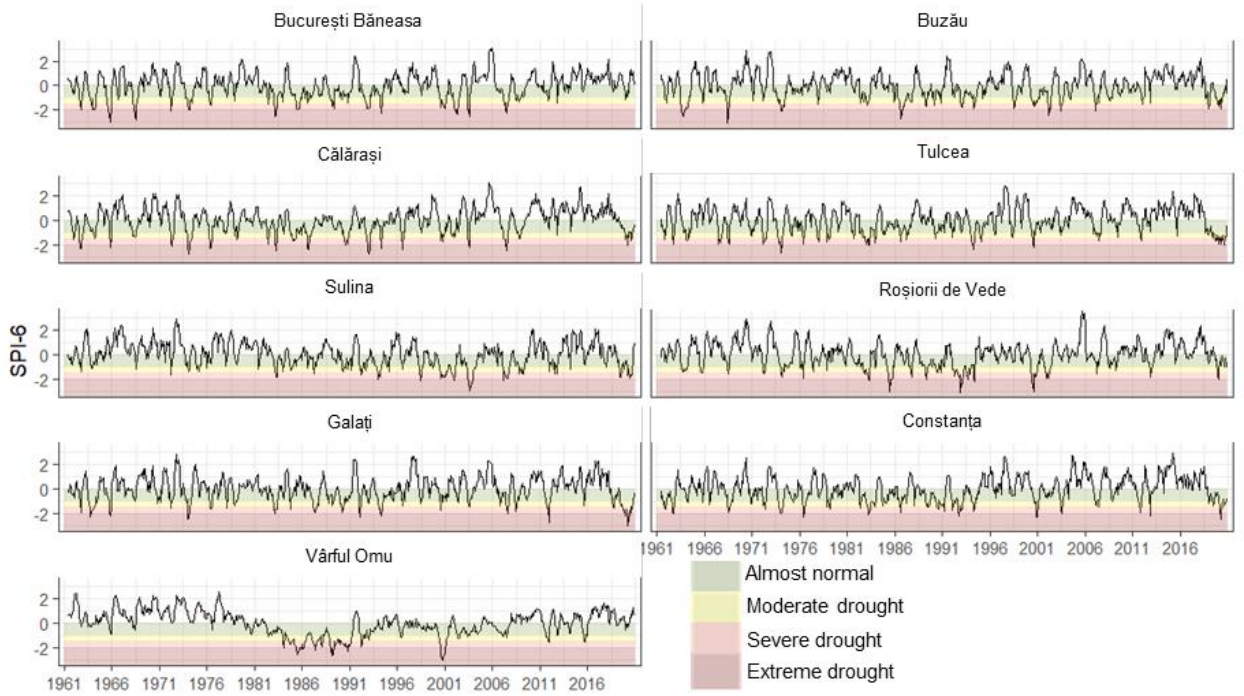

Figure 5.15 Monthly variability of SPI-6 at meteorological stations in south-eastern Romania between 1961 and 2020. Only classes indicating drought are highlighted (legend in **Table 3.16**).

Because precipitation is a crucial control factor of river runoff, assessing drought conditions with potential impact on water resources can be made using indicators at longer time scales such as the **SPI at 12-month time scale (Figure 5.16).** The SPI-12 for September is used here, which integrates the precipitation amount during the hydrological year beginning in October of the previous year. The same period is used to assess drought conditions in the agricultural year.

The driest hydrological/agricultural years, according to the SPI-12 in September, were 1961 – 1962 (Călărași), 1984 – 1985 (București Băneasa, Vârful Omu), 1985 – 1986 (Buzău), 1992 – 1993 (Roșiorii de Vede), 2006 – 2007 (Sulina), and 2019 – 2020 (Tulcea, Galați, Constanța).

For the calendar years (January – December), drought conditions can be assessed using the SPI-12 for December, which showed that the driest years were 1983 (Tulcea, Constanța), 1985 (București Băneasa, Vârful Omu), 1986 (Buzău), 1990 (Călărași), 1992 (Roșiorii de Vede), 2003 (Sulina), and 2019 (Galați).

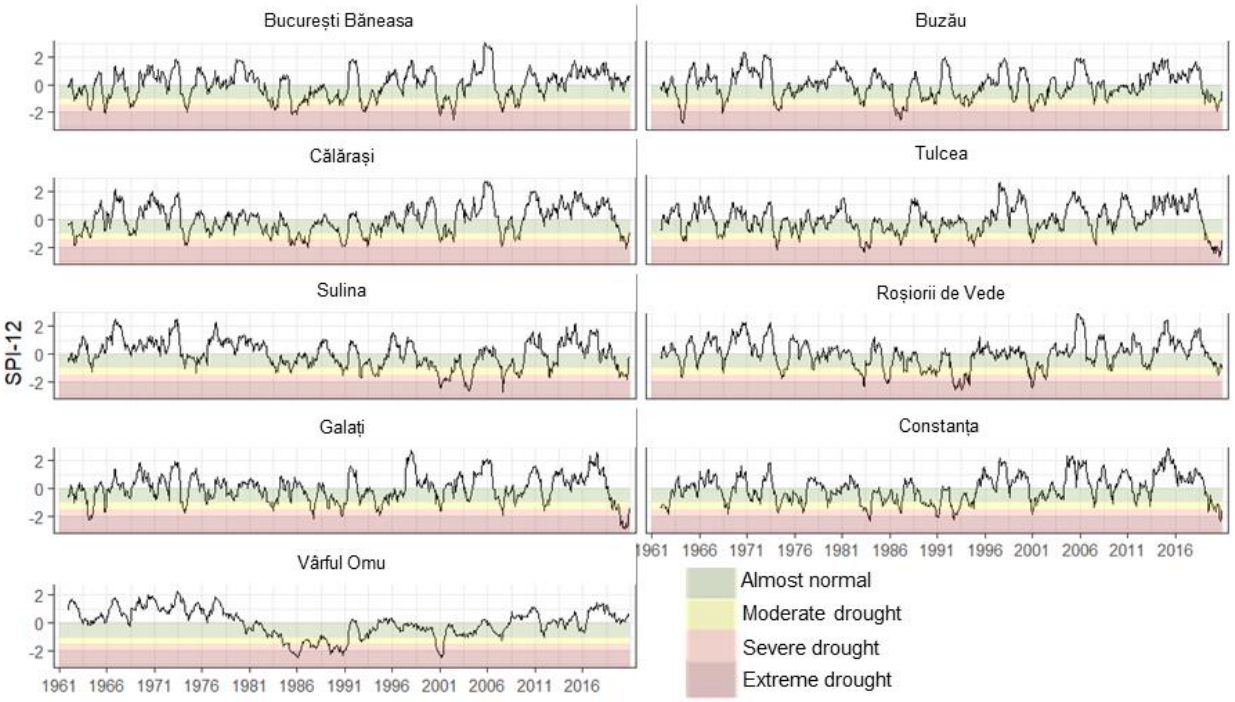

Figure 5.16 Monthly variability of SPI-12 at meteorological stations in south-eastern Romania between 1961 and 2020. Only classes indicating drought are highlighted (legend in **Table 3.16**).

5.2.1.2. Standardized Precipitation Evapotranspiration Index (SPEI)

The **SPEI at 3-month time scale** integrates the influence of the water balance (difference between precipitation and potential evapotranspiration) of the last three months and it is suitable for identifying seasonal trends. In the later part of the analysed interval, the frequency of extreme drought months increased at most stations (**Figure 5.17**).

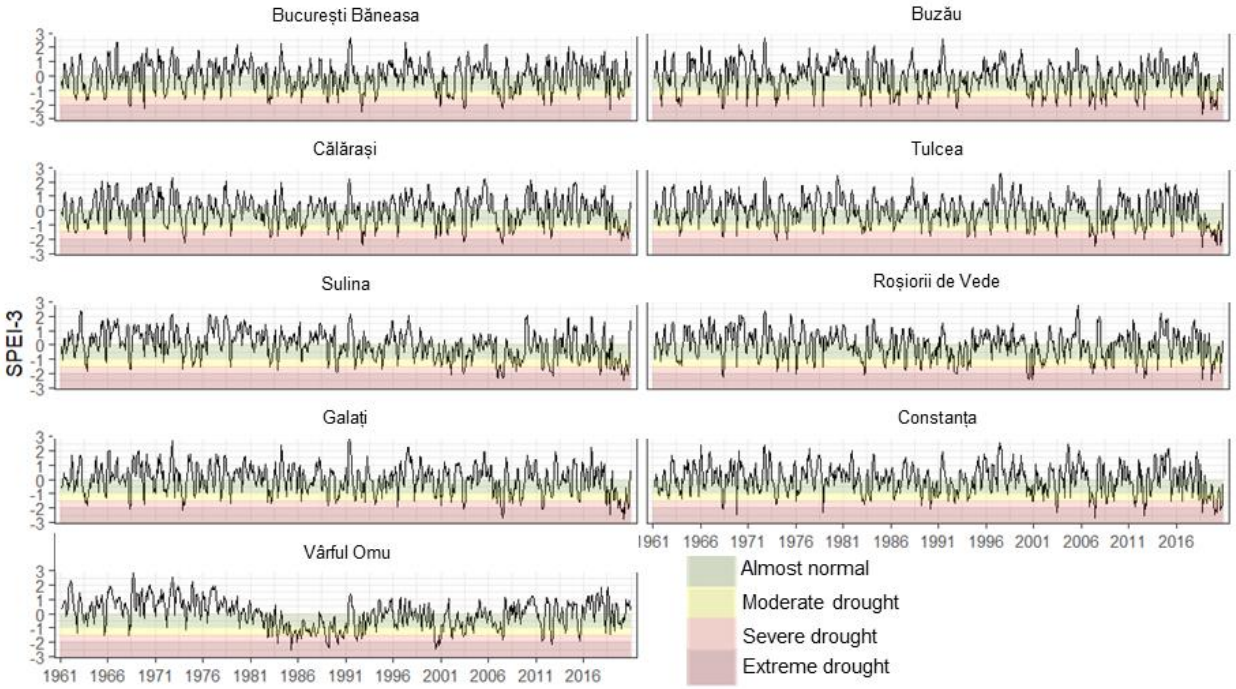

Figure 5.17 Monthly variability of SPEI-3 at meteorological stations in south-eastern Romania between 1961 and 2020. Only classes indicating drought are highlighted (legend in **Table 3.16**).

The driest months identified using the SPEI-3 are mainly found in the latter part of the analysed interval. Using the SPEI-3 for August, which integrates precipitation of June, July and August, the driest summers have been identified during the years 2000 (Roșiorii de Vede), 2003 (București Băneasa), 2007 (Tulcea, Sulina, Galați) and 2012 (Buzău, Călărași, Constanța). June and August 2007 were also extremely dry, marking the importance of temperatures in the drought development in that year's summer season.

The index for May shows that the driest springs were in 1968 at all stations except Sulina and Galați (where the spring of 2020 was the driest) and Vârful Omu (where 1985 had the lowest

value). The highest winter deficit, according to SPEI-3 for February, was in 1974 (Călărași, Tulcea), 1976 (Roșiorii de Vede), 1994 (București Băneasa), 2002 (Sulina), and 2020 (Buzău, Constanța, Galați). The most significant fall deficit, identified using SPEI-3 for November, was in 1969 (București Băneasa, Călărași, Constanța), 1994 (Tulcea), 2011 (Galați), 2012 (Sulina, Roșiorii de Vede), and 2018 (Buzău), indicating a very large accumulated deficit for those three months.

The October **SPEI, calculated at the 7-month time scale** integrates the April – October period, therefore potentially assessing insufficient water resources for vegetation. For this reason, it was considered in the drought analysis. The variation of the SPEI-7 for all the months between 1961 and 2020 is shown in **Figure 5.18**. The driest years according the October SPEI-7 were 1986 (Buzău, Călărași), 2000 (Roșiorii de Vede), 2007 (București Băneasa), 2012 (Sulina), 2018 (Galați), and 2020 (Constanța, Tulcea).

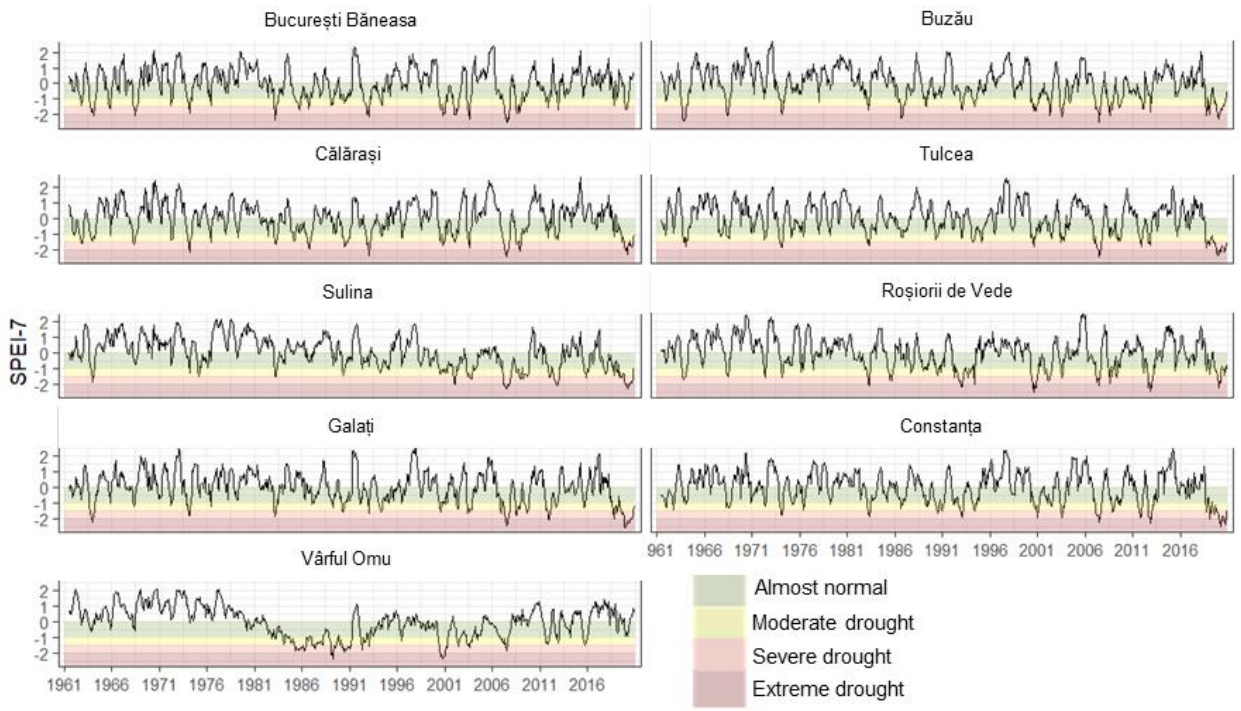

Figure 5.18 Monthly variability of SPEI-7 at meteorological stations in south-eastern Romania between 1961 and 2020. Only classes indicating drought are highlighted (legend in **Table 3.16**).

The **12-month SPEI** integrates the climate water deficit over the previous year, and it is used to identify potential risks to components with a longer response time, such as large rivers, lakes and groundwater resources.

Because the hydrological year starts in October and ends in September, the September SPEI-12 can be used to assess meteorological drought conditions with a potential influence on water resources. In addition, September SPEI-12 can also characterise drought conditions in the agricultural year. Years with the lowest September SPEI-12 were 2000 (Vârful Omu), 2003 (Roșiorii de Vede), 2007 (București Băneasa, Călărași, Sulina), and 2020 (Buzău, Tulcea, Galați, Constanța) (**Figure 5.19**).

Using the December SPEI-12, the drought conditions during the calendar year can be assessed. Thus, the driest years identified were 2000 (Roșiorii de Vede), 2007 (Sulina), 2008 (Buzău, București Băneasa, Călărași), 2019 (Galați), and 2020 (Tulcea, Constanța).

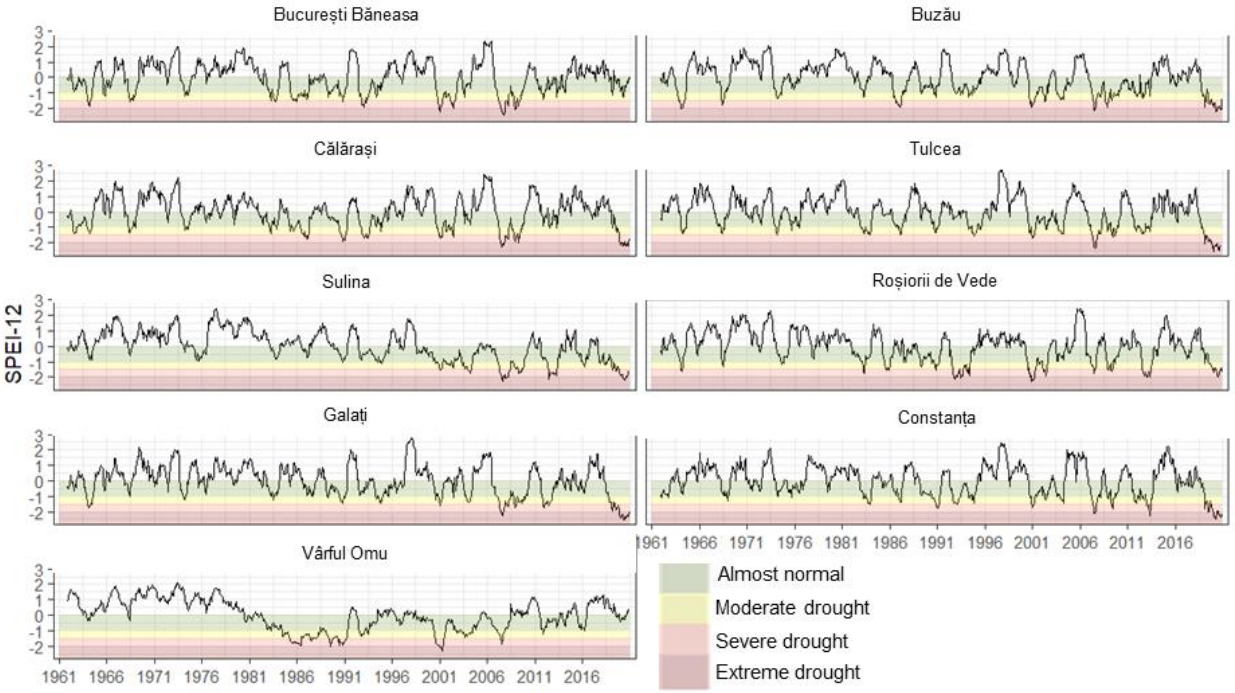

Figure 5.19 Monthly variability of SPEI-12 at meteorological stations in south-eastern Romania between 1961 and 2020. Only classes indicating drought are highlighted (legend in **Table 3.16**).

5.2.1.3. Differences between SPI and SPEI

The difference between SPI and SPEI variability (calculated for each month in the study period, resulting in 720 values for each indicator) was analysed at the meteorological stations in south-eastern Romania at 3- and 12-month aggregation periods (**Figure 5.20** and **Figure 5.21**), highlighting how the SPI values deviate from SPEI on a monthly scale.

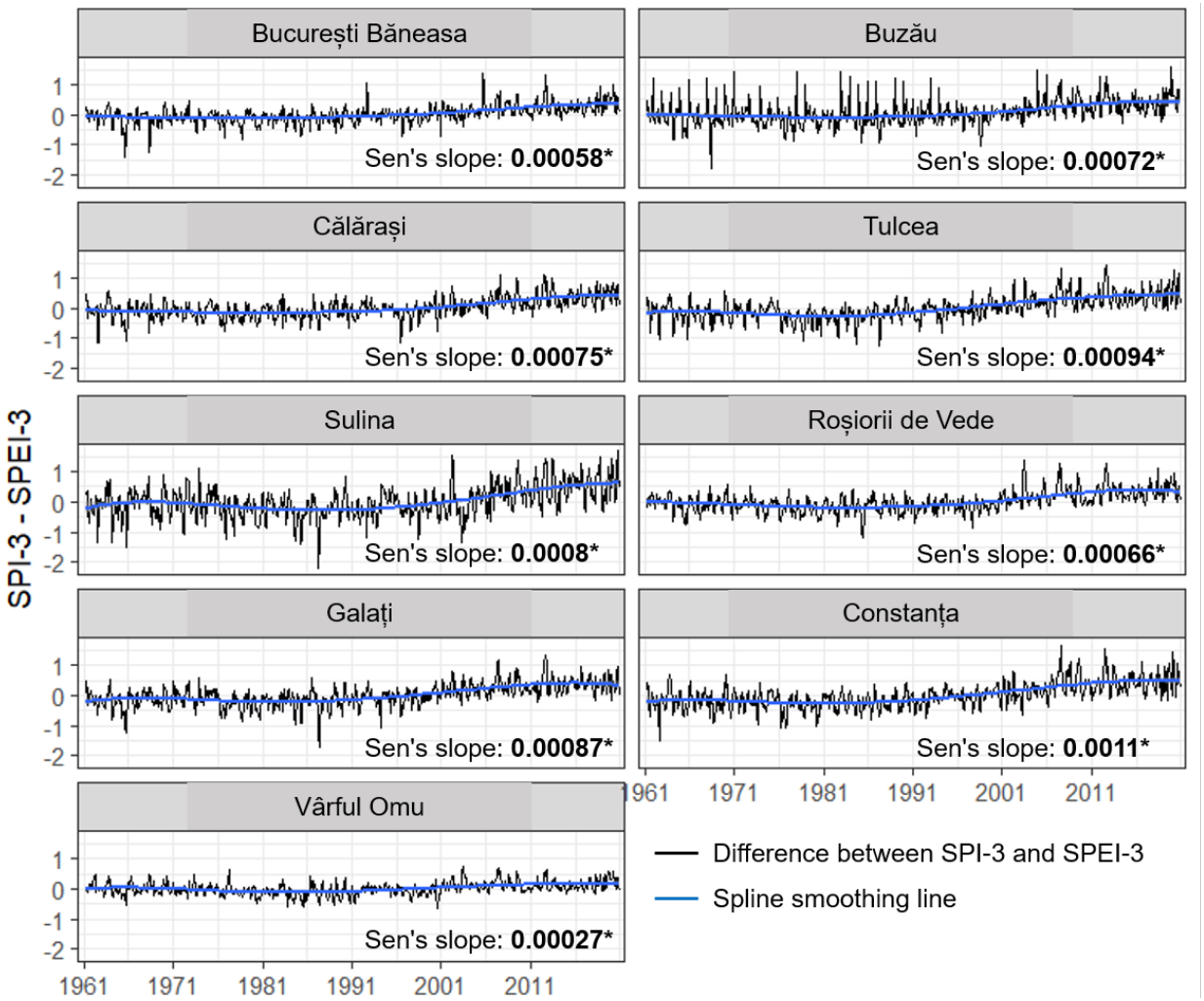

Figure 5.20 Difference between SPI-3 and SPEI-3, spline smoothing line and the Sen's slope of the difference between 1961 – 2020. The significance of the trend test (p-value < 0.05) is shown with an asterisk.

Thus, a positive deviation shows that the SPI indicates a month with higher wetness than the SPEI. They also show the Sen's slope values and the significance of the trend in difference. In

addition, a spline smoothing line has been included for visualization, enabling a smoother representation of the underlying trend in the data.

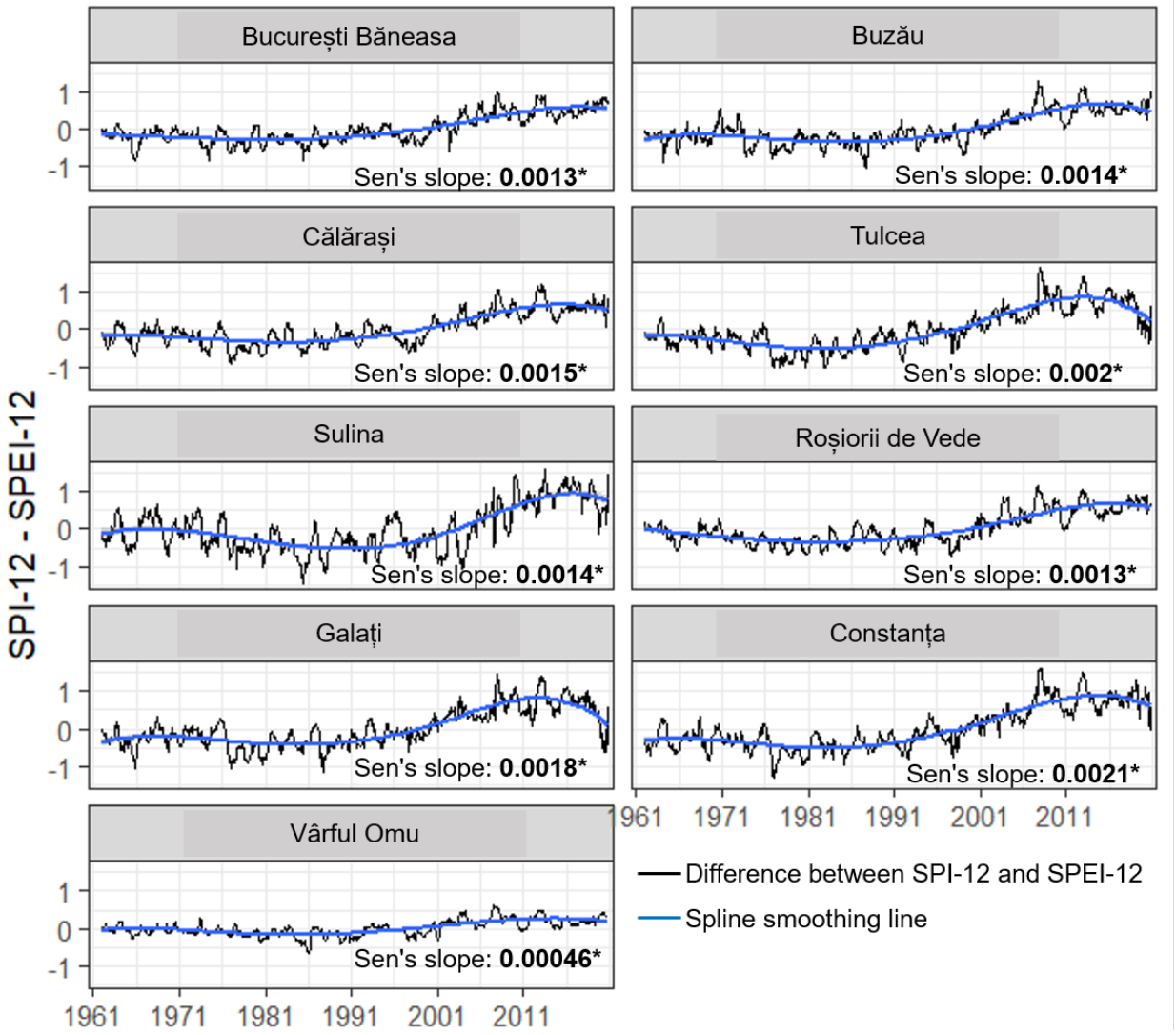

Figure 5.21 Difference between SPI-12 and SPEI-12 spline smoothing line and the Sen's slope of the difference between 1961 – 2020. The significance of the trend test (p-value < 0.05) is shown with an asterisk.

At all stations, an increase in differences is observed in the last part of the study period, starting in the 1990s and increasing in the last two decades. Possible factors causing this difference are the positive trend of temperatures and potential evapotranspiration at all stations. A higher variance of this difference appears at Sulina and Constanța meteorological stations, while the lowest is at București Băneasa. A higher occurrence of meteorological drought determined by a

deficit of precipitation, or a downward trend in precipitation, could be a factor of decreasing differences in the last study period at Galați, Constanța, and Tulcea.

The trends of the differences between the SPI and SPEI indices are significant for the 3- and 12-month time scales. The most pronounced trend in the difference at both scales is at Constanța. On the other hand, the lowest Sen slope is at București Băneasa, at 3- and 12-month scales.

The highest positive differences between SPI and SPEI (SPI indicated wetter conditions than SPEI) at the 3-month time scale were in June 2003 (Roșiorii de Vede), September 2005 (București Băneasa), August 2007 (Constanța), in 2012 in July (Călărași), August (Tulcea), September (Galați), December 2019 (Buzău) and October 2020 (Sulina) (**Figure 5.20**).

The most considerable positive difference between SPI-12 and SPEI-12 was mainly identified in 2007, except for Constanța (2008) and Călărași and Sulina (2013) (**Figure 5.21**). As some of these years were previously identified as very dry (such as 2003, 2007, 2008, 2012, or 2020), the significant differences between SPI and SPEI may indicate temperature's critical role in developing these events.

A divergence between the SPI and SPEI indices of drought frequency and drought-affected areas has been observed across Europe (Stagge et al., 2017). This difference is due to the positive temperature trend, which causes an increase in potential evapotranspiration, resulting in a high water deficit.

5.2.1.4. Spatialised trends in the SPI and the SPEI

The trends in SPI and SPEI were estimated at all meteorological stations, as mentioned in **Chapter 3.3.3**, using the Mann-Kendall and Sen's slope statistical tests at the different temporal scales. The Sen's slopes were then spatially interpolated to represent the regional trends. This approach is useful for identifying spatial patterns and potential changes in the occurrence of drought.

The SPI-3 trends for the winter (SPI-3 for February), spring (SPI-3 for May), summer (SPI-3 for August) and autumn (SPI-3 for November) seasons are shown in **Figure 5.22**.

SPI-3 trends in winter show significant downward trends at Sulina and Vârful Omu, while insignificant decreasing trends are at Roșiorii de Vede, Buzău and Tulcea. There are only insignificant trends in spring and summer, and only București Băneasa, Tulcea, and Constanța show upward trends. In autumn, there are mainly increasing trends, significant only in Călărași and insignificantly decreasing in Vârful Omu and Sulina. The upward trends in autumn could be explained by the increasing precipitation trends (Busuioc et al., 2015; Cheval et al., 2014).

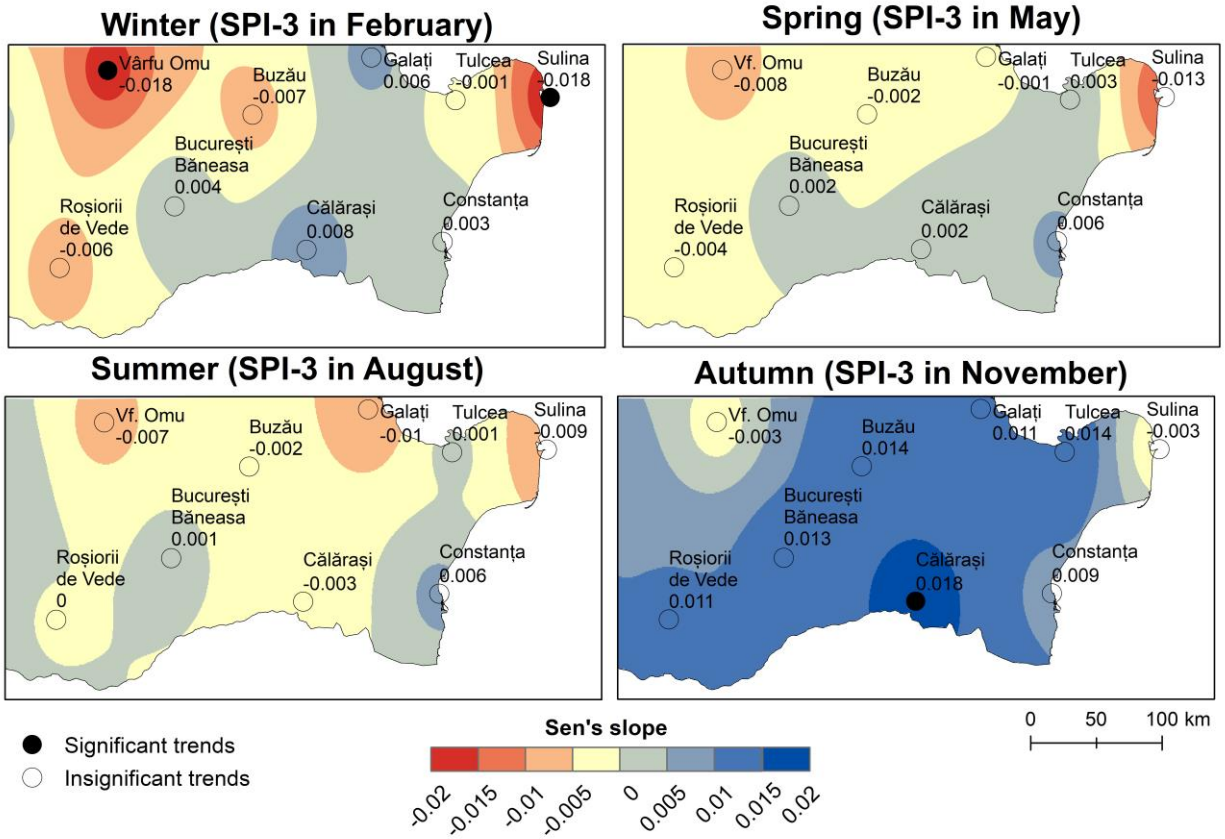

Figure 5.22 SPI-3 trends in February, May, August, and November between 1961 – 2020

SPI-12 for September (relevant to the assessment of climatic conditions in the agricultural and hydrological year) shows mainly increases, but insignificant, and decreases in Sulina (significant) and Vârful Omu (insignificant) (**Figure 5.23**).

The SPI-12 for December (calendar year) (**Figure 5.23**) shows a similar trend distribution; however, Roșiorii de Vede displays in this case insignificant decreasing trends.

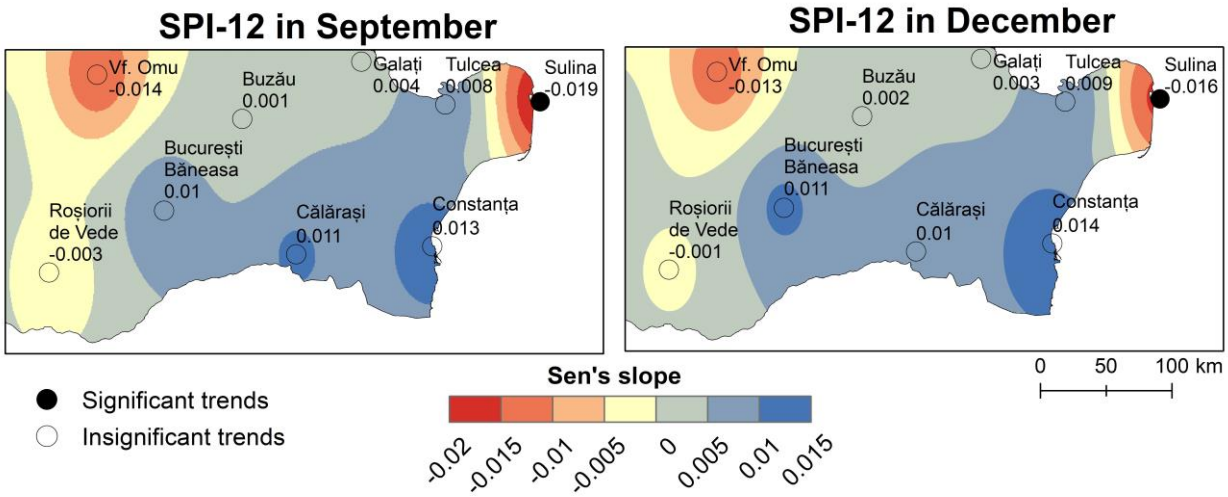

Figure 5.23 SPI-12 trends for September and December between 1961 – 2020

The seasonal trends, determined using the SPEI-3 index for February, May, August, and September are shown in **Figure 5.24**.

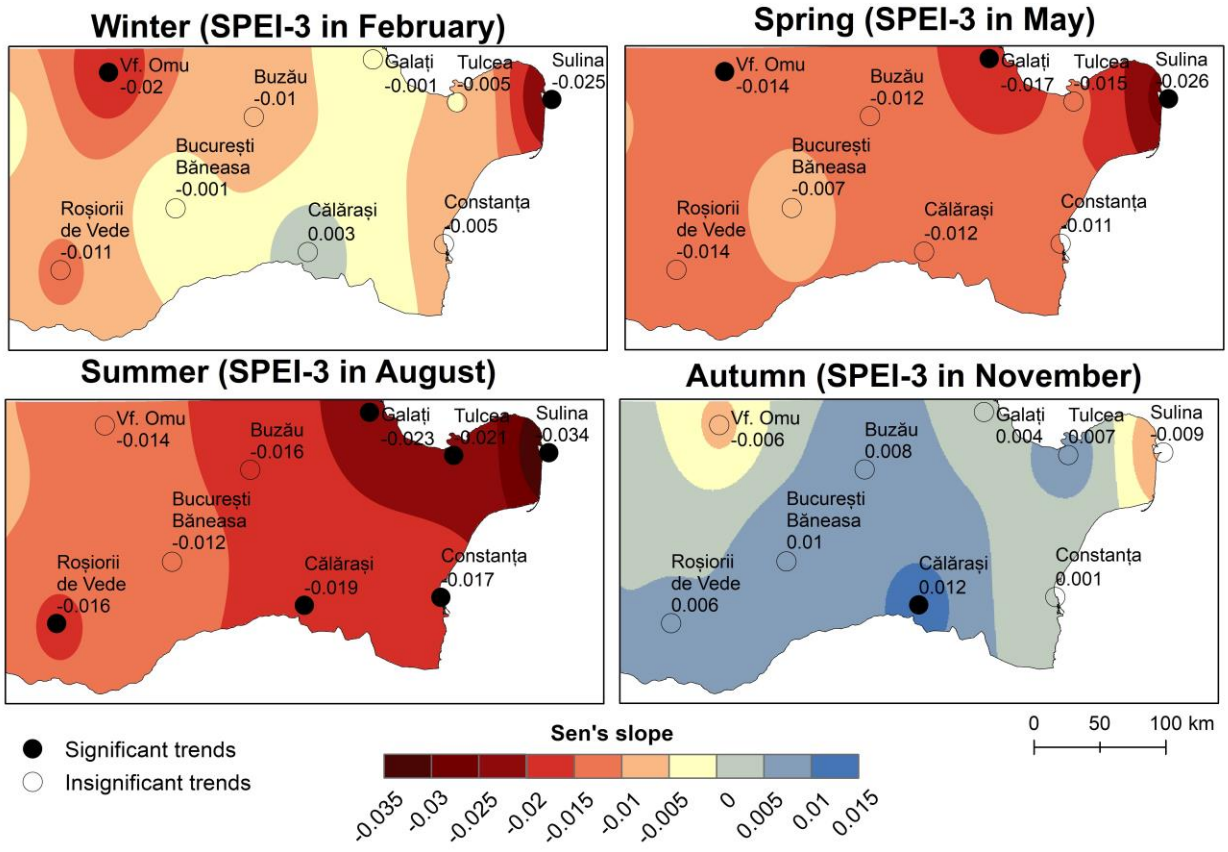

Figure 5.24 SPEI-3 trends for February, May, August, and November between 1961 – 2020

In winter, there are mainly decreasing trends (except Călărași), which are significant only at Sulina and Vârful Omu. SPEI-3 for May shows only decreasing trends, which are also significant in Sulina, Vârful Omu and Galați. Similarly, in summer, there are only decreasing trends which are significant at all the stations in the eastern part of the study area (Călărași, Tulcea, Sulina, Galați, Constanța) and Roșiorii de Vede. SPEI-3 for November shows only insignificant trends, predominantly increasing (except Sulina and Vârful Omu). Similar to the trends of SPI-3, SPEI-3 in autumn highlights a tendency towards increased wetness.

The trends of SPEI-7 for October are decreasing at all stations and are significant at Buzău, Călărași, Sulina, Galați and Vârful Omu (**Figure 5.25**). This result highlights trends that may lead to more frequent drought conditions in the study area.

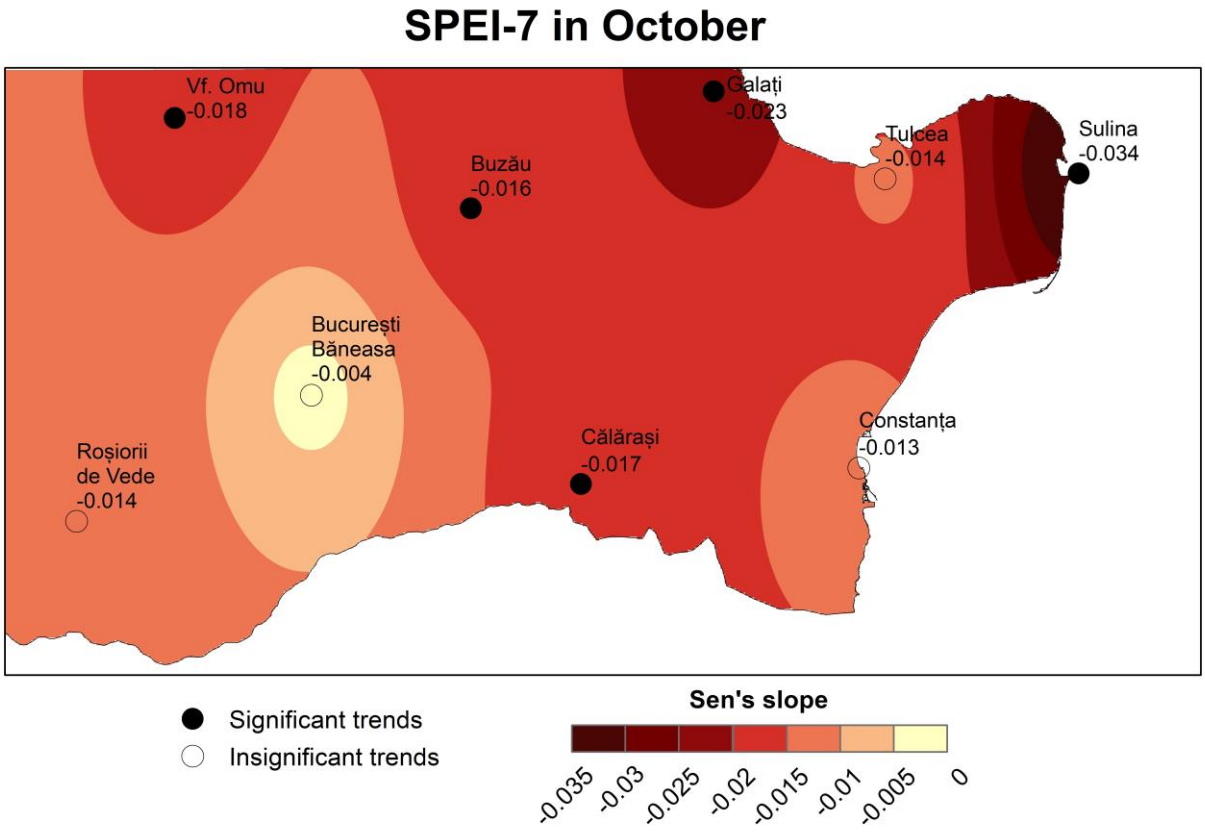

Figure 5.25 SPEI-7 trends for October over the 1961 – 2020 period

SPEI-12 from both September and December show decreases at all stations, which are significant at Buzău, Sulina, Roșiorii de Vede, Galați, Vârful Omu (and Tulcea, for SPEI-12 in

December) (**Figure 5.26**). Compared to a rainfall-based index, SPEI shows an increasing trend towards drier conditions due to rising temperatures leading to a higher water deficit.

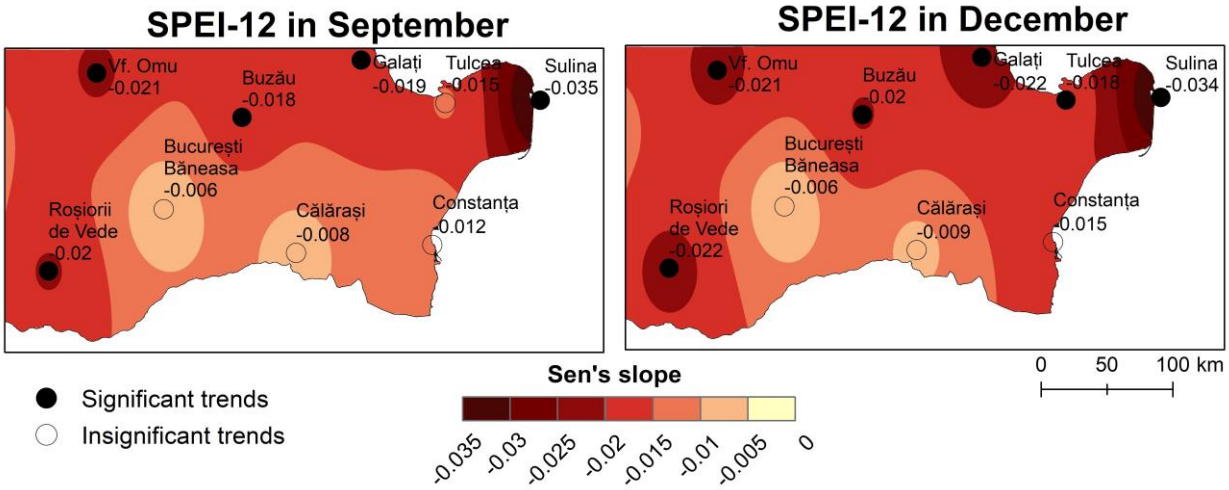

Figure 5.26 SPEI-12 trends in December and September over the 1961 – 2020 period

5.2.2. Standardized Streamflow Index (SSI)

The SSI was calculated as a measure of hydrological drought in the region, using streamflow values at four gauging stations on four different rivers, as presented in **Chapter 3.3.3.3**. This resulted in 540 SSI values for each month, station, and time scale in the 45 studied years (1966 – 2010).

The monthly variability of SSI for the 3- and 12-month scales between 1966 – 2010 is shown in **Figure 5.27** and **Figure 5.28**.

A decrease in the index values can be observed at both scales from 1981 to the mid-1990s. After this decrease period, the index shows a period of increased values, which were higher at the Budești and Coșereni gauging stations than at the Alexandria and Racovița stations.

Although these figures present the variations of all months in the time series, a seasonal analysis can be performed by subsetting the last month of the season.

By analysing the data series for the **SSI at the 3-month time scale** for February, the driest winters were in 1993 (Coșereni), 1995 (Budești), and 2001 (Alexandria and Racovița).

The driest springs (SSI-3 for May) were in 1990 (Buzău), 1994 (Budești, Coșereni), and 2002 (Alexandria). The driest summers (SSI-3 for August) were in 1968 (Coșereni), 1993 (Budești), 2007 (Racovița), and 2008 (Alexandria).

Finally, the driest autumn season was identified using the SSI-3 for November in 1990 (Coșereni, Racovița), 1994 (Budești), and 2008 (Alexandria).

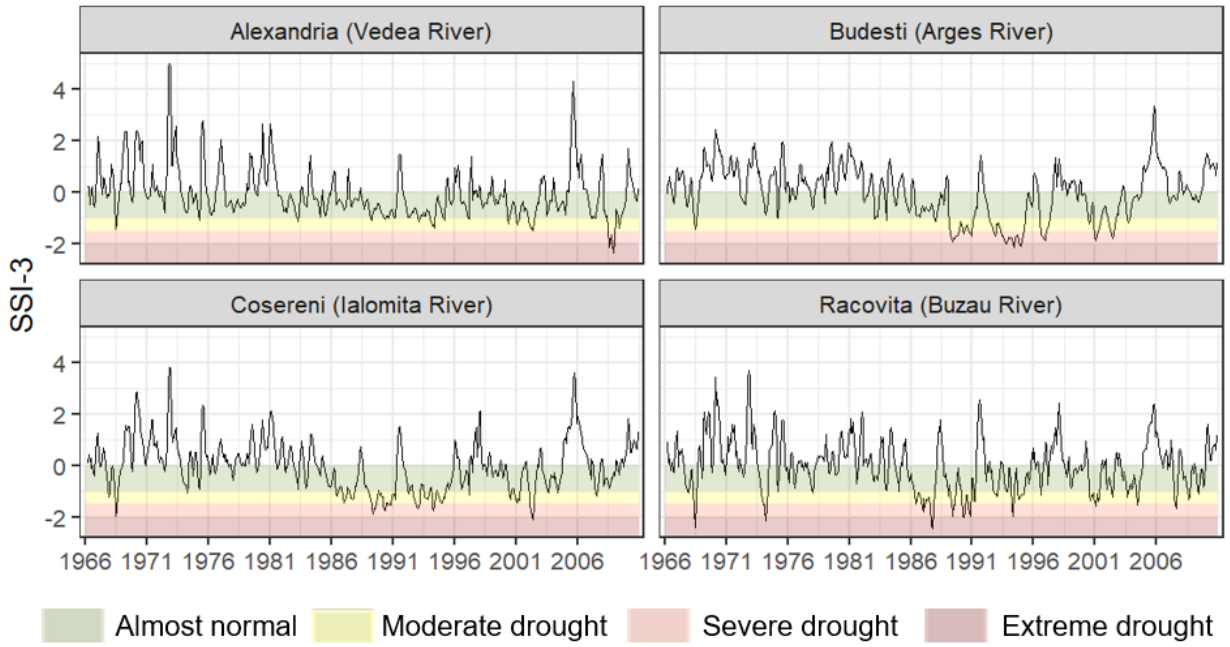

Figure 5.27 Monthly variability of SSI-3 at the Alexandria (on Vedea River), Budești (on Argeș River), Coșereni (on Ialomița River) and Racovița (on Buzău River) gauging stations between 1966 – 2010. Only classes indicating drought are highlighted (legend in **Table 3.16**).

The **SSI calculated on a 12-months scale** highlights variations over a longer period through the averaging effect of this time scale.

The SSI at the 12-month time scale for September can assess conditions during the hydrological year. The hydrological years with the highest deficit relative to average conditions were: 1987 (Racovița), 1990 (Coșereni), 2002 (Alexandria), and 1994 (Budești).

On the other hand, the driest calendar years (represented by SSI-12 for December) were 1989 (Coșereni), 1990 (Racovița), 2008 (Alexandria), and 1994 (Budești).

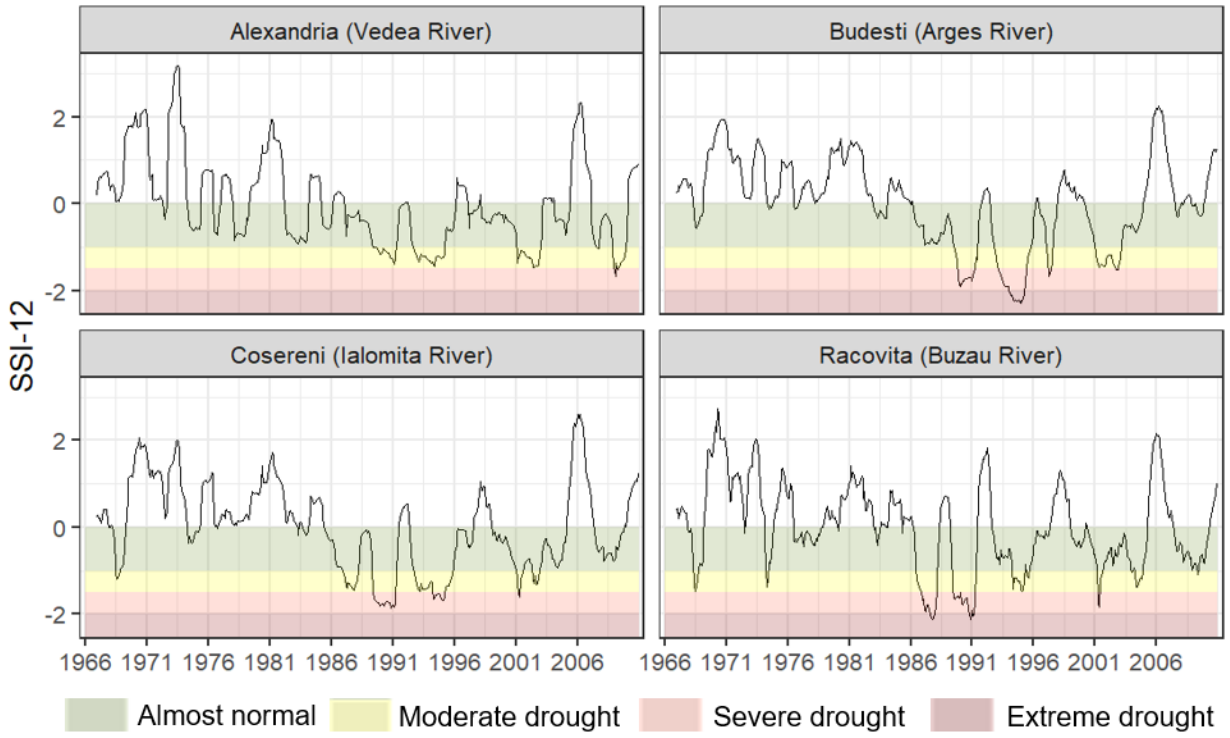

Figure 5.28 Monthly variability of SSI-12 at the Alexandria (on Vedea River), Budești (on Argeș River), Coșereni (on Ialomița River) and Racovița (on Buzău River) gauging stations between 1966 – 2010. Only classes indicating drought are highlighted (legend in **Table 3.16**).

5.2.3. Drought events

Meteorological drought events were identified with SPI and SPEI at the 3- and 12-month time, while hydrological drought events were identified with SSI at the 3-month scale, as described in **Chapter 3.3.3.4**. These were characterized in terms of duration, severity, and intensity. The droughts with the longest duration, highest magnitude and intensity are presented in **Table 5.2**.

The lengths of the longest meteorological droughts varied between stations and range from 13 (București Băneasa) to 24 months (Sulina) for SPI-3, from 12 (București Băneasa) to 31 months (Tulcea) for SPEI-3, from 30 (Galați) to 55 months (Sulina) for SPI-12 and from 31 months (Tulcea) to 79 months (Sulina) for SPEI-12.

Common periods with the most prolonged droughts at different stations highlight years of significant water stress. For SPI-3 and SPEI-3, these were in 1986 at București Băneasa and Buzău, and in 2018/2019 – 2020 at Călărași, Tulcea, Galați and Constanța. For SPI and SPEI at 12 months

scale, common periods occurred in 1984/1985 – 1988 at București Băneasa, Călărași, Tulcea, between 1988 – 1991 at Roșiorii de Vede and Galați, between 1992 – 1995 at Buzău, Roșiorii de Vede, Constanța, between 1998/2000 – 2003 at Tulcea and Sulina and between 2006 – 2010/2012 at București Băneasa, Buzău, Călărași, Galați. Between 2019 – 2020, there was also a common period in terms of drought severity at Buzău, Călărași, Tulcea, Sulina, Galați and Constanța. 1965 represented a common episode of intense drought at Tulcea and Sulina and 1968 in București Băneasa and Buzău.

In the 1961 – 2020 period, between 33 % (SPI-3 at Călărași) and 39 % (SPI-3 at Tulcea and Sulina) or between 34 % (SPEI-12 at Roșiorii de Vede) and 44 % (SPI-12 at Constanța) of months were included in a drought event.

The number of these drought events varied with indicator and time scale. In general, more drought events were identified at shorter time scales than at longer ones. For SPI-3, the number of events varied from 39 events (Călărași) to 48 events (Galați), while for SPEI-3, these varied between 37 (Galați) and 44 (Călărași and Tulcea).

On the 12-month scale, SPI showed from 11 events (București Băneasa) to 16 (Galați), and SPEI showed from 7 (Sulina) to 16 events (București Băneasa). A higher number of events at a station could suggest a higher variability of that indicator and time scale compared to the other stations.

Similarly, hydrological drought events were highlighted using sequences of negative values in the SSI-3 values, during the 1966 – 2010 period. The main events identified during this period and their characteristics are summarized in **Table 5.3**. Between 33 % (Alexandria) and 39% (Racovița) of the months in the considered period were included in a hydrological drought event.

Compared to the SPI and SPEI, the number of hydrological drought events is lower (between 8 and 16 events at Alexandria and Racovița, respectively), but these are of longer duration (from 32 up to 50 months at Buzău and Coșereni, respectively) (**Table 5.3**). In particular, 1991/1992 – 1995 is commonly identified as the longest and most severe drought event at Alexandria, Budești and Coșereni gauging stations. Moreover, hydrological drought events marked the period between 1988 – 1991: it was the longest observed event at Racovița (Buzău River) and the most intense at Coșereni (Ialomița River).

Table 5.2 Characteristics of the main meteorological drought events identified based on SPI and SPEI at 3- and 12-month scale for the 1961 – 2020 period

Meteorological stations	Scale	Index	Max. duration	Max. severity	Max. intensity	% time in drought	No. events
Băneasa	**3**	**SPI**	June 1973 – June 1974 (13 months)	September 2001 – June 2002	March 1968 – August 1968	35	45
		SPEI	February 1985 – January 1986 (12 months)	November 2006 – September 2007	October 1969 – November 1969	34	42
	12	**SPI**	March 1985 – September 1988 (43 months)		August 2000 – December 2002	39	11
		SPEI	October 2006 – January 2010 (40 months)			41	16
Buzău	**3**	**SPI**	May 1986 – October 1987 (18 months)		March 1968 – July 1968	36	43
		SPEI	May 1963 – July 1964 (15 months)	July 2019 – June 2020		34	43
	12	**SPI**	July 1992 – August 1995 (38 months)	May 1986 – March 1988		42	14
		SPEI	December 2006 – April 2012 (65 months)		October 2018 – December 2020	42	13
Călărași	**3**	**SPI**	July 2019 – October 2020 (16 months)		October 1969 – November 1969	33	39
		SPEI	March 2019 – November 2020 (21 months)		October 1969 – November 1969	37	44
	12	**SPI**	August 1984 – September 1988 (50 months)		July 2019 – December 2020	41	13
		SPEI	December 2006 – January 2010 (38 months)		February 2019 – December 2020	37	12
Tulcea	**3**	**SPI**	August 2018 – November 2020 (28 months)		October 1965 – November 1965	39	44
		SPEI	May 2018 – November 2020 (31 months)		June 2015 – September 2015	38	44
	12	**SPI**	February 1985 – February 1988 (37 months)	October 2018 – December 2020		35	13
		SPEI	July 2000 – January 2003 (31 months)	July 2018 – December 2020		39	14

Sulina	**3**	**SPI**	March 2000 – February 2002 (24 months)		October 1965 – November 1965	39	43
		SPEI	February 2008 – November 2009 (22 months)	February 2019 – October 2020	November 2006 – October 2007	37	38
	12	**SPI**	July 1998 – January 2003 (55 months)		March 2003 – February 2005	42	12
		SPEI	August 1998 – February 2005 (79 months)		September 2017 – December 2020	37	7
Roșiori de Vede	**3**	**SPI**	November 1991 – October 1993 (24 months)		April 1968 – July 1968	37	42
		SPEI	November 1991 – February 1993 (16 months)		April 1968 – July 1968	37	42
	12	**SPI**	November 1988 – June 1991 (32 months)	May 1992 – September 1994		34	14
		SPEI	May 1992 – February 1995 (34 months)			37	13
Galați	**3**	**SPI**	March 2019 – November 2020 (21 months)		June 1996 – August 1996	38	48
		SPEI	March 2019 – November 2020 (21 months)			35	37
	12	**SPI**	November 1988 – April 1991 (30 months)	October 2018 – December 2020		35	16
		SPEI	July 2006 – May 2010 (47 months)		June 2018 – December 2020	33	12
Constanța	**3**	**SPI**	January 1990 – April 1991 (16 months)		June 1962 – October 1962	37	43
		SPEI	February 2019 – December 2020 (23 months)		July 2012 – November 2012	35	40
	12	**SPI**	October 1973 – April 1977 (43 months)	May 1992 – February 1995	February 2019 – December 2020	44	15
		SPEI	May 1992 – February 1995 (34 months)	October 2018 – December 2020		40	14
Vârful Omu	**3**	**SPI**	September 1983 – May 1991 (93 months)		April 2000 – June 2001	35	23
		SPEI	May 1984 – March 1988		June 2015 – October 2015	36	30
	12	**SPI**	May 1982 – September 1991			36	4
		SPEI	May 1982 – July 1991			39	6

Finally, the overlapping periods of meteorological drought at București Băneasa meteorological station and hydrological droughts at Coșereni and Budești gauging stations are represented graphically in **Figure 5.29**. These were selected for representation because of their relative geographical proximity. The figure enables a comparative analysis of the two types of droughts, facilitating the identification of synchronous or lagged dry periods. For instance, the long hydrological drought period starting at the end of the 1980s occurred after the start of the meteorological drought events identified with SPI and SPEI.

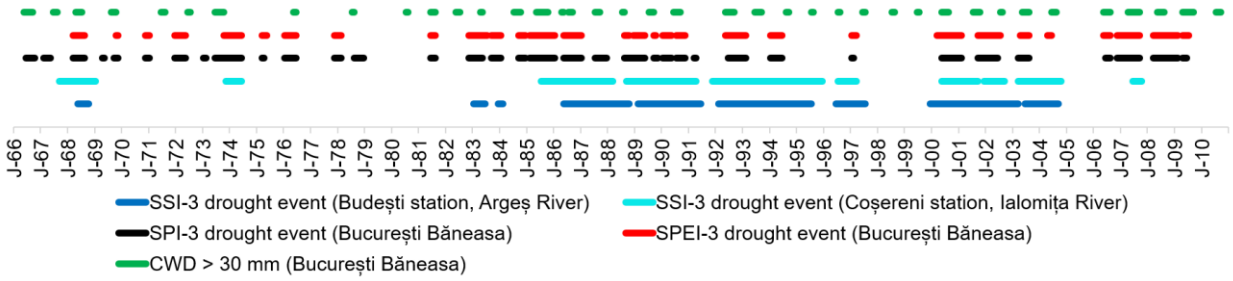

Figure 5.29 Synthesis of meteorological drought (represented by the Standardized Precipitation Index [SPI], Standardized Precipitation Evapotranspiration Index [SPEI] and climatic water deficit [CWD]) and hydrological drought (represented by the Standardized Streamflow Index [SSI]) events at the București Băneasa meteorological station and Budești (on Argeș River) and Coșereni (on Ialomița River) gauging stations between 1966 – 2010

Table 5.3 Characteristics of main hydrological drought events identified based on the Standardized Streamflow Index at 3-month scale between 1966 – 2010

Gauging station/River	Max. duration	Max. severity	Max. intensity	% time in drought	No. events
Alexandria/Vedea	November 1991 – May 1995 (43 months)		March 2008 – December 2009	33	8
Budești/Argeș	February 1992 – July 1995 (42 months)			34	9
Coșereni/Ialomița	November 1991 – December 1995 (50 months)		September 1988 – April 1991	37	10
Racovița/Buzău	September 1988 – April 1991 (32 months)		October 1985 – February 1988	39	16

Conclusion

This part of the thesis has delved into the variability of hydroclimatic parameters relevant for drought and the occurrence and changes in meteorological and hydrological drought characteristics at multiple time and spatial scales. Several periods of important water deficit have been identified and described over the 1961 – 2020 period at meteorological stations, and over the 1966 – 2010 period at hydrometric stations.

All the analyzed meteorological stations in the study area had positive temperature and potential evapotranspiration trends at the annual scale and for the summer months between 1961 – 2020. However, precipitation trends were relatively stable, with some exceptions: there were significant trends that were positive in Constanța and negative in Sulina meteorological stations. In October, there was an upward significant trend in monthly precipitation at most stations. In January, a significant upward trend was noted for Călărași station. Negative and significant trends were observed at Sulina in February and May, at Vârful Omu in April and at Galați in August.

The main drought periods identified using the Standardized Precipitation Index, the Standardized Precipitation Evapotranspiration Index and the Climatic Water Deficit were 1963 – 1964, 1968 – 1969, 1973 – 1974, 1984 – 1989, 1991 – 1995, 2000 – 2003, 2012, and 2018 – 2020. The Standardized Streamflow Index was employed for investigating hydrological drought, highlighting the streamflow reductions in the 1966 – 1969, 1991 – 1995, 2000 – 2004, and 2007 – 2009 intervals.

In particular, the Climatic Water Deficit indicated a higher occurrence of arid months in the summer season, especially in August. This was additionally emphasized by the significant positive trend (Sen slopes between 0.7 and 1.13 mm/year) of the water deficit in the same month at all the studied meteorological stations. The increasing deficit is probably related to the positive trends in air temperatures.

In addition, when comparing the results obtained using the Standardized Precipitation Evapotranspiration Index with the Standardized Precipitation Index, a higher frequency of drought is observed, which is also probably due to effect of higher temperatures.

Finally, climatic factors were the main influence (63.1% – 80% climate contribution) behind the observed streamflow reduction at the end of the 1980s and 1990s in the Vedea, Argeş, Ialomiţa and Buzău catchments, but anthropic factors also contributed (19.8% – 36.9%).

It is important to have a critical approach by acknowledging the limitations of this research, hence stimulating further improvement work. Firstly, each data source (climatic, hydrological, vegetation) has its own availability limitation and accuracy issues. Climatic and hydrological data could be affected by the various uncertainties related to the measuring errors (instrument or human-related), missing data and the methods used to gap-fill them. Secondly, the study was limited also by the temporal and spatial availability of climatic and hydrological data, as we intended to use mostly publicly available datasets. Specifically, there is a limited number of meteorological stations with an open access data policy for climate data within the study area. Similarly, for hydrological data, there is a temporal limit of access to the time series. Thirdly, the study is limited mostly to a monthly and annual temporal resolution and did not investigate hydroclimatic drought indicators at a finer time scale.

In addition to these limitations, modelling could be affected by the inherent sources of errors. For example, the results of the CWD modelling inherit the uncertainties of the different data sources and are limited by the fixed available water capacity parameter. Moreover, the catchment water balance was estimated in a simplified way, as it did not account for water storage changes or artificial inputs and outputs in the system.

In the next section (**Part III**), the consequences of meteorological drought periods previously identified in the 2001 – 2020 period will be further explored in relation to overall vegetation health response using remote sensing methods.

PART III

DROUGHT IMPACT ON VEGETATION

This part presents the results of the investigations on vegetation dynamics as responses to drought variability in south-eastern Romania. In the first chapter (**Chapter 6**), the methodology used in this part is presented. In the second chapter (**Chapter 7**), the analysis regarding vegetation trends and their differences between land covers is performed at the regional level. The last chapter (**Chapter 8**) focuses on the study at the local level. A comparative analysis of broadleaf forest vegetation responses to drought is made between five selected areas corresponding to different ecoregions representing the region's different ecological conditions for the 2001 – 2020 period and more detailed in two drought periods (2007 – 2008 and 2019 – 2020).

6. METHODOLOGY FOR ASSESSING DROUGHT IMPACT ON VEGETATION

This chapter first presents the delineation of the study area and the characteristics of the five selected sample sites (**Chapter 6.1**). This is followed by a description of the vegetation data used in this part (**Chapter 6.2**) and by the methods and techniques to process and analyse the data (**Chapter 6.3**).

6.1. Study area at the regional scale and sample sites

At the regional scale, the drought impact on vegetation dynamic is considered in the same study area defined in **Chapter 2.1**, excluding the Buzău catchment.

In addition to the analysis at the regional land cover level, the response of broadleaf forests to drought occurrence was explored in different ecoregions of the study area. Existing literature points towards the importance of drought impact and climate warming on broadleaf forests in southern Romania, as reviewed in **Chapter 1.3**, thus highlighting the relevance of analysing this vegetation type (**Figure 6.1**).

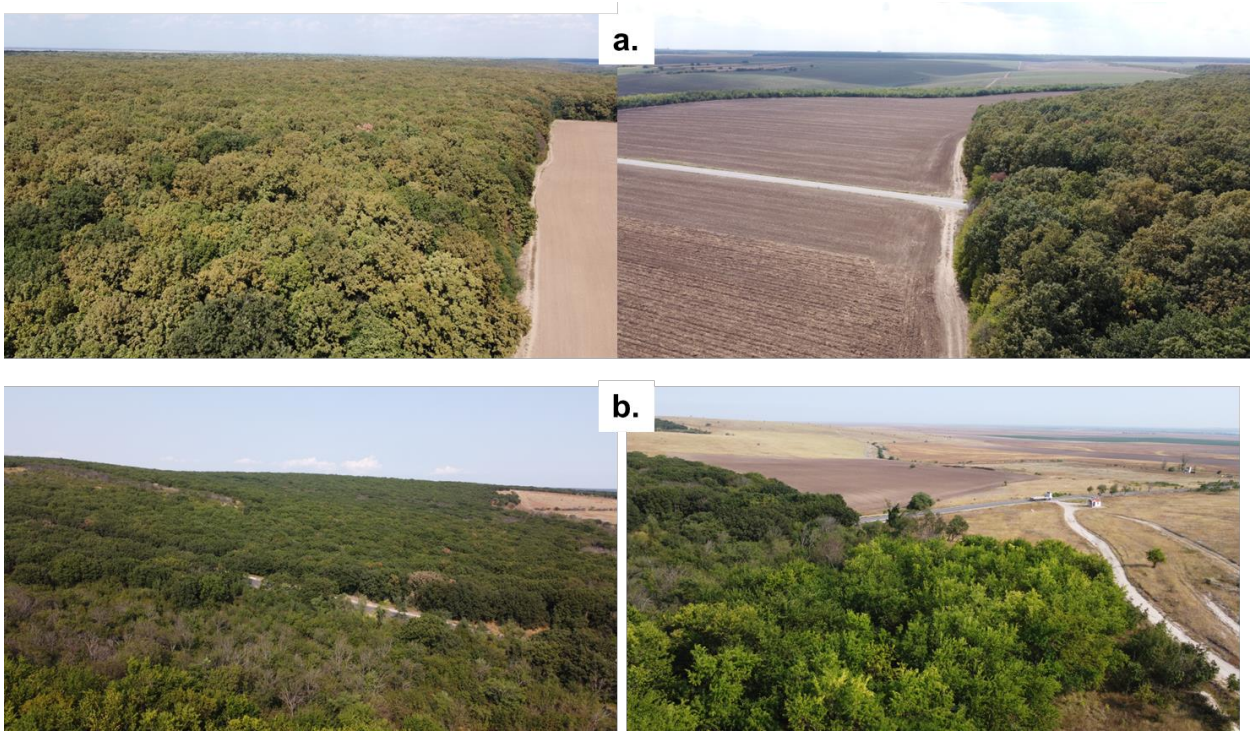

Figure 6.1 Comana (a.) and Babadag broadleaf forests (b.) (drone photography taken by Maria-Alexandra Chelu)

Moreover, these areas are selected to be included for the most part in a protected area to minimize the influence of human intervention and to retain the climatic signal influencing the vegetation dynamics to the greatest degree possible. Because of the lack of detailed spatial data on the distribution of crops, a more detailed analysis could not be performed for cropland.

The ecological regions dataset used is the Terrestrial Ecosystems of the World, distributed by WWF (Olson et al., 2001). Five major ecoregions are represented in the study area: Pontic steppe, East European Forest Steppe, Central European Mixed Forests, Balkan Mixed Forests, and Carpathian Montane Forests. The representative study sites selected within these five ecoregions are (**Figure 6.2** and **Table 6.1**):

- Babadag Forest *(Pădurea Babadag),* in the Pontic Steppe ecoregion;
- Ialomița Corridor (*Coridorul Ialomiței)*, in the East European Forest steppe;
- Comana Forest (*Pădurea Comana*), within the Comana Natural Park (*Parcul Natural Comana*) and surrounding forests (in the Balkan Mixed Forests ecoregion);
- Cândești Forests in the Southern Cândești Piedmont Forests (*Pădurile din Sudul Piemontului Cândești)* protected area and in surrounding areas, for Central European Mixed Forests;
- broadleaf forests in the Bucegi Mountains for Carpathian Montane Forests.

Table 6.1 Characteristics of the five selected study areas

Study area	Terrestrial ecoregion (Olson et al., 2001)	Morphological units (Posea and Badea, 1984) and average altitudes of sample areas	Natura 2000 protected areas[1]	Forest habitat distribution[2]
Babadag Forest	Pontic Steppe	Babadag Plateau and Casimcea Plateau, subdivisions of the Dobrogea Plateau; 224 m.a.s.l.	Northern Dobrogea Plateau (*Podișul Nord Dobrogean*, ROSCI0201) and Babadag Forest (*Pădurea Babadag*, ROSPA0091)	Eastern white oak woods (91AA), Euro-Siberian steppic woods with *Quercus* spp. (91I0), Dacian oak-hornbeam forests (91Y0), Pannonian-Balkanic turkey oak-sessile oak forests (91M0), *Salix alba* and *Populus alba* galleries (92A0)

[1] Ministerul Mediului, "Arii naturale protejate", Accessed 4 July 2022, http://www.mmediu.ro/articol/arii-naturale-protejate/33
[2] European Environment Agency, "Habitat types search", Accessed 4 July 2022, https://eunis.eea.europa.eu/habitats.jsp

Study area	Terrestrial ecoregion (Olson et al., 2001)	Morphological units (Posea and Badea, 1984) and average altitudes of sample areas	Natura 2000 protected areas[1]	Forest habitat distribution[2]
Ialomița Corridor	East European Forest Steppe	Vlăsia Plain and Titu-Sărata Plain in the Ialomița Plain; Bărăgan Plain, subdivisions of the Romanian Plain; 63 m.a.s.l.	Ialomița Corridor (*Coridorul Ialomiței*, ROSCI0290 and ROSPA0152)	Riparian mixed forests of *Quercus robur*, *Ulmus laevis* and *Ulmus minor*, *Fraxinus excelsior* or *Fraxinus angustifolia*, along the great rivers (Ulmenion minoris) (91F0), Euro-Siberian steppic woods with *Quercus* spp. (91I0), *Salix alba* and *Populus alba* galleries (92A0)
Comana Forest	Balkan Mixed Forests	Gănvanu-Burdea Plain, Burnas Plain, subdivisions of the Romanian Plain; 88 m.a.s.l.	Comana (ROSCI0043 and ROSPA0022)	Euro-Siberian steppic woods with *Quercus* spp. (91I0), Pannonian-Balkanic turkey oak-sessile oak forests (91M0), Dacian oak & hornbeam forests (91Y0)
Cândești Forests	Central European Mixed Forests	Cândești Piedmont and Prahova Subcarpathians; 354 m.a.s.l.	Southern Cândești Piedmont Forests (*Pădurile din Sudul Piemontului Cândești*, ROSCI0344)	*Asperulo-Fagetum* beech forests (9130), *Galio-Carpinetum* oak-hornbeam forests (9170), Pannonian-Balkanic turkey oak-sessile oak forests (91M0), Dacian oak & hornbeam forests (91Y0)
Bucegi Forests	Carpathian Montane Forests	Bucegi Mts. – Postăvaru Mountains (southern part of the Bucegi massif, Gurguiatu Mts., southern Leaota Mts.); 956 m.a.s.l.	Southern part of Bucegi (ROSCI0013)	*Luzulo-Fagetum* beech forests (9110), *Asperulo-Fagetum* beech forests (9130), *Tilio-Acerion* forests of slopes, screes and ravines (9180), Alluvial forests with *Alnus glutinosa* and *Fraxinus excelsior* (*Alno-Padion*, *Alnion incanae*, *Salicion albae*) (91E0*),* Dacian Beech forests (*Symphyto-Fagion*) (91V0), Acidophilous *Picea* forests of the montane to alpine levels (*Vaccinio-Piceetea*) (9410), Alpine *Larix decidua* and/or *Pinus cembra* forests (9420)

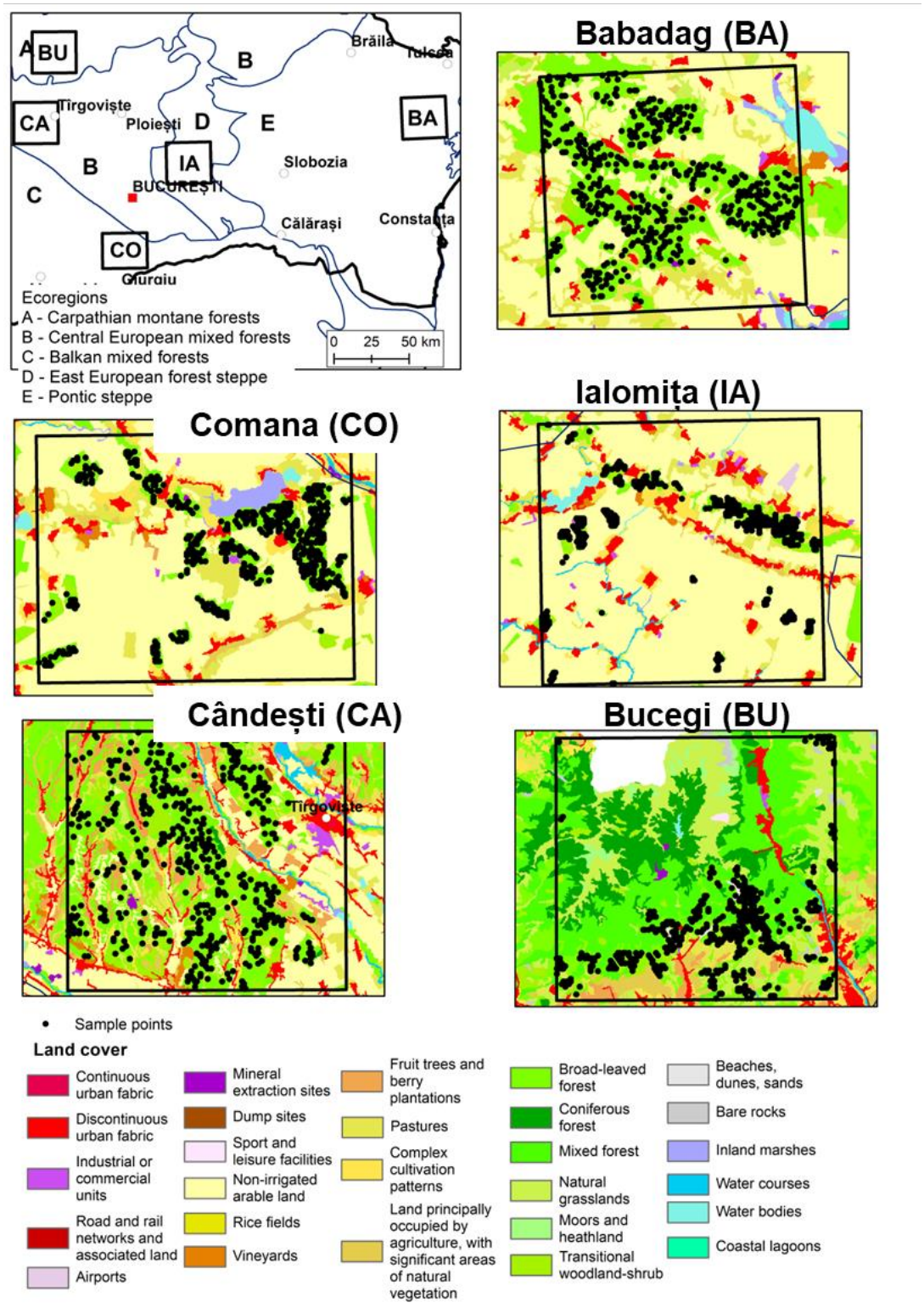

Figure 6.2 Sample sites selected within the study area and 500 random sample points in the broadleaved forests. BA – Babadag Forest; CO – Comana Forest; IA – Ialomița Corridor; CA – Cândești Forests; BU – Forests in the Bucegi Mountains.

6.2. Data and tools

The analyses in this part are mainly based on satellite image processing. The Normalized Difference Vegetation Index (NDVI) from the Moderate Resolution Imaging Spectroradiometer (MODIS) MOD13Q1 product from the Terra platform (Didan, 2015) was used to explore surface vegetation dynamics between 2001 – 2020. The MOD13Q1 product has a 16-day temporal resolution and a 250 m spatial resolution. Another indicator, the Enhanced Vegetation Index, could have been used because it has several advantages over the NDVI — it is less sensitive to background reflectance and has fewer saturation effects at high biomass (Rocha and Shaver, 2009). However, the NDVI was selected in this study because it is the most common indicator to evaluate biomass vigour in drought monitoring so that it could allow comparison with other studies.

The data were downloaded and processed using the R package *MODIStsp* (Busetto and Ranghetti, 2016). *MODIStsp* allowed downloading the data as GeoTiffs in the WGS 84 coordinate system (EPSG:4326) for the area bounded by 24.399879 (West), 28.972189 (East), 43.685805 (South), 45.593889 (North), applying the Scale/Offset option, and finally obtaining the time series as an R Raster Stack.

The Corine Land Cover (CLC) raster with 100 m spatial resolution was used to extract the land covers for the years 2000 and 2018 (EEA, 2019a,b).

Data regarding yield (in tons) and cultivated area (in hectares) between 2001 – 2020 for the main crops (maize, winter wheat, sunflower) at the county level was downloaded from TEMPO Online, the open-access database of the National Institute of Statistics.

6.3. Methods

This chapter presents the methods and techniques used in Part III. The data processing steps for evaluating the response of vegetation to drought are schematized in **Figure 6.3**. Firstly, the data was processed by interpolation for missing data and smoothing (**Chapter 6.3.1**). The MODIS pixels to be analysed were then selected based on the existence of stable land cover between 2000 and 2018 (**Chapter 6.3.2**). Next, vegetation was analysed at the regional level in terms of trends (**Chapter 6.3.3**), anomalies (**Chapter 6.3.4**) and in five selected sample areas using

multiple statistical tests (**Chapter 6.3.5**, **Chapter 6.3.6**). Finally, the methodology to identify phenological metrics based on MODIS data is presented in **Chapter 6.3.7**.

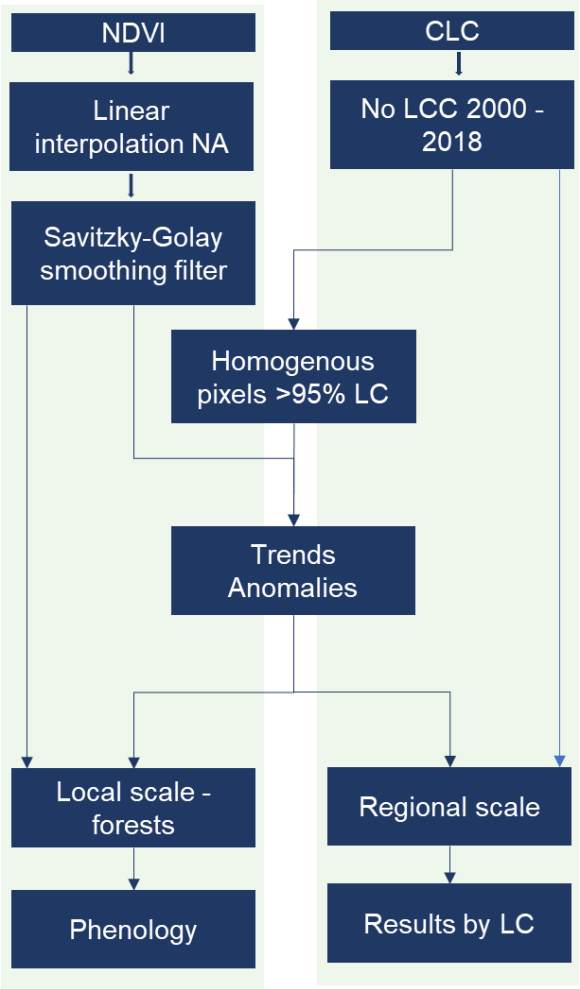

Figure 6.3 Processing steps of the Normalized Vegetation Index (NDVI) and the Corine Land Cover (CLC) to assess the response of vegetation to drought. NA = Not available (missing pixels). LC = Land Cover.

6.3.1. Interpolation and smoothing

The missing data was gap-filled using linear interpolation (function *approxNA* from the package *raster* in R programming language). Next, the data were filtered with a Savitzky-Golay Filter (SGF) (Chen et al., 2004; Savitzky and Golay, 1964), using a filter order of one and a window length of three. The usefulness of the SGF in smoothing vegetation indices was demonstrated in previous studies for reducing the noise in time series caused by atmospheric effects or sensor issues

(Arvor et al., 2008; Leroux et al., 2019; Li et al., 2020; Zhang et al., 2013). These parameters were subjectively chosen by comparing the climatology of the unfiltered NDVI from several extracted pixels (in forest and grassland coverages) with the climatology of the NDVI of the same pixels, filtered using various windows. The main criterion was maintaining the average NDVI's shape and not excessively smoothing the data. For example, an SGF window of three was used by Bart et al. (2017) for filtering the MOD13Q1 NDVI to analyse grassland phenology. An example of filtering using the unfiltered and filtered average NVDI in the forest of Comana is shown in **Figure 6.4**.

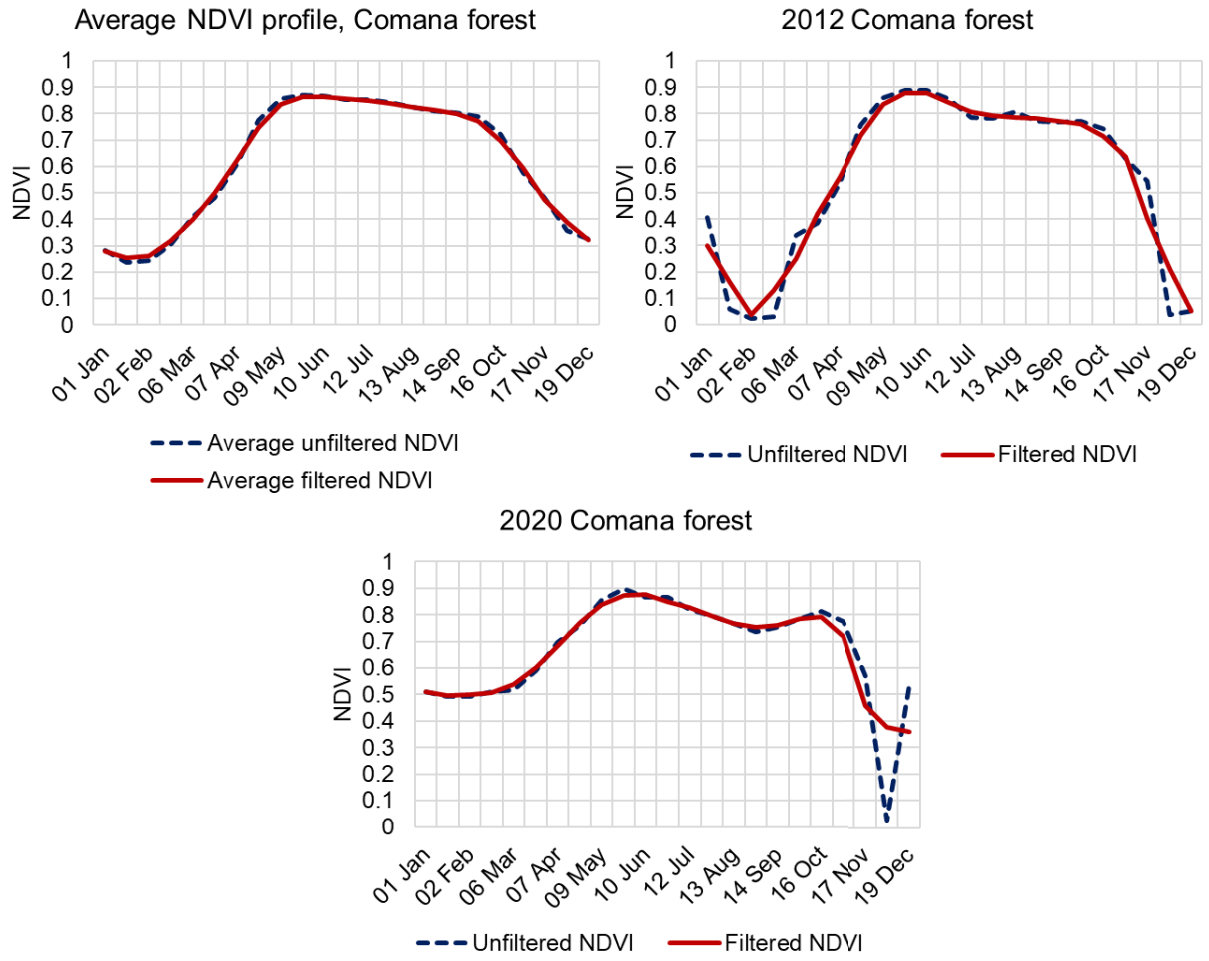

Figure 6.4 Comparison between raw NDVI and NDVI filtered with the Savitzky-Golay filter in the Comana Forest

6.3.2. Identification of stable pixels

Firstly, pixels that have not changed their land cover for the period of interest and whose land cover class covered the MODIS pixel by a minimum of 95% were identified. For this, land cover data from the CLC classification was used for the years 2000 and 2018, the most recent. A difference between CLC2018 and CLC2000 was made, and the CLC pixels whose land cover changed were discarded. In addition, a spatial analysis was made between CLC and NDVI pixels to identify those NDVI pixels that were covered by at least 95% of the same land cover. The regional analysis was performed further in the following land covers: *arable land* (*non-irrigated arable land* - 211 and *rice fields* - 213), *pastures* (231), *broadleaved forests* (311), *coniferous forests* (312), *mixed forests* (313), *natural grasslands* (321), and *inland marshes* (411). The numbers between brackets refer to the CLC codes.

6.3.3. Estimating monthly and growing season trends

To generate monthly series, the maximum NDVI of each month between 2001 – 2020 was selected. Trends in NDVI were calculated for each pixel, using the Mann-Kendall trend test (Kendall, 1975; Mann, 1945) for the monthly series and the average during the growing season of each year (April to October).

6.3.4. Estimating NDVI standardized anomalies

The anomalies were calculated for the monthly, biweekly, and growing season series as simple anomalies and standardized anomalies relative to the 2001 – 2020 average.

6.3.5. Assessing local drought response in broadleaf forests

6.3.5.1. Selection of drought years

To explore the differential response of forest vegetation during drought periods, the drought years were selected based on the station-CWD_{CRU} (**Chapter 3.3.2**). An anomaly of the total CWD during the vegetation period (April – October) was computed at the meteorological stations to obtain a synthetic and comparable index of the deficit in the study area (**Figure 6.5**). Positive values indicate a deficit above average conditions, while negative values show less deficit (therefore less water stress). The most relevant years and periods in which most stations experienced deficit above average conditions were 2003, 2007 – 2009, 2011 – 2012, 2015, and

2018 – 2020. These years were selected to compare if the response of vegetation to drought conditions was significantly different between the five study areas. In addition, the droughts of 2007 – 2008 and 2019 – 2020 were analysed further.

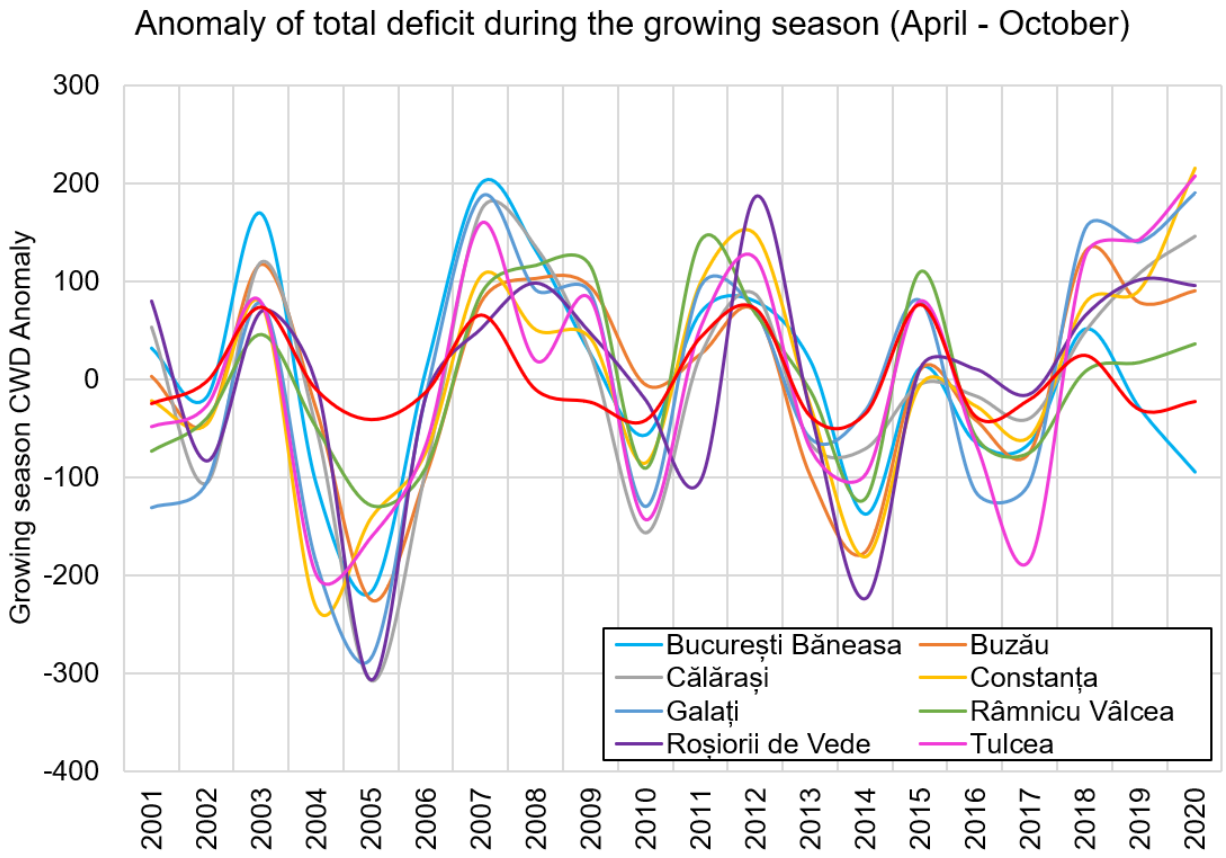

Figure 6.5 Anomaly of the total station-CWD_{CRU} during the growing season (April – October), relative to the 2001 – 2020 average

6.3.5.2. Sampling of NDVI in the study sites

Five hundred random points were selected for the broadleaved forests in each of the five sample areas, using the stable pixels as constraining shapes. This sampling was selected for having equal sample pixels in the five areas. These were used further to extract the anomaly of the mean growing season (April – October) NDVI from the Savitzky-Golay filtered MODIS 250 m data.

6.3.5.3. Statistical testing of differences in the response of NDVI

The growing season NDVI anomalies, extracted from the 500 sample points, were checked for each selected year with drought and study site to explore whether they had a normal distribution

using the Shapiro-Wilk normality test (Shapiro and Wilk, 1965). The homogeneity of variance across study zones was also checked for each year using Levene's test (Levene, 1960).

The Kruskal-Wallis test (Kruskal and Wallis, 1952) was used to explore whether there are statistical differences between the study areas for each selected drought year for these NDVI anomalies. Dunn's multiple comparison test (Dunn, 1964) with the Bonferroni Adjustment (Bonferroni and Bonferroni, 1935) was used to identify between which groups there are statistically significant differences.

6.3.6. Correlations between NDVI anomaly and CWD

Correlations between monthly NDVI anomaly (relative to the 2001 – 2020 period) and monthly CWD were performed for each month between April – October using Pearson's correlation coefficient, at the 0.05 significance level, for each study site. NDVI was extracted as the average of the 500 sample points in the broadleaf forest stable pixels. To compare the different CWD time series, the average NDVI was correlated with the CWD obtained through three methods: 1) the mean *raster-CWD* (described in **Chapter 5.1.2**), computed as an areal average of the gridded dataset in the areas covered by forests for each study site; 2) the *station-*CWD_{CRU} (**Chapter 3.3.2**) at the closest meteorological stations; 3) the *station-*CWD_{Turc} (**Chapter 3.3.2**) at the closest meteorological stations.

6.3.7. Phenological metrics

The 16-day NDVI filtered with SGF was used further to obtain phenological metrics and anomalies in each study area and to explore the influence of drought on phenological variation. The *greenbrown* package was used in R to calculate phenological metrics (Forkel and Wutzler, 2015; Forkel et al., 2013, 2015), such as the Start of Season (SOS) and End of Season (EOS). There are multiple methodologies available for performing this step. The *greenbrown* package offers the possibility of using multiple algorithms for smoothing data and deriving phenology.

For smoothing the data for extracting phenological metrics, two methods were used from the *greenbrown* package: *linear interpolation* and *splines*. Splines, Savitzky-Golay or local regression methods could capture the variability of ground-measured NDVI during the vegetation period when applied to MODIS NDVI (Cai et al., 2017). The spline method aims to minimize a mathematical function by finding the spline function for a particular smoothing parameter (Cai et

al., 2017). Spline smoothing is a simple method, requiring fewer computational resources and having few assumptions about the underlying data variability (Musial et al., 2011). The cubic spline is implemented in *greenbrown* package (Forkel and Wutzler, 2015). The linear method gap-fills the data through linear interpolation and smooths the data with a running median filter with a window-size of three (Forkel and Wutzler, 2015; Forkel et al., 2015). A disadvantage of the linear-median filter method is that it can generate abrupt variations in the data (Forkel et al., 2015).

Identification of the most suitable algorithm for determining phenological metrics would be performed ideally by validation with ground measurements, but this is difficult at large scales and when this data is lacking. Moreover, fitting a phenological method with region-specific ground data could result in incorrect phenological estimations when applied to other regions (Forkel et al., 2015). Therefore, using multiple phenological identification methods is preferrable.

Two phenology extraction methods were used: *white* and *deriv*. The *white* approach (White et al., 1997) estimates the SOS and EOS based on a threshold of 0.5 in the upward direction (and downward direction, respectively) on the greenness curve represented by an $NDVI_{ratio}$, which takes the annual minimum and maximum into consideration. This method is motivated by the assumption that the fastest green-up (in spring) and senescence (in autumn) are at the 0.5 threshold (White et al., 1997). An advantage of this method based on the $NDVI_{ratio}$ is the applicability irrespective of location and land cover (de Beurs and Henebry, 2010).

The *deriv* approach estimates the first derivative of the greenness curve (Forkel et al., 2015; Tateishi and Ebata, 2004), and similarly to the *white* method, it assumes that the SOS and EOS occur during the fastest change in greenness. A lower threshold might be more accurate in estimating SOS (White et al., 2014), but it might also increase the risk of inaccuracy due to snow cover, clouds or soil reflectance (Forkel et al., 2015).

Both the threshold method (*white*) and the derivative method (*deriv*) have the disadvantage of not supplying the associated errors of the method, therefore making it challenging to interpret if the results stem from natural variability or significant changes (de Beurs and Henebry, 2010). Moreover, a drawback of the *deriv* method is that the identification of SOS and EOS is difficult when the greenness curve does not quickly increase or decrease, which can be made more challenging, particularly for EOS, due to maximum value compositing that can alter the senescence period in the NDVI profile (de Beurs and Henebry, 2010).

In the absence of ground measurements, one way of evaluating the phenological results from the multiple algorithms could be significant correlations with relevant climate variables such as temperature and precipitation (García et al., 2019). Therefore, we used the average preseason temperature for SOS (SOS preseason is defined here as February – March) and average preseason temperature and total precipitation for EOS (EOS preseason is defined here as September – October) as an attempt to select a physically relevant approach for each region. The Pearson correlation coefficient (with a statistical significance level at 0.05) was used to correlate climate variables and SOS and EOS. In Europe, the SOS of temperate forests is mainly influenced by temperature and light availability (Forkel et al., 2015). Therefore, it is likely that an earlier SOS in broadleaf forests would be associated with increased temperature during the preseason (Bórnez et al., 2021). The EOS response was less sensitive to climate and varied more geographically; however, an early EOS was generally associated with higher temperatures in the preseason (Bórnez et al., 2021).

Moreover, the count of pixels with missing results (NA – not available pixels) was made annually for each approach.

7. DROUGHT IMPACT ON VEGETATION AT THE REGIONAL LEVEL

This chapter focuses on the analysis based on the NDVI regarding vegetation stress at the regional level. Two main approaches are adopted to investigate changes in vegetation greenness. Firstly, the monthly trends are explored and discussed in the context of climate and phenological changes in **Chapter 7.1**. Secondly, the annual NDVI anomalies are investigated in **Chapter 7.2**. These are discussed in relation to the occurrence of drought and are analysed by land cover type.

7.1. Seasonal changes in vegetation activity

In this section, the NDVI monthly trends are explored for arable lands (**Chapter 7.1.1**), grasslands and pastures (**Chapter 7.1.2**) and forests (**Chapter 7.1.**3). These trends allow us to understand the drought occurrence within the larger context of seasonal vegetation dynamics and phenological changes.

7.1.1. Arable lands

This chapter first presents the distribution and dynamics of the cultivated surfaces and yields of the main crops in south-eastern Romania between 2001 and 2020 at the county level, based on data provided by the National Institute of Statistics. Afterwards, the spatial distribution of the monthly NDVI results in arable land (in stable pixels) is reported and summarized at regional and county levels. These results are then discussed in the context of phenological changes and climate change, with implications for seasonal water availability and the timing of drought. In addition, the seasonal trends in precipitation, temperature and CWD are analysed for the 2001 – 2020 period to understand better the climatic context of the identified changes in cropland. Finally, a literature summary of these main crops' potential future phenological changes is discussed.

7.1.1.1. Spatial distribution and trends in cultivated areas and yield of the main crops in south-eastern Romania

In south-eastern Romania, most of the arable lands are cultivated with cereals, particularly winter wheat (*Triticum aestivum* L.) and maize (*Zea mays* L.). Large surfaces are also cultivated with sunflower (*Helianthus annuus* L.). The spatial distribution of the cultivated surfaces of the main crops at the county level is illustrated in **Figure 7.1**. In 2020, wheat was the main crop in the counties along the Danube River (Olt, Teleorman, Giurgiu, Călărași), as well as in Ilfov, Argeș

and the counties in Dobrogea (Constanța and Tulcea) crop, whereas maize is the main crop in Dâmbovița, Prahova, Buzău, Brăila and Ialomița counties.

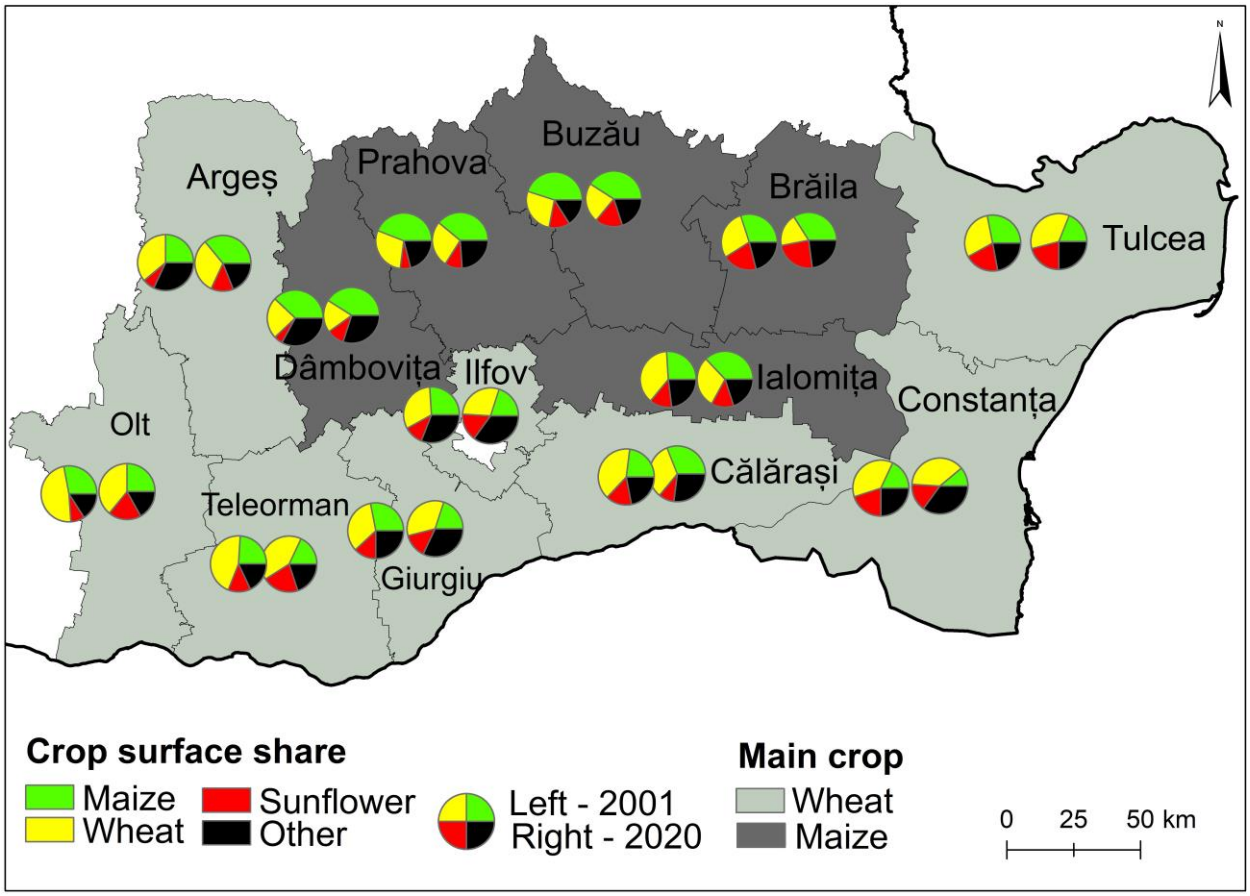

Figure 7.1 Distribution of the main crops at the county level in south-eastern Romania in 2001 and 2020. The regions in dark grey have maize as the main crop, and light grey shows wheat as the main crop (data from the National Institute of Statistics).

The linear trends between 2001 and 2020 for the annual surface proportion from total cultivated areas and yields of the main crops at the county level are summarized in **Table 7.1**. For maize, most counties show negative area trends, while for winter wheat and sunflower, most counties show an increase in surface share. Regarding yield, there is mainly a positive trend in all three main crops.

Table 7.1 Linear trends in the annual cultivated areas and yields of the main crops between 2001 – 2020

Counties	*Trend slope 2001 – 2020 for cultivated surfaces (as shares of total cultivated areas)*			*Trend slope 2001 – 2020 for yields*		
	Maize	*Wheat*	*Sunflower*	*Maize*	*Wheat*	*Sunflower*
Brăila	↓	↓	↑	↑	↑	↑
Buzău	↓	↑	↑	↑	↑	↑
Constanța	↓	↑	↓	↑	↑	↑
Tulcea	↓	↑	↓	↓	↑	↑
Argeș	↑	↑	↑	↑	↑	↑
Călărași	↑	↓	↓	↑	↑	↓
Dambovița	↓	↓	↑	↑	↑	↑
Giurgiu	↓	↑	↓	↑	↑	↑
Ialomița	↑	↑	↓	↑	↑	↑
Prahova	↓	↑	↑	↑	↑	↑
Teleorman	↓	↓	↑	↑	↑	↑
Ilfov	↓	↑	↑	↓	↑	↑
Olt	↓	↓	↑	↑	↑	↑

The sowing period for winter wheat is September – October, while harvesting is done in June – July. In southern Romania, the optimal period for sowing wheat is 25 September – 10 October (Roman et al., 2011). Wheat can be affected by drought both in autumn and spring. Water requirements increase in spring and are the highest during flowering and grain-filling (Ion, 2010). Negative impacts on winter wheat occur especially due to heat and water stress in May – June (ANM, 2014). For winter wheat, the average growing season is about 274 days at Buzău and 284 days at Grivița meteorological stations (ANM, 2014).

For maize, the growing season is between April and September. The sowing period is usually between 1 – 15 April in south and south-eastern Romania in steppe areas and between 10 – 20 April in the forest-steppe (Roman et al., 2011), while the harvesting is done in August – September. Maize is a thermophilic crop, but high temperatures in July and August impact yield. The effects are severe if hot temperatures are associated with drought periods. Temperature is the driving meteorological factor during the first phenological phases, considering the soil water accumulated during the cold season (Vâtcă et al., 2021). Due to increased water requirements, water availability becomes crucial between June and August, particularly in July – August. The critical period for water requirements is between 10 – 20 June and 10 – 20 August (Ion, 2010;

Panaitescu et al., 2012). Drought associated with hot temperatures during flowering and grain development, when maize is highly sensitive, negatively influences production. Precipitation is less important in September, as this month coincides with the end of the growing season. In southern Romania, the vegetation period of maize requires between 110 – 155 days. For maize, the average growing season is 138 days at Buzău and 148 days at Grivița (ANM, 2014).

For sunflower, the sowing period is between 25 March – 5 April (Ion, 2010), and the harvesting is in August – September. The highest water requirements for sunflower are in the flowering period, which develops in June and the first part of July (Ion, 2010).

7.1.1.2. Monthly trends of NDVI in arable lands

The monthly trends in the variations of MODIS NDVI for arable lands between 2001 – 2020 are shown in **Figure 7.2**. A pattern that stands out is the contrast between the predominantly positive NDVI trends in the spring and the beginning of summer (in June) and extended decreasing trends in August and September. For example, more than 45% of the pixels had positive trends in May. On the contrary, about 38% of pixels had negative trends in September.

For most of the spring months, there are primarily positive trends. In April, there is a higher density of positive trend pixels in the Dobrogea Plateau and the eastern and southern Romanian Plain. In May, the month with the most positive trends, the density of significant pixels increases in most areas with cropland, which is particularly dense in Central Bărăgan. In June, there is a transition of the positive trends (**greening** process) towards the centre and west, where the positive trends appear mainly in the northern and western parts of the Romanian Plain, particularly in Central Bărăgan, Brăila Plain, Titu-Sărata Plain, in the Argeș Floodplain and Prahova's Piedmont Plain (landform names according to Posea (2005).

This pattern was reversed in July, August, and September — extensive negative trends developed in arable lands. In July, the negative trends occur mainly in the Dobrogea Plateau (especially in the central part) but also in the southern Romanian Plain (Central Bărăgan, Vlăsia Plain, Găvanu-Burdea Plain, Boianu and Burnas Plains). In contrast, some positive trends are concentrated in the Danube Floodplain and the northern parts of the Romanian Plain. In August and September, there are predominantly and extensive negative trends in NDVI variability for

arable lands in the Romanian Plain and the Dobrogea Plateau and in contrast, there are only a few patches of positive trends in the Danube Floodplain.

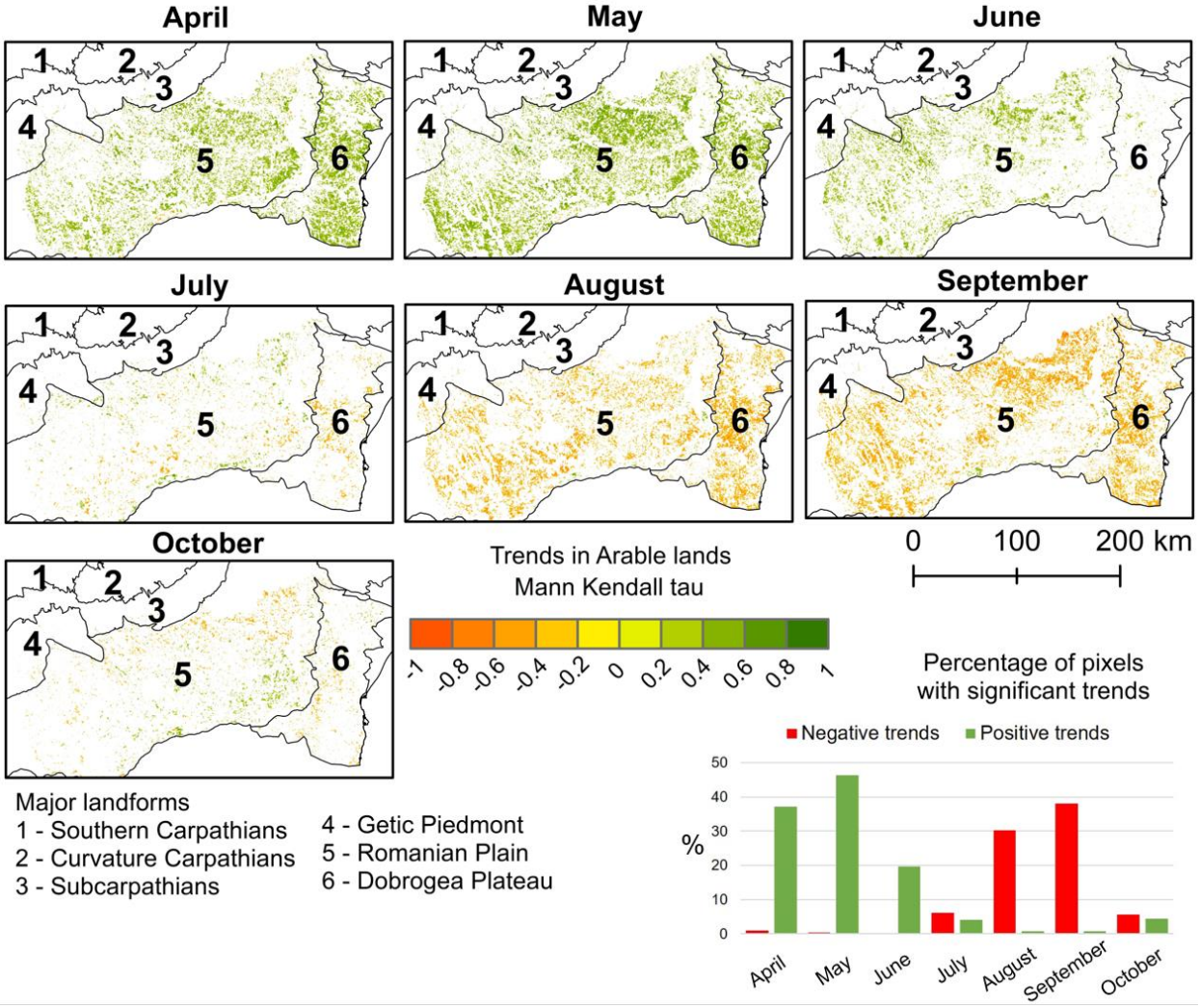

Figure 7.2 Significant monthly NDVI trends in arable lands between 2001 – 2020 in stable pixels. The graph shows the percentage of pixels with significant trends from the total stable pixels of arable lands.

In October, the situation shifted towards fewer pixels with significant trends, with about the same shares (less than 10% of pixels either positive or negative). Greening trends are found mainly in the southern parts of the Romanian Plain (especially in Southern Bărăgan Plain), and decreased trends (**browning** process) are concentrated in southern and central parts of the

Dobrogea Plateau, in the north and west of the Romanian Plain and sparsely in the Danube Floodplain.

Additionally, the temporal distribution of trends was summarized by county (**Figure 7.3**). It was calculated as the proportion of significant monthly trends (April to September) relative to each county's total number of stable arable land pixels. The trends were related to the number of pixels present in each county because not all counties had data for their entire surface, depending on how they were included in the NDVI data boundary.

The highest percentages of positive trends (greening) appear in Constanța in April and May (over 60% and over 50%, respectively, of arable lands) and in Buzău county in May (over 60%). The highest percentages of negative trends (browning) appear in Constanța in August and September (almost 50%), in Brăila in September (50%) and in Buzău county in September (60%).

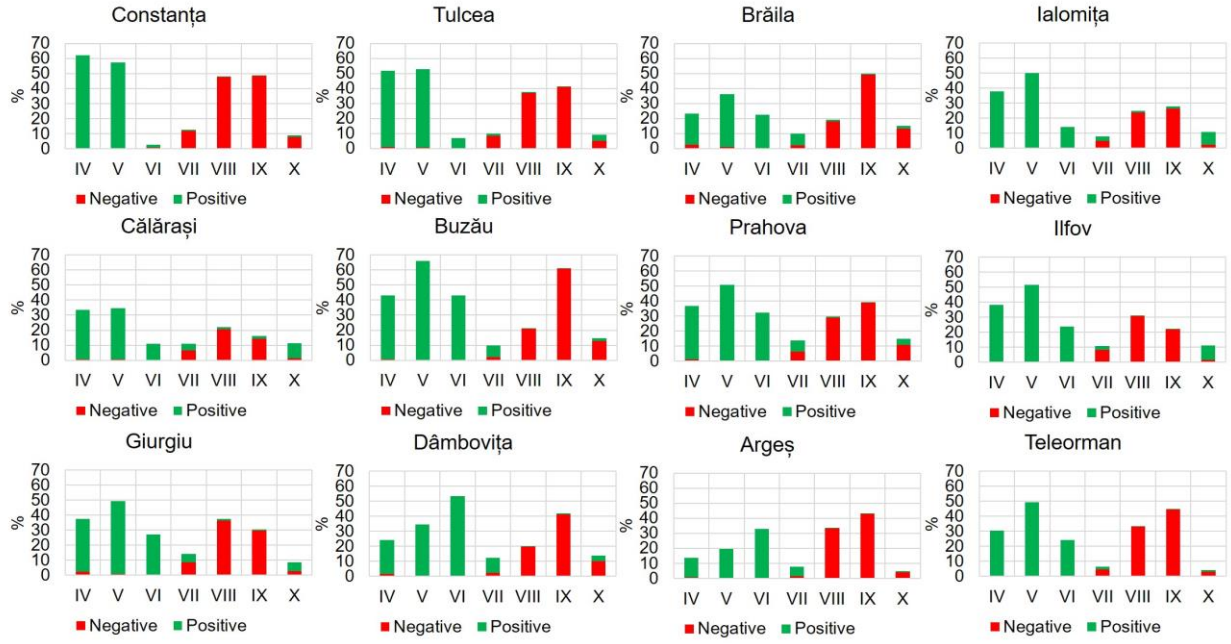

Figure 7.3 Percentage of positive and negative trends (2001 – 2020) in NDVI from the total of stable pixels (present in the study area) in arable lands by county between April and October

These results suggest a change in the phenology of agricultural vegetation, which could have implications regarding the timing of drought for water stress on plants.

Similarly, an analysis based on the Drought Severity Index (DSI), which takes into account evapotranspiration, potential evapotranspiration and the NDVI showed positive values in the

Bărăgan Plain between 30 March – 27 July, and in contrast, negative values between 28 July – 29 September, thus underlining some of the results found in our study (Angearu et al., 2020).

7.1.1.3. Discussion on the observed changes in the phenology of the main crops

The results above are consistent with the observed trends of an earlier spring activity and are likely related to warming. Even though it has been observed that the rate of advancement in phenological phases has decreased in the last decades as a response to the change in the temperature increase rate (Menzel et al., 2020), a positive trend in NDVI at the beginning of the growing season in cropland can suggest that the earlier spring trend has continued between 2001 – 2020.

Multiple processes determine crop response to climate change: shorter periods for grain filling, increased water use efficiency due to higher CO_2 concentration which could be beneficial in conditions of water limitation, as well as decisions of farmers, such as modifications in the planting date or cultivar change (Harrison and Butterfield, 1996).

The advance of the growing season onset between 1961 – 2010 was noticed in Romania in a study based on mean temperatures and the histophenogram method, but also a lengthening of the potential growing season and the phenological phases, especially after 1981, except the fruiting and dissemination phases which were reduced (Bandoc et al., 2022). Between 1971 – 2006, temperature-based simulations indicated an advancement of anthesis and maturity phases in winter wheat in Romania (Croitoru et al., 2012). However, a shorter period for crop growth cycles is expected due to warming (Sima et al., 2015). Increased temperatures can accelerate crop growth, which decreases biomass development time, which could negatively influence yield (Jacobs et al., 2019; Sima et al., 2015). For example, a shorter generative period in crops and a shorter farmers' season were observed after 1989 in Germany, Austria and Switzerland (Menzel et al., 2020). For wheat, a shorter crop growth cycle was observed in France (Beauvais, 2022). A shorter vegetative period was also noticed in Germany (Rezaei et al., 2018).

As mentioned before, the observed NDVI greening trends in spring could result from advanced crop phenological phases, which the interaction between warming and farming decisions could determine. For example, observations between 1950 – 2013 in winter wheat in Germany

showed an earlier heading and flowering related to temperature and modern cultivar choice (Rezaei et al., 2018). Some farmers in Normandy have noticed an earlier seeding date and an advance of the harvest date in wheat (Beauvais, 2022). In maize, a shift towards earlier sowing has been observed in Germany in response to higher temperatures, even though the yield was limited by cold spring weather and adaptation options such as cultivar choice (Parker et al., 2017). Similarly, an advancement in farmer activity in spring (sowing and leafing), which was related to increased temperature, was observed in Germany, Austria and Switzerland in the last two decades, particularly between mid-May and mid-June (Menzel et al., 2020).

Cultivar choice is an essential factor for crops and phenology. Agroclimatic experts have noticed important modifications in the Pannonian zone (where Romania, Bulgaria, Hungary and Serbia were included) in the cultivation timing to avoid heat and water stress, as well as the usage of new cultivars (Olesen et al., 2011). Due to the critical impact of climate change on crops in Romania, a set of financed measures, among which modifying the time of sowing, were suggested for farmers (Jacobs et al., 2019; MADR, 2015). In Romania, a study on the farmers' perception of climate change in the Bărăgan region showed that they adopted adaptation measures such as the annual use of a mix of cultivars – Romanian varieties of drought-resistant cultivars and foreign varieties that perform well in normal conditions (Sima et al., 2015). In winter wheat, one study showed that yield in newer cultivars increased between 1991 – 2012, in contrast to old (control) cultivars, suggesting adaptation through an earlier phenological development and a decreased sensitivity to heat stress in the grain-filling phase (Marinciu et al., 2013). A significant influence of total precipitation between April and June and yield in both new and old cultivars was observed, and it was higher in the new cultivars (Marinciu et al., 2013). Overall, earlier plant and farming activities could also have contributed to the observed greening trends.

Earlier phenology has implications for water availability for plants by shifting the phases towards periods with different rainfall conditions that could benefit (by taking advantage of improved soil water reserves) or threaten crop yields in rainfed systems when transitioning towards a season with less precipitation (Harrison et al., 2011; Jacobs et al., 2019). These modifications towards earlier phenological phases could mitigate climate impact by avoiding drought and heat stress during critical phases (Rezaei et al., 2015; Semenov et al., 2009). Marinciu et al. (2013) suggested that the advanced heading did not affect yield in the new wheat cultivars in southern

Romania due to avoiding the heat stress period. Shifting agricultural activities could also mean taking advantage of improved soil water reserves.

Negative trends in NDVI occur on large surfaces in August and September. These trends could be related to the shifted phenological calendar and possibly earlier harvesting. A trend towards earlier farming activity in summer has been observed in Central Europe in the last two decades, particularly between mid-June to mid-September, also related to warming (Menzel et al., 2020). Future changes in the crop calendar suggest a shift of the ending of wheat harvesting towards the end of June, a shift towards the end of maize harvesting towards August and an end of sunflower harvesting towards mid-August (Sima et al., 2015).

The NDVI trend results showed some positive trends in greenness in October in some regions (**Figure 7.2** and **Figure 7.3**), which could be due to earlier agricultural activity. For example, other authors showed that autumn farmers' activity (autumn sowing, germination and leafing) in Germany, Switzerland and Austria had mainly an advancing trend, and the earlier activity anomalies were noticeable starting in October (Menzel et al., 2020).

7.1.1.4. Changes in the relevant climatic parameters influencing the main crops in the study area during the 2001 – 2020 period

As previously mentioned, multiple potential factors could be responsible for the observed greening trends in cropland in spring, but the temperature is recognized as the primary driver of earlier spring phenology (Menzel et al., 2006; Post et al., 2018; Wolkovich et al., 2012). Earlier onsets of phenological phases in response to temperature increase have been observed in maize (Harrison et al., 2011; Parker et al., 2017), winter wheat (Rezaei et al., 2018) or sunflower (Tariq et al., 2018).

The temperature trends for the 2001 – 2020 period at the main meteorological stations relevant for areas with crops in the study area are presented in **Table 7.2**. Results show that the warming trend continues for this period, but the trends are mostly insignificant, which could be due to the shorter analysis period. In winter, the trend slopes are higher than in spring or summer, showing a faster temperature increase for this period. Significant trends occur is summer in the eastern part of the study area, at Galați, Constanța and Tulcea stations.

Table 7.2 Mann-Kendall trend (T), the significance of trends (denoted with an asterisk) and Sen's Slope (S, in ºC/year) for the average temperature in winter (December, January and February [DJF]), spring (March, April and May [MAM]) and summer (June, July and August [JJA]) for the 2001 – 2020 period at meteorological stations in the study area

		Roșiorii de Vede	București Băneasa	Buzău	Călărași	Galați	Constanța	Tulcea
DJF	**T**	+	+	+	+	+	+	+
	S	0.14	0.14	0.12	0.14	0.12	0.13	0.11
MAM	**T**	+	+	+	+	+	+	+*
	S	0.02	0.07	0.04	0.04	0.05	0.06	0.06
JJA	**T**	+	+	+	+	+*	+*	+*
	S	0.04	0.04	0.04	0.04	0.06	0.05	0.06

Crops' condition is correlated to water availability (precipitation, soil moisture) at short-term scales (Angearu et al., 2020; Dobri et al., 2021; Páscoa et al., 2020). Most arable lands are rainfed, highlighting crop productivity's dependence on climatic conditions. In the Oltenia Plain (located in the south-west of Romania), for example, correlations between crop yield (wheat, maize, sunflower) and SPI of the corresponding growing season became significant after 1990 due to a decreased use of irrigation (Onțel and Vlăduț, 2015).

A study based on NDDI (Normalized Difference Drought Index, which integrates NDVI and the Normalized Difference Water Index, a measure of agricultural drought) in croplands in Romania showed low correlations between NDDI and same-month precipitation in March and April (Dobri et al., 2021) between 2001 – 2020. However, from mid-May towards mid-August, the authors found increased importance of same-month (the highest at the end of May) and 1-lagged correlations (highest at the end of June) between NDDI and precipitation, whereas the 2-lagged correlations were higher from the end of June towards September. At the growing season scale, there were negative correlations between NDDI and precipitation in most of the region; these were statistically significant, except for some areas with increased water availability (Danube floodplain and some small irrigated areas) (Dobri et al., 2021).

Soil moisture anomalies are positively correlated to NDVI, and the relationship is stronger between July – September in contrast to April – June (Onțel et al., 2021). This could suggest that water is not a limiting factor during spring due to sufficient water reserves, while it becomes a determining factor in summer.

Regarding climatic water availability in spring, for the long-term period of 1961 – 2020 (as mentioned in **Part II**), the SPI-3 in May showed mostly statistically insignificant trends — positive in the south-east and negative in the west, north-west and the Danube Delta. On the other hand, in the same period, the CWD showed significant increases in May at Galați and Sulina meteorological stations.

In the case of the 2001 – 2020 sub-period (**Table 7.3**), there is generally an increase in water availability *in spring* (total precipitation and decrease in total deficit) in the western and central part of the study area (at Roșiorii de Vede, București Băneasa and Buzău). In contrast, the stations located on the eastern side show the opposite (Galați, Constanța, Tulcea). Călărași shows both increased precipitation and deficit, suggesting a more significant influence of temperature changes. Nevertheless, these trends are statistically insignificant (except the precipitation trend at București Băneasa station). *In summer*, on the other hand, most stations show a decrease in total precipitation (except Constanța) and an increase in deficit (except București Băneasa on both parameters), but the trends are not statistically significant.

Table 7.3 Mann-Kendall trend (T, the plus and minus signs show positive and negative trends, respectively), the significance of trend (denoted with *), Sen's slope (S, mm/year) for total precipitation (precip) and station-CWD_{CRU} in spring (March, April and May [MAM]) and summer (June, July and August [JJA]) for the 2001 – 2020 period

		Râmnicu Vâlcea	Roșiorii de Vede	București Băneasa	Buzău	Călărași	Galați	Constanța	Tulcea
MAM precip	**T**	+	+	+*	+	+	-	-	-
	S	3.5	0.9	5.7	2.6	0.4	-0.6	-0.7	-0.02
MAM CWD	**T**	-	-	-	-	+	+	+	+
	S	-0.4	-1.3	-2.6	-1.9	0.3	0.7	0.4	0.4
JJA precip	**T**	-	-	+	-	-	-	+	-
	S	-2.9	-1.8	2.1	-2.2	-2.4	-3.3	1.05	-2.8
JJA CWD	**T**	+	+	-	+	+	+	+	+
	S	0.1	3.2	-4.2	1.4	4.5	5.8	1.3	4.9

The general increasing air temperatures and the greater water availability in certain areas in spring could have played a role in the spring greening. At the same time, higher temperatures, and decreased water availability in summer in most of the stations could have affected the activity of crops during this season. Nevertheless, these trends are mostly insignificant.

7.1.1.5. Expected changes in crop response to climate change in southern Romania

Decreased total annual precipitation in future climate scenarios, particularly in summer precipitation, when water requirements are the highest, could affect maize (ANM, 2014).

When considering future climate change, a shorter growing season in winter wheat and maize was projected for 2020 – 2050 in Romania (ANM, 2014; Cuculeanu et al., 2002; Mateescu and Alexandru, 2010). For winter wheat, crop simulations showed earlier anthesis and maturity in response to an increase in daily temperature by 1 – 2°C (Lazăr and Lazăr, 2010).

Simulations for 2020 – 2050 show that winter wheat and especially maize will have a shortened vegetation period considering climate change scenarios in south-eastern Romania, with less time for ripening (Mateescu and Alexandru, 2010). Maize had a higher vulnerability to climatic change, as seen from the change in vegetation period that was higher than for winter wheat, but also due to decreased water availability during grain filling (Mateescu and Alexandru, 2010). In addition, the positive CO_2 influence is less important because maize is a C_4 plant. The increase in yield in winter wheat was attributed to a beneficial effect of CO_2 on water use efficiency, despite the shortening of the growing season (Cuculeanu et al., 2002; Mateescu and Alexandru, 2010; Mitrică et al., 2013). Other simulations show, on the contrary, decreases in winter wheat (ANM, 2014). Sunflower, another thermophilic plant, could behave similarly to maize — shorter growing season and lower yields (Potop et al., 2014). Even so, the beneficial influence of CO_2 fertilization might not compensate for the effects of climate change (Jacobs et al., 2019).

A rise in daily air temperatures of about 1°C would suit the current wheat phenology, whereas a 2°C increase would require crop phenological adaptation (Lazăr and Lazăr, 2010). As an adaptation to climate change, simulations suggest that sowing in 2021 – 2050 could be performed later for winter wheat (25 October – 10 November for the Muntenia region, or starting from 30 October for the Dobrogea region) and earlier for corn (25 March – 10 April for Muntenia or up to 5 April for Dobrogea) between 2021 – 2050, compared to the 1 – 25 April, which was suitable for 1961 – 1990 (ANM, 2014). Earlier cultivars and cultivars with higher heat and water stress resistance during grain filling and resistance to spring frost represent an adaptation option to climate change (ANM, 2014).

For example, in the Bărăgan Plain, the air temperature is expected to increase both in winter-spring, implying an earlier spring phenology, and during sensitive phenological phases (Sima et al., 2015). Regarding maximum temperatures, the highest increases between 2021 – 2050 are expected in July and August, which would impact maize crops (Sima et al., 2015).

7.1.2. Grassland and pastures

For grasslands and pastures, there are primarily positive trends in NDVI, especially between April and July (**Figure 7.4**). However, a contrast is highlighted between grasslands and pastures: while at the regional level, grasslands show the most positive trends in April (19% of total grassland pixels), pastures show the most positive trends in June (44% of total pasture pixels). Negative trends occur mainly between August and October for both land covers, with the highest percentage in September. Nevertheless, the percentage of affected surface differs: 38% of all pasture pixels show significant negative trends in September, and only 10% of grasslands. Generally, there are lower surfaces with significant NDVI trends in grasslands compared to pastures.

Due to the inhomogeneous spatial and temporal distribution of pastures and grasslands, **Figure 7.4** presents the trends of NDVI in three regions for two months. Like arable lands, the positive trends in pastures are more extensive in April in Dobrogea Plateau (zone A in **Figure 7.4**), while from May to July, their area also increases in the other regions. Therefore, positive trends occur in April and May in the Dobrogea Region (Babadag Plateau, Casimcea Plateau and Mangalia Plateau) and the Romanian Plain (Buzău-Siret Plain). In June and July, the distribution of positive NDVI trends in pastures increases in the Teleorman Plain within the Romanian Plain (zone B) and the Subcarpathians (zone C) and decreases in the Dobrogea Plateau. In August, negative trends are noticed in the Dobrogea Plateau, increasing and extending in September here and in the Romanian Plain.

Most grasslands are in the Subcarpathians, Carpathians and Dobrogea Plateau. In April, there were some positive trends in the Carpathian Mts. (in Baiu Mts.) and the Dobrogea Plateau (Casimcea and Oltina Plateaus). In July, most of the positive trend pixels occurred in the Subcarpathians (particularly in Ialomița Subcarpathians) and the Carpathians (particularly in Baiu Mts.). In September, most of the negative trend pixels were found in Dobrogea (Casimcea and Oltina Plateaus), and the positive trends in the Carpathian Mts.

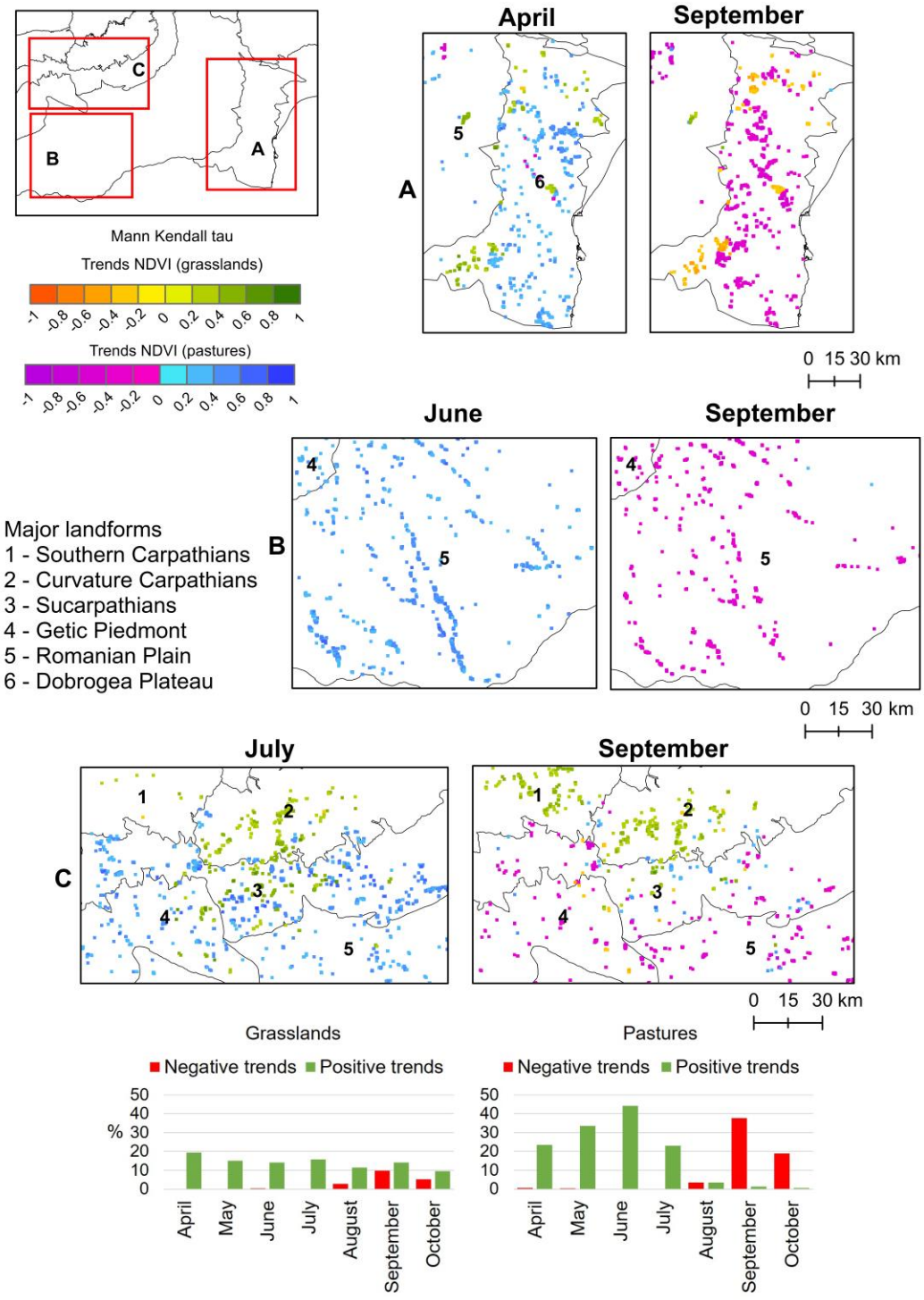

Figure 7.4 Significant monthly NDVI trends in grasslands and pastures between 2001 – 2020 in stable pixels. Pixels were exaggerated for visibility. The graph shows the percentage of pixels with significant trends from the total stable pixels for each land cover class. A) Dobrogea Plateau, B) Teleorman Plain, C) Subcarpathians.

The seasonality of trends in the lowland pastures is similar to the trends in the arable lands — larger positive trends in the first part of the growing season and more extensive negative trends in the second part. In this regard, the patterns of NDVI trends in grasslands throughout the growing season are similar to the forest trend pattern, which are primarily positive (**Figure 7.4**). These trends could be related to the heightened activity due to the positive effects of increased temperature in spring (**Table 7.2**), land cover change and CO_2 availability. On the other hand, the negative trends in pastures could be related to the increased water deficit in summer (**Table 7.3**).

The higher productivity measured by increased NDVI could occur in some areas due to higher temperatures and sufficient water supply (Alberton et al., 2017). Generally, agro-climatic experts expect a lengthened vegetation period in grasslands with climate change and increased productivity in areas of adequate water availability (Olesen et al., 2011); however, drought will continue to be a limiting factor.

Positive correlations between NDVI and SPEI-6 were shown in grasslands of south-eastern Europe in more than 50% of the area in July and up to more than 65% in September, highlighting the response to water stress and higher temperatures (Páscoa et al., 2020). Furthermore, the study of Páscoa et al. (2020) highlighted the dependence of these correlations on altitude and length of estimation period — more grasslands being positively influenced by increasing SPEI-6 at lower altitudes in July and negatively influenced by SPEI-1 in June at higher altitudes. Therefore, increasing water deficit in summer could have led to decreased greenness in grasslands and pastures, especially at low altitudes.

Despite identifying stable pixels, there are limitations regarding the availability of land cover data from 2018 at the latest. Therefore, the observed trends could have resulted from the development of woody vegetation in the grassland areas. Potential factors could include a higher timberline due to increased temperatures and decreased livestock pressure on mountain pastures and grasslands, the latter factor being lessened by the EU-supported traditional management of grasslands (Munteanu et al., 2014, 2017).

7.1.3. Forests

Trends in NDVI for **broadleaf forests** are primarily positive, particularly between April – July and especially in the Subcarpathian and Getic Piedmont regions (**Figure 7.5**). In May, there is the highest percentage of positive trends in broadleaf forests (about 50%). In terms of negative trends, these occur sparsely throughout the year. In August, there are groups of pixels with negative trends in Vlăsia Plain, Prahova's Piedmont Plain, and northern Găvanu-Burdea Plain. In September, there were negative trends in broadleaved forests in the Northern Dobrogea Plateau, the Vlăsia Plain and Prahova's Piedmont Plain.

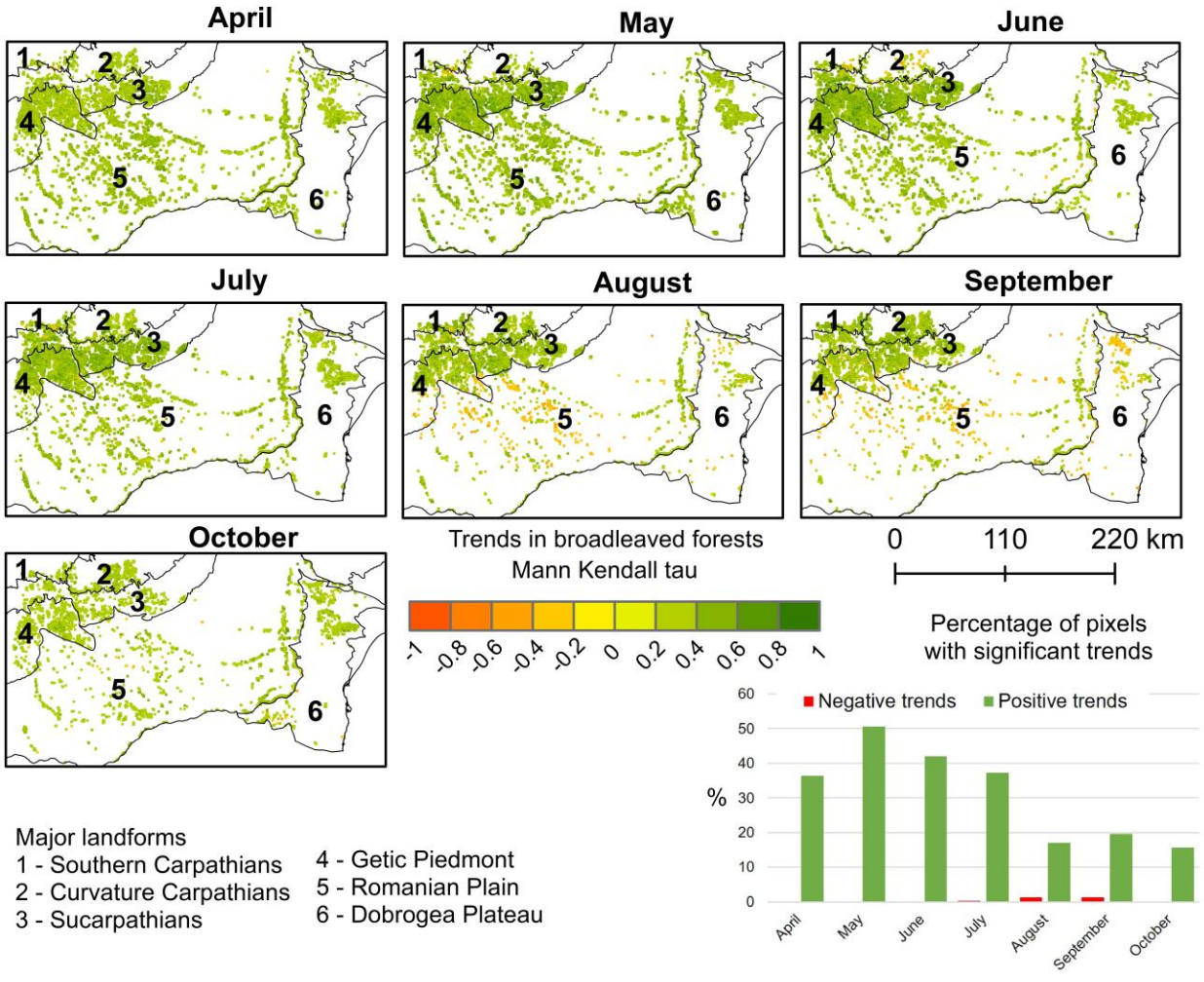

Figure 7.5 Monthly NDVI trends for broadleaf forests (pixels shown have significant trends, only in stable pixels). Pixels are exaggerated for visibility.

The significant trends in **mixed and coniferous forests** show mostly positive NDVI trends (**Figure 7.6**). In mixed forests, these occur mainly in September (60% of pixels). In coniferous forests, positive trends occur in April and between August – October but on smaller surfaces (25% in September).

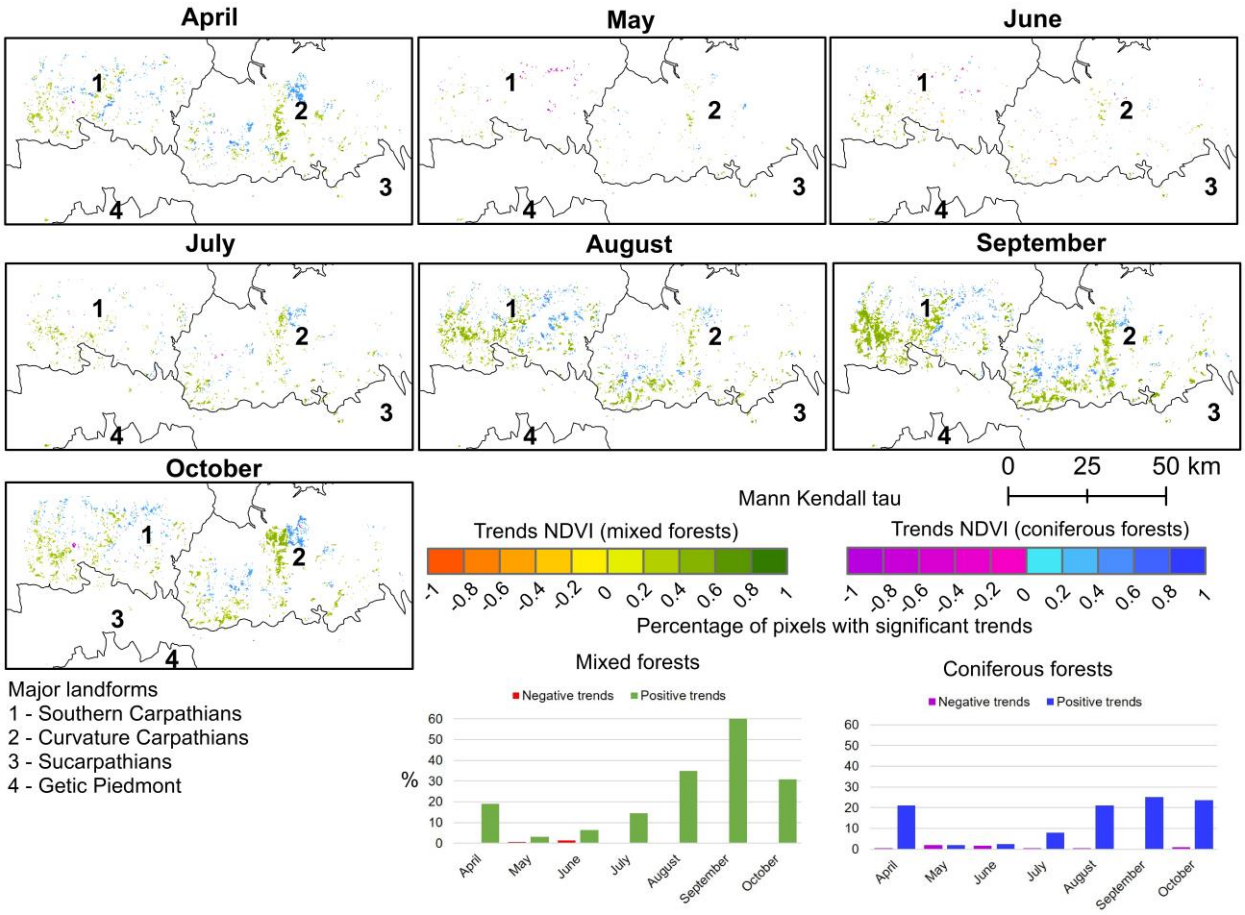

Figure 7.6 Monthly NDVI trends for mixed and coniferous forests (pixels shown have significant trends, and only in stable pixels)

In April, the positive trends for mixed forests are concentrated especially in Baiu Mts. and Loviștea Mts., while for coniferous forests, these occur especially in Făgăraș Mts., Iezer Mts., Leaota Mts., Bucegi Mts. and Baiu Mts.

In May and June, there are very few significant trends in both types of forests. However, from July to September, the spatial distribution of positive trends increases. In July, positive trends in both types appeared, particularly in Loviștea Mts., Leaota Mts., Clăbucetele Predealului Mts. and Baiu Mts.

In August and September, positive trends were found in most areas, with extensive patches of positive trends in September. These are especially continuous in August – September for mixed forests in Loviștea Mts., Leaota Mts., Bucegi Mts. and for coniferous forests in Iezer Mts., Leaota Mts. and Clăbucetele Predealului Mts.

The trends in mixed forests in October are concentrated especially in Clăbucetele Predealului Mts. but are also found in Loviștea Mts. and Leaota Mts. For coniferous forests in October, these are found particularly at the Clăbucetele Predealului Mts. – Baiu Mts. limit and in Bucegi Mts. and Făgăraș Mts. In addition, there is a small patch of negative trends in Făgăraș Mts.

A previous study showed generally increasing trends in LAI in semi-natural vegetation in Europe between 2000 – 2015, especially in temperate climates, which could support a more extended vegetation season (Buitenwerf et al., 2018). Mostly advancing but insignificant trends in the start of season of broadleaf forests in Europe between 2000 – 2018 were found by Bórnez et al. (2021), also based on LAI. Moreover, Bandoc et al. (2022) modelled an increase in the climatic growing season in the south and south-east of Romania based on the histophenogram method through an earlier potential onset and later offset of vegetation activity in the 1981 – 2010 period.

Significant correlations between NDVI and SPEI-6 were shown to be positive between July (>30% of the area) and September (>40% of the area) in broadleaf forests in Romania and the Republic of Moldova (Páscoa et al., 2020), suggesting that the decreasing water availability during these months could have contributed to some small surfaces of significant trends of decreasing NDVI in broadleaf forests. However, their study also showed significant negative correlations (increasing SPEI leading to lowered NDVI) for coniferous and mixed forests in May and June, with ~ 70% of the area with significant correlations in June for SPEI-1, and also for broadleaf forests, to a lesser degree, in May – June (Páscoa et al., 2020).

Considering that the mixed and coniferous forests are situated in energy-limited conditions (at higher altitudes), the increasing trends in temperature could benefit these types of forests, which could be illustrated in the increasing NDVI. Moreover, broadleaf forests could also benefit from increased temperatures in the first part of the growing season, with sufficient water availability. Dependence on altitude and length of estimation period is therefore highlighted: more broadleaf forests were shown to be positively influenced by SPEI-6 in July at low altitudes (increasing NDVI

with wetter conditions), and more coniferous forests are negatively influenced by SPEI-1 and SPEI-6 in June at high altitudes (lowered NDVI with wetter conditions) (Páscoa et al., 2020).

A Landsat based evaluation of summer season NDVI between 1987 – 2018 showed mostly greening trends in the Carpathian region (where NDVI was mostly correlated to temperature) and browning trends in the lowlands (where NDVI correlated with the climatic water balance, evapotranspiration and precipitation); however, most of the trends were statistically insignificant (Prăvălie et al., 2022).

In March – April, high temperatures were beneficial to vegetation at high altitudes in Romania (mixed and coniferous forests and grasslands), while in May – June and July – September, high temperatures were frequently simultaneous to very low NDVI values (and the reverse in July – September) in the lowlands in southern Romania (croplands, pastures, grasslands and broadleaved forests) (Baumbach et al., 2017).

7.2. Interannual variability of stressed vegetation condition

This chapter focuses on the exploration of the negative NDVI standardized anomalies of less than -1, considered here as *stressed vegetation*, in the 2001 – 2020 period. These are first presented at the regional scale and analysed by land cover type (**Chapter 7.2.1**). Secondly, they are interpreted in relation to meteorological drought occurrence (**Chapter 7.2.2**).

7.2.1. Overview of NDVI negative anomalies in the study area between 2001 – 2020

The **interannual variability of standardized anomalies** of the average growing season NDVI is shown in **Figure 7.7**. The constraint of an NDVI standardized anomaly that is less than -1 was selected for generating this map. The spatial distribution of these results highlights that 2001, 2003, 2007, 2008, 2012, and 2020 had widespread areas of stressed vegetation.

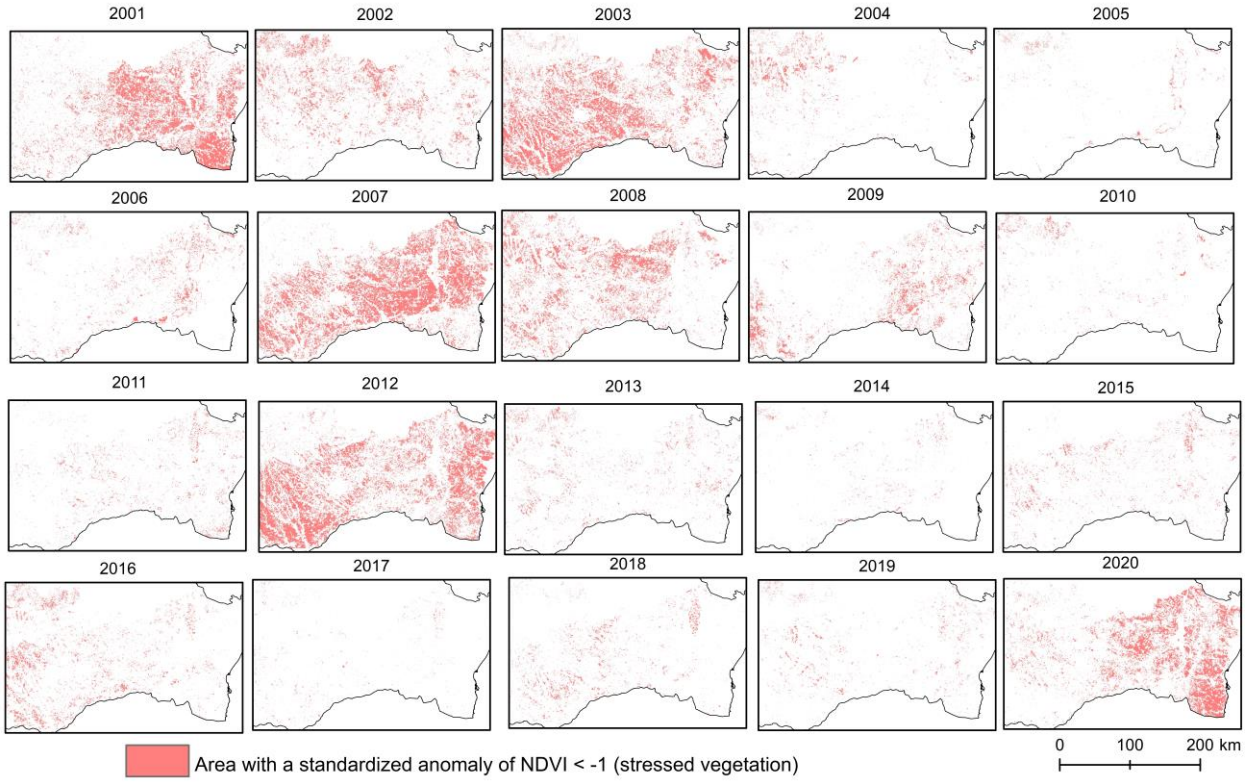

Figure 7.7 Spatial distribution of stressed vegetation during the growing season, where the standardized anomaly of the NDVI has values of less than -1

The spatial distribution of the year with the **lowest standardized anomaly of the average NDVI during the growing season (April – October)** is shown in **Figure 7.8**, while the breakdown by land cover type is presented in **Figure 7.9**. The map in **Figure 7.8** shows that in 2007 there was the most extensive spatial distribution of pixels where the lowest NDVI anomaly occurred. Specifically, it shows large regions of stressed vegetation this year in the Romanian Plain and Dobrogea Plateau.

2012 had the second most pixels with the lowest growing-season NDVI values, covering large areas, especially in the western part of the study area (mainly in Teleorman Plain and northern Ialomița Plain), but also some areas in Northern and Central Dobrogea Plateaus. The pixels with the lowest values in 2003 (the year with the third most pixels with lowest values) similarly extend in the Teleorman Plain and Ialomița Plain (in Ialomița Plain, however, a more significant extension compared to 2012), as well as northern Dobrogea Plateau.

Areas with the lowest anomalies in 2001 were in the eastern part of the study area, particularly in the Bărăgan Plain, Southern and Central Dobrogea Plateaus. Likewise, the pixels with the lowest values in the year 2020 appear in Bărăgan Plateau, Danube Floodplain (Balta Brăilei and Balta Ialomiței), and in Southern Dobrogea Plateau.

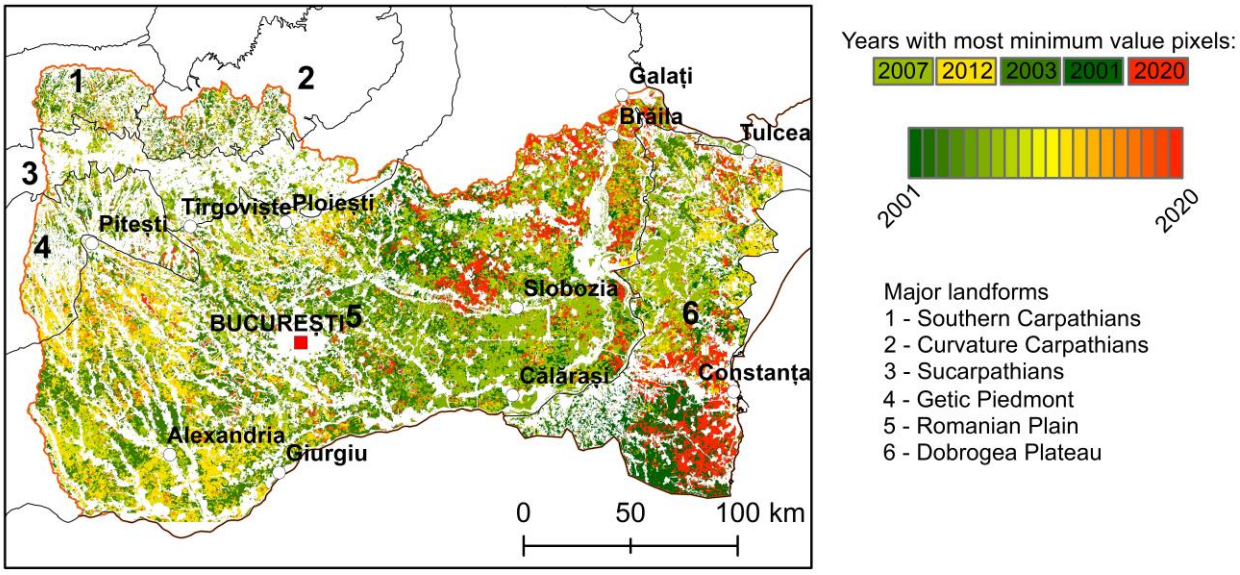

Figure 7.8 The year for each pixel with the lowest standardized anomaly of the average 16-day NDVI during the growing season (April – October, 2001 – 2020)

The spatial distribution of the lowest standardized anomaly by year is illustrated by land cover types in **Figure 7.9**. Except for natural grasslands, the top three years identified to have the lowest anomaly were dominant in the resulting statistics. These accounted for more than 50% of pixels with the lowest-value NDVI. For example, in arable lands, 2007, 2012 and 2003 were the most frequent years to have the lowest anomaly in the pixels included in the study area.

The year 2012 recorded the most pixels with the lowest value for pastures and natural grasslands, and 2002 for mixed and coniferous forests. In mixed forests, the first identified year (2002) has a very large percentage within these statistics, almost 50%. Similarly, in inland marshes, the first two identified years (2005 and 2006) occurred in more than half of the pixels, while the other years have low shares. The results of inland marshes, as presented in this figure, is relatively different from that of the other land-covers, suggesting different influencing dynamics.

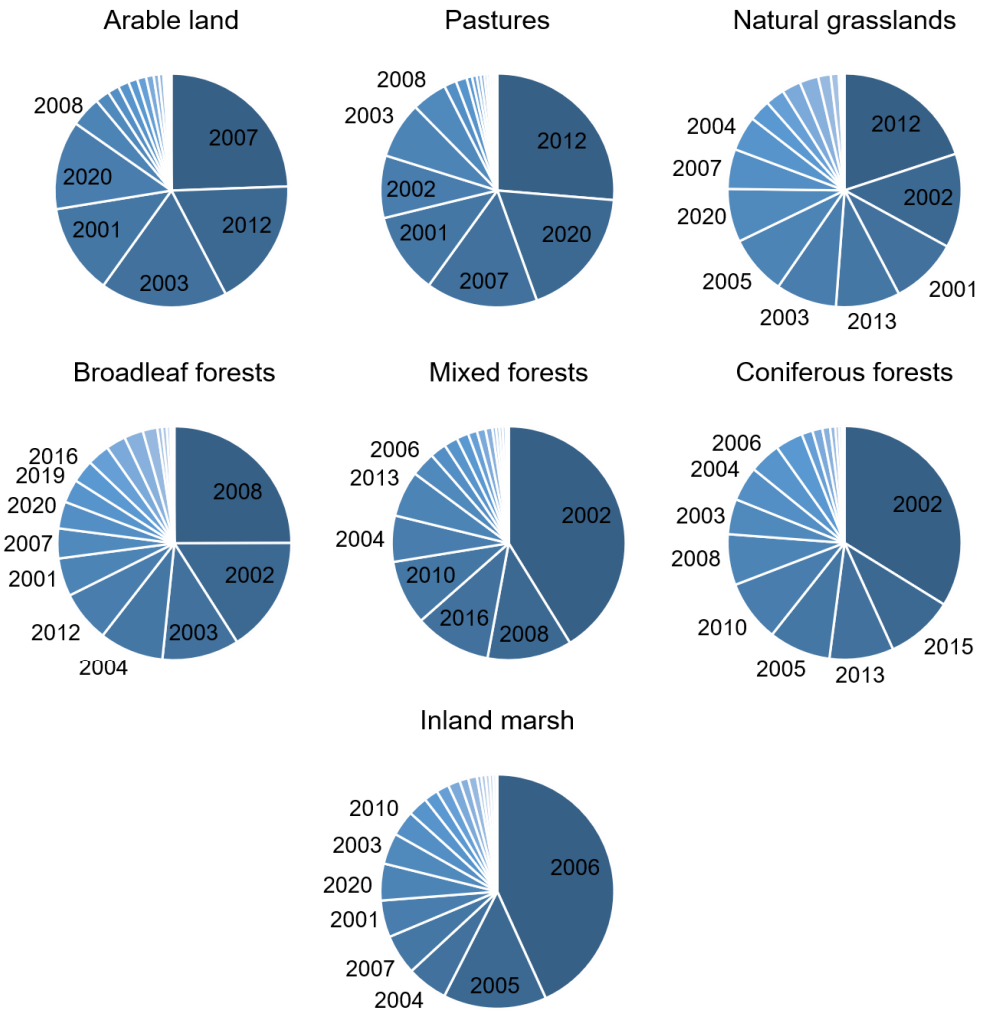

Figure 7.9 Percentage of pixels with minimum growing season (April – October, 2001 – 2020) NDVI each year in different land covers

The **annual percentage of area with stressed vegetation** for each land cover class is shown in **Figure 7.10**. Here, the threshold of NDVI standardized anomaly less than -1 was also selected. For each land cover class, the top three years with the highest percentages of affected areas were highlighted, and the position in the graph shows its hierarchy.

For arable lands, pastures and grassland, the year 2012 was a common year, particularly for pastures and grasslands, where it had the highest percentage of stressed vegetation (57% and 47% respectively affected area). 2007 had the highest percentage of stressed vegetation in arable lands (56% of the area affected) and the second highest for the pastures land cover (52%). The

year 2003 had the third most percentage of stressed vegetation for both arable land (45%) and grassland (32%).

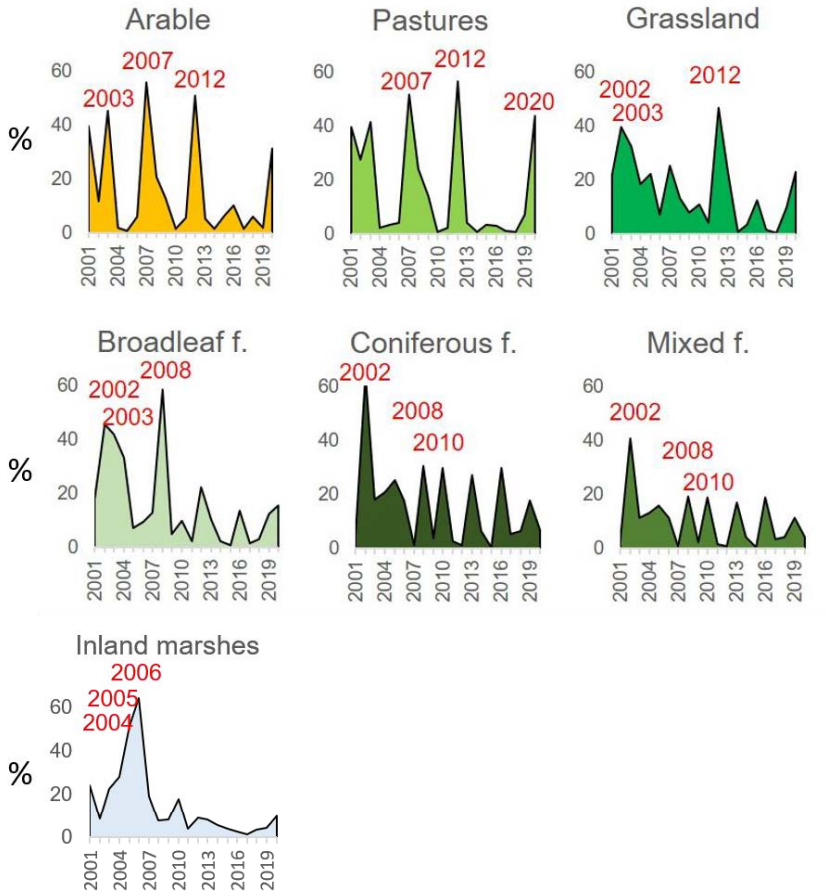

Figure 7.10 Area in drought – the percentage of pixels in each land cover with mean growing season anomaly of NDVI less than -1 (mean growing season = average of the 16-day values between April – October, 2001 – 2020)

In general, these findings regarding negative NDVI anomalies could have resulted because of multiple influencing factors. Droughts could have played a major role, but other natural processes such as floods or lower temperatures could similarly influence NDVI values. Moreover, the general greening trends could have generated more negative anomalies in the first part of the study period, which could have influenced these results. Therefore, in the following sections, the NDVI negative anomalies are interpreted in relation to the CWD, standardized indicators and results provided by other authors.

7.2.2. Negative NDVI anomalies in the context of drought occurrence

In the main vegetation drought years of 2001, 2003, 2007 and 2012, all meteorological stations had positive anomalies of the total CWD between April and October. In 2020, only the station of București Băneasa showed wetter conditions, while at the rest of the stations, the CWD had positive anomalies.

The average of all stations' growing season CWD anomalies, relative to the 1991 – 2020 interval, were positive: 3 mm in 2001, 110 mm in 2003, 141 mm in 2007, 118 in 2012 and 114 mm in 2020. However, relative to the 2001 – 2020 period, the average of all stations' growing season CWD anomalies were slightly lower: -15 mm in 2001, 91 mm in 2003, 123 mm in 2007, 100 mm in 2012 and 96 mm in 2020.

These dry years were characterized by significant temperature anomalies (Busuioc et al., 2007; Micu et al., 2017). 2007 and 2012 had hot summers in the Romanian Plain (with average temperature anomalies between 2.9ºC and 3.2º C, relative to 1961 – 2013), while 2003 was a warm summer (with average temperature anomalies between 0.9ºC and 2.1ºC) (Micu et al., 2017). Other authors have also highlighted these dry years using heat indicators (ANM, 2014), aridity indicators (Prăvălie and Bandoc, 2015), soil moisture (Onțel et al., 2021), vegetation indicators such as NDVI, NDDI (Dobri et al., 2021; Páscoa et al., 2020) or composite indicators such as DSI (Angearu et al., 2020).

At the European scale, clustering based on SPEI-12 variability between 1999 and 2010 highlights regions of similar anomalies: Romania was grouped with the Balkan peninsula and the Pannonian, Mediterranean and Caucasus regions, with marked drought occurrence between 1999 – 2002 and in 2007 – 2008 (Ivits et al., 2014).

7.2.2.1. Response of arable lands to drought

Most of the arable land (the most severe condition) had the lowest NDVI standardized anomaly in 2007, 2012 or 2003, which were also the years with the largest area in drought for this type of land cover (**Figure 7.9** and **Figure 7.10**), with a dominant spatial distribution of stressed vegetation throughout the region (**Figure 7.7**). These results suggest that the response of vegetation to drought was both extended and severe in these years.

Previous studies found significant relations in the analysed area between maize yield and temperature, climatic water balance and precipitation (Prăvălie et al., 2020; Prăvălie et al., 2017). However, correlations between PET and maize yields were not significant in Argeș, Giurgiu, Constanța and Tulcea counties and showed significance in the other counties (Prăvălie et al., 2020). In one study, heat stress indices (between May and September) were found as significant predictors of maize interannual changes in production in the study area, whereas wheat and sunflower did not show significance in most counties (Micu et al., 2017). These results highlight the dependence of crop yields, particularly summer crops, on annual climatic conditions.

When analysing the drought of **2000 – 2001**, the patterns of NDVI anomalies mainly followed the persistence of drought according to SPEI, especially regarding cropland (Páscoa et al., 2020).

The drought of **2003** was an exceptional event that affected most of Europe on account of high temperatures and precipitation deficits, which led to a decrease in net primary productivity (NPP) in cropland (Ciais et al., 2005); this occurred especially in maize because winter wheat had almost finished their development when the event unfolded. The most significant NPP decreases were in Romania and Ukraine, about -20% compared to the average between 1998 – 2002 (Ciais et al., 2005).

In 2003, the minimum anomaly pixels for cropland were mostly extended in the western and central part of the Romanian Plain (mainly the counties of Teleorman, Giurgiu, Călărași, Ilfov, Dâmbovița) (**Figure 7.8**). At București Băneasa, there was an extreme drought event from March to August, based on SPI-3 (**Chapter 5.2**), with the fourth highest drought intensity from all the droughts identified at this station for this indicator. Moreover, this year was preceded by two extreme and severe drought years (2000 – 2001). Similarly, SPEI-3 shows a drought event between April – August 2003 with the second-highest intensity of all drought events identified here. The Buzău station also showed an extreme event lasting from March (April) to August, based on SPI-3 (SPEI-3).

At Roșiorii de Vede meteorological station, SPI does not identify a drought event in 2003 (the indicator shows almost normal conditions), but SPEI does. A moderate drought event in 2003 lasted from March to September, based on SPEI-3. These results could suggest that the drought

was mainly temperature-driven at Roșiorii de Vede. At Călărași station, an extreme event lasted from April to August 2003 based on SPI-3 and SPEI-3.

The most extensive areas with the minimum NDVI standardized anomaly in **2007** for cropland were in the Bărăgan Plain (Ialomița, Călărași counties), but also in the Dobrogea Plateau (especially north of Constanța County and south of Tulcea county) (**Figure 7.8**).

The moisture deficiency started in the previous year. In 2007 at Călărași meteorological station, SPI-3 and SPEI-3 showed extreme drought events. The former identifies a drought event that starts in October 2006, and the latter shows an event starting in July 2006, and both end in September 2007. Similarly, for București Băneasa, both SPI-3 and SPEI-3 showed an extreme drought event starting in November 2006 and ending in September 2007. At Constanța, there was a severe drought event from November 2006 to July 2007, based on SPI-3, and more prolonged and extreme, from October 2006 to September 2007, based on SPEI-3.

Very high temperatures were recorded at Adamclisi (the maximum value in July 2007 reached 41.8º C) and at Turnu Măgurele (43.4ºC), for example (ANM, 2014). Simulated winter wheat LAI showed an earlier development in 2007 in spring (Lazăr et al., 2009). On a larger scale, the 2007 drought event was extended mostly in south-eastern Europe and central Italy, with the onset in winter (European Drought Center, 2013).

In **2012**, the minimum anomaly pixels in cropland were mainly in the western Romanian Plain (in Argeș, Teleorman, and Giurgiu counties), Prahova, and eastern Tulcea county (**Figure 7.8**). In 2012, at Roșiorii de Vede, an autumn-winter precipitation deficit was shown by the severe drought event based on SPI-3 from October 2011 to January 2012, suggesting that soil water reserves might not have been replenished, and a moderate drought event from July 2012 to January 2013. SPEI-3 in Roșiorii de Vede also shows a severe event from November 2011 to January 2012 and an extreme event from April 2012 to January 2013. At București Băneasa, SPI-3 and SPEI-3 identified a moderate drought and an extreme event, respectively, from August to November 2012. The previous year (2011) was also very dry at București Băneasa, based on SPI-3 and SPEI-3.

In Romania, November 2011 was the driest month up until 2012 of the previous 52 years (Mateescu et al., 2013). In July 2012, maximum values of 42.4ºC and 37.5ºC were reached at Giurgiu and Medgidia, respectively (ANM, 2014). In Romania, 5.9 million hectares of cropland

were affected in 2011 – 2012 (Sima et al., 2015). Ion et al. (2013) mentioned that sunflower performed better than maize in 2012 (with lower-than-average yields) and argued that sunflower is more adapted to the water stress of southern Romania.

The most recent drought in the studied dataset was in **2020** when large areas of stressed vegetation occurred in the eastern part of the region (**Figure 7.7**). Minimum values in cropland were reached in 2020 in the eastern part of the Romanian plain (especially Ialomița and Brăila counties), but also in the Dobrogea Plateau (Constanța and Tulcea counties) (**Figure 7.8**). Since 2012, no other year has had such a large surface of affected areas (**Figure 7.10**). Long drought events were observed at Constanța and Galați meteorological stations. At Constanța, the extreme drought was identified based on SPI-3 and SPEI-3 from December 2019 to December 2020 and from February 2019 to December 2020, respectively. These events could be longer, but the data series stop in December 2020. At Galați, SPI-3 and SPEI-3 show extreme drought between March 2019 and November 2020.

Winter wheat had earlier activity in the agricultural year 2019 – 2020 due to the positive temperature anomalies in January (Berca et al., 2021). Due to the winter-spring drought and warmer temperatures of 2019 – 2020, as well as an inadequate moisture supply in the 2018 – 2019 agricultural year, winter wheat was affected due to lowered soil moisture in a study site at Călărași and had an earlier development which led to a reduced number of grains and therefore to a lower yield (Berca et al., 2021).

The years with large areas of affected vegetation mainly relate to drought conditions. The year 2005, which was a wet year, had the lowest surface with affected vegetation; the pixels with the minimum value in 2005 were situated in the Danube Floodplain. During normal or wet years, affected crops generally have a low extension (**Figure 7.9**).

A shorter growing period in crops, determined by the advanced phenological phases, could determine lower yields. In the analysed counties, yields have mainly increased (**Table 7.1**, **Figure 7.11**), but a decrease is still observed during drought years, suggesting a vulnerability to drought events. Despite the markedly increasing trend visible since 2007, in 2020, there was a sharp drop in crop yield.

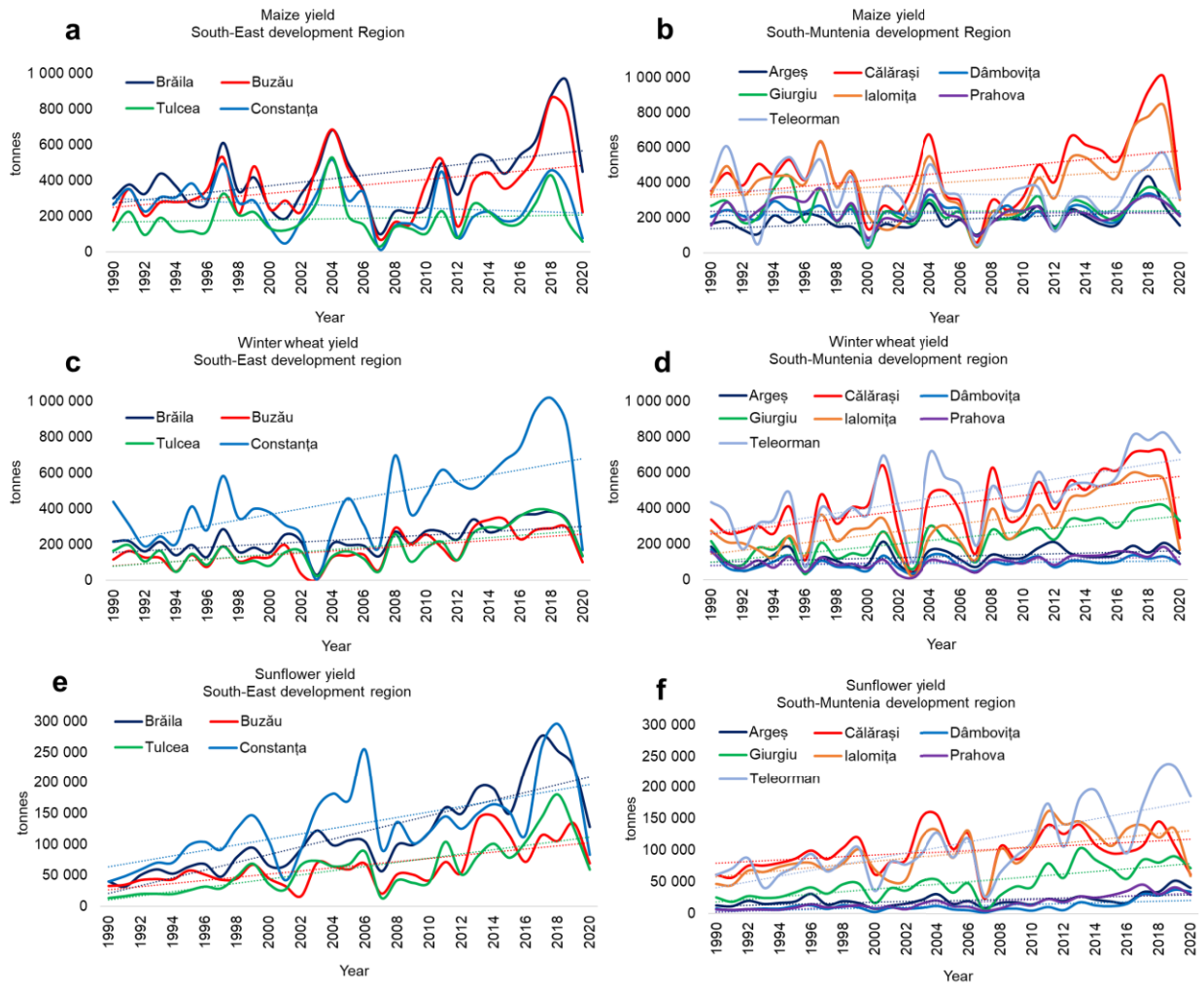

Figure 7.11 Variability of maize yield in (a) the South-East development region and (b) South-Muntenia development region; winter wheat in (c) the South-East development region and (d) South-Muntenia development region; sunflower yield in (e) the South-East development region and (f) South-Muntenia region. The coloured lines represent the counties in each development region.

7.2.2.2. Response of forests to drought

Forests had a different dynamic: most areas of stressed vegetation were in 2002 and 2008 (more than 45%), but the magnitude in 2008 was less important for coniferous and mixed forests than broadleaf forests (**Figure 7.9**, **Figure 7.10**). For forests and semi-natural vegetation, 2002 was a year with large surfaces of affected areas; coniferous forests had a very high percentage of

the affected area, about 64%. The third most affected year differed between the types of forests: for broadleaved forests, it was 2003 (42%), and for coniferous and mixed forests, it was 2010 (30% and 19%, respectively). This difference could be due to water-limited forests versus energy-limited forests.

For forests at higher altitudes, limited by energy availability (coniferous), 2010 and 2005 appeared to have more pixels of low NDVI anomalies. In 2010, there were low PET values, with slight negative anomalies at Râmnicu Vâlcea meteorological station and positive precipitation anomalies in May and June. At Vârful Omu station, there were relatively high positive anomalies in precipitation and slight negative anomalies in PET. There was a similar situation in 2005, with wetter conditions. The previously mentioned correlations between NDVI and SPEI, which are dependent on altitude in the study area from the study of Páscoa et al. (2020), strengthen this idea of lowered NDVI values at higher altitude forests during very wet years.

In 2008, most of the minimum pixels within broadleaf forests were concentrated at higher altitudes (in the Subcarpathians and Getic Plateau), contrasting with the eastern part of the study area, where there is a lower density. In the former areas, there was a drought also identified in 2008 for almost the entire year: at București Băneasa, the drought was moderate according to SPI-3 (from March 2008 to February 2009) or severe (according to SPEI-3, from March 2008 to February 2009); at Râmnicu Vâlcea, there was severe drought (according to SPI-3, from February 2008 to October 2008) or extreme (according to SPEI-3, from January 2008 to October 2008); in Buzău, the drought was according to SPI-3, extreme from January to April and severe from June to October, while according to SPEI-3 it was extreme from January to October. Therefore, the drought stress of 2008 probably accumulated the impact on forest greenness with the water stress from the previous drought year (2007).

In 2002, the minimum values pixels of NDVI standardized anomalies (**Figure 7.8**) in broadleaf forests were located in the western part of the study area and at higher altitudes. At București Băneasa, there was a severe drought from September 2001 to June 2002, according to SPI-3, and an extreme drought from September 2001 to July 2002, according to SPEI-3. At Vârfu Omu, the SPI-3 shows a moderate drought from December 2001 to September 2002. Buzău station had an extreme SPI-3 and SPEI-3 drought from December 2001 to June 2002.

Oaks are sensitive to previous autumn, spring and the beginning of the summer precipitation, particularly in April (Ciceu et al., 2020). For example, in north-western France, studies on oaks showed the lowest tree ring growth when droughts were recorded in spring and summer (Planchon et al., 2008). Therefore, the 2002 and 2008 droughts could have impacted the greenness of forests.

8. REGIONAL DIFFERENCES IN VEGETATION RESPONSE TO DROUGHT

This chapter explores in more detail the response of vegetation to hydrometeorological drought in south-eastern Romania. For this purpose, five sites were selected in the ecoregions within the study area:

- Babadag Forest in the Pontic Steppe ecoregion; Ialomița Corridor in the East European Forest steppe;
- Comana Forest, within the Comana Natural Park and surrounding forests (in the Balkan Mixed Forests ecoregion);
- Cândești Forests in the Southern Cândești Piedmont Forests protected area and in surrounding areas, for Central European Mixed Forests;
- broadleaf forests in the Bucegi Mountains for Carpathian Montane Forests.

Multiple methods were employed to compare vegetation and CWD dynamics between these sites: the average growing season anomaly (**Chapter 8.1**), correlations between each site's NDVI anomaly and the CWD (**Chapter 8.2**) and statistical tests (**Chapter 8.3**). In addition, the results of phenological identification are evaluated in **Chapter 8.4**.

Finally, vegetation dynamics and drought occurrence are analysed in two selected drought periods: 2007 – 2008 (**Chapter 8.5**) and 2019 – 2020 (**Chapter 8.6**).

8.1. Average growing season anomaly

The variability of the average growing season anomaly of the NDVI (calculated on the 16-day values) in the five sites selected with the study region is shown in **Figure 8.1**, highlighting the years of stressed vegetation (of negative anomalies).

These periods where NDVI indicated a lower vitality of vegetation were noted between 2001 – 2003, 2007 – 2009, 2006 – 2009, 2012, and 2019 – 2020. Conversely, mostly positive anomalies marked the period 2013 – 2018.

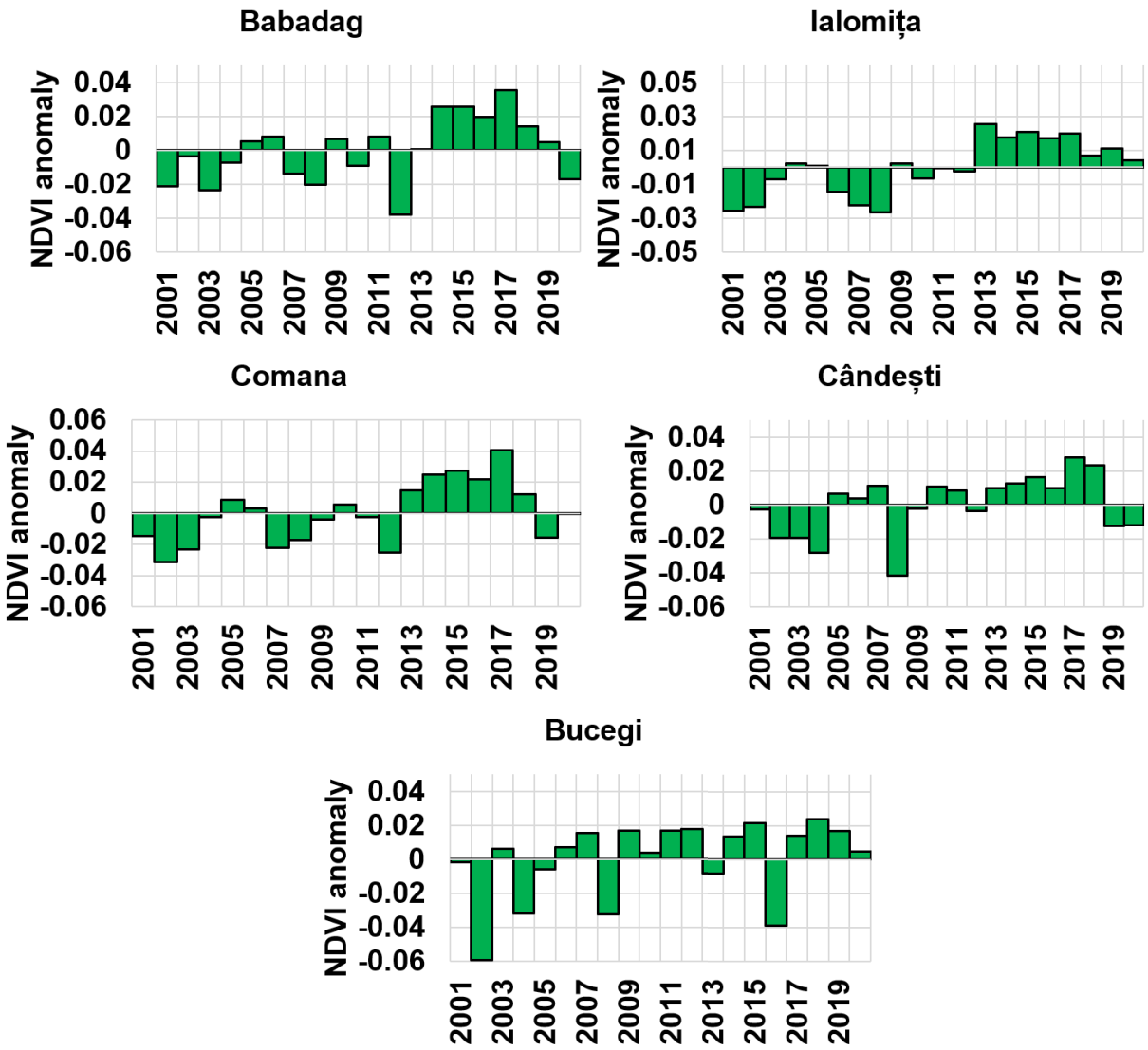

Figure 8.1 Anomaly of the average growing season NDVI in the five selected sites within the study area: Babadag, Ialomița, Comana, Cândești and Bucegi

8.2. Correlations between NDVI and CWD

In this chapter, the findings of the correlation analysis between the monthly NDVI anomaly and the CWD are presented. The aim is to gain insights into meteorological variability and vegetation patterns by investigating the interdependence between these two variables throughout the growing season (April – October).

Correlations between the NDVI and the CWD could offer valuable predictive information regarding the response pattern of vegetation to drought. Because the relationship between NDVI

and CWD can vary depending on data sources, the NDVI anomaly was correlated monthly with 3 sources of CWD: the CWD at the closest meteorological stations calculated with PET_{CRU} (station-CWD_{CRU}) and with PET_{Turc} (station-CWD_{Turc}), but also with the spatialised CWD (raster-CWD).

In the Babadag area, most correlations between the NDVI and CWD are negative and significant from May to July with station-CWD_{Turc} (**Table 8.1**). In addition, significant negative correlations are shown in July for all deficit sources.

Table 8.1 Pearson correlation coefficient between monthly NDVI anomaly in the Babadag area, the station-CWD_{CRU} and station-CWD_{Turc} at Tulcea meteorological station (2001 – 2020), and the raster-CWD (2001 – 2017). Bolded and starred values are statistically significant (p-value < 0.05).

Babadag area	*April*	*May*	*June*	*July*	*August*	*September*	*October*
Tulcea, station-CWD_{CRU}	0.28	-0.39	-0.39	**-0.54***	-0.31	-0.048	-0.2
Tulcea, station-CWD_{Turc}	0.28	**-0.53***	**-0.53***	**-0.6***	-0.38	0.12	-0.12
raster-CWD	0.17	-0.47	-0.48	**-0.71***	-0.37	0.09	-0.30

In the Ialomița area, most of the correlations are negative (**Table 8.2**). NDVI shows a high correlation with station-CWD_{CRU} and station-CWD_{Turc} at the București Băneasa meteorological station in May and from July to the end of the growing season. The Pearson correlation coefficient also shows a statistical relationship between the raster-CWD and NDVI anomalies in May, July, August and October.

Table 8.2 Pearson correlation coefficient between monthly NDVI anomaly in the Ialomița area, the station-CWD_{CRU} and station-CWD_{Turc} at București Băneasa meteorological station (between 2001 – 2020), and the raster-CWD (2001 – 2017). Bolded and starred values are significant (p-value < 0.05).

Ialomița area	*April*	*May*	*June*	*July*	*August*	*September*	*October*
București Băneasa, station-CWD_{CRU}	0.072	**-0.47***	-0.036	**-0.53***	**-0.61***	**-0.58***	**-0.63***
București Băneasa, station-CWD_{Turc}	0.042	**-0.59***	-0.15	**-0.57***	**-0.45***	**-0.48***	-0.45
raster-CWD	0.004	**-0.62***	-0.34	**-0.55***	**-0.64***	-0.36	**-0.54***

The Comana area has significant negative relationships between the anomaly of NDVI and station-CWD_{CRU} at București Băneasa and Roșiorii de Vede in May and from July to October (**Table 8.3**). The strongest correlations are in July and May, particularly with raster-CWD.

Table 8.3 Pearson correlation coefficient between monthly NDVI anomaly in the Comana area, the station-CWD_{CRU} and station-CWD_{Turc} at București Băneasa and Roșiorii de Vede meteorological stations (2001 – 2020), and the raster-CWD (2001 – 2017). Bolded and starred values are significant (p-value < 0.05).

Comana area	*April*	*May*	*June*	*July*	*August*	*September*	*October*
București Băneasa, station-CWD_{CRU}	-0.028	**-0.57***	-0.26	**-0.6***	**-0.55***	**-0.51***	**-0.49***
București Băneasa, station-CWD_{Turc}	-0.076	**-0.69***	-0.35	**-0.65***	**-0.42***	-0.34	-0.27
Roșiorii de Vede, station-CWD_{CRU}	-0.016	**-0.56***	-0.17	**-0.59***	**-0.52***	**-0.59***	**-0.55***
Roșiorii de Vede, station-CWD_{Turc}	-0.028	**-0.65***	-0.36	**-0.64***	**-0.51***	**-0.52***	-0.43
raster-CWD	-0.24	**-0.69***	-0.38	**-0.67***	**-0.57***	-0.34	-0.34

In the Cândești area, the significant correlations (negative) only appear in May (for station-CWD_{CRU} and station-CWD_{Turc} at the Râmnicu Vâlcea station) and August (for most sources) (**Table 8.4**).

Table 8.4 Pearson correlation coefficient between monthly NDVI anomaly in the Cândești area, the station-CWD_{CRU} and station-CWD_{Turc} at București Băneasa and Râmnicu Vâlcea meteorological stations (2001 – 2020), and the raster-CWD (2001 – 2017). Bolded and starred values are significant (p-value < 0.05).

Cândești area	*April*	*May*	*June*	*July*	*August*	*September*	*October*
București Băneasa, station-CWD_{CRU}	0.15	-0.21	-0.03	-0.26	**-0.53***	-0.19	-0.27
București Băneasa, Station-CWD_{Turc}	-0.018	-0.39	-0.15	-0.37	-0.38	-0.029	-0.094
Râmnicu Vâlcea, station-CWD_{CRU}	0.058	**-0.54***	-0.088	-0.16	**-0.55***	-0.033	-0.31
Râmnicu Vâlcea, station-CWD_{Turc}	0.12	**-0.53***	-0.096	-0.25	**-0.56***	0.046	-0.19
raster-CWD	0.02	-0.47	-0.18	-0.26	**-0.60***	0.16	-0.03

In the Bucegi area, the only significant relationship (positive) was found in April, and only with Vârful Omu station-CWD_{Turc} (**Table 8.5**).

Table 8.5 Pearson correlation coefficient between monthly NDVI anomaly in the Bucegi area and the station-CWD_{CRU} and station-CWD_{Turc} at Vârful Omu meteorological station (2001 – 2020), and the raster-CWD (2001 – 2017). Bolded and starred values are significant (p-value < 0.05).

Bucegi area	*April*	*May*	*June*	*July*	*August*	*September*	*October*
Vârful Omu, station-CWD_{CRU}	0.37	0.27	0.23	0.095	0.2	0.3	0.089
Vârful Omu, station-CWD_{Turc}	**0.52***	0.25	-0.016	0.12	0.21	0.27	0.03
raster-CWD	0.27	0.40	0.39	0.20	-0.03	0.4	0.1

The results for Bucegi suggest that the climatic water deficit is not a determinant variable in broadleaf greenness in this area. In the Comana, Ialomița and Cândești areas, in June, there are no significant correlations, which could be due to the high rainfall that is usual in this month, suggesting that moisture availability is not a constraining factor. In the Babadag area, however, there is a significant correlation in June with Tulcea station-CWD_{Turc}, which might suggest a limiting influence of water availability on vegetation.

8.3. Statistical analysis of NDVI in drought years

This section focuses on the results regarding the statistical significance of the differences in vegetation response (growing season NDVI anomaly) between the five study areas in years characterised by significant hydrometeorological drought. The analysed drought years were selected based on the anomaly of the total growing season CWD (**Chapter 6.3.5.1**).

According to the Shapiro-Wilk normality test, the data does not follow a normal distribution for most years and study areas. Levene's test shows that the variance across study zones is unequal for every year.

Because the data were not normally distributed and the variance across groups was not homogenous, the Kruskal-Wallis test was used to explore for statistically significance differences in NDVI between the sites, followed by the Dunn's test for multiple pairwise comparison. The

results of the Kruskal Wallis and Dunn's tests and the mean anomaly for each study area are presented in **Table 8.6**.

Table 8.6 Comparison of growing season NDVI anomalies in broadleaf forests between the five study sites in selected drought years, using the Kruskal-Wallis test and the Dunn's test. Results should be interpreted by rows.

Year	*Sig*	*Babadag*		*Ialomița*		*Comana*		*Cândești*		*Bucegi*	
		Median	Dunn's test	Median	Dunn's test	Median	Dunn's test	Median	Dunn's test	Median	Dunn's test
2003	*	-0.024	A	-0.006	D	-0.021	A, C	-0.019	C	0.009	B
2007	*	-0.009	A	-0.018	A, D	-0.015	D	0.013	C	0.018	B
2008	*	-0.02	A	-0.02	D	-0.02	A	-0.04	C	-0.03	B
2009	*	0.0085	A	0.0014	D	-0.0017	C	0.0004	C	0.0192	B
2011	*	0.0103	A	0.0007	D	-0.0014	C	0.0090	A	0.0179	B
2012	*	-0.037	A	-0.001	C	-0.021	D	-0.002	C	0.019	B
2015	*	0.03	A	0.02	B	0.03	A	0.02	C	0.02	B
2018	*	0.012	A	0.008	C	0.015	A	0.026	B	0.025	B
2019	*	0.006	A	0.011	D	-0.013	C	-0.015	C	0.020	B
2020	*	-0.016	A	0.007	B	-0.002	D	-0.011	C	0.009	B

Sig: significance of the Kruskal-Wallis test. * shows statistical significance (p-value < 0.05).
Dunn's test: A, B, C, D – Letters from the Dunn's test reporting multiple pairwise comparisons for rows. The same capital letter in one row shows no statistically significant difference between sites in that specific year. Different capital letters in the same row show statistically significant differences between the corresponding sites.

The results show significant differences in the anomalies of broadleaf forest NDVI between the five study areas during each of the selected drought years. These results and the boxplots shown in **Figure 8.2** illustrate the variability of vegetation response in different conditions.

The letter grouping results from the Dunn's test (**Table 8.6**) show that the Babadag and Comana areas were grouped the most often (did not show statistically different responses in the magnitude of the anomaly) — in 2003, 2008, 2015 and 2018. Comana and Cândești did not have statistically different responses in 2003, 2009 and 2019.

The letter grouping for the Ialomița area frequently demonstrated significant differences from the other groups (2003, 2008, 2009, 2011, 2018 and 2019). In the case of the Bucegi site, the response showed statistically significant differences from the other sites in most years.

The variability of NDVI response (in the 500 points) in the selected areas and drought years is illustrated in **Figure 8.2**. Some years show larger contrasts between the responses in broadleaf forests (2003, 2007, 2012, 2019) regarding response direction (negative/positive), spread and interquartile range. Other years, such as 2008, 2015 or 2018, show a more consistent response.

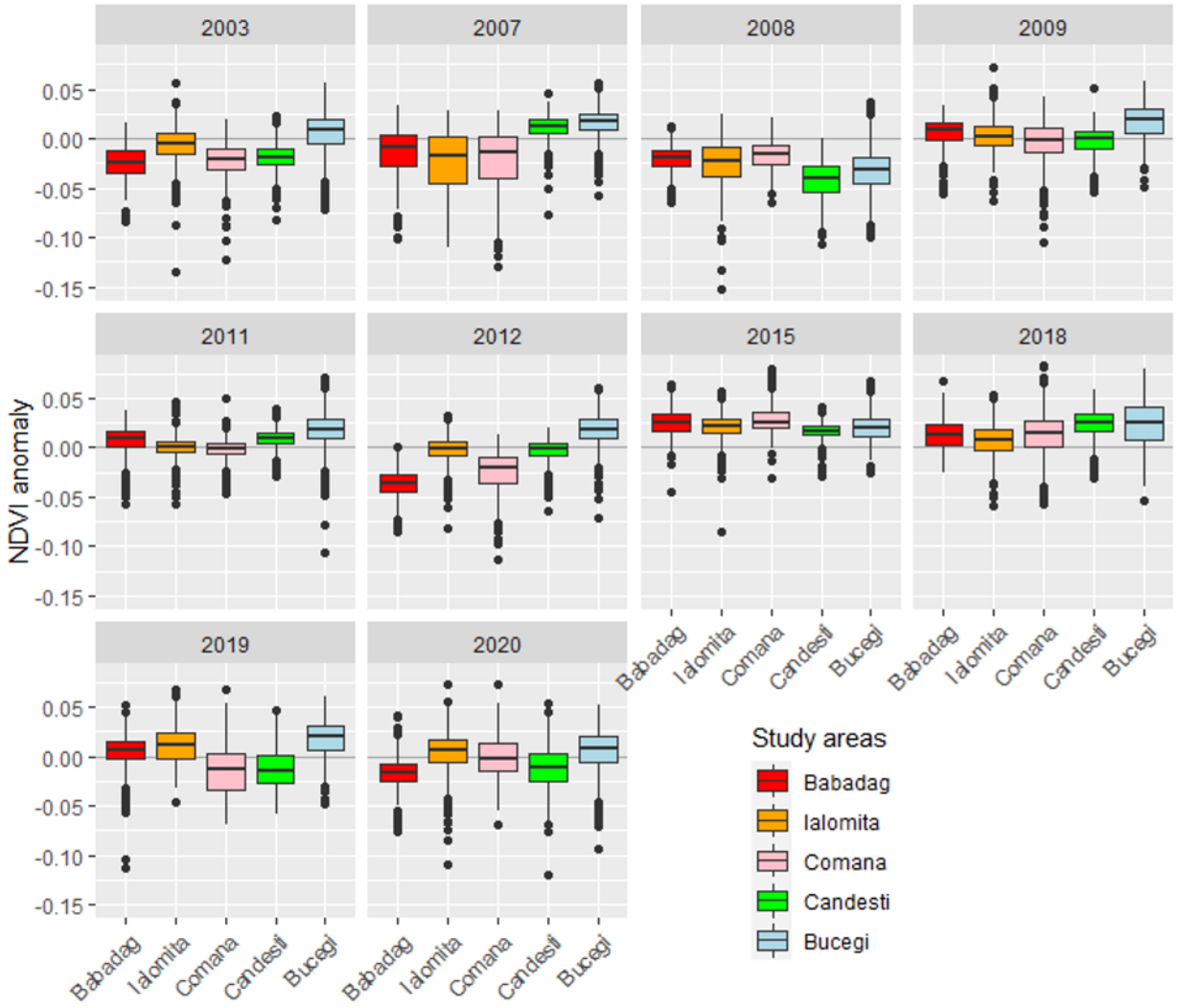

Figure 8.2 Variability of growing season NDVI anomalies during drought years in the five study areas for broadleaved forests

8.4. Quality assessment of phenology results

This chapter examines the results of the analysis on phenology metrics, the Start of Season (SOS) and End of Season (EOS) identified with the *greenbrown* package in R. These were generated by four approaches, resulting from the combination of two smoothing methods (linear and spline) and two phenological identification methods (*white* and *deriv*). Firstly, the percentage of missing pixels is presented because there were missing values in many cases. Next, the correlations between climatic variables and phenological metrics are investigated.

The percentage of missing pixels from the 500 sampling points for SOS and EOS for each year, approach and location, which could result from the failure of the method, are shown in **Figure 8.3** and **Figure 8.4**.

While there are less than 10% missing results for SOS in most years, there are a few cases where this percentage is higher. For example, such cases appeared in Babadag, Comana, Ialomița and Bucegi areas in 2020 or Comana and Ialomița areas in 2007. Similarly, most EOS results have <10% missing values; however, in 2007 – 2009 and 2017 – 2019, the percentage exceeded 20 – 30 % and even 40%.

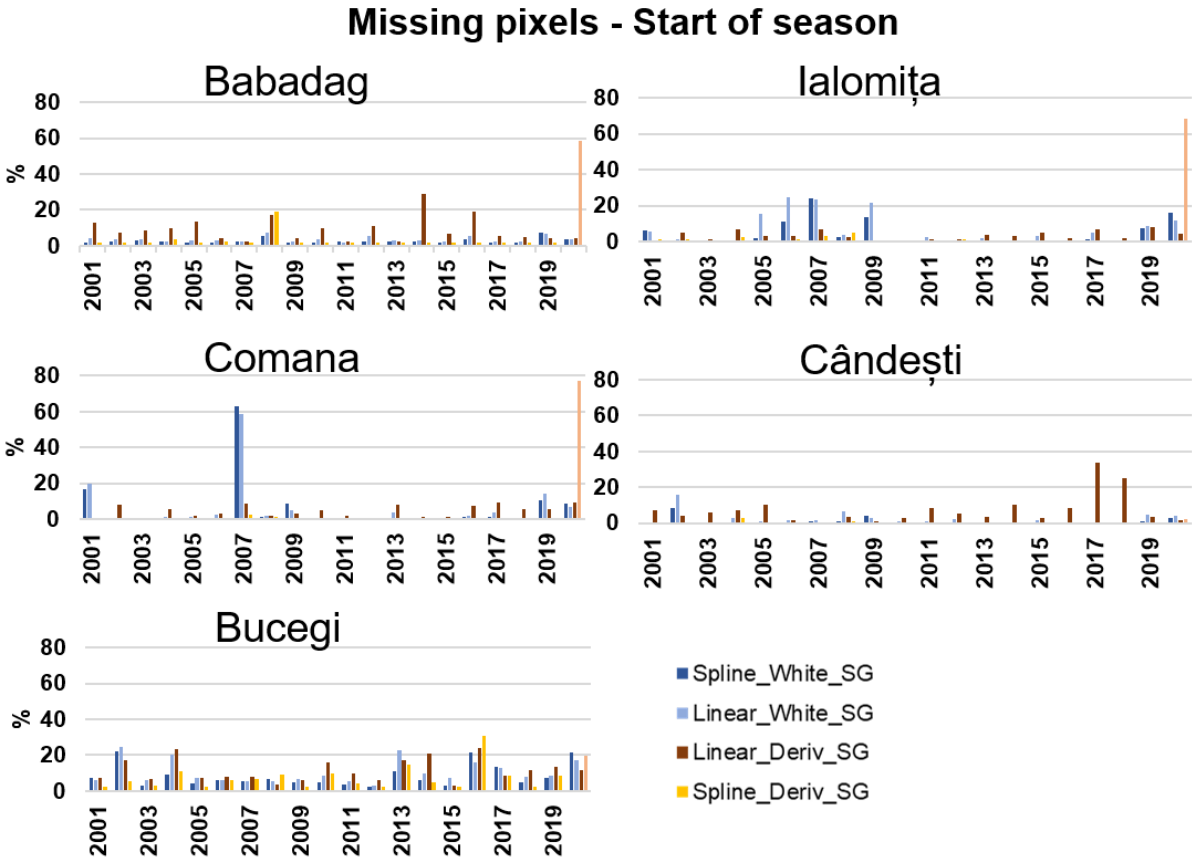

Figure 8.3 Percentage of annual missing values for each phenology approach for the Start of Season (SOS) between 2001 – 2020, in the five selected areas

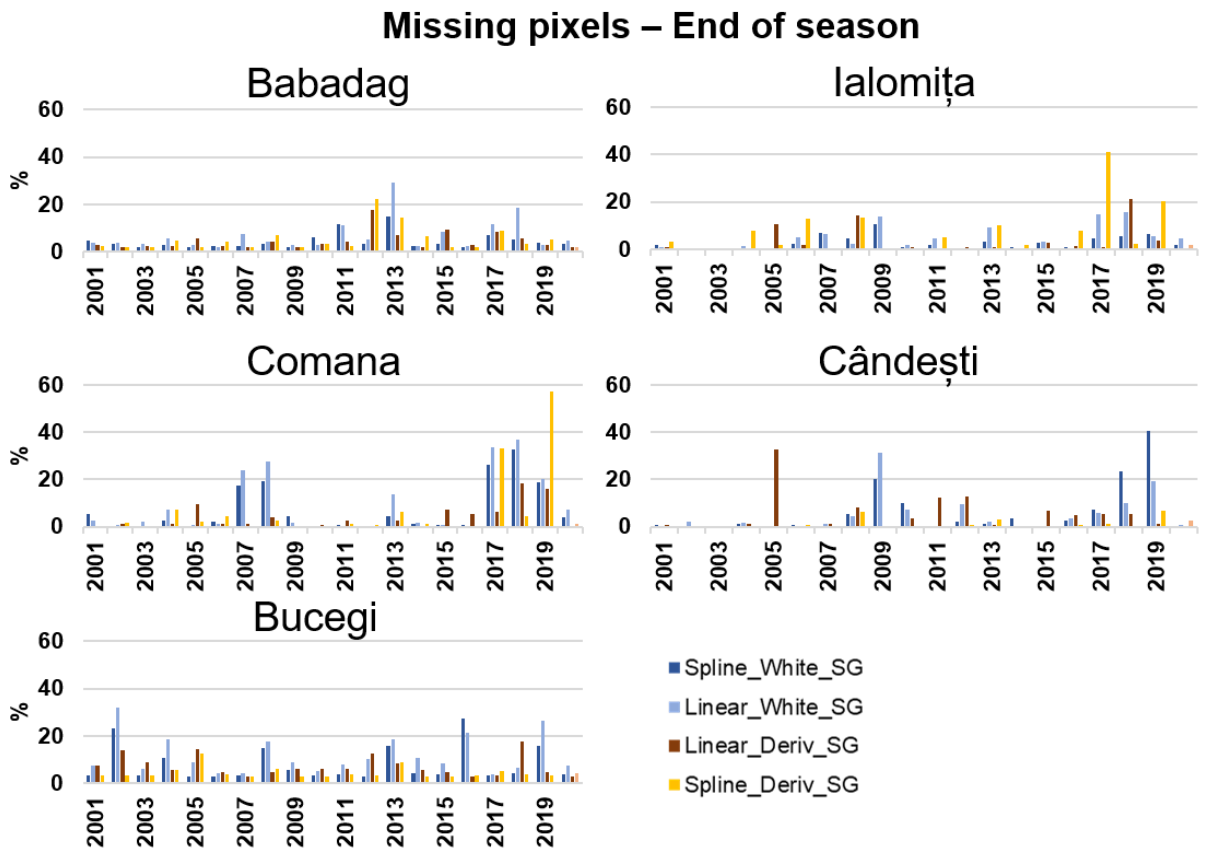

Figure 8.4 Percentage of annual missing values for each phenology approach for End of Season (EOS) between 2001 – 2020, in the five selected areas

The correlations between each phenological approach that identified SOS in the five study sites and the average preseason temperature (average February – March) at the closest meteorological station(s) or from the E-OBS gridded dataset are shown in **Table 8.7**. Except for Bucegi, all correlations are negative (the higher the preseason temperature, the earlier the SOS).

For the Comana, Ialomița and Babadag areas, it seems that two algorithms obtained higher significant correlation coefficients: firstly, the spline interpolation with *white* thresholds, followed by linear interpolation with *white* thresholds (therefore, there were higher coefficients for *white* thresholding). In the case of the Bucegi area, the highest significant correlation coefficient was obtained for the *linear-deriv* algorithm with the E-OBS average temperature. In the Cândești area, there were no significant correlations; however, the highest coefficient was obtained for the *spline-white* approach.

Table 8.7 Pearson correlation coefficient between the Start of Season (SOS) obtained through four approaches and the average temperature at meteorological stations and obtained from the gridded E-OBS data between February – March (2001 – 2020). Bolded and starred values represent significance at a 0.05 significance level.

SOS	*Linear-white*	*Linear-deriv*	*Spline-white*	*Spline-deriv*
Babadag				
Tulcea	**-0.62***	-0.43	**-0.67***	**-0.49***
E-OBS	**-0.61***	-0.43	**-0.66***	**-0.48***
Ialomița				
București Băneasa	**-0.47***	-0.29	**-0.56***	-0.30
E-OBS	-0.45	-0.22	**-0.57***	-0.30
Comana				
București Băneasa	**-0.47***	-0.24	**-0.55***	-0.25
Roșiorii de Vede	**-0.51***	-0.21	**-0.60***	-0.29
E-OBS	**-0.5***	-0.19	**-0.59***	-0.30
Cândești				
București Băneasa	-0.25	-0.01	-0.39	-0.03
Râmnicu Vâlcea	-0.29	-0.11	-0.38	-0.04
E-OBS	-0.30	-0.07	-0.42	-0.04
Bucegi				
Vârful Omu	0.38	0.41	0.24	0.32
E-OBS	**0.47***	**0.52***	0.33	**0.45***

In the following, the relation between SOS and the average temperature in February – March obtained from the E-OBS gridded dataset is analysed. While the growing degree-days measure is mainly used for estimating phenological stages (Comps et al., 1987; Lepage and Bourgeois, 2012), the average temperature can also represent a useful tool for evaluating phenological metrics.

The linear regression between the average temperature for February – March and the SOS shows a change of ~ -1.77 days/^{o}C in Cândești, ~ -2.65 days/^{o}C for Babadag, ~ -2.79 days/^{o}C for Comana, ~ -2.74 days/^{o}C for Ialomița (**Figure 8.5**). In Bucegi, there is an opposite relation; this might suggest that the selected smoothing and phenological identification methods might not be suitable for this region, or this correlation method might not be appropriate.

Bórnez et al. (2021) found a mean sensitivity of SOS to temperature in broadleaf forests of about -2.45 days/^{o}C globally, going to about -5 days/^{o}C in Eurasia.

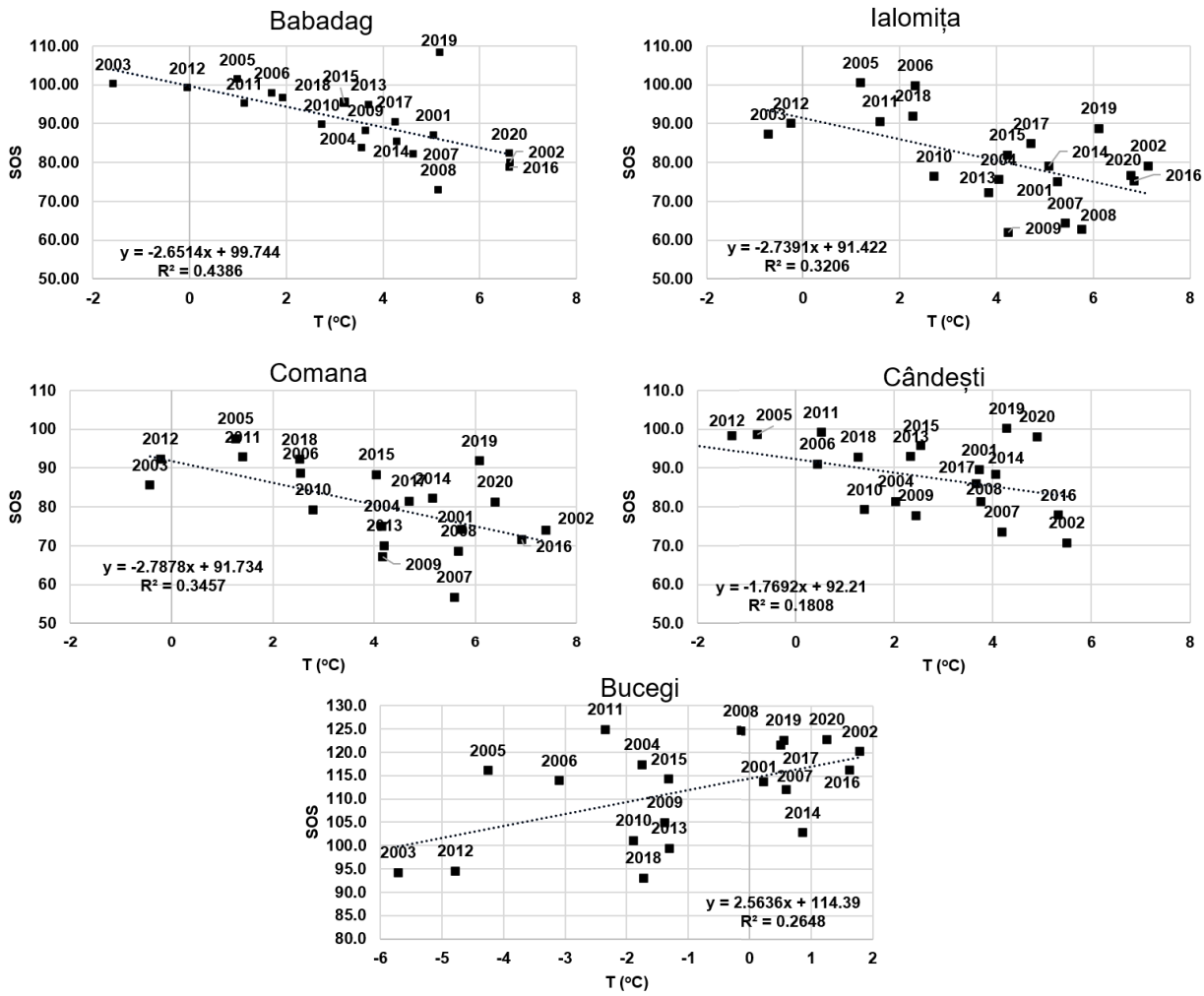

Figure 8.5 Linear regression between average temperature (average gridded E-OBS) in February – March (2001 – 2020) and Start of Season (SOS) obtained from spline smoothing and *white* phenology identification method in the Babadag, Ialomița, Comana, Cândești areas and from linear smoothing and *deriv* phenology identification method in the Bucegi area

The sensitivity of EOS to temperature was estimated in the Northern Hemisphere at -0.5 days/ºC (earlier EOS with higher temperature) while to precipitation at 0.5 days/10 mm (delayed EOS with higher precipitation) (Bórnez et al., 2021). Considering the comparable results between the correlations and temperature in meteorological stations versus E-OBS in the case of SOS, only the correlations with E-OBS are performed for the EOS (**Table 8.8**). They are mostly insignificant. The only significant (negative) correlations appear in the case of the Ialomița area, between the average temperature (September – October) and *linear-white* and *spline-white* approaches, as well

as in the Bucegi area for total precipitation (September – October) and *linear-white* approach. Except for Bucegi, although mostly insignificant, correlations between average preseason temperature and EOS are mostly negative, suggesting an earlier EOS with higher preseason temperature. Finally, **Figure 8.6** shows the linear relationship between average temperature and EOS in the Ialomița area, suggesting an advance of ~ -4.6 days/^{o}C.

Table 8.8 Pearson correlation coefficient between the End of Season (EOS) obtained through four different approaches and total precipitation and average temperature between September – October (2001 – 2020) from E-OBS. Bolded and starred values represent significance at a 0.05 significance level.

EOS	*linear-white*	*linear-deriv*	*spline-white*	*spline-deriv*
Babadag				
Total precipitation	0.03	0.41	0.02	0.33
Average temperature	-0.05	0.04	-0.14	0.02
Ialomița				
Total precipitation	0.39	0.40	0.33	0.19
Average temperature	**-0.47***	-0.13	**-0.5***	-0.25
Comana				
Total precipitation	0.23	0.38	0.23	0.43
Average temperature	-0.34	-0.21	-0.40	-0.42
Cândești				
Total precipitation	0.26	0.42	0.20	0.32
Average temperature	-0.31	0.00	-0.22	0.20
Bucegi				
Total precipitation	**-0.48***	0.05	-0.44	-0.30
Average temperature	0.14	0.15	0.07	0.29

The results of Bórnez et al. (2021) suggest that in Romania, an earlier EOS is associated with higher precipitation at higher altitude areas, while lowlands gravitate towards a later EOS with higher precipitation (Bórnez et al., 2021). The significant correlation coefficient between total precipitation and EOS (*linear-white*) in the Bucegi area would be consistent with these results. The negative correlation between precipitation and EOS in this area could be because increased precipitation is associated with increased cloudiness, which limits solar radiation and productivity in these forest biomes. In the forests in other regions, the correlations with precipitation are weak but positive, suggesting that higher precipitation could promote a more extended season (or the reverse, a deficit/lower precipitation tends to advance the EOS). Overall, these results would

suggest that drought in the preseason (low precipitation and increased temperatures) would advance the EOS; however, the relationships between variables are weak.

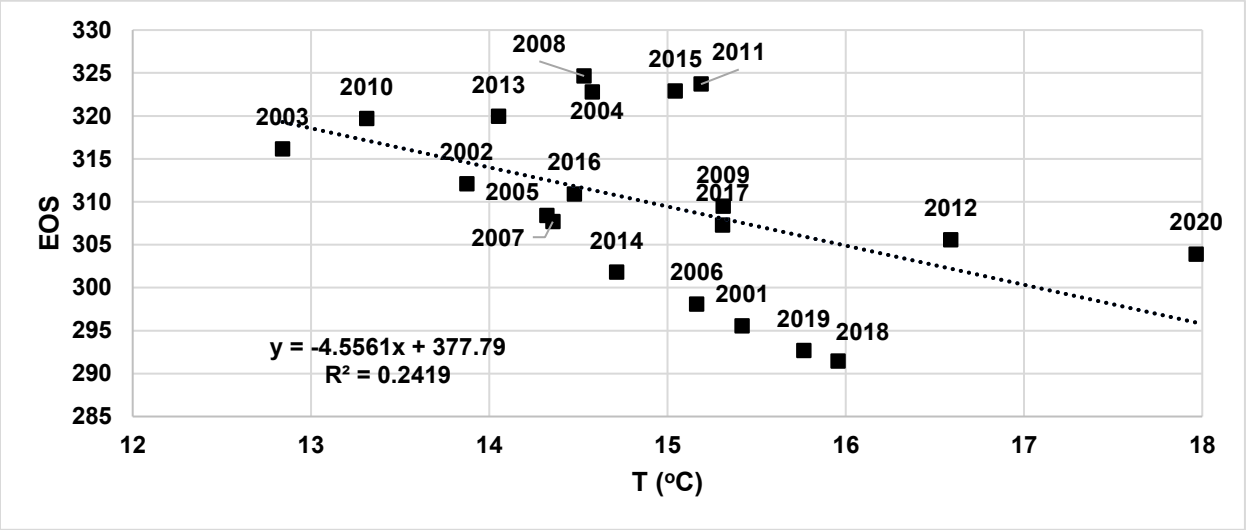

Figure 8.6 Linear relationship between the End of Season (EOS) (spline smoothing, *white* phenology approach) and average temperature, in the Ialomița area, in September – October (2001 – 2020)

The correlations of EOS with raster-CWD between April – October shown in **Table 8.9** are mostly insignificant. The only significant results are obtained for the *linear-white* approach in the Ialomița and Babadag areas, where there is a positive correlation, suggesting that the higher the deficit, the later the EOS. These results contrast the previously obtained correlations for EOS (negative correlations with temperature and positive correlations with precipitation). Bórnez et al. (2021) found mostly weak and positive relationships between EOS and SPEI.

Table 8.9 Pearson correlation coefficient between End of Season (EOS) obtained through four approaches and raster-CWD between April – October (2001 – 2020). Bolded and starred values represent significance at a 0.05 significance level.

EOS	*linear-white*	*linear-deriv*	*spline-white*	*spline-deriv*
Babadag	0.38	0.24	0.3	0.21
Ialomița	**0.58***	-0.21	0.44	0.34
Comana	**0.58***	-0.12	0.44	0.26
Cândești	0.42	-0.068	0.41	0.28
Bucegi	0.17	-0.22	0.086	0.032

8.5. Vegetation response to the 2007 – 2008 drought

The 2007 – 2008 period was marked by one of the most severe droughts in the last decades, with impacts encompassing multiple sectors. This applied to both cropland and natural vegetation, as demonstrated in previous chapters. In the case of broadleaf forests, low values of the NDVI anomaly occurred in 2007 and 2008 in the lowland areas of Babadag, Ialomița and Comana, and in 2008 also at higher altitudes in the Cândești and Bucegi areas. According to the Dunn's test results (**Table 8.6**), in 2007, the Babadag, Ialomița and Comana areas had a similar response, while in 2008, the Babadag and Comana areas had a similar response. In 2007, the site with the lowest NDVI anomalies was Ialomița, while in 2008, Cândești had the lowest anomalies. These results have motivated a more thorough analysis of the study sites for 2007 and 2008.

The evaluation deals with multiple aspects. Firstly, the regional CWD conditions from both years at meteorological stations and spatially distributed (raster-CWD) are described. Secondly, the vegetation condition during the drought is evaluated by analysing the spatial distribution of monthly NDVI standardized anomalies and the temporal profile of the 16-day NDVI in the five study sites.

8.5.1. Climatic conditions

8.5.1.1. Growing season and monthly climatic water deficit at meteorological stations

Relative to the 1991 – 2020 period, there were positive values of the total growing season deficit anomaly (station-CWD_{CRU}) in 2007 at all meteorological stations, but especially at București Băneasa (+220 mm), Galați (+224 mm), Tulcea (+199 mm), and Călărași (+187 mm). In 2008, the anomaly decreased in most of the stations but increased in Buzău, Râmnicu Vâlcea, and Roșiorii de Vede.

The CWD anomaly in the growing seasons increased in 2008 to +117 mm from +88 mm in 2007 in Râmnicu Vâlcea, which probably compounded the plant water stress, where the average growing season NDVI anomaly was positive in 2007 in the Cândești area and severely low in 2008 (**Table 8.6**, **Figure 8.1**). The Bucegi area also followed a similar trajectory.

Based on the CWD, the drought of 2007 developed from mid-spring to mid-summer (April – July), as seen in the positive anomalies of the CWD at most of the meteorological stations. The highest positive anomalies occurred in June at București Băneasa, Buzău (+ 88 mm and + 70 mm respectively), and in July at the other stations (+ 91 mm at Galați and + 96 mm at Tulcea, for example). In August, the situation reverses with negative anomalies of the CWD (wetter conditions), driven by the positive anomalies of precipitation (+38 mm at București Băneasa, +87 mm at Buzău, +90 mm at Râmnicu Vâlcea) and average PET. Afterwards, there were relatively normal to slightly drier conditions until the end of the year.

In 2008, following a slightly drier March and a slightly wetter April, higher positive CWD anomalies developed in most stations from May to August. The positive anomaly was the highest in August at most stations. The strongest anomalies were at Râmnicu Vâlcea and București Băneasa (+84 mm and +63 mm, respectively). These high CWD values in 2007 and 2008 could explain the low NDVI anomalies in both years, especially the very low value of NDVI in the Cândești area in 2008.

The high deficit in the two years resulted from negative precipitation anomalies and high positive PET anomalies. For example, strong negative anomalies of precipitation were observed at București Băneasa (-59 mm and -47 mm below average in June and July 2007 and -41 mm and -40 mm below average in June and August 2008), Râmnicu Vâlcea (-46 mm and -59 mm below average in June and July 2007 and -53 mm and -78 mm below average in June and August 2008) and Tulcea (-21 mm and -56 mm below average in June and July 2007).

Between the two years, the highest values above average for PET were in June and July, with most stations recording more than +30 mm. For most stations, June is, on average, the month with the highest total precipitation; therefore, the strong negative anomalies in June 2007 could have had a significant impact on water storage available to forests.

The strong contrasts in 2007 could be explained by the fact that despite the water deficit conditions during this year, there might have been soil water that was not yet depleted in all sites (considering that 2005 was a water surplus year; in 2006, higher positive anomalies of the deficit were recorded mainly at București Băneasa, Galați and Roșiori de Vede). In addition, in 2007 at Râmnicu Vâlcea, there were wetter conditions from August to the end of the growing season.

The variability in NDVI response, as seen from the boxplot in **Figure 8.2**, is more uniform in 2008 than in 2007, because all selected sites showed strong negative anomalies. Moreover, some areas showed less variability in their response (especially Babadag and Comana) than in 2007.

8.5.1.2. Spatial distribution of the climatic water deficit

To understand the spatial distribution of the CWD, the monthly anomalies of the raster-CWD (**Chapter 3.3.2**) in 2007 and 2008 were analysed (**Figure 8.7**).

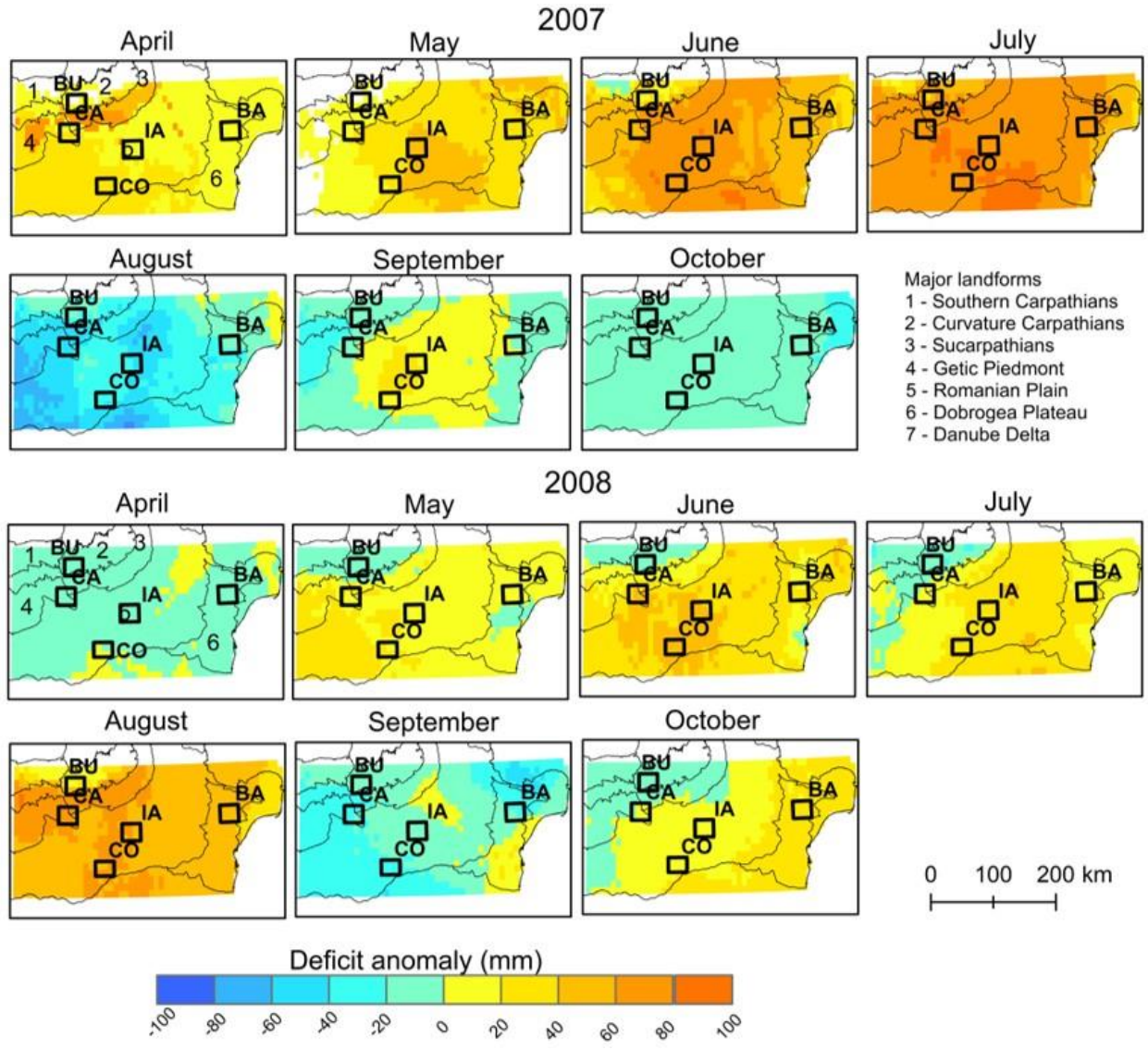

Figure 8.7 Monthly raster-CWD anomaly in 2007 and 2008 in five study sites: Babadag (BA), Bucegi (BU), Cândești (CA), Comana (CO) and Ialomița (IA) areas

As shown in **Figure 8.7**, a generally high water deficit in the growing season occurred in 2007. The month of July 2007 seems remarkable in terms of spatial distribution and severity of the deficit. August presents a wetter-than-usual situation across the entire study area, while in September, slight positive deficit anomalies continue to affect the Comana and Ialomița study areas. In 2008, the positive anomalies of the deficit occurred from May to August and in October.

The driest conditions occurred in August, where the highest values were found in the western part of the study area. The Comana, Ialomița and Cândești study areas were the most affected by drier-than-usual conditions in 2008.

8.5.2. Vegetation response to the 2007 – 2008 drought

8.5.2.1. Mean NDVI profiles of forests in 2007 and 2008

The 16-day NDVI profiles in 2007, 2008 and the average for the 2001 – 2020 period are presented in **Figure 8.8**. This allows a comparison both with average and between the two drought years.

In the Babadag, Ialomița and Comana areas, the 16-day NDVI profile was affected more in 2007 than in 2008, while the Cândești and Bucegi areas had the reverse situation (**Figure 8.8**).

In the Babadag area, in 2007, the values were generally lower than average during the growing season until the end of August, with a trough in July – August; after, values became higher than average until the end of the growing season (**Figure 8.8**). In 2008, the values of the NDVI were higher than average from the beginning of the growing season until the beginning of May; after, they were lower than average until the growing season's end, with a trough in August – September.

In the Cândești area in 2007 (**Figure 8.8**), the profile was higher than the 2001 – 2020 average at the beginning of the growing season, becoming close to the average until the end of the growing season. In 2008, the values were slightly lower than average until August, followed by a trough until the growing season's end.

In the Ialomița and Comana areas, the profile is similar in 2007 (**Figure 8.8**). Here the NDVI profile shows higher values than average at the beginning of the growing season, then much lower values compared to average, from the beginning of May to the end of August, and almost

normal/slightly higher until the end of the growing season. In 2008, the situation was different between the two locations. In the Comana area, in 2008, NDVI was slightly higher than usual at the beginning of the growing season, then close to average until the beginning of July, after which the profile was lower than average until the end of the growing season. In the Ialomița area, in 2008, the profile was higher than average from the beginning of the growing season through May; afterwards, it descended steadily until the growing season's end.

In the Bucegi area, in 2007 (**Figure 8.8**), the NDVI profile was higher than average or close to average for most of the growing season. In 2008, the profile was lower than average from April until the beginning of May, then close to average until the beginning of August; afterwards, similar to Cândești, the profile was much lower until the growing season's end.

8.5.2.2. Spatial distribution of NDVI anomalies in the five study areas

In 2007, the most severe anomalies (stressed vegetation) occurred in July (**Figure 8.9**), after which vegetation started to recover.

While in July 2007, all forests had negative anomalies of greenness compared to the average in the Babadag, Comana, Ialomița and Cândești areas, some hotspots seemed more affected than others. It also seems that the Cândești area had a lesser severity of vegetation anomalies, while in the Bucegi area, there were very few patches of stressed vegetation.

In July 2007, forests in Babadag, Comana and Ialomița areas responded more acutely than the surrounding land covers (arable land, pastures).

In 2008 (**Figure 8.10**), more severe NDVI greenness anomalies appeared in the latter part of the growing season, starting from August. This difference between 2007 and 2008 can also be observed in the average NDVI profiles (**Figure 8.8**). Moreover, the extent and severity of the negative anomalies were remarkable in September at higher altitudes (in the Cândești and Bucegi areas).

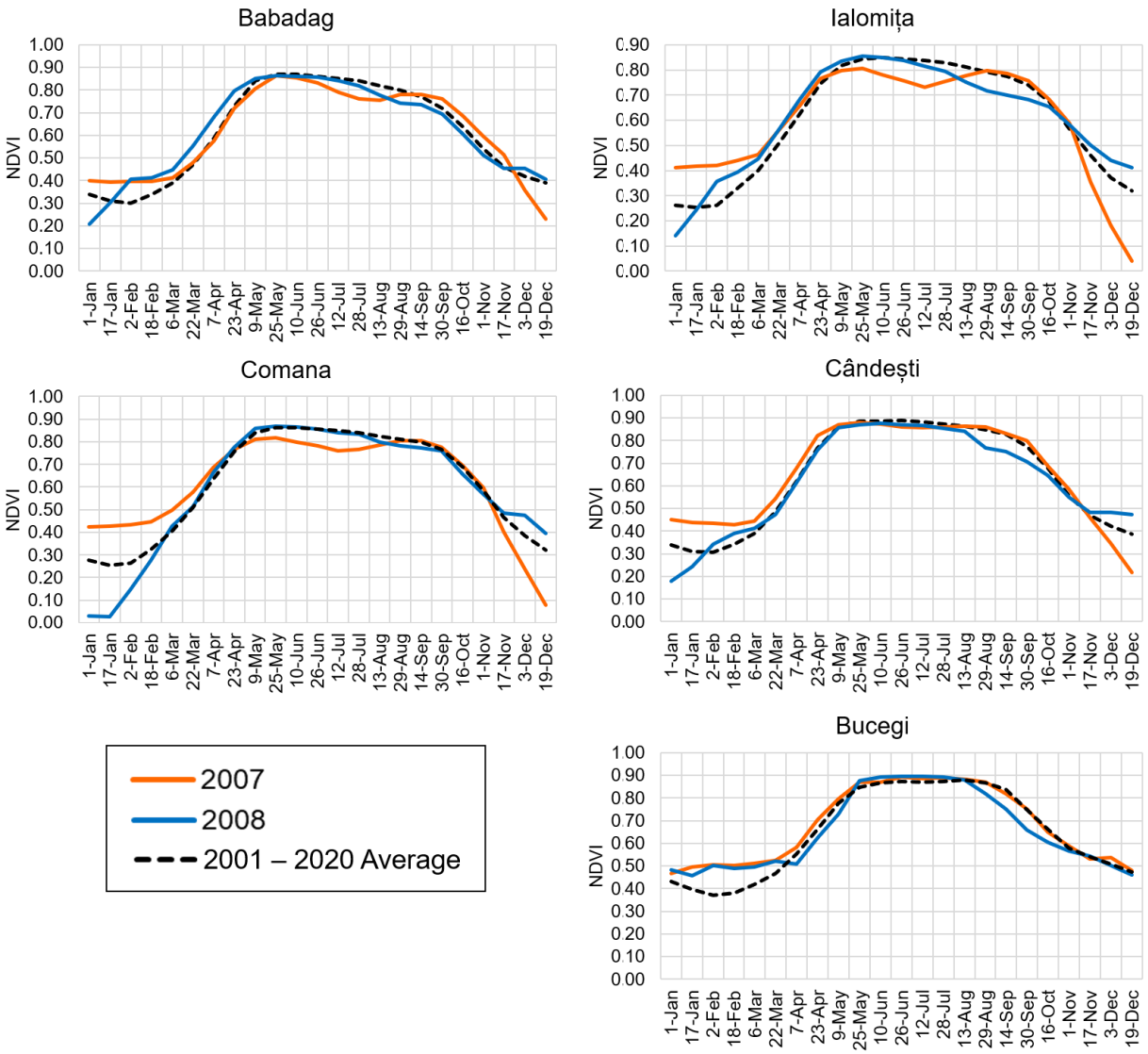

Figure 8.8 16-day NDVI profiles in 2007, 2008 and averaged over 2001 – 2020 in broadleaf forests in the selected study areas

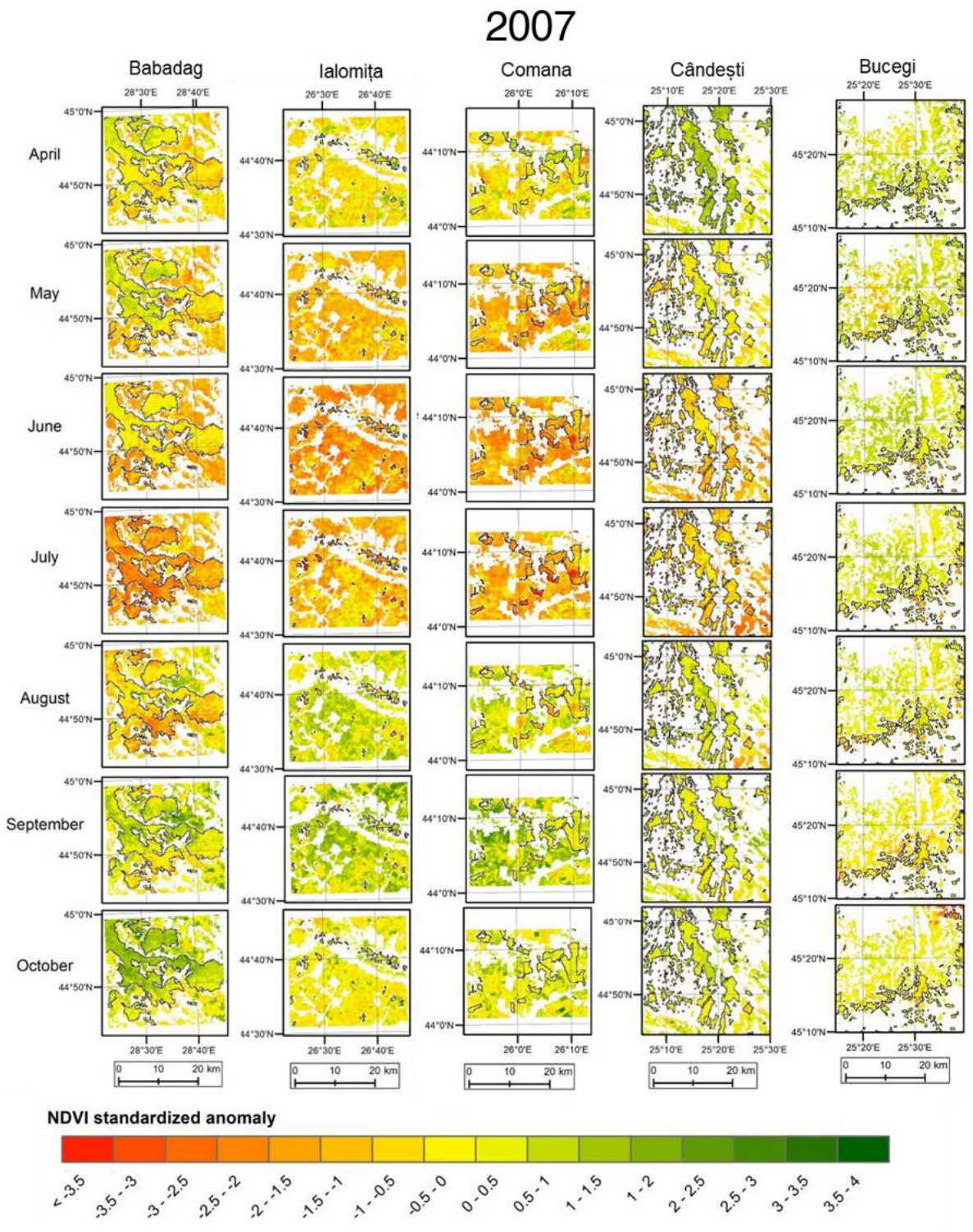

Figure 8.9 Monthly NDVI standardized anomalies in April – October 2007 in the five study areas, relative to 2001 – 2020. Green colours show a positive anomaly (higher vegetation activity than average); red colours show negative anomalies (lower vegetation activity than average).

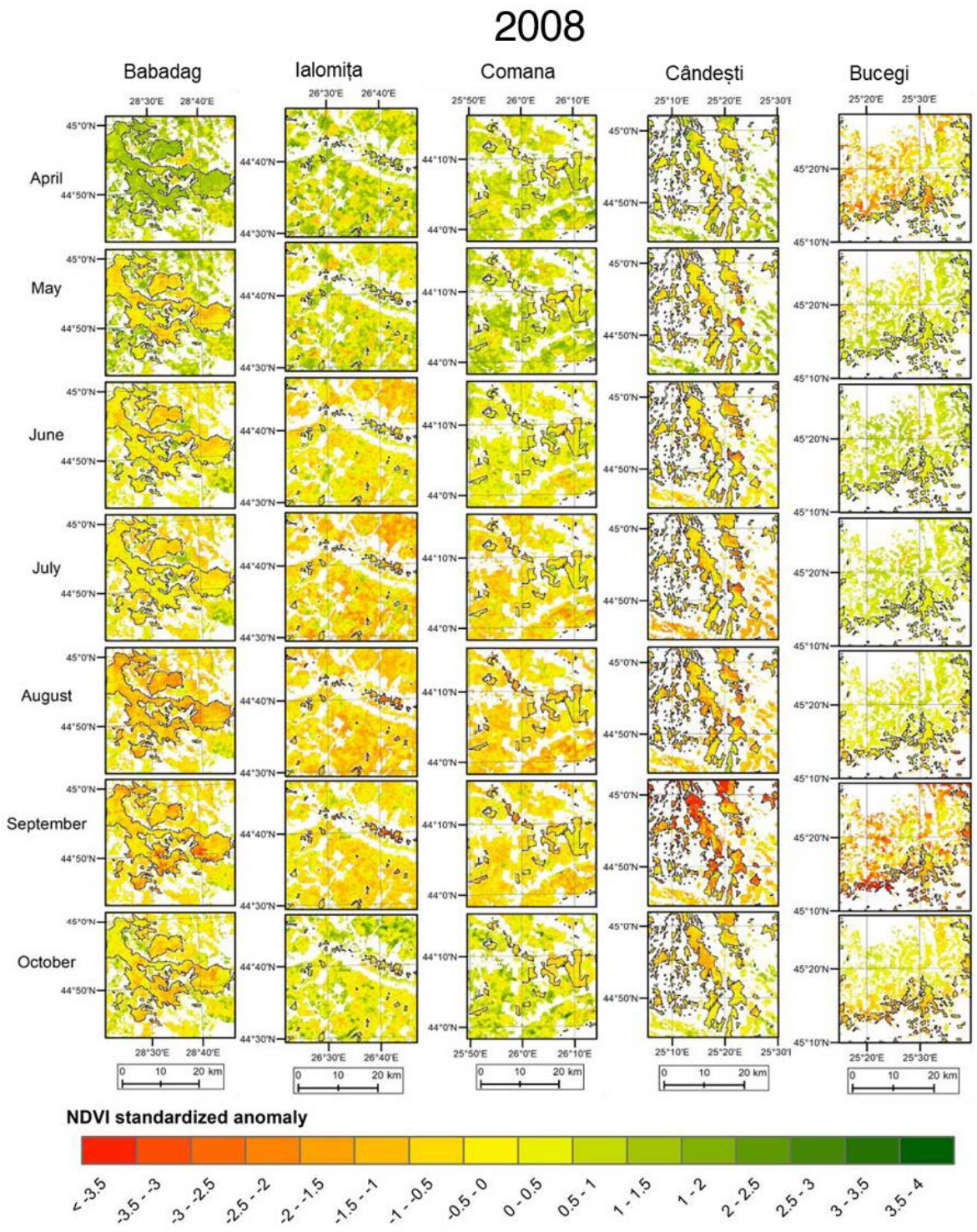

Figure 8.10 Monthly NDVI standardized anomalies in April – October 2008 in the five study areas relative to 2001 – 2020. Green colours show a positive anomaly (higher vegetation activity than average); red colours show negative anomalies (lower vegetation activity than average).

8.5.2.3. Phenology of forests in 2007 and 2008

In 2007, the phenological identification methods mostly showed an earlier SOS and, excepting the Bucegi area, most of the sites showed a later EOS (**Figure 8.11**); this can also be observed in the 2007 NDVI profile, where in most of the cases, the end of the growing season had slightly higher than average values (**Figure 8.8**). In 2008, most sites (except Bucegi) showed an earlier SOS (**Figure 8.12**). Compared to EOS, the results are generally clearer for SOS (the methods generally agree more in sign: positive or negative changes).

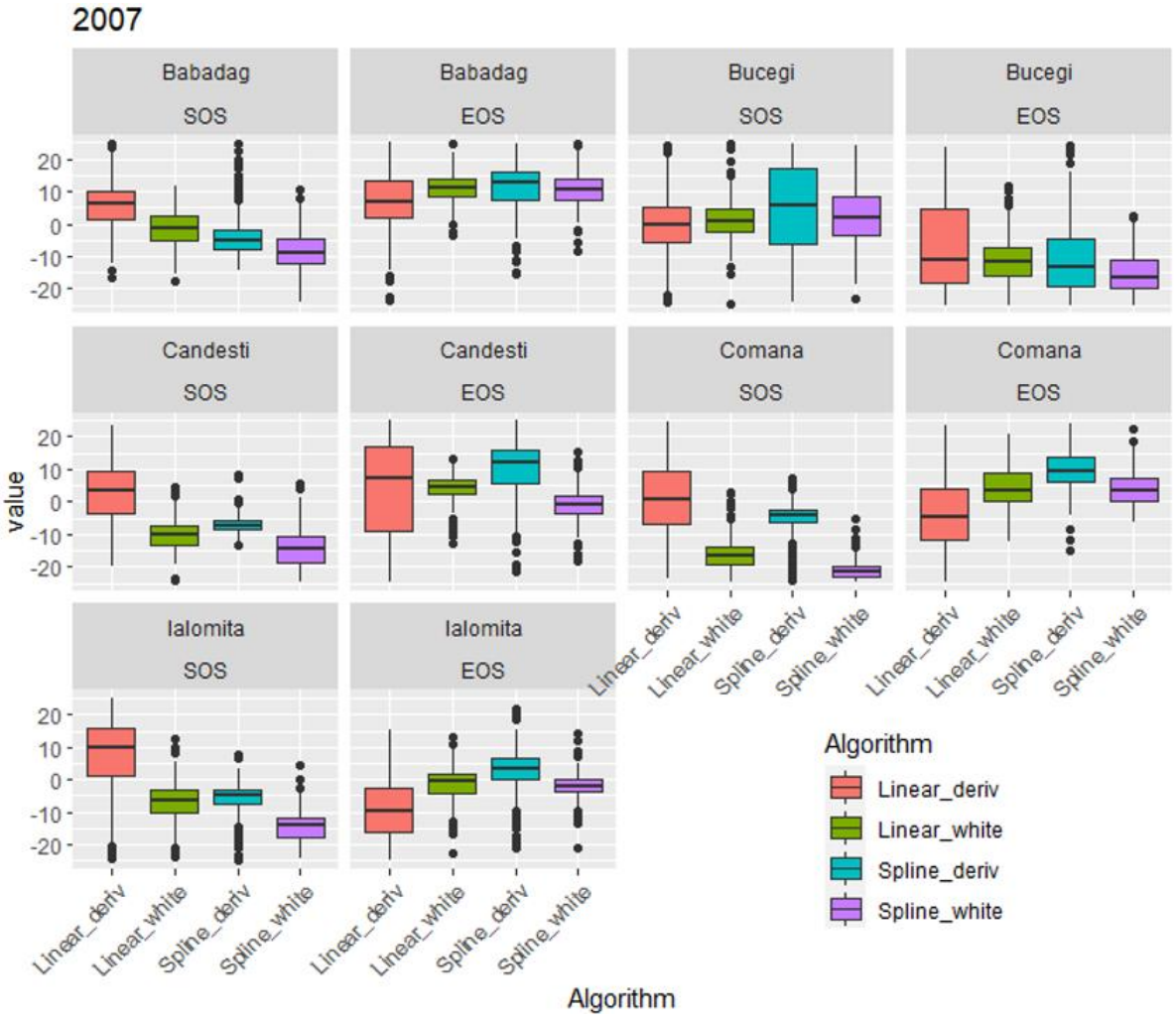

Figure 8.11 Anomalies in 2007 of the Start of Season (SOS) and End of Season (EOS) relative to 2001 – 2020 in the five sites, using two smoothing methods (linear interpolation and splines) and two phenological identification methods (*white* and *deriv* methods). Outliers of more than ±30 days were excluded.

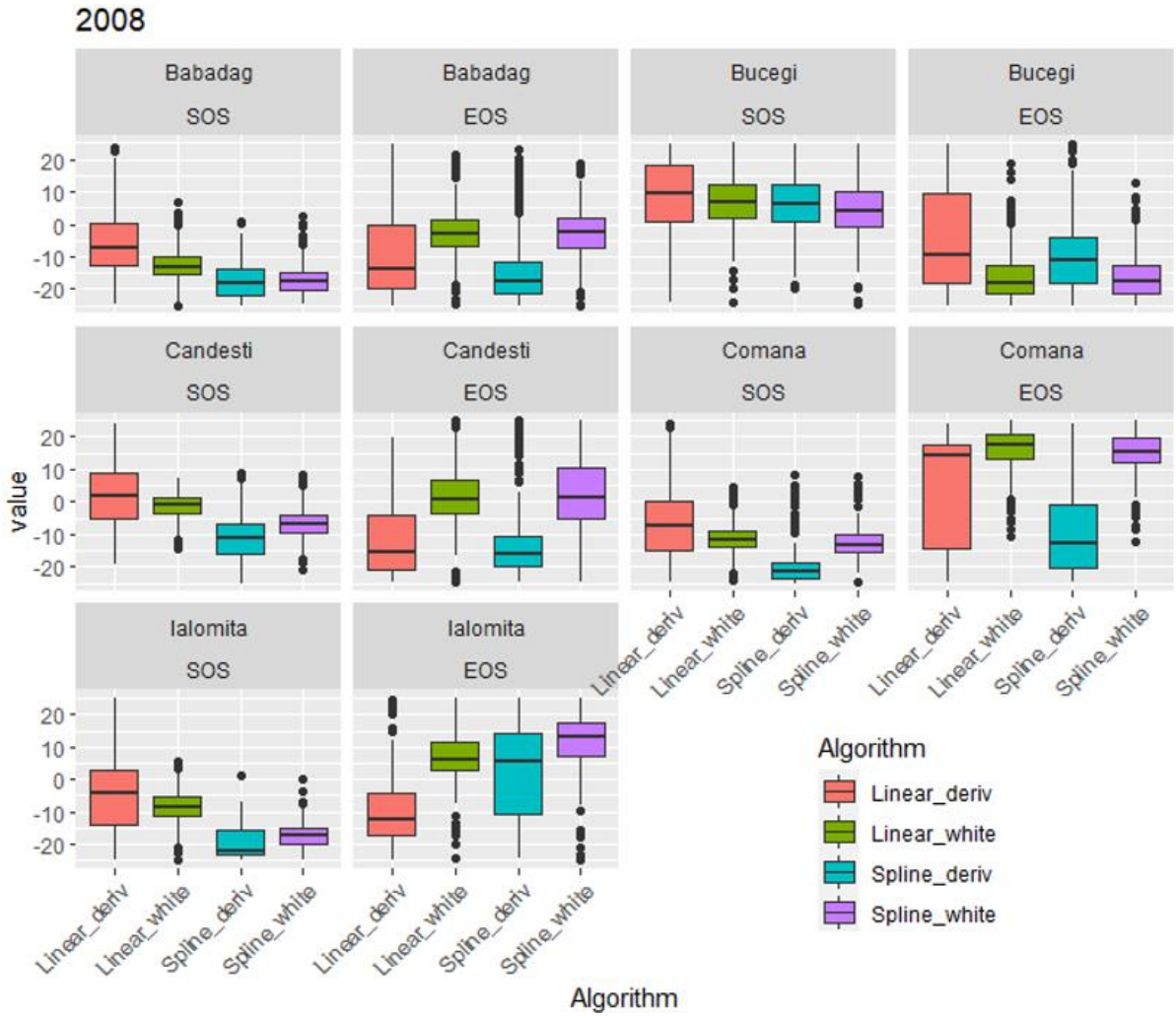

Figure 8.12 Anomalies in 2008 of Start of Season (SOS) and End of Season (EOS) relative to 2001 – 2020 in the five sites, using two smoothing methods (linear interpolation and splines) and two phenological identification methods (*white* and *deriv* methods). Outliers of more than ±30 days were excluded.

The 2007 NDVI profile was slightly higher or higher than average in 2007 at the start of the growing season in all stations. The higher-than-average NDVI values could have been due to the general trend of an early SOS in response to increased temperatures; the high preseason temperatures could have intensified these. The higher correlations between preseason temperature and the *spline-white* algorithm in the Babadag, Ialomița and Comana areas would suggest the potential suitability of this algorithm for SOS identification in this area. The spatial distribution of SOS and EOS anomalies in 2007 and 2008 is shown in **Figure 8.13** and **Figure 8.14**. In both 2007

and 2008, there was a predominantly earlier SOS, probably due to the increased temperatures in the preseason. Some authors found an earlier EOS due to summer drought (Bórnez et al., 2021; Ge et al., 2021). While some forest patches showed earlier EOS in 2007 (Ialomița, Cândești and Comana areas), Babadag had mostly a later EOS. The later EOS could be due to the improved conditions starting from August 2007. However, the Ialomița area had mainly water deficit conditions in 2007 (**Figure 8.7**). In 2008, mostly the Babadag and Cândești areas had an earlier EOS. In the Cândești area, this could be due to the high water deficit condition in August, which is confirmed by the severe negative NDVI anomalies in September (**Figure 8.10**).

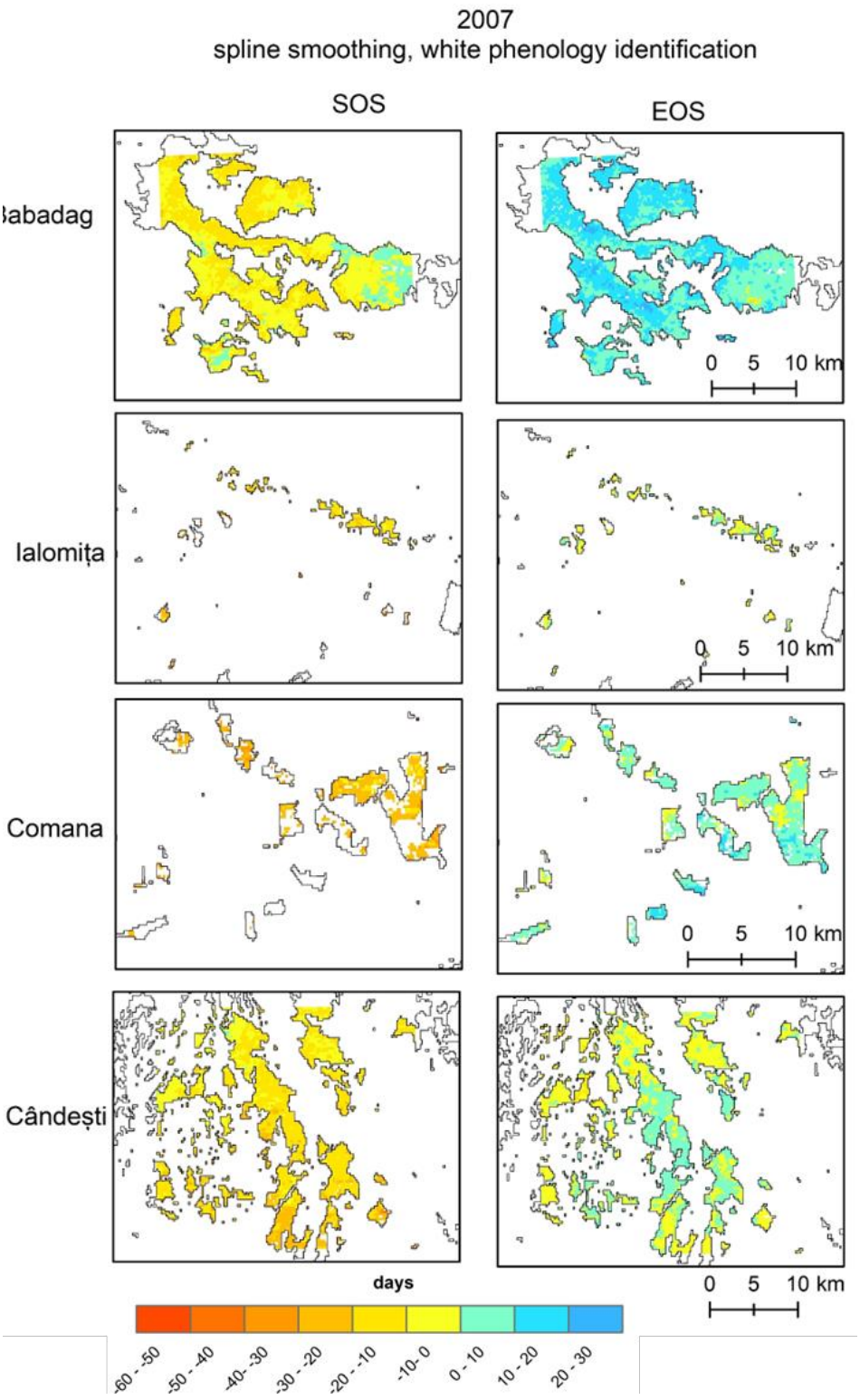

Figure 8.13 Spatial distribution of anomalies in 2007 of Start of Season (SOS) and End of Season (EOS) relative to 2001 – 2020, in the five sites, using *spline* smoothing and *white* phenology identification method

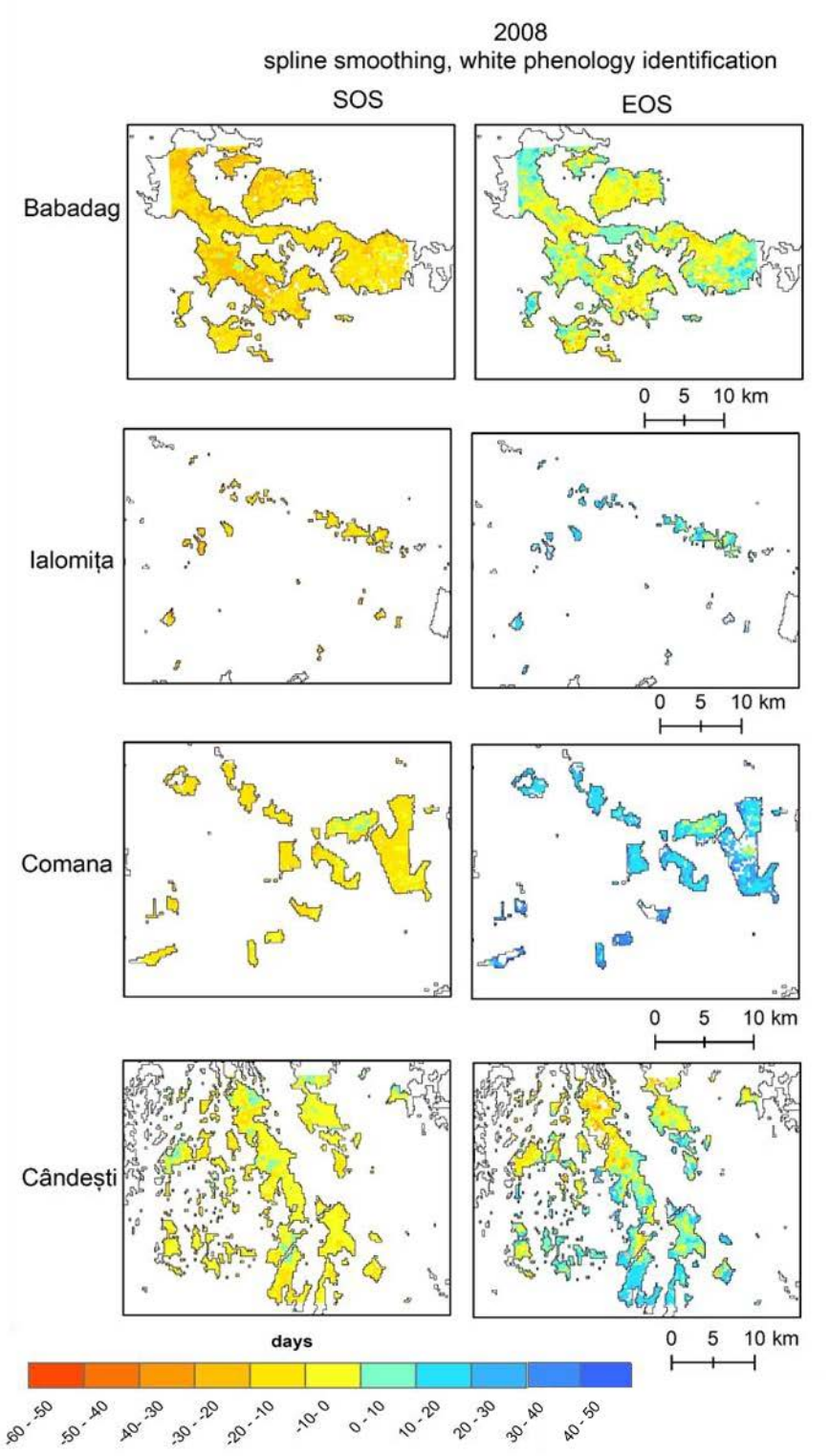

Figure 8.14 Spatial distribution of anomalies in 2008 of Start of Season (SOS) and End of Season (EOS) relative to the 2001 – 2020 period, in the five study areas, using *spline* smoothing and *white* phenology identification method

8.6. Vegetation response to the 2019 – 2020 drought

Part II demonstrated based on the CWD and standardized indicators that there were significantly dry conditions in the study area in the 2019 – 2020 period. This affected vegetation health, as noticed from the NDVI greenness. For example, negative values of the NDVI anomaly occurred in 2019 and 2020 in Cândești and Comana (similar responses according to the Dunn's test results), but also in 2020 in Babadag. The lowest median values occurred in Cândești in 2019 (-0.015) and in Babadag in 2020 (-0.016) (**Table 8.6**). Due to these reasons, and because it is the most recent in the analysed period, the analyses in this chapter are focused on the 2019 – 2020 drought.

8.6.1. Climatic conditions

8.6.1.1. Growing season and monthly climatic water deficit at meteorological stations

Relative to the 1991 – 2020 period, there were positive anomalies of the total growing season climatic water deficit anomaly (station-CWD_{CRU}) in most meteorological stations, except for București Băneasa and Vârful Omu. The deficit was particularly pronounced in the eastern part of the study area, where it increased in 2020 compared to 2019: at Călărași (+123 mm in 2019 and +160 mm in 2020), Constanța (+121 mm in 2019 and +244 mm in 2020), Galați (+178 mm in 2019 and +228 mm in 2020), Tulcea (+182 mm in 2019 and +247 mm in 2020), but also at Roșiorii de Vede (+102 mm in 2019 and +96 mm in 2020).

Based on the CWD, a drought was found in 2019 for most stations in summer and the beginning of autumn, while in 2020, it also developed in spring. There were slightly water deficient conditions in 2019 already since February/March at the Constanța, Călărași, Tulcea and Galați stations, which developed into stronger anomalies in June to September (+56 mm at Constanța and Tulcea and +32 mm at Galați in June 2019, +51 mm at Călărași and +46 mm at Tulcea in September 2019). The persistence of months with water deficit conditions was remarkable in 2019 at Călărași (9 months, March to November), Constanța (7 months, February to August), Galați (11 months, February to December) and Tulcea (10 months, February to November). In the other stations, there were deficit conditions in August and September (+ 55 mm at Roșiorii de Vede, + 49 mm at București Băneasa, +28 mm at Râmnicu Vâlcea in September, + 60 mm at Buzău in

August). In 2020, all stations had high positive water deficit anomalies in April and August – September. Persistent deficit conditions were found especially at Constanța (ten months, from January to October), Galați (also ten months, from January to October, which adds up to 21 months of deficit when also considering 2019) and Tulcea (seven months, from March to September). The wettest conditions during the two years were found at București Băneasa, with negative anomalies of the deficit between April – July 2019 and May – July 2020.

The high deficit was driven by the prolonged precipitation deficit at the stations in the eastern part of the study area (negative precipitation anomalies in most months in both 2019 – 2020 at Buzău, Călărași, Galați, Tulcea). In addition, PET had high positive anomalies in all stations, particularly in March, June, August – September 2019 and February – April and August – September 2020.

8.6.1.2. Spatial distribution of the climatic water deficit

The spatial distribution of the monthly anomalies of the raster-CWD for 2020 is shown in **Figure 8.15**. The raster-CWD presents significant inaccuracies in 2018 and 2019, as analysed in **Chapter 5.1.2**, therefore only the 2020 spatial distribution is shown here. The Babadag area had positive deficit anomalies for most of the growing season (except September). The months with the most extensive areas with positive deficit anomalies were April, July, and August in 2020.

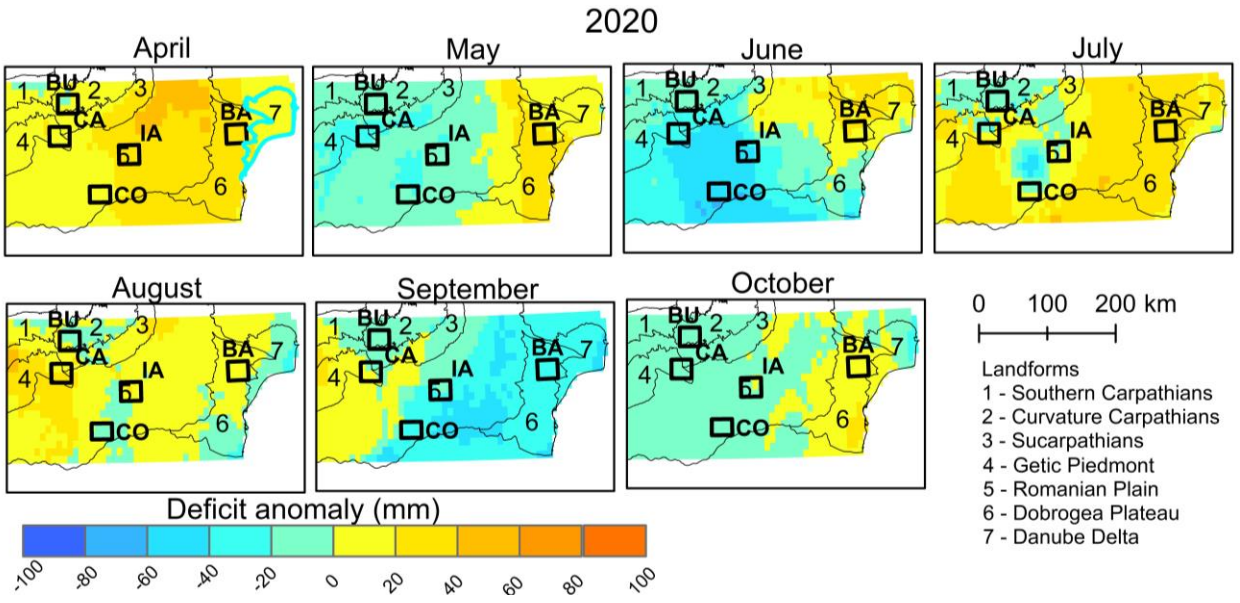

Figure 8.15 Monthly raster-CWD anomaly in 2020 in five study sites: Babadag (BA), Bucegi (BU), Cândești (CA), Comana (CO) and Ialomița (IA) areas

8.6.2. Vegetation response to the 2019 – 2020 drought

8.6.2.1. Mean NDVI profiles of forests in 2019 and 2020

Babadag was the most affected area in 2020 (**Figure 8.2**, **Table 8.6**), probably driven by the persistent water deficit throughout the growing season. The NDVI profile was above the 2001 – 2020 average in spring (from March to the end of April), after which it was always below average until the end of September (**Figure 8.16**).

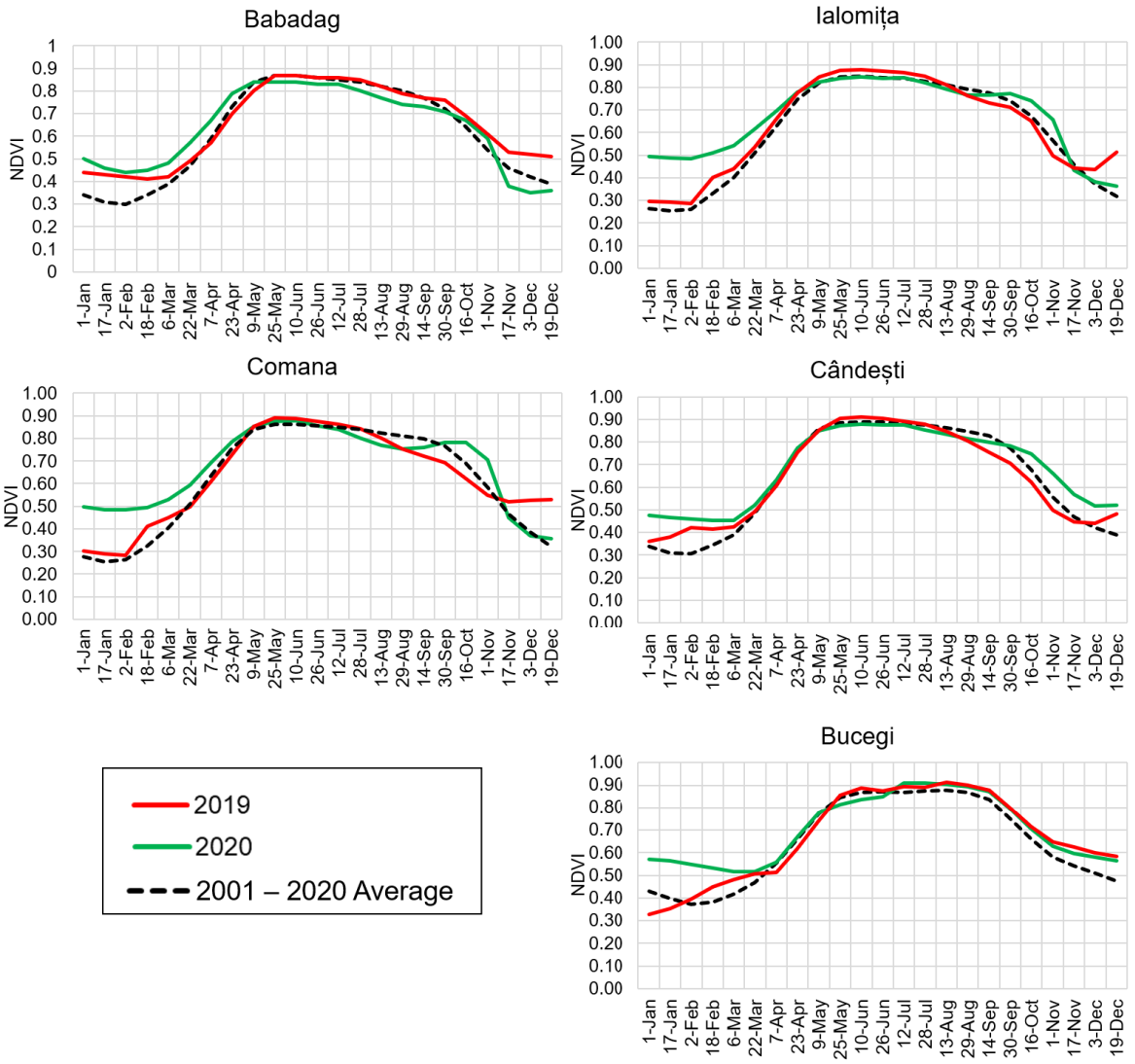

Figure 8.16 16-day NDVI profiles in 2019, 2020 and averaged over 2001 – 2020 in broadleaf forests in the five selected areas

In the Ialomița area, the 2019 NDVI profile was higher than the multiannual average until August; afterwards, it was lower until the end of the growing season. In 2020, there is a trough in August until mid-September, after which vegetation greenness recovers (in October) (**Figure 8.16**).

In the Comana area, the 2020 NDVI profile shows higher values in the first part of the growing season (April to the beginning of June) than the 2001 – 2020 average, after which the values descend (**Figure 8.16**). There is a trough in the NDVI activity between mid-July and mid-September, and in October, the NDVI profile shows an increased activity compared to the average. The trough could be due to the higher water deficit in April and August – September. In 2019, the NDVI profile was lower than average from mid-August. However, average growing season anomalies are mostly around average (**Figure 8.2**). The wetter-than-average conditions in May – June and the average conditions in October could have contributed to the average NDVI anomalies, despite the higher deficit in August and September.

In the Cândești area, the 2019 profile decreased compared to average conditions, starting in mid-August (**Figure 8.16**). The 2020 profile approaches average conditions until mid-July and decreases between mid-July and mid-September, after which it has higher values than average. Cândești was the second most affected area by drought in 2020.

In the Bucegi area, the 2019 profile also had higher values than the 2001 – 2020 average from July to the end of the growing season, which suggests a positive influence (**Figure 8.16**). Despite lowered values in May – June, the NDVI profile is also higher than the average from July to the end of the growing season, similar to 2019.

8.6.2.2. Spatial distribution of NDVI anomalies in the five study areas

The patterns of the positive anomalies of the water deficit (drought in summer and beginning of autumn) are also observed in the spatial distribution of monthly NDVI anomalies in April – October 2019, particularly in Ialomița, Comana and Cândești areas (**Figure 8.17**). In 2019, there were extensive areas of negative NDVI anomalies in the Cândești between August – October, especially in September. The forests in the Comana site also exhibited large areas with strong negative anomalies in August and September. The negative median of the growing season NDVI anomalies in 2019 in the Comana and Cândești areas also reflects these findings (**Table 8.6**). The

other sites had a positive median of growing season NDVI in 2019. In general, except for the Bucegi area (where slight anomalies appeared mostly in April), the strongest negative NDVI anomalies in all sites in 2019 were in September.

In 2020, the forests in the Babadag area were affected during an extensive period, between May and September. Significant negative NDVI anomalies were noticed also in the Cândești area between July and September. Regarding the Comana area, results for 2020 showed the most significant impact in August. On the other hand, in the Bucegi and the Ialomiţa areas, anomalies did not seem to have had a significant impact on vegetation.

When analysing 2020 compared to 2007 (**Chapter 8.5.2.2**, **Figure 8.9**), it seems there is a lower intensity of drought anomalies; however, these are spread over more months (**Figure 8.18**). For example, while in September and October 2007, it seems that vegetation had reached almost normal conditions for those months, in September 2020, there were still extensive negative anomalies in the study zones.

The median of NDVI anomalies in 2020 was negative in the Babadag, Comana and Cândești areas and positive in Ialomița and Bucegi (**Table 8.6**). In the Babadag area, the interquartile range (**Figure 8.2**) was smaller in 2020 than for the rest of the sites, showing a consistent/similar response throughout the 500 points in broadleaf forests, which was probably a response to the high water deficit observed in the eastern part of the study area.

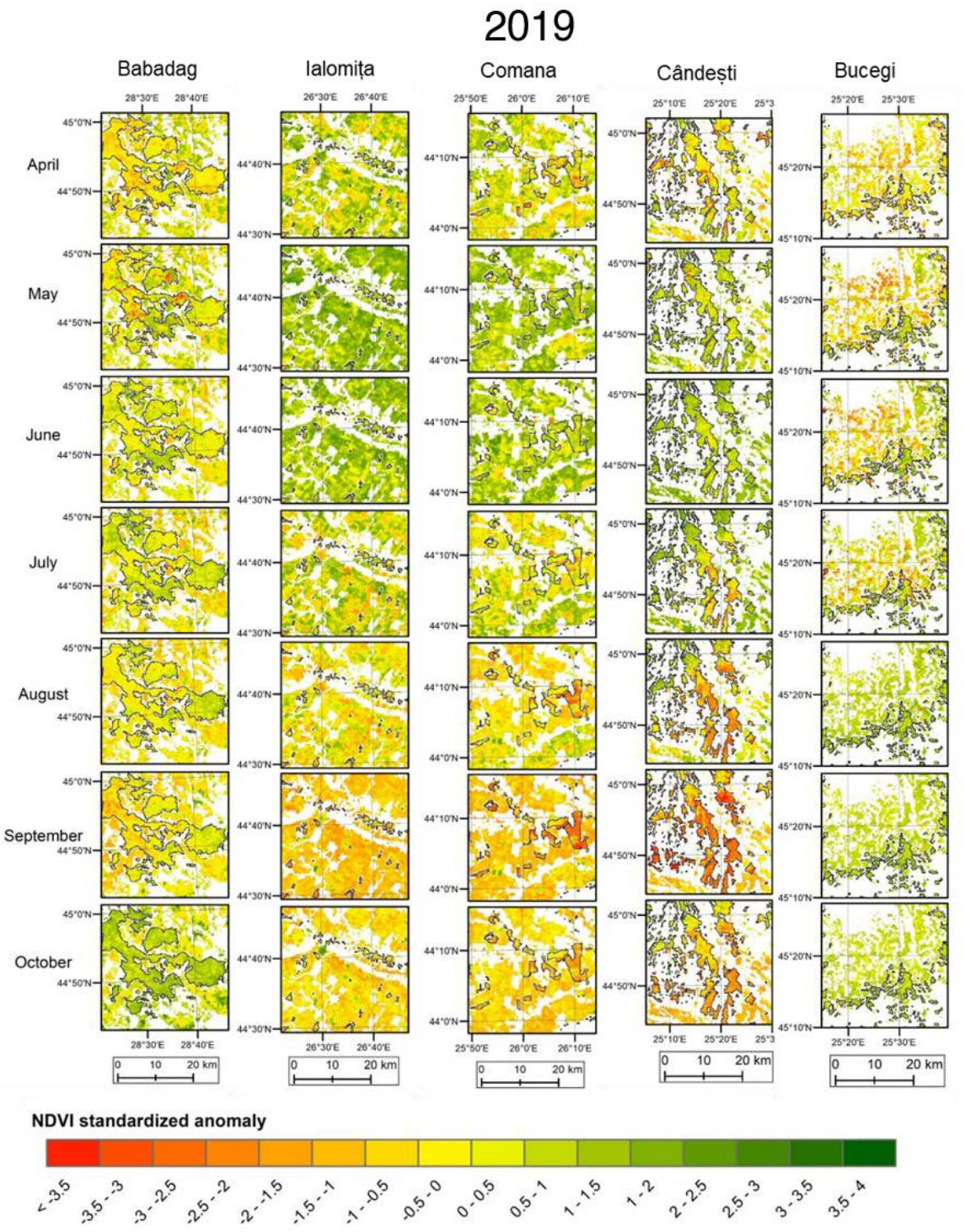

Figure 8.17 Monthly NDVI standardized anomalies during 2019 in the five study areas relative to the 2001 – 2020 period. Green colours show a positive anomaly (higher vegetation activity than average), while red colours show negative anomalies (lower vegetation activity than average).

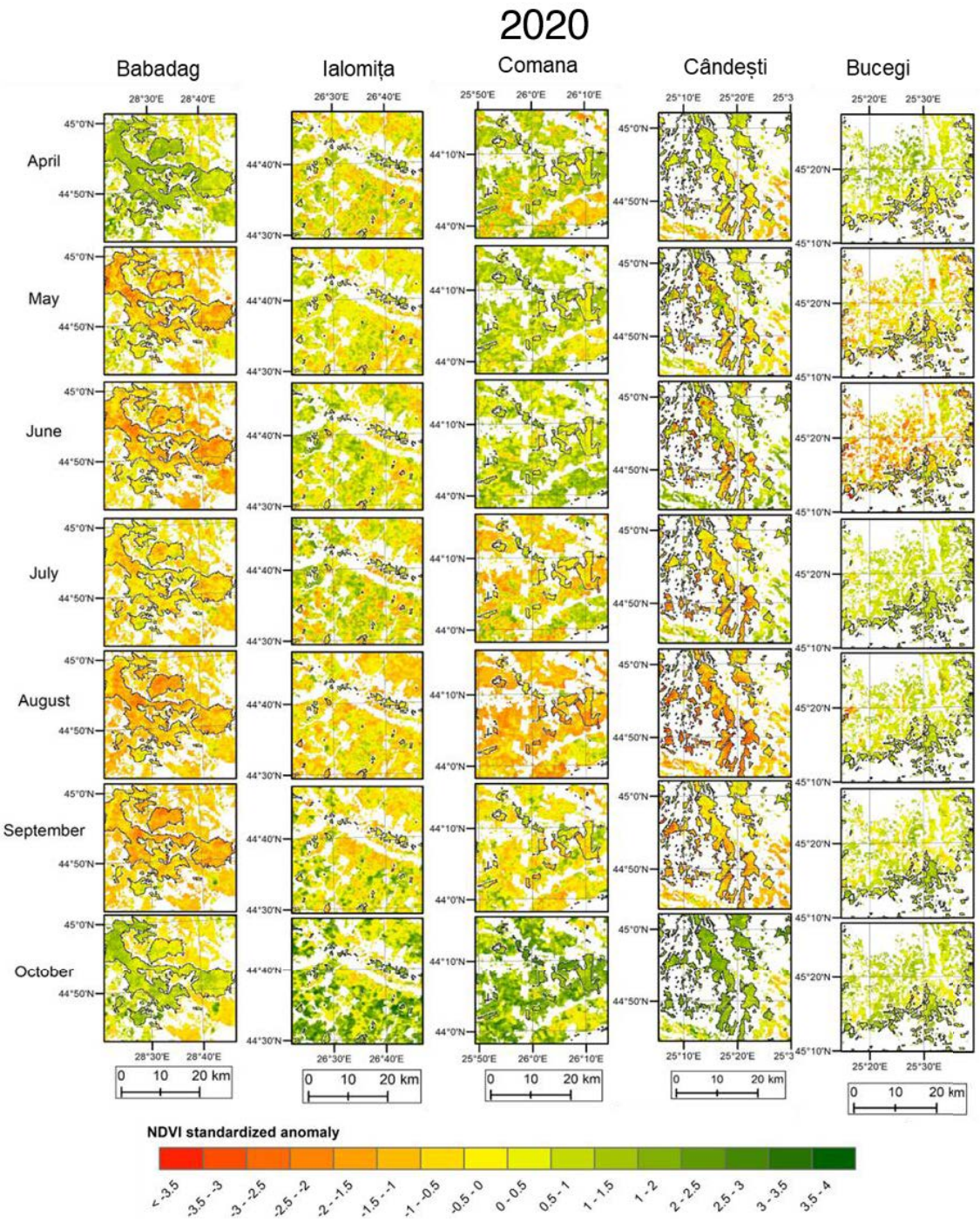

Figure 8.18 Monthly NDVI standardized anomalies during 2020 in the five study areas relative to the 2001 – 2020 period. Green colours show a positive anomaly (higher vegetation activity than average), while red colours show negative anomalies (lower vegetation activity than average).

8.6.2.3. Phenology of forests in 2019 and 2020

In 2019, most of the points showed a later SOS and an earlier EOS in all sites (except EOS in Bucegi, where algorithms do not agree) (**Figure 8.19**).

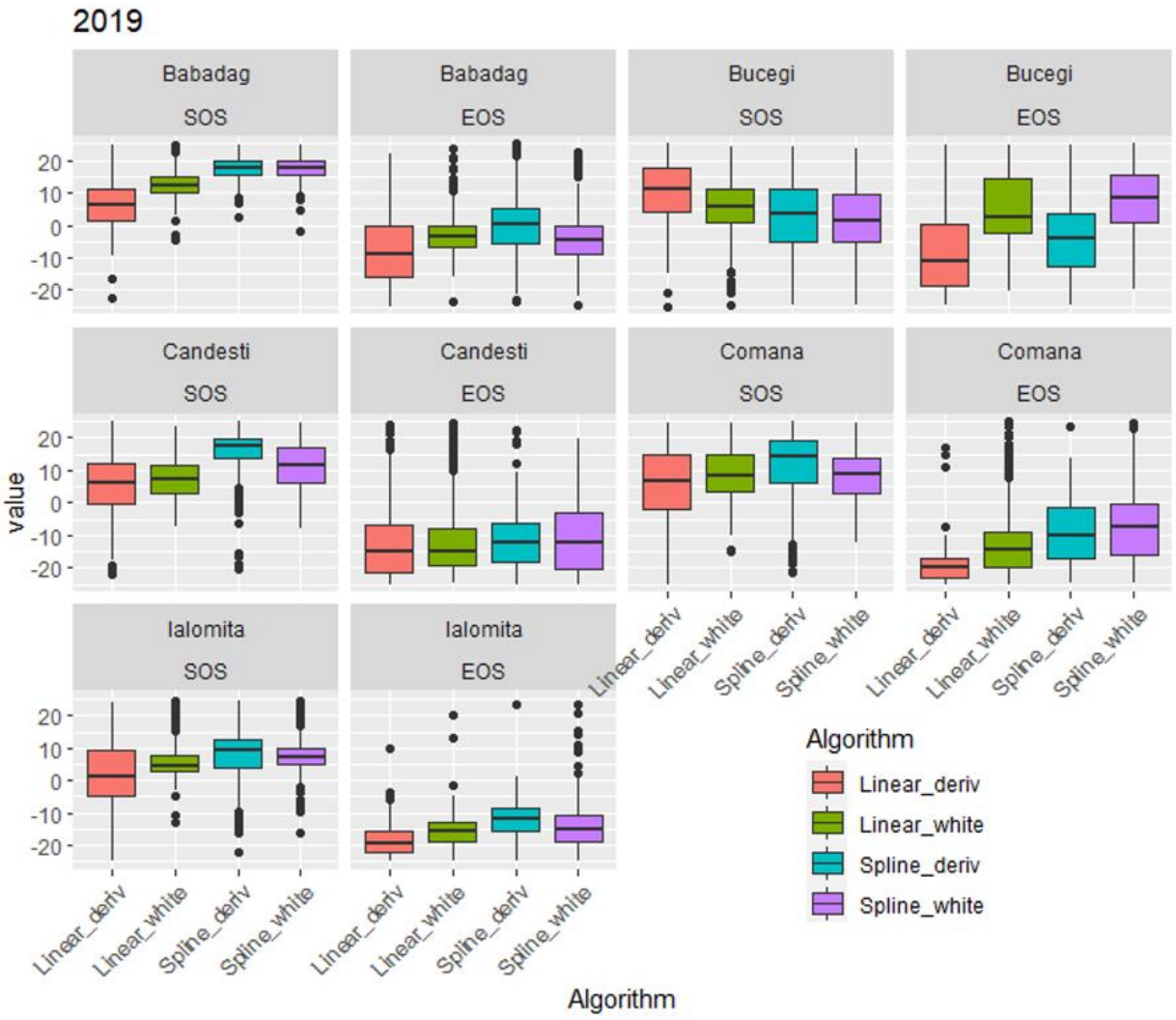

Figure 8.19 Anomalies in 2019 of Start of Season (SOS) and End of Season (EOS) relative to the 2001 – 2020 period in the five study areas, using two smoothing methods (linear interpolation and splines) and two phenological identification methods (*white* and *deriv* methods)

In 2020, most points showed a later SOS in the Bucegi, Cândești, and Comana areas (**Figure 8.20**). On the other hand, in the Ialomița and Babadag areas, the response was very variable. There is mostly an earlier EOS in Babadag, Bucegi, Comana, and Ialomița, while Cândești EOS is uncertain.

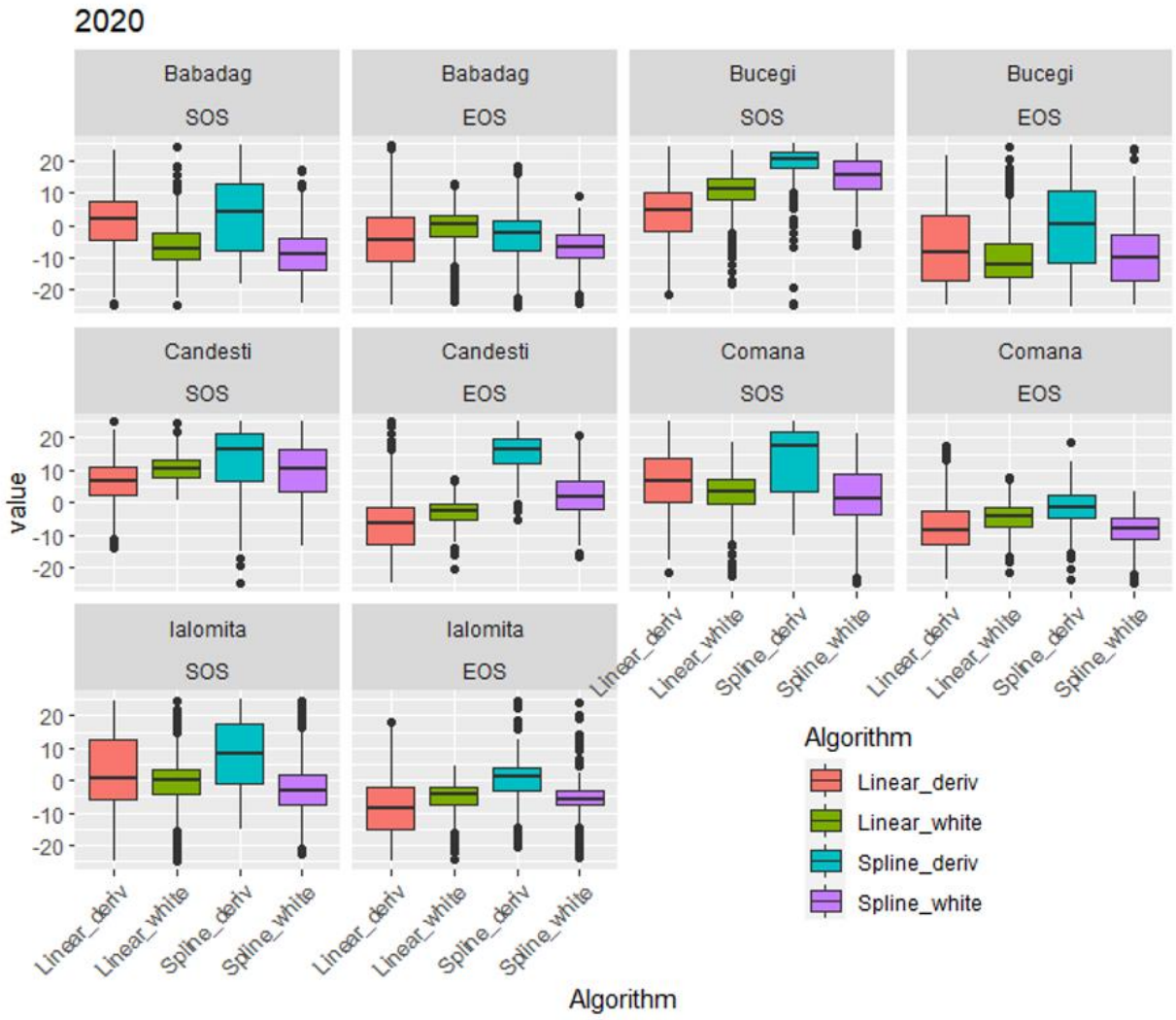

Figure 8.20 Anomalies in 2020 of Start of Season (SOS) and End of Season (EOS) relative to the 2001 – 2020 period in the five study areas, using two smoothing methods (linear interpolation and splines) and two phenological identification methods (*white* and *deriv* methods)

Figure 8.21 and **Figure 8.22** show the spatial distribution of SOS and EOS anomalies in 2019 and 2020, respectively, using the phenology results obtained through *spline* smoothing and *white* phenology identification methods. Despite positive preseason temperature anomalies, the SOS at most sites in 2019 and at Cândești and Comana in 2020 shows mostly later dates than average. In 2019 and 2020, there were mostly negative anomalies of the EOS (earlier senescence), possibly due to the high deficit throughout the growing season, especially towards the end.

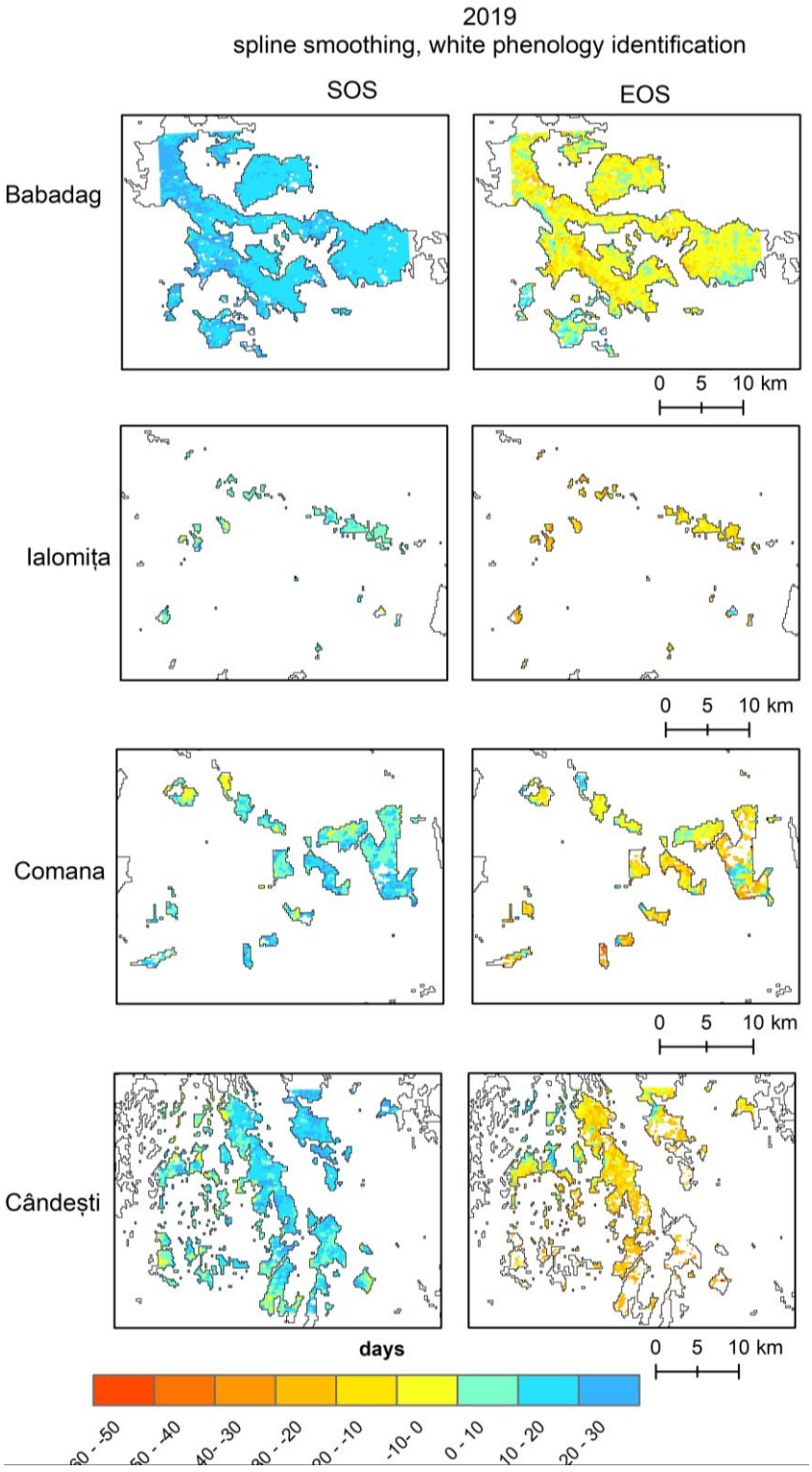

Figure 8.21 Spatial distribution of anomalies in 2019 of Start of Season (SOS) and End of Season (EOS) relative to the 2001 – 2020 period in the five study areas, using *spline* smoothing and *white* phenology identification method

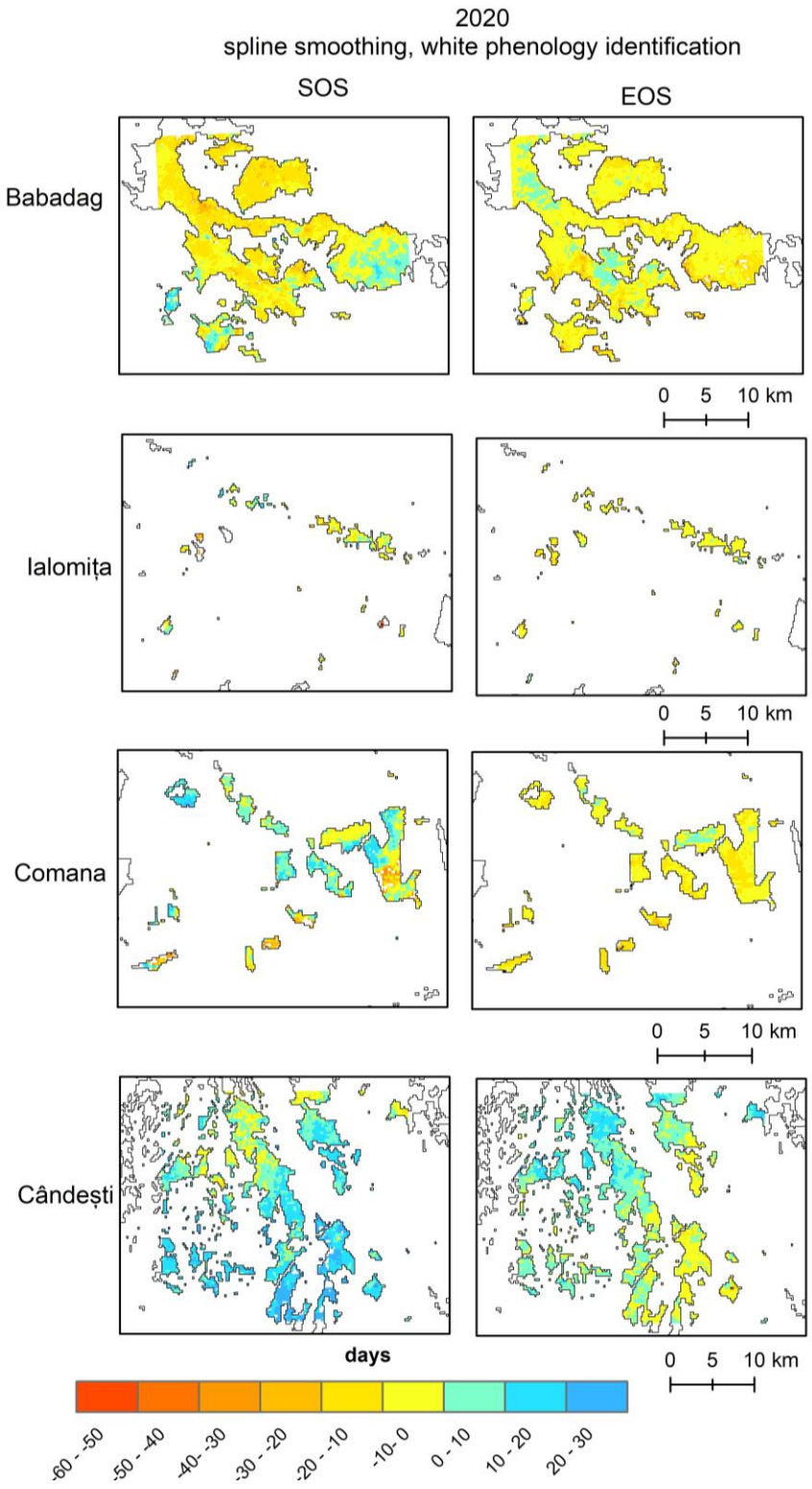

Figure 8.22 Spatial distribution of anomalies in 2020 of Start of Season (SOS) and End of Season (EOS) relative to the 2001 – 2020 period in the five study areas, using *spline* smoothing and *white* phenology identification method

Conclusion

This chapter has explored the variability of the NDVI with the aim of investigating the response of vegetation to drought in the study area.

First, there were different patterns of NDVI trends when analysing this indicator in various land covers at the regional level in the study area. Between 2001 – 2020, arable lands had positive trends between April and June, and negative trends in August and September. In pastures, there were positive trends between April and July, and negative trends in September in October. On the other hand, forests had a different pattern as response to drought. Broadleaf forests showed mostly positive trends throughout the growing season, with the highest areas of positive trends in May. Mixed forests had positive trends, particularly towards the end of the growing season (about 60% of the studied pixels showing significant trends in September). Coniferous forests did not have large areas of significant trends (the highest share of significant trends was about 25%, in September), and they were mostly positive. As discussed above (**Chapter 7.1**), the trends could be related to shifts in phenological phases due to warmer temperatures, changes in precipitation distribution during the year, effect of higher CO_2 concentrations, and farmer decisions in the case of agricultural land, with implications on biomass production in plants. In addition, despite the condition to exclude areas of land cover change between 2000 and 2018, land cover change after 2018 could have also influenced the results.

The interannual analysis of the NDVI highlighted years of significant stress in different types of land covers, as shown by the decreased vegetation greenness: 2001, 2003, 2007, 2008, 2012 and 2020. These years of stressed vegetation are associated to drought events identified by standardized drought indicators (SPI, SPEI, **Chapter 5.1**) and to periods of months and years with high values of the CWD (**Chapter 5.2**). Moreover, other authors have obtained similar results regarding the temporal distribution of vegetation drought (Pascoa et al., 2020; Angearu et al., 2020; Dobri et al., 2021).

A detailed NDVI analysis was performed in five sample sites representing different ecoregions in the study area. Firstly, for low-altitude broadleaf forests, the correlations with the CWD have revealed significant negative correlations in July in Babadag Forest, in May and from July to September in Comana Forest and the Ialomița Forest Corridor. The higher altitude

broadleaf forests showed a significant negative correlation in August in the Cândești Forest. In general, the correlations between the NDVI and the CWD were not significant for the forests in the southern part of the Bucegi Mountains. Next, the Kruskal Wallis has shown there were significant differences in the broadleaf forest NDVI anomalies between the five sites in each of the selected drought year. However, the Dunn's test revealed which sites did not have significant differences for each selected year. For example, the Babadag and Comana areas were grouped the most often, while the Bucegi site had a different response than the other sites in most of the selected years.

Finally, two particular drought periods (2007 – 2008 and 2019 – 2020) were then selected for investigating the spatial distribution of CWD, NDVI and phenological metrics anomalies. In 2007, meteorological drought occurred between April and July in the entire study area, with the highest CWD anomaly occurring in July 2007. In 2008, the positive anomalies of the deficit occurred from May to August on almost the entire area, with the highest anomaly values occurring in August in the Subcarpathian area. These conditions negatively influenced vegetation in spring and summer 2007, particularly in the Babadag, Comana, Ialomița and Cândești areas. In 2008, more severe NDVI anomalies appeared in the latter part of the growing season and their extent and severity was remarkable in September at higher altitudes. The phenological algorithms mainly showed an earlier Start of Season in 2007 and 2008, in most sites, possibly related to warm temperatures. In 2007, the algorithms generally showed a later End of Season (except in the Bucegi area) which could be related to the improved climatic conditions starting from August, while in 2008, the results were very mixed between the different methods.

In 2019, drought developed in spring and autumn, with a remarkable persistence of months with water deficit in the eastern part of the study area. These patterns of water deficit were also observed in the spatial distribution of NDVI anomalies, particularly in the Ialomița, Comana and Cândești areas. There were water deficient conditions in 2020 in April and August – September at all stations, but at stations in the easternmost area of the study area drought was identified throughout the entire growing season. This was also reflected in the extensive period with negative NDVI anomalies in the Babadag area in 2020. Low values of the NDVI anomalies occurred also in Comana and Cândești areas between July and September 2020. Regarding phenology, there was a later SOS in most areas in 2019 and in Bucegi, Cândești and Comana in 2020. Most areas showed

an earlier EOS in 2019 and 2020, which could be related to the prolonged drought conditions during these years.

Analysing the climatic and vegetation conditions at regional level and for different ecoregions yielded more insight into the relationships between drought occurrence and vegetation stress in south-eastern Romania. However, it is important to acknowledge the limitations of this study. As previously mentioned for hydroclimatic indices, the study is limited mostly to a monthly and annual temporal resolution and did not investigate vegetation drought indicators at a finer time scale. While the downloaded NDVI MODIS data had originally a 16-day temporal resolution for exploring vegetation time series, it was important to aggregate data at a common monthly resolution with the climate data.

Potential biases regarding vegetation analysis could have affected sampling (study areas and sampling points). Additionally, results regarding vegetation health are affected by the inherent errors that present when working with satellite data, such as sensor issues, atmospheric effects and influencing factors on the ground. Finally, this study is limited by the absence of ground vegetation and phenological measurements, which restricted the validation of phenological metrics.

GENERAL CONCLUSIONS

Drought is a significant hazard that affects south-eastern Romania, which should be studied from multiple perspectives due to its complex development and impacts. Therefore, this research has focused on this region, aiming to analyse the spatio-temporal variability of the hydrometeorological drought and how this variability impacts vegetation and streamflow. This general objective was achieved using different methods and approaches to highlight the occurrence and the drought characteristics, considering the phenomenon's complexity, as shown by different climatic, hydrological and vegetation indicators and indices.

Following the **introductory Part I**, which presented the research context (**Chapter 1**) and the study area (**Chapter 2**), the **second part** was dedicated to the exploration of the hydroclimatic variability and of the drought occurrence in south-eastern Romania. This part was based on the climate data processing (air temperature, precipitation and evapotranspiration) during the 1961 – 2020 period, at the scale of the meteorological stations (București Băneasa, Buzău, Călărași, Constanța, Craiova, Galați, Râmnicu Vâlcea, Roșiorii de Vede, Sulina, Tulcea, Vârful Omu) and the scale of the E-OBS gridded dataset at 0.1° spatial resolution, as well as on a hydrological dataset (average discharges) between 1966 – 2010 at four gauging stations located on the main rivers draining the study area (Alexandria on Vedea River, Budești on Argeș River, Coșereni on Ialomița River and Racovița on Buzău River).

Firstly, in **Chapter 3**, the data, methods, and tools used in the second part are presented. In **Chapter 4**, entitled *Hydroclimatic variability in south-eastern Romania*, the variability of the main factors responsible for the development of meteorological and hydrological drought in south-eastern Romania was analysed (temperature, precipitation, evapotranspiration, streamflow), and the contributions of climatic and anthropogenic factors to streamflow were assessed in four major watersheds (Argeș, Ialomița, Buzău and Vedea) at the multiannual time scale.

In **Chapter 5** (*Hydroclimatic drought characterization in south-eastern Romania*) the occurrence and changes in drought variability are investigated based on drought indicators — the climatic water deficit (CWD) and standardized indicators for the 1961 – 2020 period. The CWD was calculated using the difference between the potential and actual evapotranspiration, the latter

being obtained through the simplified Thornthwaite water balance method. The standardized drought indicators used in the analyses were the Standardized Precipitation Index (SPI), the Standardized Precipitation Evapotranspiration Index (SPEI) and the Standardized Streamflow Index (SSI).

The last part (**Part III**) was dedicated to the analysis of the impact of drought on vegetation in the study area between 2001 – 2020. Only stable pixels were considered, defined here as NDVI grids where the land cover has not changed between 2000 and 2018 (according to the Corine Land Cover database) and the same land cover overlapping it over at least 95%. The NDVI was investigated at the regional level and in more detail, in five selected study sites (Babadag Forest, Ialomița Corridor, Comana Forest, Cândești Forests and Bucegi Forests) that are representative of the different ecoregions in the study area. The methodology used in this part was presented in **Chapter 6**.

In **Chapter 7**, entitled *Drought impact on vegetation at the regional level*, the NDVI indicator was used to identify the occurrence of drought based on the vegetation anomalies that highlighted its spatial development in the years with drought, at the level of the entire study area, by discriminating between land cover classes (arable lands, pastures, natural grasslands, broadleaf forests, mixed forests and coniferous forests).

In **Chapter 8** (*Regional differences in vegetation response to drought*) the response of deciduous forests to drought was compared using the NDVI and CWD in the five representative study sites for the five ecological regions selected in the study area. Moreover, the spatial and temporal development of meteorological drought indicators and the impact on vegetation (from the point of view of vegetation condition and phenological dynamics) were investigated in the five study sites in two periods marked by severe drought: 2007 – 2008 and 2019 – 2020. For analysing the phenological dynamics, multiple smoothing and identification algorithms were tested.

In summary, the outcome of the research carried out in this PhD thesis has indicated the following main points:

- All stations have significant positive trends between 1961 – 2020 in the annual and summer months air temperatures and potential evapotranspiration. Precipitation does not have a very clear trend in the region during the analysed period. Annually, there

were significant precipitation trends only in Constanța (positive) and Sulina (negative) meteorological stations. On the monthly scale, most stations had positive significant trends in October and there was a significant increasing trend in January in Călărași. Significant negative monthly trends occurred at Sulina in February and May, at Vârful Omu in April and at Galați in August.

- Meteorological indicators highlighted periods of drought, either induced by rainfall deficit (as reflected by the Standardized Precipitation Index, SPI), climatic water balance (precipitation minus potential evapotranspiration, as reflected by the Standardized Precipitation Evapotranspiration Index, SPEI) or climatic water deficit (CWD, potential evapotranspiration minus actual evapotranspiration) in 1963 – 1964, 1968 – 1969, 1973 – 1974, 1984 – 1989, 1991 – 1995, 2000 – 2003, 2012, and 2018 – 2020. From a hydrological point of view, the streamflow was affected by drought in the 1966 – 1969, 1991 – 1995, 2000 – 2004, and 2007 – 2009 intervals, coinciding with or following meteorological droughts.
- A divergence was noticed between the SPI (based on precipitation) and the SPEI (calculated based on the climatic water balance) after 1990. This could be due mainly to the trend of increasing temperatures, which causes increased evapotranspiration.
- The analysis of the climatic water deficit (CWD) between 1961 – 2020 showed a higher frequency of arid months in the summer, particularly in August, and a significant positive trend of the water deficit in August at all meteorological stations (Sen slopes between 0.7 and 1.13 mm/year), which is also probably related to the increased evapotranspiration due to higher air temperatures.
- The observed streamflow reduction in the four studied catchments at the end of the 1980s and in the 1990s was mainly determined by climatic factors (63.1% – 80% contribution of climate), but anthropic factors also contributed (19.8% – 36.9%).
- Monthly NDVI trends showed different patterns when comparing agricultural land to forest types. For example, while arable lands show positive NDVI trends between April and June and negative trends in August and September, broadleaf forests mostly show positive trends throughout the growing season, especially in spring. Mixed and coniferous forests show positive NDVI trends, particularly towards the end of the growing season.

- The interannual variability of stressed vegetation, based on the anomalies of the NDVI in the 2001 – 2020 period, highlighted widespread areas of low-vitality vegetation in 2001, 2003, 2007, 2012 and 2020. These years also have the broadest spatial distribution in the study area when identifying the year of the lowest negative anomaly.
- Low-altitude broadleaf forests showed significant negative correlations between the NDVI and climatic water deficit in July in Babadag Forest, in May and from July to September in Comana Forest and the Ialomița Forest Corridor. On the other hand, higher altitude broadleaf forests showed a significant negative correlation in August in the Cândești Forest. Generally, no significance for the forests in the southern part of the Bucegi Mountains.
- Significant differences were found in the response of the NDVI anomaly in the growing season during drought years. In some years, vegetation had a more contrasting response (2003, 2007, 2012, 2019), while other years showed a more consistent response (2008, 2015). The vegetation response had a lower intensity of drought anomalies but spread over a longer time during the drought of 2020 compared to 2007.
- The phenological analysis showed varied responses depending on the phenological phase identification algorithm. Future improvements could address ground validation of phenological metrics obtained using NDVI time series.

Despite limitations related to data availability or quality, temporal and spatial scales, limited modelling parametrisations or biases, this study certainly provided valuable information that allows a better understanding of hydroclimatic drought characteristics in south-eastern Romania and its relation to vegetation health and streamflow. While the research contributed to the existing body of knowledge on drought variability in a specific context, the findings could also be relevant to areas of similar climatic and vegetation conditions. In the context of climate change, it is crucial to investigate the effects of this hazard on the different parts of the global mosaic of geographical conditions. Moreover, this study added another foundation layer for further exploration of drought-related issues.

Moving forward, there is a wide range of potential research opportunities. Future research could add greater complexity to the modelling approaches used in this study. The results could be improved by increasing the temporal and spatial resolution of the indicators. Moreover, future

studies could potentially focus also on drought forecasting methods, with an emphasis on reducing the devastating impacts of drought.

Finally, tackling the underlying drivers that intensify the effects of drought, such as global warming, land degradation or human practices, requires cross-disciplinary, international collaboration and long-term engagement. By prioritizing these future perspectives of resilience and water security, communities will be better equipped for drought mitigation and adaptation to a changing climate.

REFERENCES

ABA Argeș-Vedea. 2015. Planul de management al riscului la inundații - Administrația Bazinală de Apă Arges-Vedea

ABA Buzău-Ialomița. 2015. Planul de management al riscului la inundații - Administrația Bazinală de apă Buzău - Ialomița

Ainsworth E.A., Long S.P. 2005. What have we learned from 15 years of free-air CO2 enrichment (FACE)? A meta-analytic review of the responses of photosynthesis, canopy properties and plant production to rising CO2

Alberton M., Andresen M., Citadino F., Egerer H., Fritsch U., et al. 2017. Outlook on climate change adaptation in the Carpathian mountains

Allen C.D., Breshears D.D., McDowell N.G. 2015. On underestimation of global vulnerability to tree mortality and forest die-off from hotter drought in the Anthropocene. *Ecosphere*. 6(8):1–55

Allen C.D., Macalady A.K., Chenchouni H., Bachelet D., McDowell N., et al. 2010. A global overview of drought and heat induced tree mortality reveals emerging climate change risk for forests. *Forest Ecology and Management*. 259(4):660–84

Allen R.G., Pereira L.S. 1998. Crop evapotranspiration - Guidelines for computing crop water requirements - FAO Irrigation and drainage paper 56

Amigues J.P., Debaeke P., Itier B., Lemaire G., Seguin B., et al. 2006. Sécheresse et agriculture. Réduire la vulnérabilité de l'agriculture à un risque accru de manque d'eau

ANAR. 2013. Planul național de amenajare a bazinelor hidrografice din România - Sinteză

ANAR. 2015a. Planul de management actualizat al spațiului hidrografic Buzău-Ialomița

ANAR. 2015b. Planul de management actualizat al spațiului hidrografic Argeș-Vedea

ANAR. 2015c. Planul de management actualizat al Fluviului Dunărea, Deltei Dunării, Spațiului Hidrografic Dobrogea și apelor costiere

Angearu C.-V., Irimescu A., Mihăilescu D., Vîsta A. 2018. Evaluation of droughts and fires in the Dobrogea Region, using MODIS satellite data. *Agriculture for Life, Life for Agriculture Conference Proceedings*. 1(1):336–45

Angearu C.V., Onțel I., Boldeanu G., Mihăilescu D., Nertan A., et al. 2020. Multi-temporal analysis and trends of the drought based on MODIS data in agricultural areas, Romania. *Remote Sensing*. 12(23):1–24

ANM. 2008. *Clima României*. București: Editura Academiei Române

ANM. 2014. Cod de bune practici agricole, în contextul schimbărilor climatice actuale și previzibile. București

Aragão L.E.O.C., Malhi Y., Roman-Cuesta R.M., Saatchi S., Anderson L.O., Shimabukuro Y.E. 2007. Spatial patterns and fire response of recent Amazonian droughts. *Geophysical Research Letters*. 34(7):1–5

Arora V.K. 2002. The use of the aridity index to assess climate change effect on annual runoff. *Journal of Hydrology*. 265(1–4):164–77

Arvor D., Jonathan M., Meirelles M.S.P., Dubreuil V., Lecerf R. 2008. Comparison of multitemporal MODIS-EVI smoothing algorithms and its contribution to crop monitoring. *International Geoscience and Remote Sensing Symposium (IGARSS)*. 2(1):958–61

Bachmair S., Stahl K., Collins K., Hannaford J., Acreman M., et al. 2016. Drought indicators revisited: the need for a wider consideration of environment and society. *Wiley Interdisciplinary reviews - Water*. 3(4):516–36

Badea O., Neagu Ş. 2007. Starea de sănătate a pădurilor din România la nivelul anului 2006, evaluată prin reţeaua naţională de sondaje permanente (4x4 km). *Revista Pădurilor*. 5:11–17

Bandoc G., Piticar A., Patriche C., Roșca B., Dragomir E. 2022. Climate Warming-Induced Changes in Plant Phenology in the Most Important Agricultural Region of Romania. *Sustainability (Switzerland)*. 14(5):

Baronetti A., Dubreuil V., Provenzale A., Fratianni S. 2022. Future droughts in northern Italy: high-resolution projections using EURO-CORDEX and MED-CORDEX ensembles. *Climatic Change*. 172(3–4):1–22

Bart R.R., Tague C.L., Dennison P.E. 2017. Modeling annual grassland phenology along the central coast of California. *Ecosphere*. 8(7):

Bastrup-Birk A., Reker J., Zal N. 2016. European forest ecosystems: State and trends

Bates B.C., Kundzewicz Z.W., Wu S., Palutikof J.P. 2008. *Climate Change and Water. Technical Paper of the Intergovernmental Panel on Climate Change*. Geneva: IPCC Secretariat

Baumbach L., Siegmund J.F., Mittermeier M., Donner R. V. 2017. Impacts of temperature extremes on European vegetation during the growing season. *Biogeosciences*. 14(21):4891–4903

Beauvais F. 2022. *Approches géographiques et agro-climatologiques des conséquences du changement climatique sur l'agrosystème céréalier de Normandie: constat et étude d'impact prospective appliqués au blé tendre d'hiver*. Université de Caen Normandie

Beck H.E., Zimmermann N.E., McVicar T.R., Vergopolan N., Berg A., Wood E.F. 2018. Present and future Köppen-Geiger climate classification maps at 1-km resolution. *Scientific Data*. 5:1–12

Berca M., Robescu V.O., Horoias R. 2021. Winter wheat crop water consumption and its effect on yields in southern Romania, in the very dry 2019-2020 agricultural year. *Notulae Botanicae Horti Agrobotanici Cluj-Napoca*. 49(2):1–13

Bigot S., Dumas D., Brou T., Curt T., Razanaka S. 2019. Feux de végétation et conditions pluviométriques à Madagascar. *32ème Colloq. l'Association Int. Climatol.*

Bigot S., Dumas D., Brou T.Y., Ramboarison R., Razanaka S., Philippon N. 2021. Studying recent hydroclimatic variability in Madagascar despite deficient measurement networks: Use of CHIRPS and GRACE data at the scale of the Mahajunga province. *Proc. Int. Assoc. Hydrol. Sci.* 384:43–48

Bîrsan M.-V. 2015. Trends in Monthly Natural Streamflow in Romania and Linkages to Atmospheric Circulation in the North Atlantic. *Water Resources Management*. 29(9):3305–13

Bîrsan M.-V. 2017. *Variabilitatea Regimului Natural Al Scurgerii Râurilor Din România*. București: Ars Docendi

Bîrsan M.-V., Dumitrescu A. 2014a. ROCADA: Romanian daily gridded climatic dataset (1961-2013) V1.0 [Dataset]

Bîrsan M.V., Dumitrescu A. 2014b. Snow variability in Romania in connection to large-scale atmospheric circulation. *International Journal of Climatology*. 34(1):134–44

Bîrsan M.V., Zaharia L., Chendeș V., Brănescu E. 2014. Seasonal trends in Romanian streamflow. *Hydrological Processes*. 28(15):4496–4505

Bloschl G., Sivapalan M., Wagener T., Viglione A., Savenije H. 2013. *Runoff Prediction in Ungauged Basins: Synthesis across Processes, Places and Scales*. Cambridge University Press

Bodner G., Nakhforoosh A., Kaul H.-P. 2015. Management of crop water under drought: a review. *Agronomy for Sustainable Development*. 35(2):401–42

Bogdan O., Țîștea D. 1983. Clima. In *Geografia României I. Geografia Fizică*, pp. 195–292. București: Editura Academiei Republicii Socialiste România

Bojariu R., Bîrsan M.-V., Cică R., Velea L., Burcea S., et al. 2015. *Schimbările Climatice - de La Bazele Fizice La Riscuri Şi Adaptare.* București: Editura Printech

Bojariu R., Chițu Z., Dascălu S.I., Gothard M., Velea L., et al. 2021. *Schimbările Climatice – de La Bazele Fizice La Riscuri Și Adaptare - Ediție Revăzută Și Adăugită*. București: Editura Printech

Bojariu R., Dumitrescu A., Burcea S., Crăciunescu V. Ș., Mătreață M., et al. 2019. Schimbarea climatică în sectorul resurselor de apă - de la bazele fizice la riscuri și adaptare. București

Bonferroni C., Bonferroni C. 1935. Il calcolo delle assicurazioni su gruppi di teste. In *Studi in Onore Del Professore Salvatore Ortu Carboni*, ed. SO Carboni, pp. 13–60. Roma: Tipografia del Senato: Bardi

Borcan M., Neculau G., Retegan M. 2014. The influence determined by the changing of mark climatic parameters upon the hydrological regime in southern Romania. *Proc. 14th GeoConference Water Resour. For. Mar. Ocean Ecosyst. 17–26 June 2014*, pp. 759–766

Bórnez K., Verger A., Descals A., Peñuelas J. 2021. Monitoring the responses of deciduous

forest phenology to 2000–2018 climatic anomalies in the Northern Hemisphere. *Remote Sensing*. 13(14):

Breshears D.D., Cobb N.S., Rich P.M., Price K.P., Allen C.D., et al. 2005. Regional vegetation die-off in response to global-change-type drought. *Proceedings of the National Academy of Sciences of the United States of America*. 102(42):15144–48

Budyko M.I. 1961. The Heat Balance of the Earth's Surface. *Soviet Geography*. 2(4):3–13

Budyko M.I. 1974. *Climate and Life*. New York: Academic Press

Buitenwerf R., Sandel B., Normand S., Mimet A., Svenning J.C. 2018. Land surface greening suggests vigorous woody regrowth throughout European semi-natural vegetation. *Global Change Biology*. 24(12):5789–5801

Busetto L., Ranghetti L. 2016. MODIStsp: An R package for automatic preprocessing of MODIS Land Products time series. *Computers & geosciences*. 97:40–48

Busuioc A., Dobrinescu A., Birsan M.-V., Dumitrescu A., Orzan A. 2015. Spatial and temporal variability of climate extremes in Romania and associated large-scale mechanisms. *International Journal of Climatology*. 35(7):1278–1300

Busuioc A., Dumitrescu A., Orzan A. 2007. Summer anomalies in 2007 in the context of extremely hot and dry summers in Romania. *Romanian Journal of Meteorology*. 9(1–2):1–17

Busuioc A., Mic R., Stefan S. 2016. CLIMHYDEX: Changes in climate extreme and associated impact on hydrological events in Romania: Summary research and results. București

Cai Z., Jönsson P., Jin H., Eklundh L. 2017. Performance of smoothing methods for reconstructing NDVI time-series and estimating vegetation phenology from MODIS data. *Remote Sensing*. 9(12):20–22

Candrea B., Candrea P., Niță D. 2008. Harta unităților de relief din România [Dataset]

Carbonnel J.P., Petrorian R., Serban P. 1997. Evolution récente du régime hydrologique de quelques rivières de Roumanie Centrale. (Courte note). *Revue des sciences de l'eau/ Journal of Water Science*. 10(4):545–52

Chaves M.M., Flexas J., Pinheiro C. 2009. Photosynthesis under drought and salt stress: Regulation mechanisms from whole plant to cell. *Annals of Botany*. 103(4):551–60

Chelu A. 2019. A typology of indices for drought assessment. *Aerul Şi Apa. Compon. Ale Mediu.* 77-90

Chelu A., Zaharia L., Dubreuil V. 2022. Estimation of climatic and anthropogenic contributions to streamflow change in southern Romania. *Hydrological Sciences Journal*. 67(10):1598–1608

Chen J., Jönsson P., Tamura M., Gu Z., Matsushita B., Eklundh L. 2004. A simple method for reconstructing a high-quality NDVI time-series data set based on the Savitzky-Golay filter. *Remote Sensing of Environment*. 91(3–4):332–44

Cheval S., Busuioc A., Dumitrescu A., Bîrsan M.-V. 2014. Spatiotemporal variability of meteorological drought in Romania using the standardized precipitation index (SPI). *Climate Research*. 60(3):235–48

Ciais P., Reichstein M., Viovy N., Granier A., Ogée J., et al. 2005. Europe-wide reduction in primary productivity caused by the heat and drought in 2003. *Nature*. 437(7058):529–33

Ciceu A., Popa I., Leca S., Pitar D., Chivulescu S., Badea O. 2020. Climate change effects on tree growth from Romanian forest monitoring Level II plots. *Science of the Total Environment*. 698:134129

Ciulache S., Ionac N. 1995. *Fenomene Geografice de Risc*. București: Editura Universității din Bucureşti

Ciulache S., Ionac N. 2003. *Dicţionar de Meteorologie Şi Climatologie*. București: Ars Docendi

Ciulache S., Ionac N. 2004. Main Types of Climate in Romania. *Analele Universităţii din Bucureşti, seria Geografie*. 53:15–23

Claverie M., Matthews J.L., Vermote E.F., Justice C.O. 2016. A 30+ year AVHRR LAI and FAPAR climate data record: Algorithm description and validation. *Remote Sensing*. 8(3):1–12

Comps B., Letouzey J., Savoie J.-M. 1987. Phénologie du couvert arborescent dans une chênaie-hêtraie d'Aquitaine. *Annales des Sciences Forestières*. 44(2):153–120

Cornes R.C., van der Schrier G., van den Besselaar E.J.M., Jones P.D. 2018. Ensemble version of the E-OBS temperature and precipitation datasets. *Journal of Geophysical Research: Atmospheres*. 123(17):9391–9409

Crausbay S.D., Betancourt J., Bradford J., Cartwright J., Dennison W.C., et al. 2020. Unfamiliar territory: Emerging themes for ecological drought research and management. *One Earth*. 3(3):337–53

Crausbay S.D., Ramirez A.R., Carter S.L., Cross M.S., Hall K.R., et al. 2017. Defining ecological drought for the twenty-first century. *Bulletin of the American Meteorological Society*. 98(12):2543–50

Croitoru A.-E., Piticar A., Dragotă C., Burada D.C. 2013a. Recent changes in reference evapotranspiration in Romania. *Global and Planetary Change*. 111:127–36

Croitoru A.-E., Piticar A., Imbroane A.M., Burada D.C. 2013b. Spatiotemporal distribution of aridity indices based on temperature and precipitation in the extra-Carpathian regions of Romania. *Theoretical and applied climatology*. 112(3–4):597–607

Croitoru A.-E., Toma F.-M. 2011. Considerations on streamflow drought in Central Romanian Plain. *Aerul Si Apa. Compon. Ale Mediu.*, pp. 147–54

Croitoru A.E., Holobâcă I.-H., Lazăr C., Moldovan F., Imbroane A. 2012. Air temperature trend and the impact on winter wheat phenology in Romania. *Climatic Change*. 111(2):393–410

Croitoru A.E., Piticar A., Burada D.C. 2016a. Changes in precipitation extremes in Romania. *Quaternary International*. 415:325–35

Croitoru A.E., Piticar A., Ciupertea A.F., Roşca C.F. 2016b. Changes in heat waves indices in Romania over the period 1961–2015. *Global and Planetary Change*. 146:109–21

Cuculeanu V., Tuinea P., Bălteanu D. 2002. Climate change impacts in Romania: Vulnerability and adaptation options. *GeoJournal*. 57(3):203–9

Dai A. 2011. Drought under global warming: A review. *Wiley Interdisciplinary Reviews: Climate Change*. 2(1):45–65

de Beurs K.M., Henebry G.M. 2010. Spatio-Temporal Statistical Methods for Modelling Land Surface Phenology. In *Phenological Research*

Destouni G., Jaramillo F., Prieto C. 2013. Hydroclimatic shifts driven by human water use for food and energy production. *Nature Climate Change*. 3(3):213–17

DeWalle D.R., Swistock B.R., Johnson T.E., McGuire K.J. 2000. Potential effects of climate change and urbanization on mean annual streamflow in the United States. *Water Resources Research*. 36(9):2655–64

Dey P., Mishra A. 2017. Separating the impacts of climate change and human activities on streamflow: A review of methodologies and critical assumptions. *Journal of Hydrology*. 548(March):278–90

Didan K. 2015. MOD13Q1 MODIS/Terra Vegetation Indices 16-Day L3 Global 250m SIN Grid V006 [Dataset]

Dobri R.V., Sfîcă L., Amihăesei V.A., Apostol L., Țîmpu S. 2021. Drought extent and severity on arable lands in Romania derived from normalized difference drought index (2001–2020). *Remote Sensing*. 13(8):

Doniță N., Popescu A., Paucă-Comănescu M., Mihăilescu S., Biriș I.-A. 2005. *Habitatele Din România*. București: Editura Tehnică Silvică

Donohue R.J., Roderick M.L., McVicar T.R. 2007. On the importance of including vegetation dynamics in Budyko's hydrological model. *Hydrology and Earth System Sciences*. 11(2):983–95

Dorigo W., Wagner W., Albergel C., Albrecht F., Balsamo G., et al. 2017. ESA CCI Soil Moisture for improved Earth system understanding: State-of-the art and future directions. *Remote Sensing of Environment*. 203:185–215

Dracup J.A., Lee K.S., Paulson E.G.J. 1980. On the Definition of Drought. *Water Resources Research*. 16(2):297–302

Dubreuil V. 1995. Spatialisation détaillée des zones à risque vis à vis de la sécheresse dans la France de l'Ouest. *Publications de l'Association Internationale de Climatologie*. 8:198–206

Dubreuil V. 1996. Synthèse géographique de la sécheresse dans les régions océaniques. *La Météorologie*. 8(15):22–34

Dubreuil V. 1997. La sécheresse dans la France de l'Ouest : une contrainte climatique trop souvent oubliée. *Sécheresse*. 8(1):47–55

Dubreuil V. 2004. Suivi de la sécheresse par télédétection : exemple de l'été 2003 en Bretagne. *Symp. Natl. Climatol.*

Dubreuil V., Lamy C., Planchon O. 2018. Les sécheresses à Rennes : passé, présent et futur. *Les Risques Nat. Dans Le Context. Chang. Clim.*, pp. 15–21

Dubreuil V., Planchon O. 2009. Bilan d'un siècle d'observation des sécheresses et des types de circulations atmosphériques associées à Rennes. *Actes Du XXIIe Colloq. l'Association Int. Climatol.*, pp. 139–44

Dumitrescu A., Bîrsan M.-V. 2015. ROCADA: a gridded daily climatic dataset over Romania (1961–2013) for nine meteorological variables. *Natural Hazards*. 78(2):1045–63

Dumitrescu A., Bojariu R., Bîrsan M.-V., Marin L., Manea A. 2015. Recent climatic changes in Romania from observational data (1961–2013). *Theoretical and Applied Climatology*. 122(1–2):111–19

Dunn O.J. 1964. Multiple comparisons using rank sums. *Technometrics*. 6(3):241–52

EEA. 2019a. Corine Land Cover (CLC) 2018, Version 2020_20u1 [Dataset]

EEA. 2019b. Corine Land Cover (CLC) 2000, Version 2020_20u1 [Dataset]

EEA. 2021a. Water resources across Europe – confronting water stress: an updated assessment

EEA. 2021b. *Forest Fires in Europe*. https://www.eea.europa.eu/ims/forest-fires-in-europe

European Drought Center. 2013. *Drought of 2007*. https://www.geo.uio.no/edc/droughtdb/edr/DroughtEvents/_2007_Event.php

Evert R.F., Eichhorn S.E. 2012. *Biology of Plants*. 8th ed.

Fischer G., Tubiello F.N., van Velthuizen H., Wiberg D.A. 2006. Climate change impacts on irrigation water requirements: Effects of mitigation, 1990-2080. *Technological Forecasting and Social Change*. 74(7):1083–1107

Forkel M., Carvalhais N., Verbesselt J., Mahecha M.D., Neigh C.S.R., Reichstein M. 2013. Trend Change detection in NDVI time series: Effects of inter-annual variability and methodology. *Remote Sensing*. 5(5):2113–44

Forkel M., Migliavacca M., Thonicke K., Reichstein M., Schaphoff S., et al. 2015. Codominant water control on global interannual variability and trends in land surface phenology and greenness. *Global Change Biology*. 21(9):3414–35

Forkel M., Wutzler T. 2015. greenbrown - land surface phenology and trend analysis. A package for the R software. Version 2.2

Frank D., Reichstein M., Bahn M., Thonicke K., Frank D., et al. 2015. Effects of climate extremes on the terrestrial carbon cycle: concepts, processes and potential future impacts. *Global Change Biology*. 21(8):2861–80

Fu B.P. 1981. On the calculation of the evaporation from land surface. *Scientia Atmospherica Sinica*. 5(1):23–31

Fuchs R., Herold M., Verburg P.H., Clevers J.G.P.W. 2013. A high-resolution and harmonized model approach for reconstructing and analysing historic land changes in Europe. *Biogeosciences*. 10(3):1543–59

Füssel H.-M., Jol A., Marx A., Hildén M., Aparicio A., et al. 2017. Climate change, impacts and vulnerability in Europe 2016 - An indicator-based report

Gao G., Fu B., Wang S., Liang W., Jiang X. 2016. Determining the hydrological responses to climate variability and land use/cover change in the Loess Plateau with the Budyko framework. *Science of the Total Environment*. 557–558:331–42

García M.A., Moutahir H., Casady G.M., Bautista S., Rodríguez F. 2019. Using hidden Markov models for land surface phenology: An evaluation across a range of land cover types in Southeast Spain. *Remote Sensing*. 11(5):

Gâștescu P., Diaconu C., Pișota I., Ujvári I., Zăvoianu I. 1983. Apele. In *Geografia României I. Geografia Fizică*, pp. 293–387. București: Editura Academiei Republicii Socialiste România

Ge W., Han J., Zhang D., Wang F. 2021. Divergent impacts of droughts on vegetation phenology and productivity in the Yungui Plateau, southwest China. *Ecological Indicators*. 127:107743

Gouveia C.M., Trigo R.M., Beguería S., Vicente-Serrano S.M. 2017. Drought impacts on vegetation activity in the Mediterranean region: An assessment using remote sensing data and multi-scale drought indicators. *Global and Planetary Change*. 151:15–27

Grecu F. 2010. *Geografia Câmpiilor României. Note de Curs*, Vol. I. București: Editura Universității din București

Griffiths P., Müller D., Kuemmerle T., Hostert P. 2013. Agricultural land change in the Carpathian ecoregion after the breakdown of socialism and expansion of the European Union. *Environmental Research Letters*. 8(4):

Gruber A., Scanlon T., van der Schalie R., Wagner W., Dorigo W. 2019. Evolution of the ESA CCI Soil Moisture Climate Data Records and their underlying merging methodology. *Earth System Science Data Discussions*. 1–37

Hamed K.H., Ramachandra Rao A. 1998. A modified Mann-Kendall trend test for autocorrelated data. *Journal of Hydrology*. 204(1–4):182–96

Hanel M., Rakovec O., Markonis Y., Máca P., Samaniego L., et al. 2018. Revisiting the recent European droughts from a long-term perspective. *Scientific Reports*. 8(1):1–11

Harpold A.A., Dettinger M., Rajagopal S. 2017. *Defining Snow Drought and Why It Matters*. https://eos.org/opinions/defining-snow-drought-and-why-it-matters

Harris I., Osborn T.J., Jones P., Lister D. 2020. Version 4 of the CRU TS monthly high-resolution gridded multivariate climate dataset [Dataset]. *Scientific Data*. 7(1):1–18

Harris R.M.B., Beaumont L.J., Vance T.R., Tozer C.R., Remenyi T.A., et al. 2018. Biological responses to the press and pulse of climate trends and extreme events. *Nature Climate*

Change. 8(7):579–87

Harrison L., Michaelsen J., Funk C., Husak G. 2011. Effects of temperature changes on maize production in Mozambique. *Climate Research*. 46(3):211–22

Harrison P.A., Butterfield R.E. 1996. Effects of climate change on Europe-wide winter wheat and sunflower productivity. *Climate Research*. 7(3):225–41

Hartmann H., Bastos A., Das A.J., Esquivel-Muelbert A., Hammond W.M., et al. 2022. Climate Change Risks to Global Forest Health: Emergence of Unexpected Events of Elevated Tree Mortality Worldwide. *Annual Review of Plant Biology*. 73:673–702

Heim R.R. 2002. A review of twentieth-century drought indices used in the United States. *Bulletin of the American Meteorological Society*. 83(8):1149–65

Holobâcă I.-H. 2010. *Studiul Secetelor Din Transilvania*. Cluj-Napoca: Presa Universitară Clujeană

Holobâcă I.-H., Sorocovschi V., Dubreuil V. 2003. Suivi par télédétection de la sécheresse de l'année 2000 dans la dépression de la Transylvanie. *Publication de l'Association Internationale de Climatologie*. 15:87–94

Hopkins A. 2010. Grasslands in Europe of high nature value. *Grass and Forage Science*. 65(3):367–367

Hopkins W.G., Huner, Norman P.A. 2008. *Introduction to Plant Physiology*. John Wiley & Sons, Inc. 4th ed.

Hounam C.E., Burgos J.J., Kalik M.S., Palmer W.C., Rodda J. 1975. Drought and agriculture - Technical note no. 138

Huning L.S., AghaKouchak A. 2020. Global snow drought hot spots and characteristics. *Proceedings of the National Academy of Sciences of the United States of America*. 117(33):19753–59

Ingrisch J., Bahn M. 2018. Towards a Comparable Quantification of Resilience. *Trends in Ecology and Evolution*. 33(4):251–59

INHGA. 2015. Ghid de gestionare a apelor mici. București

Iojă I.-C. 2008. *Metode Şi Tehnici de Evaluare a Calităţii Mediului În Aria Metropolitană a Municipiului Bucureşti*. București: Editura Universităţii din Bucureşti

Ion V. 2010. *Fitotehnie [Lecture Notes]*. București: Facultatea de Horticultură. Universitatea de Științe Agronomice și Medicină Veterinară

Ion V., Dicu G., Bășa A.G., State D. 2013. Yield components at some hybrids of sunflower (Helianthus annuus L.) under drought conditions from south Romania. *AgroLife Scientific Journal*. 2(2):9–14

Ioniță M. 2014. The impact of the East Atlantic/Western Russia pattern on the hydroclimatology of Europe from mid-winter to late spring. *Climate*. 2(4):296–309

Ioniță M., Chelcea S., Rimbu N., Adler M.J. 2014. Spatial and temporal variability of winter

streamflow over Romania and its relationship to large-scale atmospheric circulation. *Journal of Hydrology*. 519(PB):1339–49

Ioniță M., Scholz P., Chelcea S. 2016. Assessment of droughts in Romania using the Standardized Precipitation Index. *Natural Hazards*. 81(3):1483–98

IPCC. 2014. *Climate Change 2014 - Impacts, Adaptation and Vulnerability. Part A: Global and Sectoral Aspects*

IPCC. 2021. *Climate Change 2021: The Physical Science Basis. Contribution of Working Group I to the Sixth Assessment Report of the Intergovernmental Panel on Climate Change*. Cambridge, United Kingdom and New York, NY, USA: Cambridge University Press

IPCC. 2022. *Climate Change 2022: Impacts, Adaptation and Vulnerability*. Cambridge, UK and New York, NY, USA: Cambridge University Press

Ivits E., Horion S., Fensholt R., Cherlet M. 2014. Drought footprint on European ecosystems between 1999 and 2010 assessed by remotely sensed vegetation phenology and productivity. *Global Change Biology*. 20(2):581–93

Jacobs C., Berglund M., Kurnik B., Dworak T., Marras S., et al. 2019. Climate change adaptation in the agriculture sector in Europe (4/2019)

Jaramillo F., Destouni G. 2015. Local flow regulation and irrigation raise global human water consumption and footprint. *Science*. 350(6265):1248–51

Jentsch A., Kreyling J., Boettcher-Treschkow J., Beierkuhnlein C. 2009. Beyond gradual warming: Extreme weather events alter flower phenology of European grassland and heath species. *Global Change Biology*. 15(4):837–49

Jiang C., Ryu Y., Fang H., Myneni R., Claverie M., Zhu Z. 2017. Inconsistencies of interannual variability and trends in long-term satellite leaf area index products. *Global Change Biology*. 23(10):4133–4146

Kallis G. 2008. Droughts. *Annual Review of Environment and Resources*. 33:85–118

Kendall M.G. 1975. *Rank Correlation Methods*. London: Griffin. 4th ed.

Klein Tank A.M.G., Wijngaard J.B., Können G.P., Böhm R., Demarée G., et al. 2002. Daily dataset of 20th-century surface air temperature and precipitation series for the European Climate Assessment. *International Journal of Climatology*. 22(12):1441–53

Kruskal W.H., Wallis W.A. 1952. Use of ranks in one-criterion variance analysis. *Journal of the American statistical Association*. 47(260):583–621

Kuemmerle T., Müller D., Griffiths P., Rusu M. 2009. Land use change in Southern Romania after the collapse of socialism. *Regional Environmental Change*. 9(1):1–12

Lambert R. 1977. Géographie et budget hydrologique. *Annales de Géographie*. 86(477):513–21

Lamy C. 2014. *Impact du changement climatique sur la fréquence et l'intensité des sécheresses en Bretagne*. Université Rennes 2

Lamy C., Dubreuil V. 2013. Impact potentiel du changement climatique sur les sécheresses

pédologiques en Bretagne au 21ème siècle. *Climatologie*. 10:107–21

Laurance W.F., Williamson G.B. 2001. Positive feedbacks among forest fragmentation, drought, and climate change in the Amazon. *Conservation Biology*. 15(6):1529–35

Lazăr C., Baruth B., Micale F. 2009. Winter wheat yield estimation for Romania, based on Normalized Difference Vegetation Index data available on MARSOP site. *Analele Institutului Naţional de Cercetare - Dezvoltare Agricolă Fundulea*. 77:251–60

Lazăr C., Lazăr D.A. 2010. Simulation of temperature increase influence on winter wheat yields and development in South - Eastern Romania. *Romanian Agricultural Research*. (27):7–15

Le Roux R., Wagner F., Blanc L., Betbeder J., Gond V., et al. 2022. How wildfires increase sensitivity of Amazon forests to droughts. *Environmental Research Letters*. 17(4):044031

Lecerf R., Planchon O., Dubreuil V., Hubert-Moy L. 2008. Impact de la variabilité climatique sur la dynamique de la végétation par télédétection moyenne résolution à l'échelle régionale: le cas de la Bretagne. *XXIe Colloq. l'Association Int. Climatol.*, pp. 385–90

Lepage M.-P., Bourgeois G. 2012. Modèles bioclimatiques pour la prédiction de la phénologie

Leroux L., Castets M., Baron C., Escorihuela M.J., Bégué A., Lo Seen D. 2019. Maize yield estimation in West Africa from crop process-induced combinations of multi-domain remote sensing indices. *European Journal of Agronomy*. 108(July 2018):11–26

Levanič T., Popa I., Poljanšek S., Nechita C. 2013. A 323-year long reconstruction of drought for SW Romania based on black pine (Pinus Nigra) tree-ring widths. *International Journal of Biometeorology*. 57(5):703–14

Levene H. 1960. Contributions to probability and statistics. *Essays in honor of Harold Hotelling*. 278:292

Li N., Zhan P., Pan Y., Zhu X., Li M., Zhang D. 2020. Comparison of remote sensing time-series smoothing methods for grassland spring phenology extraction on the Qinghai–Tibetan plateau. *Remote Sensing*. 12(20):1–26

Liang W., Bai D., Wang F., Fu B., Yan J., et al. 2015. Quantifying the impacts of climate change and ecological restoration on streamflow changes based on a Budyko hydrological model in China's Loess Plateau Wei. *WATER RESOURCES RESEARCH*. 6500–6519

Liu L., Hong Y., Bednarczyk C.N., Yong B., Shafer M.A., et al. 2012. Hydro-Climatological Drought Analyses and Projections Using Meteorological and Hydrological Drought Indices: A Case Study in Blue River Basin, Oklahoma. *Water Resources Management*. 26(10):2761–79

Lloyd-Hughes B., Saunders M.A. 2002. A drought climatology for Europe. *INTERNATIONAL JOURNAL OF CLIMATOLOGY*. 22(13):1571–92

Lu J., Sun G., McNulty S.G., Amatya D.M. 2005. A comparison of six potential evapotranspiration methods for regional use in the southeastern United States. *Journal of the American Water Resources Association*. 41(3):621–33

Lup A., Miron L., Alim I.D. 2017. Irrigation Investments in Romania. Size, Results, Efficiency

(1965-1989). *Bulletin of University of Agricultural Sciences and Veterinary Medicine Cluj-Napoca. Horticulture*. 74(1):93–100

Lupu L., Boroneanţ C., Dogaru D. 2018. Evaluation of the socioeconomic effects of drought in the Turnu Măgurele – Giurgiu sector of the Romanian Danube Valley. *Romanian Journal of Geography*. 62(1):49–70

MADR. 2015. Programul Național de Dezvoltare Rurală pentru perioada 2014 – 2020

Mallinis G., Petrila M., Mitsopoulos I., Lorenţ A., Neagu Ș., et al. 2019. Geospatial Patterns and Drivers of Forest Fire Occurrence in Romania. *Applied Spatial Analysis and Policy*. 12(4):773–95

Mann H.B. 1945. Non-Parametric Test Against Trend. *Econometrica*. 13(3):245–59

Marin L., Bîrsan M.-V., Bojariu R., Dumitrescu A., Micu D.M., Manea A. 2014. An overview of annual climatic changes in Romania: Trends in air temperature, precipitation, sunshine hours, cloud cover, relative humidity and wind speed during the 1961-2013 period. *Carpathian Journal of Earth and Environmental Sciences*. 9(4):253–58

Marinciu C., Mustățea P., Șerban G., Ittu G., Săulescu N. 2013. Effects of climate change and genetic progress on performance of wheat cultivars, during the last twenty years in south Romania. *Romanian Agricultural Research*. (30):

Maskey S., Trambauer P. 2015. Hydrological Modeling for Drought Assessment. In *Hydro-Meteorological Hazards, Risks, and Disasters*, eds. JF Shroder, P Paron, G Di Baldassarre, pp. 263–82. Elsevier

Mateescu E. 2014. *ADER 1.1.1. Sistem de indicatori geo-referențiali la diferite scări spațiale și temporale pentru evaluarea vulnerabilității și măsurile de adaptare ale agroecosistemelor față de schimbările globale*. Seminar privind diseminarea rezultatelor cercetarilor din domeniul mecanizarii, economiei agrare, pedologiei, agrochimiei si combaterii eroziunii solului, imbunatatirilor funciare, meteorologiei si hidrologiei [online]. http://www.madr.ro/attachments/ article/139/ANM-ADER-111.pdf

Mateescu E., Alexandru D. 2010. Management recommendations and options to improve crop systems and yields on south-east Romania in the context of regional climate change scenarios over 2020-2050. *Scientific Papers, UASVM Bucharest. Series A*. LIII:328–34

Mateescu E., Smarandache M., Jeler N., Apostol V. 2013. Drought conditions and management strategies in Romania

McCabe G.J., Wolock D.M. 2011. Century-scale variability in global annual runoff examined using a water balance model. *International Journal of Climatology*. 31(12):1739–48

McKee T.B., Doesken N.J., Kleist J. 1993. The relationship of drought frequency and duration to time scales. *Proc. 8th Conf. Appl. Climatol. 17-22 January 1993*, pp. 179–84. http://ccc.atmos.colostate.edu/relationshipofdroughtfrequency.pdf

Menzel A., Sparks T.H., Estrella N., Koch E., Aasa A., et al. 2006. European phenological response to climate change matches the warming pattern. *Global Change Biology*. 12(10):1969–76

Menzel A., Yuan Y., Matiu M., Sparks T., Scheifinger H., et al. 2020. Climate change fingerprints in recent European plant phenology. *Global Change Biology*. 26(4):2599–2612

Mianabadi A., Davary K., Pourreza-Bilondi M., Coenders-Gerrits A.M.J. 2020. Budyko framework; towards non-steady state conditions. *Journal of Hydrology*. 588(February):125089

Micu D., Havriș L.-E., Dragotă C., Mărculeț C. 2014. Changes in summer types in relation to drought occurrence in the Romanian Plain region. *Aerul Și Apa. Compon. Ale Mediu.* Cluj-Napoca: Universitatea Babeş-Bolyai

Micu D., Popovici E.-A., Havriș L.-E., Dragotă C. 2017. Heat stress-crop yields interactions under summer warming trends: Insights for the southern cropping lowlands of Romania. *Revue Roumaine de Géographie/Romanian Journal of Geography*. 61(2):169–92

Mihai G., Alexandru A.M., Stoica E., Bîrsan M.-V. 2021. Intraspecific growth response to drought of Abies alba in the Southeastern Carpathians. *Forests*. 12(4):1–23

Millennium Ecosystem Assessment. 2005. *Ecosystems and Human Well-Being: Synthesis*. Washington, DC: Island Press

Ministerul Mediului. 1992. Atlasul cadastrului apelor din România

Mishra A.K., Singh V.P. 2010. A review of drought concepts. *Journal of Hydrology*. 391(1–2):204–16

Mishra A.K., Singh V.P. 2011. Drought modeling - A review. *Journal of Hydrology*. 403(1–2):157–75

Mitof I., Prăvălie R. 2014. Temporal trends of hydroclimatic variability in the lower Buzău catchment. *Geographia Technica*. 9(1):87–100

Mitrică B., Mateescu E., Dragotă C., Busuioc A., Grigorescu I., Popovici E.-A. 2013. Climate change impacts on agricultural crops in the Oltenia Plain (Romania). *13th SGEM GeoConference Energy Clean Technol. SGEM2013 Conf. Proc. (June 16-22)*, pp. 573–84

Mjejra M., Dubreuil V., Hénia L. 2015. Suivi de la sécheresse agro-climatique à partir du déficit d'évaporation dans le bassin versant de la Mejerda (Tunisie). *XXVIIIe Colloq. l'Association Int. Climatol.*, pp. 369–74

MMSC. 2012. Strategia Naţională a României privind Schimbările Climatice 2013 - 2020

Modarres R. 2007. Streamflow drought time series forecasting. *Stochastic Environmental Research and Risk Assessment*. 21(3):223–33

Monacelli G., Galluccio M.C., Abbafati M. 2005. Drought assessment and forecasting - Drought Within The Context Of The Region VI

Mounier J. 1965. Les besoins en eau d'une région, d'après Thornthwaite. Essai d'application à la Bretagne. *Norois*. 48(1):437–48

Mounier J. 1977. Aspects et fréquences de la sécheresse en Bretagne : essai de définition de la sécheresse en Europe océanique. *Revue de géographie de Lyon*. 52(2):167–76

Munteanu C., Kuemmerle T., Boltiziar M., Butsic V., Gimmi U., et al. 2014. Forest and agricultural land change in the Carpathian region-A meta-analysis of long-term patterns and drivers of change. *Land Use Policy*. 38:685–97

Munteanu C., Radeloff V., Griffiths P., Halada L., Kaim D., et al. 2017. Land change in the Carpathian region before and after major institutional changes. In *Land-Cover and Land-Use Changes in Eastern Europe after the Collapse of the Soviet Union in 1991*, pp. 57–90. Springer

Musial J.P., Verstraete M.M., Gobron N. 2011. Technical Note: Comparing the effectiveness of recent algorithms to fill and smooth incomplete and noisy time series. *Atmospheric Chemistry and Physics*. 11(15):7905–23

Mutti P.R. 2020. *Drought characterization in the Northeast Brazil: a multiscale watershed analysis and remote sensing monitoring*. Université Rennes 2; Universidade Federal do Rio Grande do Norte

Mutti P.R., Dubreuil V., Bezerra B.G., Arvor D., Funatsu B.M., Santos e Silva C.M. 2022. Long-term meteorological drought characterization in the São Francisco watershed, Brazil: a climatic water balance approach. *International Journal of Climatology*

Nagavciuc V., Scholz P., Ioniță M. 2022. Hotspots for warm and dry summers in Romania. *Natural Hazards and Earth System Sciences*. 22(4):1347–69

Nechita C., Chiriloaei F. 2018. Interpreting the effect of regional climate fluctuations on Quercus robur L. trees under a temperate continental climate (southern Romania). *Dendrobiology*. 79:77–89

Nechita C., Cufar K., Macovei I.I., Popa I., Badea O.N., et al. 2019a. Testing three climate datasets for dendroclimatological studies of oaks in the South Carpathians. *Science of the Total Environment*. 694:

Nechita C., Macovei I., Popa I., Badea O.N., Apostol E.N., Eggertsson Ó. 2019b. Radial growth-based assessment of sites effects on pedunculate and greyish oak in southern Romania. *Science of the Total Environment*. 694:133709

Nechita C., Popa I., Eggertsson Ó. 2017. Climate response of oak (Quercus spp.), an evidence of a bioclimatic boundary induced by the Carpathians. *Science of the Total Environment*. 599–600:1598–1607

Norman S.P., Koch F.H., Hargrove W.W. 2016. Review of broad-scale drought monitoring of forests: Toward an integrated data mining approach. *Forest Ecology and Management*. 380:346–58

Olesen J.E., Trnka M., Kersebaum K.C., Skjelvag A.O., Seguin B., et al. 2011. Impacts and adaptation of European crop production systems to climate change. *European Journal of Agronomy*. 34(2):96–112

Olofsson P., Kuemmerle T., Griffiths P., Knorn J., Baccini A., et al. 2011. Carbon implications of forest restitution in post-socialist Romania. *Environmental Research Letters*. 6(4):045202

Olson D.M., Dinerstein E., Wikramanayake E.D., Burgess N.D., Powell G.V.N., et al. 2001.

Terrestrial ecoregions of the world: A new map of life on Earth. *BioScience*. 51(11):933–38

Onțel I., Irimescu A., Boldeanu G., Mihailescu D., Angearu C.V., et al. 2021. Assessment of soil moisture anomaly sensitivity to detect drought spatio-temporal variability in Romania. *Sensors*. 21(24):8371

Onțel I., Vlăduț A. 2015. Impact of drought on the productivity of agricultural crops within the Oltenia Plain, Romania. *Geographica Pannonica*. 19(1):9–19

Padrón R.S., Gudmundsson L., Greve P., Seneviratne S.I. 2017. Large-scale controls of the surface water balance over land: Insights from a systematic review and meta-analysis. *Water Resources Research*. 53(11):9659–78

Păltineanu C., Mihailescu I.F., Seceleanu I., Dragotă C., Vasenciuc F. 2007a. Using aridity indices to describe some climate and soil features in Eastern Europe: A Romanian case study. *Theoretical and Applied Climatology*. 90(3–4):263–74

Păltineanu C., Mihăilescu I.F., Seceleanu I., Dragotă C., Vasenciuc F. 2007b. *Ariditatea, Seceta, Evapotranspirația Și Cerințele de Apă Ale Culturilor Agricole În România*. Constanța: Ovidius University Press

Panaitescu L., Lungu M., Niță S. 2012. The influence of the semi-dry climate of Dobruja on the maize production. *Present Environment and Sustainable Development*. 6(2):381–86

Parker P.S., Shonkwiler J.S., Aurbacher J. 2017. Cause and consequence in maize planting dates in Germany. *Journal of Agronomy and Crop Science*. 203(3):227–40

Páscoa P., Gouveia C.M., Russo A.C., Bojariu R., Vicente-Serrano S.M., Trigo R.M. 2020. Drought impacts on vegetation in southeastern Europe. *Remote Sensing*. 12(13):1–21

Peñuelas J., Canadell J.G., Ogaya R. 2011. Increased water-use efficiency during the 20th century did not translate into enhanced tree growth. *Global Ecology and Biogeography*. 20(4):597–608

Peñuelas J., Sardans J., Estiarte M., Ogaya R., Carnicer J., et al. 2013. Evidence of current impact of climate change on life: A walk from genes to the biosphere. *Global Change Biology*. 19(8):2303–38

Petrițan A.M., Petrițan I.C., Hevia A., Walentowski H., Bouriaud O., Sánchez-Salguero R. 2021. Climate warming predispose sessile oak forests to drought-induced tree mortality regardless of management legacies. *Forest Ecology and Management*. 491:119097

Pettitt A.N. 1979. A non-parametric approach to the change-point problem. *Journal of the Royal Statistical Society. Series C (Applied Statistics)*. 28(2):126–35

Pișota I., Zaharia L. 2003. *Hidrologia Uscatului*. București: Credis

Pișota I., Zaharia L., Diaconu D. 2010. *Hidrologie*. București: Editura Universitară. II ed.

Planchon O., Dubreuil V., Bernard V., Blain S. 2008. Contribution of tree-ring analysis to the study of droughts in northwestern France (XIX-XXth century). *Climate of the Past Discussions*. 4(1):249–70

Popa I., Leca S., Crăciunescu A., Sidor C., Badea O. 2013. Dendroclimatic response variability of Quercus species in the Romanian intensive forest monitoring network. *Notulae Botanicae Horti Agrobotanici Cluj-Napoca*. 41(1):326–32

Popova-Cucu A., Doniță N., Boșcaiu N. 1983. Flora și vegetația. In *Geografia României I. Geografia Fizică*, pp. 388–441

Popovici E.A., Bălteanu D., Kucsicsa G. 2016. Utilizarea terenurilor și dezvoltarea actuală a agriculturii. In *România. Natură Şi Societate*, eds. D Bălteanu, M Dumitraşcu, S Geacu, B Mitrică, M Sima, pp. 329–74. București: Editura Academiei Române

Pörtner H.-O., Roberts D.C., Adams H., Adelekan I., Adler C., et al. 2022. Technical Summary. In *Climate Change 2022: Impacts, Adaptation and Vulnerability. Contribution of Working Group II to the Sixth Assessment Report of the Intergovernmental Panel on Climate Change*, eds. H-O Pörtner, DC Roberts, ES Poloczanska, K Mintenbeck, M Tignor, et al., pp. 37–118. Cambridge, UK and New York, NY, USA: Cambridge University Press

Posea G. 2005. *Geomorfologia României*. București: Editura Fundației "România de Mâine." 2nd ed.

Posea G., Badea L. 1984. România. Unitățile de relief (Regionarea geomorfologică)

Post E., Steinman B.A., Mann M.E. 2018. Acceleration of phenological advance and warming with latitude over the past century. *Scientific Reports*. 8(1):1–8

Potop V., Mateescu E., Boroneanţ C., Zahradníček P., Constantinescu F., et al. 2014. Modelling climate change impacts on thermophilic crops production in central and southern Europe

Prăvălie R., Bandoc G. 2015. Aridity variability in the last five decades in the Dobrogea region, Romania. *Arid Land Research and Management*. 29(3):265–87

Prăvălie R., Patriche C.V., Sirodoev I., Bandoc G., Dumitraşcu M., Peptenatu D. 2016. Water deficit and corn productivity during the post-socialist period. Case study: Southern Oltenia drylands, Romania. *Arid Land Research and Management*. 30(3):239–57

Prăvălie R., Piticar A., Roșca B., Sfîcă L., Bandoc G., et al. 2019. Spatio-temporal changes of the climatic water balance in Romania as a response to precipitation and reference evapotranspiration trends during 1961–2013. *Catena*. 172:295–312

Prăvălie R., Sîrodoev I., Nita I.A., Patriche C., Dumitraşcu M., et al. 2022. NDVI-based ecological dynamics of forest vegetation and its relationship to climate change in Romania during 1987–2018. *Ecological Indicators*. 136(August 2021):

Prăvălie R., Sîrodoev I., Patriche C., Roșca B., Piticar A., et al. 2020. The impact of climate change on agricultural productivity in Romania. A country-scale assessment based on the relationship between climatic water balance and maize yields in recent decades. *Agricultural Systems*. 179(March):

Prăvălie R., Bandoc G., Patriche C., Tomescu M. 2017. Spatio-temporal trends of mean air temperature during 1961-2009 and impacts on crop (maize) yields in the most important agricultural region of Romania. *Stochastic Environmental Research and Risk Assessment*. 31:1923–1939

Reichstein M., Bahn M., Ciais P., Frank D., Mahecha M.D., et al. 2013. Climate extremes and the carbon cycle. *Nature*. 500(7462):287–95

Retegan M., Borcan M. 2011. Estimating the tendency and the variability of the rainfall amount in Ialomița river basin and their influence upon the liquid run-off. *Aerul Și Apa. Compon. Ale Mediu. (18-19 March 2011)*, pp. 178–84

Rezaei E.E., Siebert S., Ewert F. 2015. Intensity of heat stress in winter wheat - Phenology compensates for the adverse effect of global warming. *Environmental Research Letters*. 10(2):024012

Rezaei E.E., Siebert S., Hüging H., Ewert F. 2018. Climate change effect on wheat phenology depends on cultivar change. *Scientific Reports*. 8(1):1–10

Richardson A.D., Keenan T.F., Migliavacca M., Ryu Y., Sonnentag O., Toomey M. 2013. Climate change, phenology, and phenological control of vegetation feedbacks to the climate system. *Agricultural and Forest Meteorology*. 169:156–73

Rocha A. V., Shaver G.R. 2009. Advantages of a two band EVI calculated from solar and photosynthetically active radiation fluxes. *Agricultural and Forest Meteorology*. 149(9):1560–63

Roman G.V., Tabără V., Gavril M., Ștefan M., Robu T., et al. 2011. *Fitotehnie - Vol. 1 - Cereale Și Leguminoase Pentru Boabe*. București: Editura Universitară

Rossi G., Vega T., Bonaccorso B. 2007. *Methods and Tools for Drought Analysis and Management*. Springer

Ruosteenoja K., Markkanen T., Venäläinen A., Räisänen P., Peltola H. 2018. Seasonal soil moisture and drought occurrence in Europe in CMIP5 projections for the 21st century. *Climate Dynamics*. 50(3–4):1177–92

Russell R.J. 1931. *Dry Climates of the United States: I. Climatic Map*, Vol. 5. University of California Press

Saini H.S., Westgate M.E. 1999. Reproductive development in grain crops during drought. *Advances in Agronomy*. 68(C):59–96

San-Miguel-Ayanz J., Durrant, T., Boca R., Maianti P., Liberta` G., Artes Vivancos T., et al. 2021. Forest fires in Europe, Middle East and North Africa 2020. Luxembourg

Savitzky A., Golay M.J.E. 1964. Smoothing and differentiation of data by simplified least squares procedures. *Analytical chemistry*. 36(8):1627–39

Schaake J., Liu C. 1989. Development and application of simple water balance models to understand the relationship between climate and water resources. . (181):343–52

Schaake J.C. 1990. From climate to flow. In *Climate Change and US Water Resources.*, ed. PE Waggoner, pp. 177–206. New York: Wiley

Seidl R., Thom D., Kautz M., Martin-Benito D., Peltoniemi M., et al. 2017. Forest disturbances under climate change. *Nature Climate Change*. 7(6):395–402

Semenov M.A., Martre P., Jamieson P.D. 2009. Quantifying effects of simple wheat traits on yield in water-limited environments using a modelling approach. *Agricultural and Forest Meteorology*. 149(6–7):1095–1104

Sen P.K. 1968. Estimates of the Regression Coefficient Based on Kendall's Tau. *Journal of the American Statistical Association*. 63(324):1379–89

Seneviratne S.I., Corti T., Davin E.L., Hirschi M., Jaeger E.B., et al. 2010. Investigating soil moisture-climate interactions in a changing climate: A review. *Earth-Science Reviews*. 99(3–4):125–61

Șerban C., Maftei C., Dobrică G. 2022. Surface water change detection via water indices and predictive modeling using remote sensing imagery: a case study of Nuntasi-Tuzla Lake, Romania. *Water (Switzerland)*. 14(4):

Shapiro S.S., Wilk M.B. 1965. An analysis of variance test for normality (complete samples). *Biometrika*. 52(3/4):591–611

Shaw S.B., Beslity J.O., Colvin M.E. 2019. Working towards a more holistic set of hydrologic principles to teach nonhydrologists: Five simple concepts within catchment hydrology. *Hydrological Processes*. 33(16):2258–62

Shukla S., Wood A.W. 2008. Use of a standardized runoff index for characterizing hydrologic drought. *Geophysical Research Letters*. 35(2):1–7

Sima M., Popovici E.-A., Bălteanu D., Micu D.M., Kucsicsa G., et al. 2015. A farmer-based analysis of climate change adaptation options of agriculture in the Bărăgan Plain, Romania. *Earth Perspectives*. 2(1):

Smith M.D. 2011. An ecological perspective on extreme climatic events: a synthetic definition and framework to guide future research. *Journal of Ecology*. 99(3):656–63

Sorocovschi V. 2009. Seceta: concept, geneză, atribute și clasificare. *Riscuri și catastrofe*. VIII(7):62–73

Spinoni J., Naumann G., Vogt J. 2015. Spatial patterns of European droughts under a moderate emission scenario. *Advances in Science and Research*. 12(1):179–86

Stagge J.H., Kingston D.G., Tallaksen L.M., Hannah D.M. 2017. Observed drought indices show increasing divergence across Europe. *Scientific Reports*. 7(1):14045

Stagge J.H., Tallaksen L.M., Gudmundsson L., Van Loon A.F., Stahl K. 2015. Candidate Distributions for Climatological Drought Indices (SPI and SPEI). *International Journal of Climatology*. 35(13):4027–40

Stahl K., Kohn I., Blauhut V., Urquijo J., De Stefano L., et al. 2016. Impacts of European drought events: Insights from an international database of text-based reports. *Natural Hazards and Earth System Sciences*. 16(3):801–19

Stan F., Zaharia L., Neculau G., Ioana-Toroimac G. 2015. Variabilité spatiale et temporelle de l'évaporation dans la Plaine roumaine. *Actes Du Colloq. l'Association Int. Climatol. 2015*. 28(November):621–26

Ștefan S., Ghioca M., Rimbu N., Boroneanț C. 2004. Study of meteorological and hydrological drought in southern Romania from observational data. *International Journal of Climatology*. 24(7):871–81

Stephenson N.L. 1990. Climatic control of vegetation distribution: the role of the water balance. *American Naturalist*. 135(5):649–70

Stephenson N.L. 1998. Actual evapotranspiration and deficit: Biologically meaningful correlates of vegetation distribution across spatial scales. *Journal of Biogeography*. 25(5):855–70

Tariq M., Ahmad S., Fahad S., Abbas G., Hussain S., et al. 2018. The impact of climate warming and crop management on phenology of sunflower-based cropping systems in Punjab, Pakistan. *Agricultural and Forest Meteorology*. 256–257(March):270–82

Tateishi R., Ebata M. 2004. Analysis of phenological change patterns using 1982-2000 Advanced Very High Resolution Radiometer (AVHRR) data. *International Journal of Remote Sensing*. 25(12):2287–2300

Teuling A.J., De Badts E.A.G., Jansen F.A., Fuchs R., Buitink J., et al. 2019. Climate change, reforestation/afforestation, and urbanization impacts on evapotranspiration and streamflow in Europe. *Hydrology and Earth System Sciences*. 23(9):3631–52

Thornthwaite C.W. 1948. An approach toward a rational classification of climate. *Geographical Review*. 38(1):55–94

Thornthwaite C.W., Mather J.R. 1955. *The Water Balance*, Vol. 8. Centerton, New Jersey: Drexel Institute of Technology, Laboratory of Climatology

Trenberth K.E., Dai A., Rasmussen R.M., Parsons D.B. 2003. The changing character of precipitation. *Bulletin of the American Meteorological Society*. 84(9):1205–17

Trenberth K.E., Dai A., van der Schrier G., Jones P.D., Barichivich J., et al. 2014. Global warming and changes in drought. *Nature Climate Change*. 4(1):17–22

Trzpit J.-P. 1978. La sécheresse en Basse-Normandie : calamité accidentelle ou mal récurrent ? *Études Normandes*. 27(1):55–74

Turc L. 1961. Evaluation des besoins en eau d'irrigation, évapotranspiration potentielle. *Annuaire Agronomie*. 12:13–49

Ujvári I. 1972. *Geografia Apelor României*. București: Editura Științifică

UNDRR. 2021. Special Report on Drought 2021

van den Besselaar E.J.M. 2021. *E-OBS daily gridded observations for Europe from 1950 to present: Product user guide*. https://confluence.ecmwf.int/display/CKB/E-OBS+daily+gridded+observations+for+Europe+from+1950+to+present%3A+Product+user+guide#EOBSdailygriddedobservationsforEuropefrom1950topresent:Productuserguide-Radiation

van der Molen M.K., Dolman A.J., Ciais P., Eglin T., Gobron N., et al. 2011. Drought and ecosystem carbon cycling. *Agricultural and Forest Meteorology*. 151(7):765–73

Van Loon A.F., Gleeson T., Clark J., Van Dijk A.I.J.M., Stahl K., et al. 2016. Drought in the Anthropocene. *Nature Geoscience*. 9(2):89–91

Van Mantgem P.J., Stephenson N.L. 2007. Apparent climatically induced increase of tree mortality rates in a temperate forest. *Ecology Letters*. 10(10):909–16

Van Vliet M.T.H., Donnelly C., Strömbäck L., Capell R., Ludwig F. 2015. European scale climate information services for water use sectors. *Journal of Hydrology*. 528:503–13

Van Vliet M.T.H., Sheffield J., Wiberg D., Wood E.F. 2016. Impacts of recent drought and warm years on water resources and electricity supply worldwide. *Environmental Research Letters*. 11(12):124021

Vanonckelen S., Van Rompaey A. 2015. Spatiotemporal analysis of the controlling factors of forest cover change in the Romanian Carpathian Mountains. *Mountain Research and Development*. 35(4):338–50

Vâtcă S.D., Stoian V.A., Man T.C., Horvath C., Vidican R., et al. 2021. Agrometeorological requirements of maize crop phenology for sustainable cropping—A historical review for Romania. *Sustainability (Switzerland)*. 13(14):1–14

Vermote E., NOAA CDR Program. 2019. NOAA Climate Data Record (CDR) of AVHRR Leaf Area Index (LAI) and Fraction of Absorbed Photosynthetically Active Radiation (FAPAR), version 5 [Dataset]

Vicente-Serrano S.M., Beguería S., López-Moreno J.I. 2010. A multiscalar drought index sensitive to global warming: The standardized precipitation evapotranspiration index. *Journal of Climate*. 23(7):1696–1718

Wada Y., Van Beek L.P.H., Bierkens M.F.P. 2011. Modelling global water stress of the recent past: On the relative importance of trends in water demand and climate variability. *Hydrology and Earth System Sciences*. 15(12):3785–3808

Wang C., Wang S., Fu B., Zhang L. 2016. Advances in hydrological modelling with the Budyko framework: A review. *Progress in Physical Geography*. 40(3):409–30

Wang D., Hejazi M. 2011. Quantifying the relative contribution of the climate and direct human impacts on mean annual streamflow in the contiguous United States. *Water Resources Research*. 47(9):

Wang S., McVicar T.R., Zhang Z., Brunner T., Strauss P. 2020. Globally partitioning the simultaneous impacts of climate-induced and human-induced changes on catchment streamflow: A review and meta-analysis. *Journal of Hydrology*. 590(March):125387

White K., Pontius J., Schaberg P. 2014. Remote sensing of spring phenology in northeastern forests: A comparison of methods, field metrics and sources of uncertainty. *Remote Sensing of Environment*. 148:97–107

White M.A., Thornton P.E., Running S.W. 1997. A continental phenology model for monitoring vegetation responses to interannual climatic variability. *Global Biogeochemical Cycles*. 11(2):217–34

Wilcock A.A. 1968. Köppen after fifty years. *Annals of the Association of American Geographers*. 58(1):12–28

Wilhite D., Glantz M. 1985. Understanding the drought phenomenon: The role of definitions. *Water International*. 10(3):111–20

Wilhite D.A. 2000. Drought as a natural hazard: concepts and definitions. In *Drought: A Global Assessment*, Volume 1, ed. DA Wilhite, pp. 3–18. London: Routledge

WMO. 2006. Drought monitoring and early warning: concepts, progress and future challenges

WMO. 2012. *Standardized Precipitation Index User Guide. WMO-No. 1090*. Geneva

WMO, GWP. 2016. *Handbook of Drought Indicators and Indices*. Geneva

Wolkovich E.M., Cook B.I., Allen J.M., Crimmins T.M., Betancourt J.L., et al. 2012. Warming experiments underpredict plant phenological responses to climate change. *Nature*. 485(7399):494–97

World Bank. 2018. *Romania Water Diagnostic Report: Moving toward EU Compliance, Inclusion, and Water Security*. Washington, DC: World Bank

Xie Y., Wang X., Wilson A.M., Silander J.A. 2018. Predicting autumn phenology: How deciduous tree species respond to weather stressors. *Agricultural and Forest Meteorology*. 250:127–37

Yang H., Yang D., Hu Q. 2014. An error analysis of the Budyko hypothesis for assessing the contribution of climate change to runoff. *Water Resources Research*. 50(12):9620–29

Yevjevich V. 1967. An objective approach to definitions and investigations of continental hydrologic droughts. *Hydrology Papers*. (23):

Zaharia L. 2004. Water resources of rivers in Romania. *Analele Universităţii Bucureşti: Geografie*. 77–85

Zaharia L., Beltrando G., Ioana-Toroimac G., Minea G., Grecu F. 2012. Les sécheresses des dernières décennies dans la Plaine Roumaine. *Actes Du Colloq. l'Association Int. Climatol.*, pp. 787–92

Zaharia L., Ioana-Toroimac G., Perju E.-R. 2020. Hydrological impacts of climate changes in Romania. In *Water Resources Management in Romania*, pp. 309–51

Zaharia L., Ioana-Toroimac G., Cocoş O., Ghiţă F.A., Mailat E. 2016. Urbanization effects on the river systems in the Bucharest City region (Romania). *Ecosystem Health and Sustainability*. 2(11):e01247

Zargar A., Sadiq R., Naser B., Khan F.I. 2011. A review of drought indices. *Environmental Reviews*. 19:333–49

Zhang L., Hickel K., Dawes W.R., Chiew F.H.S., Western A.W., Briggs P.R. 2004. A rational function approach for estimating mean annual evapotranspiration. *Water Resources Research*. 40(2):1–14

Zhang N., Hong Y., Qin Q., Liu L. 2013. VSDI: A visible and shortwave infrared drought index

for monitoring soil and vegetation moisture based on optical remote sensing. *International Journal of Remote Sensing*. 34(13):4585–4609

Zheng H., Zhang L., Zhu R., Liu C., Sato Y., Fukushima Y. 2009. Responses of streamflow to climate and land surface change in the headwaters of the Yellow River Basin. *Water Resources Research*. 45(7):1–9

Zhu Z., Piao S., Myneni R.B., Huang M., Zeng Z., et al. 2016. Greening of the Earth and its drivers. *Nature Climate Change*. 6(8):791–95

LIST OF FIGURES

LIST OF TABLES

APPENDIX A. Trends in hydroclimatic variables

Table A.1 Monthly and annual trends in average air temperature (T, ºC) at meteorological stations between 1961 – 2020 using the Mann-Kendall and Sen's slope statistical tests (data from ECA&D)

T	Roșiorii de Vede		București Băneasa		Buzău		Călărași		Galați		Constanța		Tulcea		Sulina		Vârful Omu		
	Z	S	Z	S	Z	S	Z	S	Z	S	Z	S	Z	S	Z	S	Z	S	
I	1.4	0.03	1.2	0.02	1.8	0.03	1.8	0.04	2.1	0.04	1.6	0.03	1.7	0.03	1.4	0.02	0.6	0.01	I
II	**1.97***	**0.04***	1.8	0.4	**2.2***	**0.04***	**2***	**0.05***	**2.5***	**0.05***	**2.2***	**0.04***	**2***	**0.04***	1.6	0.03	1.2	0.02	II
III	**2.6***	**0.05***	**2.2***	**0.04***	**3***	**0.06***	**2.6***	**0.05***	**3.3***	**0.07***	**3.3***	**0.06***	**2.8***	**0.05***	**2.4***	**0.04***	0.8	0.01	III
IV	1.4	0.02	0.5	0.006	1.7	0.02	1.3	0.19	2.0	0.03	**2.6***	**0.03***	1.5	0.02	**2.2***	**0.02***	0.6	0.01	IV
V	1.3	0.02	0.4	0.005	**2***	**0.02***	**2.2***	**0.02***	**2.6***	**0.03***	**4.0***	**0.04***	**2.1***	**0.02***	**2.7***	**0.03***	1.6	0.02	V
VI	**3.5***	**0.04***	**2.8***	**0.03***	**4.05***	**0.04***	**4.2***	**0.04***	**4.2***	**0.05***	**4.8***	**0.04***	**4.1***	**0.03***	**3.2***	**0.03***	**3.8***	**0.05***	VI
VII	**4.3***	**0.04***	**2.6***	**0.02***	**4.25***	**0.04***	**4.5***	**0.04***	**4.6***	**0.05***	**5.1***	**0.05***	**4.4***	**0.04***	**3.9***	**0.04***	**4.3***	**0.04***	VII
VIII	**4.5***	**0.06***	**3.3***	**0.04***	**4.9***	**0.06***	**4.7***	**0.06***	**5.1***	**0.06***	**5.8***	**0.06***	**5.1***	**0.05***	**4.8***	**0.05***	**5.0***	**0.06***	VIII
IX	**2.1***	**0.03***	0.7	0.008	**2.3***	**0.03***	**3.1***	**0.03***	**2.7***	**0.04***	**3.4***	**0.04***	**2.9***	**0.03***	1.9	0.02	0.9	0.01	IX
X	1.3	0.02	-0.1	-0.001	1.6	0.02	1.6	0.02	1.8	0.02	2.0	0.02	1.7	0.02	1.2	0.01	1.4	0.02	X
XI	0.8	0.01	0.1	0.002	0.7	0.01	0.4	0.008	0.9	0.02	0.3	0.01	0.3	0.01	0.2	0.00	1.4	0.03	XI
XII	1.6	0.02	1.1	0.02	1.7	0.03	1.2	0.02	**2.1***	**0.03***	1.5	0.02	1.4	0.02	1.4	0.02	1.5	0.02	XII
A	**4.7***	**0.03***	**2.7***	**0.02***	**5.2***	**0.03***	**4.8***	**0.03***	**5.1***	**0.04***	**5.5***	**0.04***	**4.7***	**0.03***	**4.3***	**0.03***	**4.7***	**0.03***	A

Z = Mann-Kendal Z; S = Sen's slope; A = Annual trend. Bolded and starred values show significance ($P \leq 0.05$).

Table A.2 Monthly and annual trends in precipitation (P, mm) at meteorological stations between 1961 – 2020 using the Mann-Kendall and Sen's slope statistical tests (data from ECA&D)

P	Roșiorii de Vede		București Băneasa		Buzău		Călărași		Galați		Constanța		Tulcea		Sulina		Vârful Omu		
	Z	S	Z	S	Z	S	Z	S	Z	S	Z	S	Z	S	Z	S	Z	S	
I	0.8	0.16	1.2	0.25	-0.7	-0.08	**2.1***	**0.40***	1.3	0.21	1.5	0.25	0.9	0.15	0.0	0.00	-1.3	-0.37	I
II	-0.8	-0.13	-0.2	0.00	-1.2	-0.17	-0.5	-0.07	-0.7	-0.11	-0.5	-0.06	-1.3	-0.17	**-2.4***	**-0.20***	-0.8	-0.21	II
III	0.6	0.13	0.8	0.15	0.7	0.08	1.1	0.17	0.6	0.09	1.0	0.16	0.1	0.02	-0.1	-0.01	0.2	0.05	III
IV	-1.1	-0.16	0.5	0.10	0.7	0.12	0.5	0.08	0.0	0.00	0.2	0.00	0.4	0.07	-1.7	-0.11	**-2.1***	**-0.59***	IV
V	0.1	0.00	-0.1	-0.02	-0.7	-0.22	-0.4	-0.12	-0.6	-0.17	0.3	0.07	-0.1	0.00	**-2.3***	**-0.24***	-1.4	-0.56	V
VI	0.9	0.26	1.2	0.37	1.1	0.26	0.2	0.09	0.0	0.00	1.1	0.24	1.3	0.31	-0.4	-0.06	-0.4	-0.23	VI
VII	-0.7	-0.17	-0.1	-0.02	0.2	0.06	-0.9	-0.23	0.2	0.05	1.1	0.18	0.7	0.17	-0.9	-0.12	-0.7	-0.46	VII
VIII	-1.3	-0.26	-1.0	-0.25	-0.9	-0.21	-0.9	-0.23	**-2.1***	**-0.35***	-1.3	-0.17	-1.8	-0.27	-0.9	-0.12	-0.6	-0.28	VIII
IX	0.8	0.13	1.2	0.28	1.2	0.24	1.1	0.29	0.3	0.06	0.6	0.12	0.5	0.15	-0.7	-0.12	0.1	0.03	IX
X	**2.7***	**0.56***	**3.1***	**0.74***	**2.9***	**0.58***	**2.5***	**0.50***	**2.5***	**0.41***	1.9	0.40	**3.4***	**0.57***	**2.1***	**0.19***	0.7	0.17	X
XI	-1.2	-0.23	-0.2	0.00	-0.8	-0.12	0.9	0.20	0.3	0.06	-0.2	-0.03	0.3	0.08	-0.2	-0.02	-1.5	-0.36	XI
XII	-0.4	-0.08	0.7	0.18	0.4	0.06	0.8	0.19	1.0	0.20	0.5	0.12	0.2	0.04	-1.4	-0.17	-1.9	-0.60	XII
A	-0.006	-0.04	1.1	1.5	0.2	0.2	1.3	1.2	0.4	0.35	**2.03***	**1.7***	1.2	1.04	**-2.01***	**-1.05***	-1.7	-4.8	A

Z = Mann-Kendal Z; S = Sen's slope; A = Annual trend. Bolded and starred values show significance ($P \leq 0.05$).

Table A.3 Monthly and annual trends in potential evapotranspiration (PET, mm) at meteorological stations between 1961 – 2020 using the Mann-Kendall and Sen's slope statistical tests (data from CRU)

PET	Roșiorii de Vede		București Băneasa		Buzău		Călărași		Galați		Constanța		Tulcea		Sulina		Vârful Omu		
	Z	S	Z	S	Z	S	Z	S	Z	S	Z	S	Z	S	Z	S	Z	S	
I	**2.2***	**0.00***	**2.5***	**0.00***	**2.3***	**0.00***	1.4	0.00	**3.3***	**0.07***	**2.2***	**0.00**	**2.6***	**0.00***	1.0	0.00	0.7	0.00	I
II	**2.6***	**0.10***	**2.4***	**0.08***	**2.3***	**0.07***	**2.2***	**0.07***	**3.1***	**0.14***	**2.9***	**0.14***	**2.9***	**0.12***	**2.2***	**0.10***	1.6	0.00	II
III	**3.4***	**0.24***	**3.4***	**0.23***	**3.6***	**0.27***	**3.7***	**0.27***	**3.8***	**0.33***	**4.2***	**0.38***	**4.1***	**0.35***	**3.8***	**0.38***	0.7	0.00	III
IV	**3.9***	**0.30***	**3.6***	**0.27***	**3.4***	**0.27***	**2.7***	**0.23***	**3.3***	**0.30***	**3.2***	**0.28***	**3.2***	**0.30***	**2.7***	**0.27***	0.5	0.03	IV
V	1.8	0.16	1.2	0.10	1.6	0.17	1.8	0.17	**2.2***	**0.26***	**2.5***	**0.25***	**2.4***	**0.27***	**2.3***	**0.27***	0.0	0.00	V
VI	**3.0***	**0.27***	**3.2***	**0.28***	**3.3***	**0.32***	**3.4***	**0.30***	**3.0***	**0.37***	**3.6***	**0.36***	**3.2***	**0.40***	**3.4***	**0.41***	1.3	0.11	VI
VII	**4.1***	**0.36***	**4.0***	**0.32***	**4.1***	**0.33***	**4.5***	**0.38***	**4.6***	**0.47***	**4.6***	**0.45***	**4.7***	**0.47***	**4.5***	**0.56***	**2.3***	**0.20***	VII
VIII	**4.6***	**0.52***	**4.5***	**0.48***	**4.8***	**0.54***	**4.7***	**0.56***	**5.2***	**0.75***	**5.3***	**0.70***	**5.3***	**0.76***	**5.2***	**0.87***	**2.1***	**0.20***	VIII
IX	**3.0***	**0.25***	**3.2***	**0.24***	**3.2***	**0.26***	**3.3***	**0.26***	**3.2***	**0.34***	**4.0***	**0.39***	**3.5***	**0.35***	**3.5***	**0.38***	-0.2	-0.01	IX
X	0.5	0.00	0.2	0.00	0.0	0.00	-0.5	0.00	0.5	0.00	0.3	0.00	0.5	0.00	0.2	0.00	0.0	0.00	X
XI	0.8	0.00	0.3	0.00	0.1	0.00	0.1	0.00	0.7	0.00	-0.1	0.00	0.8	0.00	-0.2	0.00	1.5	0.03	XI
XII	1.5	0.00	1.5	0.00	1.2	0.00	0.9	0.00	**2.6***	**0.00***	**2.3***	**0.00***	**2.3***	**0.00***	1.5	0.00	1.1	0.00	XII
A	**5.6***	**2.4***	**5.2***	**2.2***	**5.3***	**2.3***	**5.2***	**2.4***	**5.6***	**3.1***	**5.8***	**3***	**5.7***	**3.3***	**5.7***	**3.3***	**2.2***	**0.6***	A

Z = Mann-Kendal Z; S = Sen's slope; A = Annual trend. Bolded and starred values show significance ($P \leq 0.05$).

Table A.4 Monthly and annual trends in actual evapotranspiration (AET, mm) at meteorological stations between 1961 – 2020 using the Mann-Kendall and Sen's slope statistical tests (AET obtained by using the Thornthwaite water balance, **Chapter 3.3.2**)

AET	Roșiorii de Vede		București Băneasa		Buzău		Călărași		Galați		Constanța		Tulcea		Sulina		Vârful Omu		
	Z	S	Z	S	Z	S	Z	S	Z	S	Z	S	Z	S	Z	S	Z	S	
I	**2.4***	**0.01***	1.8	0.00	**2.4***	**0.00***	1.2	0.00	**2.5***	**0.08***	**2.3***	**0.07***	**2.3***	**0.03***	1.1	0.05	1.4	0.00	I
II	**2.0***	**0.08***	**2.4***	**0.09***	1.0	0.03	**2.5***	**0.11***	**2.3***	**0.11***	1.8	0.08	**2.2***	**0.11***	0.3	0.01	**2.5***	**0.00***	II
III	**3.1***	**0.16***	**3.6***	**0.19***	**4.0***	**0.20***	**3.6***	**0.21***	**3.0***	**0.22***	**3.8***	**0.28***	**4.3***	**0.26***	**2.7***	**0.17***	0.7	0.02	III
IV	0.8	0.08	**2.1***	**0.16***	**2.1***	**0.20***	**2.0***	**0.18***	1.6	0.16	1.2	0.09	0.7	0.08	**-2.2***	**-0.21***	0.5	0.03	IV
V	-0.3	-0.05	0.4	0.06	-0.1	-0.02	-0.5	-0.10	-1.3	-0.21	-0.2	-0.05	-0.4	-0.07	**-3.0***	**-0.38***	0.1	0.00	V
VI	0.9	0.18	1.3	0.32	1.3	0.24	-0.1	-0.02	-0.6	-0.14	0.7	0.15	0.7	0.19	-1.1	-0.17	1.1	0.10	VI
VII	-1.0	-0.27	0.1	0.03	-0.7	-0.17	-1.3	-0.28	-0.3	-0.06	0.8	0.14	0.9	0.16	-1.2	-0.15	1.4	0.12	VII
VIII	-1.5	-0.31	-0.7	-0.22	-1.3	-0.36	-1.3	-0.28	**-2.3***	**-0.39***	-1.3	-0.20	**-2.1***	**-0.30***	-1.1	-0.13	1.2	0.08	VIII
IX	0.7	0.13	1.3	0.25	1.3	0.20	1.2	0.29	0.4	0.06	0.9	0.17	0.7	0.15	-0.8	-0.14	-0.1	-0.02	IX
X	**3.3***	**0.36***	**2.9***	**0.22***	**3.2***	**0.32***	**2.3***	**0.23***	**2.4***	**0.32***	1.8	0.28	**3.2***	**0.41***	**2.1***	**0.18***	0.1	0.00	X
XI	-0.6	0.00	0.5	0.00	-0.1	0.00	1.1	0.01	0.6	0.00	-0.1	0.00	-0.5	0.00	-0.5	-0.03	1.2	0.03	XI
XII	0.0	0.00	0.8	0.00	0.8	0.00	0.0	0.00	**2.4***	**0.05***	1.4	0.00	**2.8***	**0.06***	-0.6	-0.02	1.1	0.00	XII
A	0.6	0.4	1.5	1.2	0.8	0.4	0.5	0.4	-0.2	-0.2	**2.3***	**1.4***	1.6	1	-1.8	-0.9	1.4	0.4	A

Z = Mann-Kendal Z; S = Sen's slope; A = Annual trend. Bolded and starred values show significance ($P \leq 0.05$).

Table A.5 Monthly and annual trends in river discharge (Q, m^3/s) at meteorological stations between 1966 – 2010 using the Mann-Kendall (or the modified Mann-Kendall for the annual trend) and Sen's slope statistical tests

Q	Vedea R., Alexandria g.s.		Argeș R., Budești g.s.		Ialomița R., Coșereni g.s.		Buzău R., Racovița g.s.		
	Z	S	Z	S	Z	S	Z	S	
I	-1.7	-0.04	-0.6	-0.13	-0.4	-0.08	0.7	0.05	I
II	**-2.3***	**-0.20***	-1.8	-0.63	-1.9	-0.42	-1.2	-0.11	II
III	**-2.4***	**-0.13***	-1.0	-0.53	-1.5	-0.39	-0.7	-0.13	III
IV	-1.2	-0.05	-1.7	-0.65	-1.7	-0.70	-1.5	-0.45	IV
V	**-2.0***	**-0.06***	**-2.1***	**-0.97***	**-2.3***	**-0.86***	-1.5	-0.44	V
VI	**-2.6***	**-0.11***	-1.7	-0.88	**-2.4***	**-0.85***	-1.9	-0.41	VI
VII	**-2.8***	**-0.09***	-1.9	-0.78	-1.9	-0.55	-1.1	-0.22	VII
VIII	-0.9	-0.01	-1.2	-0.39	-1.2	-0.26	-1.2	-0.20	VIII
IX	**-2.5***	**-0.03***	-0.7	-0.23	-0.8	-0.13	-0.3	-0.05	IX
X	-1.0	-0.01	-0.1	-0.02	0.6	0.07	0.5	0.05	X
XI	**-3.2***	**-0.04***	-1.6	-0.45	-0.4	-0.09	-0.3	-0.02	XI
XII	-1.7	-0.04	-1.6	-0.50	-0.2	-0.07	0.2	0.03	XII
A	**-2.8***	**-0.114***	-1.71	-0.55	-1.53	-0.47	**-2.34***	**-0.29***	A

Z = Mann-Kendal Z; S = Sen's slope; A = Annual trend; R. =River; g.s. = gauging station. Bolded and starred values show significance ($P \leq 0.05$).

THESE DE DOCTORAT DE

L'UNIVERSITE RENNES 2 EN CO-TUTELLE AVEC
UNIVERSITATEA BUCUREȘTI

ECOLE DOCTORALE N° 645
Espaces, Sociétés, Civilisations
Spécialité : *Géographie*

Par

Maria-Alexandra CHELU

Hydroclimatic drought and its impacts on vegetation in south-eastern Romania

Thèse présentée et soutenue à Rennes, le 19 décembre 2023
Unité de recherche : LETG (Littoral - Environnement - Télédétection - Géomatique) UMR 6554

Résumé

Rapporteurs avant soutenance :

Nadège MARTINY	Maître de Conférences-HDR, Université Bourgogne-Franche-Comté, Dijon
Iulian-Horia HOLOBÂCĂ	Professeur, Universitatea Babeș-Bolyai, Cluj-Napoca

Composition du Jury :

Examinateurs : Sylvain BIGOT	Professeur, Université Grenoble Alpes, Grenoble
Nadège MARTINY	Maître de Conférences-HDR, Université Bourgogne-Franche-Comté, Dijon
Iuliana ARMAȘ	Professeure, Universitatea din București, Bucarest
Iulian-Horia HOLOBÂCĂ	Professeur, Universitatea Babeș-Bolyai, Cluj-Napoca
Dir. de thèse : Vincent DUBREUIL	Professeur, Université Rennes 2, Rennes
Co-dir. de thèse : Liliana ZAHARIA	Professeure, Universitatea din București, Bucarest

Université de Bucarest

Faculté de Géographie

École Doctorale Simion Mehedinți - Natură și dezvoltare durabilă

Université Rennes 2

LETG UMR 6554

École Doctorale Espaces, Sociétés, Civilisations

THÈSE DE DOCTORAT

La sécheresse hydroclimatique et ses impacts sur la végétation dans le sud-est de la Roumanie

Hydroclimatic drought and its impacts on vegetation in south-eastern Romania

RÉSUMÉ

par

Maria-Alexandra CHELU

DIRECTEURS DE THÈSE:

Vincent DUBREUIL

Liliana ZAHARIA

SOMMAIRE DE LA THÈSE

INTRODUCTION GÉNÉRALE

La sécheresse est l'un des risques naturels les plus dommageables en Europe, le stress hydrique affectant en moyenne 30 % de la population chaque année (EEA, 2021). Elle affecte plusieurs secteurs socio-économiques et écosystèmes naturels. Au cours des dernières décennies, le changement climatique a affecté le cycle mondial de l'eau (IPCC, 2022), aggravé par l'influence anthropique, avec des implications pour tous les secteurs dépendant de l'eau.

En Roumanie, la sécheresse est un risque naturel qui survient fréquemment, en particulier dans les régions du sud et de l'est. Ces régions sont vulnérables à la sécheresse en raison de leurs caractéristiques géographiques spécifiques, telles qu'un bilan hydrique climatique déficitaire pendant la saison de végétation (Prăvălie et al., 2019), une tendance à l'augmentation des températures et des vagues de chaleur qui peuvent accroître l'intensité de la sécheresse (Bojariu et al., 2021 ; Dumitrescu et al., 2015) et l'aridité (Bojariu et al., 2019 ; Banque mondiale, 2018). La stratégie nationale sur le changement climatique pour la période 2013-2020 souligne que ces régions de la Roumanie sont les plus vulnérables à la sécheresse (MMSC, 2012).

Objectifs

Dans ce contexte, cette thèse vise à étudier la variabilité temporelle et spatiale de la sécheresse dans le sud-est de la Roumanie et à explorer l'influence du déficit en eau sur la végétation dans ce contexte géographique. Trois objectifs spécifiques majeurs sont poursuivis :

1. Analyse de la variabilité des paramètres hydroclimatiques liés à la sécheresse dans le sud-est de la Roumanie.

2. Analyse de la variabilité de la sécheresse à différentes échelles temporelles et spatiales et identification des caractéristiques de la sécheresse (notamment, occurrence de la sécheresse, changements dans la fréquence et les tendances, caractéristiques des événements de sécheresse).

3. Étude de la réponse de la végétation à la sécheresse à différentes échelles spatiales et temporelles, en tenant compte des différentes occupations des sols et écorégions, sur la base de données de télédétection.

Structure de la thèse

La thèse est organisée en trois parties principales : la Partie **I** présente les aspects généraux et la région d'étude, la Partie **II** est consacrée à l'analyse de la variabilité hydroclimatique et de la sécheresse dans le sud-est de la Roumanie, et la **Partie III** se concentre sur l'évaluation de la réponse de la végétation à la sécheresse. Les échelles spatiales et temporelles considérées dans les approches de cette thèse sont résumées dans la **Figure 1**.

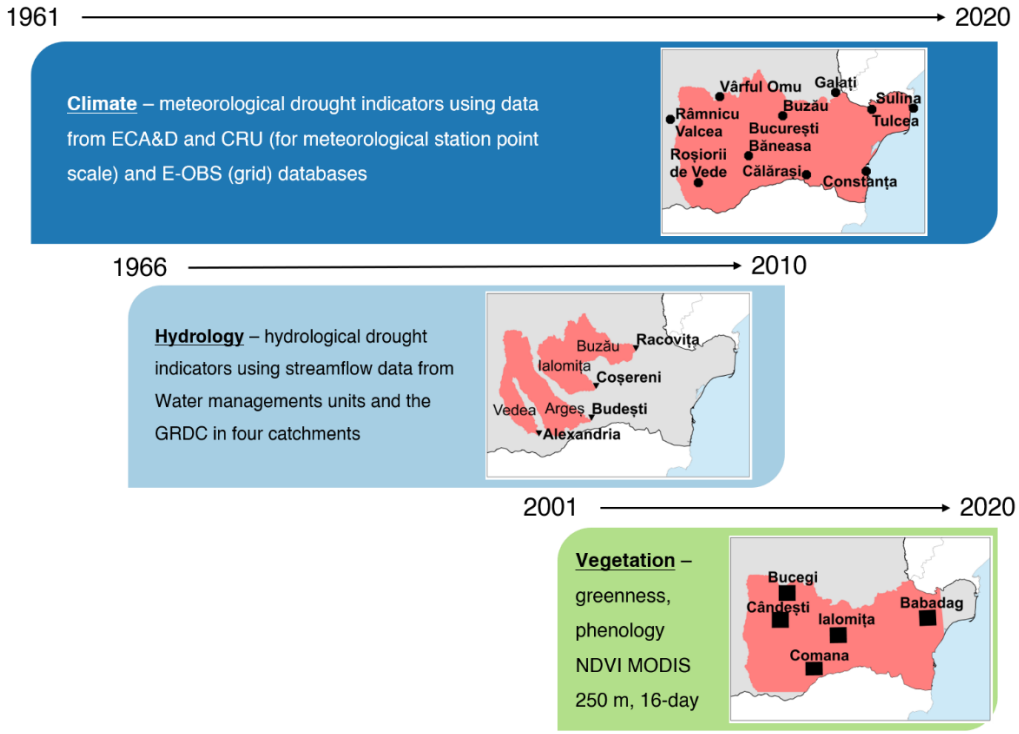

Figure 1 Aperçu des échelles temporelles et spatiales de l'analyse et des données utilisées dans l'étude

PARTIE I - INTRODUCTION ET CONTEXTE

Cette partie s'est attachée à présenter le contexte théorique dans lequel s'inscrit le présent travail et à donner un aperçu des caractéristiques géographiques de la région étudiée.

1. CADRE THÉORIQUE ET REVUE DE LITTERATURE

La sécheresse est une caractéristique temporaire et récurrente de tout climat et n'est pas synonyme d'aridité. D'un point de vue conceptuel, la sécheresse est définie comme un déficit de précipitations par rapport aux conditions moyennes (IPCC, 2021), avec des températures élevées et un fort déficit de saturation (Ciulache et Ionac, 2003) générant un impact sur les activités anthropogéniques et l'environnement. L'apparition de la sécheresse est principalement associée à la persistance de conditions anticycloniques (Holobâcă, 2010). Une approche régionale est recommandée pour définir la sécheresse en prenant en compte les conditions climatiques, géographiques et socio-économiques régionales qui augmentent le risque de sécheresse (Dubreuil, 1996). L'occurrence de la sécheresse dans les zones ayant des tendances à l'aridité, comme le sud-est de la Roumanie, impose des problèmes plus graves liés aux ressources en eau régionales que dans d'autres régions (Păltineanu et al., 2007).

Les sécheresses sont généralement classées en quatre types principaux, en fonction de la composante dans laquelle le déficit d'eau se manifeste : *sécheresse météorologique*, sécheresse *pédologique*, sécheresse *hydrologique, sécheresse socio-économique* et sécheresse *écologique* (Crausbay et al., 2017 ; Zargar et al., 2011).

Si les sécheresses sont un phénomène courant dû aux variations de la circulation atmosphérique, le réchauffement climatique a exacerbé les tendances à l'assèchement dans de nombreuses régions du monde, ce qui a augmenté la probabilité et la gravité des impacts de la sécheresse sur l'environnement, la société et l'économie (Pörtner et al., 2022). Le réchauffement climatique observé et prévu pourrait exacerber les phénomènes extrêmes tels que la sécheresse ; celle-ci pourrait survenir plus tôt et être plus intense (Trenberth et al., 2014) augmentant ainsi l'impact potentiel sur les ressources en eau et la végétation.

2. ZONE D'ÉTUDE

La région de recherche est située dans le sud-est de la Roumanie, bordée par la mer Noire à l'est et par le Danube au sud et au nord-est (**Figure 2.1**). Les bassins hydrographiques des principales rivières de la région (Argeș, Ialomița et Buzău) ont été considérés comme les limites occidentale et septentrionale. La superficie totale de la région étudiée est d'environ 63 820 km^2 (environ 26 % du territoire roumain).

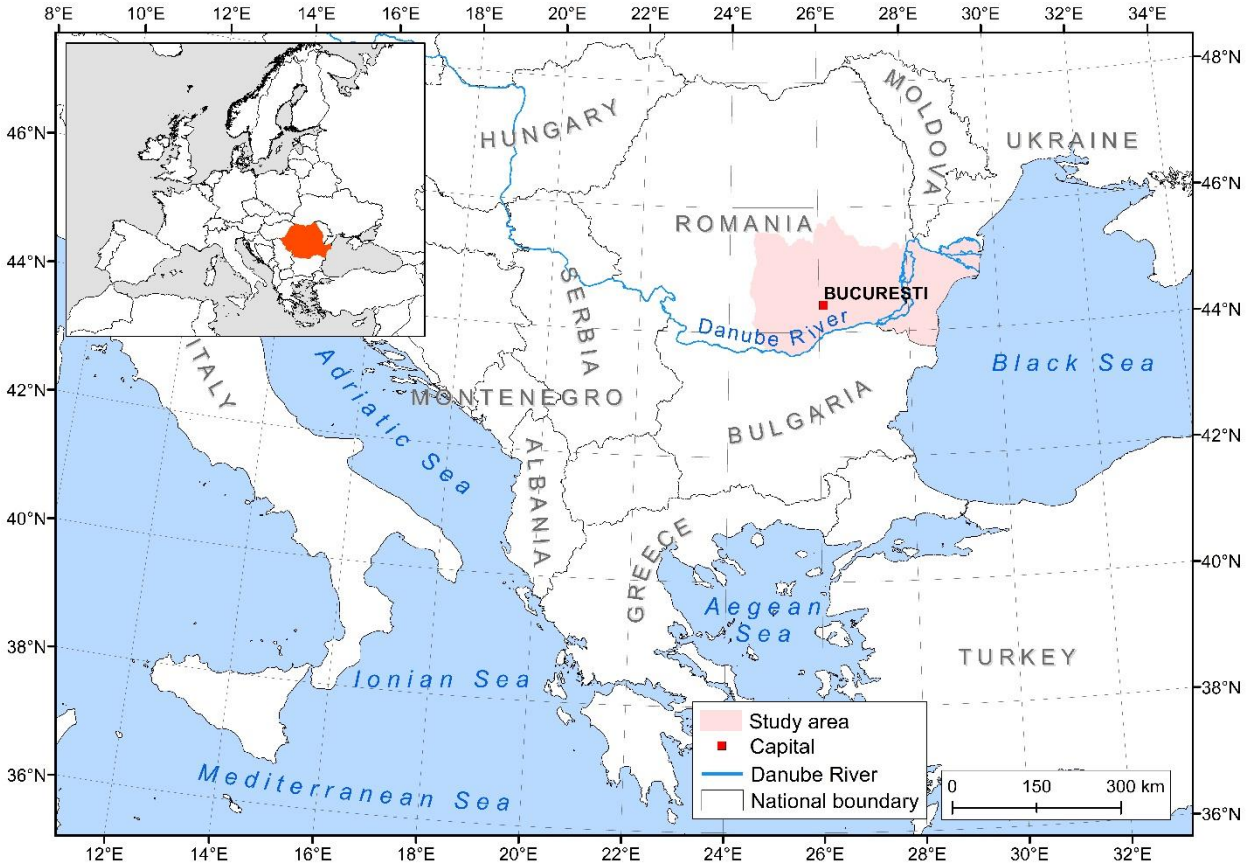

Figure 2.1 Localisation de la zone d'étude en Roumanie et par rapport aux pays de l'Europe du Sud-Est et aux mers voisines

De manière générale, la localisation de la zone d'étude détermine les caractéristiques d'un climat continental tempéré. Plus précisément, dans la classification climatique de Köppen-Geiger (Beck et al., 2018), les climats semi-arides (classe Bsk), continentaux (classes Dfa, Dfb et Dfc) et toundra/alpin (classe ET) sont présents. La plus grande influence des structures anticycloniques

continentales dans le sud et le sud-est de la Roumanie entraîne des sécheresses plus fréquentes et plus graves (ANM, 2008; Bogdan și Țîștea, 1983).

La température annuelle moyenne de l'air dans la majeure partie de la zone d'étude se situe entre 10 et 12 °C, tombant entre 6 et 8°C dans les Subcarpates et moins de 6 °C dans les Carpates. Les valeurs des précipitations annuelles augmentent dans les régions du delta du Danube et de Dobrogea (respectivement moins de 400 mm/an et 500 mm/an) à plus de 700 mm/an à des altitudes plus élevées. L'évapotranspiration potentielle est élevée dans les zones basses de la région (>800 mm/an) et diminue à moins de 650 mm en altitude. La vulnérabilité à la sécheresse de cette région est amplifiée par l'évapotranspiration potentielle plus élevée que les précipitations printanières et estivales. Cela conduit à un déficit climatique élevé, en particulier dans la région de Dobrogea (Prăvălie et al., 2019).

La plupart des rivières qui drainent la zone d'étude sont des affluents du Danube (Vedea, Argeș et Ialomița sont parmi les principaux affluents). Ce sont les principales ressources en eau de la région et elles sont principalement alimentées par des sources de surface. Le débit moyen pluriannuel des rivières varie de 7,39 m^3/s (Vedea) à 45,23 m^3/s (Argeș). L'écoulement est inférieur à 50 mm dans la région de Dobrogea et dans certaines parties de la Plaine Roumaine, et augmente jusqu'à plus de 1000 mm/an aux altitudes les plus élevées (Ujvári, 1972). Les rivières du sud de la Roumanie se rétablissent généralement plus lentement après les périodes de sécheresse en raison des influences climatiques continentales (Zaharia, 2004). En outre, le réchauffement climatique a eu un impact sur la variabilité des débits des fleuves en diminuant les débits en été en raison d'une évapotranspiration plus élevée et en augmentant les débits dans certaines rivières en hiver en raison de l'augmentation des précipitations liquides (Bîrsan, 2015 ; Zaharia et al., 2020).

La diversité des conditions géographiques de la région étudiée a favorisé la présence de plusieurs écorégions : la steppe pontique, la steppe boisée, les forêts mixtes d'Europe centrale, les forêts mixtes des Balkans et les forêts d'altitude des Carpates. La vulnérabilité à la sécheresse est amplifiée par les vastes zones cultivées qui font de la zone d'étude l'une des principales régions agricoles de Roumanie, ainsi que par la présence d'agglomérations urbaines dont les besoins en eau sont importants.

PARTIE II - VARIABILITE HYDROCLIMATIQUE ET SECHERESSE DANS LE SUD-EST DE LA ROUMANIE

3. MÉTHODOLOGIE POUR L'IDENTIFICATION ET L'ANALYSE DE LA VARIABILITÉ HYDROCLIMATIQUE ET DE LA SÉCHERESSE

3.1. Données

Pour l'analyse des données climatiques (**précipitations, température de l'air, évapotranspiration potentielle, rayonnement solaire**), une période de 60 ans a été prise en compte, de 1961 à 2020. Les sources de données suivantes ont été utilisées pour les données climatiques : projet European Climate Assessment & Dataset (ECA&D) (Klein Tank et al., 2002) pour les données des stations météorologiques (**figure 3.1**) et les ensembles de données maillées E-OBS (Cornes et al., 2018) ; Romanian Climatic Dataset (ROCADA) (Bîrsan et Dumitrescu, 2014) et Climate Research Unit (CRU) (Harris et al., 2020).

Les données hydrologiques (**débit mensuel moyen en m^3/s**) enregistrées dans les stations hydrométriques (s.h.) situées sur les principaux cours d'eau des bassins versants sélectionnés ont été fournies par les administrations des bassins hydrographiques d'Argeș-Vedea et de Buzău-Ialomița pour trois cours d'eau : la rivière Argeș (s.h. de Budești), la rivière Vedea (s.h. d'Alexandria) et la rivière Buzău (s.h. Racovița) (**figure 3.1**). Pour la rivière Ialomița (Coșereni s.h.), les données de débit ont été extraites du Global Runoff Data Center (GRDC)[1]. Les données ont été utilisées à l'échelle mensuelle (en m^3/s) et à l'échelle annuelle (en m^3/s et mm) pour la période 1966 - 2010.

Les autres jeux de données utilisés dans cette partie sont : le jeu de données Historic Land Dynamics Assessment (HILDA) version 2.0 pour l'**occupation et l'utilisation des sols** pour deux années (1960 et 2010) ; la version 5 du National Oceanic and Atmospheric Administration Climate Data Record of **Leaf Area Index** (NOAA CDR LAI) (Vermote et NOAA CDR Program, 2019); données du **modèle numérique de terrain** (MNT) de la Shuttle Radar Topography Mission

[1] Institut fédéral d'hydrologie, "BfG - GRDC", consulté le 20 juillet 2020, http://www.bafg.de/GRDC.

(SRTM)[2] à une résolution spatiale de 30 m ; **humidité des sols** provenant de l'ensemble de données combinées de l'ESA Climate Change Initiative v05.2 (ESA-CCI) (Dorigo et al., 2017 ; Gruber et al., 2019).

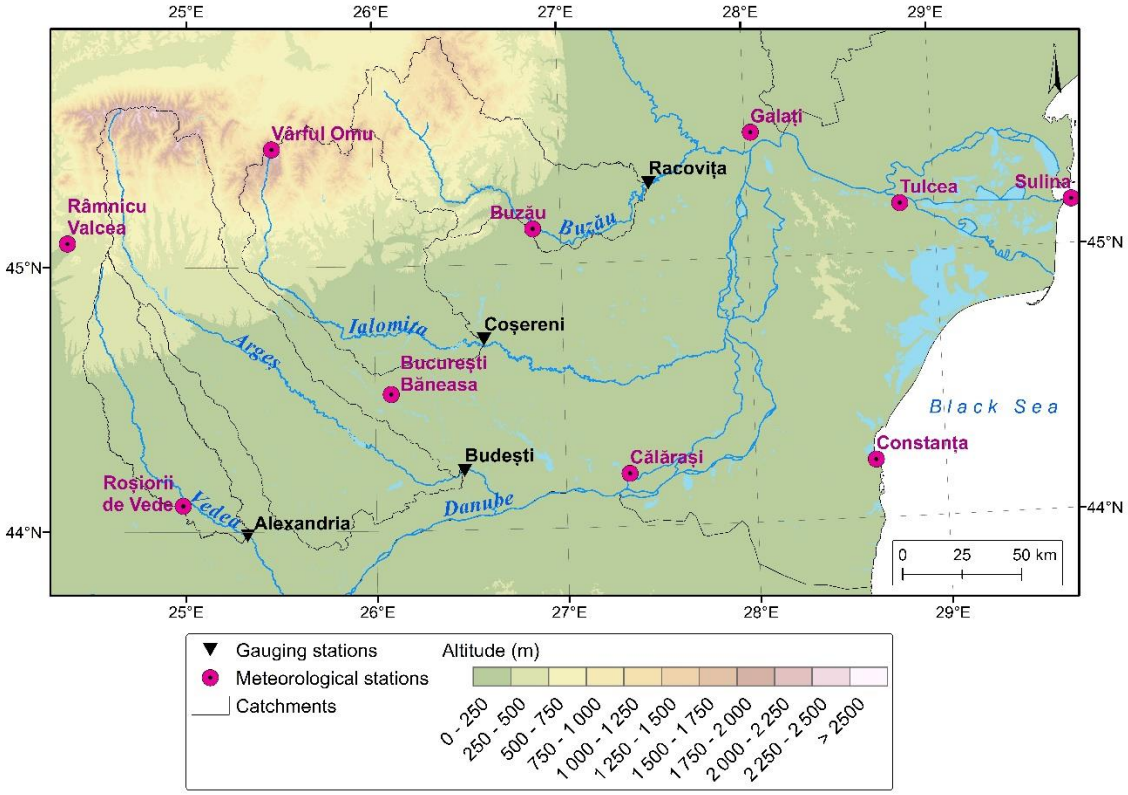

Figure 3.1 Emplacement des stations météorologiques et hydrométriques dans la zone étudiée

Trois ensembles de données de précipitations maillées (ROCADA et E-OBS à 0,1° et 0,25°) ont été comparés aux mesures des stations météorologiques (ECA&D) entre 1961 et 2013 afin d'évaluer s'ils pouvaient sous-estimer ou surestimer l'occurrence de la sécheresse. Les résultats de l'évaluation de la qualité des ensembles de données de précipitations maillées montrent que l'ensemble de données ROCADA est le plus performant. Cependant, la période de disponibilité plus courte (1961 - 2013) par rapport à l'E-OBS (1950 - aujourd'hui) est un facteur limitant. Le jeu de données ROCADA est ensuite utilisé pour analyser les influences climatiques et

[2] CGIAR - Consortium pour l'information spatiale, "CGIAR-CSI SRTM - SRTM 90m DEM Digital Elevation Database", consulté le 20 juillet 2020 https://srtm.csi.cgiar.org/.

anthropogéniques sur les changements de l'écoulement, tandis que le jeu de données E-OBS à une résolution de 0,1° est utilisé pour spatialiser le déficit d'évaporation.

La plupart des stations sont relativement bien représentées par les jeux de données mensuels maillés, à l'exception des stations Vârful Omu et Sulina. Le désaccord entre les jeux de données à Vârful Omu pourrait être lié à la complexité topographique et aux erreurs de mesure, car cette station est située à 2 504 mètres d'altitude. La station de Sulina est située à l'extrémité est de la zone d'étude, sur le littoral de la mer Noire, à une altitude de 3 m, ce qui pourrait avoir un impact sur les différentes méthodes d'interpolation en raison de l'absence de stations proches.

3.2. Méthodes et techniques d'analyse de la sécheresse

3.2.1. Analyse de la variabilité hydroclimatique

La variabilité des précipitations et des températures moyennes extraites de ECA&D, évapotranspiration potentielle CRU et évapotranspiration réelle du bilan hydrique de Thornthwaite (Thornthwaite, 1948; Thornthwaite et Mather, 1955) ont été analysées à l'échelle annuelle et mensuelle dans des stations météorologiques représentatives pour la période 1961-2020. La variabilité hydrologique a été étudiée sur la base des débits fluviaux moyens (annuels et mensuels) enregistrés dans les quatre stations hydrométriques au cours de la période 1966-2010. En outre, le test de Mann-Kendall avec les tests de pente Sen (Kendall, 1975 ; Mann, 1945) sont appliqués aux échelles mensuelle et annuelle pour estimer les tendances de ces paramètres. Pour le débit à l'échelle annuelle, le test statistique de Mann-Kendall modifié est utilisé (Hamed et Ramachandra Rao, 1998 ; Kendall, 1975 ; Mann, 1945).

La variabilité des précipitations, de l'évapotranspiration potentielle et de l'écoulement est également analysée dans les quatre bassins versants à l'échelle annuelle entre 1966 et 2010. Les tests statistiques de Mann-Kendall modifié (Hamed et Ramachandra Rao, 1998 ; Kendall, 1975 ; Mann, 1945) et le test de Sen (Sen, 1968) sont utilisées pour estimer les tendances de ces paramètres, ainsi que le test de Pettitt (Pettitt, 1979) pour identifier les points de rupture.

3.2.2. Déficit d'évaporation (CWD)

Le CWD est défini comme la différence entre l'évapotranspiration potentielle (PET) et l'évapotranspiration réelle (AET) (en mm). Le CWD et les composantes hydrologiques requises

sont obtenus ici par la méthode du **bilan hydrique** simplifié (Thornthwaite, 1948 ; Thornthwaite et Mather, 1955). Les données sur les précipitations de l'ECA&D et l'évapotranspiration potentielle du CRU (PET_{CRU}) ont été utilisées comme données d'entrée dans le modèle de bilan hydrique à chaque station météorologique pour calculer le CWD (*station-*CWD_{CRU}) entre 1961 et 2020. En outre, la même méthodologie est appliquée en utilisant l'évapotranspiration basée sur la formule de Turc PET_{Turc}, calculée à partir d'ensembles de données E-OBS maillées et extraites aux stations météorologiques (Turc, 1961); le CWD qui en résulte est ci-après dénommé *station-*CWD_{Turc} (utilisé dans la **partie III**). La même approche décrite ci-dessus pour les stations météorologiques a été appliquée au niveau du pixel en utilisant le jeu de données de précipitations mensuelles maillées E-OBS à 0,1° et PET_{Turc}. Le jeu de données maillées résultant est ci-après dénommé *raster-CWD*.

Les CWD mensuels ont ensuite été classés dans différentes classes d'ampleur de la sécheresse (Mounier, 1977) (**Tableau 3.15**). Deux périodes d'étude (1961 - 1990 et 1991 - 2020) ont ensuite été sélectionnées pour étudier les changements dans la fréquence de chaque classe. La tendance entre 1961 - 2020 dans les CWD a été examinée pour chaque mois à l'aide des tests de Mann-Kendall et de Sen.

Tableau 3.15 Classes de déficit d'évaporation (CWD) (Dubreuil, 1996 ; Mounier, 1977)

Classe	Conditions du mois	
Hyper humide	**P>PET**	ST_m = AWC
Humide		ST_m < AWC
Faible déficit	**P<PET**	CWD < 30mm
Mois subsec		30 <= CWD < 60 mm
Sec		60 <= CWD < 120 mm
Aride		CWD >= 120 mm

P = précipitations mensuelles (P) ; PET = évapotranspiration potentielle mensuelle, AWC = réserve utile; ST_m = réserve hydrique. Les unités pour tous les paramètres sont en mm.

3.2.3. Indices de sécheresse standardisés

Les indices suivants ont été calculés à l'échelle mensuelle : **L'indice standardisé des précipitations** (SPI) (McKee et al., 1993) en utilisant les précipitations ECA&D sur des périodes d'accumulation de 3, 6 et 12 mois dans les stations météorologiques ; **l'indice standardisé d'évapotranspiration et de précipitations** (Vicente-Serrano et al., 2010), utilisant les précipitations ECA&D et l'évapotranspiration potentielle CRU pour des périodes d'accumulation

de 3, 6, 7 et 12 mois dans les stations météorologiques ; **l'indice standardisé des débits** (SSI) (Modarres, 2007) en utilisant les débits moyens mensuels sur des périodes d'accumulation de 3 et 12 mois dans les stations hydrométriques.

Les tests de Mann-Kendall et de Sen ont été appliqués pour estimer les tendances de l'indice SPI et de l'indice SPEI dans toutes les stations météorologiques. Après avoir calculé l'indice SPI, l'indice SPEI et l'indice SSI, les périodes de sécheresse peuvent être identifiées sur la base de la classification selon l'écart par rapport à la moyenne de 0 (**Tableau 3.16**). Sur la base de ces indices, les événements de sécheresse ont ensuite été identifiés et caractérisés en termes de durée, de gravité et d'intensité. Dans cette étude, la définition d'un événement de sécheresse (Spinoni et al., 2015) a été adaptée comme suit : l'événement commence lorsque l'indicateur devient négatif, atteint au moins une fois la valeur de -1 et se termine lorsqu'il redevient positif.

Tableau 3.16 Classes pour SPI, SPEI et SSI (McKee et al., 1993)

Valeur	Classe	Probabilité d'événement (%)
> 2	Extrêmement humide	2.3
1,5 à 2	Sévèrement humide	4.4
1 à 1,5	Modérément humide	9.2
1 à -1	Presque normal	68.2
-1 à -1,5	Sécheresse modérée	9.2
-1,5 à -2	Sécheresse sévère	4.4
≤ -2	Sécheresse extrême	2.3

3.2.4. Analyse de la contribution des facteurs climatiques et anthropiques au changement de l'écoulement fluvial

La méthodologie décrite dans cette section et les résultats obtenus ont été présentés dans Chelu et al. (2022). Les poids des contributions des facteurs climatiques et anthropogéniques au changement de débit ont été estimés sur la base de la méthode Budyko (Budyko, 1961, 1974) et la méthode de l'élasticité climatique du débit (Schaake et Liu, 1989 ; Zheng et al., 2009). L'équation de Fu a été utilisée (Fu, 1981 ; Zhang et al., 2004).

4. VARIABILITÉ HYDROCLIMATIQUE DANS LE SUD-EST DE LA ROUMANIE

Ce chapitre commence par présenter la variabilité et les tendances des principaux paramètres climatiques et hydrologiques liés à la sécheresse dans les stations météorologiques et

hydrométriques (température de l'air, précipitations, évapotranspiration potentielle et réelle et débit des rivières). Ensuite, une analyse de l'ensemble des données sur l'humidité du sol est présentée, ainsi que les moyennes saisonnières et la variabilité de cet ensemble de données. Enfin, la variabilité hydroclimatique à l'échelle du bassin versant a été étudiée et une analyse de contribution a été réalisée dans le cadre de la méthode de Budyko afin d'évaluer l'influence des facteurs climatiques et anthropogéniques sur les changements de débit.

4.1. Variabilité hydroclimatique dans les stations météorologiques et hydrométriques

4.1.1. Température de l'air, précipitations et évapotranspiration

Toutes les stations météorologiques analysées dans la zone d'étude ont connu une évolution positive de la température et de l'évapotranspiration potentielle à l'échelle annuelle et pour les mois d'été au cours de la période 1961-2020. En revanche, l'évolution des précipitations a été relativement stable, à quelques exceptions : il y a eu des tendances positives significatives dans les stations météorologiques de Constanța et des tendances négatives à Sulina. En octobre, une tendance significative à la hausse des précipitations mensuelles a été observée dans la plupart des stations.

4.1.2. Débit des fleuves

À l'échelle annuelle, le test de Mann-Kendall modifié appliqué aux débits des rivières de 1966 à 2010 n'a montré des modifications significatives que sur les rivières Vedea et Buzău, où les tendances sont négatives (avec des pentes de tendance de -0,114 m^3/s et -0,29 m^3/s respectivement).

4.2. Humidité des sols

Cette étude utilise le jeu de données ESA-CCI sur l'humidité du sol uniquement pour donner un aperçu de la dynamique spatiale et temporelle globale et n'est pas considérée comme reflétant les valeurs absolues/actuelles de l'humidité du sol. Après avoir évalué la qualité de l'ensemble de données, l'humidité du sol est analysée pour la période 1992 - 2019. La période antérieure à 1992 n'a pas été prise en compte en raison de la faible couverture spatiale. La variation des anomalies standardisées d'humidité du sol pour la période 1992 - 2019 dans l'intervalle mars -

novembre dans quatre régions du sud-est de la Roumanie a montré des déficits pour les périodes 1992 - 1993, 1994, 2000 - 2001, 2007 - 2009, 2011 - 2012 et 2019.

4.3. Variabilité hydroclimatique à l'échelle du bassin versant et analyse de la contribution des facteurs climatiques et anthropiques au changements de l'écoulement fluvial

Les résultats présentés dans cette section ont été publiés dans Chelu et al. (2022).

Sur la période 1966-2010, le test de Mann-Kendall modifié a montré des tendances à la baisse du débit annuel mesuré, qui n'étaient significatives que dans deux bassins versants : le Vedea et le Buzău (**figure 4.12).** Il y a eu des points de rupture statistiquement significatifs dans la deuxième partie des années 1980 dans les quatre bassins versants, comme le montre le test de Pettitt : en 1981 dans le Vedea, 1984 dans le Ialomița et 1985 dans les bassins versants de l'Argeș et du Buzău (**Figure 4.12**). Les points de rupture ont été utilisés pour séparer les périodes avant et après le changement. Au cours de la deuxième période, le débit a diminué de pourcentages compris entre -53,4% dans le bassin de Vedea et -28,1% dans le bassin de Buzău (**Tableau 4.2**) (Chelu et al., 2022).

Tableau 4.2 Changements entre les périodes après et avant changement (définies par les points de rupture indiqués dans la **figure 4.12**) dans les précipitations (ΔP), l'évapotranspiration potentielle (ΔPET), le débit (ΔQ) et l'indice d'évaporation (ΔAET/P) (Chelu et al., 2022)

	ΔP		ΔPET		ΔQ		ΔAET/P
Bassin versant	mm	%	mm	%	mm	%	
Vedea	-104.3	-15.8	49.7	6.1	-57.5	-53.4	0.06
Argeș	-63.3	-8.8	50.4	6.7	-77.2	-39.6	0.05
Ialomita	-89.2	-11.7	46.8	6.6	-90.3	-35.1	0.06
Buzău	-47.9	-7.3	50.0	6.8	-55.9	-28.1	0.04

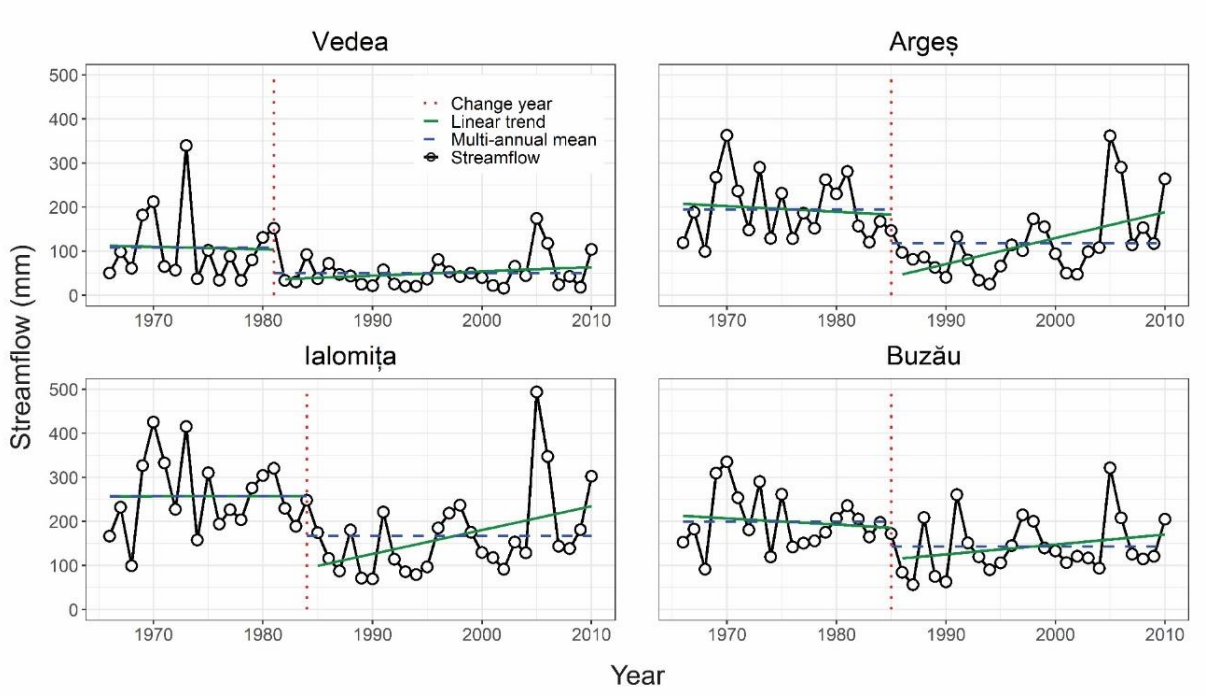

Figure 4.12 Variation, tendances linéaires, moyennes pluriannuelles et points de rupture de la série des débits annuels moyens dans les bassins des rivières Vedea, Argeș, Ialomița et Buzău. (Chelu et al., 2022)

L'écoulement dans le bassin versant augmente avec la diminution du paramètre ω du bassin versant (de 3,3 à 2,5). D'un point de vue climatique, le débit des cours d'eau dans les quatre bassins versants est le plus sensible aux précipitations, comme l'indiquent les valeurs plus élevées de l'élasticité des précipitations par rapport à l'élasticité de la PET (**Tableau 4.3**).

Tableau 4.3 Paramètre du bassin versant (ω) de l'équation de Fu et élasticité du débit par rapport aux précipitations (ε_P) et à l'évapotranspiration potentielle (ε_{PET}) (Chelu et al., 2022)

Bassin versant	ω	ε_P	ε_{PET}
Vedea	3.3	3.0	-2.0
Argeș	2.9	2.4	-1.4
Ialomita	2.6	2.2	-1.2
Buzău	2.5	2.1	-1.1

Les résultats ont montré que les facteurs climatiques étaient la principale influence (contribution climatique de 63,1 % à Argeș à 80 % à Vedea) de la réduction des débits observée à la fin des années 1980 et dans les années 1990 dans les bassins versants de Vedea, Argeș, Ialomița

et Buzău, mais les facteurs anthropiques y ont également contribué (19,8 % à Vedea et 36,9 % à Argeș) (**Tableau 4.4**).

Tableau 4.4 Contribution des précipitations (ΔQ_P), de l'évapotranspiration potentielle (ΔQ_{PET}), des facteurs climatiques (ΔQ_c) et des facteurs anthropiques (ΔQ_h) aux changements de débit entre les périodes avant et après les changements (Chelu et al., 2022)

Bassin versant	ΔQ_P		ΔQ_{PET}		ΔQ_c (%)		ΔQ_h	
	mm	%	mm	%	mm	%	mm	%
Vedea	-37.7	65.6	-8.4	14.6	-46.1	80.2	-11.4	19.8
Argeș	-34.6	44.8	-14.2	18.4	-48.8	63.1	-28.5	36.9
Ialomita	-56.2	62.2	-15.4	17.0	-71.5	79.2	-18.7	20.8
Buzău	-27.3	48.8	-12.6	22.5	-39.8	71.2	-16.1	28.8

5. CARACTÉRISATION HYDROCLIMATIQUE DE LA SÉCHERESSE DANS LE SUD-EST DE LA ROUMANIE

Ce chapitre est consacré à l'analyse des sécheresses météorologiques et hydrologiques en utilisant deux types d'indicateurs de sécheresse : le déficit d'évaporation (CWD) et les indicateurs standardisés : l'indice de précipitations standardisé (SPI), l'indice d'évapotranspiration et de précipitations standardisé (SPEI) et l'indice de débit standardisé (SSI). Les analyses ont été effectuées pour la période 1961 - 2020 pour la sécheresse météorologique et 1966 - 2010 pour la sécheresse hydrologique.

5.1. Évaluation de la sécheresse d'après le déficit d'évaporation

La CWD a indiqué une fréquence plus élevée de mois arides pendant la saison estivale, en particulier au mois d'août (**Figure 5.4**). 1980 et 2010 ont connu le plus grand nombre de mois arides. Ceci a été souligné par la tendance positive significative (pentes Sen entre 0,7 et 1,13 mm/an) du déficit d'évaporation au cours du même mois dans toutes les stations météorologiques. En octobre, le nombre de mois humides a augmenté dans toutes les stations dans la deuxième période, ce qui est également démontré par la tendance significative à la baisse de CWD en octobre dans la plupart des stations. En moyenne, les dix années où les totaux de CWD ont été les plus élevés ont été 2020, 2007, 2012, 2019, 2000, 2008, 2003, 1990, 2018 et 2009, ce qui accentue l'intensité accrue du déficit au cours des dernières décennies. Les déficits les plus élevés ont été atteints au cours des mois d'été des années susmentionnées. Au niveau mensuel, le mois de juillet

2007 a connu le CWD le plus élevé dans toutes les stations, à l'exception de Buzău, où le déficit mensuel le plus intense a été observé en août 2018. L'augmentation de l'occurrence des mois arides et de la fréquence des années sèches au cours de la dernière période d'étude est probablement liée à l'augmentation de la PET dans toutes les saisons sauf l'automne (Croitoru et al., 2013) qui entraîne un déficit plus important.

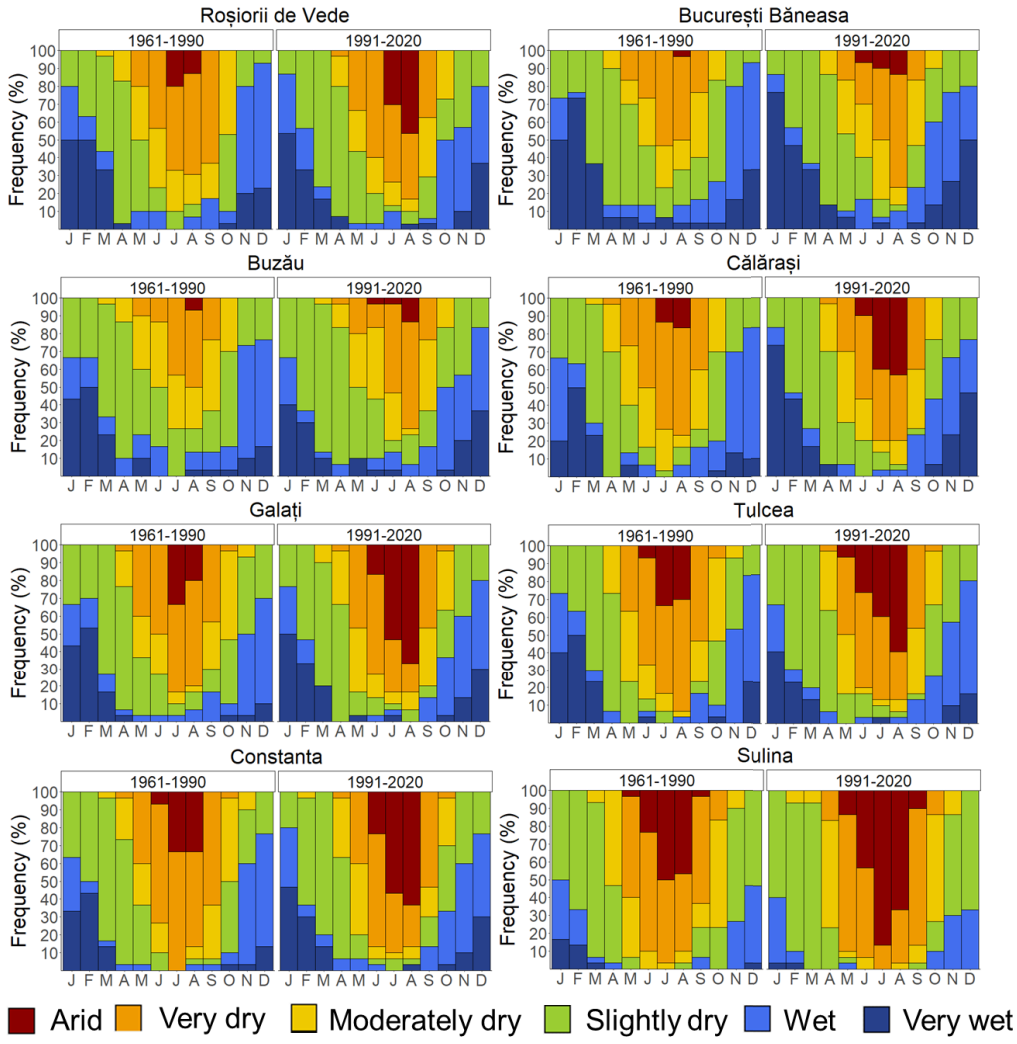

Figure 5.4 Fréquence mensuelle (%) des classes de CWD entre 1961 - 1990 et 1991 - 2020

La différence entre les données spatialisées raster-CWD et station-CWD_{CRU} a mis en évidence des différences substantielles en 2018 et 2019. Ces différences sont liées à des valeurs de rayonnement solaires anormales en 2018 et 2019 dans les données d'entrée de raster-CWD. En raison de cette anomalie, qui se propage dans l'évapotranspiration potentielle et, par conséquent,

dans le raster-CWD, **trois années (2018, 2018 et 2020) sont exclues de la suite de l'analyse dans cette partie.**

Les différences de CWD au cours des mois de printemps de la période 1991 - 2017 par rapport à la période 1961 - 1990 sont faibles en mars et avril (± 5 mm). En mai, autour de Buzău et dans la région du delta du Danube, certaines zones présentent des différences positives plus importantes.

Pendant les mois d'été (**Figure 5.12**), les augmentations les plus significatives de la moyenne raster-CWD et avec la plus grande couverture spatiale sont en août : 5 - 10 mm dans la plupart des zones et 10 - 15 mm dans la partie nord-est de la zone d'étude (Delta du Danube et régions de Galați). Une zone de diminution apparaît en juillet dans la partie sud de la zone d'étude. Cela pourrait s'expliquer par les valeurs plus élevées des précipitations moyennes de juillet dans cette région dans le jeu de données E-OBS au cours de la période 1991 - 2017 par rapport à 1961 - 1990. En automne, les différences montrent des diminutions significatives du déficit dans la majeure partie de la zone pour septembre et octobre, atteignant des valeurs inférieures à -15 mm. En septembre, la région du delta du Danube montre une augmentation du déficit.

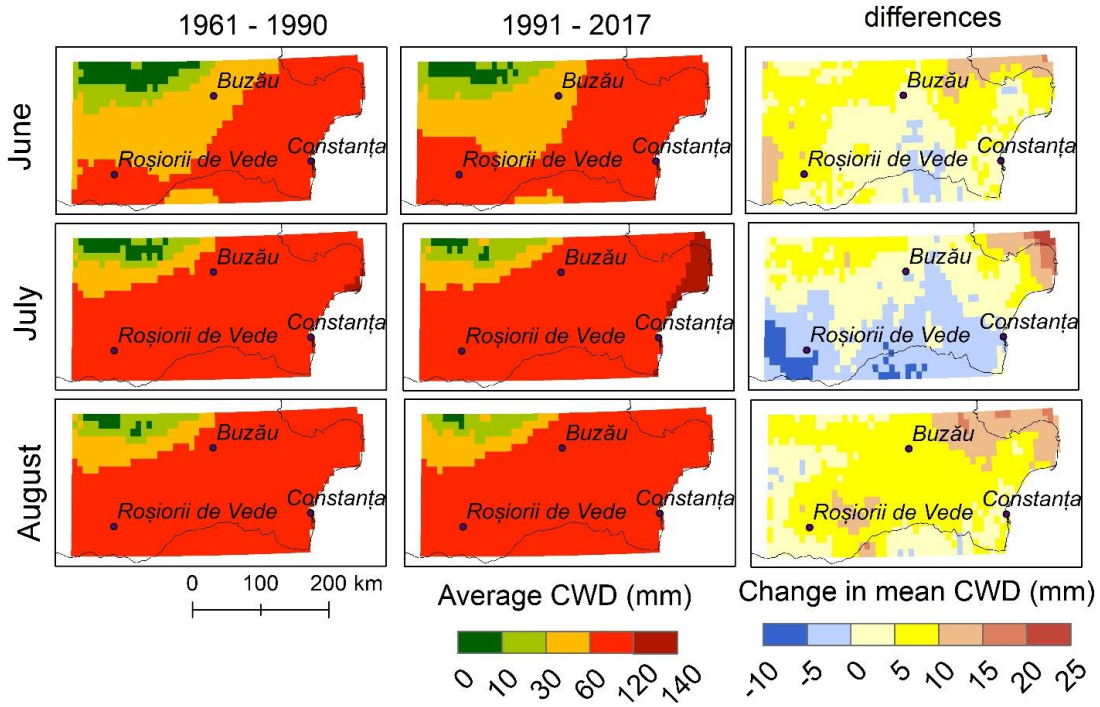

Figure 5.12 Moyenne pluriannuelle raster-CWD en été et différences entre 1991 - 2017 et 1961 - 1990

5.2. Évaluation de la sécheresse d'après les indicateurs standardisés

5.2.1. Variabilité des indicateurs de sécheresse entre 1961 et 2020

5.2.1.1. Indice standardisé des précipitations (SPI)

Une période de valeurs SPI plus faibles, indiquant une sécheresse, peut être observée du début des années 1980 au milieu des années 1990 dans les stations de București Băneasa, Călărași, Roșiorii de Vede, Galați, Buzău.

Les hivers les plus secs (avec le déficit de précipitations le plus élevé), identifiés avec **SPI-3 pour février**, étaient en 1974 (Buzău, Călărași, Constanța), 1976 (Roșiorii de Vede), 1989 (București Băneasa, Vârful Omu), 1994 (Tulcea, Galați), et 2002 (Sulina). Les printemps les plus secs (identifiés à l'aide de **SPI-3 en mai**) ont été observés en 1968 (București Băneasa, Buzău, Călărași, Tulcea, Galați, Constanța), 1985 (Roșiorii de Vede, Vârful Omu), et 2003 (Sulina). Pour la période estivale, **SPI-3 pour août** a indiqué les périodes le plus sèches en 1962 (Călărași, Tulcea, Sulina, Constanța), 1963 (Buzău), 1965 (București Băneasa), 1996 (Galați) et 2000 (Roșiorii de Vede, Vârful Omu). Les automnes les plus secs identifiés à l'aide de **SPI-3 en novembre** ont été observés en 1969 (București Băneasa, Călărași, Constanța), 1983 (Sulina, Vârful Omu), 1992 (Roșiorii de Vede), 1994 (Tulcea), 2011 (Galați), et 2018 (Buzău). Les années hydrologiques/agricoles les plus sèches, selon le **SPI-12 de septembre**, ont été 1961 - 1962 (Călărași), 1984 - 1985 (Băneasa, Vârful Omu), 1985 - 1986 (Buzău), 1992 - 1993 (Roșiorii de Vede), 2006 - 2007 (Sulina) et 2019 - 2020 (Tulcea, Galați, Constanța).

5.2.1.2. Indice standardisé d'évapotranspiration et de précipitations (SPEI)

Dans la dernière partie de l'intervalle analysé, la fréquence des mois de sécheresse extrême identifiés avec SPEI à l'échelle de temps de 3 mois a augmenté dans la plupart des stations. Les années avec le SPEI-12 septembre le plus bas ont été 2000 (Vârful Omu), 2003 (Roșiorii de Vede), 2007 (București Băneasa, Călărași, Sulina) et 2020 (Buzău, Tulcea, Galați, Constanța). Les mois les plus secs identifiés à l'aide de SPEI-3 se trouvent principalement dans la dernière partie de l'intervalle analysé.

En utilisant **SPEI-3 pour le mois d'août**, les étés les plus secs ont été identifiés en 2000 (Roșiorii de Vede), 2003 (București Băneasa), 2007 (Tulcea, Sulina, Galați) et 2012 (Buzău, Călărași, Constanța). **SPEI-2 pour le mois de mai** montre que les printemps les plus secs ont eu

lieu en 1968 dans toutes les stations sauf Sulina et Galați (où le printemps 2020 a été le plus sec) et Vârful Omu (où 1985 a eu la valeur la plus basse). Le déficit hivernal le plus élevé, selon **SPEI-3 pour février**, a été enregistré en 1974 (Călărași, Tulcea), 1976 (Roșiorii de Vede), 1994 (Bucarest Băneasa), 2002 (Sulina) et 2020 (Buzău, Constanța, Galați). Le déficit automnal le plus important identifié à l'aide de **SPEI-3 pour le mois de novembre** a été enregistré en 1969 (Bucarest Băneasa, Călărași, Constanța), 1994 (Tulcea), 2011 (Galați), 2012 (Sulina, Roșiorii de Vede) et 2018 (Buzău), ce qui indique un déficit cumulé très important pour ces trois mois.

Si l'on compare les résultats obtenus avec SPI et SPEI, on constate qu'après 1990, la fréquence de la sécheresse est plus élevée avec SPEI, ce qui est probablement dû à l'effet des températures plus élevées.

5.2.1.3. Tendances spatiales de SPI et de SPEI

Les pentes Sen de SPI et SPEI ont été interpolées dans l'espace pour représenter les tendances régionales. Les tendances de SPI-3 pendant l'hiver montrent des tendances significatives à la baisse à Sulina et Vârful Omu, tandis que des tendances à la baisse non significatives sont observées à Roșiorii de Vede, Buzău et Tulcea. Au printemps et en été, les tendances sont insignifiantes et seuls Bucarest Băneasa, Tulcea et Constanța affichent des tendances à la hausse. En automne, on observe principalement des tendances à la hausse, significatives uniquement à Călărași et en baisse non significative à Vârful Omu et Sulina. Les tendances à la hausse en automne pourraient s'expliquer par les tendances à la hausse des précipitations (Busuioc et al., 2015 ; Cheval et al., 2014).

Concernant le SPEI-3, pendant l'hiver, on observe des tendances prédominantes à la baisse (à l'exception de Călărași), qui ne sont significatives qu'à Sulina et Vârful Omu (**Figure 5.24**). L'indice SPEI-3 en mai ne montre que des tendances à la baisse, qui sont également significatives à Sulina, Vârful Omu et Galați. De même, pendant l'été, il n'y a que des tendances à la baisse, qui sont significatives dans toutes les stations de la partie orientale de la zone d'étude (Călărași, Tulcea, Sulina, Galati, Constanța) et à Roșiorii de Vede. L'indice SPEI-3 en novembre ne montre que des tendances insignifiantes, principalement à la hausse (à l'exception de Sulina et Vârful Omu). Comme les tendances de l'indice SPI-3, l'indice SPEI-3 pour l'automne montre une tendance à l'augmentation de l'humidité.

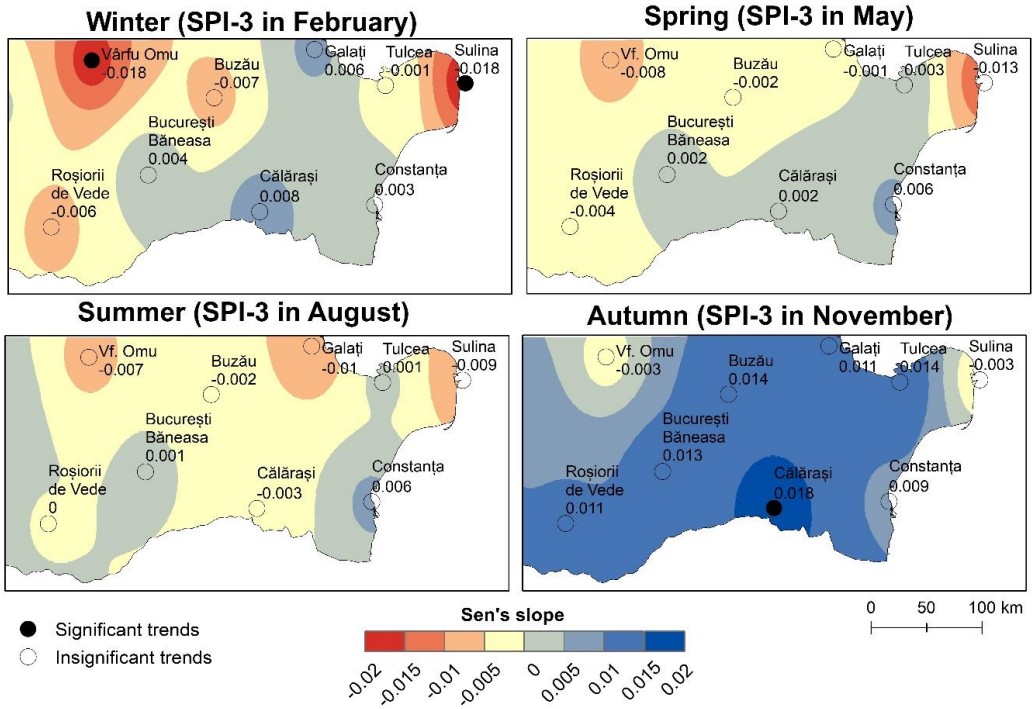

Figure 5.22 Tendances SPI-3 en février, mai, août et novembre sur la période 1961-2020

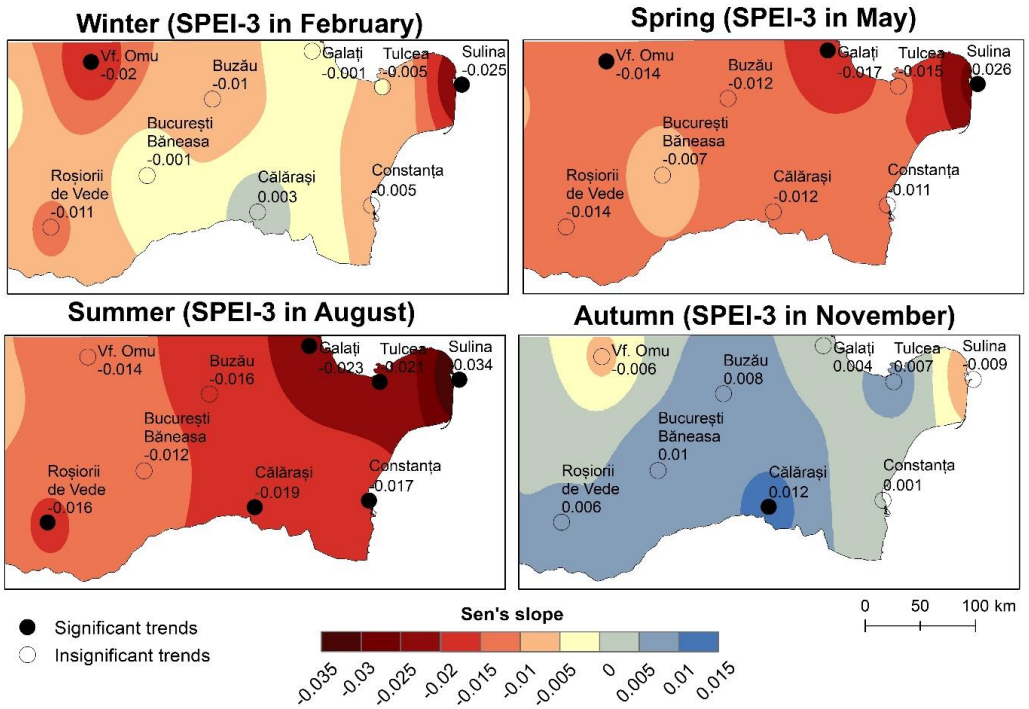

Figure 5.24 Tendances SPEI-3 pour février, mai, août et novembre sur la période 1961-2020

Par rapport à l'indice SPI, l'indice SPEI montre une tendance croissante vers des conditions plus sèches en raison de la hausse des températures, ce qui entraîne un déficit hydrique plus important.

5.2.1.4. Indice standardisé des débit (SSI)

Une diminution des valeurs de l'indice peut être observée sur les deux échelles (3 et 12) de 1981 au milieu des années 1990. Après cette période de diminution, l'indice montre une période d'augmentation des valeurs, qui étaient plus élevées aux stations hydrométriques de Budești et Coșereni qu'aux stations d'Alexandrie et de Racovița.

En analysant la série de données **SSI-3 pour février**, les hivers les plus secs ont été enregistrés en 1993 (Coșereni), 1995 (Budești) et 2001 (Alexandria et Racovița). Les printemps les plus secs (**SSI-3 pour mai**) ont été enregistrés en 1990 (Buzău), 1994 (Budești, Coșereni) et 2002 (Alexandrie). Les étés les plus secs (**SSI-3 pour août**) ont été enregistrés en 1968 (Coșereni), 1993 (Budești), 2007 (Racovița) et 2008 (Alexandrie). Les automnes les plus secs (**SSI-3 pour novembre)** ont été observés en 1990 (Coșereni, Racovita), 1994 (Budești) et 2008 (Alexandria). Les **SSI-12 pour septembre** a montré le plus grand déficit par rapport aux conditions moyennes en 1987 (Racovița), 1990 (Coșereni), 2002 (Alexandria) et 1994 (Budești).

5.2.1.5. Evènements de sécheresse

Les événements de sécheresse ayant la durée la plus longue, la magnitude la plus élevée et l'intensité la plus forte sont présentés dans le **Tableau 5.2**. Les périodes communes avec les sécheresses les plus longues à différentes stations mettent en évidence les années de stress hydrique important. Pour SPI-3 et SPEI-3, il s'agit de 1986 à București Băneasa et Buzău, et de 2018/2019 - 2020 à Călărași, Tulcea, Galați et Constanța. Pour SPI et SPEI à l'échelle de 12 mois, les périodes communes ont été 1984/1985 - 1988 à București Băneasa, Călărași, Tulcea, entre 1988 - 1991 à Roșiorii de Vede et Galați, entre 1992 - 1995 à Buzău, Roșiorii de Vede, Constanța, entre 1998/2000 - 2003 à Tulcea et Sulina et entre 2006 - 2010/2012 à București Băneasa, Buzău, Călărași, Galați. La période 1991/1992 - 1995 est communément identifiée comme l'événement de sécheresse hydrologique le plus long et le plus sévère aux stations hydrométriques d'Alexandria, de Budești et de Coșereni. En outre, des événements de sécheresse hydrologique ont marqué la période 1988 - 1991 : c'est l'événement le plus long observé à Racovița (rivière Buzău) et le plus intense à Coșereni (rivière Ialomița).

Tableau 5.2 Caractéristiques des principaux épisodes de sécheresse climatique identifiés sur la base des SPI et SPEI à l'échelle de 3 et 12 mois pour la période 1961-2020

Stations météorologiques	Scara	Index	Durée maximale	Gravité maximale	Intensité maximale	% de temps de sécheresse	Nombre d'événements
Băneasa	**3**	**SPI**	Juin 1973 - juin 1974 (13 mois)	Septembre 2001 - juin 2002	Mars 1968 - août 1968	35	45
		SPEI	Février 1985 - janvier 1986 (12 mois)	Novembre 2006 - septembre 2007	Octobre 1969 - Novembre 1969	34	42
	12	**SPI**	Mars 1985 - septembre 1988 (43 mois)		Août 2000 - décembre 2002	39	11
		SPEI	Octobre 2006 - janvier 2010 (40 mois)			41	16
Buzău	**3**	**SPI**	Mai 1986 - octobre 1987 (18 mois)		Mars 1968 - Juillet 1968	36	43
		SPEI	Mai 1963 - juillet 1964 (15 mois)	juillet 2019 - juin 2020		34	43
	12	**SPI**	Juillet 1992 - août 1995 (38 mois)	Mai 1986 - mars 1988		42	14
		SPEI	Décembre 2006 - avril 2012 (65 mois)		Octobre 2018 - décembre 2020	42	13
Călărași	**3**	**SPI**	Juillet 2019 - octobre 2020 (16 mois)		Octobre 1969 - Novembre 1969	33	39
		SPEI	Mars 2019 - novembre 2020 (21 mois)		Octobre 1969 - Novembre 1969	37	44
	12	**SPI**	Août 1984 - septembre 1988 (50 mois)		juillet 2019 - décembre 2020	41	13
		SPEI	Décembre 2006 - janvier 2010 (38 mois)		Février 2019 - décembre 2020	37	12
Tulcea	**3**	**SPI**	Août 2018 - novembre 2020 (28 mois)		Octobre 1965 - Novembre 1965	39	44
		SPEI	Mai 2018 - novembre 2020 (31 mois)		Juin 2015 - septembre 2015	38	44
	12	**SPI**	Février 1985 - février 1988 (37 mois)	Octobre 2018 - décembre 2020		35	13

		SPEI	Juillet 2000 - janvier 2003 (31 mois)	Juillet 2018 - décembre 2020		39	14
Sulina	**3**	**SPI**	Mars 2000 - février 2002 (24 mois)		Octobre 1965 - Novembre 1965	39	43
		SPEI	Février 2008 - novembre 2009 (22 mois)	Février 2019 - octobre 2020	Novembre 2006 - octobre 2007	37	38
	12	**SPI**	Juillet 1998 - janvier 2003 (55 mois)		Mars 2003 - février 2005	42	12
		SPEI	Août 1998 - février 2005 (79 mois)		Septembre 2017 - décembre 2020	37	7
Roșiori de Vede	**3**	**SPI**	Novembre 1991 - octobre 1993 (24 mois)		Avril 1968 - Juillet 1968	37	42
		SPEI	Novembre 1991 - février 1993 (16 mois)		Avril 1968 - Juillet 1968	37	42
	12	**SPI**	Novembre 1988 - juin 1991 (32 mois)	Mai 1992 - septembre 1994		34	14
		SPEI	Mai 1992 - février 1995 (34 mois)			37	13
Galati	**3**	**SPI**	Mars 2019 - novembre 2020 (21 mois)		Juin 1996 - août 1996	38	48
		SPEI	Mars 2019 - novembre 2020 (21 mois)			35	37
	12	**SPI**	Novembre 1988 - avril 1991 (30 mois)	Octobre 2018 - décembre 2020		35	16
		SPEI	Juillet 2006 - mai 2010 (47 mois)		Juin 2018 - décembre 2020	33	12
Constanța	**3**	**SPI**	Janvier 1990 - avril 1991 (16 mois)		Juin 1962 - Octobre 1962	37	43
		SPEI	Février 2019 - décembre 2020 (23 mois)		Juillet 2012 - Novembre 2012	35	40
	12	**SPI**	Octobre 1973 - avril 1977 (43 mois)	Mai 1992 - février 1995	Février 2019 - décembre 2020	44	15
		SPEI	Mai 1992 - février 1995 (34 mois)	Octobre 2018 - décembre 2020		40	14
Vârful Omu	**3**	**SPI**	Septembre 1983 - mai 1991 (93 mois)		Avril 2000 - juin 2001	35	23
		SPEI	Mai 1984 - mars 1988		Juin 2015 - Octobre 2015	36	30
	12	**SPI**	Mai 1982 - septembre 1991			36	4
		SPEI	Mai 1982 - juillet 1991			39	6

6. PARTIE III - IMPACT DE LA SÉCHERESSE SUR LA VÉGÉTATION

Cette partie présente les résultats de la recherche sur la dynamique de la végétation en relation avec la variabilité de la sécheresse dans le sud-est de la Roumanie. Le premier chapitre présente la méthodologie utilisée dans cette partie. Dans le deuxième chapitre, les résultats de l'analyse des tendances de la végétation et ses différences entre les occupations du sol au niveau régional sont détaillés. Le dernier chapitre se concentre sur les analyses au niveau local. Une étude comparative des réponses à la sécheresse des forêts de feuillus est menée entre cinq zones sélectionnées correspondant à différentes écorégions dans la région étudiée, pour la période 2001 - 2020 et plus en détail dans deux périodes de sécheresse sévère (2007 - 2008 et 2019 - 2020).

6.1. MÉTHODOLOGIE D'ÉVALUATION DE L'IMPACT DE LA SÉCHERESSE SUR LA VÉGÉTATION

Pour évaluer l'impact de la sécheresse sur la dynamique de la végétation, deux approches ont été envisagées :

- analyse régionale, dans le sud-est de la Roumanie (à l'exception du bassin versant de Buzau et du delta du Danube)
- analyse dans cinq zones d'étude de cas sélectionnées avec des forêts de feuillus dans différentes écorégions (Olson et al., 2001) de la zone d'étude (**Figure 6.2**):
    - *La forêt de Babadag,* dans l'écorégion de la steppe pontique ;
    - *Le corridor de Ialomița* dans la steppe boisée d'Europe de l'Est ;
    - *La forêt de Comana*, dans le *Parc Naturel de Comana* et ses forêts voisines (dans l'écorégion des forêts mixtes des Balkans) ;
    - *Forêts du sud du Piémont Cândești* et des régions voisines pour les forêts mixtes d'Europe Centrale ;
    - des forêts de feuillus des monts Bucegi pour les forêts d'altitude des Carpates.

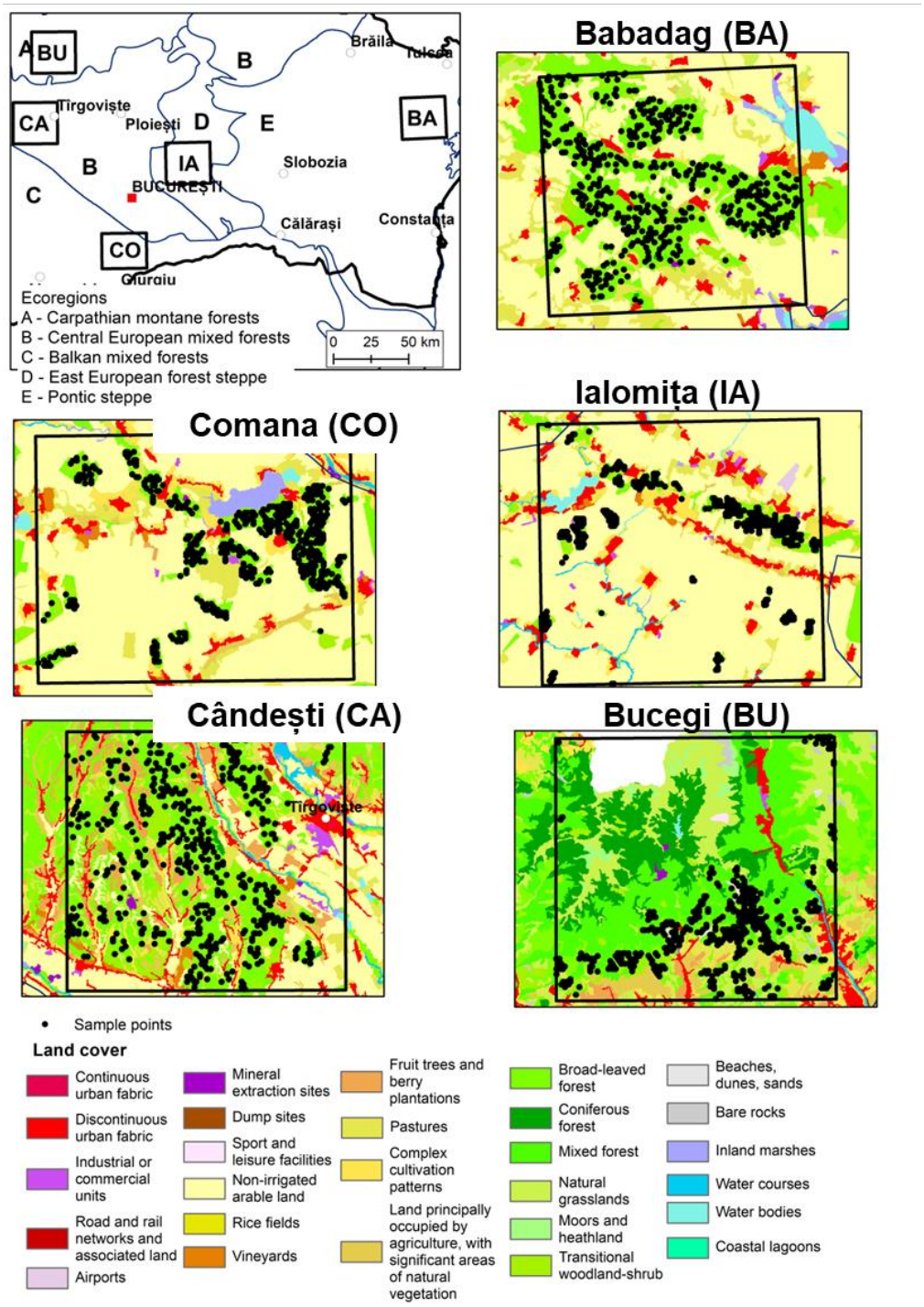

Figure 6.2 Zones sélectionnées dans la zone d'étude de cas et 500 points d'échantillonnage aléatoires dans les forêts de feuillus. BA - Forêt de Babadag ; CO - Forêt de Comana ; IA - Corridor de Ialomiţa ; CA - Forêts de Cândești ; BU - Forêts des monts Bucegi.

Les données utilisées dans cette partie sont les suivantes : **l'indice de végétation par différence normalisée (NDVI)** MOD13Q1 de Moderate Resolution Imaging Spectroradiometer (MODIS) (Didan, 2015) pour la période 2001-2020, avec une résolution temporelle de 16 jours et une résolution spatiale de 250 m ; **occupations des sols** Corine Land Cover (CLC) avec une résolution spatiale de 100 m pour les années 2000 et 2018 (AEE, 2019a,b) ; le **rendement** (en tonnes) et la **superficie cultivée** (en hectares) pour les principales cultures, extraites de la base de données de l'Institut National de la Statistique.

Au niveau régional, les tendances mensuelles et annuelles de la période de végétation (test de tendance de Mann-Kendall) et les anomalies de NDVI au niveau régional ont été analysées. Au niveau de l'étude de cas, les anomalies du NDVI ont été analysées à l'aide de tests statistiques multiples au cours des principales années de sécheresse identifiées sur la base du déficit d'évaporation station-CWD_{CRU}. Le NDVI a également été utilisé par la suite pour dériver des métriques et des anomalies phénologiques à l'aide du package *greenbrown* de R (Forkel et Wutzler, 2015 ; Forkel et al., 2013, 2015) : début de saison (SOS) et fin de saison végétative (EOS).

6.2. IMPACT DE LA SÉCHERESSE SUR LA VÉGÉTATION AU NIVEAU RÉGIONAL

6.2.1. Changements saisonniers dans l'activité de la végétation

La distribution spatiale des tendances mensuelles du NDVI dans les terres arables (dans les pixels stables) est étudiée au niveau régional. Ces résultats sont ensuite discutés dans le contexte des changements phénologiques et climatiques, avec des implications sur la disponibilité saisonnière de l'eau et le moment d'apparition des sécheresses.

Tout d'abord, l'analyse de cet indicateur dans les différents types d'occupation du sol de la zone d'étude a révélé des tendances différentes de l'indice NDVI. De 2001 à 2020, les terres arables ont connu des tendances positives entre avril et juin et des tendances négatives en août et septembre (**Figure 7.2**)**.** Dans le cas des prairies, les tendances sont positives entre avril et juillet et négatives en septembre et octobre. D'autre part, les forêts ont réagi différemment à la sécheresse. Les forêts de feuillus ont montré des tendances majoritairement positives tout au long de la saison de croissance, avec les plus grandes zones de tendances positives en mai (**Figure 7.5**). Les forêts mixtes ont montré des tendances positives, en particulier vers la fin de la saison de croissance (environ 60 % des pixels étudiés ont montré des tendances significatives en septembre). Les forêts

de conifères ne présentaient pas de grandes zones couvertes par des tendances significatives (la proportion la plus élevée de tendances significatives était d'environ 25 % en septembre), et celles-ci étaient principalement positives. Les tendances pourraient être liées à des changements dans les phases phénologiques dus à des températures plus élevées, à des changements dans la répartition des précipitations au cours de l'année, à l'effet des concentrations plus élevées de CO_2 et aux pratiques agricoles dans les terres arables et les prairies, avec des implications pour la production de biomasse végétale. En outre, malgré la condition d'exclure les zones où l'occupation du sol a changé entre 2000 et 2018, les changements d'après 2018 pourraient également avoir influencé les résultats.

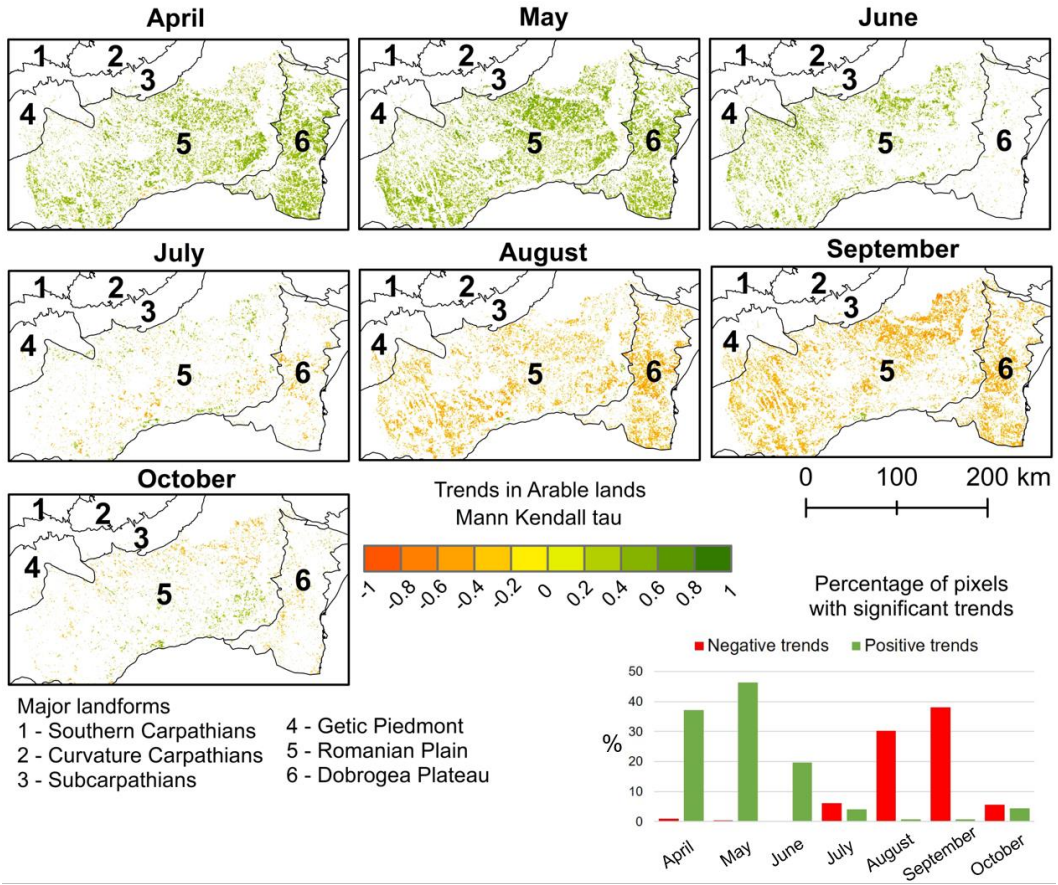

Figure 7.2 Tendances mensuelles significatives du NDVI dans les terres arables entre 2001 et 2020 dans les pixels stables. Le graphique montre le pourcentage de pixels présentant des tendances significatives sur l'ensemble des pixels stables des terres arables.

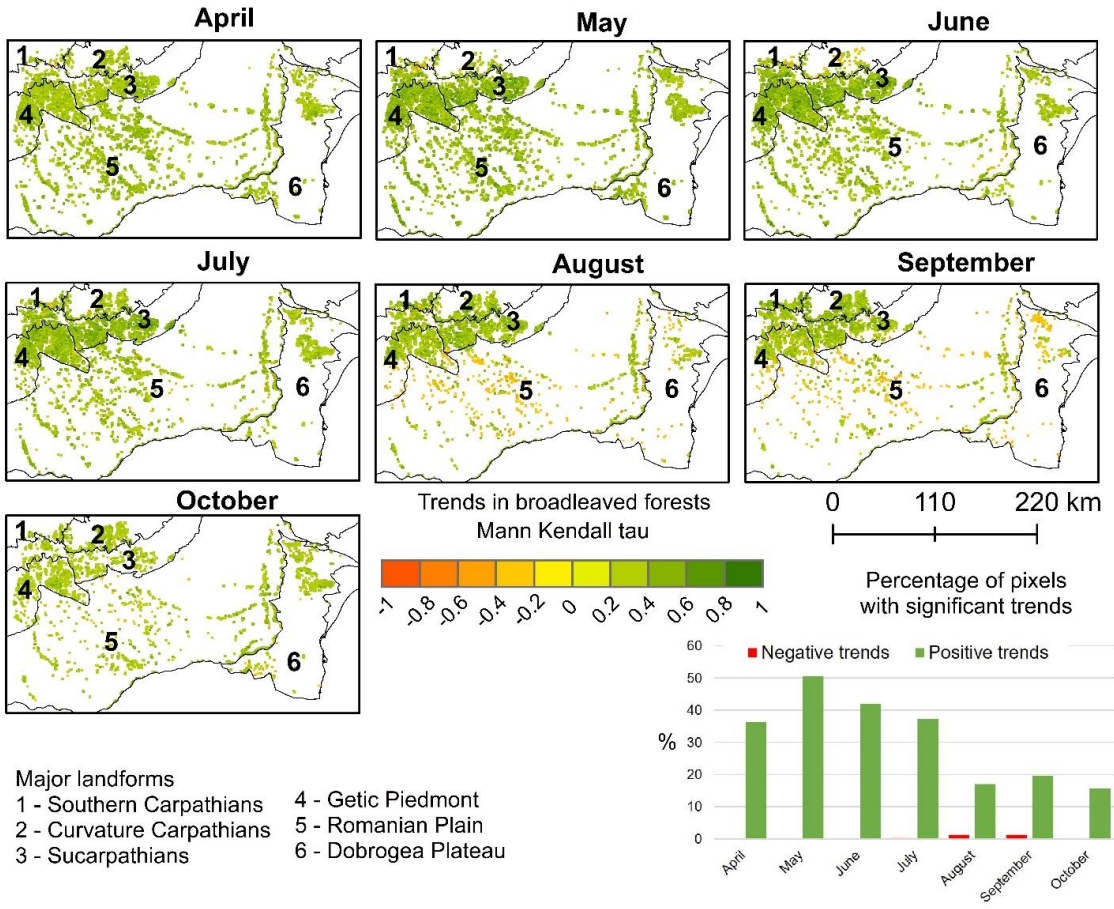

Figure 7.5 Tendances mensuelles du NDVI pour les forêts de feuillus (les pixels indiqués ont des tendances significatives, seulement dans les pixels stables). Les pixels sont exagérés pour des raisons de visibilité.

6.2.2. Variabilité interannuelle de l'état de santé de la végétation

Ce chapitre se concentre sur l'étude des anomalies négatives standardisées du NDVI inférieures à -1, considérées ici comme une *végétation affectée*, sur la période 2001-2020. Ces anomalies sont d'abord présentées à l'échelle régionale et analysées par type d'occupation du sol. Ensuite, elles sont interprétées en relation avec l'occurrence de la sécheresse météorologique

L'analyse interannuelle du NDVI a révélé des années de stress important dans différents types de d'occupation du sol, comme le montrent les baisses inférieures à la moyenne du NDVI : 2001, 2003, 2007, 2008, 2012 et 2020. Ces années de stress de la végétation sont associées à des événements de sécheresse identifiés par des indicateurs de sécheresse normalisés (SPI, SPEI) et à des mois et des années présentant des valeurs élevées de CWD.

La distribution spatiale de l'année présentant la **plus grande anomalie standardisée du NDVI moyen pendant la saison de croissance (avril - octobre)** est présentée dans la **Figure 7.8**. Elle montre que c'est en 2007 que la distribution spatiale des pixels présentant la plus faible anomalie de NDVI a été la plus large. Cela indique de vastes régions de végétation stressée en 2007 dans la Plaine Roumaine et sur le Plateau de Dobrogea.

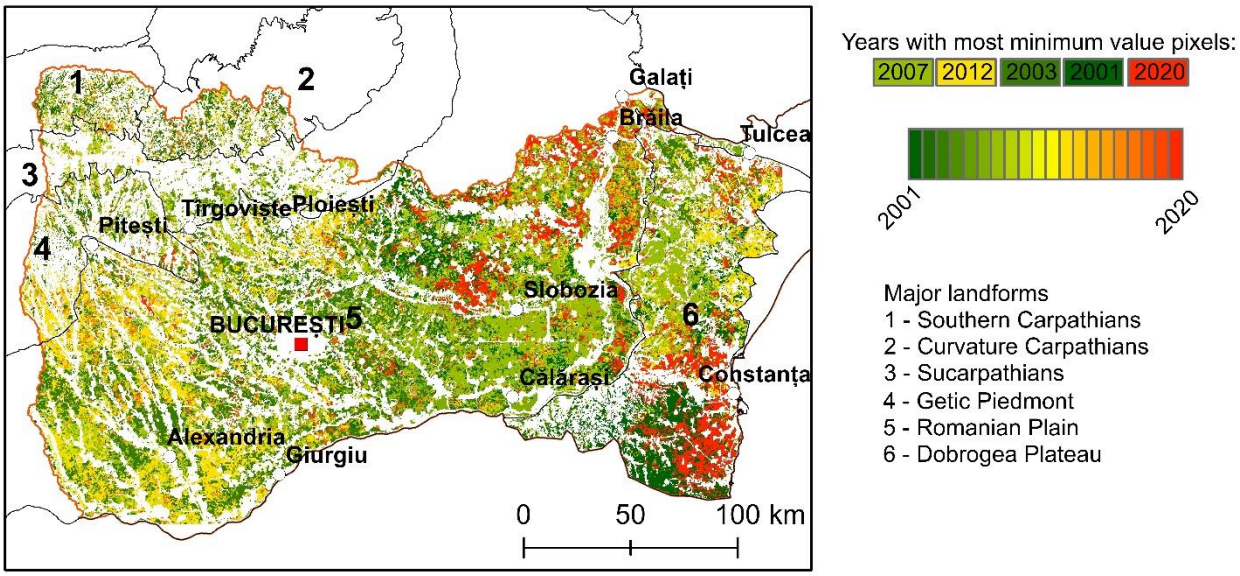

Figure 7.8 Année pour chaque pixel présentant la plus grande anomalie moyenne normalisée de NDVI sur 16 jours pendant la période de végétation (avril - octobre, 2001 - 2020)

6.3. DIFFÉRENCES RÉGIONALES DANS LA REPONSE DE LA VÉGÉTATION À LA SÉCHERESSE

Une analyse détaillée du NDVI a été réalisée dans cinq zones d'étude représentant différentes écorégions de la zone d'étude, seulement dans des forêts de feuillus. La variabilité de l'anomalie NDVI moyenne de la forêt de feuillus pendant la saison de croissance sur les cinq sites indique une vitalité végétale plus faible entre 2001 et 2003, 2007 et 2009, 2006 et 2009, 2012 et 2019 et 2020 (**Figure 8.1**). En revanche, des anomalies positives prédominantes ont été observées pendant la période 2013-2018.

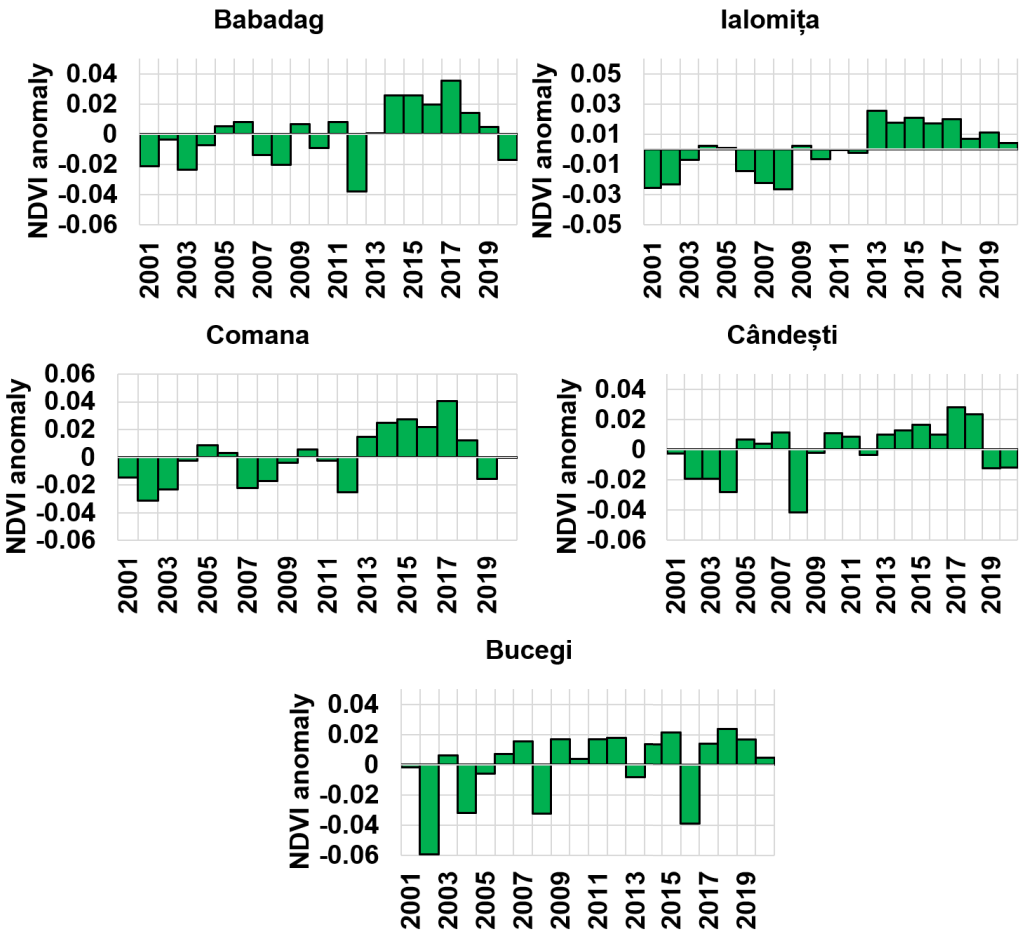

Figure 8.1 Anomalie moyenne du NDVI au cours de la période de végétation dans les cinq zones sélectionnées dans la zone d'étude : Babadag, Ialomița, Comana, Cândești et Bucegi

Pour les forêts de feuillus dans la zone de plaine, les coefficients de Pearson appliqués à la relation entre le NDVI et le CWD ont montré des corrélations négatives significatives en juillet dans la forêt de Babadag, en mai et de juillet à septembre dans la forêt de Comana et dans le corridor de Ialomița. Les forêts de feuillus situées à des altitudes plus élevées ont montré une corrélation négative significative en août dans la forêt de Cândești. En général, les corrélations entre le NDVI et le CWD n'étaient pas significatives pour les forêts de la partie sud des monts Bucegi. En outre, le test de Kruskal-Wallis a montré qu'il existait des différences significatives dans les anomalies du NDVI entre les cinq sites pour chacune des années de sécheresse sélectionnées (**Tableau 8.6**). Cependant, le test de Dunn a montré quels sites ne présentaient pas de différences significatives pour chaque année sélectionnée. Par exemple, les zones de Babadag

et de Comana ont été regroupées le plus souvent, tandis que la zone de Bucegi a eu une réponse différente des autres sites pour la plupart des années sélectionnées.

Tableau 8.6 Comparaison des anomalies du NDVI pendant la période de végétation dans les forêts de feuillus des cinq zones d'étude au cours de certaines années de sécheresse, à l'aide du test de Kruskal-Wallis et du test de Dunn. Les résultats doivent être interprétés au niveau de la ligne du tableau.

Année	*Sig*	*Babadag*		*Ialomita*		*Comana*		*Chanter*		*Bucegi*	
		Médiane	Test de Dunn	Médiane	Test de Dunn	Médiane	Test de Dunn	Médiane	Test de Dunn	Médiane	Test de Dunn
2003	*	-0.024	A	-0.006	D	-0.021	A, C	-0.019	C	0.009	B
2007	*	-0.009	A	-0.018	A, D	-0.015	D	0.013	C	0.018	B
2008	*	-0.02	A	-0.02	D	-0.02	A	-0.04	C	-0.03	B
2009	*	0.0085	A	0.0014	D	-0.0017	C	0.0004	C	0.0192	B
2011	*	0.0103	A	0.0007	D	-0.0014	C	0.0090	A	0.0179	B
2012	*	-0.037	A	-0.001	C	-0.021	D	-0.002	C	0.019	B
2015	*	0.03	A	0.02	B	0.03	A	0.02	C	0.02	B
2018	*	0.012	A	0.008	C	0.015	A	0.026	B	0.025	B
2019	*	0.006	A	0.011	D	-0.013	C	-0.015	C	0.020	B
2020	*	-0.016	A	0.007	B	-0.002	D	-0.011	C	0.009	B

Sig : signification du test de Kruskal-Wallis. * indique une signification statistique (valeur $p < 0,05$).
Test de Dunn : A, B, C, D - Lettres du test de Dunn indiquant les comparaisons multiples par paire pour les lignes. La même lettre majuscule dans une ligne indique qu'il n'y a pas de différence statistiquement significative entre les sites pour l'année en question. Des lettres majuscules différentes dans une même ligne indiquent des différences statistiquement significatives entre les sites correspondants.

La régression linéaire entre la température moyenne de février-mars et le début de la saison (SOS) en utilisant la technique de lissage *spline* et la méthode d'identification de la phénologie *white* montre une variation de ~ -1,77 jours/ºC à Cândești, ~ -2,65 jours/ºC à Babadag, ~ -2,79 jours/ºC à Comana, ~ -2,74 jours/ºC à Ialomița. Dans le Bucegi, on observe une relation inverse, ce qui pourrait suggérer que les méthodes de lissage et d'identification phénologique sélectionnées ne conviennent pas à cette région, ou que cette méthode de corrélation n'est pas appropriée. À l'exception de la région de Bucegi, et bien que non significatives pour la plupart, les corrélations entre la température moyenne pré-saison et la fin de saison (EOS) sont pour la plupart négatives, suggérant une EOS plus précoce avec une température pré-saison plus élevée.

6.3.1. Réponse de la végétation à la sécheresse en 2007-2008

La période 2007-2008 a été marquée par l'une des sécheresses les plus graves entre 1961-2020, dont les effets se sont fait sentir dans plusieurs secteurs. Cela s'est vérifié tant pour les terres

arables que pour la végétation naturelle, comme cela a été démontré dans les chapitres précédents. Dans le cas des forêts de feuillus, des valeurs basses de d'anomalie du NDVI ont été enregistrées en 2007 et 2008 dans les zones de basse altitude de Babadag, Ialomița et Comana, et en 2008 et à des altitudes plus élevées dans les régions de Cândești et Bucegi. Selon les résultats du test de Dunn (**Tableau 8.6**), les zones de Babadag, Ialomița et Comana ont eu une réponse similaire en 2007, tandis qu'en 2008, les zones de Babadag et Comana ont eu une réponse similaire. En 2007, le site présentant les anomalies de NDVI les plus faibles était celui de Ialomița, tandis qu'en 2008, c'est celui de Cândești qui présentait les anomalies les plus faibles. Ces résultats ont motivé une analyse plus détaillée des sites étudiés en 2007 et 2008.

6.3.1.1. Conditions climatiques

D'après le CWD, la sécheresse météorologique de 2007 s'est développée du milieu du printemps au milieu de l'été (avril à juillet) dans l'ensemble de la zone d'étude (**Figure 8.7**).

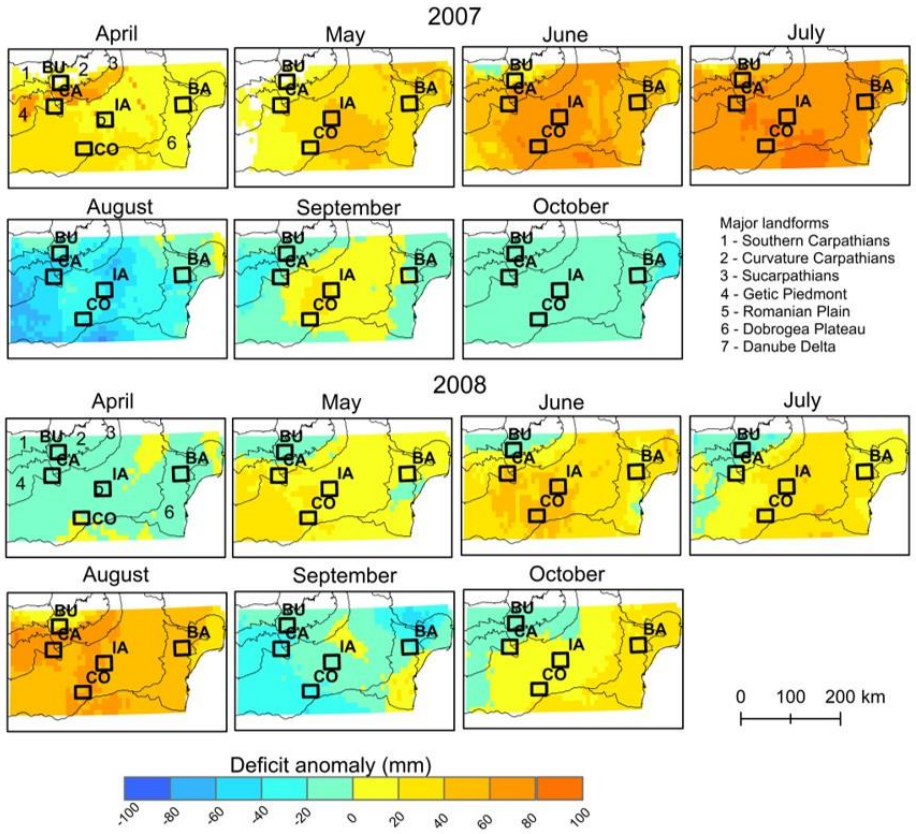

Figure 8.7 Anomalie raster-CWD mensuelle en 2007 et 2008 dans cinq zones d'étude : Babadag (BA), Bucegi (BU), Cândești (CA), Comana (CO) et Ialomița (IA).

Par rapport à la période 1991 - 2020, des valeurs positives de l'anomalie du déficit total de la saison de croissance (station-CWD_{CRU}) ont été enregistrées en 2007 dans toutes les stations météorologiques, mais surtout à București Băneasa (+220 mm), Galați (+224 mm), Tulcea (+199 mm) et Călărași (+187 mm). En 2008, l'anomalie a diminué dans la plupart des stations, mais a augmenté à Buzău, Râmnicu Vâlcea et Roșiorii de Vede. Des anomalies positives de déficit se sont produites de mai à août sur la quasi-totalité de la zone, les valeurs d'anomalie les plus sévères étant enregistrées en août dans la région des Subcarpates.

6.3.1.2. Réponse de la végétation à la sécheresse en 2007-2008

Les conditions déficitaires ont eu une influence négative sur la végétation au printemps et à l'été 2007 (surtout en juillet), en particulier dans les régions de Babadag, Comana, Ialomița et Candesti (**figure 8.9**). En juillet 2007, les forêts des régions de Babadag, Comana et Ialomița ont eu une réponse plus sévère que les autres types d'occupation du sol (terres arables, pâturages). En 2008, des anomalies plus sévères du NDVI se sont produites dans la dernière partie de la saison de croissance, et leur ampleur et leur gravité ont été remarquables en septembre à des altitudes plus élevées (dans les régions de Cândești et de Bucegi).

Les algorithmes phénologiques ont principalement montré un début de saison plus précoce en 2007 et 2008 dans la plupart des zones d'étude, ce qui pourrait être lié à des températures plus élevées. En 2007, les algorithmes ont généralement montré une fin de saison plus tardive (sauf dans la région de Bucegi), ce qui pourrait être lié à l'amélioration des conditions climatiques à partir du mois d'août, tandis qu'en 2008, les résultats variaient considérablement entre les différentes méthodes.

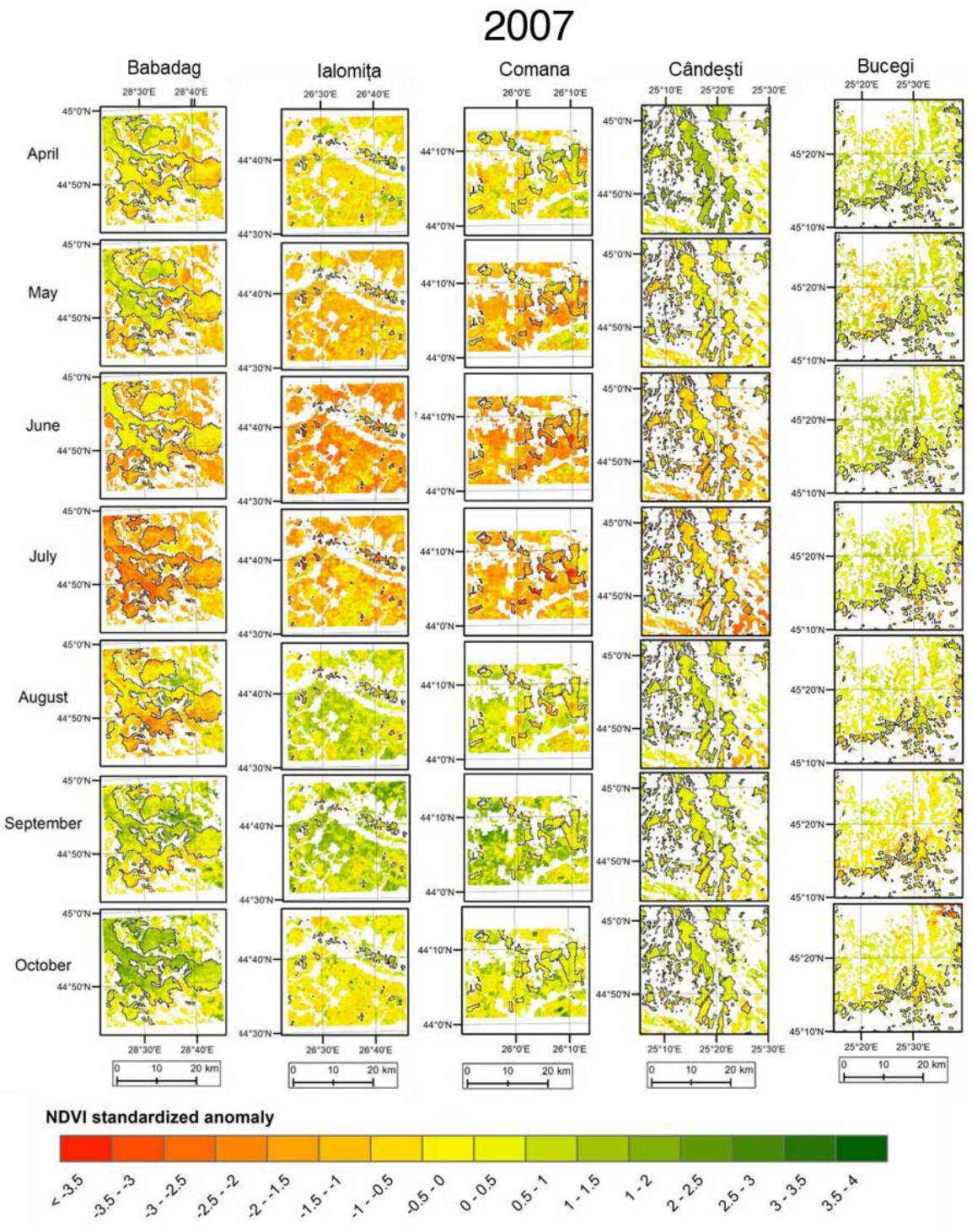

Figure 8.9 Anomalies mensuelles standardisées du NDVI d'avril à octobre 2007 dans les cinq zones d'étude, par rapport à la période 2001-2020. Les couleurs vertes indiquent une anomalie positive (activité supérieure à la moyenne) ; les couleurs orange indiquent des anomalies négatives (activité inférieure à la moyenne).

6.3.2. Réponse de la végétation à la sécheresse en 2019 - 2020

La partie II a démontré, sur la base des indicateurs CWD et normalisés, que la zone d'étude a connu une sécheresse importante entre 2019 et 2020, ce qui a affecté la santé de la végétation telle qu'observée à partir de l'indice NDVI. Par exemple, des valeurs d'anomalie NDVI négatives sont apparues en 2019 et 2020 à Cândești et Comana (réponses similaires selon les résultats du test de Dunn), mais aussi en 2020 à Babadag. Les valeurs médianes les plus faibles sont apparues à Cândești en 2019 (-0,015) et à Babadag en 2020 (-0,016) (**Tableau 8.6**). Pour ces raisons et parce qu'elle est la plus récente de la période analysée, l'analyse de ce chapitre se concentre sur la sécheresse de 2019 - 2020.

6.3.2.1. Conditions climatiques

Par rapport à la période 1991 - 2020, des anomalies positives de l'anomalie du déficit total d'évaporation de la saison de croissance (station-CWD_{CRU}) ont été enregistrées dans la plupart des stations météorologiques, à l'exception de București Băneasa et Vârful Omu. Le déficit a été particulièrement prononcé dans la partie orientale de la zone d'étude, où il a augmenté en 2020 par rapport à 2019 : à Călărași (+123 mm en 2019 et +160 mm en 2020), Constanța (+121 mm en 2019 et +244 mm en 2020), Galați (+178 mm en 2019 et +228 mm en 2020), Tulcea (+182 mm en 2019 et +247 mm en 2020), mais aussi à Roșiorii de Vede (+102 mm en 2019 et +96 mm en 2020).

La distribution spatiale des anomalies mensuelles raster-CDW pour 2020 est présentée dans la **Figure 8.15**. La région de Babadag a connu des anomalies de déficit positives pendant la majeure partie de la saison de croissance (à l'exception du mois de septembre). Les mois avec les plus grandes zones d'anomalies de déficit positives ont été avril, juillet et août en 2020.

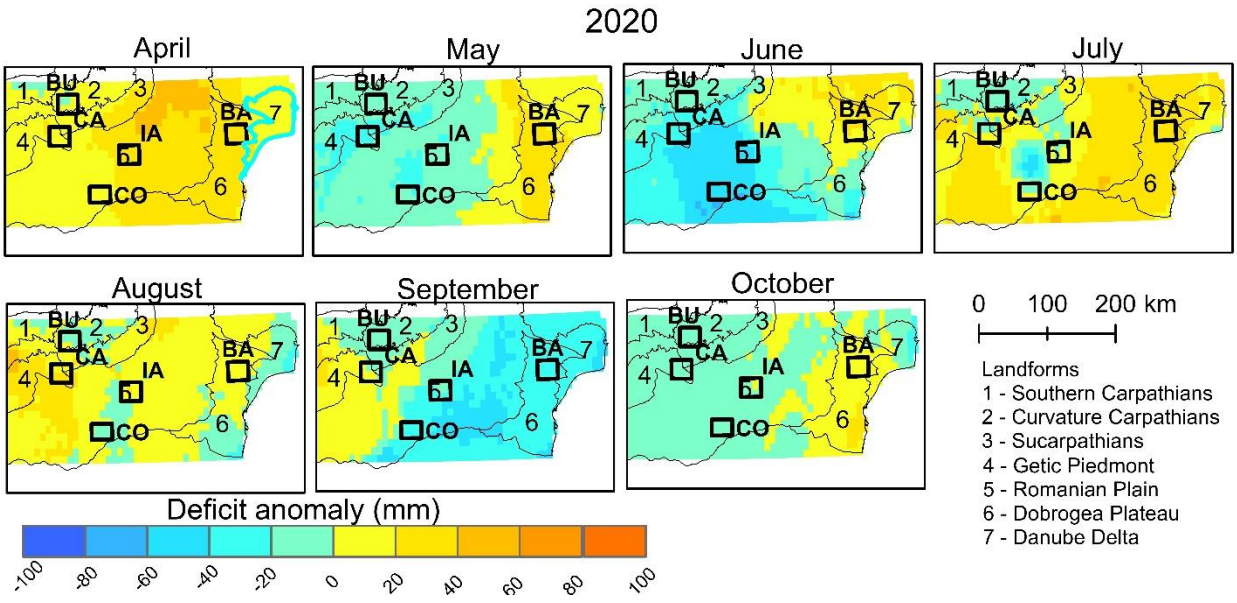

Figure 8.15 Anomalie raster-CWD mensuelle en 2020 dans cinq zones d'étude : Babadag (BA), Bucegi (BU), Cândești (CA), Comana (CO) et Ialomița (IA).

6.3.2.2. Réponse de la végétation à la sécheresse en 2019 - 2020

En 2019, la sécheresse s'est développée au printemps et en automne, avec une persistance remarquable des mois de déficit d'évaporation dans la partie orientale de la zone d'étude. Ces distributions de déficit d'évaporation ont également été observées dans la distribution spatiale des anomalies de NDVI, en particulier dans les zones de Ialomița, Comana et Cândești. Des conditions déficitaires ont été observées en 2020 en avril et en août-septembre dans toutes les stations, mais dans les stations situées dans la partie la plus orientale de la zone d'étude, la sécheresse a été identifiée tout au long de la période de végétation. Cela se reflète également dans la période prolongée d'anomalies négatives du NDVI dans la région de Babadag en 2020 (**figure 8.18**). De faibles anomalies du NDVI ont également été observées dans les régions de Comana et de Cândești entre juillet et septembre 2020.

En termes de phénologie, un EOS plus tardif a été enregistré en 2019 dans la plupart des zones, et à Bucegi, Cândești et Comana en 2020. La plupart des zones ont montré un EOS plus précoce en 2019 et 2020, ce qui pourrait être lié aux conditions de sécheresse prolongées au cours de ces années.

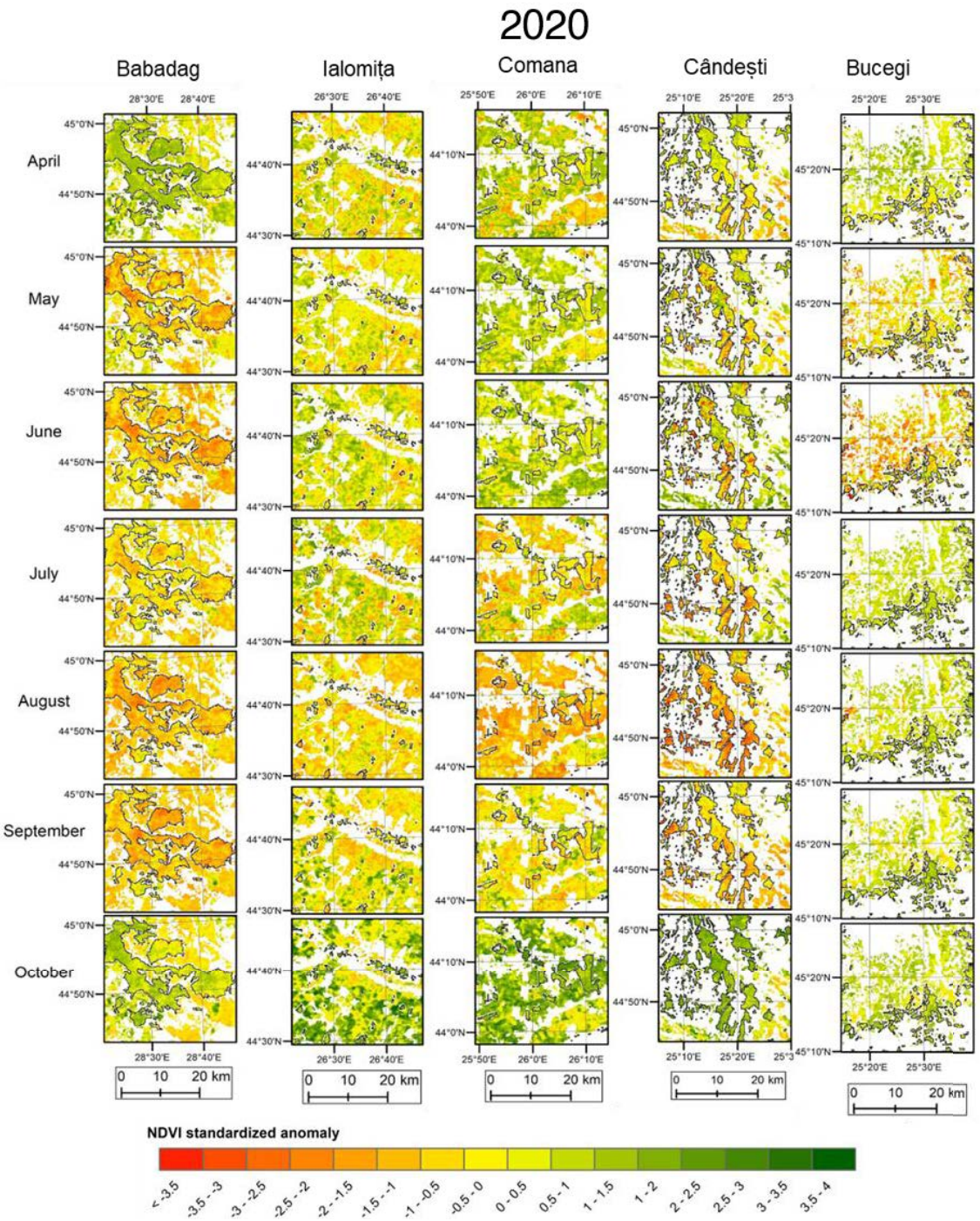

Figure 8.18 Anomalies mensuelles normalisées du NDVI en 2020 dans les cinq zones d'étude par rapport à la période 2001-2020. Les couleurs vertes indiquent une anomalie positive (activité végétale supérieure à la moyenne), tandis que les couleurs rouges indiquent des anomalies négatives (activité végétale inférieure à la moyenne).

7. CONCLUSIONS GÉNÉRALES

La sécheresse est un risque naturel important qui affecte le sud-est de la Roumanie et qui doit être étudié sous plusieurs angles en raison de son évolution et de son impact complexes. Par conséquent, la présente recherche s'est concentrée sur cette région, dans le but d'analyser la variabilité spatiale et temporelle de la sécheresse hydrométéorologique et la manière dont cette variabilité affecte la végétation et le débit des cours d'eau. Cet objectif général a été atteint en utilisant différentes méthodes et approches basées sur l'utilisation d'indicateurs et d'indices climatiques, hydrologiques et de végétation qui ont mis en évidence la complexité du phénomène de sécheresse et son impact sur l'écoulement des rivières et la végétation.

Les résultats de la recherche menée dans le cadre de cette thèse de doctorat ont mis en évidence les principaux aspects suivants :

- Toutes les stations météorologiques analysées ont montré des tendances positives significatives entre 1961 et 2020 dans les valeurs annuelles et estivales de la température de l'air et de l'évapotranspiration potentielle. Les précipitations ne montrent pas une tendance très claire dans la région étudiée au cours de la période analysée. A l'échelle annuelle, des tendances significatives des précipitations ont été observées uniquement aux stations météorologiques de Constanța (positives) et de Sulina (négatives). A l'échelle mensuelle, la plupart des stations ont enregistré des tendances positives significatives en octobre et une tendance à la hausse significative en janvier à Călărași. Des tendances mensuelles négatives significatives ont été observées à Sulina en février et en mai, à Vârful Omu en avril et à Galați en août.
- Les indicateurs climatiques ont montré des périodes de sécheresse, induites soit par un déficit de précipitations (reflété par l'indice standardisé de précipitations, SPI), soit par le bilan hydrique climatique (précipitations moins évapotranspiration potentielle, reflété par l'indice standardisé d'évapotranspiration et de précipitations, SPEI) ou par le déficit d'évaporation (CWD, évapotranspiration potentielle moins évapotranspiration réelle) en 1963-1964, 1968-1969, 1973-1974, 1984-1989, 1991-1995, 2000-2003, 2012 et 2018-2020. Sur le plan hydrologique, le débit des cours d'eau a été affecté par la sécheresse dans les intervalles 1966

- 1969, 1991 - 1995, 2000 - 2004 et 2007 - 2009, qui ont coïncidé avec la sécheresse météorologique ou l'ont suivie.

- Après 1990, une divergence a été observée entre SPI (basé sur les précipitations) et SPEI (basé sur le bilan hydrique climatique). Cela pourrait être principalement dû à la tendance à la hausse des températures, qui entraîne une augmentation de l'évapotranspiration.
- L'analyse du déficit d'évaporation (CWD) entre 1961 et 2020 a montré une plus grande fréquence de mois arides en été, en particulier en août, et une tendance positive significative du déficit d'évaporation en août dans toutes les stations météorologiques (pentes Sen entre 0,7 et 1,13 mm/an), qui est aussi probablement liée à l'augmentation de l'évapotranspiration due à des températures de l'air plus élevées.
- La réduction de l'écoulement observée dans les quatre bassins versants étudiés à la fin des années 1980 et dans les années 1990 est principalement due à des facteurs climatiques (63,1 % - 80 % de contribution climatique), mais aussi à des facteurs anthropiques (19,8 % - 36,9 %).
- Les tendances mensuelles du NDVI ont montré une saisonnalité différente entre les terres agricoles et les forêts. Par exemple, alors que les terres arables présentent des tendances positives du NDVI entre avril et juin et des tendances négatives en août et septembre, les forêts de feuillus ont des tendances majoritairement positives tout au long de la période de végétation, en particulier au printemps. Les forêts mixtes et de conifères montrent des tendances NDVI positives, surtout vers la fin de la période de végétation.
- La variabilité interannuelle de la végétation affectée, basée sur les anomalies du NDVI au cours de la période 2001-2020, a révélé de vastes zones de végétation à faible vitalité en 2001, 2003, 2007, 2012 et 2020. Ces années présentent également la distribution spatiale la plus large dans la zone d'étude lorsque l'on identifie l'année présentant l'anomalie négative la plus faible.
- Les forêts de feuillus dans les zones de basse altitude ont montré des corrélations négatives significatives entre le NDVI et le déficit hydrique climatique en juillet dans la forêt de Babadag, en mai et de juillet à septembre dans la forêt de Comana et le corridor de Ialomița. D'autre part, les forêts de feuillus de plus haute altitude ont montré une corrélation négative significative en août dans la forêt de Cândești. En général, aucune corrélation significative n'a été trouvée pour les forêts de la partie sud des monts Bucegi.

- Des différences significatives ont été constatées dans la réponse de l'anomalie NDVI pendant la saison de croissance au cours des années de sécheresse. Certaines années, la végétation a réagi de manière plus contrastée (2003, 2007, 2012, 2019), tandis que d'autres années ont montré une réaction plus uniforme (2008, 2015). La réponse de la végétation a été moins marquée par les anomalies liées à la sécheresse, mais elle s'est étendue sur une période plus longue pendant la sécheresse de 2020 que pendant celle de 2007.
- L'analyse phénologique a montré des réponses variées en fonction de l'algorithme d'identification de la phase phénologique. Les améliorations futures pourraient porter sur la validation sur le terrain des paramètres phénologiques obtenus à l'aide des séries chronologiques de NDVI.

Malgré les limitations liées à la disponibilité ou à la qualité des données, à l'échelle temporelle et spatiale ou aux incertitudes, cette étude a contribué à une meilleure compréhension des caractéristiques hydroclimatiques de la sécheresse dans le sud-est de la Roumanie et de sa relation avec l'état de la végétation et le débit des cours d'eau. Bien que la recherche ait contribué à l'ensemble des connaissances existantes sur la variabilité de la sécheresse dans un contexte spécifique, les résultats pourraient également être pertinents pour des zones présentant des conditions similaires climatiques et de végétation. Dans le contexte du changement climatique, il est essentiel d'étudier les effets de ce risque sur différentes parties de la mosaïque mondiale des conditions géographiques.

Pour l'avenir, il existe un large éventail de directions de recherche potentielles. Les études futures pourraient complexifier davantage les approches de modélisation utilisées dans la présente étude. Les résultats pourraient être améliorés en augmentant la résolution temporelle et spatiale des indicateurs pris en compte dans les analyses. En outre, les études futures pourraient également se concentrer sur les méthodes de prévision de la sécheresse en vue de réduire l'impact négatif de la sécheresse.

L'étude de la sécheresse et des facteurs qui sous-tendent l'intensification de la sécheresse et ses effets, tels que le réchauffement climatique, la dégradation des sols ou les pratiques agricoles, nécessite une approche transdisciplinaire et internationale ainsi qu'un engagement à long terme.

8. BIBLIOGRAPHIE SÉLECTIVE

ANM. 2008. *Climat de la Roumanie*. Bucarest : Maison d'édition de l'Académie roumaine

Beck H.E., Zimmermann N.E., McVicar T.R., Vergopolan N., Berg A., Wood E.F. 2018. Cartes de classification climatique Köppen-Geiger actuelles et futures à une résolution de 1 km.*Données scientifiques*. 5:1-12

Bîrsan M.-V. 2015. Trends in Monthly Natural Streamflow in Romania and Linkages to Atmospheric Circulation in the North Atlantic. *Water Resources Management*. 29(9):3305-13.

Bîrsan M.-V., Dumitrescu A. 2014. ROCADA : Romanian daily gridded climatic dataset (1961-2013) V1.0 [Dataset].

Bogdan O., Țîștea D. 1983. Climate. In *Geografia României I. Physical Geography*, pp. 195-292. Bucarest : Editura Academiei Republicii Socialiste România.

Bojariu R., Chițu Z., Dascălu S.I., Gothard M., Velea L., et al. 2021. Le *changement climatique - Des bases physiques aux risques et à l'adaptation - Édition révisée et augmentée*. Bucarest : Printech Publishing House

Bojariu R., Dumitrescu A., Burcea S., Crăciunescu V. Ș., Mătreață M., et al. 2019. Le changement climatique dans le secteur des ressources en eau - des bases physiques aux risques et à l'adaptation. Bucarest

Budyko M.I. 1961. Le bilan thermique de la surface de la terre. *Géographie soviétique*. 2(4):3-13

Budyko M.I. 1974. *Climate and Life*. New York : Academic Press

Busuioc A., Dobrinescu A., Birsan M.-V., Dumitrescu A., Orzan A. 2015. Variabilité spatiale et temporelle des extrêmes climatiques en Roumanie et mécanismes associés à grande échelle. *International Journal of Climatology*. 35(7):1278-1300

Chelu A., Zaharia L., Dubreuil V. 2022. Estimation des contributions climatiques et anthropogéniques au changement du débit des cours d'eau dans le sud de la Roumanie. *Journal des sciences hydrologiques*. 67(10):1598-1608

Cheval S., Busuioc A., Dumitrescu A., Bîrsan M.-V. 2014. Spatiotemporal variability of meteorological drought in Romania using the standardized precipitation index (SPI). *Climate Research*. 60(3):235-48

Ciulache S., Ionac N. 2003. *Dictionnaire de météorologie et de climatologie*. Bucarest : Ars Docendi

Cornes R.C., van der Schrier G., van den Besselaar E.J.M., Jones P.D. 2018. Ensemble version of the E-OBS temperature and precipitation datasets ", *Journal of Geophysical Research : Atmospheres*, 123(17):9391-9409.

Crausbay S.D., Ramirez A.R., Carter S.L., Cross M.S., Hall K.R., et al. 2017. Defining ecological drought for the twenty-first century ", *Bulletin of the American Meteorological*

Society, 98(12):2543-50.

Croitoru A.-E., Piticar A., Dragotă C., Burada D.C. 2013. Recent changes in reference evapotranspiration in Romania. *Global and Planetary Change*. 111:127-36

Didan K. 2015. MOD13Q1 MODIS/Terra Vegetation Indices 16-Day L3 Global 250m SIN Grid V006 [Dataset].

Dorigo W., Wagner W., Albergel C., Albrecht F., Balsamo G., et al. 2017. ESA CCI Soil Moisture for improved Earth system understanding : State-of-the art and future directions.*Remote Sensing of Environment*. 203:185-215

Dubreuil V. 1996. Synthèse géographique de la sécheresse dans les régions océaniques. *Météorologie*. 8(15):22-34

Dumitrescu A., Bojariu R., Bîrsan M.-V., Marin L., Manea A. 2015. Recent climatic changes in Romania from observational data (1961-2013). *Theoretical and Applied Climatology*. 122(1-2):111-19

AEE. 2019a. Corine Land Cover (CLC) 2000, Version 2020_20u1 [Dataset].

AEE. 2019b. Corine Land Cover (CLC) 2018, Version 2020_20u1 [Dataset].

AEE. 2021. Les ressources en eau en Europe - faire face au stress hydrique : une évaluation actualisée

Forkel M., Carvalhais N., Verbesselt J., Mahecha M.D., Neigh C.S.R., Reichstein M. 2013. Trend Change detection in NDVI time series : Effects of inter-annual variability and methodology ", *Remote Sensing*, 5(5), 2113-44.

Forkel M., Migliavacca M., Thonicke K., Reichstein M., Schaphoff S., et al. 2015. Codominant water control on global interannual variability and trends in land surface phenology and greenness. *Global Change Biology*. 21(9):3414-35.

Forkel M., Wutzler T. 2015. greenbrown - land surface phenology and trend analysis. Un paquetage pour le logiciel R. Version 2.2

Fu B.P. 1981. On the calculation of the evaporation from land surface. *Scientia Atmospherica Sinica*. 5(1):23-31

Gruber A., Scanlon T., van der Schalie R., Wagner W., Dorigo W. 2019. Évolution des enregistrements de données climatiques sur l'humidité du sol de l'ESA CCI et de leur méthodologie de fusion sous-jacente. *Discussions sur les données scientifiques du système terrestre*. 1-37

Hamed K.H., Ramachandra Rao A. 1998. A modified Mann-Kendall trend test for autocorrelated data. *Journal of Hydrology*. 204(1-4):182-96

Harris I., Osborn T.J., Jones P., Lister D. 2020. Version 4 du CRU TS monthly high-resolution gridded multivariate climate dataset [Dataset]. *Données scientifiques*. 7(1):1-18

Holobaca I.-H. 2010. *L'étude des sécheresses en Transylvanie*. Cluj-Napoca : Cluj University Press

GIEC. 2021. *Changement climatique 2021 : les bases scientifiques. Contribution du groupe de travail I au sixième rapport d'évaluation du groupe d'experts intergouvernemental sur l'évolution du climat*. Cambridge, Royaume-Uni et New York, NY, États-Unis : Cambridge University Press.

GIEC. 2022. *Climate Change 2022 : Impacts, Adaptation and Vulnerability*, Cambridge, UK et New York, NY, USA : Cambridge University Press.

Kendall M.G. 1975. *Rank Correlation Methods*. Londres : Griffin. 4e éd.

Klein Tank A.M.G., Wijngaard J.B., Können G.P., Böhm R., Demarée G., et al. 2002. Daily dataset of 20th-century surface air temperature and precipitation series for the European Climate Assessment. *International Journal of Climatology*. 22(12):1441-53

Mann H.B. 1945. Non-Parametric Test Against Trend. *Econometrica*. 13(3):245-59

McKee T.B., Doesken N.J., Kleist J. 1993. The relationship of drought frequency and duration to time scales. *Proc. 8th Conf. Appl. Climatol. 17-22 janvier 1993*, pp. 179-84. http://ccc.atmos.colostate.edu/relationshipofdroughtfrequency.pdf.

MMSC. 2012. Stratégie nationale de lutte contre le changement climatique de la Roumanie 2013 - 2020

Modarres R. 2007. Streamflow drought time series forecasting. *Stochastic Environmental Research and Risk Assessment*. 21(3):223-33

Mounier J. 1977. Aspects et fréquences de la sécheresse en Bretagne : essai de définition de la sécheresse en Europe océanique. *Revue de géographie de Lyon*. 52(2):167-76

Olson D.M., Dinerstein E., Wikramanayake E.D., Burgess N.D., Powell G.V.N., et al. 2001. Terrestrial ecoregions of the world : A new map of life on Earth (Écorégions terrestres du monde : une nouvelle carte de la vie sur Terre). *BioScience*. 51(11):933-38

Păltineanu C., Mihăilescu I.F., Seceleanu I., Dragotă C., Vasenciuc F. 2007. *Aridité, sécheresse, évapotranspiration et besoins en eau des cultures agricoles en Roumanie*. Constanta : Ovidius University Press

Pettitt A.N. 1979. A non-parametric approach to the change-point problem", *Journal of the Royal Statistical Society. Series C (Applied Statistics)*. 28(2):126-35

Pörtner H.-O., Roberts D.C., Adams H., Adelekan I., Adler C., et al. 2022. Résumé technique. Dans *Climate Change 2022 : Impacts, Adaptation and Vulnerability : Contribution of Working Group II to the Sixth Assessment Report of the Intergovernmental Panel on Climate Change (Changement climatique 2022 : impacts, adaptation et vulnérabilité : contribution du groupe de travail II au sixième rapport d'évaluation du groupe d'experts intergouvernemental sur l'évolution du climat)*, eds. H-O Pörtner, DC Roberts, ES Poloczanska, K Mintenbeck, M Tignor, et al, pp. 37-118. Cambridge, UK et New York, NY, USA : Cambridge University Press.

Prăvălie R., Piticar A., Roșca B., Sfîcă L., Bandoc G., et al. 2019. Changements spatio-temporels du bilan hydrique climatique en Roumanie en réponse aux tendances des précipitations et de l'évapotranspiration de référence pendant 1961-2013.*Catena*. 172:295-312

Schaake J., Liu C. 1989. Development and application of simple water balance models to understand the relationship between climate and water resources (Développement et application de modèles simples de bilan hydrique pour comprendre la relation entre le climat et les ressources en eau). . (181):343-52

Sen P.K. 1968. Estimates of the Regression Coefficient Based on Kendall's Tau. *Journal of the American Statistical Association*. 63(324):1379-89

Spinoni J., Naumann G., Vogt J. 2015. Spatial patterns of European droughts under a moderate emission scenario. *Advances in Science and Research*. 12(1):179-86.

Thornthwaite C.W. 1948. Une approche vers une classification rationnelle du climat. *Geographical Review*. 38(1):55-94

Thornthwaite C.W., Mather J.R. 1955. *The Water Balance*, Vol. 8. Centerton, New Jersey : Drexel Institute of Technology, Laboratory of Climatology.

Trenberth K.E., Dai A., van der Schrier G., Jones P.D., Barichivich J., et al. 2014. global warming and changes in drought. *Nature Climate Change*. 4(1):17-22.

Turc L. 1961. Evaluation des besoins en eau d'irrigation, évapotranspiration potentielle. *Annuaire Agronomie*. 12:13-49

Ujvári I. 1972. *Géographie des eaux roumaines*. Bucarest : Editura Științifică

Van Loon A.F., Gleeson T., Clark J., Van Dijk A.I.J.M., Stahl K., et al. 2016. Drought in the Anthropocene. *Nature Geoscience*. 9(2):89-91

Vermote E., NOAA CDR Program. 2019. NOAA Climate Data Record (CDR) of AVHRR Leaf Area Index (LAI) and Fraction of Absorbed Photosynthetically Active Radiation (FAPAR), version 5 [Dataset].

Vicente-Serrano S.M., Beguería S., López-Moreno J.I. 2010. A multiscalar drought index sensitive to global warming : The standardized precipitation evapotranspiration index", *Journal of Climate*, 23(7):1696-1718.

Banque mondiale. 2018. *Romania Water Diagnostic Report : Moving toward EU Compliance, Inclusion, and Water Security*. Washington, DC : Banque mondiale.

Zaharia L. 2004. Ressources en eau des rivières en Roumanie. *Annales de l'Université de Bucarest : Géographie*. 77-85

Zaharia L., Ioana-Toroimac G., Perju E.-R. 2020. Impacts hydrologiques des changements climatiques en Roumanie. Dans *Water Resources Management in Romania*, pp. 309-51.

Zargar A., Sadiq R., Naser B., Khan F.I. 2011. A review of drought indices ", *Environmental Reviews*. 19:333-49

Zhang L., Hickel K., Dawes W.R., Chiew F.H.S., Western A.W., Briggs P.R. 2004. A rational function approach for estimating mean annual evapotranspiration", *Water Resources Research*, 40(2), p. 1-14.

Zheng H., Zhang L., Zhu R., Liu C., Sato Y., Fukushima Y. 2009. Responses of streamflow to

climate and land surface change in the headwaters of the Yellow River Basin. *Water Resources Research*. 45(7):1-9

COLLEGE DOCTORAL BRETAGNE
ESPACES SOCIETES CIVILISATIONS

UNIVERSITÉ RENNES 2

Titre : La sécheresse hydroclimatique et ses impacts sur la végétation dans le sud-est de la Roumanie

Mots clés : sécheresse, déficit d'évaporation, bilan hidrique, dynamique de la végétation, cadre Budyko

Résumé : La partie sud-est de la Roumanie est particulièrement vulnérable à la sécheresse. La présente étude a pour objectif d'analyser la sécheresse hydroclimatique dans cette région et son impact sur la végétation naturelle et cultivée. La variabilité des paramètres hydroclimatiques pertinents pour la sécheresse est analysée - précipitations, températures, évapotranspiration, débit des rivières. Ensuite, la sécheresse est étudiée en utilisant des indices de sécheresse standardisés et le déficit d'évaporation obtenu par la méthode du bilan hydrique. La partie finale de la thèse est focalisée sur l'évaluation de la réponse de la végétation à la sécheresse, basée sur l'indice de végétation par différence normalisée (NDVI), dans différents types de couverture terrestre et écorégions. Au niveau régional, les tendances du NDVI et la variabilité interannuelle des anomalies du NDVI dans différents types de couverture terrestre sont examinées (terres arables, forêts, pâturages et prairies). En plus, la variabilité du NDVI est étudiée en détail dans les forêts de feuillus dans cinq zones d'étude. Les résultats révèlent des variations de l'état de la végétation et des paramètres phénologiques en réponse à la sécheresse entre 2001 et 2020, en particulier au cours de deux périodes sèches sélectionnées (2007 – 2008 et 2019 – 2020).

Title : Hydroclimatic drought and its impacts on vegetation in south-eastern Romania

Keywords : drought, climatic water deficit, water balance, vegetation dynamic, Budyko framework

Abstract : The south-eastern part of Romania is particularly vulnerable to drought. The aim of this study is to analyze hydroclimatic drought in this region and its impact on natural and cultivated vegetation. The variability of hydroclimatic parameters relevant to drought is analyzed: precipitation, temperatures, evapotranspiration and river flow. Drought is then studied using standardized drought indices and the evaporation deficit obtained using the water balance method. The final part of the thesis focuses on assessing the response of vegetation to drought, based on the Normalised Difference Vegetation Index (NDVI), in different land cover types and ecoregions. At the regional level, NDVI trends and interannual variability of NDVI anomalies in different land cover types (arable land, forest, pasture and grassland) are examined. In addition, NDVI variability is studied in detail in deciduous forests in five study areas. The results reveal variations in vegetation condition and phenological parameters in response to drought between 2001 and 2020, particularly during two selected dry periods (2007 - 2008 and 2019 - 2020).